5-1-2022

DENSITY FUNCTIONAL THEORY STUDIES OF FERMI RESONANCE IN SMALL ARYL AZIDE VIBRATIONAL PROBES

Gammanage Sathya Madhuwanthi Perera
Southern Illinois University Carbondale, sathya.perera@siu.edu

DENSITY FUNCTIONAL THEORY STUDIES OF FERMI RESONANCE IN SMALL ARYL AZIDE VIBRATIONAL PROBES

by

Gammanage Sathya Madhuwanthi Perera

B.S., University of Ruhuna, 2017

A Thesis
Submitted in Partial Fulfillment of the Requirements for the
Master of Science Degree

School of Chemical and Biomolecular Sciences
in the Graduate School
Southern Illinois University Carbondale
May 2022

THESIS APPROVAL

DENSITY FUNCTIONAL THEORY STUDIES OF FERMI RESONANCE IN SMALL ARYL AZIDE VIBRATIONAL PROBES

by

Gammanage Sathya Madhuwanthi Perera

A Thesis Submitted in Partial

Fulfillment of the Requirements

for the Degree of

Master of Science

in the field of Chemistry

Approved by:

Lichang Wang, Chair

Sean D. Moran

Kyle N. Plunkett

Graduate School
Southern Illinois University Carbondale
April 5, 2022

AN ABSTRACT OF THE THESIS OF

Gammanage Sathya Madhuwanthi Perera, for the Master of Science degree in Chemistry, presented on April 5, 2022, at Southern Illinois University Carbondale.

TITLE: DENSITY FUNCTIONAL THEORY STUDIES OF FERMI RESONANCE IN SMALL ARYL AZIDE VIBRATIONAL PROBES

MAJOR PROFESSOR: Dr. Lichang Wang

Site-specific study of the protein using time-resolved IR spectroscopy with the assistance of vibrational probes (VPs) has been the most promising research discipline. However, azide VPs that are absorbed within the protein transparent window generate a complex absorption profile due to Fermi resonance (FR). In the current study, the azide absorption profiles of three aryl-azide compounds: 4-azidotoluene, 4-azido-N-phenylmaleimide, and 4-azidoacetanilide have been explored with basis set effect, solvent effect, intramolecular effect, and the effect of rotational isomerism. Basis set effect was studied using seven basis sets namely: 6-31G(d,p), 6-31+G(d,p), 6-31++G(d,p), 6-311G(d,p), 6-311+G(d,p), 6-311++G(d,p) and 6-311++G(df,pd) with DFT/B3LYP. Geometry optimization and anharmonic frequency calculations have been carried out using two solvents, NNDMA and THF. Peak intensities, relative peak positions to the azido asymmetric stretch, cubic force constants, and the third-order Fermi resonance constants were analyzed. 4-azidoacetanilide has a more complex azide absorption profile that cannot explain both basis set effect and solvent effect. The DFT results show that FR patterns change with para substitution, and the azide asymmetric stretch blue shifts with substitution of methyl to maleimide, or NNDMA to THF. It has been found that rotamers depict the same features in the azide absorption profile. Moreover, theoretical vibrational spectra with the 6-311+G(d,p) basis set can describe the FTIR spectra qualitatively, but it was identified that more accidental FRs would impact on azide absorption profile than that observed in FTIR spectra.

ACKNOWLEDGMENTS

I express my deep sense of gratitude to Dr. Lichang Wang for all of her stimulating motivation, valuable guidance, support, supervision through this research project. Thanks also go to Dr. Sean Moran for his constant support and teaching me the concepts of this research project. Dr. Kyle Plunkett for his advice and support throughout. I would like to thank everyone in the chemistry department for providing me a pleasant working environment to work throughout of my master's degree, especially, my computational group members Thomas Testoff, Domoina Holiharimanana, Zaheer Masood, Ruitao Wu, and Rotimi Ore for giving me constant feedback and support. I would like to thank Taylor Hill for providing me the experimental data and Tenyu Aikawa for the python code.I sincerely thank to all my friends for their encouragement offered during this research project. I would like to thank my loving mother, sister, and Becky for giving me enormous support throughout.

TABLE OF CONTENTS

LIST OF TABLES

LIST OF FIGURES

CHAPTER 1

INTRODUCTION

1.1 Vibrational (Infrared) Spectroscopy

When a molecule interacts with electromagnetic radiation, it can undergo various changes (e.g., rotation about its center of gravity, stretching and bending of the bonds, etc.) due to the transitions between different types of quantized energy levels, such as electronic, vibrational, rotational, and translational. Infrared (IR) light has an energy of ~ 400 – 4000 cm^{-1} that corresponds to the energy involved in the vibrational motions of molecules. Vibrational transitions are allowed observed by IR if the dipole moment of the molecule changes during a particular vibration. Hence, homonuclear diatomic molecules, symmetric polyatomic molecules, and symmetric stretching and bending vibrations of some heteronuclear molecules are IR inactive. Two atoms in a molecule are connected by an elastic bond, like a spring, that vibrates around an average position (equilibrium bond length). This elastic bond has an intrinsic vibrational or oscillation frequency depending on the reduced mass and force constant which obeys Hooke's law. Thus, lighter atoms and stronger bonds with more s-character and polar character particularly have high wavenumbers.[1] IR spectroscopy is a widely used tool for studying the functional groups in organic compounds because particular functional groups vibrate in a characteristic region of the IR spectrum. If an organic compound is irradiated with IR light, some frequencies will get absorbed by the compound and the rest will pass through the compound without being absorbed. IR spectrometer measures "Transmittance", the percentage of IR light that passes through the compound. Therefore, ~100% transmittance indicates that the compound doesn't consist of such types of bonds whilst a low percentage of transmittance indicates that the compound does have that particular functional group.

1.1.1 Vibrational Degrees of Freedom

The Heisenberg uncertainty principle states that it is impossible to accurately determine both the position and momentum of a particle simultaneously because molecules are constantly in motions such that they possess three general types of motions: translations, rotations, and vibrations. The "Degree of Freedom" defines the number of variables used to describe the motions of an atom. In 3-D space, each atom has three degrees of freedom. Thus, a molecule containing N number of atoms has a 3N total number of degrees of freedom. Each translational and rotational motions use three degrees of freedom around its center of mass. However, for linear molecules, only two rotational degrees of freedom are counting due to rotation around its axis leaving the molecule unchanged. The rest of the remaining degrees of freedom describe the vibrational motions of the molecule. Therefore, a linear molecule has 3N-5 vibrational degrees of freedom while a non-linear molecule has 3N-6 vibrational degrees of freedom.

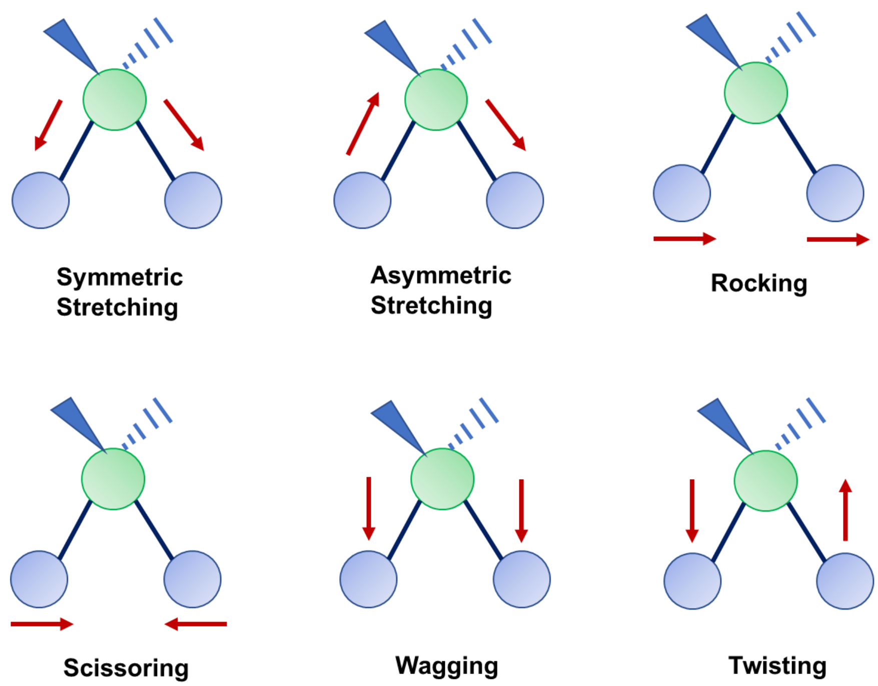

Figure 1.1 – Types of vibrational modes of chemical bonds.

1.1.2 Vibrational Modes

Vibrational modes are defined as different independent vibrational motions of atoms. Vibrational modes can be represented by stretching and bending vibrations (Figure 1.1). Stretching vibration is a change of bond length and the number of stretching modes are equal to the number of bonds in the molecule of interest. Stretching vibrations can be symmetric or asymmetric. Only asymmetric stretching vibrations are IR active whereas symmetric vibrations are Raman active. Bending vibration is a change of bond angle and there are two types of bending vibrations: In-plane Bending and Out-of-plane Bending. In-plane bending vibrations are rocking and scissoring while out-of-plane vibrations are wagging and twisting. Twisting vibrations are also IR inactive.[2]

1.1.3 Harmonic Oscillator & Anharmonic Oscillator

Vibrational transitions of a molecule can be demonstrated by two models: Simple Harmonic Oscillator (SHO) and Morse Potential. In harmonic oscillator approximation, the molecule is at rest at equilibrium bond length r_e, and the change of energy of the bond is similar when it stretches and compresses by the same distance (obeying Hooke's law), see Figure 1.2. The energy of a vibrational level is given by equation 1, derived by 1-D Schrödinger equation, where v is the vibrational quantum number, h is the Planck's constant, and ω_e is the oscillation frequency. When v = 0, a molecule has non-zero vibrational energy which means that atoms can never be completely at rest relative to each other. This energy is known as "Zero-point energy" (equation 1.2).

$$E_v = \left(v + \frac{1}{2}\right) h\omega_e \tag{1.1}$$

$$E_0 = \frac{1}{2} h\omega_e \tag{1.2}$$

Solutions to the Schrödinger equation restrict vibrational transitions to $\Delta v = \pm 1$ (selection rule), and at room temperature, only the ground state is populated. Therefore, the harmonic spectrum of a molecule shows only "Fundamental" vibrations which are defined as the transitions from the ground state ($v = 0$) to the first excited state ($v = 1$). For harmonic oscillator, $E_v \rightarrow \infty$ when $v \rightarrow \infty$, the molecule is still intact. Actual chemical bonds do not obey Hooke's law as they are dissociated at larger internuclear separations. Hence, the anharmonic oscillator approximation also known as Morse Potential, suggested by P. M. Morse, shows a more accurate description of the vibrational energies. [3] The energy of a vibrational level is then modified to equation 1.3, where x_e denotes the anharmonicity constant.

$$E_v = \left(v + \frac{1}{2}\right) h\omega_e - \left(v + \frac{1}{2}\right)^2 h\omega_e x_e + \left(v + \frac{1}{2}\right)^3 h\omega_e y_e + \ldots. \qquad (1.3)$$

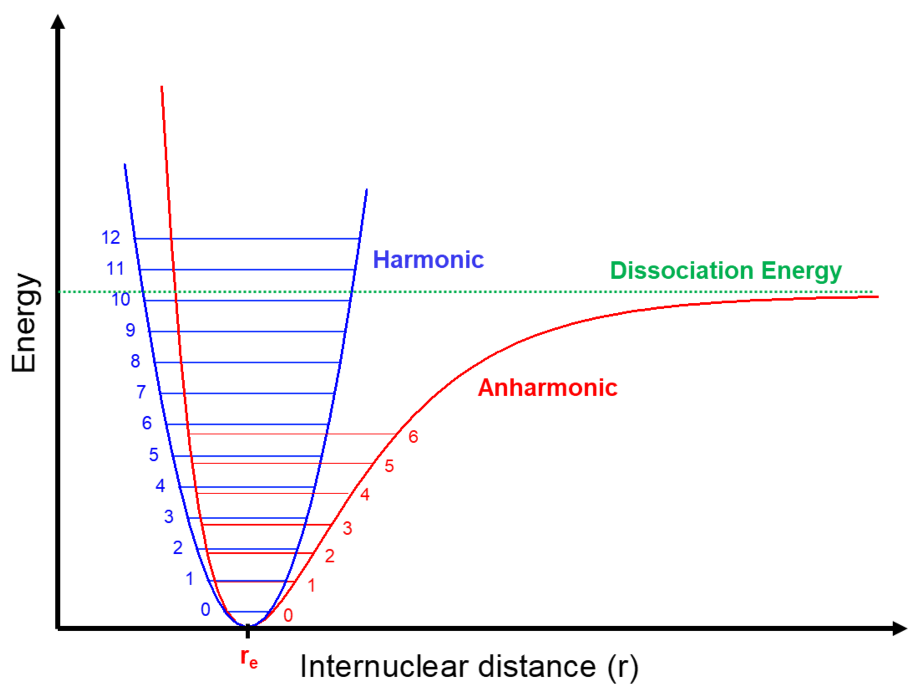

Figure 1.2 – The energy profile of harmonic oscillator (blue) and the Morse potential (red). r_e is the equilibrium bond length, and the bond dissociates at dissociation energy.

1.1.4 Types of Vibrational Transitions

For an anharmonic oscillator, the selection rule is $\Delta v = \pm1, \pm2, \pm3 \ldots$, reflecting that a transition from the ground state ($v = 0$) to the higher energy levels are allowed. These vibrational transitions are known as "Overtones". At room temperature, some molecules have a significant population in the $v = 1$ state, and transitions from this excited state are known as hot bands. Combination bands are generated due to the excitations of two or more different fundamental vibrations simultaneously. Figure 1.3 demonstrates the energy profiles of different kinds of vibrational transitions.

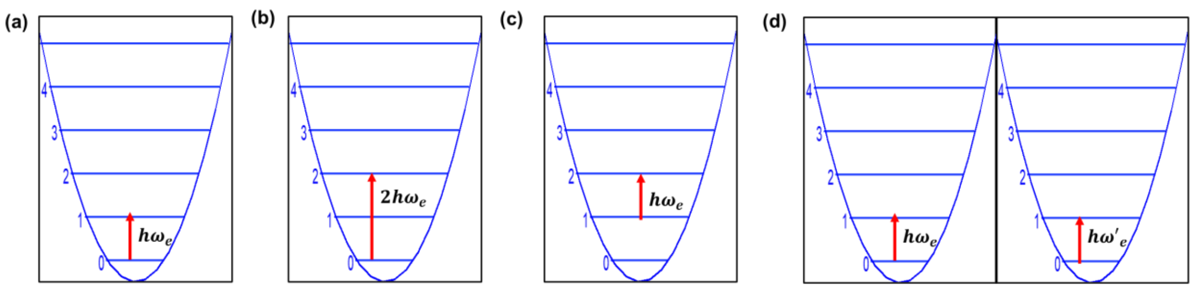

Figure 1.3 - The vibrational energy profiles of (a) a fundamental ($\Delta E = \boldsymbol{h\omega}_e$), (b) a first overtone ($\Delta E = 2\boldsymbol{h\omega}_e$), (c) hot bands ($\Delta E = \boldsymbol{h\omega}_e$), and (d) a combination band ($\Delta E = \boldsymbol{h\omega}_e + \boldsymbol{h\omega}'_e$).

1.2 Fermi Resonance

Fermi resonance (FR) is the resonance between a fundamental vibration and a combination band or an overtone band with similar energy and symmetry of the fundamental vibration. In general, combination bands or overtones are unnoticeable in the IR spectrum. However, if a combination band or overtone is located near to the fundamental vibration, energy transfer from fundamental vibration to combination band or overtone will happen and it results in an increased intensity of combination band or overtone while a decreased intensity of fundamental vibration (Figure 1.4). Moreover, this will create a splitting of the absorption profile of fundamental vibration and frequency shift in both modes.[4] Therefore, the fundamental absorption profile becomes more complex and broader. FRs play a major role in vibrational energy transfer in proteins. Therefore, understanding FRs and vibrational coupling would provide additional information about the environment of a protein and its dynamics. [5, 6]

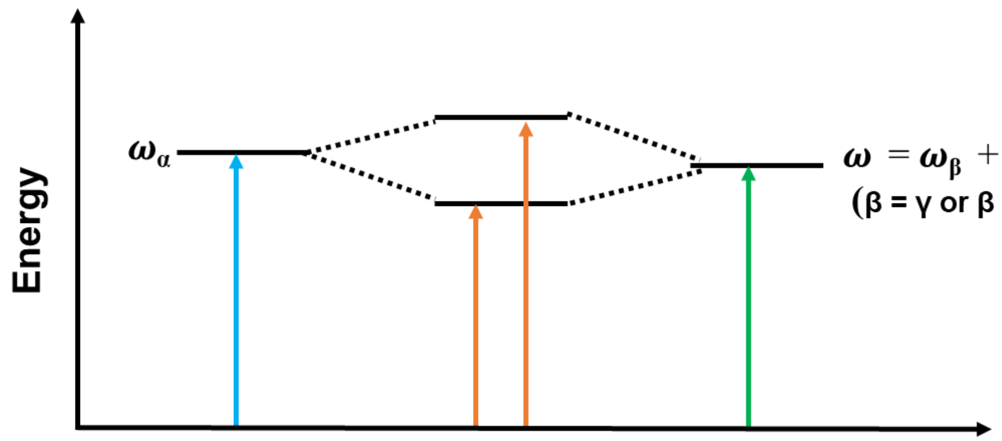

Figure 1.4 – The energy profile of a Fermi resonance, where $\boldsymbol{\omega}_\alpha$ is the fundamental frequency and $\boldsymbol{\omega}_\beta$ and $\boldsymbol{\omega}_\gamma$ are fundamental frequencies of the combination band ($\beta \neq \gamma$) or overtone ($\beta = \gamma$).

1.3 Vibrational Probes

Vibrational spectroscopy has been a vital tool in the investigation of biological systems such as RNAs, proteins, and peptides. Proteins are built from twenty amino acids and are limited to a few atoms (C, H, N, O, and S). Thus, vibrational spectra of proteins are congested, broadened, and complicated due to the similarities in vibrational modes, diverse intermolecular and intramolecular interactions, and vibrational coupling. Interestingly, vibrational spectra of proteins have a “transparent window” between 1800-2300 cm^{-1} where no native protein vibrations occur. Small organic molecule-based “vibrational probes” (VPs) that generate signals within this region have been used in structure elucidation and dynamic studies of proteins. [7-10]

The most common VPs that absorb within this region are small molecules containing carbon-deuterium bonds (C-D), nitriles (-CN), thiocyanates (-SCN), azides ($-N_3$), cyanamides (-

NCN), transition metal-carbonyl complexes $M(CO)_n$, alkynes (C≡C), or C-F groups. [11-31] Spectral characteristics of VPs should include large transition dipole strength, narrow bandwidth, and long vibrational lifetime. Large transition dipole strength facilitates the analysis of protein solutions at micro-to lower millimolar concentrations with a high signal-to-noise ratio. For example, the major challenge of using C-D, C≡C, and -CN as VPs is their low transition dipole strength compared to metal-carbonyl complexes and azide VPs. In addition, vibrational lifetime plays a major role when selecting a VP for time-resolved nonlinear IR spectroscopy. In general, vibrational lifetimes are very short for many VPs, but attempts have been made to increase vibrational lifetimes by a combination of isotopic labeling and heavy atom effects. Kossowska et al. showed that the incorporation of S, Si, or Se atoms adjacent to a C≡C bond can increase vibrational lifetimes by an order of 2, 10, or 16, respectively.[32, 33] Park et al. have also shown that incorporation of S and Se atoms can enhance the vibrational lifetime of nitrile-derivatized prolines.[34] Chalyavi et al. have reported that the use of heavy atoms like Si and Sn, or heavy ^{15}N isotope can increase vibrational lifetimes from ~2 ps to ~300 ps.[35]

Moreover, steric perturbative effects, solvothermal stability, and sensitivity of the VP must be considered when determining the appropriate VP for a specific application. Levin et al. have reported the relative ranking of VPs based on these parameters.[36] It shows that transition metal-carbonyl compounds are least favorable in terms of their bulkiness, which can produce undesired perturbations to the protein structure. Isonitrile probes have desirable traits such as high transition dipole strength, sensitivity to H-bonding environment, and comparatively longer vibrational lifetimes, but they are chemically unstable under acidic conditions.[37] Furthermore, VP must be sensitive to the protein environment and not to the vibrational coupling within the VP. For example, -CN and C≡C probes each show a single peak within the transparent window whereas azide probes show complex and broad adsorption profiles resulting from accidental FRs.[38-40] These FRs can be eliminated through isotopic labeling. Lipkin et al. have shown that single or multiple isotopic labels can simplify the complex adsorption profile of 3-azidopyridine by red shifting the frequency by almost 100 cm^{-1}.[41] Because FR is a result of vibrational coupling between transitions with similar energies, isotopic substitution is the most effective way to alter the energies of the transitions by changing the reduced mass. When considering the aforementioned characteristics, azide-modified compounds are some of the most promising VPs and an alternative strategy to using isotopic labeling to simplify their complex absorption profiles.

1.4 Overview

This chapter briefly explains the background to the vibrational spectroscopy and vibrational probes because the study is mainly focusing on understanding anharmonic vibrational coupling and Fermi resonance in the azide absorption profile of small aryl-azide compounds. Chapter 2 demonstrates how computer simulations are utilized to study the anharmonic IR spectra of aryl-azides. Then, Chapter 3 lays out DFT studies of vibrational coupling and Fermi resonance in 4-azidotoluene and 4-azidoacetanilide. Chapter 4 focuses on the impact of rotational isomers on IR spectra of 4-azido-N-phenylmaleimide. The last chapter compares theoretically calculated IR spectra of three aryl-azides with the experimental FTIR spectra as well as the conclusion of this research and future work.

CHAPTER 2

METHODOLOGY

2.1 Computational Chemistry

The branch of chemistry that solves chemical problems with the assistance of computers is known as computational chemistry. Computational chemistry helps to determine the structures and properties of molecules, gases, liquids, and solids. Therefore, properties like energies, charges, dipole moments, frequencies, ionization potentials, electron affinities, and HOMO-LUMO gaps can be obtained by using computational chemistry. There are several computational modeling methods such as Quantum mechanical calculations, Molecular mechanics, Monte Carlo simulation, and Molecular dynamics. These methods have their features and differ from other methods. Quantum mechanical methods describe the electrons and nuclei in a system and the properties that depend upon the electronic distribution can be determined. Molecular mechanics ignores electron motions and the molecule is considered as a collection of spheres joined by springs. The motions of these atoms are described by the laws of classical mechanics and are suitable for larger systems consisting of thousands of atoms. There are several software packages related to computational chemistry. One of the most widely used software is Gaussian,[42] which allows to calculate numerous properties of a particular atom or molecule.

In this study, Gaussian 16W software was used for geometry optimization and frequency calculations of three aryl-azide compounds: 4-azidotoluene, 4-azidoacetanilide, and 4-azido-N-phenylmaleimide in two solvents: NNDMA (N,N-dimethylacetamide) and THF. The Density Functional Theory (DFT) calculations were carried out using B3LYP exchange and correlation functional, and seven different basis sets namely: 6-31G(d,p), 6-31+G(d,p), 6-31++G(d,p), 6-311G(d,p), 6-311+G(d,p), 6-311++G(d,p), and 6-311++G(df,pd) to determine which basis set is optimum to deconvolute the complex absorption profile of azide VPs. The polarizable continuum model using the integral equation formalism variant (IEFPCM), was used to model the solvent. Hence, this work provides deep insights into the intramolecular effect, basis set effect, and solvent effect on the azide absorption profile.

2.2 Density Functional Theory (DFT)

In this study, density functional theory (DFT) is used to compute the electronic structure of molecules. As the name implies, it allows determining all the properties based on the electron density as a function of space and time rather than using wave functions. Therefore, the computational cost is very low compared to the other traditional methods like the Hartree Fock theory. Molecular geometries, frequencies, ionization energies, electric and magnetic properties can be calculated by using this theory. DFT is based on the Hohenberg-Kohn (HK) theorem, which expresses the ground-state electronic energy of an atom or a molecule as a function of the electron density (ρ) of the molecule. ρ is a function of the coordinates of the electrons. The total electronic energy can be denoted as,

$$E = T + V_{nucl} + V_{rep} + E_{xc} \tag{2.1}$$

where T is the electronic kinetic energy, V_{nucl} is the attraction of the electrons(2.2) to the nuclei(α), V_{rep} is the interelectronic Coulomb repulsion, and E_{xc} is the exchange-correlation energy.

$$V_{nucl} = -\sum_{\alpha} \int \frac{Z_{\alpha}\rho(1)}{r_{1\alpha}} d\tau_1 \tag{2.2}$$

$$V_{rep} = -\frac{1}{2} \iint \frac{\rho(1)\rho(2)}{r_{12}}\, d\tau_1 d\tau_2 \tag{2.3}$$

$$T = \frac{3}{10}(3\pi^2)^{2/3} \int \rho^{5/3} d\tau \tag{2.4}$$

$$T = -\frac{1}{2}\sum_i \int \psi_i \nabla^2 \psi_i d\tau \tag{2.5}$$

$$E_{xc} = -\frac{9}{8}\left(\frac{3}{\pi}\right)^{1/5} \alpha \int \rho(1)^{4/3}\, d\tau_1 \tag{2.6}$$

Since the T in terms of ρ is quite complicated and completely unknown, T involving the wavefunctions is used. Also, E_{xc} is solved using a variety of approximations methods, and the simplest approximation is local density approximation, which is given in the E_{xc} equation (2.6). Later, wavefunctions that are obtained from self-consistent field calculations are used due to the difficulty of obtaining high accuracy from ρ functions directly, which is known as Kohn-Sham formulations shown below.[43, 44]

$$F\psi = \varepsilon\psi \tag{2.7}$$

$$F(1) = -\frac{1}{2}\nabla_1^2 - \sum_\alpha \left(\frac{Z_\alpha}{r_{1\alpha}}\right) + \sum_j J(1) + V_{xc} \tag{2.8}$$

$$V_{xc} = \frac{\partial E_{xc}}{\partial \rho} \tag{2.9}$$

$$\rho = \sum_i |\psi_i|^2 \tag{2.10}$$

2.3 B3LYP Functional

B3LYP functional, which stands for Becke, 3-parameter, Lee-Yang-Parr, is a hybrid functional, constructed with a part of exact exchange from Hartree-Fock theory with exchange and correlation from other methods (ab initio or semi-empirical), equations 2.11 and 2.12. For further details about the B3LYP, we refer the reader to the literature.[45-48] B3LYP is the widely used functional because it shows significant improvement from Hartree-Fock results and is generally faster. Also, it gives very good results compared to the other functionals for small organic molecules. A hybrid exchange-correlation (E_x-E_c) functional is generally given as a linear combination of the Hartree-Fock exact exchange functional.[49] Barone et al. have shown that B3LYP exchange and correlational functional offer an excellent compromise between accuracy and computational cost, and provides satisfactory results for studying the vibrational spectroscopic details of small organic molecules.[50]

$$E_X^{B3LYP} = 0.8E_X^{LDA} + 0.2E_X^{HF} + 0.72\Delta E_X^{B88} \quad (2.11)$$

$$E_C^{B3LYP} = 0.19E_C^{VWN3} + 0.81E_C^{LYP} \quad (2.12)$$

2.4 Basis Sets

In quantum calculations, molecule orbitals (MOs) are written as the linear combinations of atomic orbitals, and it is called Linear Combination of Atomic Orbitals-Molecular Orbitals [LCAO-MO].

$$\Psi_i = \sum_{\mu}^{n} c_{i\mu}\phi_\mu \quad (2.13)$$

Usually, i, j, k, l ….. are used for the MOs, and μ, v, λ, δ ... for AOs. n is the number AOs. An atomic orbital is a wave function for a single electron in an atom.[51]

2.4.1 Slater-type and Gaussian-type Orbitals

Initially, the Slater-type Orbitals (STOs) were used as the basis functions because of their similarity to AOs of the hydrogen atom.[52]

$$\psi_{nlmA}(r_A, \theta_A, \phi_A) = f_n(r_A)\, Y_l^m(\theta_A, \phi_A) \quad (2.14)$$

$$f_n^{STO}(r_A) = r_A^{n-1}\, e^{-\zeta r_A} \quad (2.15)$$

Here, ζ is the screening constant depends on various basis functions. (r_A, θ_A, ϕ_A) are spherical coordinates, and $f_n(r_A)$ and $Y_l^m(\theta_A, \phi_A)$ are the radial and angular momentum parts. n, l, and m are principle, angular momentum, and magnetic quantum numbers, respectively. The STOs are exponential functions on distance from the nucleus (A) which is similar to the AOs of hydrogen orbitals and converge rapidly with an increasing number of functions. These functions are not suitable for fast calculations due to the calculation of three and four center integrals.

Then, it was found that the use of Gaussian-type orbitals (GTOs) is much simpler instead of STOs. However, a single GTO is not sufficient to describe AOs. Therefore, a linear combination of GTOs (contracted GTO or CGTO) is used to describe the AOs as follows,

$$f_l^{GTO}\ (r_A) = r_A^l\, e^{-\alpha r_A^2} \qquad (2.16)$$

$$f_l^{CGTO}\ (r_A) = r_A^l \sum_i d_i e^{-\alpha_i r_A^2} \qquad (2.17)$$

where α is also a coefficient depending on the various basis functions. The use of ten GTOs is much faster than STOs. STO is a minimal basis set where only enough functions are used to accommodate all electrons.[53]

2.4.2 Split Basis Sets

The minimal basis sets (STO-nGTO) do not adequately describe anisotropic electron distribution in molecules. Each split basis set has a set of two (or more) functions of different sizes or radial distributions, allowing more flexibility. In a minimal or single-zeta (SZ) basis set, the first-row elements have five AOs (1s, 2s, and 2p). For the double-zeta (DZ) basis set, there are two sets of basis functions for each sub-shell. Hence, for the first-row elements, twelve AOs are allocated (1s, 1s´ 2s, 2s´, 2p, and 2p´). All the functions that are used to double are called outer functions (1s´, 2s´ and 2p´) while minimal basis functions are called 'inner' functions. The inner function has a larger ζ exponent and therefore it is tighter, the outer has smaller ζ , and it is more diffused. Similarly, triple-zeta (TZ), quadruple-zeta (QZ), and quintuple (5Z)… basis sets are also used. Since the core electrons are chemically insignificant and constant, Split-valence basis sets are used to improve the flexibility of the valence region and use a single (contracted) set of functions for the core electrons. Hence, the valence double-zeta basis set double the number of basis functions in the valence region only. For example, the first row elements then have ten AOs (1s, 2s, 2s´, 2p, and 2p´). Moreover, polarization basis functions were also added to improve the description of anisotropic electron distribution. Thus, normally p orbitals are added to the H and He atoms, d orbitals are added to first-row atoms, and f orbitals are added to second-row atoms. Normal split valence basis sets describe electron distribution not far away from the nucleus. Some cases have electron distribution far away from nuclear centers (e.g., anions, molecules with lone pairs of electrons, excited states, transition states). One adds additional s (for H and He) and p (for heavy atoms) functions with very diffuse radial distributions.[54-56]

2.4.3 Pople Style Basis Sets

The notation for the split-valence basis sets was first introduced by John Pople's group. The basis set notation looks like k-nlm++G** or k-nlm++G(idf,jpd), where k primitive GTOs for core electrons, n primitive GTOs for inner valence orbitals, l primitive GTOs for medium valence orbitals, and m primitive GTOs for outer valence orbitals. "+" means 1 p diffuse functions added to heavy atoms and "++" means 1 p diffuse functions added to heavy atoms and 1 s diffuse functions added to H atom. "*" means 1 d polarization functions added to heavy atoms. "**" means 1 d polarization functions added to heavy atoms and 1 p polarization functions added to H atom. "idf" means i d and 1 f polarization functions added to heavy atoms. "idf,jpd" means i d and 1 f polarization functions added to heavy atoms and j p and 1 d polarization functions added to H atom. In DZ split valence basis sets, inner valance basis orbitals are the minimal basis functions (ex; 2s, 2p), medium and outer valance orbitals are the set of added basis functions (2s′,2p′). In TZ split valence basis sets, inner valance basis orbitals are the minimal basis functions (ex; 2s, 2p), medium valance basis orbitals are the first set of added basis functions (2s′,2p′) and outer valance orbitals are the second set of added basis functions (2s″,2p″).[57-61]

Example: DZ split valance : 3-21G, 6-31G, 3-21G*,3-21+G*, 6-31+G**, 6-31++G(d,p)

TZ split valance : 6-311G, 6-311+G(2df,p), 6-311++G(df,pd)

In this study, the IR spectra of three aryl-azides were calculated using seven basis sets: 6-31G(d,p), 6-31+G(d,p), 6-31++G(d,p), 6-311G(d,p), 6-311+G(d,p), 6-311++G(d,p) and 6-311++G(df,pd) to understand the basis set effect on Fermi resonance in azide absorption profile.

2.5 Gaussian 16W software

Gaussian 16W is a computer program designed for computational chemistry calculations.[42] It is the latest version in the Gaussian series of electronic structure programs. The calculated properties using Gaussian software include the energies, molecular geometries, frequencies of molecules, etc. It can be used to study intermediates that are impossible to observe experimentally. The GaussView 6.0.16 (Figure 2.1) is a graphical user interface that enables to input structure to Gaussian 16W and to examine the output structures generated after calculations from Gaussian. Hence, GaussView software helps to visualize the results of Gaussian calculations by using different types of graphical techniques such as optimized molecular structures, IR, Raman, NMR, and other spectra, molecular orbital diagrams, and atomic charge distributions, and so on.

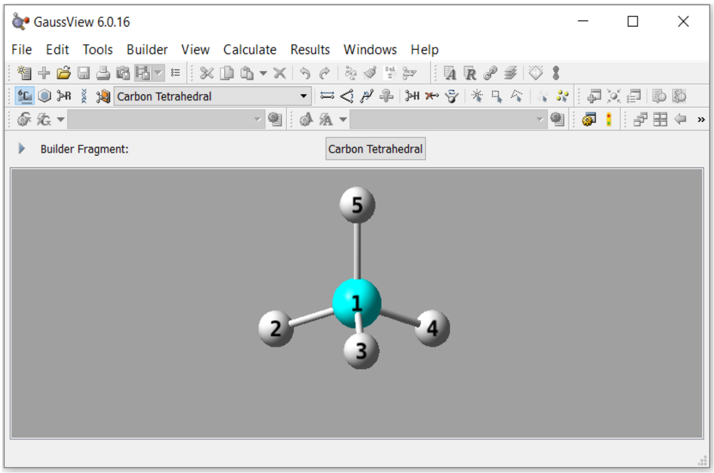

Figure 2.1 – The graphical user interface of the GaussView 6.0.16

2.6 Geometry Optimization

Geometry optimization is a process used to obtain the minimum energy configuration of a molecule. When a molecule is built-in GaussView software the initial geometry is not a stable configuration. Thus, that energy optimization for each molecule is necessary. This process is called geometry optimization. The stable structure can be corresponding to the local minima or global minima. In the process of geometry optimization, searching for minimum energy from the initial structure take place, see Figure 2.2.[62]

The geometry optimization is necessary before the anharmonic frequency calculations of the aryl-azides. It is necessary to check whether the geometry optimization calculations are successfully converged at the default settings of convergence (i.e., opt without any additional information sets the RMS force criterion to $3*10^{-4}$). Once the current values of all four criteria fall below the threshold, the optimization is completed. The next step is to perform harmonic frequency calculations and no imaginary frequencies should be found when a structure is at the minimum.

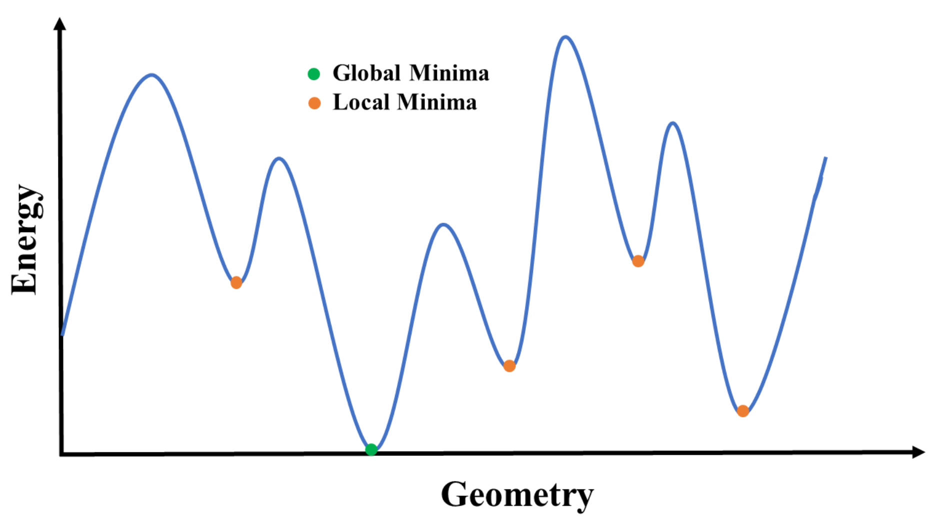

Figure 2.2 - Schematic diagram of geometry optimization

2.7 Anharmonic Frequency Calculations

Anharmonic frequency calculations are needed to understand the presence of FRs by determining the frequencies, intensities, and cubic force constants of overtones and combination bands. Thus, DFT analysis was carried out on three aryl-azide compounds for combined geometry optimization and frequency calculations along with anharmonic corrections. In this study, cubic force constants K_{ijk} were obtained using triple of modes i, j, and k, (where k, is fundamental, and i and j are combination band or overtone modes, respectively). To read out cubic force constant values from the Gaussian output file, the mode numbers of i, j, and k are needed to convert into (N - i + 1), (N - j + 1), and (N - k + 1), respectively, where N is the degrees of freedom of the molecule. The third-order Fermi resonance parameter (TFR) for the triple of modes i, j, and k using resonance distance (Δω) was calculated as follows,

$$\Delta\omega = |\omega_i + \omega_j - \omega_k| \tag{2.18}$$

$$\text{TFR} = \left|\frac{K_{ijk}}{\Delta\omega}\right| \tag{2.19}$$

Modes are considered resonant when TFR is of order ~1 or larger.[63-65] This value provides insights into what possible FRs are present in the complex absorption profile of azide compounds more directly than using cubic force constants. In this work, we make recommendations for the choice of basis set based on comparing four parameters: peak intensities, peak positions relative to the fundamental vibration, cubic force constant, and TFR values. Relative peak position (Δω') is calculated as,

$$\Delta\omega' = \omega_{ij} - \omega_k \tag{2.20}$$

where, ω_{ij} and ω_k are wavenumbers of the combination band or overtone and fundamental vibration, respectively.

2.8 IEFPCM Solvent Model

The polarizable continuum model (PCM) using the integral equation formalism variant (IEFPCM) was used to model the solvent. The SCRF keyword in Gaussian specifies that calculation needs to be performed in a solvent by placing the molecule of interest (solute) into a void cavity within a continuous dielectric medium mimicking the solvent. The shape and size of the cavity are different for various versions of the continuum models. In Gaussian, the default SCRF method is the IEFPCM solvent model. In this model, the solute cavity creates via a set of overlapping spheres. For further details of the solvent model, see Tomasi et. al.[66-74] The NNDMA and THF were used to study the solvent effect on azide absorption profile. The dielectric constants (ε) of the NNDMA and THF are 37.8 and 7.58, respectively. Since the higher dielectric constant indicates higher polarity, NNDMA is much more polar than THF solvent.

2.9 Overview

In this chapter, we provided an overview of the computational background of the Gaussian software, DFT, B3LYP functional, basis sets, and IEFPCM solvent model. The combined geometry optimization, harmonic frequency, and anharmonic frequency calculations were carried out using seven basis sets: 6-31G(d,p), 6-31+G(d,p), 6-31++G(d,p), 6-311G(d,p), 6-311+G(d,p), 6-311++G(d,p), and 6-311++G(df,pd) to investigate intramolecular, solvent, and basis set effects on azide absorption profiles of three modified aryl-azide compounds: 4-azidotoluene, 4-azidoacetanilide and 4-azido-N-phenylmaleimide. The next chapter emphasizes vibrational coupling and Fermi resonance in 4-azidotoluene and 4-azidoacetanilide, and Chapter 4 focuses on 4-azido-N-phenylmaleimide. Peak intensities, peak positions relative to the azide asymmetric stretch, cubic force constants, and the TFR constants were extensively discussed.

CHAPTER 3

DFT STUDIES OF VIBRATIONAL COUPLING AND FERMI RESONANCE IN 4-AZIDOTOLUENE AND 4-AZIDOACETANILIDE

3.1 Introduction

Understanding protein structures and structural changes in response to their surroundings is challenging. Aryl-azides have shown promise as powerful vibrational probes for site-specific studies of proteins because of the high transition dipole strength of the azide asymmetric stretch. However, azide probes have broad bandwidths and complex absorption profiles due to Fermi resonances (FRs). Thus, understanding these complex absorption profiles using computational calculations could lead to the wider use of azide-based vibrational probes. The major advantages of computational studies are that they directly tabulate how many vibrational modes exist, indicate what types of modes they are, and provide 3D animations of these stretching and bending vibrations. By running anharmonic frequency calculations of azide compounds, we can readily identify fundamental vibrations, overtones, and combination bands and from that deduce accidental FRs. Additionally, it is helpful to understand the vibrational spectrum of an azide compound before experimental analysis. By running a single computational calculation, it can be determined if the absorption profile is too complicated to yield an understanding of protein structure and dynamics from experimental results without too much time or difficulty. Thus, computational calculations can provide a basic idea of whether an azide VP is suitable for understanding protein local environment and dynamics in a specific application. Although computational studies have been carried out to understand complex adsorption profiles of VPs, there has been no work done to understand the complex adsorption profile of azide VPs using different basis sets. Herein we report how different basis sets predict the vibrational spectra of two aryl azide compounds, 4-azidotoluene and 4-azidoacetanilide, see Figure 1. Recently, 4-azido-L-phenylalanine, the unnatural amino acid modified with an azide moiety has been studied experimentally and theoretically.[75-79] Thus, we chose to investigate 4-azidotoluene, which is a simple analog to 4-azido-L-phenylalanine. Since 4-azidoacetanilide has a linker that mimics a peptide bond, it can produce a peptide bond and clip the aryl azide to the protein site of interest. It has been shown that the use of 4-azidoacetanilide as a VP is less likely due to a more complex azide asymmetric adsorption profile compared to 4-azidotoluene. Studying these two aryl-azide compounds also provides an opportunity to understand the impact of intramolecular interactions on their vibrational spectra as the only difference between 4-aziodtoluene and 4-azidoacetanilide is the addition of a peptide bond. To understand the solvent effect, NNDMA and THF solvents were used with the IEFPCM solvent model. This study has shown that these aryl-azides VPs are less sensitive to the solvent suggesting that they would be useful when solvent composition changes throughout the experimental time scale. For ease of understanding, the azide absorption profiles of the two molecules are described in each solvent separately.

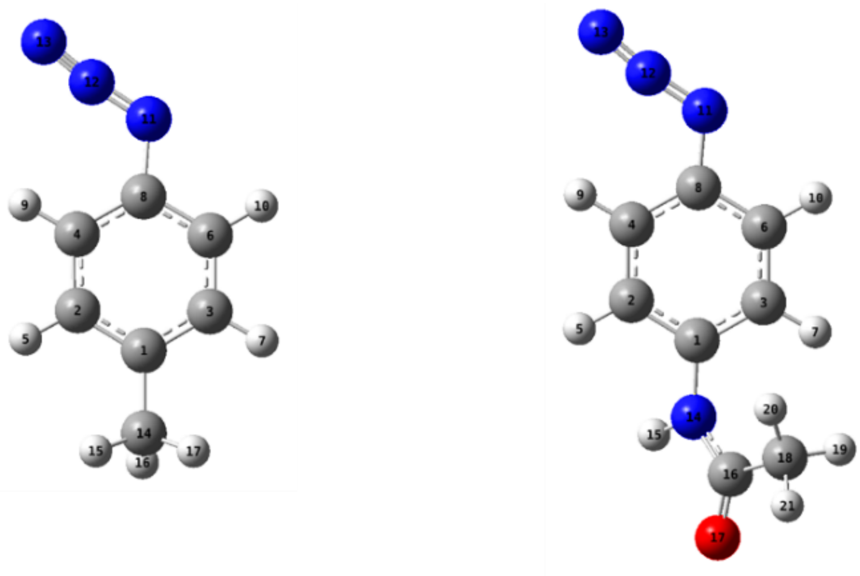

Figure 3.1 - Optimized Structures of 4-azidotoluene (left) and 4-azidoacetanilide (right)

3.2 4-azidotoluene

First, the structural parameters of optimized 4-azidotoluene were studied to understand the basis sets effect and solvent effect on bond distances, bond angles, and dihedral angels because the force constant depends on these structural parameters. Table 3.1-3.3 shows structural parameters for both solvents and seven basis sets. For ease of reading, atoms are numbered in Figure 3.1, and bond distances, angles, and dihedral angles are labeled. In 4-azidotoluene, the azide group and benzene ring are in the same plane (D9 ≈ 180^0). There's no significant change in the bond distances and bond angles. However, dihedral angels of the D12, D13, and D14 are changing considerably with different basis sets and solvents. Since the methyl group has sp^3 hybridization, all sp^3 C-H bonds can easily rotate, and this will change the strength of the bonds.

Then, the DFT calculated frontier molecular orbitals HOMO and LUMO of 4-azidotoluene are illustrated in Figure 3.2. The HOMO orbital is distributed in the region perpendicular to the bond axis only avoiding hydrogen atoms in the benzene ring while the LUMO orbital is localized parallel to the bond axis and only covers the azide region and three carbon atoms close to the azide group. The HOMO and LUMO orbitals are the same for all basis sets and both solvents except for a slight electron density change around the methyl group of the HOMO orbital of 6-31+G(d,p), 6-311+G(d,p), 6-311++G(d,p), and 6-311++G(df,pd) basis sets. In these basis sets, the shape of the orbital is a little bit deviated from the other HOMO orbital. However, Tables 3.4 and 3.5 show that the energies and HOMO-LUMO gaps are similar in 6-31+G(d,p)/6-31++G(d,p) and 6-311+G(d,p)/6-311++G(d,p) pairs separately. Moreover, both NNDMA and THF have a similar HOMO-LUMO gap for each basis set. Here, we can see how the dihedral angle changes in the methyl group describe the changes in the HOMO orbital.

Table 3.1 – Bond distances (Å) of 4-azidotoluene with seven basis sets: 6-31G(d,p), 6-31+G(d,p), 6-31++G(d,p), 6-311G(d,p), 6-311+G(d,p), 6-311++G(d,p), 6-311++G(df,pd) and two solvents, NNDMA (N) and THF (T).

Label	Definition	6-31G(d,p)		6-31+G(d,p)		6-31G++(d,p)		6-311G(d,p)		6-311+G(d,p)		6-311++G(d,p)		6-311++G(df,pd)	
		N	**T**	**N**	**T**	**N**	**T**	**N**	**T**	**N**	**T**	**N**	**T**	**N**	**T**
R1	R(1,2)	1.402	1.402	1.402	1.402	1.403	1.403	1.399	1.399	1.400	1.399	1.400	1.399	1.396	1.396
R2	R(1,3)	1.403	1.403	1.405	1.405	1.404	1.404	1.400	1.400	1.401	1.401	1.401	1.402	1.399	1.399
R3	R(2,4)	1.394	1.393	1.397	1.397	1.396	1.396	1.392	1.392	1.393	1.393	1.393	1.394	1.391	1.391
R4	R(2,5)	1.087	1.087	1.087	1.087	1.087	1.087	1.085	1.085	1.085	1.085	1.085	1.085	1.084	1.084
R5	R(3,6)	1.392	1.392	1.393	1.393	1.394	1.394	1.390	1.390	1.391	1.390	1.391	1.390	1.387	1.387
R6	R(3,7)	1.087	1.087	1.087	1.087	1.087	1.087	1.085	1.085	1.085	1.085	1.085	1.085	1.084	1.084
R7	R(4,8)	1.400	1.400	1.400	1.400	1.401	1.401	1.398	1.398	1.398	1.397	1.398	1.397	1.395	1.395
R8	R(6,8)	1.399	1.399	1.401	1.400	1.400	1.400	1.397	1.397	1.397	1.397	1.397	1.398	1.395	1.395
R9	R(4,9)	1.086	1.086	1.086	1.086	1.086	1.086	1.084	1.084	1.084	1.084	1.084	1.084	1.083	1.083
R10	R(6,10)	1.085	1.085	1.085	1.085	1.085	1.085	1.083	1.083	1.083	1.083	1.083	1.083	1.082	1.082
R11	R(8,11)	1.424	1.424	1.425	1.425	1.425	1.425	1.423	1.423	1.424	1.424	1.424	1.424	1.422	1.421
R12	R(11,12)	1.235	1.235	1.235	1.235	1.235	1.235	1.231	1.231	1.230	1.230	1.230	1.230	1.228	1.228
R13	R(12,13)	1.142	1.142	1.142	1.142	1.142	1.142	1.134	1.134	1.134	1.134	1.134	1.134	1.132	1.132
R14	R(1,14)	1.510	1.510	1.511	1.511	1.511	1.511	1.509	1.509	1.509	1.509	1.509	1.509	1.507	1.507
R15	R(14,15)	1.094	1.094	1.094	1.094	1.094	1.094	1.092	1.092	1.092	1.092	1.092	1.092	1.090	1.090
R16	R(14,16)	1.097	1.097	1.097	1.097	1.097	1.097	1.096	1.096	1.096	1.095	1.096	1.095	1.094	1.094
R17	R(14,17)	1.094	1.094	1.095	1.095	1.094	1.094	1.092	1.092	1.092	1.093	1.092	1.093	1.092	1.092

Table 3.2 – Bond angels of 4-azidotoluene with different basis sets: 6-31G(d,p), 6-31+G(d,p), 6-31++G(d,p), 6-311G(d,p), 6-311+G(d,p), 6-311++G(d,p), 6-311++G(df,pd) and two solvents, NNDMA (N) and THF (T).

Label	Definition	6-31G(d,p)		6-31+G(d,p)		6-31G++(d,p)		6-311G(d,p)		6-311+G(d,p)		6-311++G(d,p)		6-311++G(df,pd)	
		N	T	N	T	N	T	N	T	N	T	N	T	N	T
A1	A(1,2,3)	117.79	117.78	117.74	117.74	117.75	117.74	117.76	117.76	117.75	117.75	117.75	117.75	117.75	117.74
A2	A(1,2,4)	121.62	121.61	121.65	121.65	121.64	121.64	121.59	121.59	121.61	121.61	121.61	121.61	121.61	121.61
A3	A(1,2,5)	119.49	119.47	119.53	119.52	119.54	119.52	119.54	119.53	119.56	119.54	119.56	119.53	119.54	119.53
A4	A(1,3,6)	121.43	121.44	121.45	121.46	121.46	121.47	121.44	121.45	121.46	121.47	121.46	121.46	121.45	121.46
A5	A(1,3,7)	119.50	119.49	119.55	119.54	119.54	119.52	119.53	119.52	119.54	119.54	119.54	119.54	119.54	119.53
A6	A(2,4,8)	119.56	119.57	119.51	119.53	119.52	119.54	119.67	119.68	119.60	119.61	119.60	119.60	119.62	119.64
A7	A(3,6,8)	119.81	119.82	119.79	119.80	119.78	119.79	119.90	119.90	119.83	119.83	119.83	119.84	119.86	119.87
A8	A(2,4,9)	119.94	119.94	119.73	119.74	119.75	119.76	119.76	119.77	119.68	119.69	119.68	119.68	119.66	119.67
A9	A(3,6,10)	120.94	120.97	120.83	120.88	120.82	120.87	120.93	120.98	120.80	120.86	120.80	120.87	120.79	120.84
A10	A(4,8,6)	119.79	119.77	119.84	119.82	119.84	119.82	119.64	119.63	119.75	119.73	119.75	119.74	119.70	119.68
A11	A(6,8,11)	116.15	116.16	116.14	116.15	116.18	116.19	116.35	116.36	116.33	116.33	116.33	116.31	116.40	116.41
A12	A(8,11,12)	118.68	118.65	118.80	118.76	118.80	118.75	118.90	118.87	119.02	119.00	119.01	118.98	119.27	119.24
A13	A(11,12,13)	172.61	172.63	172.75	172.77	172.77	172.78	172.92	172.94	172.88	172.92	172.81	172.93	172.80	172.82
A14	A(1,2,14)	121.11	121.14	121.34	121.34	121.15	121.14	121.14	121.15	121.15	121.24	121.14	121.32	121.32	121.33
A15	A(1,14,15)	111.42	111.42	111.33	111.34	111.37	111.39	111.36	111.37	111.35	111.35	111.35	111.33	111.31	111.31
A16	A(1,14,16)	111.15	111.18	111.09	111.10	111.03	111.05	111.00	111.02	110.94	110.97	110.95	111.03	111.00	111.03
A17	A(1,14,17)	111.40	111.40	111.34	111.36	111.35	111.37	111.34	111.35	111.33	111.34	111.33	111.32	111.30	111.31
A18	A(15,14,16)	107.26	107.28	107.62	107.59	107.36	107.35	107.38	107.39	107.40	107.50	107.40	107.60	107.62	107.63
A19	A(15,14,17)	108.23	108.18	108.16	108.12	108.26	108.20	108.27	108.22	108.31	108.23	108.30	108.17	108.26	108.19
A20	A(16,14,17)	107.18	107.17	107.12	107.14	107.28	107.29	107.31	107.31	107.33	107.27	107.32	107.20	107.17	107.19

Table 3.3 – Dihedral angels of 4-azidotoluene with different basis sets: 6-31G(d,p), 6-31+G(d,p), 6-31++G(d,p), 6-311G(d,p), 6-311+G(d,p), 6-311++G(d,p), 6-311++G(df,pd) and two solvents, NNDMA (N) and THF (T).

Label	Definition	6-31G(d,p)		6-31+G(d,p)		6-31G++(d,p)		6-311G(d,p)		6-311+G(d,p)		6-311++G(d,p)		6-311++G(df,pd)	
		N	T	N	T	N	T	N	T	N	T	N	T	N	T
D1	D(4,2,1,3)	0.29	0.28	0.20	0.21	0.30	0.30	0.25	0.25	0.29	0.27	0.30	0.23	0.24	0.22
D2	D(5,2,1,3)	-179.60	-179.62	-179.72	-179.71	-179.59	-179.58	-179.61	-179.61	-179.58	-179.60	-179.56	-179.67	-179.66	-179.69
D3	D(6,3,1,2)	-0.28	-0.28	-0.20	-0.21	-0.31	-0.32	-0.25	-0.25	-0.29	-0.28	-0.31	-0.24	-0.25	-0.23
D4	D(7,3,1,2)	179.60	179.61	179.71	179.70	179.59	179.58	179.60	179.61	179.57	179.60	179.56	179.67	179.66	179.69
D5	D(8,6,3,1)	0.10	0.11	0.07	0.07	0.13	0.13	0.08	0.08	0.10	0.09	0.10	0.08	0.09	0.08
D6	D(9,4,2,1)	-179.85	-179.84	-179.90	-179.89	-179.85	-179.85	-179.85	-179.84	-179.86	-179.87	-179.87	-179.89	-179.90	-179.90
D7	D(10,6,3,1)	179.85	179.86	179.91	179.91	179.87	179.86	179.84	179.84	179.86	179.88	179.87	179.91	179.91	179.92
D8	D(11,8,6,3)	179.86	179.84	179.92	179.91	179.87	179.87	179.88	179.88	179.87	179.88	179.87	179.91	179.91	179.91
D9	D(12,11,8,6)	-179.91	-179.95	-179.95	-179.96	-179.97	-179.96	-179.90	-179.90	-179.93	-179.96	-179.93	-179.94	-179.95	-179.97
D10	D(13,12,11,8)	-179.99	-179.98	-179.97	-179.99	-179.90	-179.89	-179.98	-179.98	180.00	-179.96	-179.65	-179.93	-179.93	-179.93
D11	D(14,1,2,4)	-178.62	-178.63	-179.00	-178.95	-178.59	-178.58	-178.63	-178.62	-178.61	-178.69	-178.62	-178.94	-178.97	-179.02
D12	D(15,14,1,2)	-28.17	-26.84	-14.33	-15.07	-27.65	-28.19	-28.14	-27.85	-28.11	-22.60	-28.09	-16.38	-16.28	-15.56
D13	D(16,14,1,2)	91.40	92.79	105.60	104.83	91.94	91.41	91.45	91.76	91.45	97.11	91.48	103.48	103.57	104.33
D14	D(17,14,1,2)	-149.14	-147.75	-135.11	-135.82	-148.59	-149.08	-149.08	-148.73	-149.09	-143.48	-149.07	-137.17	-137.15	-136.35

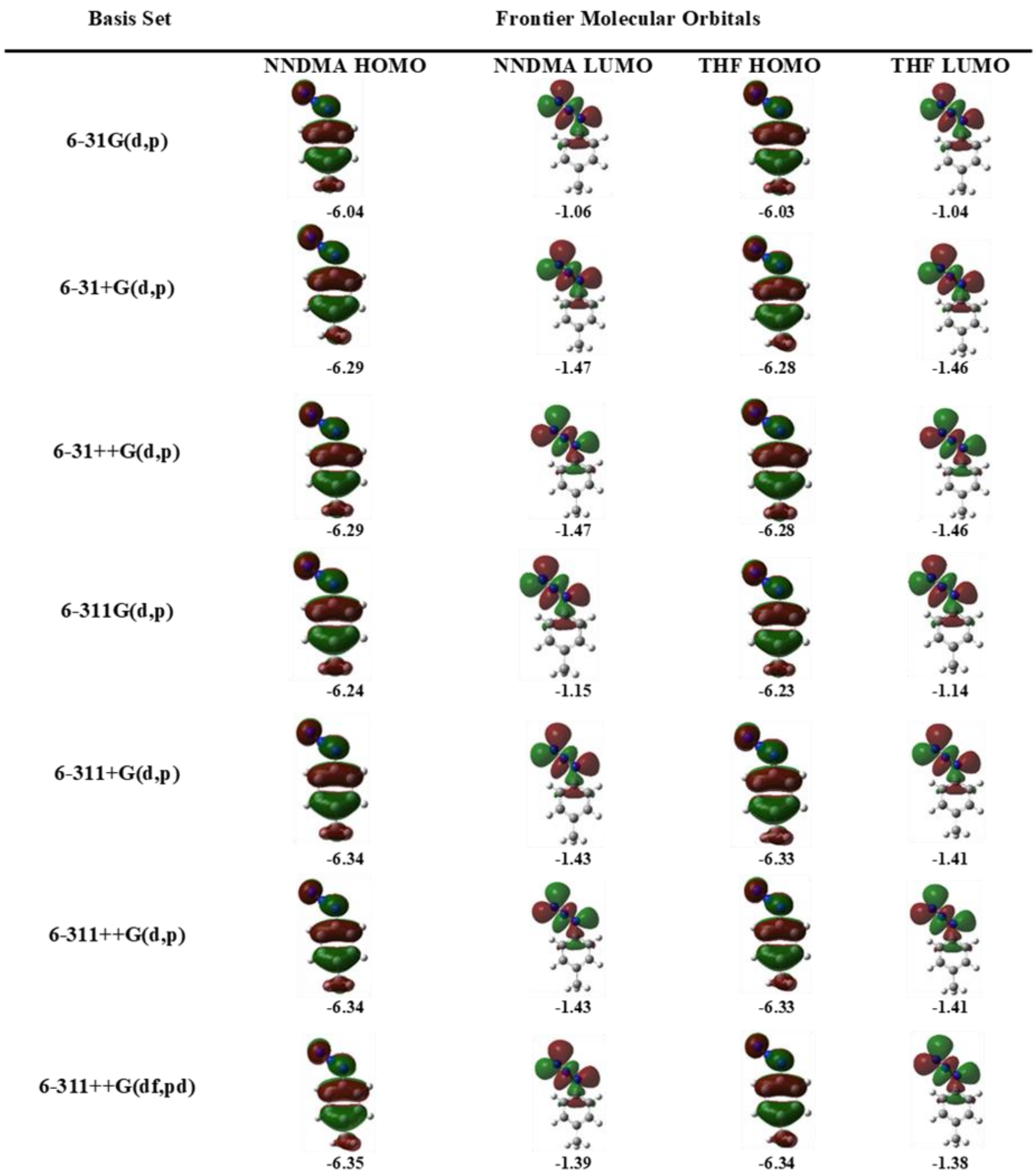

Figure 3.2 - Spatial distributions of HOMO and LUMO frontier molecular orbitals of 4-azidotoluene in NNDMA and THF solvents for seven basis sets. Orbital energy eigenvalues (in eV) are shown below each molecular orbital. The red and green color lobes correspond to the two different phases of the orbital wave function with positive and negative signs, respectively.

As mentioned before, the slight change in the HOMO orbital in 6-31+G(d,p), 6-311+G(d,p), 6-311++G(d,p), and 6-311++G(df,pd) basis sets is due to the changes in the dihedral angle of the methyl group. According to Table 3.3, the dihedral angles D12, D13, and D14 are greatly changing for both solvents in 6-31+G(d,p) and 6-311++G(df,pd) and for THF solvent in 6-311+G(d,p) and 6-311++G(d,p) basis sets, separately. Hence, this will result in huge changes in the strength of the vibrational modes consisting of methyl group. The energies of the molecule decrease (more negative) from 6-31G(d,p) to 6-311++G(df,pd) and ~0.02 eV high in NNDMA solvent. But HOMO-LUMO gap has the order of 6-311G(d,p) > 6-31G(d,p) > 6-311++G(df,pd) > 6-311+G(d,p)/6-311++G(d,p) > 6-31+G(d,p)/6-31++G(d,p) and similar for both solvents.

Table 3.4 – Energies and HOMO-LUMO gap for the 4-azidotoluene in NNDMA.

Basis set	Energy (au)	HOMO(au)	HOMO(eV)	LUMO(au)	LUMO(eV)	HL gap (eV)
6-31G(d,p)	-435.170516	-0.22	-6.04	-0.04	-1.06	4.99
6-31+G(d,p)	-435.185925	-0.23	-6.29	-0.05	-1.47	4.82
6-31++G(d,p)	-435.186090	-0.23	-6.29	-0.05	-1.47	4.82
6-311G(d,p)	-435.268606	-0.23	-6.24	-0.04	-1.15	5.09
6-311+G(d,p)	-435.274933	-0.23	-6.34	-0.05	-1.43	4.91
6-311++G(d,p)	-435.275006	-0.23	-6.34	-0.05	-1.43	4.91
6-311++G(df,pd)	-435.292966	-0.23	-6.35	-0.05	-1.39	4.95

Table 3.5 – Energies and HOMO-LUMO gap for the 4-azidotoluene in THF.

Basis set	Energy (au)	HOMO(au)	HOMO(eV)	LUMO(au)	LUMO(eV)	HL gap (eV)
6-31G(d,p)	-435.169858	-0.22	-6.03	-0.04	-1.04	4.99
6-31+G(d,p)	-435.185180	-0.23	-6.28	-0.05	-1.46	4.83
6-31++G(d,p)	-435.185345	-0.23	-6.28	-0.05	-1.46	4.82
6-311G(d,p)	-435.267869	-0.23	-6.23	-0.04	-1.14	5.09
6-311+G(d,p)	-435.274154	-0.23	-6.33	-0.05	-1.41	4.92
6-311++G(d,p)	-435.274230	-0.23	-6.33	-0.05	-1.41	4.92
6-311++G(df,pd)	-435.292202	-0.23	-6.34	-0.05	-1.38	4.96

3.2.1 4-azidotoluene in NNDMA

Combined geometry optimization and anharmonic frequency calculations of 4-azidotoluene were performed in NNDMA solvent using seven different basis sets: 6-31G(d,p), 6-31+G(d,p), 6-31++G(d,p), 6-311G(d,p), 6-311+G(d,p), 6-311++G(d,p), and 6-311++G(df,pd). These calculations provide IR spectra of both anharmonic and harmonic vibrational transitions. In 4-azidotoluene, there are 17 atoms, so 45 (3N-6) fundamental vibrational modes can be seen. Figure 3.2 shows the harmonic spectrum of 4-azidotoluene using the 6-311+G(d,p) basis set. The highest intensity peak corresponds to the azide asymmetric stretching vibration, which is located at 2213.7 cm^{-1} with a molar absorptivity coefficient of ~6000 M^{-1} cm^{-1}. Moreover, this azide asymmetric stretching vibration (38th Mode, Fund(38)) is the only visible fundamental vibration within the transparent window (~1800 - 2300 cm^{-1}). Mode 30 has the second-highest molar absorptivity coefficient with ε over 1000 M^{-1} cm^{-1}, which indicates that transition dipole strength or population density of modes 38 and 30 are relatively high. All other fundamental bands have an intensity less than 1000 M^{-1} cm^{-1}.

Table 3.4 shows the peak position and intensity of high-intensity peaks for 4-azidotoluene in NNDMA using the 6-311+G(d,p) basis set. Figure 3.2 also presents both harmonic and anharmonic vibrations, and it shows that the intensity of the anharmonic vibrations is lower than the harmonic vibrations. In the harmonic analysis, only a single sharp peak within the transparent window is observed, while in the anharmonic spectrum, there are several peaks within the transparent window. However, only one fundamental band is present, and the other peaks are combination bands or overtones. In general, combination bands and overtones have less intensity and are barely noticeable in the IR spectrum. However, strong vibrational coupling between these bands and the azide asymmetric stretch may result in higher intensities.

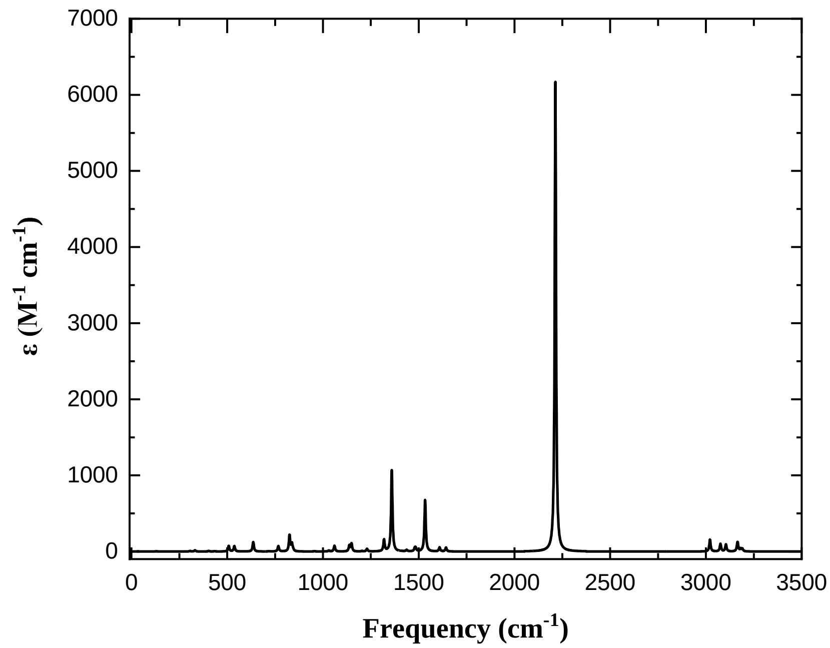

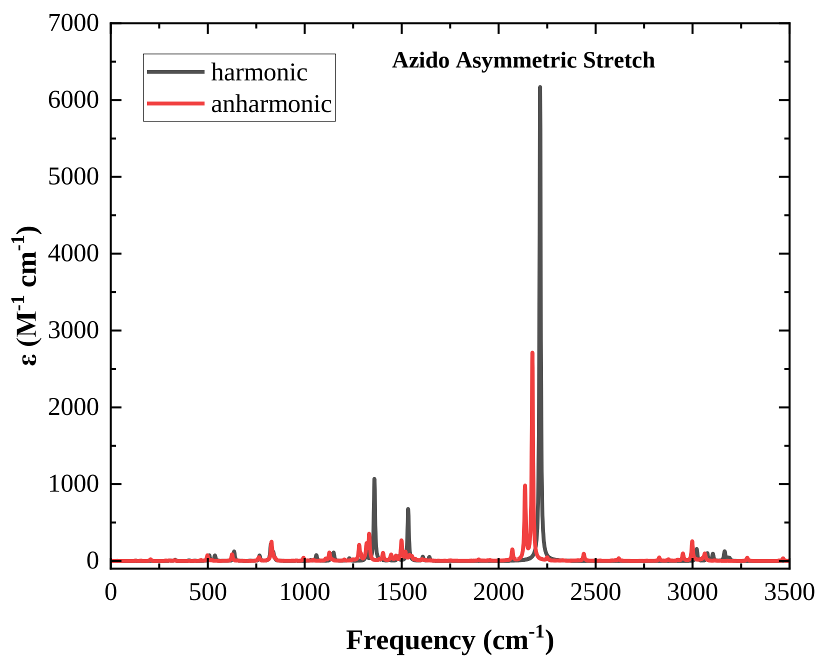

Figure 3.3 – IR spectra of harmonic (top), both anharmonic and harmonic (bottom) of 4-azidotoluene in NNDMA using B3LYP/6-311+G(d,p) level in Gaussian-16.

Table 3.6 - Normal Modes of 4-azidotoluene in NNDMA using B3LYP/6-311+G(d,p)

Mode	Vibration	$\upsilon_{(harmonic)}$ / cm^{-1}	$\upsilon_{(anharmonic)}$ / cm^{-1}	$I_{(harmonic)}$ / km mol^{-1}	$I_{(anharmonic)}$ / km mol^{-1}
38	N_3 asymmetric stretch	2213.7	2173.9	1795.4	780.9
35	4-H sp^2 C-H in plane + Benzene ring vibration	1533.4	1499.5	197.6	62.5
30	N_3 Sym stretch + C-N stretch + ring vibrations + all C-H in-plane	1359.4	1319.1	312.1	49.8

To get deeper insights into the vibrational coupling and FRs, the peak intensities, peak positions relative to the fundamental vibration, cubic force constants (K_{ijk}), and TFR values were compared. Appendix A shows these values for combination bands and overtones that occur within ± 130 cm^{-1} from the fundamental vibration for seven basis sets.

Although there are more than one hundred vibrational modes within the transparent window, only a few modes show high intensity or vibrational coupling strength. Figures 3.4 and 3.5 present intensities and cubic force constants of combination bands or overtones that can make resonance with the azide asymmetric stretch. Unexpectedly, for the 6-31G(d,p) basis set, the combination band Comb(22 26) has the highest intensity (~1200 km mol^{-1}), and the fundamental vibration has a much lower intensity compared to the other six basis sets. Thus, the use of the 6-31G(d,p) basis set for anharmonic frequency calculations is questionable.

All other basis sets show azide asymmetric stretch intensity greater than 740 km mol^{-1}. Then, Comb(18 30) and Comb(15 30) have the second and third highest intensity of ~270 km mol^{-1} and ~35 km mol^{-1}, respectively for more diffused basis sets (i.e., 6-31+G(d,p), 6-31++G(d,p), 6-311+G(d,p) and 6-311++G(d,p)). But comparatively, both Comb(18 30) and Comb(15 30) have less intensity for 6-31G(d,p) and 6-311G(d,p) basis sets, whereas when a more diffused and polarized basis set 6-311++G(df,pd) is used, the intensity is relatively high.

Moreover, Comb(17 30) has ~30 km mol^{-1} intensity for triple-zeta basis sets except for 6-311++G(df,pd), and very low intensity for double-zeta basis sets. The overtone Over(25), which is very far away in frequency from Fund(38) has an intensity of ~10 km mol^{-1} for all basis sets. All other vibrational modes have an intensity of less than 10 km mol^{-1} for every basis set. However, these vibrational modes can be FR with a small intensity or cubic force constant. If a combination band or overtone mode is very close to the fundamental vibration, and the cubic force constant is greater than 1 cm^{-1}, then there's a great chance of that mode resonant couple with the azide asymmetric stretch. But, if a particular mode is very far away from the fundamental vibration, then to produce FR, it should have a higher cubic force constant.

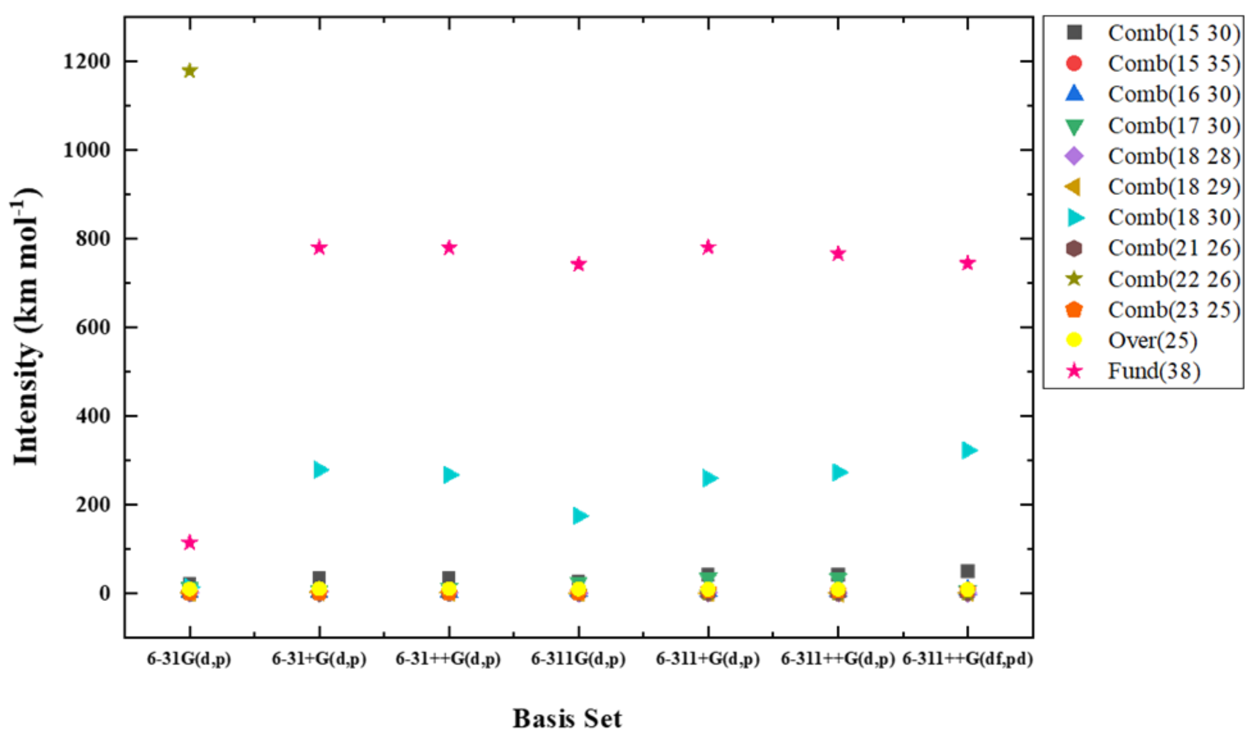

Figure 3.4 – Intensities of vibrational modes that can potentially couple with the azide asymmetric stretch of 4-azidotoluene for 6-31G(d,p), 6-31+G(d,p), 6-31++G(d,p), 6-311G(d,p), 6-311+G(d,p), 6-311++G(d,p), 6-311++G(df,pd) basis sets in NNDMA.

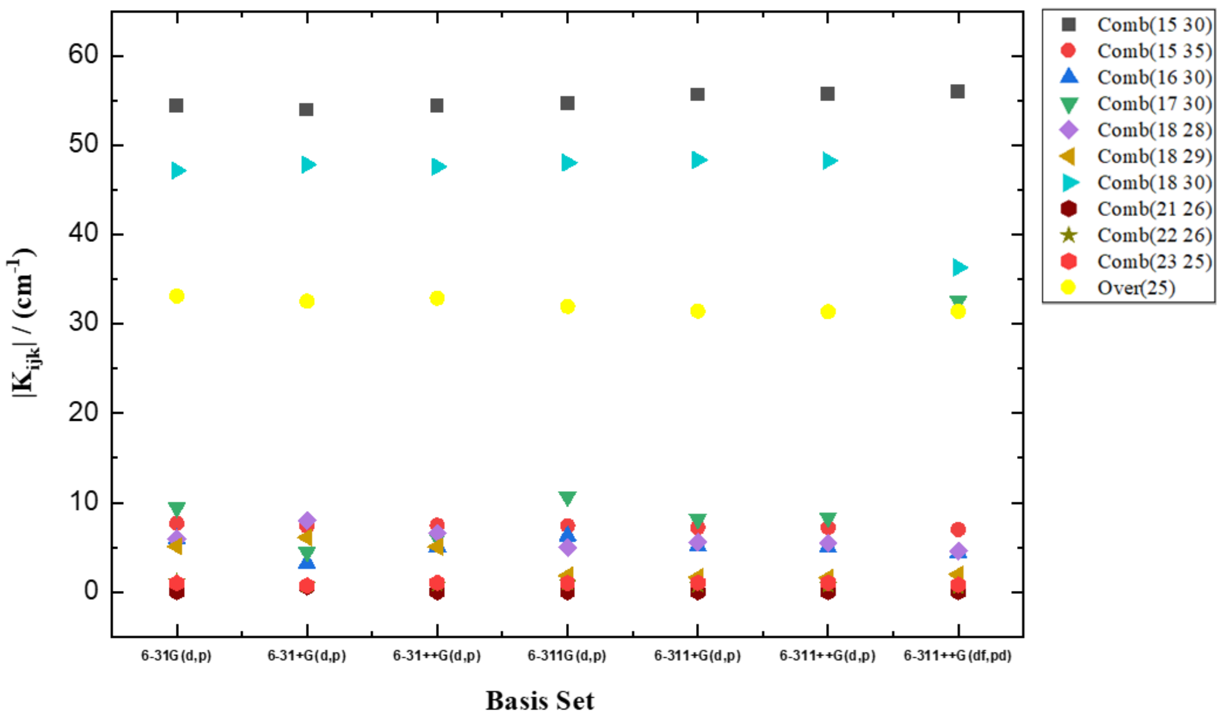

Figure 3.5 – Cubic force constants of vibrational modes that can potentially couple with the azide asymmetric stretch of 4-azidotoluene for 6-31G(d,p), 6-31+G(d,p), 6-31++G(d,p), 6-311G(d,p), 6-311+G(d,p), 6-311++G(d,p), 6-311++G(df,pd) basis sets in NNDMA.

According to Figure 3.5, Comb(15 30) has the highest cubic force constant ~55 cm^{-1} for all basis sets, indicating that Comb(15 30) is possibly involved in FR. For six of the seven basis sets, Comb(18 30) and Over(25) have the second and third highest coupling constants, ~48 cm^{-1} and ~32 cm^{-1}, respectively. Surprisingly, for the 6-311++(df,pd) basis set, the cubic force constants for Comb(18 30) and Comb(17 30) were quite different from those obtained with the other basis sets while the cubic force constant for Over(25) was similar. This more polarized basis set shows an increased cubic force constant of ~31 cm^{-1} for Comb(17 30) and decreased cubic force constant of ~32 cm^{-1} for Comb(18 30). Interestingly, Comb(17 30) has a cubic force constant of less than 10 cm^{-1} for all basis sets other than 6-311++G(df,pd). For all seven basis sets, vibrational modes other than Comb(15 30), Comb(18 30), and Over(25) (and Comb(17 30) in the case of 6-311++G(df,pd)) within the transparent region have cubic force constants less than 10 cm^{-1}. Interestingly, we can see the relationship between intensity and cubic force constant by studying the peak positions of those possible FRs.

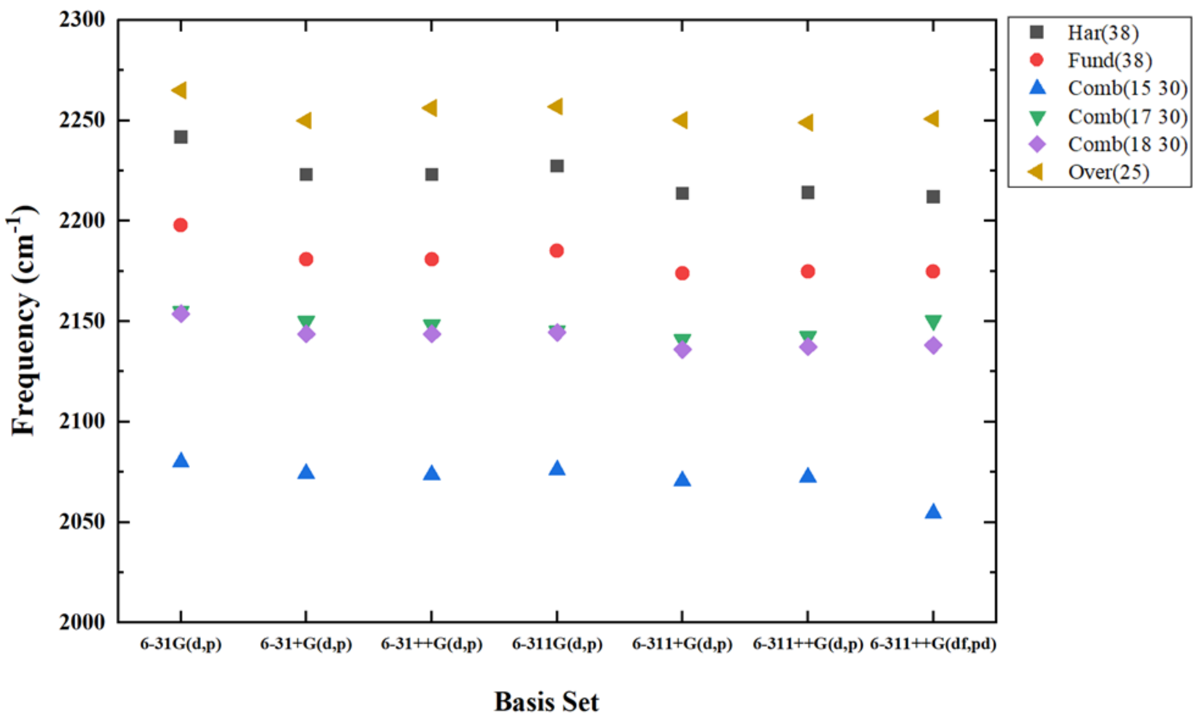

Figure 3.6 – Frequencies of vibrational modes that can potentially couple with the azide asymmetric stretch of 4-azidotoluene for 6-31G(d,p), 6-31+G(d,p), 6-31++G(d,p), 6-311G(d,p), 6-311+G(d,p), 6-311++G(d,p), 6-311++G(df,pd) basis sets in NNDMA.

Figure 3.6 shows the peak positions for combination bands or overtones that can potentially couple with azide asymmetric stretch with the seven basis sets. Qualitatively, the frequencies for each vibrational mode show similar trends for all the basis sets. The frequencies of harmonic azide asymmetric stretch Har(38) are always greater than anharmonic frequencies Fund(38) for all basis sets. Even though Comb(15 30) has a high cubic force constant, it is very far ($\Delta\omega'$ ~100 cm^{-1}) from the fundamental vibration, which causes it to have lower intensity compared to Comb(18 30), which is near the fundamental vibration ($\Delta\omega'$ ~37 cm^{-1}). Over(25) also shows less intensity because of the large Δω’ from the fundamental vibration (Δω’ ~74 cm^{-1}). Comb(17 30) and Comb(18 30) have very similar relative peak positions. Thus, it is apparent that the larger cubic force constant is why Comb(18 30) has a higher intensity than Comb(17 30). All these observations can be directly summarized by TFR values.

Table 3.7 gives TFR values for most possible modes that can make FRs with azide asymmetric stretch within the transparent window. If the TFR value is higher than 1, then the particular combination band or overtone is said to be strongly coupled with fundamental vibration. A TFR between 1 and 0.3, indicates that the overtone or combination band is weakly coupled to the fundamental vibration. Table 3.7 shows that Comb(18 30) has a TFR value greater than 1 for each basis set calculation, which reflects that Comb(18 30) is strongly coupled to the azide asymmetric stretch. Although both Comb(15 30) and Over(25) are very far away in frequency from the fundamental vibration, they show TFR values of ~0.6 and ~0.4, respectively for all basis sets. Therefore, both Comb(15 30) and Over(25) are weakly coupled to the azido asymmetric stretch. Also, Comb(17 30) is weakly coupled to the azide asymmetric stretch due to the moderate cubic force constant and its relative peak position.

Table 3.7 - TFR values for combination or overtone bands that can potentially couple with azide asymmetric stretch in 4-azidotoluene in NNDMA solvent

Mode	6-31G(d,p)	6-31+G(d,p)	6-31++G(d,p)	6-311G(d,p)	6-311+G(d,p)	6-311++G(d,p)	6-311++G(df,pd)
Comb(15 30)	0.48	0.56	0.58	0.55	0.58	0.60	0.41
Comb(15 35)	0.11	0.10	0.09	0.10	0.08	0.09	0.51
Comb(16 30)	0.10	0.05	0.10	0.11	0.10	0.10	0.06
Comb(17 30)	0.22	0.45	0.37	0.58	0.46	0.58	4.28
Comb(18 28)	0.12	0.13	0.12	0.07	0.09	0.09	0.08
Comb(18 29)	0.15	0.16	0.17	0.06	0.07	0.06	0.03
Comb(18 30)	1.77	2.95	3.00	1.70	1.86	2.05	1.68
Comb(21 26)	0.00	0.01	0.00	0.00	0.00	0.00	0.00
Comb(22 26)	0.11	0.01	0.03	0.04	0.02	0.02	0.01
Comb(23 25)	0.52	0.06	0.33	0.05	0.26	0.29	0.07
Over(25)	0.47	0.45	0.43	0.43	0.40	0.41	0.41

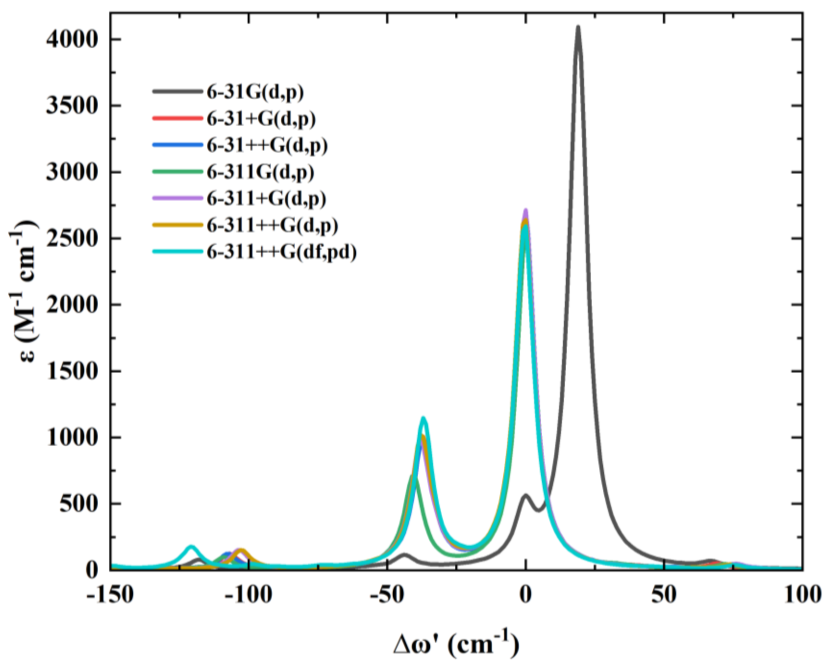

Figure 3.7 – Vibrational spectra (transparent window) of 4-azidotoluene for 6-31G(d,p), 6-31+G(d,p), 6-31++G(d,p), 6-311G(d,p), 6-311+G(d,p), 6-311++G(d,p), 6-311++G(df,pd) basis sets in NNDMA. $\Delta\omega' = \omega_{ij} - \omega_k$ (ω_{ij} and ω_k are wavenumbers of combination band or overtone and fundamental vibration, respectively).

Figure 3.7 shows that the 6-31G(d,p) basis set produces a completely different absorption profile for 4-azidotoluene by generating a high-intensity peak for a combination band. For other basis sets, the absorption profiles are similar, but they clearly show that the absorption profiles are red-shifted with a more polarized and diffused character in the basis set. We have shown that 6-31G(d,p), 6-311G(d,p), and 6-311G(df,pd) basis sets are not suitable for studying FRs while 6-31+G(d,p), 6-31++G(d,p), 6-311+G(d,p), and 6-311++G(d,p) are suitable for predicting FRs for 4-azidotoluene in NNDMA. Since 6-31+G(d,p) has the lowest computational cost out of these four basis sets, the 6-31+G(d,p)/B3LYP combination is preferred for these types of frequency calculations.

3.2.2 4-azidotoluene in THF

It is important to understand how different solvents affect vibrational coupling and FRs. In this section, we report vibrational coupling and FRs of 4-azidotoluene in THF solvent. This would help us to understand whether our calculated vibrational coupling and FRs are translatable to other solvents. The dielectric constant for NNDMA and THF are 37.8 and 7.6, respectively. Figure 3.8 and Table 3.8 show that modes 38 and 30 have the highest intensities in THF as in NNDMA solvent. Appendix B show vibrational modes occurring within ±130 cm^{-1} of the fundamental vibration for the seven basis sets.

Table 3.8 - Normal modes of 4-azidotoluene in THF using B3LYP/6-311+G(d,p)

Mode	Vibration	$\upsilon_{(harmonic)}$ / cm^{-1}	$\upsilon_{(anharmonic)}$ / cm^{-1}	$I_{(harmonic)}$ / km mol^{-1}	$I_{(anharmonic)}$ / km mol^{-1}
38	N_3 asymmetric stretch	2217.8	1323.4	1620.7	742.6
35	4-H sp^2 C-H in plane + Benzene ring vibration	1534.2	1497.4	184.8	25.7
30	N_3 Sym stretch + C-N stretch + ring vibrations + all C-H in-plane	1361.2	2177.1	279.7	132.6

Figure 3.9 presents high-intensity vibrational modes within the transparent region. The highest intensity corresponds to the azide asymmetric stretch Fund(38). The intensity of Fund(38) in THF is around 740 km mol^{-1}, which is lower than in NNDMA. Also, intensity of Fund(38) slightly less for 6-31G(d,p) and decreased by ~300 km mol^{-1} for 6-311++G(df,pd). As in NNDMA solvent, the second and third highest intensity peaks correspond to Comb(18 30) and Comb(15 30), respectively.

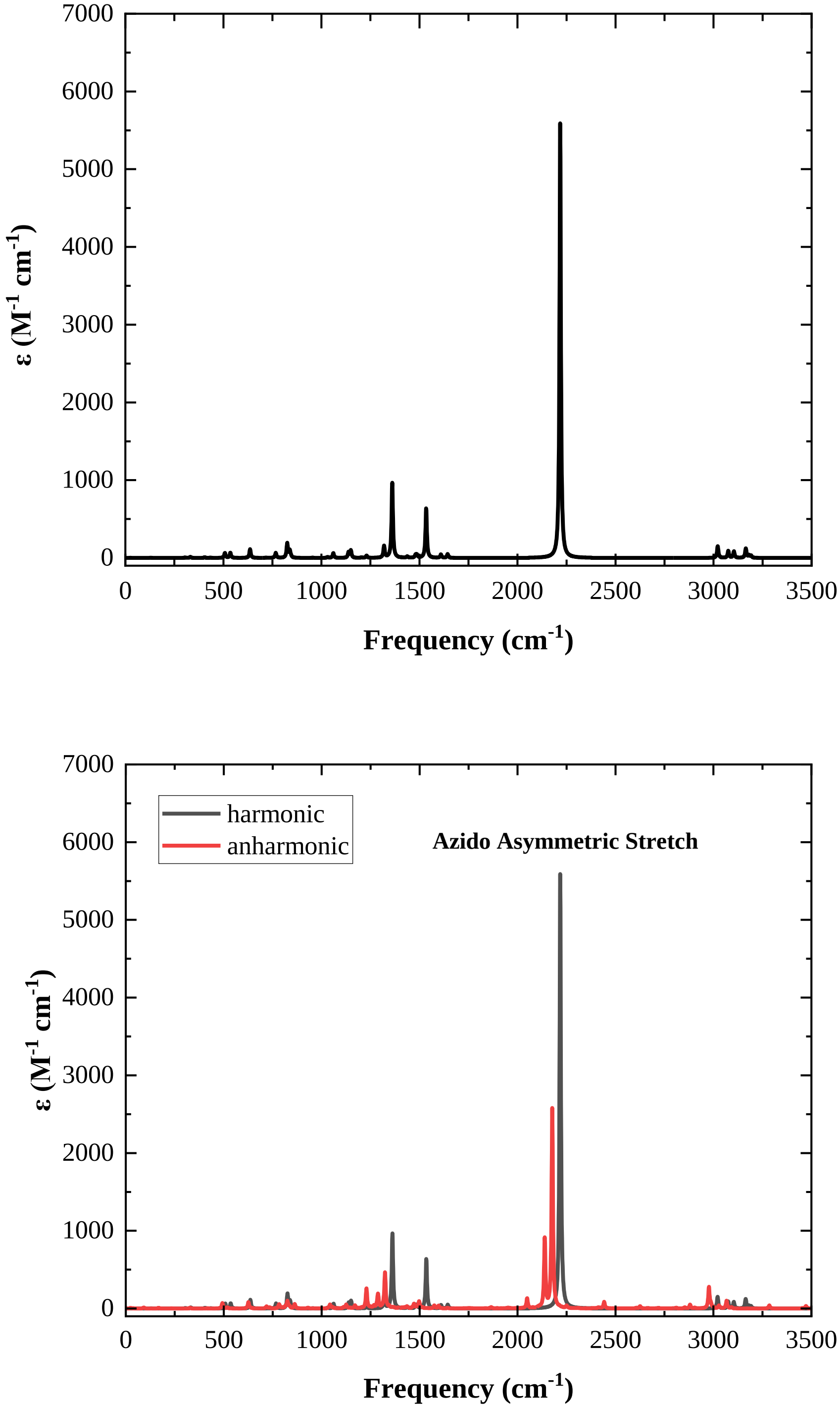

Figure 3.8 - IR spectra of harmonic (top), both anharmonic and harmonic (bottom) of 4-azidotoluene in THF using B3LYP/6-311+G(d,p) level in Gaussian-16.

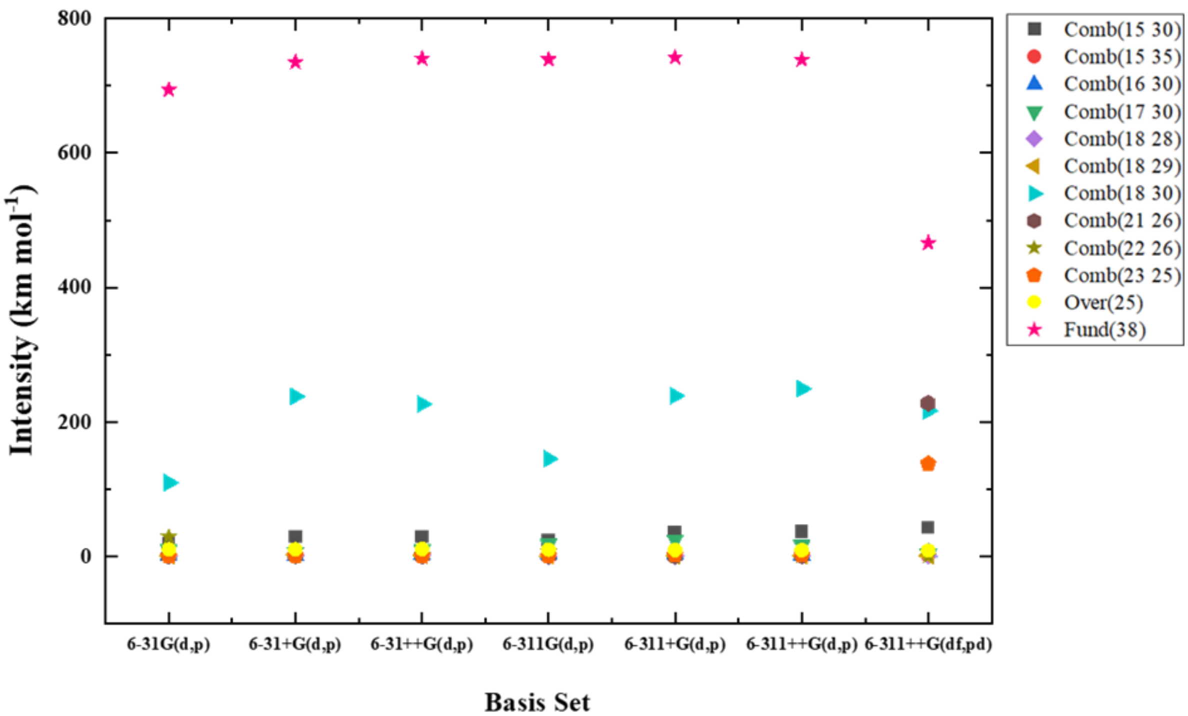

Figure 3.9 – Intensities of vibrational modes that can potentially couple with the azide asymmetric stretch of 4-azidotoluene for 6-31G(d,p), 6-31+G(d,p), 6-31++G(d,p), 6-311G(d,p), 6-311+G(d,p), 6-311++G(d,p), 6-311++G(df,pd) basis sets in THF.

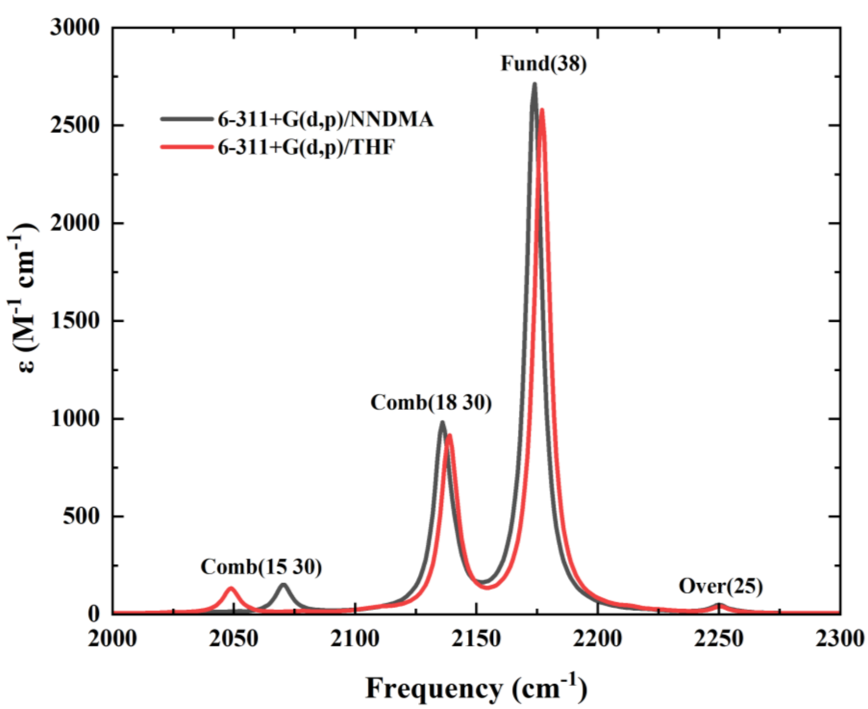

Figure 3.10 - Vibrational spectra of 4-azidotoluene in NNDMA and THF solvents with B3LYP/6-311+G(d,p) level of theory.

Figure 3.10 shows that THF solvent blue shifts both azide asymmetric stretch and Comb(18 30) bands. The intensity of these modes is also lower in THF compared to NNDMA, but they have a similar trend in both solvents. The major differences in these two solvents are, (i) 6-311++G(df,pd) basis set introduces two more high-intensity peaks (i.e., Comb(23 25) and Comb(21 26)) in THF which are not intense in NNDMA or other basis set calculations in THF, and (ii) the high-intensity peak, Comb(22 26) in 6-31G(d,p) in NNDMA solvent is less intense in THF solvent (29 km mol^{-1}). Figure 3.11 presents the azide asymmetric stretch adsorption profiles in seven basis sets. It clearly shows that 6-31G(d,p) and 6-311++G(df,pd) basis sets are different from the rest of the basis set adsorption profiles. Therefore, these calculations verify that these two basis sets are not suitable for studying vibrational coupling and FRs. The intensity of Comb(17 30) is varying for different basis sets as it was in NNDMA. Over(25) has an intensity of ~10 km mol^{-1}, and all other vibrational modes within the transparent window have lower intensity than 10 km mol^{-1}.

These observations verify that changing the solvents does not influence the identity of FRs, but the intensity of each vibrational transition in all basis set calculations is lower with THF. According to Figure 3.12, not only intensity values but also cubic force constants have similar trends in both solvents. The highest cubic force constant of ~55 cm^{-1} is observed for Comb(15 30) with all basis sets, and the second-highest cubic force constant ~48 cm^{-1} is for Comb(18 30). Like in NNDMA solvent, the cubic force constant of Comb(18 30) drops to ~36 cm^{-1}, and that of Comb(17 30) increases to ~32 cm^{-1} for 6-311++G(df,pd) basis set. Over(25) has ~32 cm^{-1} cubic force constant for all basis sets, and Comb(17 30) has a force constant less than 10 cm^{-1} for all basis sets except for 6-311G(d,p). All the rest of the vibrational modes within the transparent window have a cubic force constant of less than10 cm^{-1}.

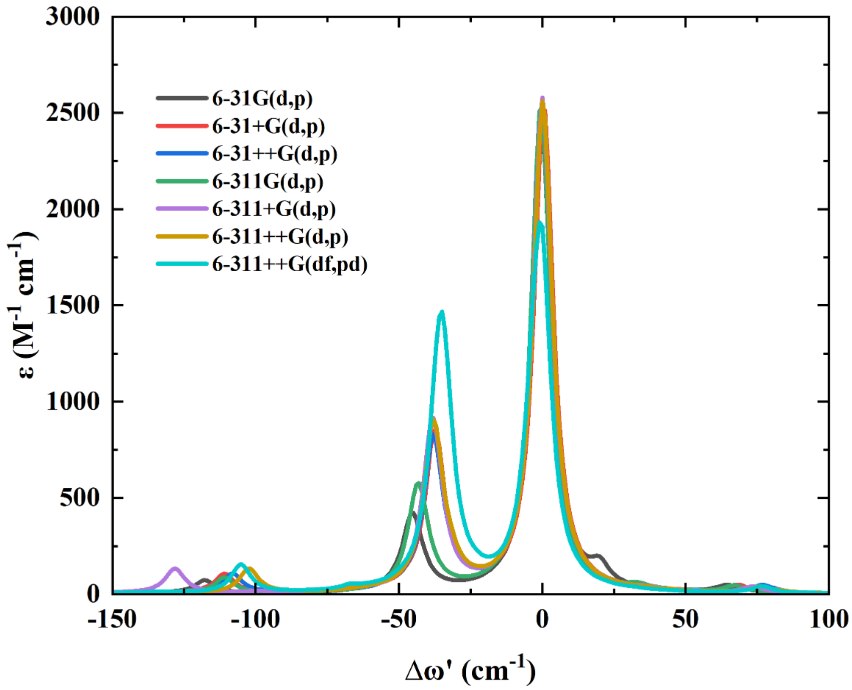

Figure 3.11 – Vibrational spectra (transparent window) of 4-azidotoluene for 6-31G(d,p), 6-31+G(d,p), 6-31++G(d,p), 6-311G(d,p), 6-311+G(d,p), 6-311++G(d,p), 6-311++G(df,pd) basis sets in THF. $\Delta\omega' = \omega_{ij} - \omega_k$ (ω_{ij} and ω_k are wavenumbers of combination band or overtone and fundamental vibration, respectively).

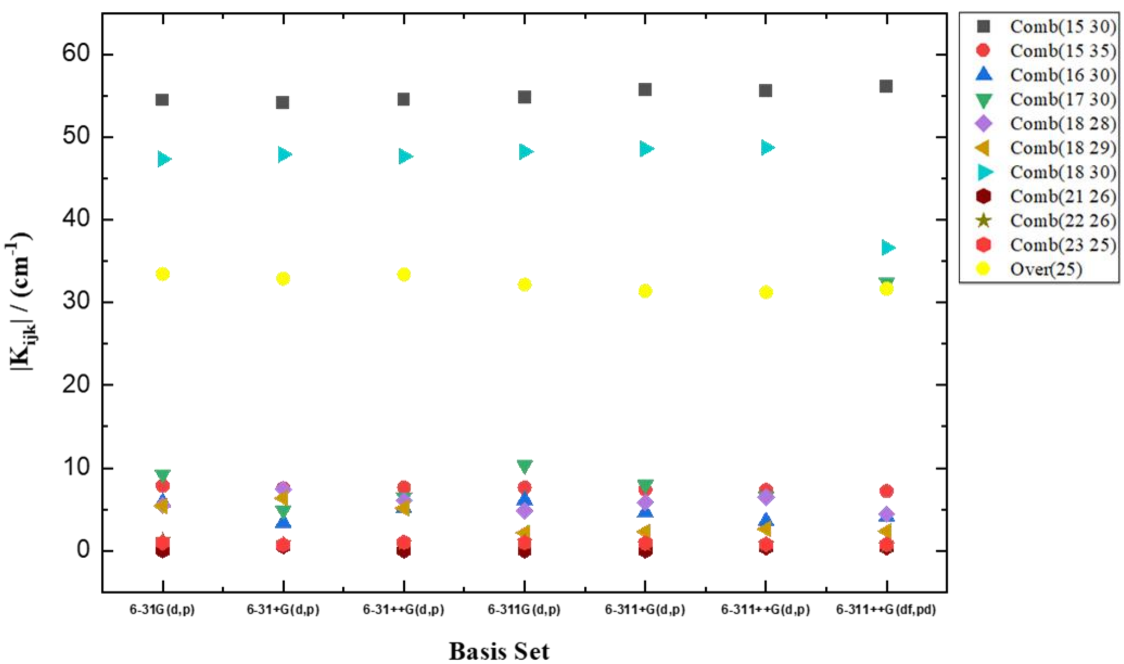

Figure 3.12 – Cubic force constants of vibrational modes that can potentially couple with the azide asymmetric stretch of 4-azidotoluene for 6-31G(d,p), 6-31+G(d,p), 6-31++G(d,p), 6-311G(d,p), 6-311+G(d,p), 6-311++G(d,p), 6-311++G(df,pd) basis sets in THF.

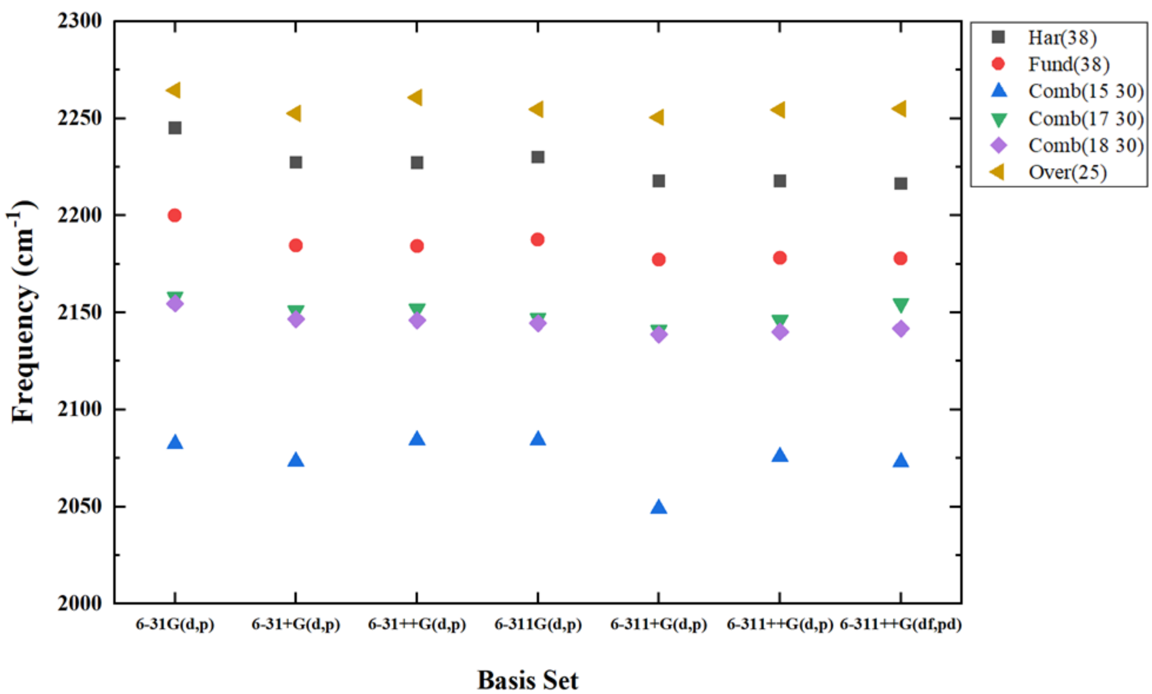

Figure 3.13 – Frequencies of vibrational modes that can potentially couple with the azide asymmetric stretch of 4-azidotoluene for 6-31G(d,p), 6-31+G(d,p), 6-31++G(d,p), 6-311G(d,p), 6-311+G(d,p), 6-311++G(d,p), 6-311++G(df,pd) basis sets in THF.

The peak positions of vibrational modes are solvent-dependent. When THF solvent was used, the azide asymmetric stretch blue shift for all basis set calculations and 6-311+G(d,p) has the lowest wavenumber for Fund(38) and combination band or overtones that can resonate with Fund(38). Qualitatively, frequencies for possible FRs show similar trends for all basis set calculations, see Figure 3.13. Like in the NNDMA solvent, Comb(15 30) and Over(25) are very far ($\Delta\omega' > 100$ cm^{-1} and > 65 cm^{-1}, respectively) away energetically from the Fund(38), and Comb(18 30) and Comb(17 30) are positioned so close.

Table 3.9 shows TFR values for possible modes that can resonantly couple with the azide asymmetric stretch for 4-azidotoluene in THF solvent. Here again, Comb(18 30) has TFR > 1 for each basis set calculation because Comb(18 30) is strongly coupled to the azide asymmetric stretch. Although both Comb(15 30) and Over(25) are very far away in frequency from the fundamental vibration, they show TFR values of ~0.55 and ~0.45, respectively. Therefore, both Comb(15 30) and Over(25) are weakly coupled to the azido asymmetric stretch. Also, Comb(17 30) is very weakly coupled to the azide asymmetric stretch due to moderate cubic force constant and relative peak position.

The vibrational modes that contribute to the FRs are shown in Figure 3.14. Interestingly, mode 30, which has the second-highest intensity is involved in making FRs. Using 4-azidotoluene, we have shown that 6-31G(d,p), 6-311G(d,p), and 6-311G(df,pd) are not optimal for studying vibrational coupling and FRs. In this case, basis sets 6-31+G(d,p), 6-31++G(d,p), 6-311+G(d,p), and 6-311++G(d,p) are suitable for studying vibrational coupling and FRs qualitatively. Since the 6-31+G(d,p) basis set has the lowest computational cost out of the four mentioned basis sets, the 6-31+G(d,p)/B3LYP combination is preferred for these types of calculations. Figure 3.10 shows that both solvents have a similar absorption profile for azide asymmetric stretch in the 6-311+G(d,p) basis set. However, recommending this level of theory by only using one aryl azide molecule is not sufficient. To get a better understanding, it is ideal to explore more modified aryl-azide compounds.

Table 3.9 - TFR values for combination or overtone bands that can potentially couple with azide asymmetric stretch in 4-azidotoluene in THF solvent.

Mode	6-31G(d,p)	6-31+G(d,p)	6-31++G(d,p)	6-311G(d,p)	6-311+G(d,p)	6-311++G(d,p)	6-311++G(df,pd)
Comb(15 30)	0.49	0.53	0.57	0.53	0.47	0.59	0.56
Comb(15 35)	0.11	0.11	0.09	0.10	0.14	0.09	0.10
Comb(16 30)	0.10	0.05	0.10	0.10	0.07	0.06	0.06
Comb(17 30)	0.35	0.21	0.36	0.53	0.28	0.29	4.28
Comb(18 28)	0.09	0.10	0.11	0.07	0.11	0.10	0.07
Comb(18 29)	0.10	0.17	0.16	0.06	0.03	0.10	0.05
Comb(18 30)	1.17	2.27	2.44	1.56	2.73	2.05	1.44
Comb(21 26)	0.00	0.02	0.00	0.00	0.00	0.19	0.02
Comb(22 26)	0.06	0.09	0.03	0.03	0.01	0.02	0.01
Comb(23 25)	0.05	0.04	0.44	0.03	0.23	0.13	0.20
Over(25)	0.50	0.45	0.43	0.46	0.43	0.40	0.41

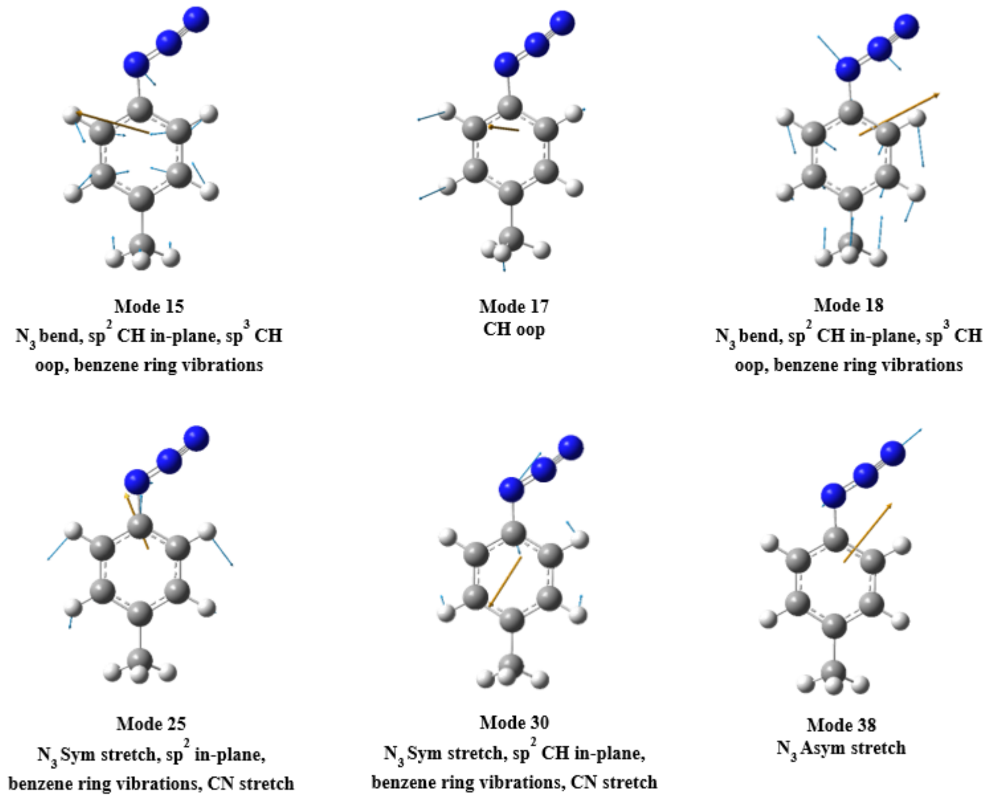

Figure 3.14 - Vibrational modes of combination or overtone bands that can potentially couple with the azide asymmetric stretch in 4-azidotoluene.

3.3 4-azidoacetanilide

The structural parameters of optimized 4-azidoacetanilide were studied to understand the basis sets effect and solvent effect on bond distances, bond angles, and dihedral angles. Table 3.10-3.12 shows structural parameters for both solvents with seven basis sets. For ease of understanding, atoms are numbered in Figure 3.1, and bond distances, angles, and dihedral angles are labeled. In 4-azidoacetanilide, the azide group and benzene ring are in the same plane (D12 ≈ 180^0). There's no significant change in the bond distances and bond angles. However, dihedral angels of the D15, D16, D18, D19, and D20 are changing considerably with different basis sets and solvents. Since the acetamide group has single bonds, all bonds can easily rotate, and this will change the strength of the bonds.

Table 3.10 – Bond distances (Å) of 4-azidoacetanilide with different basis sets: 6-31G(d,p), 6-31+G(d,p), 6-31++G(d,p), 6-311G(d,p), 6-311+G(d,p), 6-311++G(d,p), 6-311++G(df,pd) and two solvents, NNDMA (N) and THF (T).

Label	Definition	6-31G(d,p)		6-31+G(d,p)		6-31G++(d,p)		6-311G(d,p)		6-311+G(d,p)		6-311++G(d,p)		6-311++G(df,pd)	
		N	**T**	**N**	**T**	**N**	**T**	**N**	**T**	**N**	**T**	**N**	**T**	**N**	**T**
R1	R(1,2)	1.403	1.403	1.403	1.403	1.403	1.403	1.400	1.400	1.399	1.399	1.399	1.399	1.397	1.397
R2	R(1,3)	1.402	1.402	1.402	1.402	1.402	1.402	1.399	1.399	1.399	1.399	1.399	1.399	1.396	1.396
R3	R(2,4)	1.390	1.390	1.393	1.393	1.393	1.393	1.389	1.389	1.390	1.390	1.390	1.390	1.387	1.387
R4	R(2,5)	1.086	1.086	1.086	1.086	1.086	1.086	1.084	1.084	1.084	1.084	1.084	1.084	1.083	1.083
R5	R(3,6)	1.391	1.391	1.393	1.393	1.393	1.393	1.389	1.389	1.389	1.389	1.389	1.389	1.387	1.387
R6	R(3,7)	1.083	1.083	1.084	1.084	1.084	1.084	1.082	1.082	1.082	1.082	1.082	1.082	1.081	1.081
R7	R(4,8)	1.402	1.401	1.402	1.402	1.402	1.402	1.399	1.399	1.399	1.399	1.399	1.399	1.397	1.397
R8	R(6,8)	1.399	1.399	1.400	1.400	1.400	1.400	1.397	1.397	1.397	1.397	1.397	1.397	1.395	1.395
R9	R(4,9)	1.085	1.086	1.086	1.086	1.085	1.086	1.084	1.084	1.084	1.084	1.084	1.084	1.083	1.083
R10	R(6,10)	1.085	1.085	1.085	1.085	1.085	1.085	1.083	1.083	1.083	1.083	1.083	1.083	1.082	1.082
R11	R(8,11)	1.421	1.421	1.422	1.422	1.422	1.422	1.420	1.420	1.421	1.420	1.421	1.420	1.418	1.418
R12	R(11,12)	1.236	1.236	1.236	1.236	1.236	1.236	1.232	1.232	1.231	1.231	1.231	1.231	1.229	1.229
R13	R(12,13)	1.141	1.141	1.141	1.141	1.141	1.141	1.133	1.133	1.133	1.133	1.133	1.133	1.131	1.131
R14	R(1,14)	1.415	1.415	1.421	1.420	1.421	1.420	1.417	1.416	1.421	1.420	1.421	1.420	1.418	1.417
R15	R(14,15)	1.014	1.014	1.015	1.014	1.015	1.014	1.013	1.013	1.013	1.013	1.013	1.013	1.012	1.012
R16	R(14,16)	1.377	1.379	1.370	1.373	1.370	1.373	1.375	1.377	1.370	1.372	1.370	1.372	1.368	1.370
R17	R(16,17)	1.230	1.229	1.238	1.236	1.238	1.236	1.225	1.223	1.231	1.229	1.231	1.229	1.229	1.227
R18	R(16,18)	1.514	1.515	1.512	1.513	1.512	1.513	1.513	1.514	1.511	1.512	1.511	1.512	1.509	1.510
R19	R(18,19)	1.095	1.095	1.095	1.095	1.095	1.095	1.093	1.093	1.093	1.093	1.093	1.093	1.092	1.092
R20	R(18,20)	1.091	1.091	1.091	1.092	1.091	1.092	1.090	1.090	1.090	1.090	1.090	1.090	1.088	1.088
R21	R(18,21)	1.091	1.091	1.091	1.091	1.091	1.091	1.089	1.089	1.089	1.089	1.089	1.089	1.088	1.088

Table 3.11 – Bond angels of 4-azidoacetanilide with different basis sets: 6-31G(d,p), 6-31+G(d,p), 6-31++G(d,p), 6-311G(d,p), 6-311+G(d,p), 6-311++G(d,p), 6-311++G(df,pd) and two solvents, NNDMA (N) and THF (T).

Label	Definition	6-31G(d,p)		6-31+G(d,p)		6-31G++(d,p)		6-311G(d,p)		6-311+G(d,p)		6-311++G(d,p)		6-311++G(df,pd)	
		N	T	N	T	N	T	N	T	N	T	N	T	N	T
A1	A(1,2,3)	118.91	118.86	119.17	119.10	119.17	119.09	118.90	118.84	119.12	119.06	119.13	119.06	119.05	118.99
A2	A(1,2,4)	120.88	120.91	120.75	120.78	120.75	120.78	120.86	120.89	120.74	120.77	120.74	120.77	120.78	120.81
A3	A(1,2,5)	119.53	119.49	119.66	119.62	119.66	119.62	119.50	119.47	119.63	119.59	119.63	119.59	119.62	119.59
A4	A(1,3,6)	120.39	120.42	120.33	120.38	120.34	120.38	120.44	120.48	120.39	120.43	120.39	120.43	120.41	120.45
A5	A(1,3,7)	120.32	120.26	120.31	120.26	120.31	120.25	120.24	120.18	120.24	120.18	120.24	120.18	120.26	120.21
A6	A(2,4,8)	119.80	119.81	119.71	119.73	119.71	119.73	119.86	119.88	119.77	119.78	119.76	119.78	119.80	119.82
A7	A(3,6,8)	120.32	120.33	120.19	120.20	120.18	120.20	120.32	120.34	120.19	120.20	120.19	120.20	120.24	120.25
A8	A(2,4,9)	119.61	119.62	119.46	119.47	119.46	119.47	119.48	119.49	119.42	119.43	119.42	119.43	119.41	119.42
A9	A(3,6,10)	120.40	120.45	120.37	120.42	120.36	120.42	120.46	120.50	120.39	120.45	120.39	120.45	120.36	120.41
A10	A(4,8,11)	124.17	124.18	124.06	124.08	124.06	124.08	124.09	124.09	123.99	124.00	123.98	123.99	123.94	123.96
A11	A(6,8,11)	116.16	116.19	116.11	116.13	116.10	116.13	116.33	116.36	116.25	116.27	116.25	116.28	116.37	116.39
A12	A(8,11,12)	118.68	118.63	118.79	118.73	118.78	118.72	118.92	118.89	119.03	118.97	119.03	118.97	119.28	119.23
A13	A(11,12,13)	172.50	172.55	172.57	172.61	172.59	172.62	172.79	172.82	172.71	172.75	172.72	172.76	172.62	172.66
A14	A(1,3,14)	122.48	122.50	122.05	122.09	122.06	122.11	122.24	122.27	121.95	121.96	121.93	121.95	122.08	122.11
A15	A(1,14,15)	116.35	116.42	116.50	116.57	116.49	116.56	116.42	116.48	116.48	116.56	116.49	116.57	116.34	116.42
A16	A(1,14,16)	131.15	131.23	130.25	130.37	130.27	130.39	130.70	130.79	130.10	130.18	130.07	130.16	130.30	130.40
A17	A(14,16,17)	119.32	119.31	119.39	119.38	119.39	119.38	119.55	119.55	119.59	119.59	119.60	119.60	119.57	119.56
A18	A(14,16,18)	119.01	118.96	119.28	119.21	119.28	119.21	118.80	118.73	118.98	118.89	118.96	118.87	119.05	118.98
A19	A(16,18,19)	110.15	110.15	109.85	109.85	109.85	109.85	109.99	109.99	109.72	109.71	109.74	109.72	109.70	109.69
A20	A(16,18,20)	113.11	113.13	113.05	113.08	113.05	113.09	113.13	113.15	113.05	113.10	113.03	113.08	113.06	113.10
A21	A(16,18,21)	107.51	107.45	107.80	107.72	107.79	107.71	107.50	107.44	107.85	107.78	107.86	107.78	107.84	107.76

Table 3.12 – Dihedral angels of 4-azidoacetanilde with different basis sets: 6-31G(d,p), 6-31+G(d,p), 6-31++G(d,p), 6-311G(d,p), 6-311+G(d,p), 6-311++G(d,p), 6-311++G(df,pd) and two solvents, NNDMA (N) and THF (T).

Label	Definition	6-31G(d,p)		6-31+G(d,p)		6-31G++(d,p)		6-311G(d,p)		6-311+G(d,p)		6-311++G(d,p)		6-311++G(df,pd)	
		N	T	N	T	N	T	N	T	N	T	N	T	N	T
D1	D(4,2,1,3)	-0.80	-0.74	-0.58	-0.54	-0.59	-0.54	-0.65	-0.61	-0.56	-0.52	-0.58	-0.54	-0.64	-0.60
D2	D(5,2,1,3)	179.55	179.64	179.69	179.78	179.67	179.76	179.63	179.72	179.67	179.77	179.68	179.77	179.63	179.72
D3	D(6,3,1,2)	1.96	1.94	1.68	1.66	1.69	1.67	1.82	1.80	1.67	1.66	1.69	1.67	1.71	1.70
D4	D(7,3,1,2)	-176.77	-176.77	-177.30	-177.25	-177.27	-177.22	-177.03	-177.01	-177.31	-177.27	-177.32	-177.27	-177.24	-177.21
D5	D(8,4,2,1)	-0.69	-0.73	-0.70	-0.74	-0.69	-0.74	-0.74	-0.77	-0.72	-0.76	-0.70	-0.74	-0.66	-179.50
D6	D(8,6,3,1)	-1.65	-1.66	-1.49	-1.50	-1.51	-1.52	-1.60	-1.62	-1.50	-1.52	-1.50	-1.51	-1.49	-1.50
D7	D(9,4,2,1)	179.98	179.96	179.98	179.97	179.98	179.97	179.92	179.91	179.96	179.95	179.96	179.95	179.96	179.95
D8	D(10,6,3,1)	179.72	179.74	179.78	179.81	179.77	179.80	179.75	179.76	179.78	179.81	179.78	179.81	179.79	179.82
D9	D(2,4,8,11)	-179.45	-179.44	-179.51	-179.49	-179.51	-179.50	-179.46	-179.45	-179.51	-179.49	-179.51	-179.49	-179.52	-179.50
D10	D(3,6,8,11)	-179.43	-179.41	-179.43	-179.42	-179.42	-179.41	-179.41	-179.39	-179.42	-179.41	-179.43	-179.42	-179.44	-179.44
D11	D(4,8,11,12)	-0.02	-0.04	-0.28	-0.26	-0.28	-0.25	-0.14	-0.13	-0.29	-0.29	-0.26	-0.27	-0.23	-0.24
D12	D(6,8,11,12)	179.53	179.51	179.33	179.36	179.34	179.37	179.45	179.46	179.32	179.33	179.35	179.34	179.36	179.36
D13	D(8,11,12,13)	-179.96	179.99	-179.83	-179.92	-179.81	-179.80	-179.93	-179.96	-179.84	-179.89	-179.83	-179.89	-179.90	-179.91
D14	D(6,3,1,14)	179.08	179.06	178.87	178.86	178.87	178.85	179.01	179.00	178.87	178.86	178.90	178.89	178.93	178.92
D15	D(3,1,14,15)	-142.31	-142.34	-136.22	-136.31	-136.37	-136.43	-138.78	-138.75	-135.10	-134.89	-135.03	-134.81	-136.41	-136.44
D16	D(1,14,16,17)	45.28	45.21	49.11	48.96	48.86	48.75	48.18	48.07	50.52	50.67	50.75	50.84	49.19	49.07
D17	D(1,14,16,18)	179.51	179.46	-179.06	-179.07	-178.97	-179.00	179.77	179.82	-179.24	-179.27	-179.39	-179.37	-179.15	-179.14
D18	D(14,16,18,19)	0.10	0.07	1.53	1.56	1.63	1.65	0.43	0.51	1.32	1.33	1.15	1.21	1.49	1.54
D19	D(14,16,18,20)	-90.13	-90.10	-91.83	-91.97	-91.93	-92.06	-89.45	-89.59	-91.86	-92.01	-91.54	-91.78	-92.11	-92.32
D20	D(14,16,18,21)	31.08	31.15	29.24	29.16	29.14	29.08	31.66	31.57	29.11	29.02	29.41	29.23	28.86	28.72

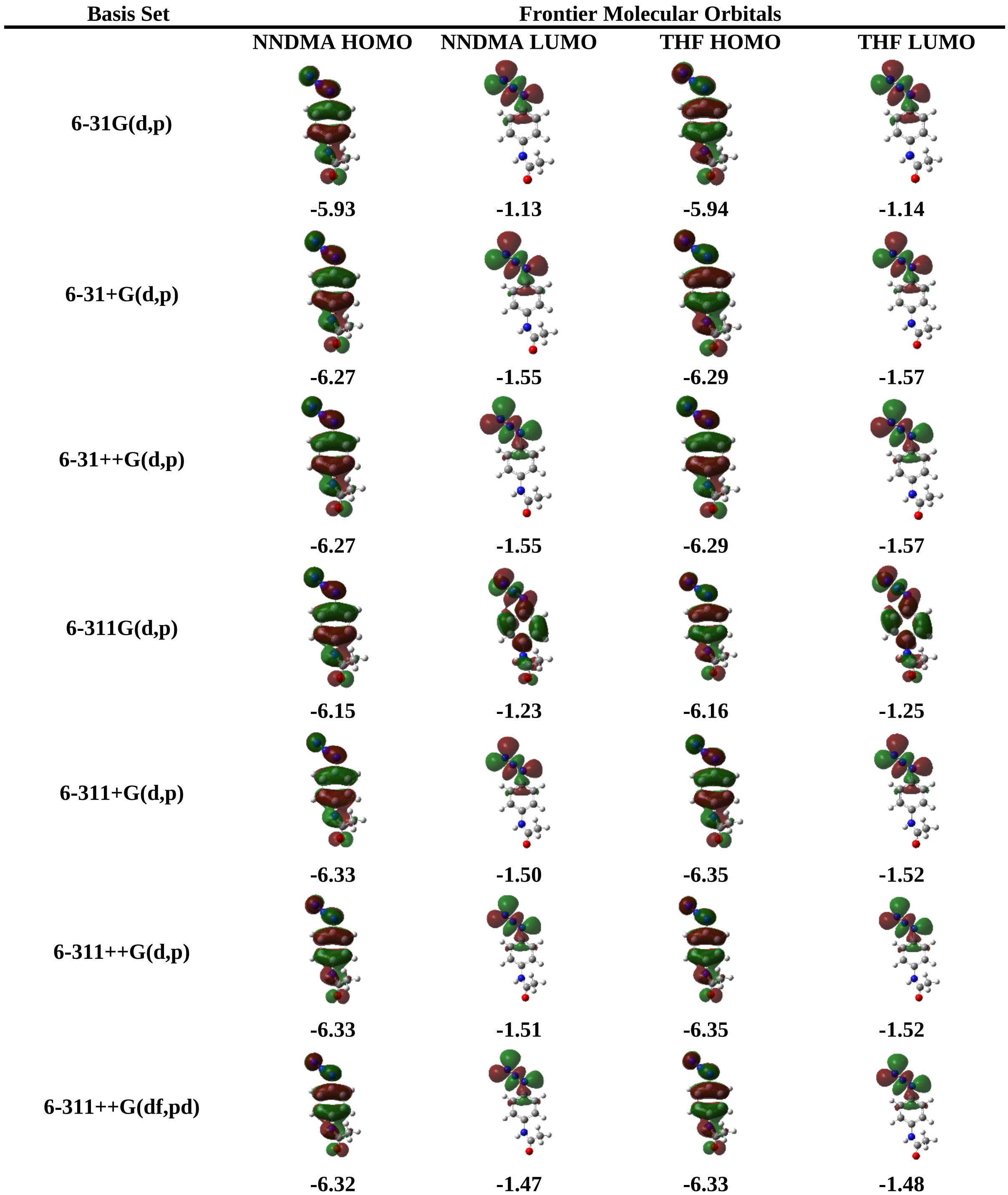

Figure 3.15 - Spatial distributions of HOMO and LUMO frontier molecular orbitals of 4-azidoacetanilide in NNDMA and THF solvents for seven basis sets. Orbital energy eigenvalues (in eV) are shown below each molecular orbital. The red and green color lobes correspond to the two different phases of the orbital wave function with positive and negative signs, respectively.

Then, the DFT calculated frontier molecular orbitals HOMO and LUMO of 4-azidoacetanilide are illustrated in Figure 3.15. The HOMO and LUMO orbitals are the same for all basis sets and two solvents except for the LUMO orbital in the 6-311G(d,p) basis set. The HOMO orbital is distributed in the region perpendicular to the bond axis avoiding all hydrogen atoms while the LUMO orbital is localized parallel to the bond axis and only covers the azide region and three carbon atoms close to the azide group. According to Table 3.12, the dihedral angles D16 and D20 greatly changed for both solvents in 6-31G(d,p) and 6-31G(d,p)/6-311G(d,p) basis sets, separately due to the free bond rotation around single bonds. Hence, this will result in huge changes in the strength of the vibrational modes consisting of the acetamide group. The energies of the molecule decrease (more negative) from 6-31G(d,p) to 6-311++G(df,pd) and ~0.06 eV high in NNDMA solvent. However, Tables 3.13 and 3.14 show that the energies and HOMO-LUMO gaps are similar in 6-31+G(d,p)/6-31++G(d,p) and 6-311+G(d,p)/6-311++G(d,p) pairs separately. But HOMO-LUMO gap has the order of 6-311G(d,p) > 6-311++G(df,pd) > 6-311+G(d,p)/6-311++G(d,p) > 6-31G(d,p) > 6-31+G(d,p)/6-31++G(d,p) and similar for both solvents.

Table 3.13 – Energies and HOMO-LUMO gap for the 4-azidoacetanilide in NNDMA.

Basis set	Energy (au)	HOMO(au)	HOMO(eV)	LUMO(au)	LUMO(eV)	HL gap (eV)
6-31G(d,p)	-603.873140	-0.22	-5.93	-0.04	-1.13	4.80
6-31+G(d,p)	-603.899573	-0.23	-6.27	-0.06	-1.55	4.72
6-31++G(d,p)	-603.899775	-0.23	-6.27	-0.06	-1.55	4.72
6-311G(d,p)	-604.016797	-0.23	-6.15	-0.05	-1.23	4.92
6-311+G(d,p)	-604.030250	-0.23	-6.33	-0.06	-1.50	4.83
6-311++G(d,p)	-604.030390	-0.23	-6.33	-0.06	-1.51	4.83
6-311++G(df,pd)	-604.054945	-0.23	-6.32	-0.05	-1.47	4.85

Table 3.14 – Energies and HOMO-LUMO gap for the 4-azidoacetanilide in THF.

Basis set	Energy (au)	HOMO(au)	HOMO(eV)	LUMO(au)	LUMO(eV)	HL gap (eV)
6-31G(d,p)	-603.871374	-0.22	-5.94	-0.04	-1.14	4.80
6-31+G(d,p)	-603.897356	-0.23	-6.29	-0.06	-1.57	4.72
6-31++G(d,p)	-603.897559	-0.23	-6.29	-0.06	-1.57	4.72
6-311G(d,p)	-604.014923	-0.23	-6.16	-0.05	-1.25	4.91
6-311+G(d,p)	-604.028050	-0.23	-6.35	-0.06	-1.52	4.83
6-311++G(d,p)	-604.028192	-0.23	-6.35	-0.06	-1.52	4.82
6-311++G(df,pd)	-604.052752	-0.23	-6.33	-0.05	-1.48	4.85

3.3.1 4-azidoacetanilide in NNDMA

The harmonic and anharmonic vibrational spectra of 4-azidoacetanilide with DFT/B3LYP/6-311+G(d,p) level in NNDMA are shown in Figure 3.16. Table 3.15 illustrates vibrational modes with high intensities in the harmonic spectrum. Both Figure 3.16 and Table 3.15 show that the azide asymmetric stretch (mode 49) has the highest intensity. Then, modes 48, 45, 40, 39, 38, and 37 have the next highest intensities. Hence, these vibrational modes can be contributing to the generation of FRs with azide asymmetric stretch.

The 4-azidoacetanilide consists of 21 atoms. Thus, 57 (3N-6) fundamental vibrational modes can be seen in the IR spectrum. The anharmonic vibrational spectra of the azide adsorption profile with seven different basis sets are shown in Figure 3.17. All the vibrational modes occurring within ±120 cm^{-1} of the fundamental vibration for seven basis sets are shown in Appendix C. Unlike the 4-azidotoluene, 4-azidoacetanilide has a very complex absorption profile for the azide asymmetric stretch. Different basis sets generate different azide absorption profiles except for 6-31+G(d,p), 6-31++G(d,p), and 6-311++G(df,pd) basis sets which have the exact absorption profile. Figure 3.18 presents high-intensity peaks within the transparent window in seven basis sets. There, some combination bands show higher intensity than azide asymmetric stretch in 6-311G(d,p), 6-311+G(d,p), and 6-311++G(d,p) basis sets. For example, Comb(20 45), Comb(22 41) and Comb(21 44) have the highest intensity in 6-311G(d,p), 6-311+G(d,p), and 6-311++G(d,p) basis sets, respectively. Moreover, Comb(24 40) and Comb(25 39) have high intensity in both 6-31G(d,p) and 6-311G(d,p) basis sets. The azide absorption profile of 4-azidoacetanilide is too complicated with many high-intensity combination bands. For example, the 6-311+G(d,p) basis set has high intensities for Comb(22 41) and Comb(16 48) modes which will be proven to be non-FRs later. To understand FRs, cubic force constants were studied for high-intensity peaks within the transparent window. As shown in Figure 3.19, Comb(24 39) has the highest cubic force constant around 50 cm^{-1}. But it is ~50 cm^{-1} away from the azide asymmetric stretch, see Figure 3.20. Both Comb(22 39) and Over(33) have a cubic force constant of ~35 cm^{-1}, but they are also very far away from the fundamental vibration, ~80 and ~95 cm^{-1}, separately. Then, Comb(24 38) has the cubic force constant > 10 cm^{-1} except for the 6-311G(d,p) basis set. But it is also ~50 cm^{-1} away from the fundamental vibration. Both Comb(25 39) and Comb(24 40) are somewhat closer to the fundamental vibration with cubic force constant < 10 cm^{-1}. Hence, the intensity of these modes is not high as expected from the vibrational coupling.

Table 3.15 – Vibrational modes of 4-azidoacetanilide in NNDMA using B3LYP/6-311+G(d,p)

Mode	Vibration	$\upsilon_{(harmonic)}$ / cm^{-1}	$\upsilon_{(anharmonic)}$ / cm^{-1}	$I_{(harmonic)}$ / km mol^{-1}	$I_{(anharmonic)}$ / km mol^{-1}
49	N_3 asymmetric stretch	2216.9	2173.9	1868.1	475.4
48	C=O stretch, C-H in plane	1679.2	1643.2	1045.4	342.2
45	sp^2 C-H in-plane	1535.3	1492.0	463.9	169.8
40	sp^3 C-H oop	1398.4	1371.2	152.0	70.4
39	N_3 Sym stretch + C-N stretch + ring vibrations + C-H in-plane	1363.5	1315.6	143.0	61.3
38	C-N stretch + ring vibrations + C-H in-plane	1342.4	1305.8	716.4	2.5
37	sp^2 C-H in-plane	1332.5	1301.8	181.7	219.3

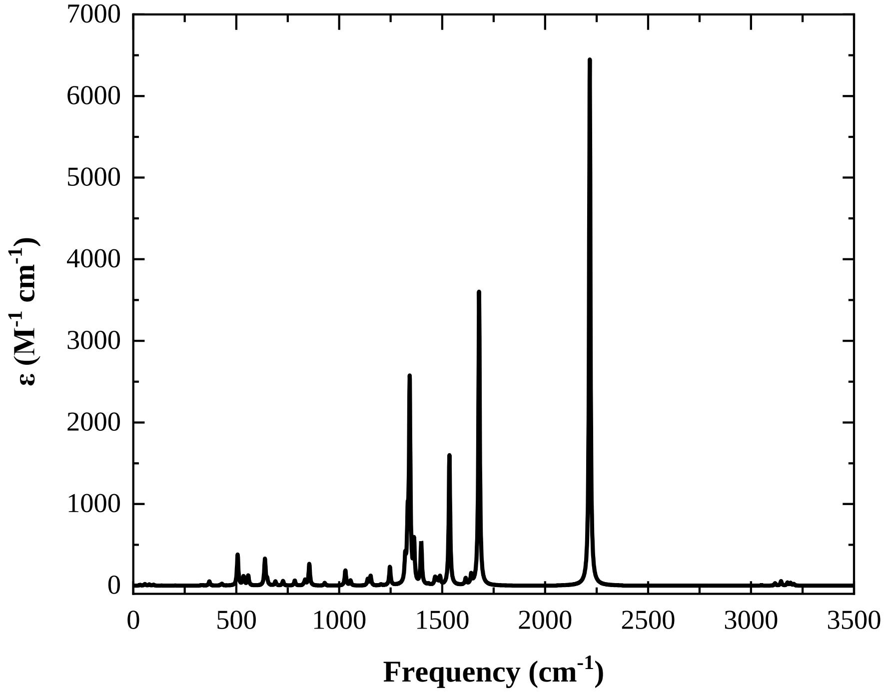

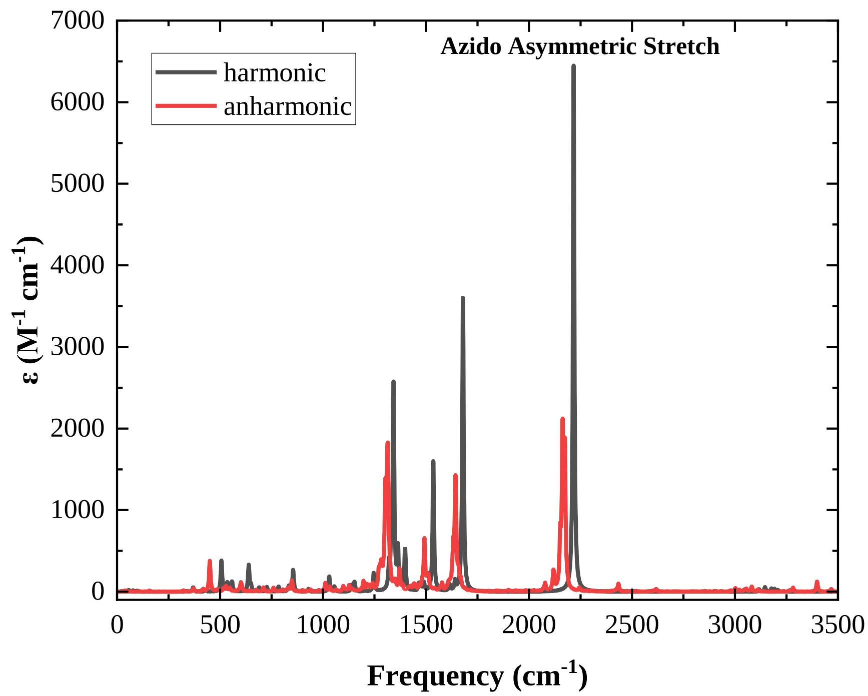

Figure 3.16 – IR spectra of harmonic (top), both anharmonic and harmonic (bottom) of 4-azidoacetanilide in NNDMA using B3LYP/6-311+G(d,p) level in Gaussian-16

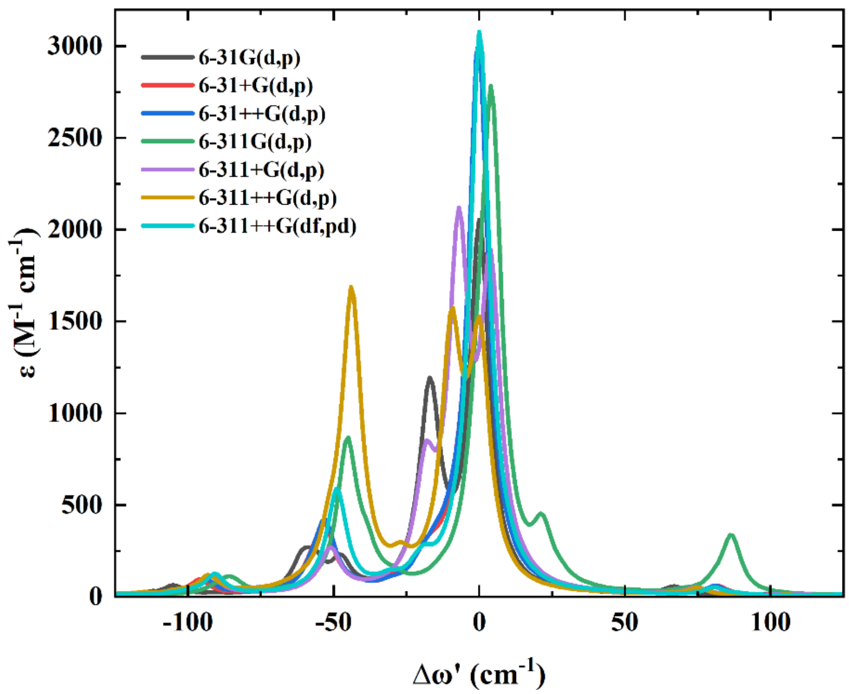

Figure 3.17 – Vibrational spectra (transparent window) of 4-azidoacetanilide for 6-31G(d,p), 6-31+G(d,p), 6-31++G(d,p), 6-311G(d,p), 6-311+G(d,p), 6-311++G(d,p), 6-311++G(df,pd) basis sets in NNDMA. $\Delta\omega' = \omega_{ij} - \omega_k$ (ω_{ij} and ω_k are wavenumbers of combination band or overtone and fundamental vibration, respectively).

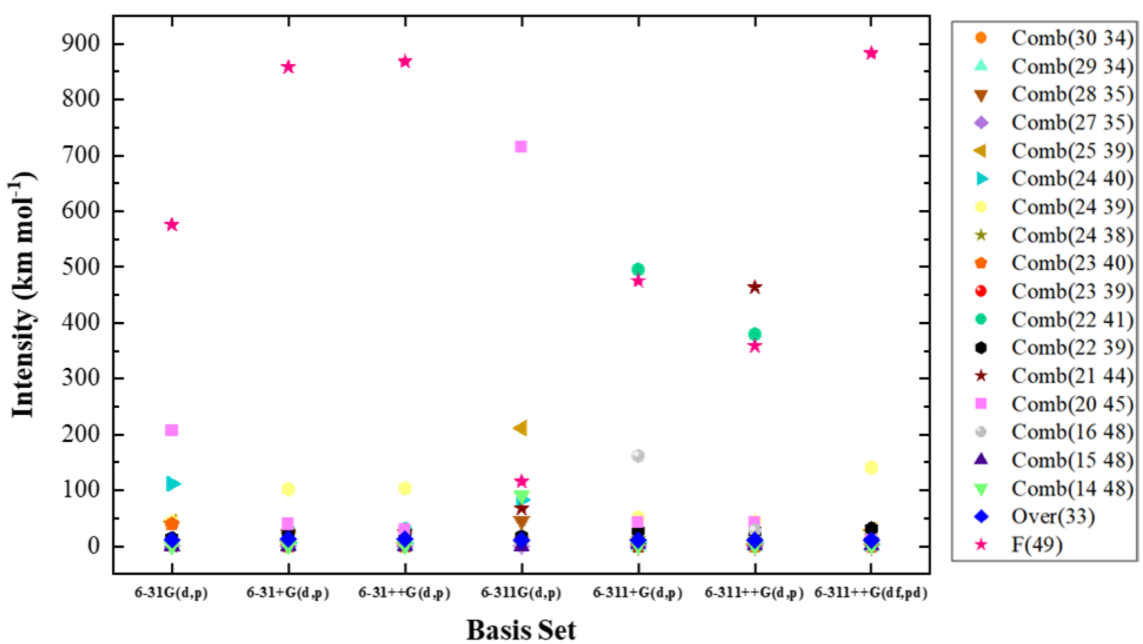

Figure 3.18 - Intensities of vibrational modes that can potentially couple with the azide asymmetric stretch of 4-azidoacetanilide for 6-31G(d,p), 6-31+G(d,p), 6-31++G(d,p), 6-311G(d,p), 6-311+G(d,p), 6-311++G(d,p), 6-311++G(df,pd) basis sets in NNDMA.

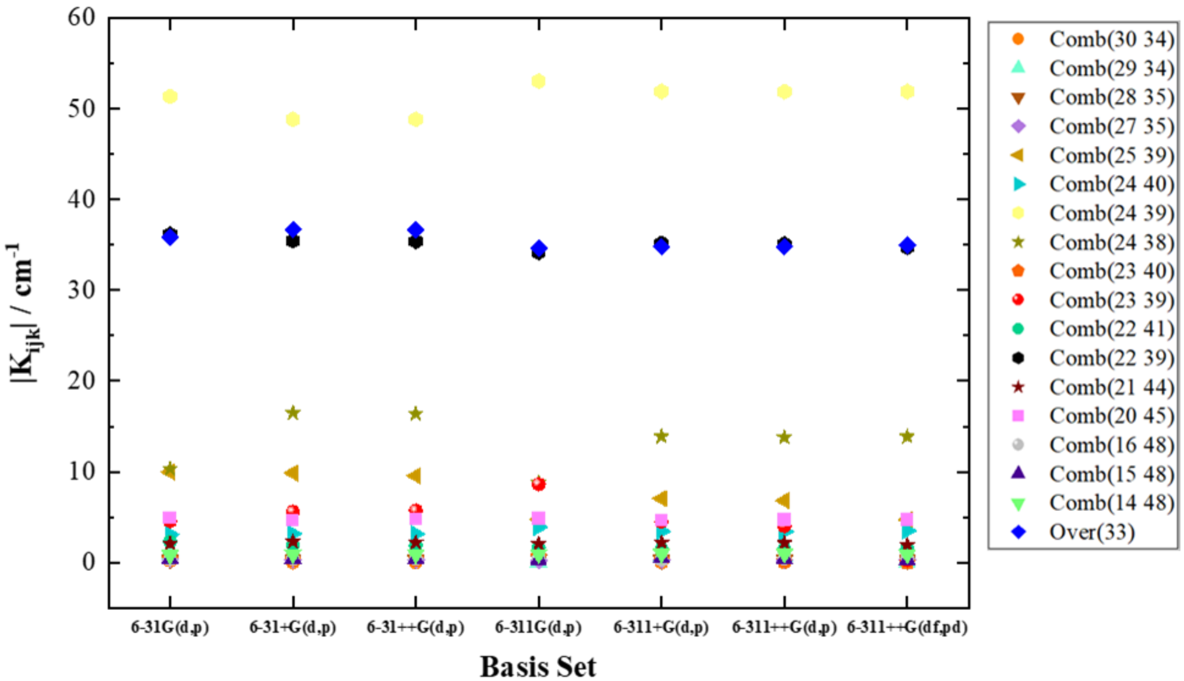

Figure 3.19 - Cubic force constants of vibrational modes that can potentially couple with the azide asymmetric stretch of 4-azidoacetanilide for 6-31G(d,p), 6-31+G(d,p), 6-31++G(d,p), 6-311G(d,p), 6-311+G(d,p), 6-311++G(d,p), 6-311++G(df,pd) basis sets in NNDMA.

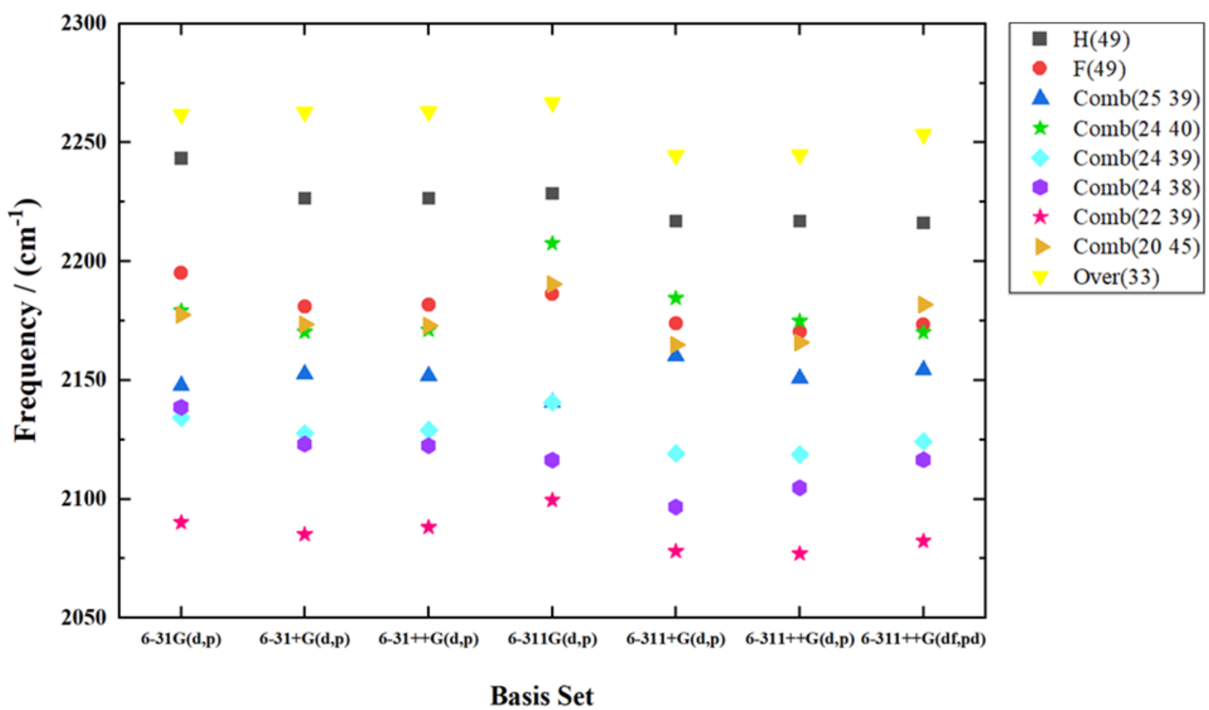

Figure 3.20 - Frequencies of vibrational modes that can potentially couple with the azide asymmetric stretch of 4-azidoacetanilide for 6-31G(d,p), 6-31+G(d,p), 6-31++G(d,p), 6-311G(d,p), 6-311+G(d,p), 6-311++G(d,p), 6-311++G(df,pd) basis sets in NNDMA.

Nevertheless, if K_{ijk} < 10 cm^{-1}, and the vibrational mode is very near to the fundamental vibration, there is a still chance to generate FRs. For example, Comb(20 45) is 10 cm^{-1} far away from the azide asymmetric stretch except for the 6-31G(d,p) basis set, and has a cubic force constant of 5 cm^{-1}. Thus, Comb(20 45) has high intensity comparatively. When comparing the general trend of frequencies (Δω') and resonance shift (Δω) of these FRs to the azide asymmetric stretch, they show the same pattern except for Comb(24 40) and Comb(20 45) due to the frequency is changing from -Δω' to +Δω' for double zeta to triple zeta basis sets. TFR values directly estimate what FRs are involved in complex azide adsorption profiles. However, lower Δω values can give exceptionally high TFR values. For example, Comb(24 40) has a high TFR value of 17.5 due to a low Δω of 0.2 cm^{-1}. To figure out FRs, the consistency of the TFR value is important. According to Table 3.17, only Comb(24 39) has TFR > 1. Hence, Comb(24 39) is strongly coupled to the azide asymmetric stretch.

Table 3.16 - TFR values for combination or overtone bands that can potentially couple with the azide asymmetric stretch in 4-azidoacetanilide in NNDMA solvent

Mode	6-31G(d,p)	6-31+G(d,p)	6-31++G(d,p)	6-311G(d,p)	6-311+G(d,p)	6-311++G(d,p)	6-311++G(df,pd)
Over(33)	0.443	0.448	0.452	0.480	0.436	0.428	0.429
Comb(30 34)	0.056	0.000	0.000	0.028	0.000	0.000	0.020
Comb(29 34)	0.034	0.132	0.294	0.000	3.314	0.102	0.000
Comb(28 35)	0.006	0.019	0.022	0.008	0.015	0.050	0.175
Comb(27 35)	0.004	0.008	0.007	0.004	0.008	0.012	0.010
Comb(25 39)	0.354	0.474	0.403	0.104	0.783	0.423	0.344
Comb(24 40)	0.121	0.258	0.292	0.121	0.234	0.830	17.541
Comb(24 39)	0.863	1.022	1.040	2.539	1.267	1.224	1.475
Comb(24 38)	0.136	0.278	0.286	0.206	0.273	0.265	0.316
Comb(23 40)	0.006	0.009	0.008	0.021	0.843	0.018	0.000
Comb(23 39)	0.051	0.079	0.079	0.099	0.081	0.069	0.004
Comb(22 41)	0.080	0.064	0.059	0.077	0.053	0.068	0.072
Comb(22 39)	0.336	0.355	0.346	0.375	0.357	0.376	0.370
Comb(21 44)	0.100	0.047	0.045	0.135	0.045	0.051	0.078
Comb(20 45)	0.427	2.452	0.914	0.473	0.636	1.383	0.379
Comb(16 48)	0.004	0.011	0.013	0.007	0.022	0.078	0.005
Comb(15 48)	0.010	0.017	0.017	0.005	0.294	0.013	0.025
Comb(14 48)	0.016	0.055	0.047	0.007	0.012	0.011	0.351

Then, Comb(20 45), Comb(25 39), Comb(22 39), and Over(33) were also considered to be weakly coupled to the azide asymmetric stretch due to TFR > 0.3. Moreover, Comb(24 40) and Comb(24 38) can be also considered as FRs due to very weak coupling (TFR ≈ 0.3). Figure 3.21 illustrates individual normal modes that contribute to making FRs.

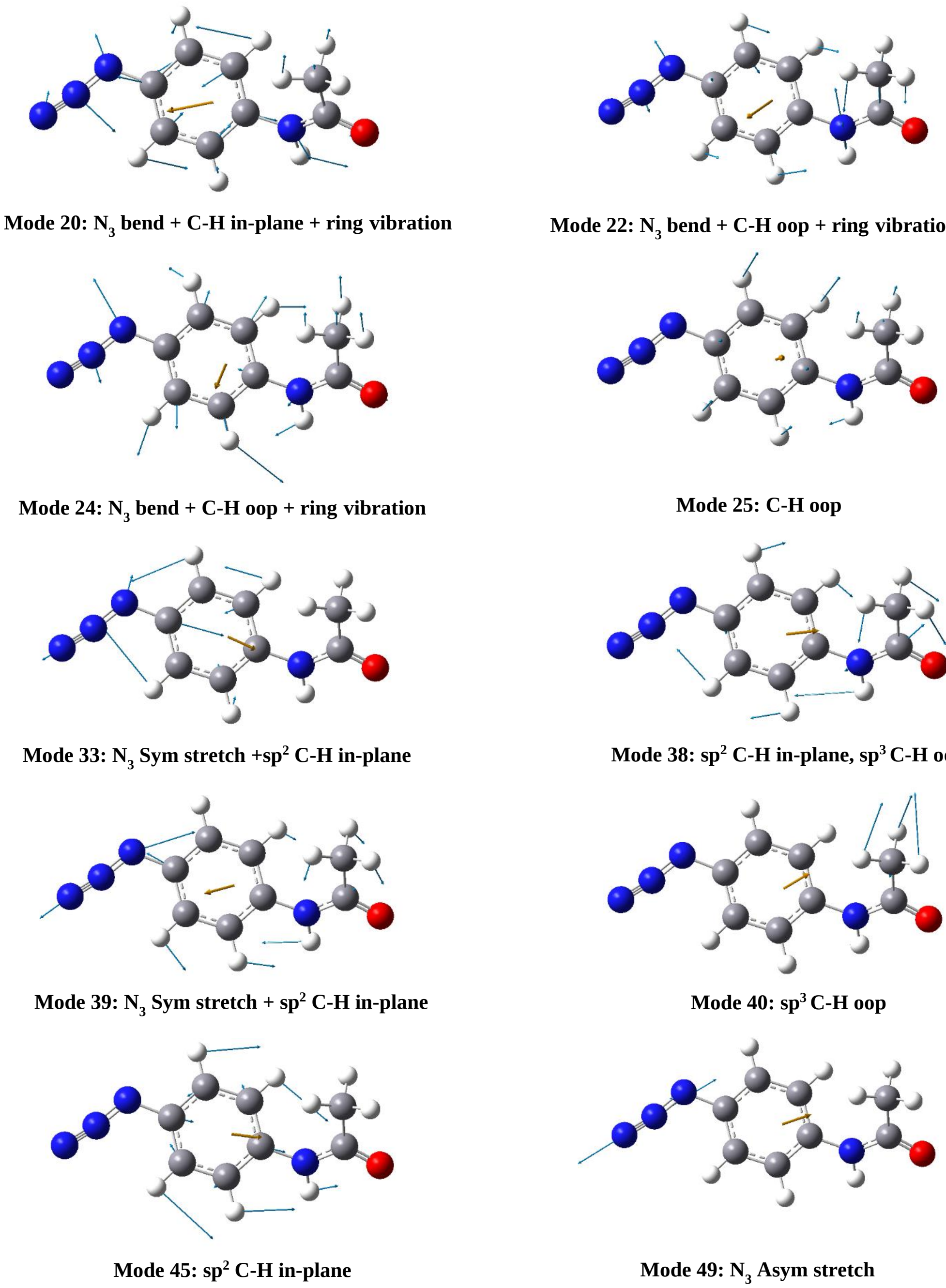

Figure 3.21 - Vibrational modes of combination or overtone bands that can potentially couple with the azide asymmetric stretch in 4-azidoacetanilide.

3.3.2 4-azidoacetanilide in THF

It has been shown how the azide absorption profile is too complicated for 4-azidoacetanilide in NNDMA. But we could be able to show FRs by using cubic force constant and TFR values, and high-intensity vibrational modes may not be FRs. Here, we present theoretical calculations for 4-azidoacetanilide in THF to study the solvent effect as well as to verify observed FRs for 4-azidoacetanilide in NNDMA. Both harmonic and anharmonic spectra are shown in Figure 3.22 and vibrational modes occurring within ±120 cm^{-1} of the azide asymmetric stretch were shown in Appendix D. Table 3.18 illustrates vibrational modes with high intensities in the harmonic spectrum. Anharmonic vibrational spectra of azide adsorption profile with seven different basis sets are shown in Figure 3.17. Like in the NNDMA solvent, 4-azidoacetanilide has a very complex absorption profile for the azide asymmetric stretch. Different basis sets generate different azide absorption profiles.

Table 3.17 – Vibrational modes of 4-azidoacetanilide in THF using B3LYP/6-311+G(d,p)

Mode	**Vibration**	**$\upsilon_{(harmonic)}$ / cm^{-1}**	**$\upsilon_{(anharmonic)}$ / cm^{-1}**	**$I_{(harmonic)}$ / km mol^{-1}**	**$I_{(anharmonic)}$ / km mol^{-1}**
49	N_3 asymmetric stretch	2220.9	2174. 4	1693.0	795.2
48	C=O stretch, C-H in plane	1690.8	1684.5	986.4	135.7
45	sp^2 C-H in-plane	1535.9	1487.9	434.7	21.1
40	sp^3 C-H oop	1399.1	1355.1	136.0	17.5
39	N_3 Sym stretch + C-N stretch + ring vibrations + C-H in-plane	1364.5	1312.7	140.6	93.1
38	C-N stretch + ring vibrations + C-H in-plane	1340.9	1294.1	631.9	112.6
37	sp^2 C-H in-plane	1332.0	1233.6	193.5	478.1

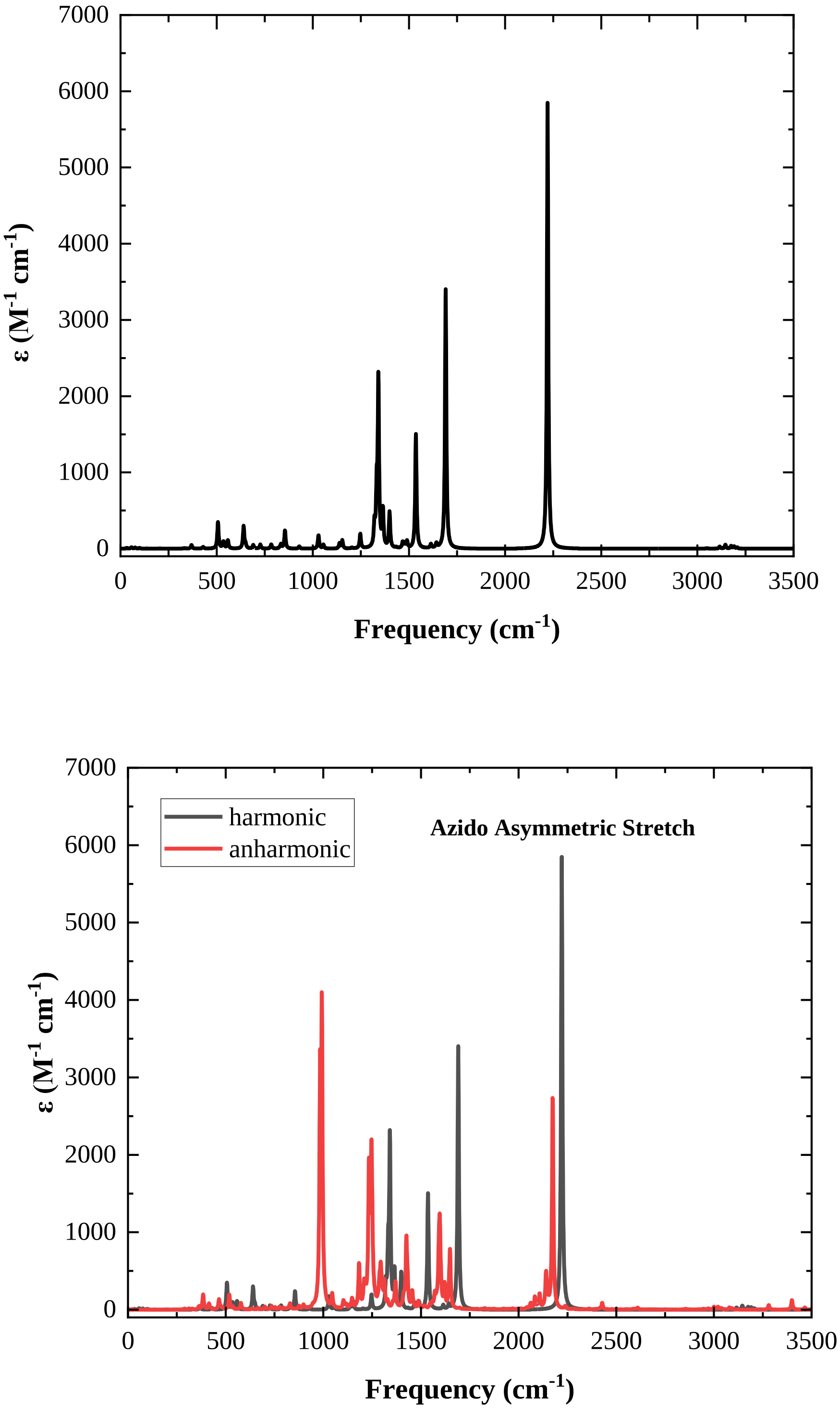

Figure 3.22 – IR spectra of harmonic (top), both anharmonic and harmonic (bottom) of 4-azidoacetanilide in THF using B3LYP/6-311+G(d,p) level in Gaussian-16.

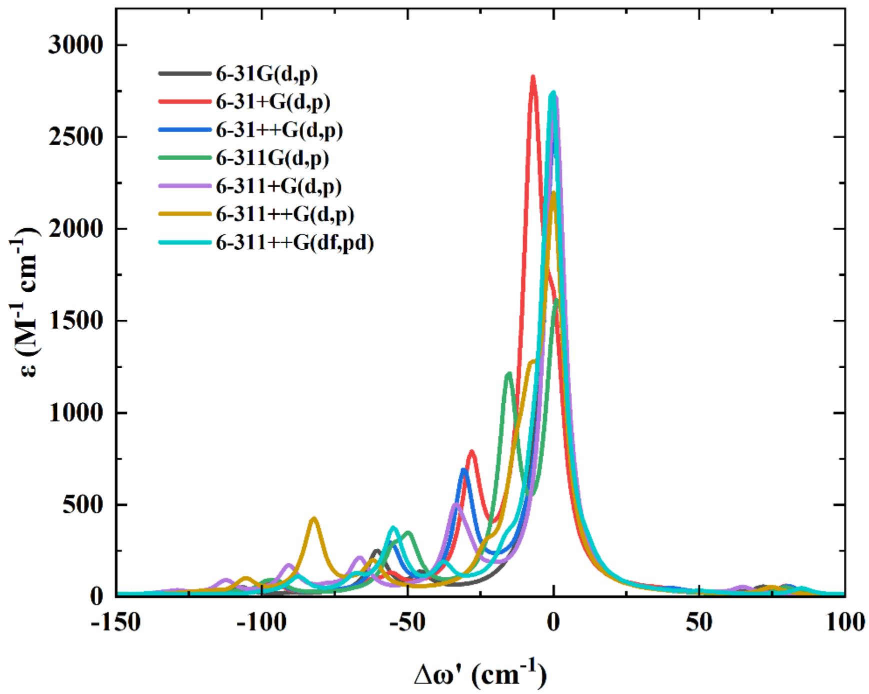

Figure 3.23 - Vibrational spectra (transparent window) of 4-azidoacetanilide for 6-31G(d,p), 6-31+G(d,p), 6-31++G(d,p), 6-311G(d,p), 6-311+G(d,p), 6-311++G(d,p), 6-311++G(df,pd) basis sets in THF. $\Delta\omega' = \omega_{ij} - \omega_k$ (ω_{ij} and ω_k are wavenumbers of combination band or overtone and fundamental vibration, respectively).

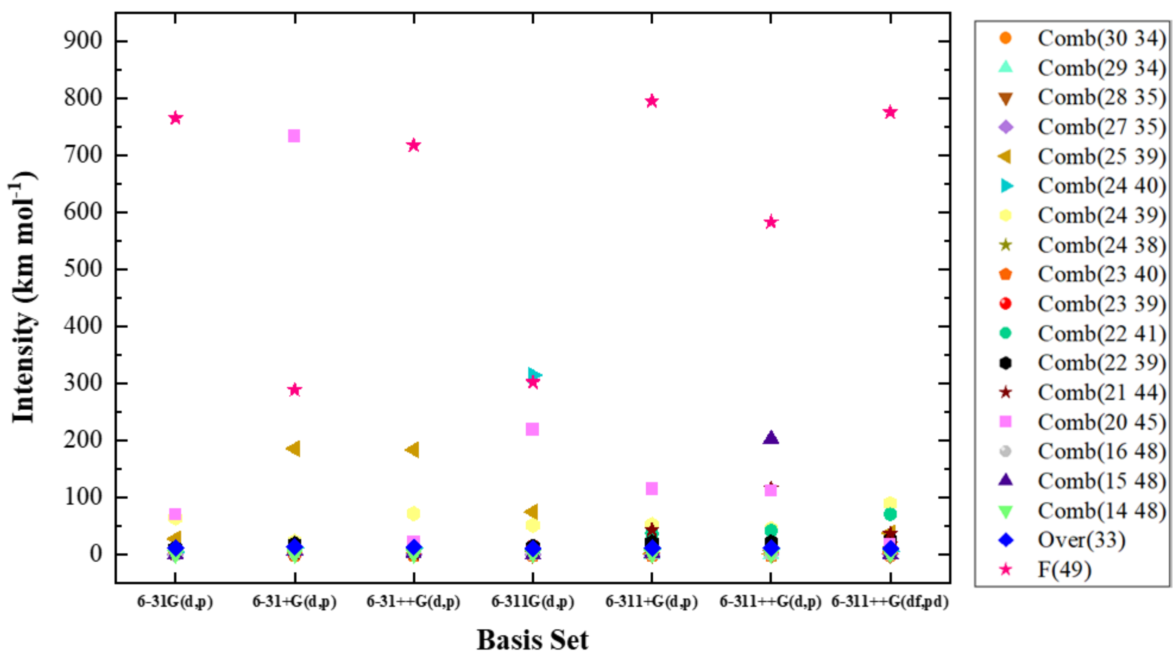

Figure 3.24 - Intensities of vibrational modes that can potentially couple with the azide asymmetric stretch of 4-azidoacetanilide for 6-31G(d,p), 6-31+G(d,p), 6-31++G(d,p), 6-311G(d,p), 6-311+G(d,p), 6-311++G(d,p), 6-311++G(df,pd) basis sets in THF.

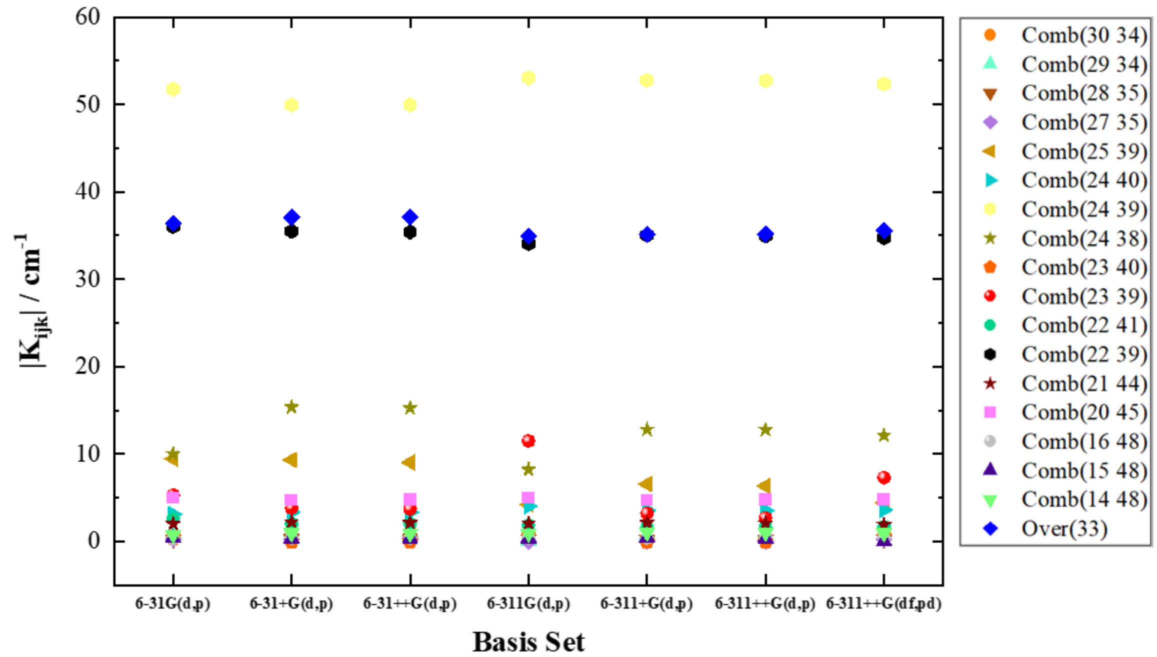

Figure 3.25 - Cubic force constants of vibrational modes that can potentially couple with the azide asymmetric stretch of 4-azidoacetanilide for 6-31G(d,p), 6-31+G(d,p), 6-31++G(d,p), 6-311G(d,p), 6-311+G(d,p), 6-311++G(d,p), 6-311++G(df,pd) basis sets in THF.

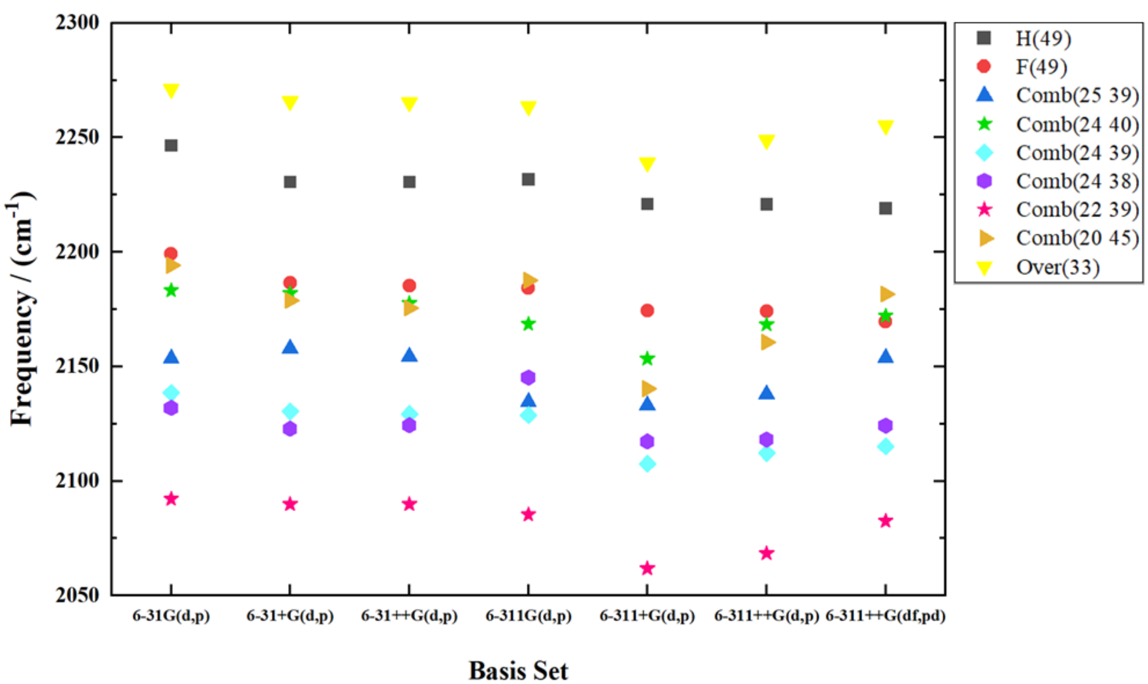

Figure 3.26 - Frequencies of vibrational modes that can potentially couple with the azide asymmetric stretch of 4-azidoacetanilide for 6-31G(d,p), 6-31+G(d,p), 6-31++G(d,p), 6-311G(d,p), 6-311+G(d,p), 6-311++G(d,p), 6-311++G(df,pd) basis sets in THF.

Figure 3.24 shows the high-intensity vibrational modes within the transparent window. As in NNDMA solvent, azide absorption profiles consist of high intensity for different vibrational modes in each basis set. For example, 6-31+G(d,p) and 6-311G(d,p) basis sets have high intensity for Comb(20 45) and Comb(24 40), separately. Furthermore, Com(22 41) and Comb(21 44) have high intensity for triple zeta basis sets which will be proven to be non FRs due to low cubic force constant (~2 cm^{-1}) and longer $\Delta\omega$' and $\Delta\omega$. Comb(15 48) has a very high intensity (203 km mol^{-1}) in 6-311++G(df,pd) basis set while in other basis sets it is zero or less than 10 km mol^{-1}. The cubic force constant of these high-intensity peaks were shown in Figure 3.25. Like in the NNDMA solvent, Comb(24 39), Comb(22 39), Comb(24 38), and Over(33) have the highest cubic force constants values. Moreover, Comb(25 39), Comb(23 39), Comb(24 40), Comb(20 45), Comb(22 41) and Comb(21 44) have cubic force constants of > 1 cm^{-1}. To ensure whether these are possible FRs, we need to consider peak position, see Figure 3.26. Although Comb(22 39) and Over(33) have high cubic force constant values, they are very far away from the azide asymmetric stretch (~100 and 80 cm^{-1}, respectively). Comb(24 39) has the highest cubic force constant, but it is $\Delta\omega$ as high as ~ 50 cm^{-1}. Therefore, Comb(24 39) shows TFR around 1, making it a strongly coupled FR, see Table 3.19. Also, Comb(20 45) is very close to the fundamental vibration and changes its peak position with different basis sets having a cubic force constant of ~5 cm^{-1}. Thus, Comb(20 45) is also considered as FR. Comb(25 39) is another possible FR due to a cubic force constant of ~12 cm^{-1} with ~25 cm^{-1} distance to the azide asymmetric stretch. In addition, Comb(24 38) and Comb(24 40) are weakly coupled to the azide asymmetric stretch due to large $\Delta\omega$ and low cubic force constant values separately. But Comb(23 39), Comb(22 41), and Comb(21 44) are not potentially coupled with the Fund(49). Figure 3.27 presents the azide absorption profile of 4-azidoacetanilide in two solvents with the 6-311+G(d,p).

Table 3.18 - TFR values for combination or overtone bands that can potentially couple with the azide asymmetric stretch in 4-azidoacetanilide in THF solvent.

Mode	6-31G(d,p)	6-31+G(d,p)	6-31++G(d,p)	6-311G(d,p)	6-311+G(d,p)	6-311++G(d,p)	6-311++G(df,pd)
Over(33)	0.498	0.456	0.448	0.427	0.355	0.454	0.410
Comb(30 34)	0.033	0.000	0.000	0.027	0.002	0.035	0.033
Comb(29 34)	0.179	0.199	0.924	0.000	0.010	0.027	0.000
Comb(28 35)	0.005	0.067	0.647	0.005	0.012	0.043	0.011
Comb(27 35)	0.004	0.006	0.005	0.000	0.000	0.000	0.007
Comb(25 39)	0.352	0.414	0.398	0.084	0.205	0.239	0.532
Comb(24 40)	0.107	5.544	0.919	4.431	0.269	0.452	0.233
Comb(24 39)	0.886	1.090	1.105	1.774	0.951	1.040	1.667
Comb(24 38)	0.121	0.259	0.267	0.161	0.173	0.192	0.315
Comb(23 40)	0.006	0.000	0.000	0.013	0.000	0.000	0.010
Comb(23 39)	0.059	0.053	0.048	0.114	0.037	0.034	0.074
Comb(22 41)	0.142	0.044	0.040	0.055	0.039	0.052	0.172
Comb(22 39)	0.356	0.351	0.328	0.323	0.276	0.286	0.469
Comb(21 44)	0.247	0.043	0.041	0.176	0.020	0.020	0.083
Comb(20 45)	2.057	1.119	0.607	0.419	0.224	0.517	0.311
Comb(16 48)	0.002	0.168	0.107	0.009	0.054	0.052	0.020
Comb(15 48)	0.007	0.027	0.031	0.006	0.007	0.058	0.000
Comb(14 48)	0.010	0.009	0.008	0.006	0.007	0.008	0.005

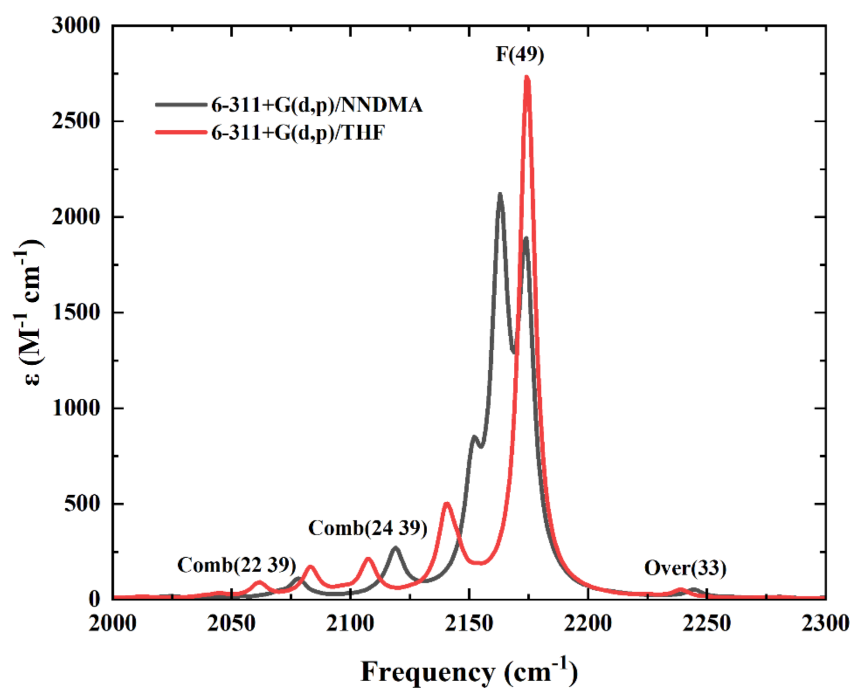

Figure 3.27 - Vibrational spectra of 4-azidoacetanilide in NNDMA and THF solvents with B3LYP/6-311+G(d,p) level of theory.

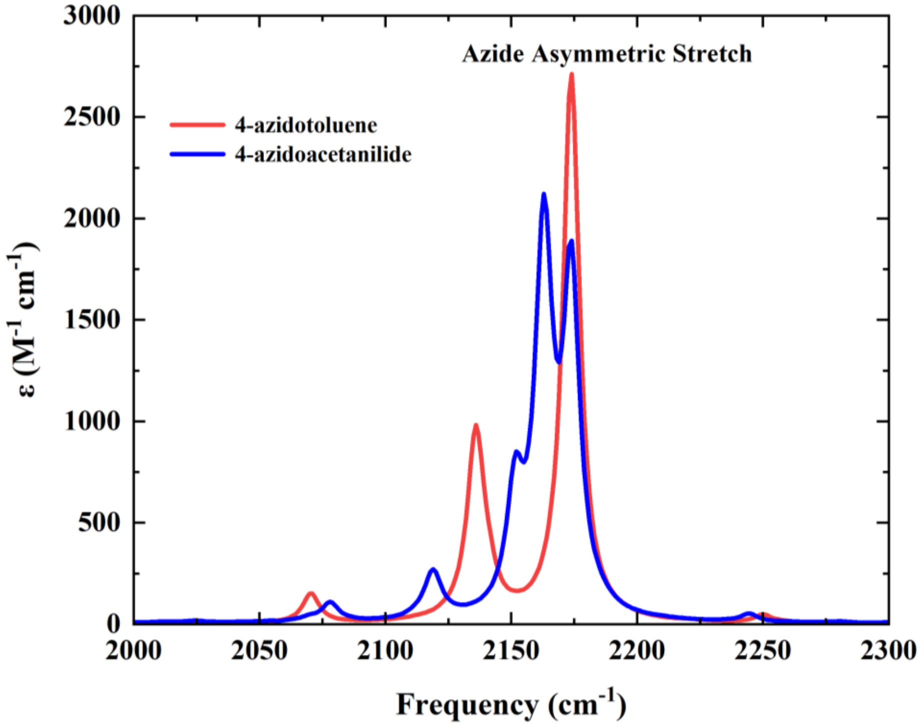

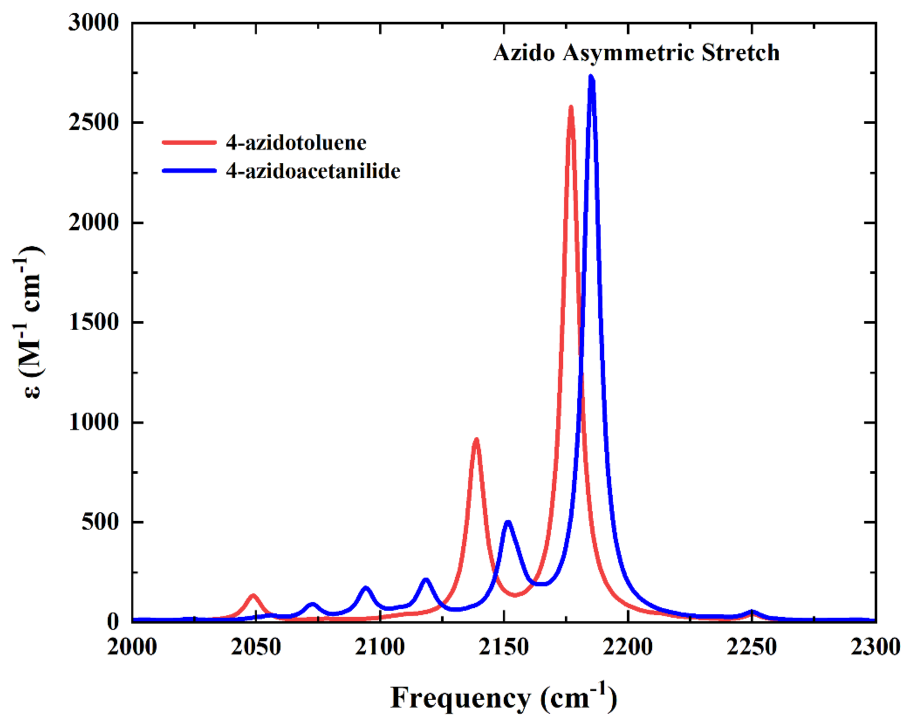

Figure 3.28 - Vibrational spectra of 4-azidotoluene and 4-azidoacetanilide in NNDMA (top) and THF (bottom) solvents with B3LYP/6-311+G(d,p) level of theory.

Neither the basis set effect nor solvent effect can be explained for 4-azidoacetanilide due to the different complex azide absorption profiles. Figure 3.28 shows both 4-azidotoluene and 4-azidoacetanilide with the 6-311+G(d,p) basis set for both solvents. This presents the intramolecular impact on the azide absorption profile. The extra peptide bond between the benzene ring and methyl group complicates the azide absorption profile.

3.4 Overview

This chapter provided a brief description of how theoretical calculations can provide insights into the vibrational coupling and FRs in two aryl-azide compounds. Studying intensities, cubic force constants, and peak positions provide insights into what vibrational modes generate the complex absorption profile of these VPs. Analyzing cubic force constants and TFR values provides a clear indication of FRs compared to intensity itself. The basis set effects, solvent effects, and intramolecular effects were explored. In general, many studies of VPs only use a single basis set for the calculations. However, our study showed that it is difficult to predict the appropriate basis set. Even a large basis set may produce erratic results. For example, the more diffused and polarized 6-311++G(df,pd) basis set provides complications to the azide absorption profile. Therefore, it is important to test several basis sets. In both molecules with two solvents, basis sets like 6-31G(d,p) and 6-311G(d,p) are also not suitable because they exhibit high intensities for combination bands that are not generating FRs. The 4-azidotoluene molecule has a simple azide absorption profile. In contrast, 4-azidoacetanilide has a very complex absorption profile. Hence, the use of theoretical calculation for these types of azide probes will be best before it uses in experimental spectroscopic analysis which will save much time and money. Because it will help us to figure out the complexity level of the azide absorption profile.

CHAPTER 4

IMPACT OF ROTATIONAL ISOMERS ON IR SPECTRA OF SMALL MOLECULES

4.1 Introduction

In the previous chapter, the azide absorption profile of two aryl-azide molecules was explored using intensities, cubic force constants, peak positions, and TFR values. Computational calculations facilitate figuring out the complexity level of the azide absorption profile easily compared to experimental techniques. It has shown how the azide absorption profile is complicated with para substitution of methyl to an acetamide group. It is also important to understand how different isomers of aryl-azides contribute to the azide absorption profile. A rotation around a single bond can form rotational isomers. For example, 4-acetanilide has two isomers due to the difference in the spatial arrangement of the acetamide group with the azide group. Since 4-azidoacetanilide has a complex azide absorption profile, we selected another aryl-azide compound, 4-azido-N-phenylmaleimide to study the impact of rotational isomers on azide absorption profile. Moreover, 4-azido-N-phenylmaleimide has been studied as a substrate for Old Yellow Enzyme.[80] In addition that this molecule has an extended conjugation and greater sensitivity to energy transfer through FRs with less spectral complexity than other aryl-azides. Thus, in this chapter, we give deep insight into the rotational isomers of 4-azido-N-phenylmaleimide. The geometry optimization and anharmonic frequency calculations were carried out using DFT with the same calculation method. For ease of understanding, the azide absorption profiles of the 4-azido-N-phenylmaleimide are described in each solvent separately. Figure 1 shows the two isomers of the 4-azido-N-phenylmaleimide. Calculated rotational energy barriers using the 6-311++G(d,p) basis set in NNDMA and THF solvents are 0.165 eV and 0.146 eV, respectively. Interestingly, these two isomers have similar energies with every basis set.

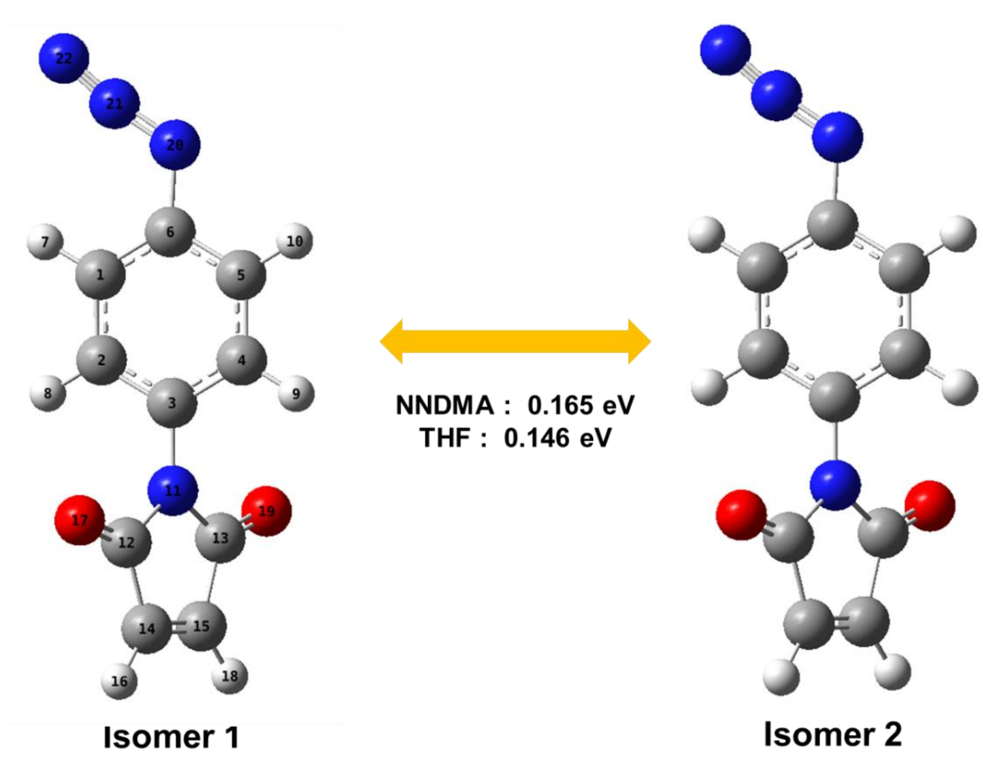

Figure 4.1 – Rotational isomers of 4-azido-N-phenylmaleimide with DFT/B3LYP/6-311++G(d,p) level of theory.

4.2 4-azido-N-phenylmaleimide

First, the structural parameters of optimized 4-azido-N-phenylmaleimide were studied to understand the basis sets effect and solvent effect on bond distances, bond angles, and dihedral angles. Table 4.1-4.3 shows structural parameters of isomer 1 for both solvents and seven basis sets. For ease of reading, atoms in isomer 1 are numbered in Figure 4.1, and bond distances, angles, and dihedral angles are labeled. In 4-azido-N-phenylmaleimide, the azide group and benzene ring are in the same plane (D9 ≈ 180^0). There's no significant change in the bond distances and bond angles. However, dihedral angles of the D8 and D9 are changing considerably with different basis sets and solvents due to the maleimide group bonded through a single bond, it can easily rotate, and this will change the strength of the bonds.

Table 4.1 – Bond distances (Å) of 4-azido-N-phenylmaleimide (Isomer 1) with seven basis sets: 6-31G(d,p), 6-31+G(d,p), 6-31++G(d,p), 6-311G(d,p), 6-311+G(d,p), 6-311++G(d,p), 6-311++G(df,pd) and two solvents, NNDMA (N) and THF (T).

Label	Definition	6-31G(d,p)		6-31+G(d,p)		6-31G++(d,p)		6-311G(d,p)		6-311+G(d,p)		6-311++G(d,p)		6-311++G(df,pd)	
		N	T	N	T	N	T	N	T	N	T	N	T	N	T
R1	R(1,2)	1.497	1.498	1.498	1.498	1.498	1.498	1.497	1.498	1.497	1.498	1.497	1.498	1.496	1.496
R2	R(2,3)	1.335	1.335	1.337	1.337	1.337	1.337	1.331	1.331	1.332	1.332	1.332	1.332	1.330	1.330
R3	R(3,4)	1.497	1.498	1.498	1.498	1.498	1.498	1.497	1.498	1.497	1.498	1.497	1.498	1.496	1.496
R4	R(4,5)	1.409	1.410	1.406	1.407	1.406	1.407	1.408	1.409	1.405	1.406	1.405	1.406	1.403	1.404
R5	R(1,5)	1.409	1.410	1.406	1.407	1.406	1.407	1.408	1.409	1.405	1.406	1.405	1.406	1.403	1.404
R6	R(2,6)	1.081	1.082	1.082	1.082	1.082	1.082	1.080	1.080	1.080	1.080	1.080	1.080	1.079	1.079
R7	R(3,7)	1.081	1.082	1.082	1.082	1.082	1.082	1.080	1.080	1.080	1.080	1.080	1.080	1.079	1.079
R8	R(5,8)	1.424	1.424	1.429	1.428	1.429	1.428	1.425	1.425	1.429	1.428	1.429	1.428	1.426	1.425
R9	R(8,9)	1.399	1.399	1.398	1.398	1.398	1.398	1.396	1.396	1.394	1.394	1.394	1.394	1.392	1.392
R10	R(8,10)	1.400	1.400	1.399	1.399	1.399	1.399	1.397	1.397	1.395	1.396	1.395	1.396	1.393	1.393
R11	R(9,11)	1.391	1.391	1.394	1.394	1.394	1.394	1.389	1.389	1.390	1.390	1.390	1.390	1.388	1.388
R12	R(9,12)	1.083	1.083	1.085	1.085	1.085	1.085	1.082	1.082	1.083	1.083	1.083	1.083	1.082	1.082
R13	R(10,13)	1.390	1.390	1.392	1.392	1.392	1.392	1.388	1.388	1.389	1.388	1.389	1.388	1.386	1.386
R14	R(10,14)	1.083	1.083	1.085	1.084	1.085	1.084	1.082	1.082	1.083	1.083	1.083	1.083	1.082	1.082
R15	R(13,15)	1.400	1.400	1.402	1.401	1.402	1.401	1.398	1.398	1.399	1.398	1.399	1.398	1.396	1.396
R16	R(11,15)	1.401	1.401	1.403	1.403	1.403	1.403	1.399	1.399	1.399	1.399	1.399	1.399	1.397	1.397
R17	R(11,16)	1.085	1.085	1.085	1.085	1.085	1.085	1.084	1.084	1.084	1.084	1.084	1.084	1.082	1.082
R18	R(13,17)	1.084	1.084	1.085	1.085	1.085	1.085	1.083	1.083	1.083	1.083	1.083	1.083	1.082	1.082
R19	R(15,18)	1.420	1.420	1.420	1.420	1.420	1.420	1.419	1.419	1.419	1.419	1.419	1.419	1.416	1.416
R20	R(18,19)	1.237	1.237	1.237	1.237	1.237	1.237	1.232	1.232	1.232	1.232	1.232	1.232	1.230	1.230
R21	R(19,20)	1.141	1.141	1.140	1.140	1.140	1.140	1.132	1.133	1.132	1.132	1.132	1.132	1.130	1.130
R22	R(4,21)	1.214	1.214	1.218	1.217	1.218	1.217	1.208	1.207	1.210	1.209	1.210	1.209	1.209	1.208
R23	R(1,22)	1.214	1.214	1.218	1.217	1.218	1.217	1.208	1.207	1.210	1.209	1.210	1.209	1.209	1.208

Table 4.2 – Bond angles of 4-azido-N-phenylmaleimide (Isomer 1) with different basis sets: 6-31G(d,p), 6-31+G(d,p), 6-31++G(d,p), 6-311G(d,p), 6-311+G(d,p), 6-311++G(d,p), 6-311++G(df,pd) and two solvents, NNDMA (N) and THF (T).

Label	Definition	6-31G(d,p)		6-31+G(d,p)		6-31G++(d,p)		6-311G(d,p)		6-311+G(d,p)		6-311++G(d,p)		6-311++G(df,pd)	
		N	T	N	T	N	T	N	T	N	T	N	T	N	T
A1	A(1,2,3)	108.88	108.89	108.89	108.75	108.72	108.75	108.95	108.97	108.84	108.88	108.84	108.87	108.85	108.88
A2	A(2,3,4)	108.87	108.89	108.89	108.75	108.72	108.75	108.94	108.96	108.84	108.87	108.84	108.87	108.84	108.88
A3	A(3,4,5)	106.29	106.45	106.45	106.42	106.46	106.42	106.16	106.15	106.26	106.23	106.26	106.23	106.25	106.22
A4	A(2,1,5)	106.29	106.29	106.29	106.42	106.45	106.42	106.16	106.15	106.26	106.23	106.26	106.23	106.25	106.22
A5	A(1,2,6)	121.83	121.76	121.76	121.89	121.98	121.89	121.73	121.64	121.92	121.82	121.91	121.83	121.96	121.86
A6	A(2,3,7)	129.29	129.35	129.35	129.35	129.29	129.35	129.32	129.39	129.24	129.30	129.24	129.29	129.19	129.25
A7	A(1,5,8)	125.16	125.17	125.17	125.17	125.17	125.17	125.11	125.11	125.10	125.10	125.09	125.11	125.12	125.10
A8	A(4,5,8)	125.17	125.17	125.17	125.18	125.18	125.18	125.10	125.12	125.10	125.10	125.10	125.10	125.08	125.11
A9	A(5,8,9)	119.98	120.00	120.00	119.87	119.85	119.88	120.03	120.04	119.89	119.92	119.89	119.92	119.92	119.94
A10	A(5,8,10)	120.08	120.09	120.09	119.95	119.93	119.96	120.10	120.12	119.97	119.99	119.97	119.99	119.98	120.01
A11	A(8,9,11)	120.17	120.17	120.17	120.12	120.12	120.13	120.21	120.21	120.15	120.16	120.15	120.15	120.17	120.17
A12	A(8,9,12)	120.00	120.01	120.01	120.00	119.96	120.00	120.03	120.05	119.94	119.99	119.94	119.99	119.94	119.98
A13	A(8,10,13)	119.98	119.99	119.99	119.94	119.92	119.95	120.05	120.07	119.98	120.01	119.98	120.01	120.01	120.04
A14	A(8,10,14)	120.03	120.04	120.04	120.02	120.00	120.02	120.04	120.05	119.96	119.99	119.96	119.99	119.95	119.98
A15	A(10,13,15)	120.10	120.13	120.13	119.93	119.90	119.93	120.12	120.14	119.92	119.95	119.92	119.95	119.95	119.97
A16	A(9,11,15)	119.85	119.63	119.63	119.67	119.62	119.67	119.89	119.93	119.67	119.72	119.67	119.72	119.71	119.75
A17	A(9,11,16)	119.59	119.57	119.57	119.52	119.55	119.53	119.47	119.46	119.50	119.48	119.50	119.48	119.50	119.48
A18	A(10,13,17)	120.60	120.61	120.61	120.67	120.65	120.67	120.64	120.65	120.66	120.67	120.66	120.67	120.65	120.66
A19	A(11,15,18)	124.06	123.94	123.94	123.94	123.94	123.94	124.00	123.99	123.87	123.88	123.87	123.87	123.82	123.83
A20	A(13,15,18)	115.99	116.03	116.03	115.90	115.85	115.90	116.15	116.20	116.01	116.06	116.01	116.06	116.13	116.16
A21	A(15,18,19)	118.62	118.57	118.57	118.71	118.75	118.70	118.88	118.82	119.00	118.95	118.99	118.95	119.28	119.18
A22	A(18,19,20)	172.41	172.50	172.50	172.48	172.42	172.49	172.70	172.76	172.55	172.62	172.55	172.63	172.49	172.52
A23	A(3,4,21)	127.92	127.83	127.83	127.87	127.94	127.87	127.99	127.90	128.05	127.98	128.05	127.97	128.06	127.99
A24	A(1,5,22)	125.78	125.88	125.88	125.71	125.61	125.71	125.85	125.95	125.69	125.79	125.69	125.80	125.69	125.78

Table 4.3 – Dihedral angles of 4-azido-N-phenylmaleimide (Isomer 1) with different basis sets: 6-31G(d,p), 6-31+G(d,p), 6-31++G(d,p), 6-311G(d,p), 6-311+G(d,p), 6-311++G(d,p), 6-311++G(df,pd) and two solvents, NNDMA (N) and THF (T).

Label	Definition	6-31G(d,p)		6-31+G(d,p)		6-31G++(d,p)		6-311G(d,p)		6-311+G(d,p)		6-311++G(d,p)		6-311++G(df,pd)	
		N	**T**	**N**	**T**	**N**	**T**	**N**	**T**	**N**	**T**	**N**	**T**	**N**	**T**
D1	D(1,2,3,4)	0.06	-0.01	0.28	0.25	0.26	0.23	0.07	0.03	0.25	0.25	0.26	0.27	0.24	0.25
D2	D(2,3,4,5)	-0.05	0.01	-0.20	-0.20	-0.18	-0.18	-0.05	-0.02	-0.20	-0.20	-0.20	-0.21	-0.17	-0.20
D3	D(3,2,1,5)	-0.04	0.01	-0.25	-0.22	-0.24	-0.21	-0.07	-0.02	-0.22	-0.22	-0.23	-0.23	-0.22	-0.21
D4	D(5,1,2,6)	-179.91	-179.89	179.97	180.00	179.98	-179.99	-179.90	-179.87	-179.99	-179.97	-180.00	-179.97	-179.99	-179.96
D5	D(1,2,3,7)	179.89	179.86	-179.96	-179.99	-179.97	-180.00	179.86	179.84	-179.99	179.98	-179.99	179.99	-180.00	179.97
D6	D(2,1,5,8)	-179.99	179.99	-179.87	-179.86	-179.89	-179.86	-179.92	180.00	-179.85	-179.87	-179.88	-179.84	-179.81	-179.89
D7	D(3,4,5,8)	-179.98	-180.00	-179.97	180.00	-179.96	180.00	179.96	-179.98	180.00	-179.98	-179.97	180.00	179.94	-179.97
D8	D(4,5,8,9)	-132.58	-134.47	-114.41	-118.89	-114.69	-119.19	-128.62	-130.96	-112.56	-118.16	-112.36	-118.00	-113.76	-118.39
D9	D(4,5,8,10)	47.44	45.55	65.62	61.13	65.34	60.82	51.41	49.09	67.47	61.84	67.67	62.01	66.26	61.62
D10	D(5,8,9,11)	-179.48	-179.50	-179.61	-179.62	-179.60	-179.63	-179.48	-179.44	-179.61	-179.64	-179.61	-179.64	-179.62	-179.64
D11	D(5,8,9,12)	0.30	0.11	0.42	0.32	0.43	0.32	0.34	0.22	0.48	0.39	0.50	0.40	0.44	0.39
D12	D(5,8,10,13)	-179.57	-179.56	-179.66	-179.58	-179.68	-179.59	-179.61	-179.66	-179.73	-179.62	-179.75	-179.63	-179.73	-179.64
D13	D(5,8,10,14)	0.18	0.02	0.37	0.32	0.37	0.33	0.23	0.01	0.41	0.38	0.40	0.39	0.42	0.37
D14	D(8,10,13,15)	-0.94	-0.93	-0.73	-0.79	-0.71	-0.77	-0.90	-0.89	-0.64	-0.72	-0.63	-0.71	-0.63	-0.70
D15	D(8,9,11,15)	-0.96	-0.94	-0.71	-0.80	-0.71	-0.79	-0.92	-0.90	-0.66	-0.75	-0.64	-0.75	-0.67	-0.74
D16	D(8,9,11,16)	179.71	179.67	179.76	179.72	179.75	179.71	179.68	179.64	179.76	179.75	179.77	179.76	179.74	179.76
D17	D(8,10,13,17)	179.73	179.69	179.77	179.69	179.77	179.69	179.74	179.72	179.82	179.74	179.83	179.74	179.83	179.75
D18	D(9,11,15,18)	-179.51	-179.52	-179.62	-179.54	-179.63	-179.54	-179.54	-179.58	-179.69	-179.57	-179.70	-179.58	-179.71	-179.59
D19	D(10,13,15,18)	-179.53	-179.54	-179.66	-179.67	-179.65	-179.68	-179.56	-179.53	-179.66	-179.69	-179.66	-179.69	-179.65	-179.69
D20	D(11,15,18,19)	-0.04	0.05	-0.24	0.03	-0.26	0.00	-0.08	-0.15	-0.19	0.08	-0.23	0.13	0.09	0.11
D21	D(13,15,18,19)	179.97	-179.94	179.79	-179.95	179.76	-179.99	179.94	179.87	179.82	-179.90	179.78	-179.87	-179.95	-179.89
D22	D(15,18,19,20)	-179.84	-179.90	179.96	-179.96	179.90	180.00	-179.87	-179.91	-179.83	-179.91	179.94	179.91	-179.94	179.94
D23	D(2,3,4,21)	179.80	179.88	179.52	179.53	179.55	179.56	179.80	179.90	179.53	179.54	179.53	179.52	179.53	179.55
D24	D(4,5,8,21)	0.16	0.13	0.30	0.26	0.29	0.25	0.11	0.09	0.26	0.27	0.29	0.25	0.24	0.28
D25	D(4,5,1,22)	-179.84	-179.97	-179.62	-179.69	-179.62	-179.71	-179.83	-179.94	-179.66	-179.69	-179.65	-179.69	-179.66	-179.68

Table 4.4 shows dihedral angle D8 in two isomers of 4-azido-N-phenylmaleimide. Isomer 1 has a -D8 while Isomer 2 has a +D8. But both D8 are similar for each solvent. Here, we can see both basis set and solvent impact on D8. The D8 has the order of 6-31G(d,p) > 6-311G(d,p) > 6-31++G(d,p)/6-31+G(d,p) > 6-311++(df,pd) > 6-311+G(d,p)/6-311++G(d,p) for both solvents. This means the angle between the planes increases with the polarization and diffusion character. However, there are no significant changes in D8 for singly and doubly diffused basis sets. Hence, calculations can be carried out using singly diffused basis sets to save the computational cost. However, the azide absorption profile can be significantly different for both 6-31G(d,p) and 6-311G(d,p) basis sets due to ~20^0 deviation from other basis sets.

Table 4.4 – Dihedral angle (D8) of rotational isomers of 4-azido-N-phenylmaleimide with different basis sets and two solvents, NNDMA and THF.

Basis set	Isomer 1		Isomer 2	
	NNDMA	THF	NNDMA	THF
6-31G(d,p)	-132.58	-134.47	132.54	134.59
6-31+G(d,p)	-114.41	-118.89	114.64	118.91
6-31++G(d,p)	-114.69	-119.19	114.71	119.15
6-311G(d,p)	-128.62	-130.96	128.58	130.91
6-311+G(d,p)	-112.56	-118.16	112.58	118.11
6-311++G(d,p)	-112.36	-118.00	112.41	118.05
6-311++G(df,pd)	-113.76	-118.39	113.80	118.77

Then, the DFT calculated frontier molecular orbitals HOMO and LUMO of 4-azido-N-phenylmaleimide isomer 1 are illustrated in Figure 4.2. Both HOMO and LUMO orbitals for isomer 1 and isomer 2 are similar. The HOMO orbital is distributed in the region perpendicular to the bond axis only avoiding hydrogen atoms and there’s less localization in the maleimide group. Moreover, this electron distribution within the maleimide group is different as in the same pattern in dihedral angle D8. Here, we can see how the dihedral angle changes in the maleimide group describe the changes in the HOMO orbital. The LUMO orbital is localized in the region perpendicular to the bond axis of the maleimide group and is similar for all basis sets. Tables 4.5 and 4.6 show that the energies and HOMO-LUMO gaps are similar in 6-31+G(d,p)/6-31++G(d,p) and 6-311+G(d,p)/6-311++G(d,p) pairs separately. Moreover, both isomers have a similar HOMO-LUMO gap but are different for two solvents for each basis set. The energies of the molecule decrease (more negative) from 6-31G(d,p) to 6-311++G(df,pd) and ~0.06 eV high in NNDMA solvent compared to THF solvent for each basis set.

Table 4.5 – The energies and HOMO-LUMO gap for both isomers of 4-azido-N-phenylmaleimide in NNDMA solvent.

Basis set	Energy (au)	Isomer 1			Isomer 2		
		HOMO (eV)	LUMO (eV)	HL gap (eV)	HOMO (eV)	LUMO (eV)	HL gap (eV)
6-31G(d,p)	-754.087785	-6.20	-2.73	3.46	-6.20	-2.73	3.46
6-31+G(d,p)	-754.118199	-6.61	-3.08	3.53	-6.61	-3.08	3.53
6-31++G(d,p)	-754.118284	-6.61	-3.08	3.53	-6.61	-3.08	3.53
6-311G(d,p)	-754.268672	-6.42	-2.88	3.53	-6.42	-2.88	3.53
6-311+G(d,p)	-754.284428	-6.67	-3.06	3.61	-6.67	-3.06	3.61
6-311++G(d,p)	-754.284547	-6.67	-3.06	3.61	-6.67	-3.06	3.61
6-311++G(df,pd)	-754.315119	-6.66	-3.05	3.61	-6.66	-3.05	3.61

Table 4.6 – The energies and HOMO-LUMO gap for both isomers of 4-azido-N-phenylmaleimide in THF solvent.

Basis set	Energy (au)	Isomer 1			Isomer 2		
		HOMO (eV)	LUMO (eV)	HL gap (eV)	HOMO (eV)	LUMO (eV)	HL gap (eV)
6-31G(d,p)	-754.085970	-6.17	-2.76	3.42	-6.17	-2.76	3.42
6-31+G(d,p)	-754.115789	-6.57	-3.10	3.48	-6.57	-3.10	3.48
6-31++G(d,p)	-754.115877	-6.57	-3.10	3.47	-6.57	-3.10	3.47
6-311G(d,p)	-754.266697	-6.39	-2.90	3.49	-6.39	-2.90	3.49
6-311+G(d,p)	-754.282019	-6.62	-3.08	3.54	-6.62	-3.08	3.54
6-311++G(d,p)	-754.282137	-6.62	-3.08	3.54	-6.62	-3.08	3.54
6-311++G(df,pd)	-754.312719	-6.62	-3.07	3.55	-6.62	-3.07	3.55

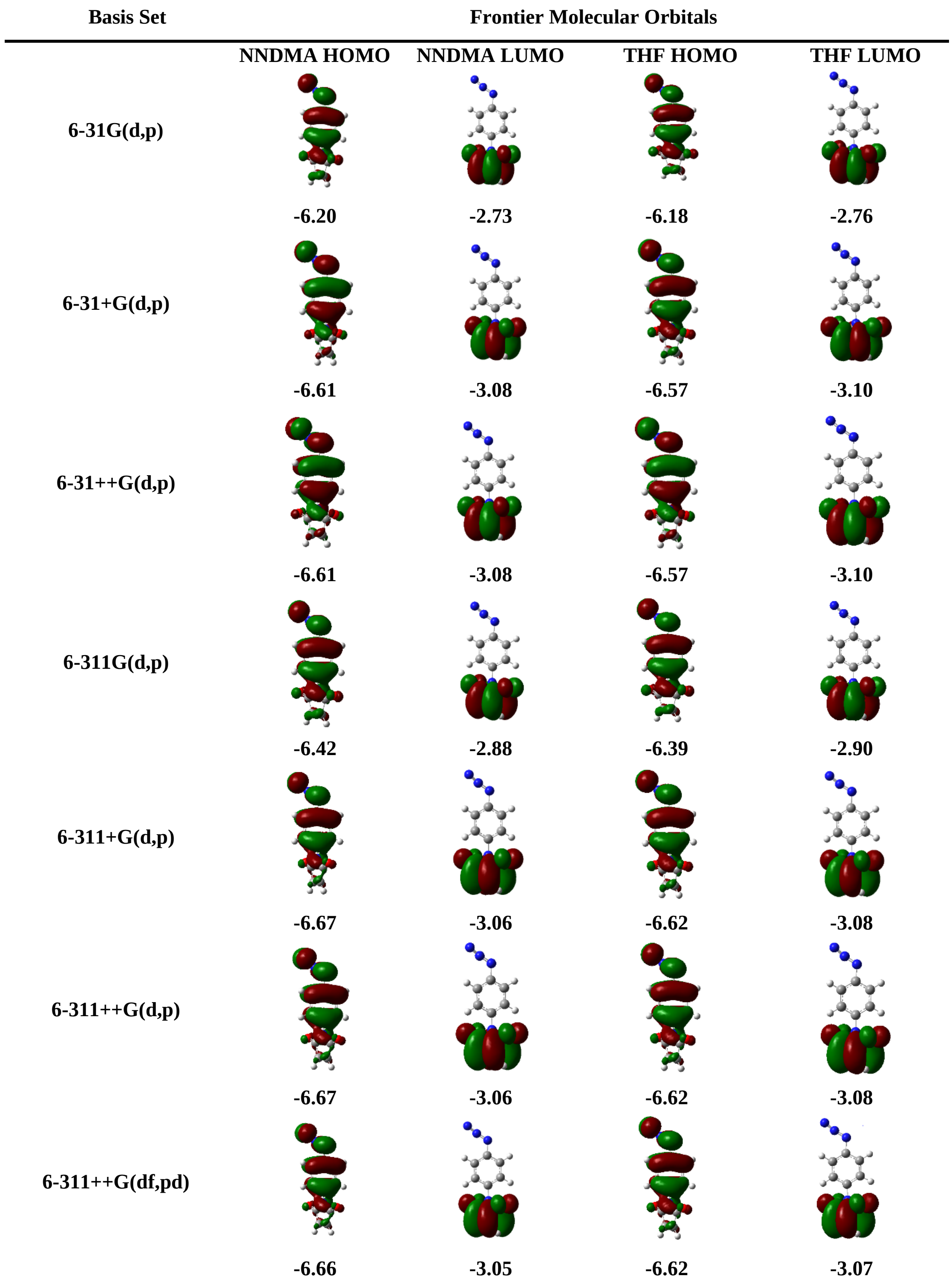

Figure 4.2 - Spatial distributions of HOMO and LUMO frontier molecular orbitals of 4-azido-N-phenylmaleimide in NNDMA and THF solvents for seven basis sets Orbital energy eigenvalues (in eV) are shown below each molecular orbital. The red and green color lobes correspond to the two different phases of the orbital wave function with positive and negative signs, respectively.

4.2.1 4-azido-N-phenylmaleimide in NNDMA

Combined geometry optimization and anharmonic frequency calculations of two rotamers of 4-azido-N-phenylmaleimide were carried out in NNDMA solvent using seven different basis sets: 6-31G(d,p), 6-31+G(d,p), 6-31++G(d,p), 6-311G(d,p), 6-311+G(d,p), 6-311++G(d,p), and 6-311++G(df,pd). The 4-azido-N-phenylmaleimide has 22 atoms. Thus, 60 fundamental vibrational modes are present. For ease of reading, first I discuss isomer 1 and then compare the results of isomer 2 with isomer 1. High-intensity modes with molar absorptivity coefficients over 1000 M^{-1} cm^{-1} for isomer 1 were shown in Table 4.7. The carbonyl stretch (mode 52), and azide asymmetric stretch (mode 54) have the highest intensities followed by modes 48, 45, and 46. Figure 4.3 shows the harmonic and anharmonic spectra with 6-311+G(d,p) basis set, and Appendix E and Appendix F provide spectroscopic details of combination and overtone bands occurring within ±135 cm^{-1} of the azide asymmetric stretch for seven basis sets for isomer 1 and isomer 2, respectively. The anharmonic frequency calculation with 6-311++G(df,pd) basis set for isomer 2 is not completed and suppose to finish in the future.

Table 4.7 - Normal Modes of 4-azido-N-phenylmaleimide (isomer 1) in NNDMA using B3LYP/6-311+G(d,p) basis set.

Mode	Vibration	$\upsilon_{(harmonic)}$ / cm^{-1}	$\upsilon_{(anharmonic)}$ / cm^{-1}	$I_{(harmonic)}$ / km mol^{-1}	$I_{(anharmonic)}$ / km mol^{-1}
54	N_3 asymmetric stretch	2221.1	2177.5	1752.8	788.8
52	C=O stretch	1731.7	1699.8	1582.4	923.0
48	4-H sp^2 C-H in plane + Benzene ring vibrations	1533.9	1504.3	393.1	180.3
46	N_3 Sym stretch + C-N stretch + both ring vibrations + all C-H in-plane	1404.0	1370.0	321.4	137.9
45	N_3 Sym stretch + C-N stretch + both ring vibrations + all C-H in-plane	1359.5	1322.3	565.3	114.8

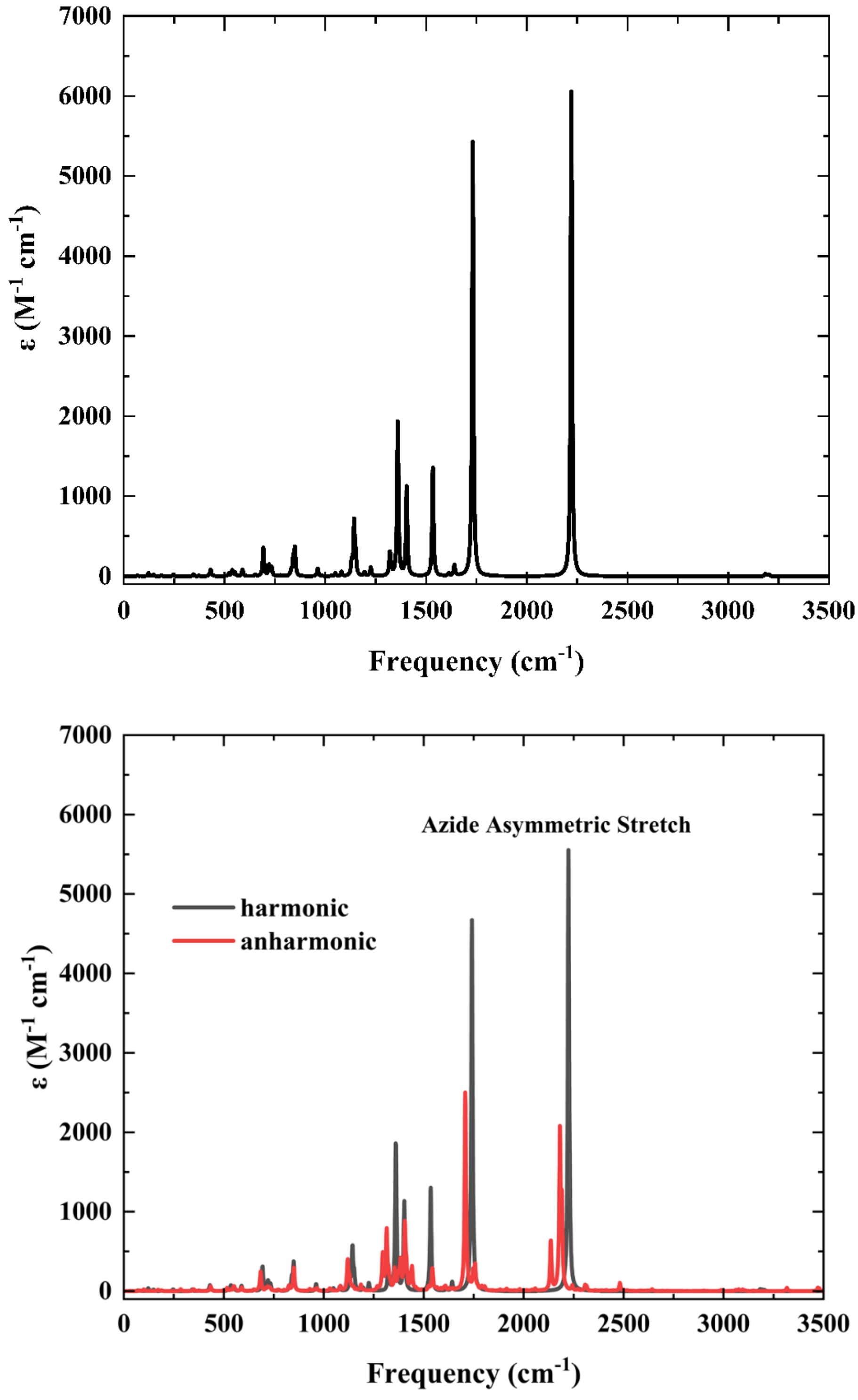

Figure 4.3 – IR spectra of harmonic (top), both anharmonic and harmonic (bottom) of 4-azido-N-phenylmaleimide (isomer 1) in NNDMA using B3LYP/6-311+G(d,p) level in Gaussian-16.

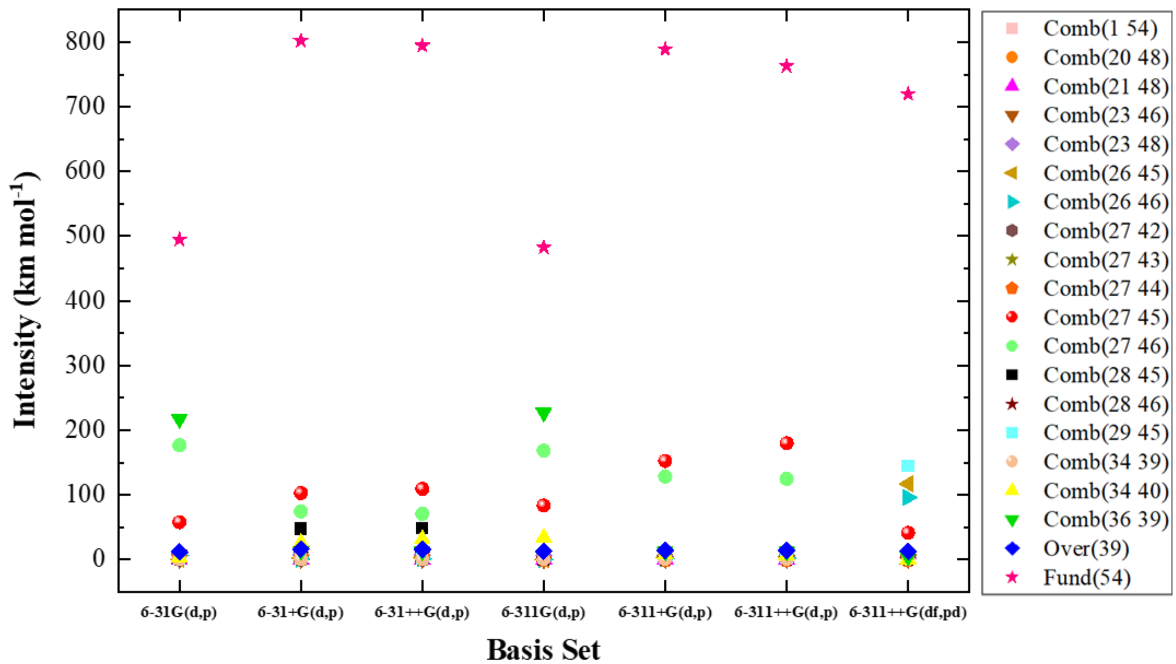

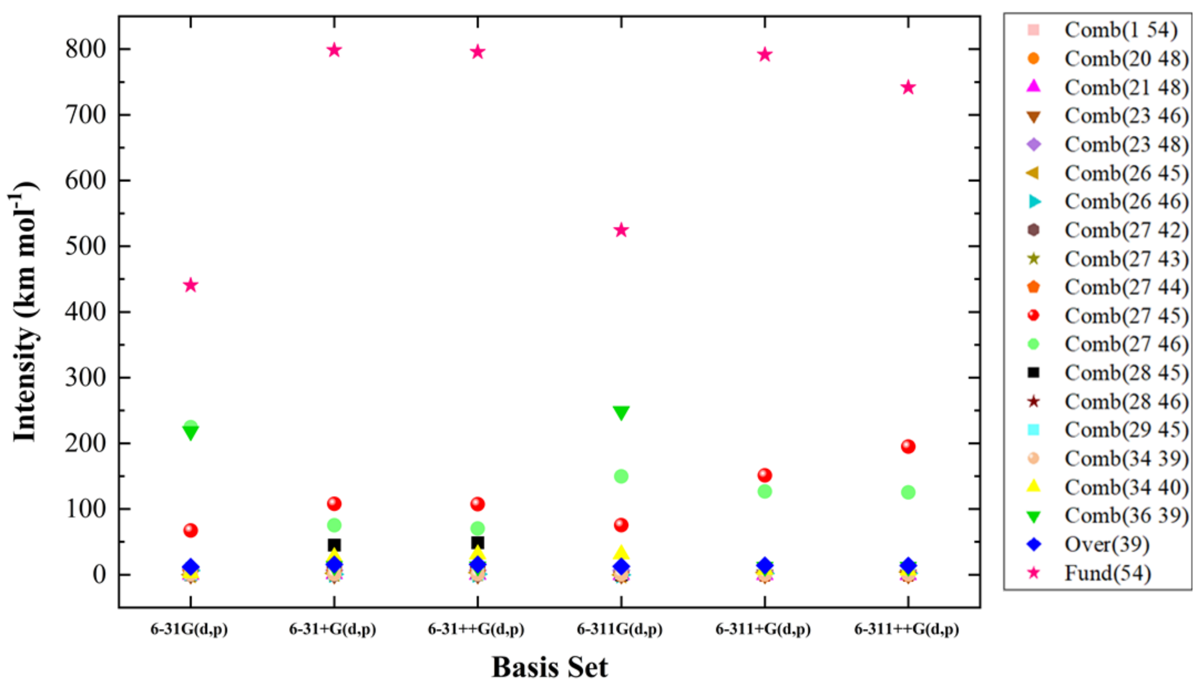

Figure 4.4 – Intensities of vibrational modes that can potentially couple with the azide asymmetric stretch of 4-azido-N-phenylmaleimide for 6-31G(d,p), 6-31+G(d,p), 6-31++G(d,p), 6-311G(d,p), 6-311+G(d,p), 6-311++G(d,p), 6-311++G(df,pd) basis sets in NNDMA of isomer 1 (top) and isomer 2 (bottom).

Figure 4.4 presents high-intensity vibrational modes within the transparent window, as well as some lower intensity peaks, which were included due to their high cubic force constant (> 1 cm^{-1}) for all basis sets. The highest intensity peak (~800 km mol^{-1}) corresponds to the azide asymmetric stretch Fund(54) and other combination bands as are a result of multiple vibrational transitions that possibly give rise to the FRs. As in 4-azidotoluene, 6-31G(d,p) and 6-311G(d,p) basis sets have ~300 km mol^{-1} dropped intensity for Fund(54). Moreover, Comb(36 39) has high intensities ~220 km mol^{-1} for 6-31G(d,p) and 6-311G(d,p) while for other basis sets, it is ~12 km mol^{-1} except 4 km mol^{-1} for more polarized 6-311++G(df,pd) basis set. In addition, Comb(27 46) and Comb(27 45) have the next highest intensity peaks and show different patterns in these basis sets. In 6-31G(d,p) and 6-311G(d,p), the Comb(27 46) has an intensity of ~170 km mol^{-1}, and it is higher than the intensity of Comb(27 45). But for other basis sets, Com(27 45) has a higher intensity than Comb(27 46). Again, 6-311++G(df,pd) basis set have comparatively lower intensities for Comb(27 45) and Comb(27 46). But like in the 4-azidotoluene, 6-311++G(df,pd) basis set shows relatively higher intensity for three combination bands: Comb(26 45), Comb(26 46), and Comb(29 45) while an intensity of ~2 km mol^{-1} for other basis sets.

Furthermore, Comb(28 45) and Comb(34 40) have high intensities in 6-31+G(d,p), 6-31++G(d,p) and 6-311G(d,p) basis sets while lower intensity in other basis sets. The overtone Over(39), which is very far away in frequency from Fund(54) has an intensity of ~14 km mol^{-1} for all basis sets. All other vibrational modes have an intensity less than 12 km mol^{-1} for every basis set. Interestingly, both isomers have a similar pattern in intensity. Figures in 4.5 show how small deviations in intensity values change the shape of the azide absorption profiles of 6-31G(d,p), 6-311G(d,p), and 6-311++G(df,pd) basis sets.

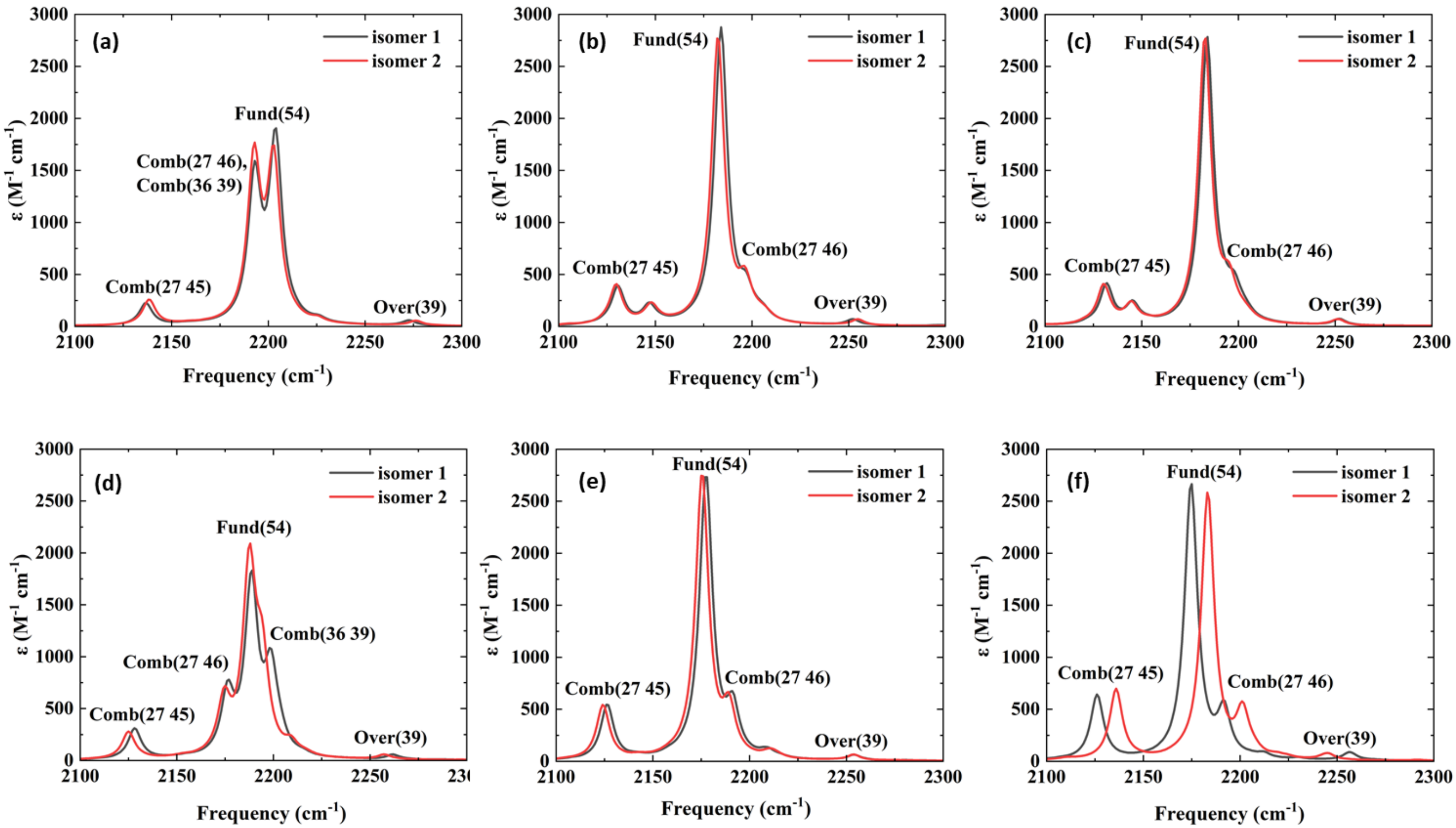

Figure 4.5 – Vibrational spectra of rotamers of 4-azido-N-phenylmaleimide in NNDMA solvent with seven basis sets: (a) 6-31G(d,p), (b) 6-31+G(d,p), (c) 6-31++G(d,p), (d) 6-311G(d,p), (e) 6-311+G(d,p), and (f) 6-311++G(d,p).

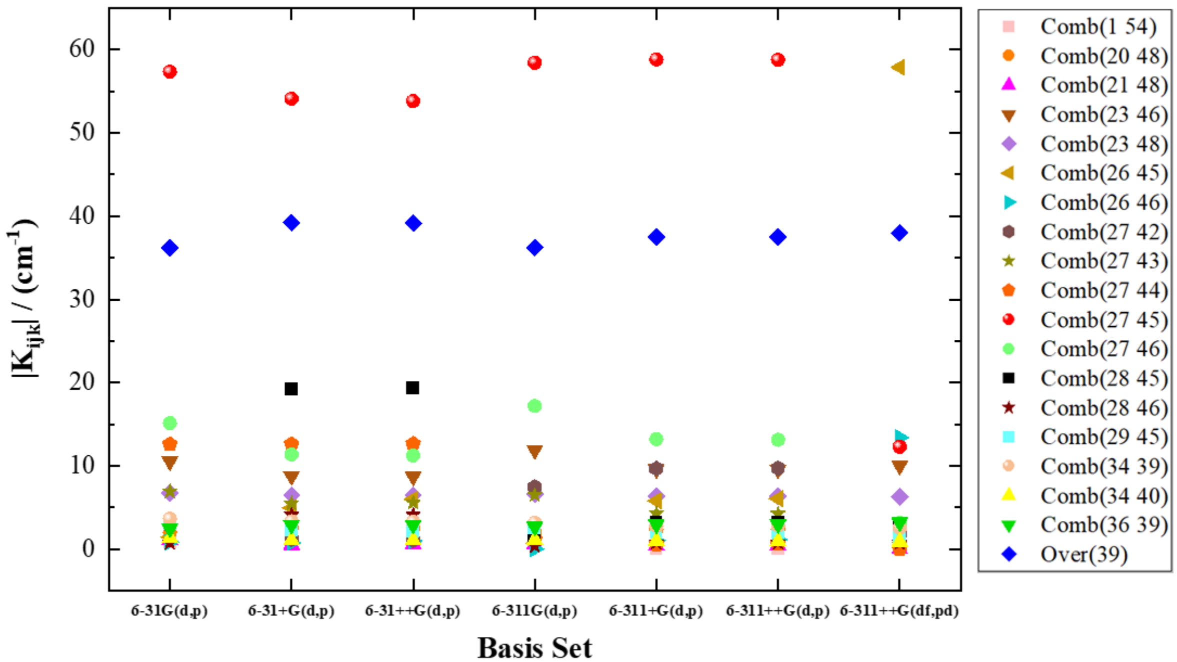

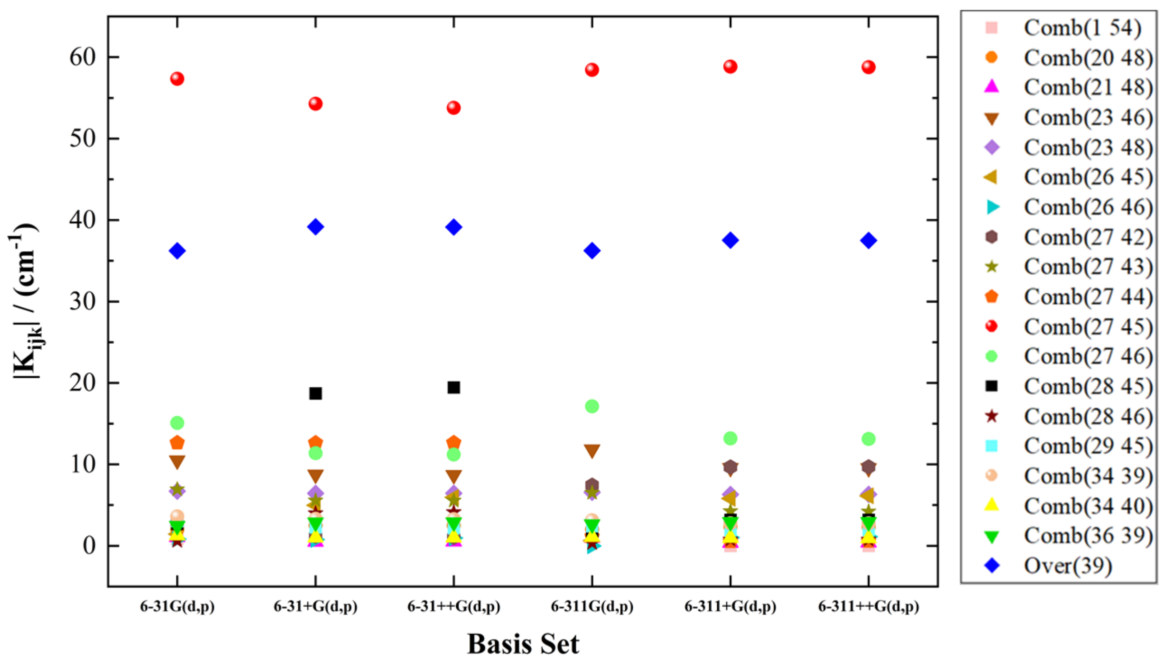

Figure 4.6 – Cubic force constants of vibrational modes that can potentially couple with the azide asymmetric stretch of 4-azido-N-phenylmaleimide for 6-31G(d,p), 6-31+G(d,p), 6-31++G(d,p), 6-311G(d,p), 6-311+G(d,p), 6-311++G(d,p), 6-311++G(df,pd) basis sets in NNDMA of isomer 1 (top) and isomer 2 (bottom).

Within the transparent window, the most likely vibrational modes that can couple with the azide asymmetric stretch would result from Comb(27 45) and Over(39), see Figure 4.6. Comb (27 45) has a cubic force constant over 50 cm^{-1} with every basis set except 6-311++G(df,pd) (12 cm^{-1}) basis set while Over(39) has the next highest cubic force constant (~37 cm^{-1}) for all basis sets. Like in the 4-azidotoluene, the more polarized 6-311++G(df,pd) basis set introduces new combination bands that can couple with azide asymmetric stretch with higher cubic force constants and intensities. For instance, Comb(26 45) has the highest cubic force constant (58 cm^{-1}) using the 6-311++G(df,pd) basis set while it is ~6 cm^{-1} for other basis sets. Also, Comb(26 46) has a cubic force constant of 13 cm^{-1} for 6-311++G(df,pd), and ~1 cm^{-1} for other basis sets. Hence, these results show that 6-311++G(df,pd) basis set is not ideal for understanding azide absorption profiles.

Although we recommend the 6-31+G(d,p) basis set using the 4-azidotoluene for predicting vibrational coupling, 4-azido-N-phenylmaleimide calculations show both 6-31+G(d,p) and 6-31++G(d,p) introduce new combination bands that can couple with azide asymmetric stretch which are absent in other basis sets. For example, Comb(28 45) has a cubic force constant of 19 cm^{-1} for 6-31+G(d,p) and 6-31++G(d,p) and ~3 cm^{-1} for other basis sets, respectively.

Then, Comb(27 46) has a cubic force constant over 10 cm^{-1}. The intensity of Comb(27 46) is higher in 6-31G(d,p) and 6-311G(d,p) basis sets when compared to other basis sets due to increased force constants. Even though Comb(27 44) has a 12 cm^{-1} force constant for double zeta basis sets, it is far away in frequency from Fund(54) to make an FR. The rest of the vibrational modes have a cubic force constant lower than 10 cm^{-1}, but these modes can couple with azide asymmetric stretch if they are very near to the azide asymmetric stretch.

Figure 4.6 shows that both isomers have similar cubic force constant values and patterns. TFR values of each mode in isomer 1 were calculated and shown in Table 4.8 to figure out whether these combinations of bands or overtone can be resonant with azide asymmetric stretch. TFR values increase when the magnitude of the cubic force constant increases and/or when resonance shift $\Delta\omega$ decreases. Generally, if TFR ≥ 1, $K_{ijk} > 10$ cm^{-1}, and $\Delta\omega < 10$ cm^{-1}, then the overall coupling strength will be significant enough to result in an accidental FR between the fundamental band and the combinations bands/overtone. For instance, both comb (27 45) and Over (39) are very far away in the frequency from the fundamental vibration, but cubic force constants are so high that can result in accidental FRs.

The 6-311G++(df,pd) basis set shows an unexpected high TFR value for Comb(26 46) and Comb(26 45) correspond to very low resonance shift (~0.01 cm^{-1}) and high cubic force constant, respectively. Moreover, 6-311G(d,p) show TFR of ~0.9 for both Comb(29 46) and Comb(1 54) because of ~1 cm^{-1} resonance shift. If we ignore the 6-311G++(df,pd) basis set, Comb(27 45) and Comb(27 46) have TFR values > 1 making them strongly coupled FRs with azide asymmetric stretch.

In addition, Over(39) has a TFR of ~ 0.5 making it a weakly coupled FR. The Comb(28 45) has TFR value of ~0.58 for both 6-31+G(d,p) and 6-31++G(d,p) basis sets, and ~0.37 for 6-311++G(d,p) basis set. Thus, Comb(28 45) is barely noticeable in the IR spectrum of the 6-311++G(d,p) basis set. However, Comb(29 45) has a TFR of ~0.5 for both 6-311+G(d,p) and 6-311++G(d,p) basis sets due to low resonance shift values, which is less than 0.3 for other basis sets. Comb(29 45) has a low intensity and cubic force constant. Therefore, we can ignore Comb(29 45).

From all these observations, all basis sets have questionable vibrational modes for identifying combination bands or overtones that can couple with the azide asymmetric stretch if we consider TFR < 0.3. Thus, it is crucial to understand what are the most possible combination or overtones that produce FRs with azide asymmetric stretch from an IR spectrum. In every basis set calculation, Comb(27 45), Comb(27 46) and Over(39) have consistent TFR values expect for 6-311++G(df,pd) basis set. If we consider 6-31+G(d,p) and 6-31++G(d,p) basis sets, Comb(28 45) is also a weakly coupled FR because of the high cubic force constant. Hence, the 6-311+G(d,p) basis set would be the best basis set for understanding vibrational coupling and FRs in 4-azido-N-phenylmaleimide.

Table 4.8 - TFR values for combination or overtone bands that can potentially couple with the azide asymmetric stretch in 4-azido-N-phenylmaleimide (isomer 1) in NNDMA solvent

Mode	6-31G(d,p)	6-31+G(d,p)	6-31++G(d,p)	6-311G(d,p)	6-311+G(d,p)	6-311++G(d,p)	6-311++G(df,pd)
Comb(1 54)	0.049	0.146	0.043	0.857	0.000	0.000	0.140
Comb(20 48)	0.045	0.062	0.062	0.045	0.094	0.239	0.064
Comb(21 48)	0.025	0.013	0.013	0.015	0.017	0.091	0.000
Comb(23 46)	0.092	0.084	0.087	0.098	0.099	0.105	0.095
Comb(23 48)	0.245	0.254	0.277	0.235	0.167	0.115	0.174
Comb(26 45)	0.026	0.072	0.065	0.008	0.170	0.130	1.582
Comb(26 46)	0.090	0.032	0.022	0.000	0.074	0.011	892.798
Comb(27 42)	0.030	0.022	0.020	0.097	0.142	0.148	0.022
Comb(27 43)	0.102	0.084	0.087	0.094	0.098	0.099	0.011
Comb(27 44)	0.175	0.218	0.201	0.022	0.011	0.167	0.000
Comb(27 45)	1.010	1.371	1.381	1.181	1.721	1.567	0.247
Comb(27 46)	1.375	2.210	1.132	1.126	0.978	0.779	0.240
Comb(28 45)	0.064	0.590	0.572	0.065	0.163	0.365	0.757
Comb(28 46)	0.510	0.338	0.271	0.023	0.027	0.017	0.017
Comb(29 45)	0.086	0.092	0.080	0.069	0.496	0.514	0.127
Comb(34 39)	0.075	0.073	0.074	0.090	0.087	0.261	0.074
Comb(34 40)	0.120	0.272	0.068	0.070	0.032	0.009	0.127
Comb(36 39)	0.290	0.134	0.150	0.253	0.090	0.077	0.085
Over(39)	0.511	0.555	0.565	0.480	0.476	0.440	0.497

Table 4.9 - TFR values for combination or overtone bands that can potentially couple with the azide asymmetric stretch in 4-azido-N-phenylmaleimide (isomer 2) in NNDMA solvent

Mode	6-31G(d,p)	6-31+G(d,p)	6-31++G(d,p)	6-311G(d,p)	6-311+G(d,p)	6-311++G(d,p)
Comb(1 54)	0.055	0.043	0.034	0.077	0.000	0.000
Comb(20 48)	0.045	0.067	0.064	0.048	0.102	0.125
Comb(21 48)	0.026	0.015	0.014	0.028	0.019	0.034
Comb(23 46)	0.086	0.098	0.087	0.113	0.101	0.102
Comb(23 48)	0.321	0.237	0.263	0.224	0.161	0.149
Comb(26 45)	0.028	0.062	0.065	0.008	0.193	0.053
Comb(26 46)	0.085	0.037	0.022	0.000	0.060	0.006
Comb(27 42)	0.030	0.020	0.019	0.094	0.143	0.127
Comb(27 43)	0.107	0.108	0.087	0.093	0.097	0.086
Comb(27 44)	0.181	0.215	0.199	0.023	0.012	0.026
Comb(27 45)	1.107	1.384	1.376	1.113	1.756	1.157
Comb(27 46)	1.495	0.545	1.245	34.244	0.962	1.182
Comb(28 45)	0.058	0.612	0.590	0.142	0.189	0.142
Comb(28 46)	0.146	0.136	0.273	0.007	0.025	0.019
Comb(29 45)	0.097	0.097	0.084	0.071	0.920	0.045
Comb(34 39)	0.080	0.092	0.077	0.097	0.091	0.056
Comb(34 40)	0.112	0.052	0.024	0.044	0.030	0.012
Comb(36 39)	0.372	0.107	0.035	0.413	0.085	0.121
Over(39)	0.482	0.481	0.550	0.503	0.464	0.572

The TFR values for isomer 2 and isomer 1 can be different due to the changes in the resonance shifts. However, both remain the same conclusions. Figure 4.7 represents frequencies for combination or overtone bands that can potentially couple with the azide asymmetric stretch. The peak position of anharmonic azide asymmetric stretch Fund(54) is always lower than harmonic vibrational mode Har(54) due to its anharmonicity. Besides, Comb(27 45) and Over(39) are always ~50 cm^{-1} and ~70 cm^{-1} far in frequency from the Fund(54), respectively. However, the peak position of Comb(27 46) varies with the basis set relative to the Fund(54) because it is very near to the Fund(54). It locates at the right for 6-31G(d,p), and 6-311G(d,p); the left for 6-31+G(d,p), 6-31++G(d,p), 6-311+G(d,p), and 6-311++G(d,p); and on for 6-311++G(df,pd) to the Fund(54). Both isomers have a similar frequency pattern for all modes. But 6-311++G(d,p) basis set has a narrow absorption profile for isomer 2 compared to isomer 1.

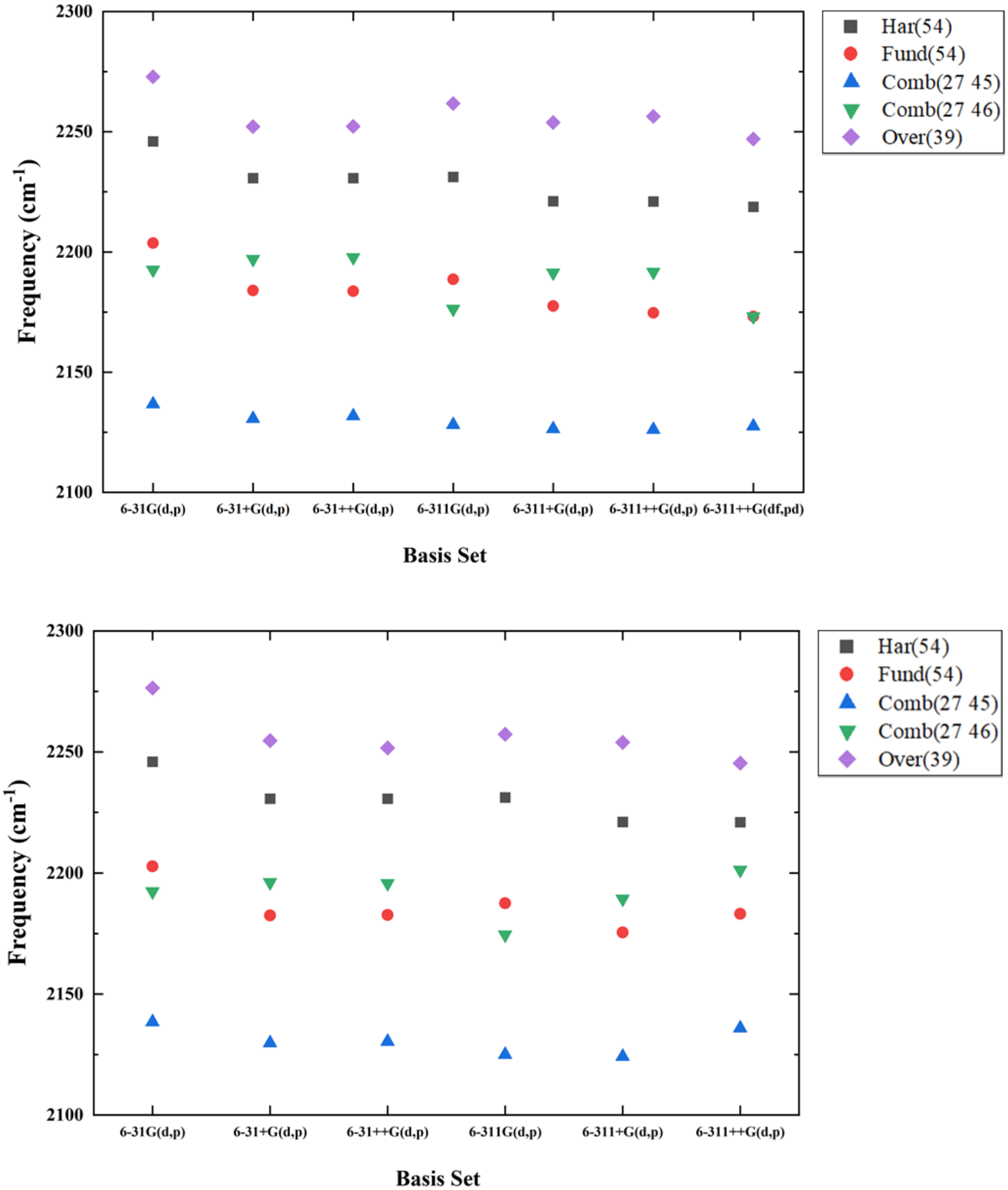

Figure 4.7 – Frequencies of vibrational modes that can potentially couple with the azide asymmetric stretch of 4-azido-N-phenylmaleimide for 6-31G(d,p), 6-31+G(d,p), 6-31++G(d,p), 6-311G(d,p), 6-311+G(d,p), 6-311++G(d,p), 6-311++G(df,pd) basis sets in NNDMA of isomer 1 (top) and isomer 2 (bottom).

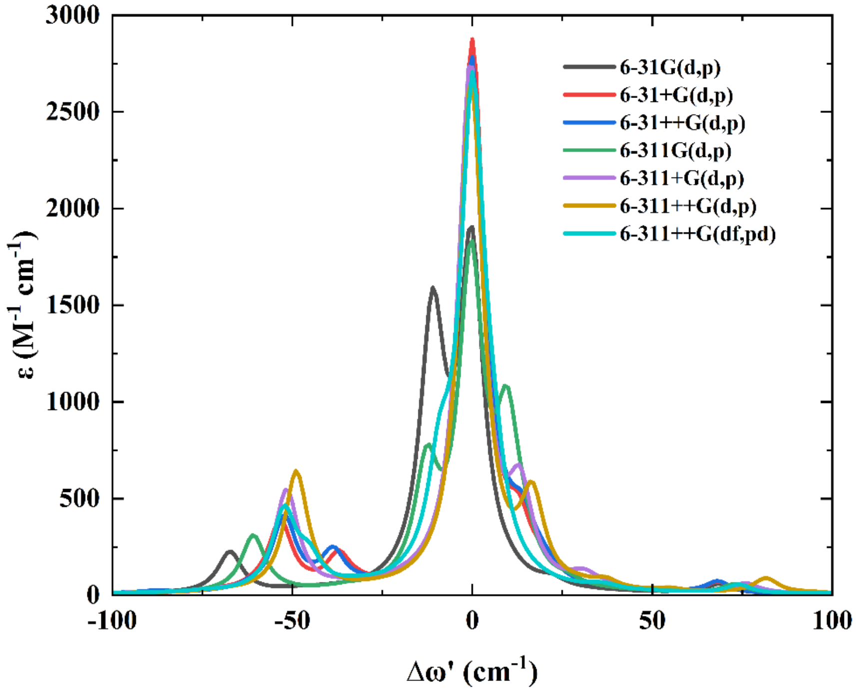

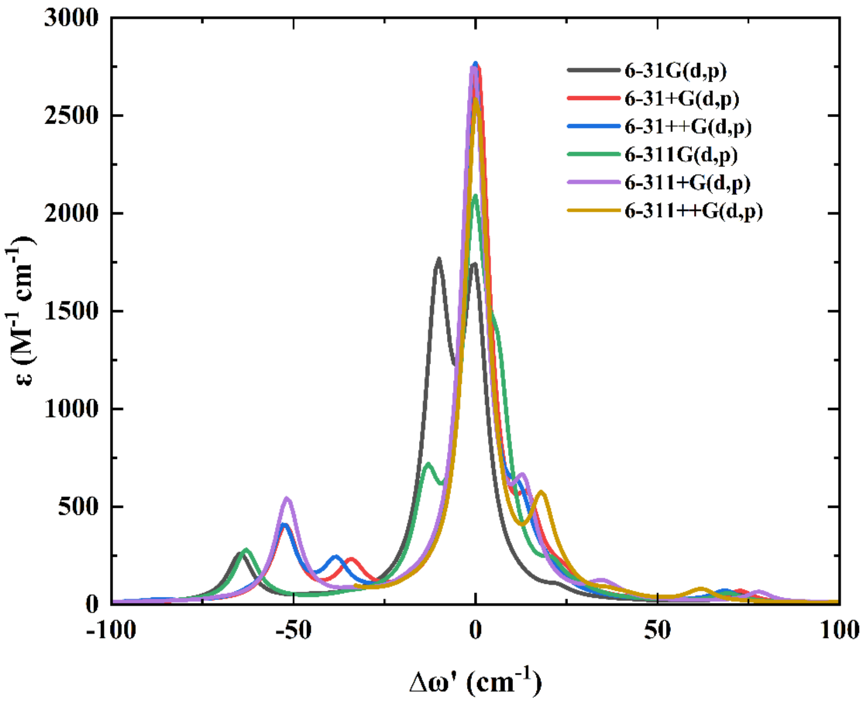

Figure 4.8 - Vibrational spectra (transparent window) of isomer 1 (top) and isomer 2 (bottom) of 4-azido-N-phenylmaleimide for 6-31G(d,p), 6-31+G(d,p), 6-31++G(d,p), 6-311G(d,p), 6-311+G(d,p), 6-311++G(d,p), 6-311++G(df,pd) basis sets in NNDMA. $\Delta\omega' = \omega_{ij} - \omega_k$ (ω_{ij} and ω_k are wavenumbers of combination band or overtone and fundamental vibration, respectively).

Figure 4.8 presents the azide asymmetric stretch adsorption profile of isomer 1 for all basis sets. Both 6-31G(d,p) and 6-311G(d,p) basis sets have a lower intensity adsorption profile comparatively. It also shows that azide asymmetric stretch red-shifted when more polarized and diffused basis sets were used. Unlike in 4-azidotoluene, 4-azido-N-phenylmaleimide introduces different vibrational modes coupled to the azide asymmetric stretch for different basis sets. Therefore, 6-311++G(df,pd) and 6-31+G(d,p)/6-31++G(d,p) basis sets have different absorption profiles compared to 6-311+G(d,p) and 6-311++G(d,p) basis sets for both isomers. As previously described, this change can be attributed to the significant change in the dihedral angle between the benzene ring and the maleimide group.

4.2.2. 4-azido-N-phenylmaleimide in THF

High-intensity modes with molar absorptivity coefficients over 1000 M^{-1} cm^{-1} for isomer 1 were shown in Table 4.10. The carbonyl stretch (Mode 52), and azide asymmetric stretch (mode 54) have the highest intensities followed by modes 48, 45, and 46. Figure 4.9 shows the harmonic and anharmonic spectra with the 6-311+G(d,p) basis set, and Appendix G and Appendix H provide spectroscopic details of combination and overtone bands occurring within ±135 cm^{-1} of the azide asymmetric stretch for seven basis sets for isomer 1 and isomer 2, respectively. Figure 4.10 shows high-intensity vibrational modes within the transparent window, as well as some lower intensity peaks, which were included due to their high cubic force constant (> 1 cm^{-1}) for all basis sets. Unlike the NNDMA, the intensity of azide asymmetric stretch is low for triple-zeta basis sets, and the 6-311G(d,p) basis set has an increased intensity for Fund(54) when compared to NNDMA solvent. Even though Comb(36 39) has high intensities in NNDMA for 6-31G(d,p) and 6-311G(d,p) basis sets, intensity of Comb(36 39) in THF is ~20 km mol^{-1} except for 6-311G(d,p) and 6-311++G(df,pd) basis sets which have even less intensities.

In addition, Comb(27 46) has a higher intensity than Comb(27 45) for all basis sets and is always greater compared to NNDMA solvent. As in NNDMA solvent, 6-311++G(df,pd) basis set shows some intensity for Comb(26 45), Comb(26 46), and Comb(29 45), but the intensities are less compared to NNDMA solvent. Moreover, Comb(34 40) was quite intense in 6-311G(d,p) in both NNDMA and THF, but unlike in the NNDMA solvent, Comb(34 40) is intense in 6-311+G(d,p) and 6-311++G(d,p), and not in the 6-31+G(d,p) and 6-31++G(d,p) basis sets. Comb(28 45) also has an intensity over 10 km mol^{-1} for 6-31+G(d,p) and 6-31++G(d,p) basis sets, but not intense as in NNDMA solvent, and has an intensity of 30 km mol^{-1} for 6-31G(d,p) basis set which is indistinct in NNDMA. Comb(28 46) has an intensity of 25 km mol^{-1} and 11 km mol^{-1} in THF and NNDMA for 6-31G(d,p), respectively, but has an intensity below 10 km mol^{-1} for all other basis sets in both solvents. Then, Over(39) shows a similar pattern in THF solvent as in NNDMA and has an intensity over 10 km mol^{-1} for all basis sets. All other vibrational modes have intensities less than 10 km mol^{-1} except for Comb(23 48) in 6-31G(d,p), and Comb(29 45) in 6-311++(df,pd) which is ~12 km mol^{-1}.

Table 4.10 - Normal Modes of 4-azido-N-phenylmaleimide (isomer 1) in THF using B3LYP/6-311+G(d,p) basis set.

Mode	Vibration	$\upsilon_{(harmonic)}$ / cm^{-1}	$\upsilon_{(anharmonic)}$ / cm^{-1}	$I_{(harmonic)}$ / km mol^{-1}	$I_{(anharmonic)}$ / km mol^{-1}
54	N_3 asymmetric stretch	2224.2	2183.3	1608.9	562.0
52	C=O stretch	1741.2	1707.9	1354.1	705.9
48	4-H sp^2 C-H in plane + Benzene ring vibrations	1534.8	1543.4	378.0	79.6
46	N_3 Sym stretch + C-N stretch + both ring vibrations + all C-H in-plane	1402.7	1354.1	325.4	202.3
45	N_3 Sym stretch + C-N stretch + both ring vibrations + all C-H in-plane	1360.4	1314.5	539.3	37.9

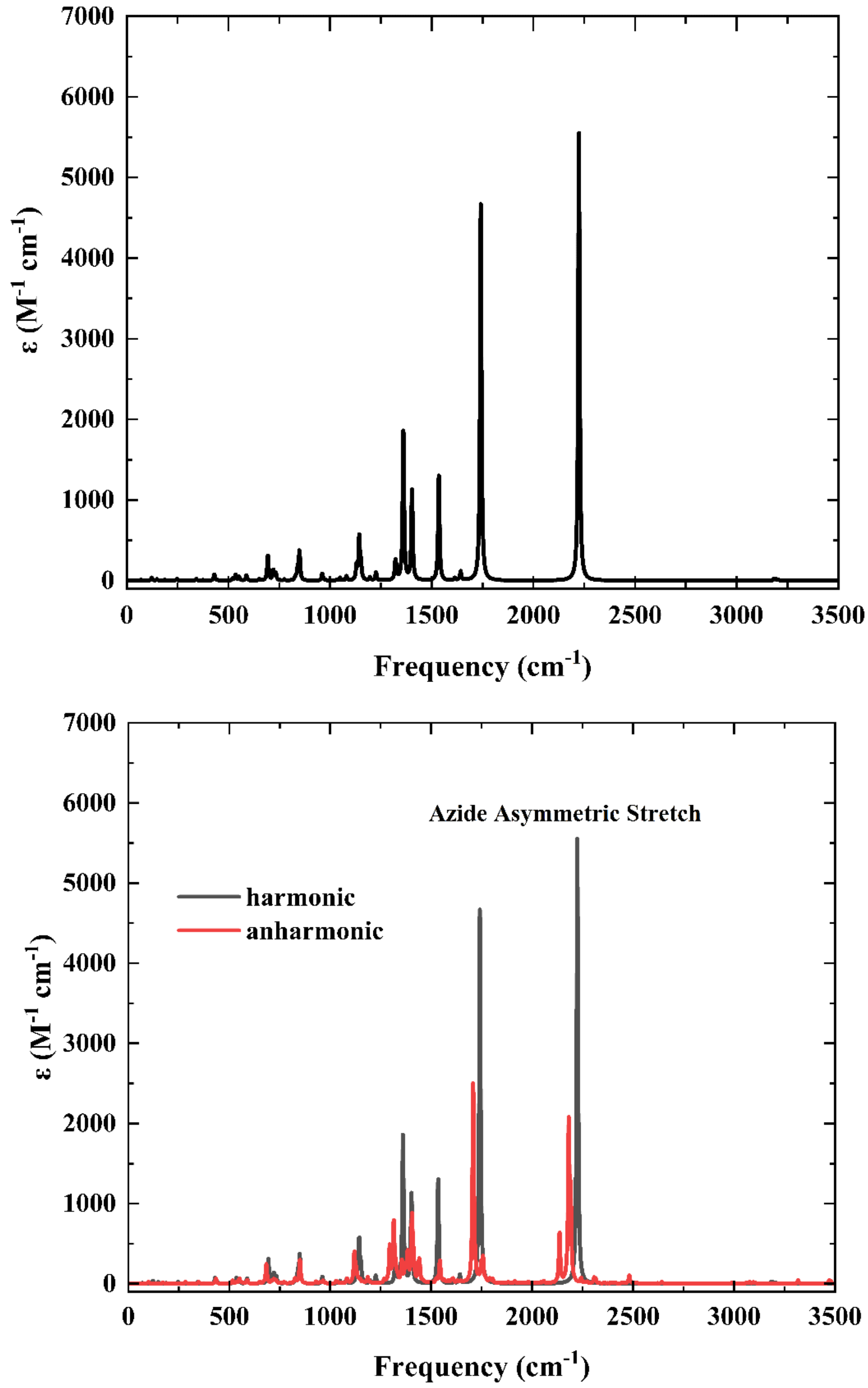

Figure 4.9 – IR spectra of harmonic (top), both anharmonic and harmonic (bottom) of 4-azido-N-phenylmaleimide (isomer 1) in THF using B3LYP/6-311+G(d,p) level in Gaussian-16.

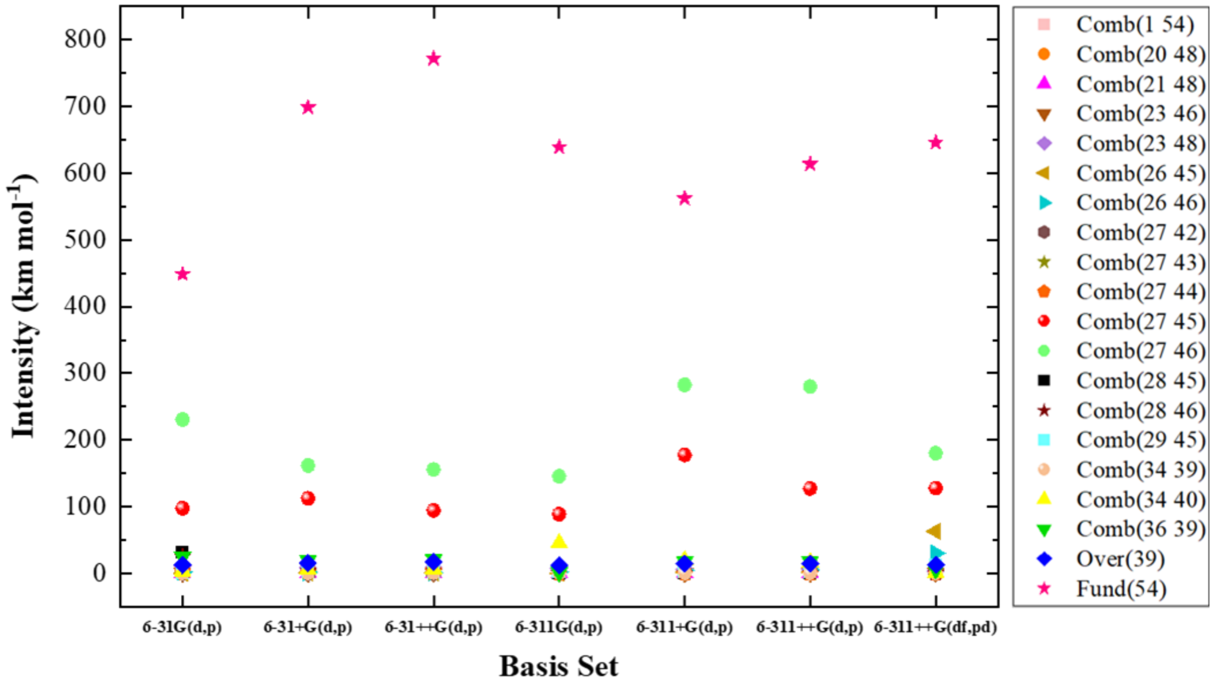

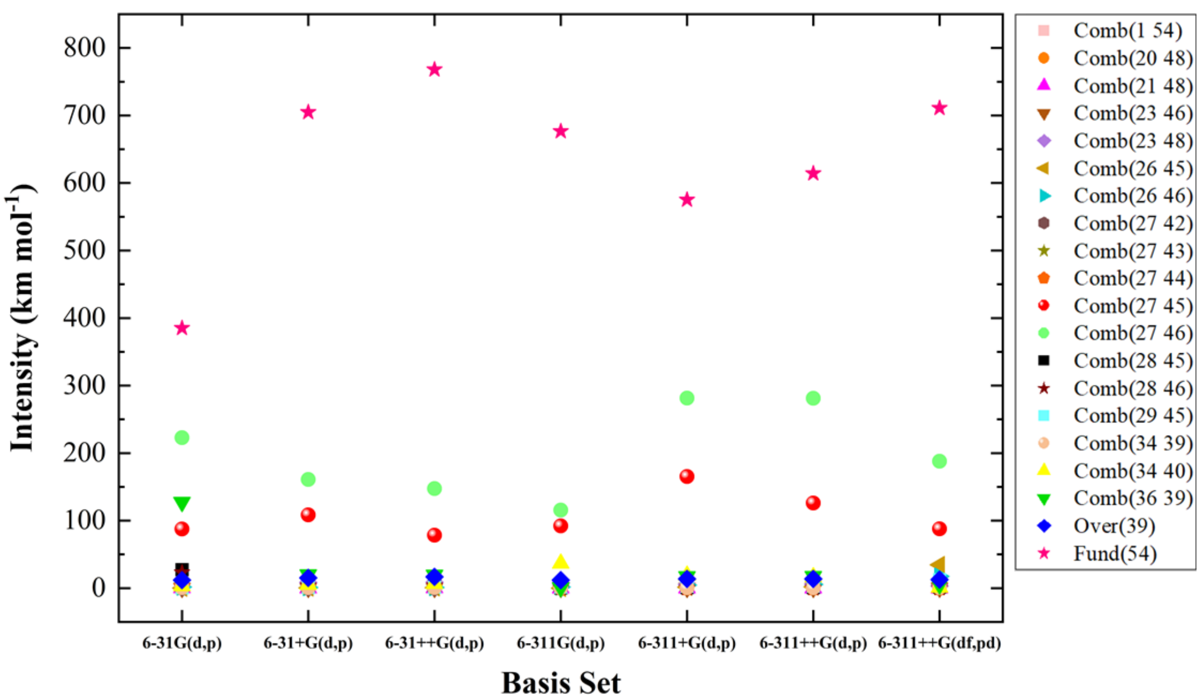

Figure 4.10 – Intensities of vibrational modes that can potentially couple with the azide asymmetric stretch of 4-azido-N-phenylmaleimide for 6-31G(d,p), 6-31+G(d,p), 6-31++G(d,p), 6-311G(d,p), 6-311+G(d,p), 6-311++G(d,p), 6-311++G(df,pd) basis sets in THF of isomer 1 (top) and isomer 2 (bottom).

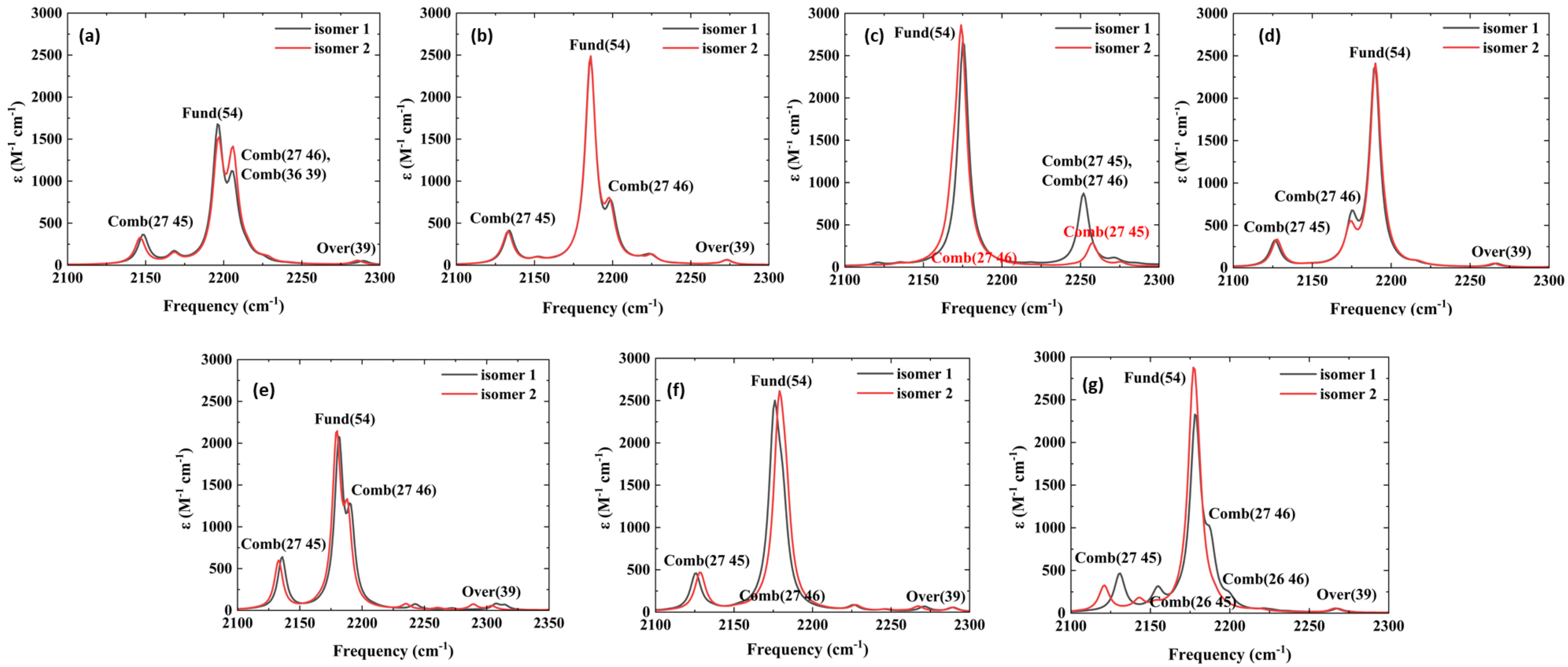

Figure 4.11 – Vibrational spectra of rotamers of 4-azido-N-phenylmaleimide in THF solvent with seven basis sets: (a) 6-31G(d,p), (b) 6-31+G(d,p), (c) 6-31++G(d,p), (d) 6-311G(d,p), (e) 6-311+G(d,p), (f) 6-311++G(d,p), and (g) 6-311++G(df,pd).

Both isomers have a similar pattern in intensity. Figures in 4.11 show how small deviations in intensity values change the shape of the azide absorption profiles of 6-31G(d,p) and 6-311++G(df,pd) basis sets. The 6-31++G(d,p) basis set shows a completely different azide absorption profile for both isomers. For isomer 1, both Comb(27 45) and Comb(27 46) are located very far from the azide asymmetric stretch while for isomer 2, only Comb(27 45) is located very far from the azide asymmetric stretch. The abnormal thing is that Comb(27 45) locates right to the fundamental vibration. Hence, studying vibrational spectra using 6-31++G(d,p) will be also questionable. From these intensity values, we can see that the intensity of combination bands is solvent-dependent. To get deep insights into the FRs, let's consider the cubic force constants values, see Figure 4.12. In THF, Comb(27 45) has a cubic force constant over 50 cm^{-1} for every basis set. Even though 6-311++G(df,pd) basis set has high intensity and cubic force constant for Comb(26 45) in NNDMA, it is low for THF solvent. Therefore, from the cubic force constants, we can directly see a strong coupling between Comb(27 45) and the azide asymmetric stretch. The second highest cubic force constant of ~35 cm^{-1} for Over(39). The intensity of both Comb(27 45) and Over(39) are not that high as they are very far in frequency from the fundamental vibration. As we mentioned, Comb(28 45) has considerable intensity and a high cubic force constant value for the 6-31G(d,p) basis set in THF. However, it has 10 cm^{-1} for 6-31+G(d,p) and 6-31++G(d,p) basis sets while less than 2 cm^{-1} for all other basis sets. Then, Comb(27 46) has a cubic force constant over 12 cm^{-1} and it is very close to the fundamental vibration ($\Delta\omega'$ = ~10 cm^{-1}). Although Comb(27 44) has a cubic force constant over 10 cm^{-1} for double zeta basis sets, it is very far in frequency to make an FR with fundamental vibration. In addition, Comb(23 46) has a cubic force constant of around 10 cm^{-1}, but it is not intense due to high $\Delta\omega'$. All other combination bands have cubic force constants less than 10 cm^{-1}.

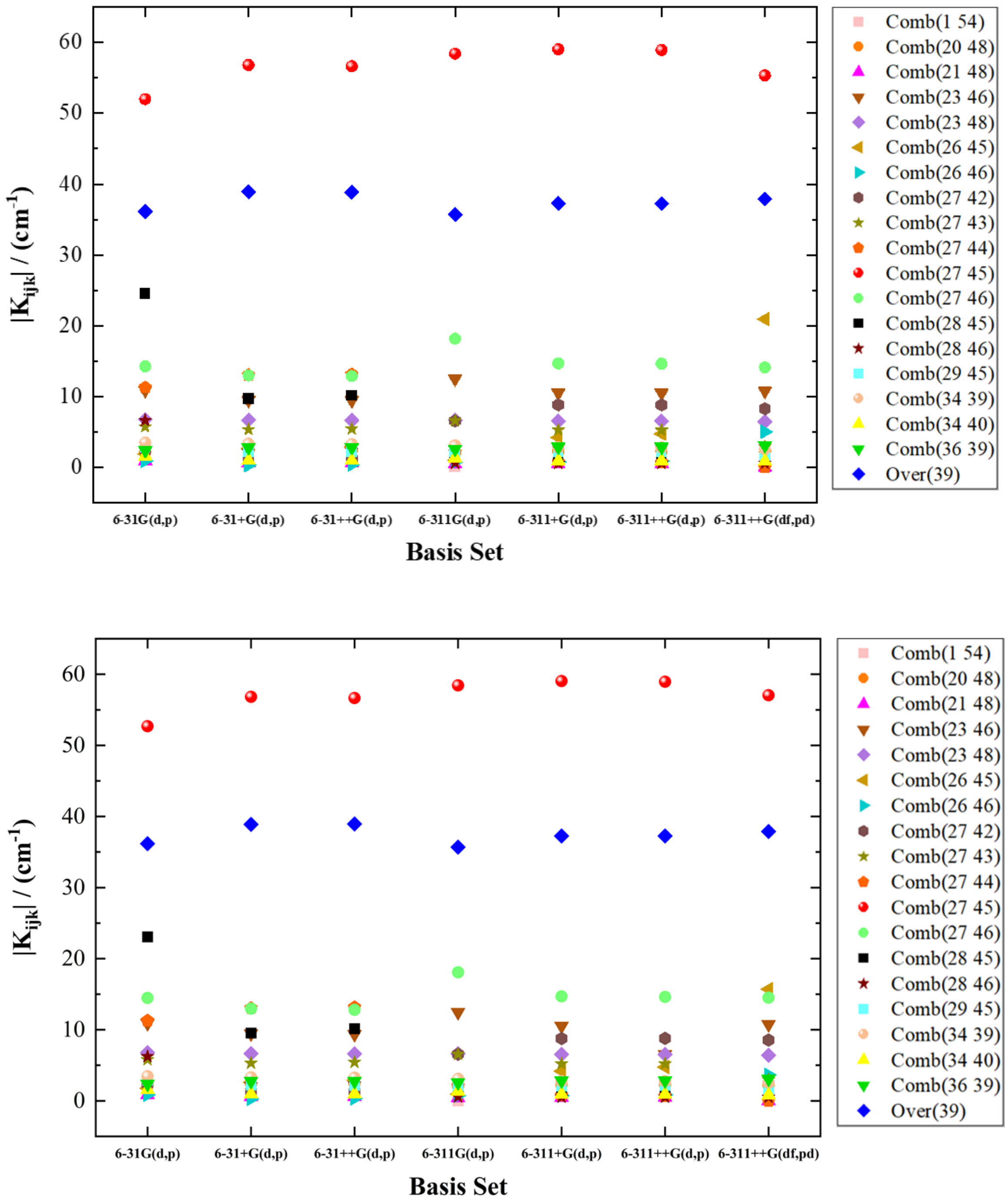

Figure 4.12 – Cubic force constants of vibrational modes that can potentially couple with the azide asymmetric stretch of 4-azido-N-phenylmaleimide for 6-31G(d,p), 6-31+G(d,p), 6-31++G(d,p), 6-311G(d,p), 6-311+G(d,p), 6-311++G(d,p), 6-311++G(df,pd) basis sets in THF of isomer 1 (top) and isomer 2 (bottom).

Table 4.11 - TFR values for combination or overtone bands that can potentially couple with the azide asymmetric stretch in 4-azido-N-phenylmaleimide (isomer 1) in THF solvent.

Mode	6-31G(d,p)	6-31+G(d,p)	6-31++G(d,p)	6-311G(d,p)	6-311+G(d,p)	6-311++G(d,p)	6-311++G(df,pd)
Comb(1 54)	0.024	2.857	0.005	0.000	0.038	0.016	0.065
Comb(20 48)	0.058	0.078	0.027	0.046	0.214	0.530	0.123
Comb(21 48)	0.025	0.025	0.009	0.011	0.032	0.283	0.000
Comb(23 46)	0.095	0.092	0.088	0.104	0.111	0.103	0.101
Comb(23 48)	0.240	0.172	0.026	0.231	0.069	0.090	0.132
Comb(26 45)	0.032	1.542	0.120	0.016	0.064	0.054	0.780
Comb(26 46)	0.054	0.006	0.004	0.030	0.028	0.015	0.402
Comb(27 42)	0.033	0.027	0.048	0.061	0.142	0.132	0.123
Comb(27 43)	0.117	0.154	0.210	0.088	0.115	0.107	0.073
Comb(27 44)	0.196	0.217	0.235	0.035	0.015	0.036	0.000
Comb(27 45)	1.324	1.328	0.787	1.117	1.393	1.524	1.408
Comb(27 46)	3.942	2.237	0.102	1.155	5.235	2.001	553.411
Comb(28 45)	0.804	0.365	1.388	0.035	0.045	0.059	0.512
Comb(28 46)	0.533	0.102	0.051	0.029	1.290	0.771	0.158
Comb(29 45)	0.186	0.029	0.008	0.054	0.131	0.222	0.489
Comb(34 39)	0.135	0.129	0.011	0.069	0.123	0.263	0.154
Comb(34 40)	0.077	0.026	0.004	0.694	0.004	0.006	0.012
Comb(36 39)	0.189	0.073	0.008	0.118	0.091	0.078	0.071
Over(39)	0.369	0.440	0.092	0.457	0.485	0.432	0.414

Both isomers have the same cubic force constant values. If a combination band is very close to fundamental vibration (< 10 cm^{-1}), then any combination band with a cubic force constant > 1 cm^{-1} can be produced FR. TFR values were shown in Table 4.11 to check what are the combination or overtone bands that can potentially couple with 4-azido-N-phenylmaleimide.

When considering TFR values, the 6-311++G(df,pd) basis set shows a very large value for Comb(27 46) and Comb(26 45) because of ~0 cm^{-1} resonance shift and large cubic force constant (-21 cm^{-1}), respectively. In the 6-31++G(d,p) basis set, the resonance shift of most of the combination bands that are coupled with azide asymmetric stretch is so high except for Comb(28 45). Therefore, this basis set is questionable for predicting FRs for 4-azido-N-phenylmaleimide. For the other five basis sets, both comb(27 46) and Comb(27 45) have TFR values over 1. Therefore, these combination bands are strongly coupled to the azide asymmetric stretch. In 6-31+G(d,p) basis set, Comb(1 54) and Comb(26 45) have high TFR values due to low resonance shift of -0.5 cm^{-1} and -1.7 cm^{-1}, respectively. Although, Comb(28 46) has a less cubic force constant values (< 1cm^{-1}) for 6-311+G(d,p) and 6-311++G(d,p) basis sets, it shows high TFR values due to less $\Delta\omega$. Likewise Comb(34 40), Comb(20 48) and Comb(29 45) show high TFR values in 6-311G(d,p), 6-311++G(d,p) and 6-311++(df,pd) basis sets, respectively because of low $\Delta\omega$. In addition, 6-31G(d,p) basis set shows TFR value of > 0.3 for both Comb(28 46) and Comb(28 45). Comb(28 45) was possibly weakly coupled FR in double zeta basis sets and 6-311++G(df,pd), but it's not possible in the other three basis sets. If we consider 0.3 cut-offs for making possible FRs, then Over(39) is also weakly coupled to the fundamental vibration. All other combination bands in Table 4.11 are very weakly coupled (< 0.3) to the fundamental vibration.

Table 4.12 - TFR values for combination or overtone bands that can potentially couple with the azide asymmetric stretch in 4-azido-N-phenylmaleimide (isomer 2) in THF solvent.

Mode	6-31G(d,p)	6-31+G(d,p)	6-31++G(d,p)	6-311G(d,p)	6-311+G(d,p)	6-311++G(d,p)	6-311++G(df,pd)
Comb(1 54)	0.025	0.110	0.007	0.000	0.061	0.772	0.472
Comb(20 48)	0.060	0.076	0.028	0.047	1.590	0.262	0.070
Comb(21 48)	0.026	0.024	0.006	0.011	0.071	0.267	0.000
Comb(23 46)	0.097	0.104	0.165	0.102	0.112	0.061	0.100
Comb(23 48)	0.214	0.186	0.033	0.228	0.075	0.098	0.171
Comb(26 45)	0.046	2.195	0.030	0.016	0.067	0.046	0.525
Comb(26 46)	0.259	0.004	0.019	0.029	0.028	0.012	0.301
Comb(27 42)	0.032	0.027	0.031	0.062	0.141	0.131	0.111
Comb(27 43)	0.127	0.149	0.128	0.087	0.115	0.106	0.060
Comb(27 44)	0.193	0.214	0.220	0.037	0.022	0.043	0.000
Comb(27 45)	1.341	1.283	0.700	1.124	1.480	1.520	1.081
Comb(27 46)	5.361	0.662	7.121	1.027	4.319	1.571	1.356
Comb(28 45)	0.821	0.383	0.219	0.034	0.047	0.057	0.044
Comb(28 46)	0.448	0.058	0.073	0.026	0.213	0.164	1.333
Comb(29 45)	0.272	0.024	0.010	0.051	0.152	0.205	0.094
Comb(34 39)	0.116	0.127	0.011	0.071	0.168	0.218	0.119
Comb(34 40)	0.064	0.027	0.004	0.321	0.005	0.007	0.034
Comb(36 39)	0.289	0.072	0.014	0.110	0.084	0.078	0.072
Over(39)	0.405	0.442	0.098	0.461	0.456	0.424	0.413

Table 4.12 presents TFR values for isomer 2 and these values can be different from isomer 1 due to different resonance shifts but they predict the same argument as isomer 1. Figure 4.13 compares the azide asymmetric stretch absorption profiles in seven basis sets. It shows that 6-31G(d,p), 6-31++G(d,p) and 6-311++G(df,pd) basis sets have different absorption profiles compared to other basis sets because 6-31G(d,p) has a lower intensity absorption profile, 6-31++G(d,p) has a completely different high-intensity blue-shifted absorption profile, and 6-311++G(df,pd) produces many peaks that are not intense in other basis sets.

From these observations, we can see how different solvents affect vibrational coupling and how different basis sets describe vibrational couplings. How far a basis set can predict the vibrational couplings are quite questionable, but we can see that only a few combination bands are involved in making FRs. If a combination band or an overtone is consistently coupled with the same coupling strength for every basis set even though it is very far away in frequency from the fundamental vibration, it can generate FR. For 4-azido-N-phenylmaleimide, Comb(27 45) and Comb(27 46) are strongly coupled with the Fund(54). Also, Over(39) is weakly coupled to the azide asymmetric stretch. Figure 4.14 presents that 6-31+G(d,p), 6-311+G(d,p), and 6-311++G(d,p) have a similar trend of frequencies for combination and overtone bands relative to the fundamental vibration except for 6-31++G(d,p) basis set. Comb(27 45) is always ~50 cm^{-1} far away in frequency from the Fund(54) and Comb(27 46) stays so close and right to the Fund(54). Over(39) is very far away in frequency from the Fund(54) which causes to have less intensity despite having a high vibrational coupling constant. We proved that it is not suitable for vibrational analysis using 6-31G(d,p), 6-31++G(d,p), 6-311G(d,p) and 6-311++G(df,pd) basis sets to understand vibrational coupling. Moreover, both 6-31+G(d,p) and 6-311++G(d,p) basis sets have more FRs compared to 6-311+G(d,p) basis set.

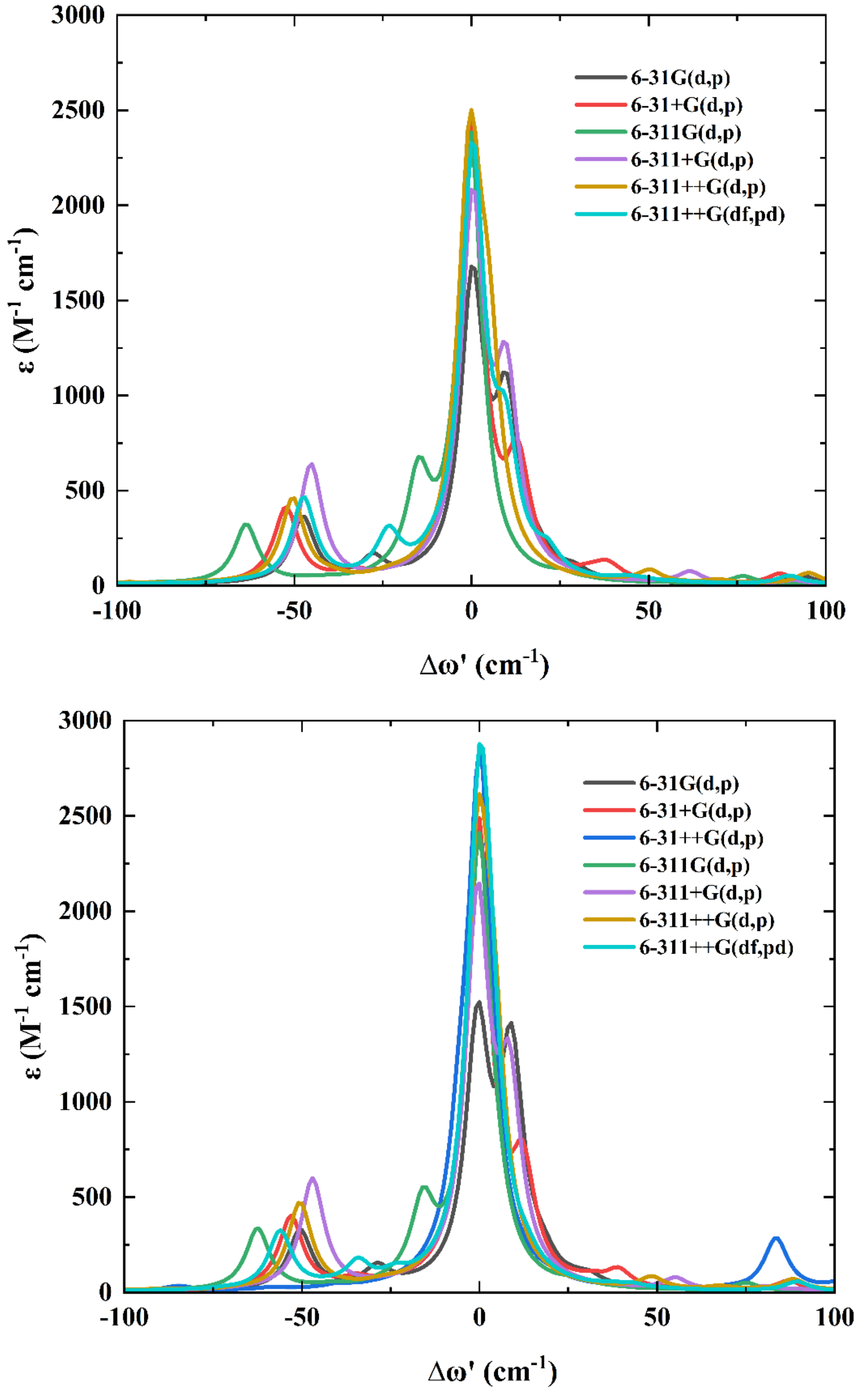

Figure 4.13 - Vibrational spectra (transparent window) of isomer 1 (top) and isomer 2 (bottom) of 4-azido-N-phenylmaleimide for 6-31G(d,p), 6-31+G(d,p), 6-31++G(d,p), 6-311G(d,p), 6-311+G(d,p), 6-311++G(d,p), 6-311++G(df,pd) basis sets in THF. $\Delta\omega' = \omega_{ij} - \omega_k$ (ω_{ij} and ω_k are wavenumbers of combination band or overtone and fundamental vibration, respectively).

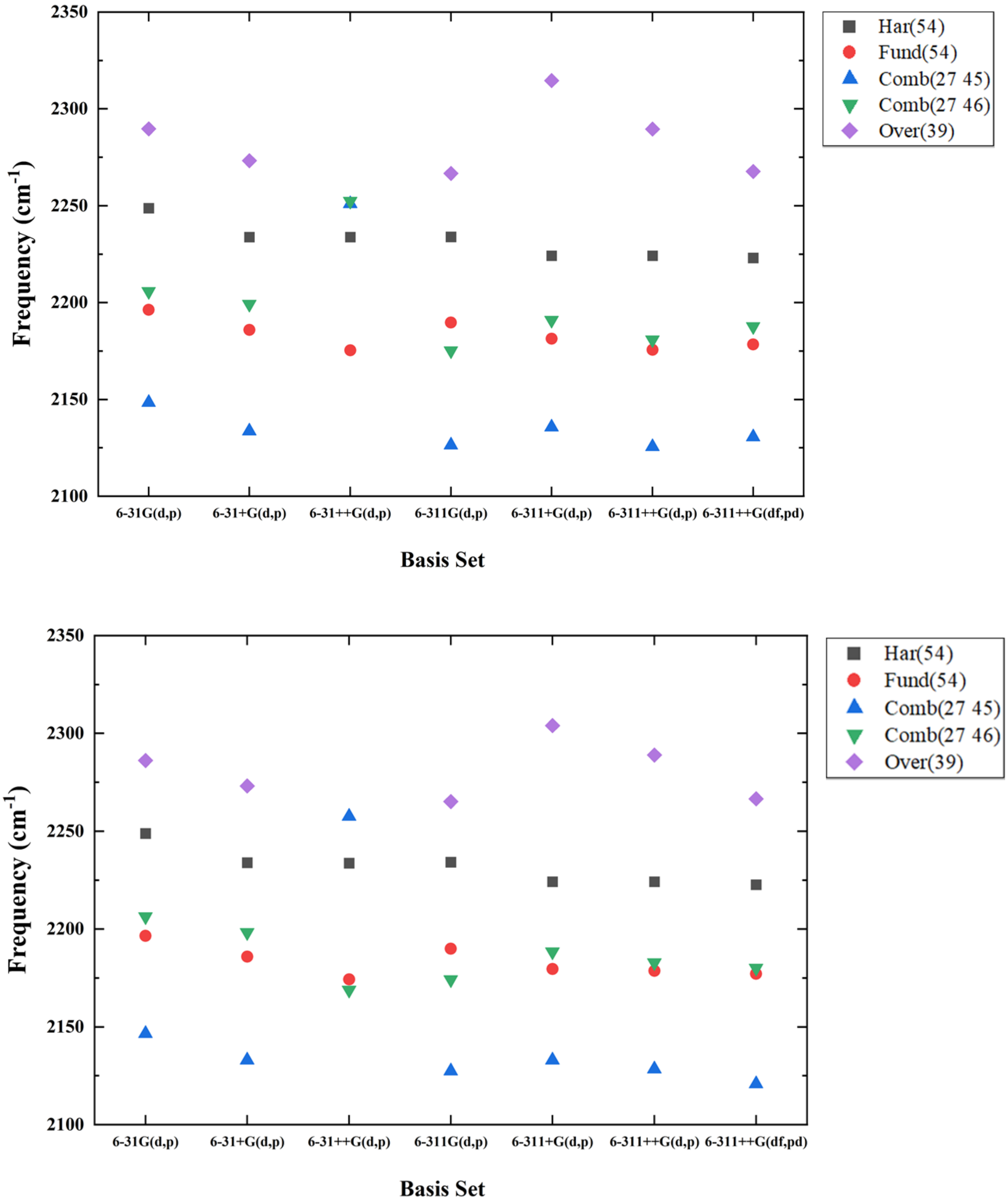

Figure 4.14 – Frequencies of vibrational modes that can potentially couple with the azide asymmetric stretch of 4-azido-N-phenylmaleimide for 6-31G(d,p), 6-31+G(d,p), 6-31++G(d,p), 6-311G(d,p), 6-311+G(d,p), 6-311++G(d,p), 6-311++G(df,pd) basis sets in THF of isomer 1 (top) and isomer 2 (bottom).

Therefore, out of seven different basis sets, it is clear that 6-311+G(d,p) basis set would be the best basis set for understanding vibrational coupling and FRs in an IR spectrum of 4-azido-N-phenylmaleimide. The solvent effect of 4-azido-N-phenylmaleimide is shown in Figure 4.15. It shows that the intensity of azide asymmetric stretch decreases while the intensity of combination bands increases. In addition, the peak position of Fund(54), Comb(27 46), and Comb(27 45) blue shift with THF. A comparison of absorption profiles of 4-azidotoluene and 4-azido-N-phenylmaleimide (Isomer 1) was shown in Figure 4.16 to investigate the intramolecular effect. When the methyl group is replaced with a maleimide group, azide asymmetric stretch blue shifts and azide adsorption profile are completely different from one another. When comparing vibrational transitions that contribute to FRs (see Figures 3.14 and 4.17), both molecules show the same vibrational modes. For example, modes 30, 15, 17, and 25 in 4-azidotoluene are similar to modes (45,46), 27, 26, and 39 in 4-azido-N-phenylmaleimide, respectively.

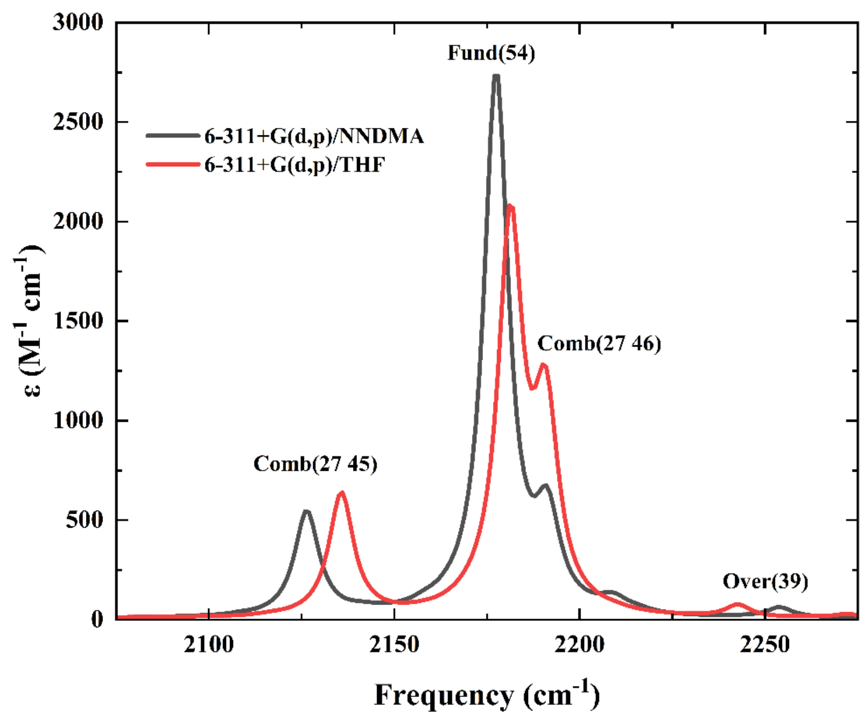

Figure 4.15 - Vibrational spectra of 4-azido-N-phenylmaleimide in NNDMA and THF solvents with DFT/B3LYP/6-311+G(d,p) level of theory.

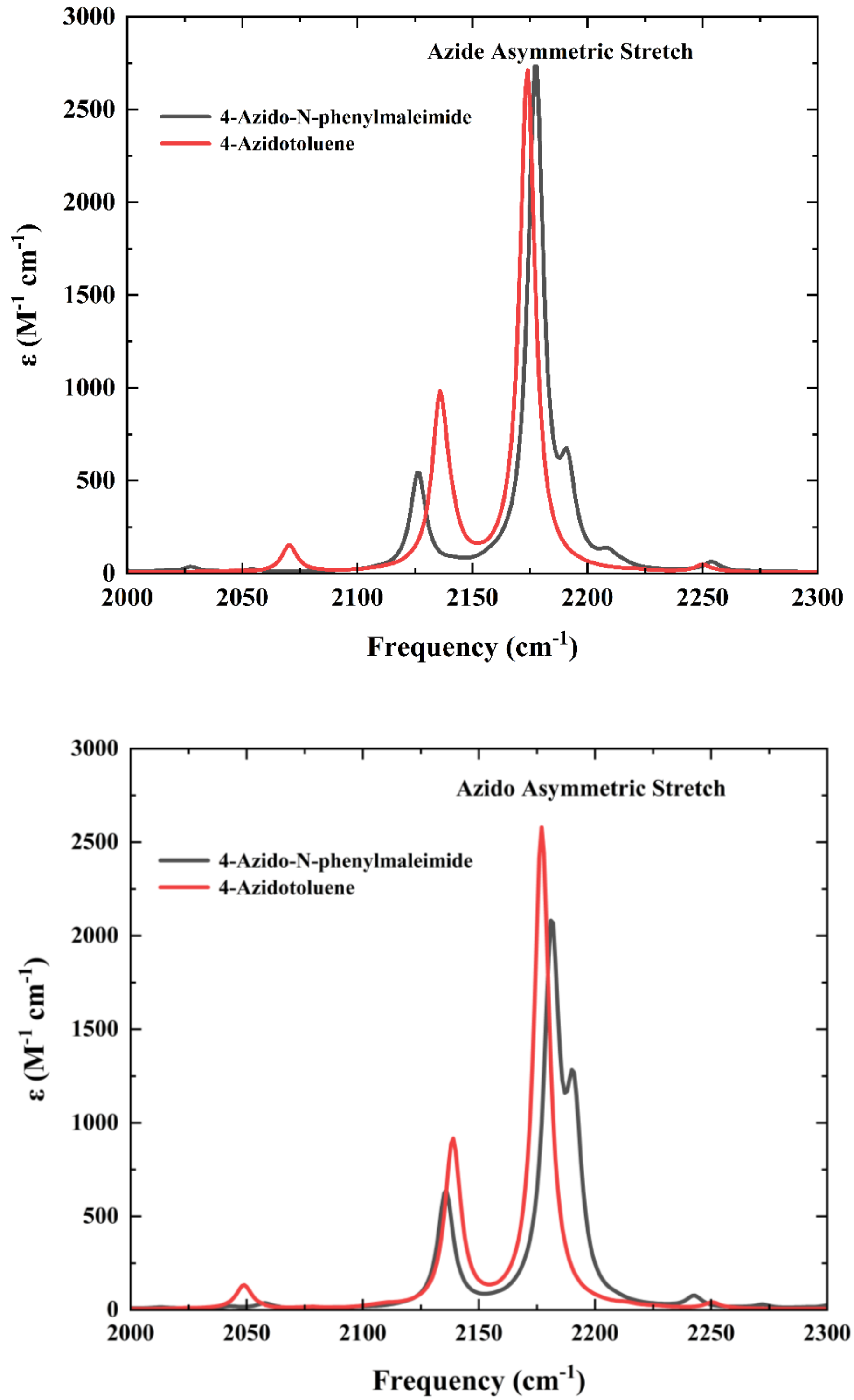

Figure 4.16 - Vibrational spectra of 4-azidotoluene and 4-azido-N-phenylmaleimide (Isomer 1) in NNDMA (a) and THF (b) solvents with B3LYP/6-311+G(d,p) level of theory

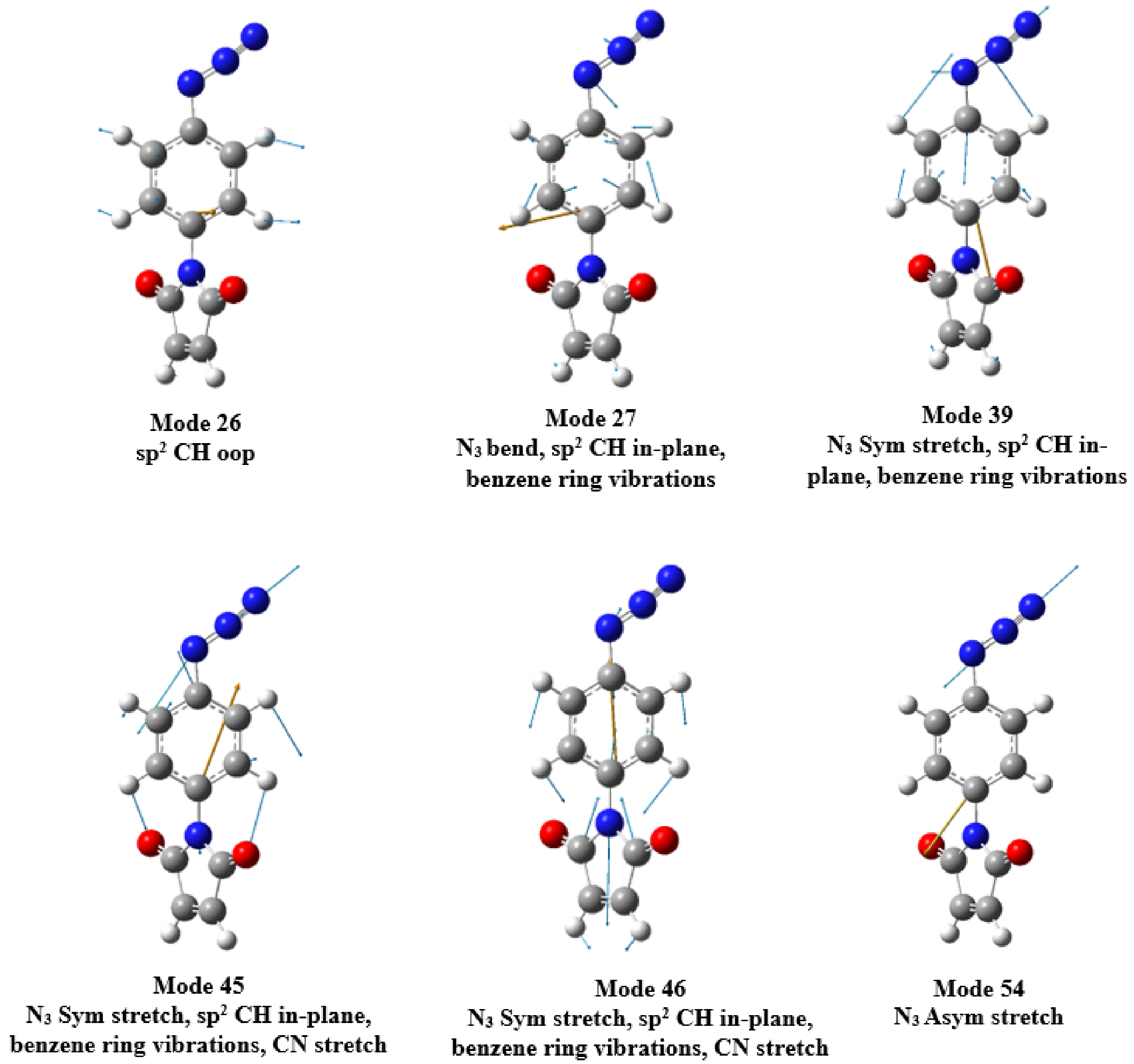

Figure 4.17 - Vibrational modes of combination or overtone bands that can potentially couple with the azide asymmetric stretch in 4-azido-N-phenylmaleimide.

4.3 Overview

This chapter mainly demonstrates two rotamers of 4-azido-N-phenylmaleimide. Both rotamers have the same cubic force constants for each mode while intensity and peak position can be different due to the changes in dihedral angles. It has been shown that the azide absorption profiles of 6-31G(d,p), and 6-311G(d,p) are completely different from the rest of the basis sets due to a dihedral angle (D8) change of ~20^0. Variations in the dihedral angle between the benzene ring and the maleimide group affect the vibrational coupling within the molecule. It was also verified by small changes in the HOMO orbital. The complexity of the azide absorption profile increases when the number of atoms increases and symmetry loses. Hence, the azide absorption profile of 4-azido-N-phenylmaleimide is less complicated than 4-azidoacetanilide and more complex than 4-azidotoluene. The 6-31++G(d,p) basis set was completely fine for 4-azidotoluene, but it produced a very different azide absorption profile for 4-azido-N-phenylmaleimide with THF solvent. Unlike in 4-azidotoluene, the 4-azido-N-phenylmaleimide has more different combination bands with high intensity for different basis sets. When a more polarized basis set is used, the complexity also increases. It was shown that the 6-311++(df,pd) basis set introduced new peaks with high intensity which are not intense in other basis sets. On top of that, there are few changes in the azide absorption profile of 4-azido-N-phenylmaleimide in 6-31+G(d,p) and 6-311+G(d,p)/6-311++G(d,p) basis sets. Hence, it is questionable to state that one basis set is perfect for anharmonic frequency analysis. However, qualitatively, 6-31+G(d,p), 6-311+G(d,p), and 6-311++G(d,p) basis sets are helpful to understand the azide absorption profile. Therefore, it is necessary to run anharmonic frequency calculations in a few basis sets to study the azide absorption profile. The consistency of intensity, peak position, cubic force constants, and TFR values can help to understand the kind of vibrational coupling and FRs exist in the azide absorption profile. The next chapter compares computational anharmonic frequency calculations with experimental FTIR spectra of three aryl-azides.

CHAPTER 5

EXPLORING SMALL ARYL-AZIDE VIBRATIONAL PROBES USING DFT AND FTIR STUDIES

5.1 Introduction

The previous chapters briefly described how DFT studies facilitate to study of azide asymmetric absorption profiles of small aryl-azide molecules. For example, anharmonic frequency calculations provide peak positions, intensities, and cubic force constants for each vibrational mode. In addition, 3D animations of these vibrational modes can be easily obtained. Hence, computer simulations are a promising method to study complex azide absorption profiles. But the actual question is, can we observe the same azide absorption profiles experimentally. It is crucial to know which computer model can generate spectra similar to the experimental infrared spectra. There are many functionals and basis sets that can be used in DFT studies. It has been shown that the B3LYP functional would be the best functional for small organic molecules.[50] In general, anharmonic frequency calculations run longer time when 6-311++G(df,pd) basis set is used. Thus, it is so important to research which basis set can generate vibrational spectra similar to the experimental vibrational spectra with lower computational cost. In this chapter, we compare computational calculations with FTIR spectra.

The combined geometry optimization and anharmonic frequency calculations were carried out using seven basis sets and two solvents. Here, we briefly discuss which basis set is compatible with experimental results and predict the solvent effect for three aryl-azides. Moreover, Hill et al. have reported synthesis, preparation, and 2DIR and FTIR spectra on these three aryl-azide compounds and our future work will report most of the basis sets can qualitatively produce azide absorption profiles similar to the FTIR spectra.[81, 82]

5.2 Comparison of DFT calculations with FTIR

The 75 mM solutions of three aryl-azide at room temperature in NNDMA and THF were used to obtain FTIR spectra. To compare the azide absorption profiles, the relative intensities were used, and frequencies of theoretical spectra were shifted to align the azide asymmetric stretch of theoretical and FTIR spectra together as follows,

$$\text{Shift} = \omega_{\text{theoretical}} - \omega_{\text{FTIR}} \tag{5.1}$$

where $\omega_{\text{theoretical}}$ is the frequency of azide asymmetric stretch in theoretical spectra and ω_{FTIR} is the frequency of azide asymmetric stretch in FTIR spectra. In FTIR spectra, the highest intensity peak corresponds to the fundamental vibration and combination bands, or overtones barely have an intensity. However, strong vibrational mixing of combination bands or overtones with fundamental vibration may increase the intensity of the combination band or overtone as high as fundamental vibration. Hence, it is hard to state which peak corresponds to the azide asymmetric stretch based on FTIR spectra. Theoretical IR spectra always differed from what we are observing from the experimental spectra. The wavenumbers of the vibrational modes are higher than that of FTIR spectra due to computational calculations being less accurate in describing the influences of other vibrational modes, such as interactions between the FRs and higher-order force constants. Moreover, another reason that might influence the calculated frequencies would be PCM model does not take into consideration the specific solvent-solute interaction or non-electrostatic effects. Also, the fitting of the experimental spectra may introduce some errors in the intensity ratio of the three states, which may contribute to the deviations. Hence, the experimental spectra are more congested while DFT spectra have wider absorption profiles comparatively. In comparison, we suppose to report what vibrational modes contribute to the accidental FRs in experimental spectra.

5.2.1 4-azido-N-phenylmaleimide

The spectral characteristics of both theoretical and FTIR spectra are shown in Tables 5.1 and 5.2 respectively. FTIR spectra of 4-azido-N-phenylmaleimide are not complicated as 4-azidotoluene or 4-azidoacetanilide. It only has two high-intensity peaks in 2095 and 2129 cm^{-1}. But DFT calculations predict two more peaks that can be suppressed by the high-intensity peaks in the FTIR spectra. The major difference between the NNDMA and THF is the intensity of the two peaks. DFT calculations also show that THF solvent has less intensity for the azide asymmetric stretch compared to the NNDMA solvent (Figure 4.15) and it increases the intensity of combinations bands. As a result, the intensity ratio of the second major peak increases (Table 5.2). This increment is high in 6-311+G(d,p) and 6-311++G(d,p) basis sets (Figure 4.10).

Table 5.1 - Spectral characteristics of FTIR spectra of 4-azido-N-phenylmaleimide

Peak	Peak Position / cm^{-1}		Frequency Shift / cm^{-1}		Relative peak Intensity	
	NNDMA	THF	NNDMA	THF	NNDMA	THF
1	2096.0	2095.3	-33.3	-33.7	0.7037	0.9824
2	2129.3	2129.0	0.0	0.0	1	1

Table 5.2 - Spectral characteristics of B3LYP/6-311+G(d,p) spectra of 4-azido-N-phenylmaleimide

Peak	Peak Position / cm^{-1}		Resonance Shift / cm^{-1}		Relative peak Intensity	
	NNDMA	THF	NNDMA	THF	NNDMA	THF
Comb(27 45)	2126..4	2135.7	-34.2	-42.4	0.1926	0.3153
F(54)	2177.5	2181.3	0.0	0.0	1	1
Comb(27 46)	2191.3	2190.9	13.5	-2.8	0.1597	0.5027
Over(39)	2253.9	2314.6	78.9	76.9	0.0179	0.0247

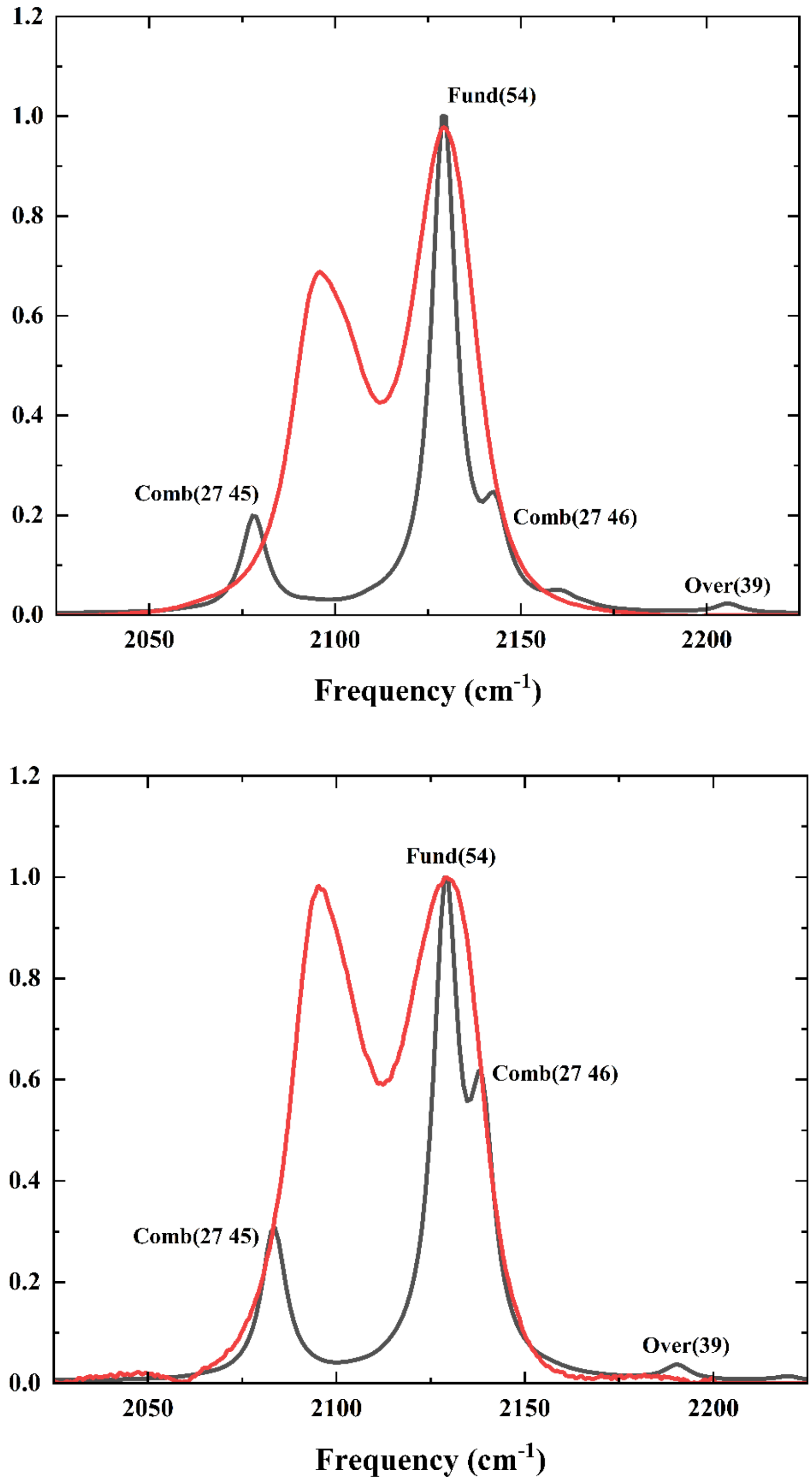

Figure 5.1 – FTIR (red) and DFT (black) spectra of 4-azido-N-phenylmaleimide in NNDMA (top) and THF (bottom) solvents.

The frequency difference between the major peaks in all three aryl-azide is relatively high. According to Table 5.1, the frequency gap between the two peaks is around 34 cm^{-1}. Hence, the peak at 2095 cm^{-1} in FTIR spectra can be assigned to the Comb(27 45). Figure 5.1 shows both theoretical spectra with the 6-311+G(d,p) basis set and the FTIR spectra in NNDMA and THF solvents. There is one high-intensity shoulder peak right to the azide asymmetric stretch which cannot be seen separately in FTIR spectra due to the frequency gap being low. These differences are 9.6 and 13.8 cm^{-1} for THF and NNDMA respectively. As in other aryl-azide compounds, there is always a small overtone peak far away from the fundamental vibration because that overtone has the second-highest cubic force constant within the transparent window. Surprisingly, in both combination bands, mode 27 is involved and modes 45 and 46 have high intensity individually. Thus, this proves that the azide asymmetric absorption profile can consist of multiple peaks and not all peaks can be visible in FTIR spectra.

5.2.2 4-azidotoluene

Figure 5.2 presents both theoretical spectra with the 6-311+G(d,p) basis set and the FTIR spectra in NNDMA and THF solvents. The frequencies, resonance shift, and relative intensities for both FTIR and theoretical spectra are tabulated in Tables 5.3 and 5.4. Four distinct peaks are visible in both solvents. The FTIR spectrum of NNDMA solvent has two high-intensity peaks at 2105 and 2127 cm^{-1}. The frequency difference between high-intensity peaks in NNDMA is 22 cm^{-1}. Surprisingly, the highest intensity peak in NNDMA solvent becomes less intense in THF solvent. THF solvent has one high-intensity peak at 2105 cm^{-1} and a shoulder peak at 2119 cm^{-1} instead of two high-intensity peaks in NNDMA due to the small frequency gap of 14 cm^{-1}. The peak at 2051 cm^{-1} in NNDMA is also visible in the same position in THF. The shoulder peak in NNDMA at 2142 cm^{-1} can be seen separately in THF at 2139 cm^{-1} due to the frequency gap of

20 cm^{-1} with the peak at 2119 cm^{-1}. DFT calculations also show four individual peaks (i.e., Comb(18 30), Comb(15 30), Over(25) and Fund(38)) within the transparent window except for 6-31G(d,p)/NNDMA, 6-311++G(df,pd)/NNDMA, 6-31G(d,p)/THF and 6-311G(d,p)/THF basis sets calculations. Thus, we can verify that these basis sets are not suitable for studying vibrational coupling. The rest of the basis set has the same azide absorption profile. Comb(15 30) matches with the peak at 2050 cm^{-1}. Our calculations showed that Comb(15 30) has the highest cubic force constant (Figures 3.5 and 3.12) with the azide asymmetric stretch within the transparent window. Even though Over(25) is too far from fundamental vibration, it can be assigned to the peak around 2140 cm^{-1} because of the third-highest cubic force constant. Why do two solvents have completely different absorption profiles? and what is the azide asymmetric stretch out of the two high-intensity peaks? are the two major questions we need to address theoretically. First, we have shown that the intensity of azide asymmetric stretch lowered with the THF solvent (Figure 3.10). Second, there's another combination band Comb(17 30) along with the Comb(18 30) that can not see separately in both FTIR and DFT spectra. Since the Comb(17 30) exists close to the Comb(18 30) and the azide asymmetric stretch, both combination bands borrow oscillator strength from the azide asymmetric stretch. When the frequency gap between the two high-intensity peaks reduces (matching energies), azide asymmetric stretch shares more oscillator strength with the nearby combination bands with matching symmetries. Interestingly, mode 30 is involved in both combination bands and it has the second-highest intensity. Since the frequency gap is low for THF, it will result in high intensity in peak at 2105 cm^{-1} in THF solvent. Thus, the shoulder peak in THF at 2119 cm^{-1} and the highest intensity peak in NNDMA is the azide asymmetric stretch. The intensity of Comb(17 30) is higher in 6-311+G(d,p) and 6-311++G(d,p) basis sets (Figures 3.4 and 3.9).

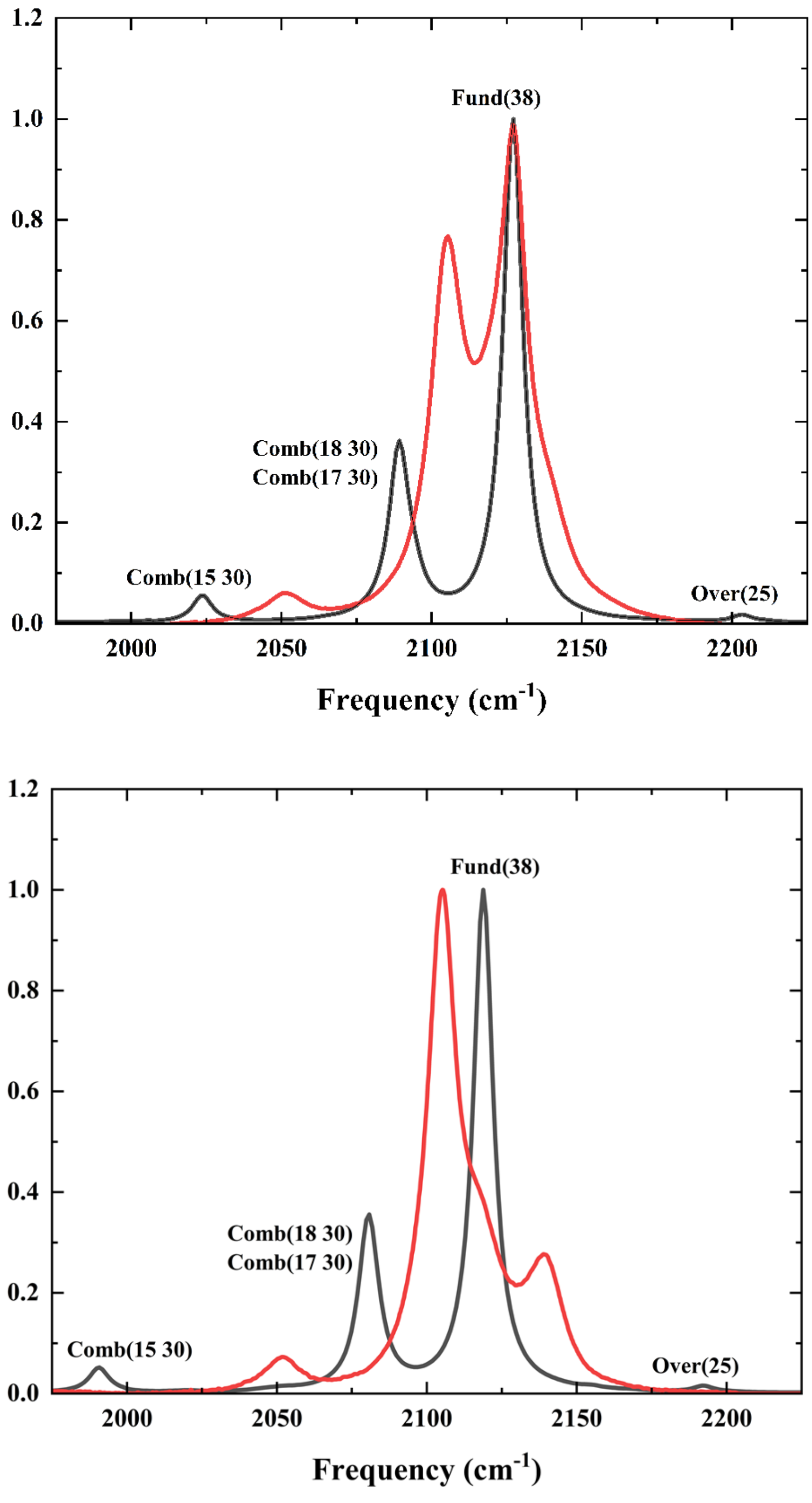

Figure 5.2 – FTIR (red) and DFT (black) spectra of 4-azidotoluene in NNDMA (top) and THF (bottom) solvents.

Table 5.3 - Spectral characteristics of FTIR spectra of 4-azidotoluene

Peak	Frequency / cm^{-1}		Frequency shift / cm^{-1}		Relative peak Intensity	
	NNDMA	THF	NNDMA	THF	NNDMA	THF
1	2050.7	2051.9	-76.4	-67.0	0.0608	0.0727
2	2105.4	2105.2	-21.7	-13.7	0.7762	1
3	2127.1	2118.9	0	0	1	0.3820
4	2142.0	2138.9	14.9	20.0	0.2477	0.2766

Table 5.4 - Spectral characteristics of B3LYP/6-311+G(d,p) spectra of 4-azidotoluene

Peak	Frequency / cm^{-1}		Resonance shift / cm^{-1}		Relative peak Intensity	
	NNDMA	THF	NNDMA	THF	NNDMA	THF
Comb(15 30)	2070.5	2048.8	-95.2	-119.3	0.0536	0.0489
Comb(17 30)	2140.9	2140.9	-17.7	-28.5	0.0440	0.0331
Comb(18 30)	2135.9	2138.6	-26.1	-17.8	0.3329	0.3213
Fund(38)	2173.9	2177.1	0	0	1	1
Over(25)	2250.0	2250.5	78.7	73.3	0.0120	0.0122

5.2.3 4-azidoacetanilide

The frequencies, resonance shift, and relative intensities for both experimental and theoretical spectra are shown in Tables 5.5 and 5.6. In FTIR spectra, four distinct peaks are visible in both solvents. A high-intensity peak at 2118 cm^{-1} and a low-intensity peak at 2081 cm^{-1} appears in both solvents. The frequency difference between these two peaks is 37 cm^{-1}. One-shoulder peak is visible at 2101 cm^{-1} for both solvents and another small peak is visible at 2147 and 2142 cm^{-1} for NNDMA and THF solvents respectively. Visibly, the FTIR spectra of 4-azidoacetanilide are simple. But, DFT calculations show that multiple combination bands can couple with the azide asymmetric stretch and generate different absorption profiles for different basis sets. Since the 6-311+G(d,p) basis set is suitable for describing the other two aryl-azide compounds, both theoretical spectra with the 6-311+G(d,p) basis set and the FTIR spectra in

NNDMA and THF solvents are shown in Figure 5.3. It shows that one peak results in higher intensity than azide asymmetric stretch in NNDMA solvent. This is due to the collection of combination bands present in it, such as Comb(25 39), Comb(20 45), and Comb(22 41). The shoulder peak next to this highest intensity peak is Comb(16 48). Based on the resonant coupling constant, both Comb(22 41) and Comb(16 48) cannot potentially couple with the azide asymmetric stretch. THF also has these high-intensity random peaks reflecting that these kinds of aryl-azides are not suitable as VPs. However, both spectra show that all these small peaks are left to the azide asymmetric stretch that can collectively contribute to the peaks in 2081 and 2101 cm^{-1} while the peak at ~2040 cm^{-1} can be Over(33).

Table 5.5 - Spectral characteristics of FTIR spectra of 4-azidoacetanilide

Peak	**Peak Position / cm^{-1}**		**Frequency shift / cm^{-1}**		**Relative peak Intensity**	
	NNDMA	**THF**	**NNDMA**	**THF**	**NNDMA**	**THF**
1	2080.6	2081.1	-37.3	-36.8	0.2941	0.2848
2	2101.1	2101.1	-16.8	-16.8	0.1379	0.1822
3	2117.9	2117.9	0	0	1	1
4	2147.1	2142.0	29.2	24.1	0.0640	0.1007

Table 5.6 - Spectral characteristics of B3LYP/6-311+G(d,p) spectra of 4-azidoacetanilide

Peak	**Frequency / cm^{-1}**		**Resonance Shift / cm^{-1}**		**Relative peak Intensity**	
	NNDMA	**THF**	**NNDMA**	**THF**	**NNDMA**	**THF**
Comb(22 39)	2078.1	2061.7	-98.6	-127.1	0.0566	0.0275
Comb(24 38)	2117.3	2096.7	-50.8	-74.1	0.0253	0.0083
Comb(24 39)	2119.2	2107.5	-41.0	-55.5	0.1091	0.0659
Comb(25 39)	2160.1	2133.0	-16.1	-31.9	0.0257	0.0018
Comb(20 45)	2165.0	2140.2	-7.3	-20.9	0.0892	0.1448
Fund(49)	2173.8	2174.4	0	0	1	1
Comb(24 40)	2184.6	2153.3	14.6	-13.1	0.0129	0.023
Over (33)	2244.6	2239.0	79.8	99.0	0.0236	0.0142

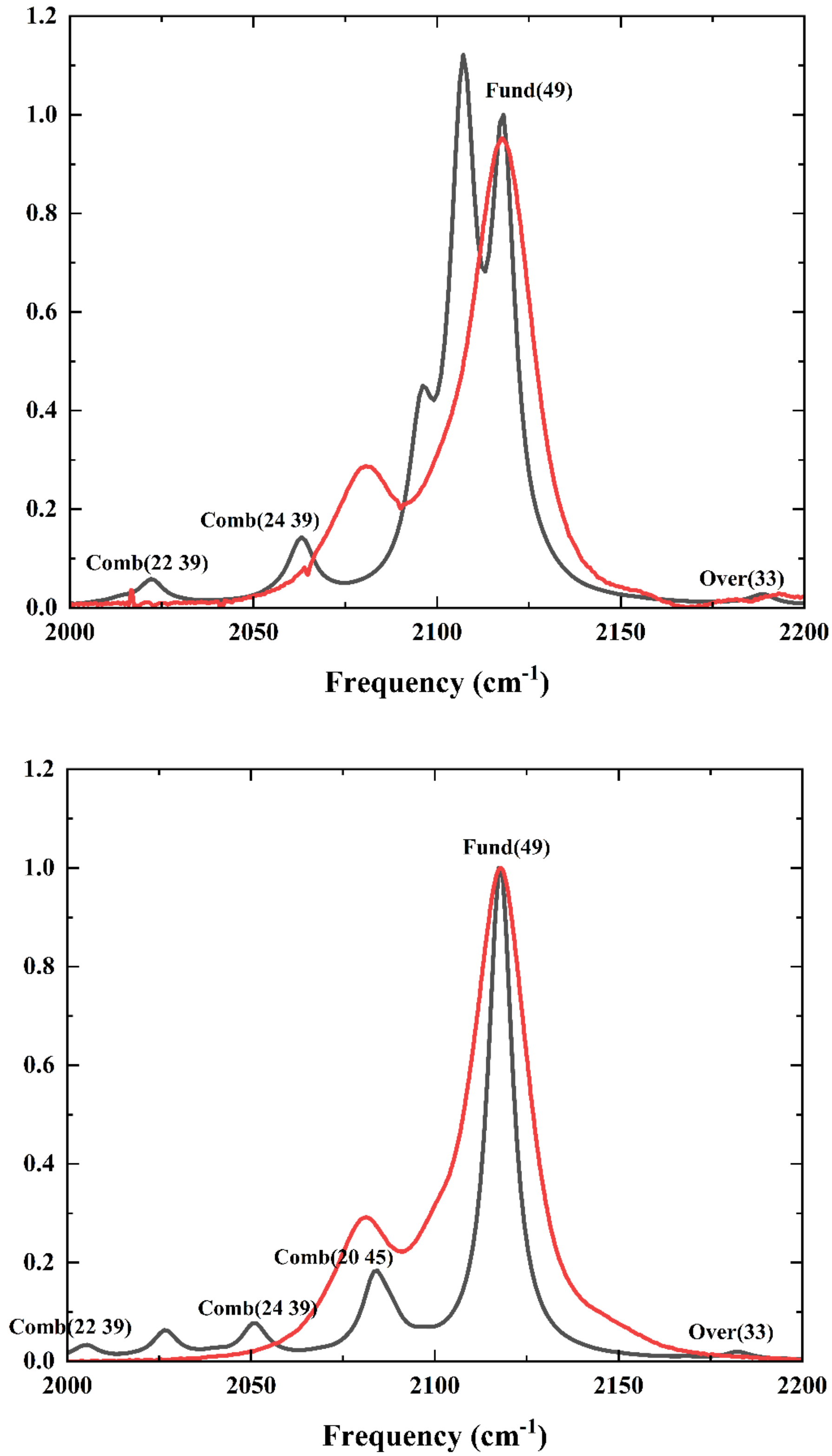

Figure 5.3 – FTIR (red) and DFT (black) spectra of 4-azidoacetanilide in NNDMA (top) and THF (bottom) solvents.

5.3 Overview

The final chapter compared the DFT calculated spectra and the FTIR spectra. DFT calculations have shown that multiple peaks are present within the azide absorption profile. Since the absorption profiles of FTIR spectra are congested, it is hard to state the number of peaks within it. On the other hand, DFT calculations have much wider azide absorption profiles. Most importantly, every basis set calculation shows the same vibrational modes contributing to the azide absorption profile except for molecules like 4-azidoacetanilide and 6-31G(d,p), 6-311G(d,p), and 6-311++G(df,pd) basis sets. Both 6-311+G(d,p) and 6-311++G(d,p) basis sets could explain the solvent effect for both 4-azidotoluene and 4-azido-N-phenylmaleimide molecules. This comparison shows how important to understand the complex absorption profile of azide asymmetric stretch before it is used in the applications such as VPs.

CHAPTER 6

CONCLUSION AND FUTURE WORK

6.1 Conclusion

Our study demonstrates how theoretical calculations can provide insight into the vibrational coupling and FRs in two aryl-azide compounds. Studying intensities, cubic force constants, and peak positions provide insight into what vibrational modes generate the complex absorption profile of these VPs. The basis set effects, solvent effects, and intramolecular effects were explored. In general, many studies of VPs only use a single basis set for the calculations. However, our study showed that it is difficult to predict the appropriate basis set. Even a high accurate basis set may produce erratic results. For example, the more diffused and polarized 6-311++G(df,pd) basis set provides unnecessary complications to the absorption profile. Therefore, it is important to test several basis sets.

The 6-31G(d,p) and 6-311G(d,p) are also not suitable because they exhibit high intensities for combination bands that are not potentially coupled with the azide asymmetric stretch due to the significant changes in dihedral angles between the azidophenyl ring and the para substituent. The changes in dihedral angle led to the changes in the region at para substituent in the HOMO orbital. Also, the 6-31++G(d,p) basis set introduces an unexpectedly intense peak for 4-azido-N-phenylmaleimide in THF solvent. After eliminating the basis sets listed above, 6-31+G(d,p), 6-311+G(d,p) and 6-311++G(d,p) basis sets are well in agreement with analyzing the vibrational spectra to understand vibrational coupling and FRs in aryl-azides except for molecules like 4-azidoacetanilide. Theoretical calculations of 4-azidoacetanilide showed a very complex absorption profile for azide asymmetric stretch when compared to 4-azidotoluene and 4-azido-N-phenylmaleimide reflecting that the use of 4-azidoacetanilide won't be a wise choice for experimental studies of protein structure and dynamics. Out of these basis sets, the 6-311+G(d,p) basis set would be the best basis set since it produces a less complicated absorption profile with less possible resonance. Although we recommended a 6-311+G(d,p) basis set to understand vibrational coupling and FRs, it also showed a high-intensity peak for combinations bands that can't couple with the azide asymmetric stretch for 4-azidoacetanilide. In this case, evaluating cubic force constants and TFR values give more insights into understanding vibrational coupling and FRs respectively.

The TFR parameter provides a direct estimation of which combination and overtone bands that can potentially couple with the azide asymmetric stretch. Since the TFR is calculated based on cubic force constants and resonance shifts, we can get a high TFR value if a combination band or overtone is very close to the fundamental vibration. In that case, we can ignore those modes based on their intensity and cubic force constant values.

In both solvents, we found that the same combination bands and overtones are involved in making FRs for all basis set calculations. In addition, those modes always consist of a high-intensity vibrational mode. For example, in 4-azidotoluene, mode 30 was involved in Comb(18 30), Comb(15 30), and Comb(17 30). In 4-azido-N-phenylmaleimide, mode 45 and mode 46 were involved in Comb(27 45) and Comb(27 46). In addition, modes 30, 15, 17, and 25 in 4-azidotoluene are similar to modes (45,46), 27, 26, and 39 in 4-azido-N-phenylmaleimide, respectively. Azide asymmetric stretch blue shift when substitution with methyl to maleimide group and solvent change from NNDMA to THF. Our study shows that azide-modified aryl compounds can be used as VPs if the absorption profile is not complicated as in 4-azidotoluene and 4-azido-N-phenylmaleimide. The anharmonic spectra of rotamers of 4-azido-N-phenylmaleimide depict similar features. DFT spectra can qualitatively describe the azide absorption profiles of FTIR spectra. But quantitively, theoretical calculations have multiple peaks within the azide absorption profile. For example, DFT calculations have shown that the azide absorption profile of 4-azidoacetanilide is more complicated than we see from the FTIR spectra.

6.2 Future Work

In this study, we mainly focused on the basis set effect, intramolecular effect, rotational isomerism effect, and solvent effect on the azide absorption profiles. The basis sets: 6-31G(d,p), 6-311G(d,p), and 6-311++G(df,pd) generate completely different absorption profiles from the other basis sets due to the structural changes in the optimized structures with different basis sets. Hence, it is interesting to study the azide absorption profile with one geometrically optimized structure with different basis set calculations for anharmonic frequency calculations. Recently, we have found that the erratic azide absorption profile of 6-31++G(d,p) basis set calculation in THF solvent for 4-azido-N-phenylmaleimide can be fixed by using 6-31G(d,p) and 6-31+G(d,p) optimized structure. It would also be great to analyze frequency calculations with different functionals other than B3LYP.

To further understand of intramolecular effect, it would be exciting to characterize azidophenyl with different electron-accepting and electron-donating para substituents. Moreover, investigating rotational isomers with different energies would be another inspiring goal. Further, aryl-azides in polar and non-polar solvents would provide more insights into the solvent effect on the azide absorption profile.

REFERENCES

1. Banwell, C. N., *Fundamentals of molecular spectroscopy*. McGraw-Hill: London; New York, 1966.

2. Merlin, J.-C.; Cornard, J.-P. A Pictorial Representation of Normal Modes of Vibration Using Vibrational Symmetry Coordinates. *J. Chem. Educ.* **2006,** *83* (9), 1393.

3. Morse, P. M. Diatomic Molecules According to the Wave Mechanics. II. Vibrational Levels. *Physical Review* **1929,** *34* (1), 57-64.

4. Fermi, E. Über den Ramaneffekt des Kohlendioxyds. *Zeitschrift für Physik* **1931,** *71* (3-4), 250-259.

5. Leitner, D. M. Energy Flow in Proteins. *Annu. Rev. Phys. Chem.* **2008,** *59* (1), 233-259.

6. Rodgers, J. M.; Abaskharon, R. M.; Ding, B.; Chen, J.; Zhang, W.; Gai, F. Fermi resonance as a means to determine the hydrogen-bonding status of two infrared probes. *Phys. Chem. Chem. Phys.* **2017,** *19* (24), 16144-16150.

7. Adhikary, R.; Zimmermann, J.; Romesberg, F. E. Transparent Window Vibrational Probes for the Characterization of Proteins With High Structural and Temporal Resolution. *Chem. Rev.* **2017,** *117*, 1927-1969.

8. Thielges, M. C. Transparent window 2D IR spectroscopy of proteins. *J. Chem. Phys.* **2021,** *155* (4), 040903.

9. Ma, J.; Pazos, I. M.; Zhang, W.; Culik, R. M.; Gai, F. Site-Specific Infrared Probes of Proteins. *Annu. Rev. Phys. Chem.* **2015,** *66*, 357-77.

10. Kim, H.; Cho, M. Infrared Probes for Studying the Structure and Dynamics of Biomolecules. *Chem. Rev.* **2013,** *113* (8), 5817-5847.

11. Choi, J.-H.; Oh, K.-I.; Lee, H.; Lee, C.; Cho, M. Nitrile and thiocyanate IR probes: Quantum chemistry calculation studies and multivariate least-square fitting analysis. *J. Chem. Phys.* **2008,** *128* (13), 134506.

12. Oh, K.-I.; Choi, J.-H.; Lee, J.-H.; Han, J.-B.; Lee, H.; Cho, M. Nitrile and thiocyanate IR probes: Molecular dynamics simulation studies. *J. Chem. Phys.* **2008,** *128* (15), 154504.

13. Choi, J.-H.; Cho, M. Vibrational solvatochromism and electrochromism of infrared probe molecules containing C≡O, C≡N, C=O, or C−F vibrational chromophore. *J. Chem. Phys.* **2011,** *134* (15), 154513.

14. Chin, J. K.; Jimenez, R.; Romesberg, F. E. Direct Observation of Protein Vibrations by Selective Incorporation of Spectroscopically Observable Carbon−Deuterium Bonds in Cytochrome c. *J. Am. Chem. Soc.* **2001,** *123* (10), 2426-2427.

15. Zimmermann, J.; Gundogdu, K.; Cremeens, M. E.; Bandaria, J. N.; Hwang, G. T.; Thielges, M. C.; Cheatum, C. M.; Romesberg, F. E. Efforts toward Developing Probes of Protein Dynamics: Vibrational Dephasing and Relaxation of Carbon–Deuterium Stretching Modes in Deuterated Leucine. *J. Phys. Chem. B* **2009,** *113* (23), 7991-7994.

16. Lam, Z.; Kong, K. V.; Olivo, M.; Leong, W. K. Vibrational spectroscopy of metal carbonyls for bio-imaging and -sensing. *Analyst* **2016,** *141* (5), 1569-1586.

17. Deiters, A.; Schultz, P. G. In vivo incorporation of an alkyne into proteins in Escherichia coli. *Bioorg. Med. Chem. Lett.* **2005,** *15* (5), 1521-4.

18. Zheng, M. L.; Zheng, D. C.; Wang, J. Non-Native Side Chain IR Probe in Peptides: Ab Initio Computation and 1D and 2D IR Spectral Simulation. *J. Phys. Chem. B* **2010,** *114* (6), 2327-2336.

19. Lee, G.; Kossowska, D.; Lim, J.; Kim, S.; Han, H.; Kwak, K.; Cho, M. Cyanamide as an Infrared Reporter: Comparison of Vibrational Properties between Nitriles Bonded to N and C Atoms. *J. Phys. Chem. B* **2018,** *122* (14), 4035-4044.

20. Fafarman, A. T.; Webb, L. J.; Chuang, J. I.; Boxer, S. G. Site-Specific Conversion of Cysteine Thiols into Thiocyanate Creates an IR Probe for Electric Fields in Proteins. *J. Am. Chem. Soc.* **2006,** *128* (41), 13356-13357.

21. Getahun, Z.; Huang, C. Y.; Wang, T.; De León, B.; DeGrado, W. F.; Gai, F. Using nitrile- derivatized amino acids as infrared probes of local environment. *J Am Chem Soc* **2003,** *125* (2), 405-11.

22. Waegele, M. M.; Tucker, M. J.; Gai, F. 5-Cyanotryptophan as an Infrared Probe of Local Hydration Status of Proteins. *Chem. Phys. Lett.* **2009,** *478* (4), 249-253.

23. Fafarman, A. T.; Boxer, S. G. Nitrile bonds as infrared probes of electrostatics in ribonuclease S. *J. Phys. Chem. B* **2010,** *114* (42), 13536-13544.

24. Thielges, M. C.; Axup, J. Y.; Wong, D.; Lee, H. S.; Chung, J. K.; Schultz, P. G.; Fayer, M. D. Two-dimensional IR spectroscopy of protein dynamics using two vibrational labels: a site-specific genetically encoded unnatural amino acid and an active site ligand. *J. Phys. Chem. B* **2011,** *115* (38), 11294-11304.

25. Bazewicz, C. G.; Lipkin, J. S.; Smith, E. E.; Liskov, M. T.; Brewer, S. H. Expanding the Utility of 4-Cyano-l-Phenylalanine As a Vibrational Reporter of Protein Environments. *J. Phys. Chem. B* **2012,** *116* (35), 10824-10831.

26. Shi, L.; Liu, X.; Shi, L.; Stinson, H. T.; Rowlette, J.; Kahl, L. J.; Evans, C. R.; Zheng, C.; Dietrich, L. E. P.; Min, W. Mid-infrared metabolic imaging with vibrational probes. *Nat. Methods* **2020,** *17* (8), 844-851.

27. Cai, K.; Liu, J.; Liu, Y.; Chen, F.; Yan, G.; Lin, H. Application of a transparent window vibrational probe (azido probe) to the structural dynamics of model dipeptides and amyloid β-peptide. *Spectrochim Acta A Mol Biomol Spectrosc* **2020,** *227*, 117681.

28. Chalyavi, F.; Adeyiga, O.; Weiner, J. M.; Monzy, J. N.; Schmitz, A. J.; Nguyen, J. K.; Fenlon, E. E.; Brewer, S. H.; Odoh, S. O.; Tucker, M. J. 2D-IR studies of cyanamides (NCN) as spectroscopic reporters of dynamics in biomolecules: Uncovering the origin of mysterious peaks. *J. Chem. Phys.* **2020,** *152* (7), 074201.

29. Gai, X. S.; Coutifaris, B. A.; Brewer, S. H.; Fenlon, E. E. A direct comparison of azide and nitrile vibrational probes. *Phys. Chem. Chem. Phys.* **2011,** *13* (13), 5926-5930.

30. Lee, H.; Choi, J.-H.; Cho, M. Vibrational solvatochromism and electrochromism of cyanide, thiocyanate, and azide anions in water. *Phys. Chem. Chem. Phys.* **2010,** *12* (39), 12658.

31. Wolfshorndl, M. P.; Baskin, R.; Dhawan, I.; Londergan, C. H. Covalently Bound Azido Groups Are Very Specific Water Sensors, Even in Hydrogen-Bonding Environments. *J. Phys. Chem. B* **2012,** *116* (3), 1172-1179.

32. Kossowska, D.; Park, K.; Park, J. Y.; Lim, C.; Kwak, K.; Cho, M. Rational Design of an Acetylenic Infrared Probe with Enhanced Dipole Strength and Increased Vibrational Lifetime. *J. Phys. Chem. B* **2019,** *123* (29), 6274-6281.

33. Kossowska, D.; Lee, G.; Han, H.; Kwak, K.; Cho, M. Simultaneous enhancement of transition dipole strength and vibrational lifetime of an alkyne IR probe via π-d backbonding and vibrational decoupling. *Phys. Chem. Chem. Phys.* **2019,** *21* (45), 24919-24925.

34. Park, K.-H.; Jeon, J.; Park, Y.; Lee, S.; Kwon, H.-J.; Joo, C.; Park, S.; Han, H.; Cho, M. Infrared Probes Based on Nitrile-Derivatized Prolines: Thermal Insulation Effect and Enhanced Dynamic Range. *J. Phys. Chem. Lett.* **2013,** *4* (13), 2105-2110.

35. Chalyavi, F.; Schmitz, A. J.; Fetto, N. R.; Tucker, M. J.; Brewer, S. H.; Fenlon, E. E. Extending the vibrational lifetime of azides with heavy atoms. *Phys. Chem. Chem. Phys.* **2020,** *22* (32), 18007-18013.

36. Levin, D. E.; Schmitz, A. J.; Hines, S. M.; Hines, K. J.; Tucker, M. J.; Brewer, S. H.; Fenlon, E. E. Synthesis and evaluation of the sensitivity and vibrational lifetimes of thiocyanate and selenocyanate infrared reporters. *RSC Adv.* **2016,** *6* (43), 36231-36237.

37. Maj, M.; Ahn, C.; Błasiak, B.; Kwak, K.; Han, H.; Cho, M. Isonitrile as an Ultrasensitive Infrared Reporter of Hydrogen-Bonding Structure and Dynamics. *J. Phys. Chem. B* **2016,** *120* (39), 10167-10180.

38. Dutta, S.; Cook, R. J.; Houtman, J. C. D.; Kohen, A.; Cheatum, C. M. Characterization of azido-NAD + to assess its potential as a two-dimensional infrared probe of enzyme dynamics. *Anal. Biochem.* **2010,** *407* (2), 241-246.

39. Nydegger, M. W.; Dutta, S.; Cheatum, C. M. Two-dimensional infrared study of 3-azidopyridine as a potential spectroscopic reporter of protonation state. *J. Chem. Phys.* **2010,** *133* (13), 134506.

40. Lieber, E.; Rao, C. N. R.; Thomas, A. E.; Oftedahl, E.; Minnis, R.; Nambury, C. V. N. Infrared spectra of acid azides, carbamyl azides and other azido derivatives: Anomalous splittings of the N3 stretching bands. *Spectrochim. Acta* **1963,** *19* (7), 1135-1144.

41. Lipkin, J. S.; Song, R.; Fenlon, E. E.; Brewer, S. H. Modulating Accidental Fermi Resonance: What a Difference a Neutron Makes. *J. Phys. Chem. Lett.* **2011,** *2* (14), 1672-1676.

42. Frisch, M. J.; Trucks, G. W.; Schlegel, H. B.; Scuseria, G. E.; Robb, M. A.; Cheeseman, J. R.; Scalmani, G.; Barone, V.; Petersson, G. A.; Nakatsuji, H., et al. *Gaussian 16 Rev. C.01*, Wallingford, CT, 2016.

43. M. A. Ratner, G. C. S., *Introduction to Quantum mechanics in Chemistry*. Prentice Hall, New Jersy, 2001.

44. Mardirossian, N.; Head-Gordon, M. Thirty years of density functional theory in computational chemistry: an overview and extensive assessment of 200 density functionals. *Mol. Phys.* **2017,** *115* (19), 2315-2372.

45. Becke, A. D. Density-functional exchange-energy approximation with correct asymptotic behavior. *Phys. Rev. A* **1988,** *38* (6), 3098-3100.

46. Lee, C.; Yang, W.; Parr, R. G. Development of the Colle-Salvetti correlation-energy formula into a functional of the electron density. *Phys. Rev. B* **1988,** *37* (2), 785-789.

47. Perdew, J. P.; Burke, K.; Wang, Y. Generalized gradient approximation for the exchange-correlation hole of a many-electron system. *Phys. Rev. B* **1996,** *54* (23), 16533-16539.

48. Perdew, J. P.; Chevary, J. A.; Vosko, S. H.; Jackson, K. A.; Pederson, M. R.; Singh, D. J.; Fiolhais, C. Atoms, molecules, solids, and surfaces: Applications of the generalized gradient approximation for exchange and correlation. *Phys. Rev. B* **1992,** *46* (11), 6671-6687.

49. Paier, J.; Marsman, M.; Kresse, G. Why does the B3LYP hybrid functional fail for metals? *J. Chem. Phys.* **2007,** *127* (2), 024103.

50. Barone, V. Anharmonic vibrational properties by a fully automated second-order perturbative approach. *J. Chem. Phys.* **2004,** *122* (1), 014108.

51. Helgaker, T.; Taylor, P. R., Gaussian Basis Sets and Molecular Integrals. In *Modern Electronic Structure Theory*, World Scientific Publishing Company: 1995; pp 725-856.

52. Slater, J. C. Atomic Shielding Constants. *Phys. Rev.* **1930,** *36* (1), 57-64.

53. Majumdar D., S. P. N., Roszak S., Leszczynski J., Slater-Type Orbitals. In *Basis Sets in Computational Chemistry*, E., P., Ed. Springer, Cham: Lecture Notes in Chemistry, 2021; Vol. 107.

54. Dunning T.H., H. P. J., Gaussian Basis Sets for Molecular Calculations. In *Methods of Electronic Structure Theory*, H.F., S., Ed. Springer, Boston, MA: Modern Theoretical Chemistry, 1977; Vol. 3.

55. Dunning, T. H. Gaussian Basis Functions for Use in Molecular Calculations. I. Contraction of (9s5p) Atomic Basis Sets for the First-Row Atoms. *J. Chem. Phys.* **1970,** *53* (7), 2823- 2833.

56. Woon, D. E.; Dunning, T. H. Gaussian basis sets for use in correlated molecular calculations. III. The atoms aluminum through argon. *J. Chem. Phys.* **1993,** *98* (2), 1358-1371.

57. Hehre, W. J.; Stewart, R. F.; Pople, J. A. Self-Consistent Molecular-Orbital Methods. I. Use of Gaussian Expansions of Slater-Type Atomic Orbitals. *J. Chem. Phys.* **1969,** *51* (6), 2657-2664.

58. Ditchfield, R.; Hehre, W. J.; Pople, J. A. Self-Consistent Molecular-Orbital Methods. IX. An Extended Gaussian-Type Basis for Molecular-Orbital Studies of Organic Molecules. *J. Chem. Phys.* **1971,** *54* (2), 724-728.

59. Hehre, W. J.; Ditchfield, R.; Pople, J. A. Self—Consistent Molecular Orbital Methods. I. Further Extensions of Gaussian—Type Basis Sets for Use in Molecular Orbital Studies of Organic Molecules. *J. Chem. Phys.* **1972,** *56* (5), 2257-2261.

60. Hariharan, P. C.; Pople, J. A. The influence of polarization functions on molecular orbital hydrogenation energies. *Theoretica chimica acta* **1973,** *28* (3), 213-222.

61. Ågren, H. Handbook of gaussian basis sets: A compendium for ab-initio molecular orbital calculations. By Raymond Poirier, Roy Kari, and Imre Csizmadia. Elsevier science publishers B.V., Amsterdem, 1985. *Int. J. Quantum Chem* **1987,** *32* (4), 549-549.

62. Schlegel, H. B. Geometry optimization. *WIREs Computational Molecular Science* **2011,** *1* (5), 790-809.

63. Pandey, H. D.; Leitner, D. M. Vibrational States and Nitrile Lifetimes of Cyanophenylalanine Isotopomers in Solution. *J. Phys. Chem. A* **2018,** *122* (34), 6856-6863.

64. Maitra, A.; Sarkar, S.; Leitner, D. M.; Dawlaty, J. M. Electric Fields Influence Intramolecular Vibrational Energy Relaxation and Line Widths. *J. Phys. Chem. Lett.* **2021,** *12* (32), 7818-7825.

65. Schmitz, A. J.; Pandey, H. D.; Chalyavi, F.; Shi, T.; Fenlon, E. E.; Brewer, S. H.; Leitner, D. M.; Tucker, M. J. Tuning Molecular Vibrational Energy Flow within an Aromatic Scaffold via Anharmonic Coupling. *J. Phys. Chem. A* **2019,** *123* (49), 10571-10581.

66. Tomasi, J.; Mennucci, B.; Cammi, R. Quantum Mechanical Continuum Solvation Models. *Chem. Rev.* **2005,** *105* (8), 2999-3094.

67. Miertuš, S.; Scrocco, E.; Tomasi, J. Electrostatic interaction of a solute with a continuum. A direct utilizaion of AB initio molecular potentials for the prevision of solvent effects. *Chem. Phys.* **1981,** *55* (1), 117-129.

68. Miertuš, S.; Tomasi, J. Approximate evaluations of the electrostatic free energy and internal energy changes in solution processes. *Chem. Phys.* **1982,** *65* (2), 239-245.

69. Tomasi, J.; Mennucci, B.; Cancès, E. The IEF version of the PCM solvation method: an overview of a new method addressed to study molecular solutes at the QM ab initio level. *Journal of Molecular Structure: THEOCHEM* **1999,** *464* (1), 211-226.

70. Mennucci, B.; Cancès, E.; Tomasi, J. Evaluation of Solvent Effects in Isotropic and Anisotropic Dielectrics and in Ionic Solutions with a Unified Integral Equation Method: Theoretical Bases, Computational Implementation, and Numerical Applications. *J. Phys. Chem. B* **1997,** *101* (49), 10506-10517.

71. Mennucci, B.; Tomasi, J. Continuum solvation models: A new approach to the problem of solute's charge distribution and cavity boundaries. *J. Chem. Phys.* **1997,** *106* (12), 5151- 5158.

72. Cancès, E.; Mennucci, B.; Tomasi, J. A new integral equation formalism for the polarizable continuum model: Theoretical background and applications to isotropic and anisotropic dielectrics. *J. Chem. Phys.* **1997,** *107* (8), 3032-3041.

73. Barone, V.; Cossi, M.; Tomasi, J. A new definition of cavities for the computation of solvation free energies by the polarizable continuum model. *J. Chem. Phys.* **1997,** *107* (8), 3210-3221.

74. Cossi, M.; Barone, V.; Cammi, R.; Tomasi, J. Ab initio study of solvated molecules: a new implementation of the polarizable continuum model. *Chem. Phys. Lett.* **1996,** *255* (4), 327-335.

75. Zhang, J.; Wang, L.; Zhang, J.; Zhu, J.; Pan, X.; Cui, Z.; Wang, J.; Fang, W.; Li, Y. Identifying and Modulating Accidental Fermi Resonance: 2D IR and DFT Study of 4-Azido-l-phenylalanine. *J. Phys. Chem. B* **2018,** *122* (34), 8122-8133.

76. Park, J. Y.; Mondal, S.; Kwon, H.-J.; Sahu, P. K.; Han, H.; Kwak, K.; Cho, M. Effect of isotope substitution on the Fermi resonance and vibrational lifetime of unnatural amino acids modified with IR probe: A 2D-IR and pump-probe study of 4-azido-L-phenyl alanine. *J. Chem. Phys.* **2020,** *153* (16), 164309.

77. Chin, J. W.; Santoro, S. W.; Martin, A. B.; King, D. S.; Wang, L.; Schultz, P. G. Addition of p-Azido-l-phenylalanine to the Genetic Code of Escherichia coli. *J. Am. Chem. Soc.* **2002,** *124* (31), 9026-9027.

78. Shao, N.; Singh, N. S.; Slade, S. E.; Jones, A. M. E.; Balasubramanian, M. K. Site Specific Genetic Incorporation of Azidophenylalanine in Schizosaccharomyces pombe. *Sci. Rep.* **2015,** *5* (1), 17196.

79. Ye, S.; Huber, T.; Vogel, R.; Sakmar, T. P. FTIR analysis of GPCR activation using azido probes. *Nat. Chem. Biol.* **2009,** *5* (6), 397-399.

80. Steinkellner, G.; Gruber, C. C.; Pavkov-Keller, T.; Binter, A.; Steiner, K.; Winkler, C.; Łyskowski, A.; Schwamberger, O.; Oberer, M.; Schwab, H., et al. Identification of promiscuous ene-reductase activity by mining structural databases using active site constellations. *Nat. Commun.* **2014,** *5* (1).

81. Hill, T. D. Enzyme Active site dynamics and substrate orientation probed via strong anharmonic coupling in an aryl-azide vibrational label using 2D IR Spectroscopy Southern Illinois University, Carbondale, 2020.

82. Perera S. M., Hill T. D., Moran S. D., Wang L. Exploring Aryl Azide Vibrational Probes Using DFT, 2D IR, and FTIR Studies. *(In preparation)* **2022**.

APPENDIX A

VIBRATIONAL MODES OF 4-AZIDOTOLUENE THAT OCCUR WITHIN ±130 CM^{-1}

FROM THE FUNDAMENTAL VIBRATION FOR SEVEN BASIS SETS IN NNDMA

i, j, k : vibrational modes ; where k = 38 (azide asymmetric stretch)

i = j → overtone & i ≠ j → combination band

K_{ijk} : cubic force constant

TFR : third-order Fermi resonance

ω(i), ω(j), ω(k) : anharmonic frequencies of i, j & k th mode

ω(ij) : anharmonic frequency of ij th mode

I(i), I(j), I(k) : anharmonic intensities of i, j & k th mode

I(ij) : anharmonic intensity of ij th mode

Δω' : ω(ij) - ω(k)

Δω : ω(i) + ω(j) - ω(k)

6-31G(d,p)

i	j	K_{ijk} / cm^{-1}	ω(i) / cm^{-1}	I(i) / km mol^{-1}	ω(j) / cm^{-1}	I(j) / km mol^{-1}	ω(ij) / cm^{-1}	I(ij) / km mol^{-1}	I(ij) / I(k)	Δω'	Δω	TFR
25	25	-33.12	1133.8	10.9	1133.8	10.9	2265.0	10.1	0.0885	67.3	69.9	0.474
24	24	-0.79	1131.0	11.6	1131.0	11.6	2261.2	0.0	0.0001	63.5	64.2	0.012
23	23	0.78	1062.0	6.3	1062.0	6.3	2090.3	0.2	0.0016	-107.4	-73.7	0.011
24	25	-2.45	1131.0	11.6	1133.8	10.9	2262.6	0.1	0.0006	65	67.1	0.037
23	27	0.71	1062.0	6.3	1211.7	2.5	2255.3	0.1	0.0007	57.6	76.1	0.009
23	26	0.70	1062.0	6.3	1202.6	1.6	2248.6	0.0	0.0003	50.9	66.9	0.010
23	25	0.99	1062.0	6.3	1133.8	10.9	2180.4	0.3	0.0022	-17.3	-1.9	0.529
22	27	-0.26	1006.0	10.5	1211.7	2.5	2226.6	0.0	0.0002	29	20.1	0.013
22	26	1.18	1006.0	10.5	1202.6	1.6	2217.0	1179.3	10.3326	19.4	10.9	0.109
22	25	3.21	1006.0	10.5	1133.8	10.9	2148.9	0.6	0.0052	-48.7	-57.9	0.055
22	24	-0.68	1006.0	10.5	1131.0	11.6	2144.8	0.0	0.0003	-52.9	-60.7	0.011
21	30	-2.53	992.9	13.9	1326.0	48.5	2322.3	0.1	0.0010	124.6	121.2	0.021

i	j	K_{ijk} / cm^{-1}	ω(i) / cm^{-1}	I(i) / km mol^{-1}	ω(j) / cm^{-1}	I(j) / km mol^{-1}	ω(ij) / cm^{-1}	I(ij) / km mol^{-1}	I(ij) / I(k)	Δω'	Δω	TFR
21	29	-0.42	992.9	13.9	1318.6	25.2	2311.7	0.0	0.0003	114.1	113.9	0.004
21	25	0.83	992.9	13.9	1133.8	10.9	2128.4	0.0	0.0004	-69.3	-71	0.012
19	30	0.89	936.6	0.6	1326.0	48.5	2265.8	0.0	0.0001	68.2	64.9	0.014
19	26	-0.32	936.6	0.6	1202.6	1.6	2139.4	0.0	0.0001	-58.2	-58.5	0.005
18	34	1.36	845.2	9.6	1487.9	9.1	2307.3	0.0	0.0002	109.6	135.4	0.010
18	31	-1.85	845.2	9.6	1396.3	5.0	2237.9	0.9	0.0082	40.2	43.8	0.042
18	30	47.16	845.2	9.6	1326.0	48.5	2153.6	14.0	0.1228	-44	-26.6	1.776
18	29	5.10	845.2	9.6	1318.6	25.2	2151.8	1.0	0.0087	-45.8	-33.9	0.151
18	28	5.94	845.2	9.6	1303.5	10.6	2138.6	0.8	0.0073	-59.1	-49	0.121
17	31	-0.44	828.9	14.9	1396.3	5.0	2231.1	0.0	0.0004	33.5	27.5	0.016
17	30	9.43	828.9	14.9	1326.0	48.5	2155.0	12.8	0.1121	-42.7	-42.9	0.220
17	29	1.04	828.9	14.9	1318.6	25.2	2144.0	0.0	0.0004	-53.7	-50.2	0.021
17	28	1.17	828.9	14.9	1303.5	10.6	2132.2	0.0	0.0003	-65.5	-65.3	0.018
16	33	0.24	809.3	12.2	1462.8	14.9	2269.9	0.0	0.0000	72.2	74.5	0.003
16	31	-0.35	809.3	12.2	1396.3	5.0	2220.8	0.1	0.0007	23.1	7.9	0.044
16	30	5.97	809.3	12.2	1326.0	48.5	2143.6	2.3	0.0202	-54	-62.4	0.096
16	29	0.52	809.3	12.2	1318.6	25.2	2136.2	0.0	0.0001	-61.5	-69.8	0.007
16	28	0.92	809.3	12.2	1303.5	10.6	2122.7	0.0	0.0002	-75	-84.9	0.011
15	35	7.68	758.7	8.9	1510.5	96.0	2270.8	1.8	0.0157	73.1	71.5	0.107
15	34	-1.35	758.7	8.9	1487.9	9.1	2231.2	0.4	0.0033	33.5	49	0.028
15	31	2.56	758.7	8.9	1396.3	5.0	2162.0	0.7	0.0065	-35.7	-42.7	0.060
15	30	-54.37	758.7	8.9	1326.0	48.5	2080.0	21.0	0.1839	-117.7	-113	0.481
15	29	-6.00	758.7	8.9	1318.6	25.2	2076.5	0.1	0.0013	-121.2	-120.4	0.050
14	35	0.40	705.8	0.0	1510.5	96.0	2217.5	0.0	0.0004	19.9	18.6	0.022
14	33	0.42	705.8	0.0	1462.8	14.9	2158.2	0.1	0.0005	-39.4	-29	0.015
13	37	0.24	644.5	1.1	1623.8	3.2	2266.5	0.0	0.0000	68.8	70.6	0.003
13	36	-0.53	644.5	1.1	1588.6	4.3	2232.0	0.0	0.0000	34.3	35.4	0.015
13	34	-0.25	644.5	1.1	1487.9	9.1	2116.9	0.0	0.0002	-80.8	-65.3	0.004
12	37	0.93	625.8	21.7	1623.8	3.2	2248.9	0.1	0.0011	51.2	51.9	0.018
12	36	1.30	625.8	21.7	1588.6	4.3	2212.4	0.6	0.0057	14.7	16.7	0.078
12	35	-4.14	625.8	21.7	1510.5	96.0	2137.7	1.1	0.0100	-59.9	-61.4	0.067
12	34	0.83	625.8	21.7	1487.9	9.1	2098.5	0.0	0.0000	-99.2	-84	0.010
3	38	-4.55	126.4	0.8	2197.7	114.1	2315.9	0.6	0.0051	118.2	126.4	0.036

6-31+G(d,p)

i	j	K_{ijk} / cm^{-1}	ω(i) / cm^{-1}	I(i) / km mol^{-1}	ω(j) / cm^{-1}	I(j) / km mol^{-1}	ω(ij) / cm^{-1}	I(ij) / km mol^{-1}	I(ij) / I(k)	Δω'	Δω	TFR
25	25	-32.55	1126.4	22.9	1126.4	22.9	2250.0	10.1	0.0130	69.1	72	0.452
24	24	-0.90	1118.3	9.8	1118.3	9.8	2234.5	0.0	0.0000	53.6	55.8	0.016
25	26	-11.54	1126.4	22.9	1185.1	2.3	2309.3	1.1	0.0014	128.5	130.6	0.088
24	26	-0.79	1118.3	9.8	1185.1	2.3	2301.2	0.5	0.0006	120.4	122.5	0.006
24	25	-3.38	1118.3	9.8	1126.4	22.9	2242.1	0.2	0.0002	61.2	63.9	0.053

i	j	K_{ijk} / cm^{-1}	ω(i) / cm^{-1}	I(i) / km mol^{-1}	ω(j) / cm^{-1}	I(j) / km mol^{-1}	ω(ij) / cm^{-1}	I(ij) / km mol^{-1}	I(ij) / I(k)	Δω'	Δω	TFR
23	27	0.54	1042.3	14.0	1203.5	4.0	2227.5	0.0	0.0000	46.7	65	0.008
23	26	0.48	1042.3	14.0	1185.1	2.3	2209.4	0.0	0.0000	28.5	46.5	0.01
23	25	0.70	1042.3	14.0	1126.4	22.9	2152.4	0.8	0.0010	-28.4	-12.2	0.058
22	27	-0.28	936.0	0.8	1203.5	4.0	2210.2	0.0	0.0000	29.3	-41.3	0.007
22	26	0.73	936.0	0.8	1185.1	2.3	2189.8	0.8	0.0010	8.9	-59.7	0.012
22	25	2.89	936.0	0.8	1126.4	22.9	2132.7	0.9	0.0012	-48.1	-118.4	0.024
22	24	-0.64	936.0	0.8	1118.3	9.8	2122.4	0.0	0.0001	-58.4	-126.5	0.005
21	29	-0.21	1060.4	4.8	1308.9	99.4	2303.3	0.0	0.0000	122.5	188.5	0.001
21	28	0.28	1060.4	4.8	1287.2	11.1	2295.2	0.1	0.0001	114.4	166.8	0.002
21	27	-0.25	1060.4	4.8	1203.5	4.0	2198.1	0.1	0.0001	17.2	83.1	0.003
21	26	-0.57	1060.4	4.8	1185.1	2.3	2180.8	0.8	0.0010	0	64.7	0.009
19	30	0.74	919.2	1.2	1330.4	6.5	2248.6	0.0	0.0000	67.7	68.7	0.011
18	34	-1.34	834.2	2.9	1512.9	9.9	2297.8	0.0	0.0000	116.9	166.3	0.008
18	33	0.25	834.2	2.9	1427.3	4.0	2238.0	0.0	0.0000	57.2	80.7	0.003
18	32	-0.31	834.2	2.9	1352.2	15.8	2244.8	0.0	0.0000	64	5.6	0.054
18	31	2.35	834.2	2.9	1392.4	4.1	2223.5	1.0	0.0013	42.7	45.8	0.051
18	30	-47.82	834.2	2.9	1330.4	6.5	2143.8	278.9	0.3578	-37.1	-16.2	2.944
18	29	-6.09	834.2	2.9	1308.9	99.4	2139.1	3.0	0.0038	-41.8	-37.7	0.162
18	28	-8.01	834.2	2.9	1287.2	11.1	2128.7	3.2	0.0041	-52.1	-59.5	0.135
17	31	-0.26	840.5	43.9	1392.4	4.1	2217.9	0.0	0.0000	37	52.1	0.005
17	30	4.47	840.5	43.9	1330.4	6.5	2149.9	7.1	0.0091	-31	-9.9	0.451
17	29	0.59	840.5	43.9	1308.9	99.4	2135.0	0.0	0.0000	-45.8	-31.4	0.019
17	28	0.74	840.5	43.9	1287.2	11.1	2123.0	0.0	0.0000	-57.9	-53.1	0.014
16	35	-0.46	780.4	10.8	1498.3	47.8	2286.9	0.0	0.0000	106.1	97.8	0.005
16	33	0.22	780.4	10.8	1427.3	4.0	2196.3	0.0	0.0000	15.4	26.8	0.008
16	31	-0.26	780.4	10.8	1392.4	4.1	2184.2	0.0	0.0000	3.3	-8	0.032
16	30	3.25	780.4	10.8	1330.4	6.5	2116.5	1.2	0.0015	-64.4	-70.1	0.046
16	29	0.31	780.4	10.8	1308.9	99.4	2101.5	0.0	0.0000	-79.3	-91.5	0.003
16	28	0.67	780.4	10.8	1287.2	11.1	2090.9	0.0	0.0000	-89.9	-113.3	0.006
15	35	7.36	753.9	12.1	1498.3	47.8	2252.0	1.6	0.0020	71.2	71.4	0.103
15	34	-1.37	753.9	12.1	1512.9	9.9	2222.9	0.3	0.0004	42	85.9	0.016
15	31	2.98	753.9	12.1	1392.4	4.1	2148.5	1.3	0.0017	-32.4	-34.5	0.086
15	30	-53.94	753.9	12.1	1330.4	6.5	2074.0	33.9	0.0435	-106.8	-96.6	0.559
15	29	-7.23	753.9	12.1	1308.9	99.4	2064.6	0.4	0.0005	-116.2	-118	0.061
15	28	-11.57	753.9	12.1	1287.2	11.1	2054.8	0.9	0.0012	-126	-139.8	0.083
14	35	0.25	681.4	0.5	1498.3	47.8	2176.0	0.0	0.0000	-4.8	-1.1	0.230
14	33	0.47	681.4	0.5	1427.3	4.0	2088.6	0.1	0.0001	-92.2	-72.1	0.007
13	37	0.28	645.0	0.6	1605.3	2.5	2253.8	0.0	0.0000	73	69.4	0.004
13	36	-0.62	645.0	0.6	1580.9	7.8	2225.3	0.0	0.0000	44.5	45.1	0.014
13	35	0.26	645.0	0.6	1498.3	47.8	2139.8	0.0	0.0000	-41	-37.6	0.007
13	34	-0.24	645.0	0.6	1512.9	9.9	2111.1	0.0	0.0000	-69.8	-23	0.011
12	37	1.05	618.2	23.7	1605.3	2.5	2228.9	0.1	0.0002	48.1	42.7	0.025
12	36	1.51	618.2	23.7	1580.9	7.8	2198.7	0.6	0.0008	17.9	18.3	0.083
12	35	-4.14	618.2	23.7	1498.3	47.8	2114.1	1.5	0.0020	-66.8	-64.3	0.064
12	34	0.86	618.2	23.7	1512.9	9.9	2085.6	0.0	0.0000	-95.3	-49.7	0.017
3	38	-5.69	117.0	1.0	2180.8	779.6	2285.4	0.7	0.0008	104.6	117	0.049

6-31++G(d,p)

i	j	K_{ijk} / cm^{-1}	ω(i) / cm^{-1}	I(i) / km mol^{-1}	ω(j) / cm^{-1}	I(j) / km mol^{-1}	ω(ij) / cm^{-1}	I(ij) / km mol^{-1}	I(ij) / I(k)	Δω'	Δω	TFR
25	25	-32.88	1128.3	14.2	1128.3	14.2	2256.1	10.3	0.0133	75.1	75.6	0.435
24	24	-0.71	1128	11.5	1128.0	11.5	2256.9	0.0	0.0000	76	75	0.009
23	23	0.64	1055.7	9.9	1055.7	9.9	2076.8	0.1	0.0001	-104.2	-69.5	0.009
24	25	-2.10	1128.0	11.5	1128.3	14.2	2256.1	0.0	0.0000	75.2	75.3	0.028
23	27	0.77	1055.7	9.9	1205.2	1.9	2241.4	0.1	0.0001	60.5	80	0.010
23	26	0.72	1055.7	9.9	1200.3	1.4	2240.1	0.0	0.0000	59.2	75	0.010
23	25	1.03	1055.7	9.9	1128.3	14.2	2169.3	1.4	0.0018	-11.7	3.1	0.338
22	26	0.85	1005.5	2.2	1200.3	1.4	2214.8	1.0	0.0013	33.8	24.8	0.034
22	25	2.90	1005.5	2.2	1128.3	14.2	2143.6	0.8	0.0011	-37.3	-47.1	0.061
22	24	-0.74	1005.5	2.2	1128.0	11.5	2141.7	0.1	0.0001	-39.3	-47.4	0.016
21	29	-0.43	985.1	31.1	1317.0	54.1	2306.2	0.0	0.0000	125.2	121.2	0.004
21	28	-0.20	985.1	31.1	1292.9	88.9	2287.6	0.0	0.0000	106.6	97.1	0.002
21	25	0.66	985.1	31.1	1128.3	14.2	2116.6	0.0	0.0001	-64.3	-67.6	0.010
19	30	0.93	940.1	2.4	1330.8	3.9	2266.8	0.0	0.0000	85.8	90	0.010
19	26	-0.27	940.1	2.4	1200.3	1.4	2142.5	0.0	0.0000	-38.5	-40.6	0.007
18	34	-1.32	834.2	3.0	1474.9	19.0	2291.9	0.0	0.0000	110.9	128.2	0.010
18	32	-0.33	834.2	3.0	1399.6	20.8	2249.0	0.0	0.0000	68.1	52.9	0.006
18	31	1.96	834.2	3.0	1381.0	2.6	2223.4	0.8	0.0010	42.4	34.3	0.057
18	30	-47.60	834.2	3.0	1330.8	3.9	2143.7	267.5	0.3431	-37.2	-15.9	2.987
18	29	-5.07	834.2	3.0	1317.0	54.1	2150.4	2.1	0.0027	-30.5	-29.7	0.171
18	28	-6.59	834.2	3.0	1292.9	88.9	2130.2	2.2	0.0028	-50.7	-53.8	0.122
17	31	-0.34	833.6	37.1	1381.0	2.6	2216.4	0.0	0.0000	35.4	33.7	0.010
17	30	6.09	833.6	37.1	1330.8	3.9	2148.1	12.2	0.0157	-32.9	-16.5	0.369
17	29	0.64	833.6	37.1	1317.0	54.1	2145.1	0.0	0.0000	-35.8	-30.3	0.021
17	28	0.86	833.6	37.1	1292.9	88.9	2122.9	0.0	0.0000	-58.1	-54.4	0.016
16	33	0.24	801.8	14.8	1451.1	12.8	2246.7	0.0	0.0000	65.8	71.9	0.003
16	31	-0.34	801.8	14.8	1381.0	2.6	2202.5	0.1	0.0001	21.6	1.9	0.181
16	30	5.06	801.8	14.8	1330.8	3.9	2135.0	2.9	0.0037	-45.9	-48.4	0.105
16	29	0.44	801.8	14.8	1317.0	54.1	2132.3	0.0	0.0000	-48.6	-62.1	0.007
16	28	0.85	801.8	14.8	1292.9	88.9	2111.3	0.0	0.0000	-69.6	-86.2	0.010
15	35	7.47	756.5	9.3	1506.4	51.0	2261.5	1.7	0.0022	80.6	81.9	0.091
15	34	-1.36	756.5	9.3	1474.9	19.0	2216.6	0.3	0.0004	35.6	50.5	0.027
15	31	2.67	756.5	9.3	1381.0	2.6	2148.4	1.1	0.0014	-32.5	-43.4	0.061
15	30	-54.40	756.5	9.3	1330.8	3.9	2073.5	33.9	0.0435	-107.5	-93.6	0.581
15	29	-5.98	756.5	9.3	1317.0	54.1	2076.1	0.2	0.0003	-104.8	-107.4	0.056
15	28	-9.95	756.5	9.3	1292.9	88.9	2056.3	0.7	0.0009	-124.7	-131.5	0.076
14	35	0.42	698.5	0.0	1506.4	51.0	2204.8	0.0	0.0001	23.9	24	0.018
14	33	0.47	698.5	0.0	1451.1	12.8	2134.8	0.1	0.0001	-46.1	-31.3	0.015
13	36	0.53	642.3	0.7	1580.4	5.6	2221.7	0.0	0.0000	40.8	41.8	0.013
12	37	1.02	621.6	26.8	1610.8	3.0	2234.2	0.1	0.0002	53.3	51.4	0.020
12	36	-1.50	621.6	26.8	1580.4	5.6	2200.1	0.6	0.0007	19.2	21	0.071
12	35	-4.17	621.6	26.8	1506.4	51.0	2126.5	1.6	0.0021	-54.4	-53	0.079
12	34	0.90	621.6	26.8	1474.9	19.0	2081.9	0.0	0.0000	-99	-84.4	0.011
3	38	-5.65	123.4	0.9	2180.9	779.5	2293.0	0.7	0.0008	112	123.4	0.046

6-311G(d,p)

i	j	K_{ijk} / cm^{-1}	ω(i) / cm^{-1}	I(i) / km mol^{-1}	ω(j) / cm^{-1}	I(j) / km mol^{-1}	ω(ij) / cm^{-1}	I(ij) / km mol^{-1}	I(ij) / I(k)	Δω'	Δω	TFR
25	25	-31.95	1129.8	11.3	1129.8	11.3	2256.9	9.8	0.0132	71.8	74.4	0.430
24	24	-1.13	1129.1	13.0	1129.1	13.0	2255.6	0.0	0.0000	70.4	73	0.015
23	23	0.56	1074.5	5.0	1074.5	5.0	2082.8	0.1	0.0001	-102.3	-36.1	0.016
24	25	-2.39	1129.1	13.0	1129.8	11.3	2255.9	0.1	0.0001	70.8	73.7	0.032
23	27	0.78	1074.5	5.0	1204.2	0.3	2244.6	0.1	0.0001	59.4	93.6	0.008
23	26	0.72	1074.5	5.0	1200.0	2.0	2242.1	0.0	0.0000	57	89.4	0.008
23	25	0.99	1074.5	5.0	1129.8	11.3	2172.5	0.5	0.0007	-12.6	19.2	0.052
22	28	1.03	1012.5	5.1	1282.0	74.8	2301.9	0.0	0.0000	116.8	109.3	0.009
22	26	1.01	1012.5	5.1	1200.0	2.0	2217.6	3.2	0.0043	32.5	27.3	0.037
22	25	2.67	1012.5	5.1	1129.8	11.3	2147.6	0.5	0.0007	-37.5	-42.9	0.062
22	24	-0.62	1012.5	5.1	1129.1	13.0	2144.8	0.0	0.0000	-40.4	-43.6	0.014
21	30	-3.15	991.6	17.8	1324.5	52.3	2312.5	0.2	0.0002	127.4	131	0.024
21	29	-0.39	991.6	17.8	1320.2	45.5	2311.0	0.0	0.0000	125.9	126.7	0.003
21	25	0.98	991.6	17.8	1129.8	11.3	2120.5	0.1	0.0001	-64.6	-63.8	0.015
19	30	-1.02	908.3	0.3	1324.5	52.3	2257.5	0.0	0.0000	72.4	47.7	0.022
19	26	0.33	908.3	0.3	1200.0	2.0	2134.4	0.0	0.0000	-50.7	-76.9	0.004
19	25	0.23	908.3	0.3	1129.8	11.3	2065.0	0.0	0.0000	-120.2	-147.1	0.002
18	34	-1.36	832.2	9.1	1484.7	15.8	2295.2	0.0	0.0000	110	131.8	0.010
18	32	-0.24	832.2	9.1	1401.4	5.6	2248.3	0.0	0.0000	63.2	48.5	0.005
18	31	2.16	832.2	9.1	1379.0	4.9	2224.6	1.2	0.0016	39.5	26.1	0.083
18	30	-48.03	832.2	9.1	1324.5	52.3	2144.4	174.9	0.2358	-40.8	-28.4	1.693
18	29	-1.82	832.2	9.1	1320.2	45.5	2152.8	0.2	0.0003	-32.3	-32.7	0.056
18	28	-4.98	832.2	9.1	1282.0	74.8	2116.7	0.4	0.0006	-68.4	-70.9	0.070
17	34	0.21	842.3	29.4	1484.7	15.8	2286.4	0.0	0.0000	101.3	141.9	0.001
17	31	-0.58	842.3	29.4	1379.0	4.9	2216.3	0.1	0.0001	31.1	36.2	0.016
17	30	10.66	842.3	29.4	1324.5	52.3	2145.2	25.3	0.0341	-39.9	-18.3	0.583
17	29	0.40	842.3	29.4	1320.2	45.5	2145.4	0.0	0.0000	-39.8	-22.6	0.018
16	34	0.23	801.9	7.3	1484.7	15.8	2277.8	0.0	0.0000	92.6	101.5	0.002
16	33	0.23	801.9	7.3	1448.5	32.3	2258.0	0.0	0.0000	72.9	65.3	0.004
16	31	-0.40	801.9	7.3	1379.0	4.9	2207.7	0.1	0.0001	22.5	-4.2	0.095
16	30	6.28	801.9	7.3	1324.5	52.3	2136.7	4.8	0.0065	-48.5	-58.7	0.107
16	28	0.73	801.9	7.3	1282.0	74.8	2101.2	0.0	0.0000	-83.9	-101.2	0.007
15	35	7.43	760.4	4.6	1502.1	7.4	2260.7	1.6	0.0022	75.5	77.3	0.096
15	34	-1.33	760.4	4.6	1484.7	15.8	2222.5	0.3	0.0004	37.4	60	0.022
15	31	2.90	760.4	4.6	1379.0	4.9	2151.6	1.0	0.0013	-33.5	-45.8	0.063
15	30	-54.60	760.4	4.6	1324.5	52.3	2076.0	26.8	0.0362	-109.2	-100.2	0.545
15	29	-1.36	760.4	4.6	1320.2	45.5	2080.9	0.0	0.0000	-104.3	-104.5	0.013
14	35	0.46	710.8	0.2	1502.1	7.4	2210.1	0.0	0.0000	25	27.8	0.016
14	33	0.50	710.8	0.2	1448.5	32.3	2153.1	0.1	0.0002	-32	-25.8	0.019
13	36	0.62	644.3	0.4	1573.4	3.7	2217.7	0.0	0.0000	32.6	32.5	0.019
13	34	-0.27	644.3	0.4	1484.7	15.8	2105.9	0.0	0.0000	-79.3	-56.2	0.005
12	37	1.03	625.9	23.1	1611.0	5.2	2235.8	0.1	0.0002	50.7	51.7	0.020
12	36	-1.16	625.9	23.1	1573.4	3.7	2198.9	0.5	0.0007	13.7	14.2	0.082
12	35	-3.98	625.9	23.1	1502.1	7.4	2126.7	1.3	0.0018	-58.5	-57.1	0.070
12	34	0.77	625.9	23.1	1484.7	15.8	2088.9	0.0	0.0000	-96.3	-74.5	0.010

6-311+G(d,p)

i	j	K_{ijk} / cm^{-1}	ω(i) / cm^{-1}	I(i) / km mol^{-1}	ω(j) / cm^{-1}	I(j) / km mol^{-1}	ω(ij) / cm^{-1}	I(ij) / km mol^{-1}	I(ij) / I(k)	Δω'	Δω	TFR
25	25	-31.44	1126.3	14.5	1126.3	14.5	2250.0	9.4	0.0120	76.1	78.7	0.399
24	24	-0.99	1127.8	17.6	1127.8	17.6	2258.3	0.0	0.0000	84.4	81.7	0.012
23	23	0.56	1043.6	3.8	1043.6	3.8	2076.5	0.0	0.0001	-97.4	-86.6	0.006
24	25	-2.30	1127.8	17.6	1126.3	14.5	2254.1	0.0	0.0001	80.2	80.2	0.029
23	27	0.81	1043.6	3.8	1203.3	3.6	2240.6	0.1	0.0001	66.7	73.1	0.011
23	26	0.73	1043.6	3.8	1205.1	1.4	2243.4	0.0	0.0000	69.5	74.9	0.010
23	25	1.04	1043.6	3.8	1126.3	14.5	2165.9	7.2	0.0092	-7.9	-4	0.262
22	28	0.94	1014.9	1.6	1280.7	56.1	2299.9	0.0	0.0000	126	121.7	0.008
22	26	0.77	1014.9	1.6	1205.1	1.4	2221.9	0.4	0.0005	48	46.1	0.017
22	25	2.46	1014.9	1.6	1126.3	14.5	2143.9	0.8	0.0010	-29.9	-32.7	0.075
22	24	-0.66	1014.9	1.6	1127.8	17.6	2145.8	0.1	0.0001	-28	-31.2	0.021
21	28	-0.29	993.6	11.9	1280.7	56.1	2275.2	0.0	0.0001	101.3	100.4	0.003
21	27	0.21	993.6	11.9	1203.3	3.6	2192.9	0.0	0.0000	19.1	23.1	0.009
21	25	0.89	993.6	11.9	1126.3	14.5	2117.4	0.1	0.0001	-56.4	-53.9	0.016
19	30	1.03	937.4	1.0	1319.1	49.8	2256.8	0.0	0.0000	82.9	82.6	0.012
19	26	-0.30	937.4	1.0	1205.1	1.4	2142.4	0.0	0.0000	-31.4	-31.3	0.010
19	25	-0.22	937.4	1.0	1126.3	14.5	2065.2	0.0	0.0000	-108.7	-110.1	0.002
18	34	-1.37	828.8	8.6	1470.3	15.8	2289.0	0.0	0.0000	115.1	125.2	0.011
18	32	-0.21	828.8	8.6	1402.4	8.2	2242.2	0.0	0.0000	68.3	57.3	0.004
18	31	2.02	828.8	8.6	1385.0	2.6	2220.8	0.7	0.0010	47	40	0.050
18	30	-48.36	828.8	8.6	1319.1	49.8	2135.9	260.0	0.3329	-37.9	-26	1.858
18	29	-1.65	828.8	8.6	1322.8	7.3	2153.1	0.4	0.0006	-20.8	-22.3	0.074
18	28	-5.58	828.8	8.6	1280.7	56.1	2112.3	1.0	0.0013	-61.6	-64.4	0.087
17	31	-0.45	837.1	14.6	1385.0	2.6	2214.9	0.0	0.0000	41	48.3	0.009
17	30	8.16	837.1	14.6	1319.1	49.8	2140.9	34.4	0.044	-33	-17.7	0.461
17	29	0.26	837.1	14.6	1322.8	7.3	2147.9	0.0	0.0000	-26	-13.9	0.019
17	28	0.95	837.1	14.6	1280.7	56.1	2106.9	0.0	0.0000	-67	-56.1	0.017
16	34	0.21	804.6	0.6	1470.3	15.8	2273.3	0.0	0.0000	99.5	101	0.002
16	33	0.25	804.6	0.6	1445.7	19.6	2252.6	0.0	0.0000	78.7	76.4	0.003
16	31	-0.34	804.6	0.6	1385.0	2.6	2205.2	0.0	0.0000	31.4	15.7	0.021
16	30	5.14	804.6	0.6	1319.1	49.8	2130.1	4.3	0.0055	-43.8	-50.2	0.102
16	28	0.68	804.6	0.6	1280.7	56.1	2097.5	0.0	0.0000	-76.4	-88.6	0.008
15	35	7.21	759.6	4.9	1499.5	62.5	2258.1	1.4	0.0018	84.2	85.2	0.085
15	34	-1.39	759.6	4.9	1470.3	15.8	2218.4	0.2	0.0002	44.5	56.1	0.025
15	31	2.77	759.6	4.9	1385.0	2.6	2151.9	1.5	0.0019	-22	-29.2	0.095
15	30	-55.62	759.6	4.9	1319.1	49.8	2070.5	41.8	0.0536	-103.4	-95.2	0.584
15	29	-1.20	759.6	4.9	1322.8	7.3	2083.2	0.0	0.0000	-90.7	-91.4	0.013
14	35	0.43	683.2	0.3	1499.5	62.5	2180.3	0.0	0.0000	6.4	8.8	0.049
14	33	0.50	683.2	0.3	1445.7	19.6	2121.7	0.2	0.0003	-52.1	-44.9	0.011
13	37	0.26	643.8	0.2	1605.4	5.7	2247.2	0.0	0.0000	73.3	75.4	0.003
13	36	0.57	643.8	0.2	1571.2	5.7	2215.2	0.0	0.0000	41.4	41.2	0.014
12	37	1.04	625.5	25.5	1605.4	5.7	2229.9	0.2	0.0002	56	57	0.018
12	36	-1.29	625.5	25.5	1571.2	5.7	2196.0	0.3	0.0004	22.2	22.8	0.056
12	35	-3.95	625.5	25.5	1499.5	62.5	2124.0	1.9	0.0025	-49.9	-48.9	0.081
12	34	0.80	625.5	25.5	1470.3	15.8	2084.6	0.0	0.0000	-89.3	-78.1	0.010
3	38	-5.60	125.6	1.1	2173.9	780.9	2302.4	0.7	0.0009	128.5	125.6	0.045

6-311++G(d,p)

i	j	K_{ijk} / cm^{-1}	ω(i) / cm^{-1}	I(i) / km mol^{-1}	ω(j) / cm^{-1}	I(j) / km mol^{-1}	ω(ij) / cm^{-1}	I(ij) / km mol^{-1}	I(ij) / I(k)	Δω'	Δω	TFR
25	25	-31.36	1125.7	16.0	1125.7	16.0	2248.8	9.4	0.0122	74.2	76.8	0.408
24	24	-0.99	1125.7	18.5	1125.7	18.5	2254.4	0.0	0.0000	79.8	76.9	0.013
23	23	0.58	1052.5	8.5	1052.5	8.5	2080.9	0.1	0.0001	-93.7	-69.6	0.008
24	25	-2.34	1125.7	18.5	1125.7	16.0	2251.4	0.0	0.0001	76.8	76.8	0.03
23	27	0.82	1052.5	8.5	1201.6	3.1	2241.7	0.1	0.0001	67.1	79.5	0.01
23	26	0.73	1052.5	8.5	1203.5	0.8	2243.5	0.0	0.0000	68.9	81.4	0.009
23	25	1.03	1052.5	8.5	1125.7	16.0	2167.5	5.8	0.0076	-7.1	3.6	0.285
22	28	0.95	1010.5	2.2	1283.8	89.9	2302.3	0.0	0.0000	127.7	119.7	0.008
22	26	0.76	1010.5	2.2	1203.5	0.8	2220.0	0.4	0.0005	45.4	39.3	0.019
22	25	2.46	1010.5	2.2	1125.7	16.0	2143.6	0.8	0.0011	-31	-38.4	0.064
22	24	-0.66	1010.5	2.2	1125.7	18.5	2144.2	0.1	0.0001	-30.4	-38.4	0.017
21	28	-0.28	990.4	23.0	1283.8	89.9	2273.8	0.0	0.0001	99.2	99.6	0.003
21	27	0.21	990.4	23.0	1201.6	3.1	2188.3	0.0	0.0000	13.7	17.4	0.012
21	25	0.88	990.4	23.0	1125.7	16.0	2113.3	0.1	0.0001	-61.3	-58.5	0.015
19	30	1.01	933.5	0.9	1321.9	38.5	2259.0	0.0	0.0000	84.4	80.8	0.013
19	26	-0.29	933.5	0.9	1203.5	0.8	2140.9	0.0	0.0000	-33.7	-37.6	0.008
18	34	-1.36	829.2	18.3	1487.1	31.9	2291.5	0.0	0.0000	116.9	141.7	0.01
18	31	2.03	829.2	18.3	1379.2	10.4	2221.8	0.8	0.0010	47.2	33.9	0.06
18	30	-48.25	829.2	18.3	1321.9	38.5	2137.3	273.1	0.3565	-37.3	-23.5	2.054
18	29	-1.59	829.2	18.3	1319.1	86.1	2151.4	0.4	0.0005	-23.2	-26.3	0.061
17	31	-0.46	838.3	36.4	1379.2	10.4	2215.6	0.0	0.0000	41	42.9	0.011
17	30	8.33	838.3	36.4	1321.9	38.5	2142.3	33.8	0.0441	-32.3	-14.5	0.576
17	29	0.25	838.3	36.4	1319.1	86.1	2146.0	0.0	0.0000	-28.6	-17.2	0.014
17	28	0.97	838.3	36.4	1283.8	89.9	2109.0	0.0	0.0000	-65.6	-52.5	0.018
16	34	0.21	801.5	4.8	1487.1	31.9	2274.8	0.0	0.0000	100.2	114	0.002
16	33	0.23	801.5	4.8	1444.1	42.8	2247.9	0.0	0.0000	73.3	71	0.003
16	31	-0.32	801.5	4.8	1379.2	10.4	2205.0	0.0	0.0000	30.4	6.2	0.052
16	30	5.00	801.5	4.8	1321.9	38.5	2132.1	4.2	0.0055	-42.5	-51.2	0.098
16	28	0.66	801.5	4.8	1283.8	89.9	2098.4	0.0	0.0000	-76.2	-89.3	0.007
15	35	7.22	760.4	6.0	1498.7	33.1	2257.9	1.4	0.0019	83.3	84.5	0.085
15	34	-1.38	760.4	6.0	1487.1	31.9	2221.2	0.2	0.0002	46.6	72.8	0.019
15	31	2.79	760.4	6.0	1379.2	10.4	2153.0	1.5	0.0019	-21.6	-35	0.08
15	30	-55.66	760.4	6.0	1321.9	38.5	2072.3	41.4	0.0541	-102.3	-92.4	0.603
15	29	-1.14	760.4	6.0	1319.1	86.1	2081.7	0.0	0.0000	-92.9	-95.1	0.012
15	28	-8.69	760.4	6.0	1283.8	89.9	2046.1	0.5	0.0006	-128.5	-130.4	0.067
14	35	0.46	689.4	0.2	1498.7	33.1	2186.8	0.0	0.0000	12.2	13.5	0.034
14	33	0.50	689.4	0.2	1444.1	42.8	2124.9	0.3	0.0003	-49.7	-41.1	0.012
13	37	0.26	643.7	0.9	1605.5	4.1	2247.2	0.0	0.0000	72.6	74.6	0.003
13	36	0.57	643.7	0.9	1571.1	6.5	2214.4	0.0	0.0000	39.8	40.1	0.014
12	37	1.04	622.7	26.2	1605.5	4.1	2227.2	0.2	0.0002	52.6	53.6	0.019
12	36	-1.28	622.7	26.2	1571.1	6.5	2192.6	0.4	0.0005	18	19.1	0.067
12	35	-3.97	622.7	26.2	1498.7	33.1	2120.8	1.9	0.0025	-53.8	-53.2	0.075
12	34	0.81	622.7	26.2	1487.1	31.9	2084.3	0.0	0.0000	-90.3	-64.8	0.012
3	38	-5.75	133.4	0.8	2174.6	766.1	2296.4	0.7	0.0009	121.8	133.4	0.043

6-311++G(df,pd)

i	j	K_{ijk} / cm^{-1}	ω(i) / cm^{-1}	I(i) / km mol^{-1}	ω(j) / cm^{-1}	I(j) / km mol^{-1}	ω(ij) / cm^{-1}	I(ij) / km mol^{-1}	I(ij) / I(k)	Δω'	Δω	TFR
26	26	-3.81	1160.8	3.4	1160.8	3.4	2238.4	0.0	0.0001	63.8	147.1	0.026
25	25	-31.40	1125.2	14.2	1125.2	14.2	2250.9	8.4	0.0113	76.3	75.7	0.415
24	24	-1.58	1054.1	19.4	1054.1	19.4	2200.1	0.0	0.0000	25.5	-66.4	0.024
23	23	0.56	1038.4	2.0	1038.4	2.0	2092.9	0.0	0.0001	-81.7	-97.8	0.006
25	26	-10.82	1125.2	14.2	1160.8	3.4	2246.5	0.8	0.0010	71.9	111.4	0.097
24	26	-1.37	1054.1	19.4	1160.8	3.4	2218.6	0.6	0.0008	43.9	40.3	0.034
24	25	-4.81	1054.1	19.4	1125.2	14.2	2225.4	0.3	0.0004	50.8	4.7	1.025
23	27	0.66	1038.4	2.0	1201.8	3.0	2241.2	0.1	0.0001	66.6	65.6	0.01
23	26	0.54	1038.4	2.0	1160.8	3.4	2168.2	0.0	0.0000	-6.4	24.6	0.022
23	25	0.80	1038.4	2.0	1125.2	14.2	2174.7	7.6	0.0102	0	-11	0.072
22	29	-0.50	1072.9	7.2	1275.3	14.9	2266.1	0.3	0.0004	91.5	173.6	0.003
22	26	0.59	1072.9	7.2	1160.8	3.4	2113.3	0.2	0.0002	-61.3	59.1	0.01
22	25	2.32	1072.9	7.2	1125.2	14.2	2122.1	1.3	0.0017	-52.6	23.4	0.099
22	24	-0.50	1072.9	7.2	1054.1	19.4	2093.9	0.1	0.0001	-80.7	-47.6	0.01
21	34	-0.92	805.3	25.0	1509.7	36.8	2281.7	0.4	0.0005	107.1	140.4	0.007
21	30	-0.53	805.3	25.0	1323.2	90.2	2250.5	0.0	0.0001	75.9	-46.2	0.011
21	29	-0.43	805.3	25.0	1275.3	14.9	2197.6	0.0	0.0000	23	-94	0.005
21	27	-0.21	805.3	25.0	1201.8	3.0	2123.6	0.1	0.0001	-51	-167.5	0.001
21	26	-0.40	805.3	25.0	1160.8	3.4	2046.3	1.2	0.0016	-128.4	-208.5	0.002
21	25	0.28	805.3	25.0	1125.2	14.2	2057.1	0.0	0.0001	-117.5	-244.1	0.001
19	30	0.85	950.6	2.0	1323.2	90.2	2227.7	0.0	0.0000	53.1	99.1	0.009
18	34	-0.97	829.8	28.2	1509.7	36.8	2192.7	0.0	0.0000	18.1	164.9	0.006
18	33	0.32	829.8	28.2	1437.6	7.6	2285.8	0.0	0.0000	111.1	92.7	0.003
18	32	-0.26	829.8	28.2	1404.3	4.4	2233.3	0.0	0.0000	58.6	59.5	0.004
18	31	1.90	829.8	28.2	1205.2	5.5	2176.4	0.5	0.0007	1.7	-139.6	0.014
18	30	-36.32	829.8	28.2	1323.2	90.2	2138.1	322.5	0.4334	-36.5	-21.7	1.673
18	29	-1.97	829.8	28.2	1275.3	14.9	2103.8	1.1	0.0015	-70.8	-69.5	0.028
18	28	-4.58	829.8	28.2	1286.7	29.2	2113.3	0.8	0.0011	-61.3	-58.1	0.079
17	34	0.82	843.8	2.4	1509.7	36.8	2189.3	0.0	0.0000	14.7	178.9	0.005
17	31	-1.79	843.8	2.4	1205.2	5.5	2173.7	0.4	0.0006	-0.9	-125.6	0.014
17	30	32.57	843.8	2.4	1323.2	90.2	2150.4	5.6	0.0076	-24.2	-7.6	4.266
17	29	1.76	843.8	2.4	1275.3	14.9	2101.1	0.8	0.0011	-73.5	-55.4	0.032
17	28	4.12	843.8	2.4	1286.7	29.2	2110.8	0.6	0.0008	-63.8	-44.1	0.094
16	35	-0.49	774.2	11.1	1473.8	26.5	2236.4	0.0	0.0000	61.8	73.4	0.007
16	31	-0.34	774.2	11.1	1205.2	5.5	2099.3	0.0	0.0000	-75.4	-195.2	0.002
16	30	4.36	774.2	11.1	1323.2	90.2	2076.4	8.7	0.0117	-98.2	-77.3	0.056
15	35	7.00	714.6	14.8	1473.8	26.5	2221.9	1.1	0.0015	47.3	13.8	0.508
15	34	-1.28	714.6	14.8	1509.7	36.8	2099.8	0.1	0.0002	-74.8	49.7	0.026
15	31	3.35	714.6	14.8	1205.2	5.5	2085.7	2.4	0.0032	-88.9	-254.8	0.013

i	j	K_{ijk} / cm^{-1}	ω(i) / cm^{-1}	I(i) / km mol^{-1}	ω(j) / cm^{-1}	I(j) / km mol^{-1}	ω(ij) / cm^{-1}	I(ij) / km mol^{-1}	I(ij) / I(k)	Δω’	Δω	TFR
15	30	-55.96	714.6	14.8	1323.2	90.2	2054.3	49.0	0.0659	-120.4	-136.9	0.409
14	35	0.31	696.9	0.2	1473.8	26.5	2176.7	0.0	0.0000	2	-4	0.078
14	33	0.51	696.9	0.2	1437.6	7.6	2150.2	0.4	0.0005	-24.5	-40.2	0.013
13	37	0.26	645.1	0.2	1598.3	11.9	2240.7	0.0	0.0000	66.1	68.8	0.004
13	36	0.63	645.1	0.2	1568.2	1.4	2214.9	0.0	0.0000	40.3	38.7	0.016
13	35	0.29	645.1	0.2	1473.8	26.5	2125.1	0.0	0.0000	-49.5	-55.7	0.005
12	37	1.08	621.1	24.6	1598.3	11.9	2217.6	0.2	0.0002	42.9	44.8	0.024
12	36	-1.21	621.1	24.6	1568.2	1.4	2190.2	0.3	0.0003	15.6	14.7	0.082
12	35	-3.86	621.1	24.6	1473.8	26.5	2101.5	2.4	0.0032	-73.2	-79.7	0.048
3	38	-5.64	107.9	0.7	2174.6	744.0	2260.0	0.7	0.0010	85.4	107.9	0.052

APPENDIX B

VIBRATIONAL MODES OF 4-AZIDOTOLUENE THAT OCCUR WITHIN ±130 CM^{-1}

FROM THE FUNDAMENTAL VIBRATION FOR SEVEN BASIS SETS IN THF

i, j, k : vibrational modes ; where k = 38 (azide asymmetric stretch)

i = j → overtone & i ≠ j → combination band

K_{ijk} : cubic force constant

TFR : third-order Fermi resonance

ω(i), ω(j), ω(k) : anharmonic frequencies of i, j & k th mode

ω(ij) : anharmonic frequency of ij th mode

I(i), I(j), I(k) : anharmonic intensities of i, j & k th mode

I(ij) : anharmonic intensity of ij th mode

Δω' : ω(ij) - ω(k)

Δω : ω(i) + ω(j) - ω(k)

6-31G(d,p)

i	j	K_{ijk} / cm^{-1}	ω(i) / cm^{-1}	I(i) / km mol^{-1}	ω(j) / cm^{-1}	I(j) / km mol^{-1}	ω(ij) / cm^{-1}	I(ij) / km mol^{-1}	I(ij) / I(k)	Δω'	Δω	TFR
25	25	-33.43	1133.6	5.8	1133.6	5.8	2264.5	10.0	0.0144	64.7	67.2	0.497
24	24	-0.81	1132.1	13.0	1132.1	13.0	2264.8	0.0	0.0000	64.9	64.3	0.013
23	23	0.75	1047.9	5.7	1047.9	5.7	2077.7	0.2	0.0003	-122.1	-104.1	0.007
24	25	-2.49	1132.1	13.0	1133.6	5.8	2264.3	0.1	0.0001	64.4	65.8	0.038
23	27	0.68	1047.9	5.7	1211.5	2.0	2248.9	0.1	0.0001	49	59.5	0.011
23	26	0.68	1047.9	5.7	1202.3	2.0	2241.7	0.0	0.0001	41.8	50.3	0.013
23	25	0.96	1047.9	5.7	1133.6	5.8	2174.0	0.2	0.0002	-25.9	-18.4	0.052
22	28	0.26	1018.4	3.7	1305.7	128.5	2322.8	0.0	0.0000	123	124.3	0.002
22	27	-0.28	1018.4	3.7	1211.5	2.0	2229.7	0.0	0.0000	29.9	30	0.009
22	26	1.26	1018.4	3.7	1202.3	2.0	2220.0	28.8	0.0415	20.2	20.8	0.061
22	25	3.27	1018.4	3.7	1133.6	5.8	2151.9	0.5	0.0008	-48	-47.9	0.068

i	j	K_{ijk} / cm^{-1}	ω(i) / cm^{-1}	I(i) / km mol^{-1}	ω(j) / cm^{-1}	I(j) / km mol^{-1}	ω(ij) / cm^{-1}	I(ij) / km mol^{-1}	I(ij) / I(k)	Δω'	Δω	TFR
22	24	-0.66	1018.4	3.7	1132.1	13.0	2150.2	0.0	0.0000	-49.7	-49.4	0.013
21	30	-2.23	982.0	13.4	1329.7	112.2	2310.8	0.1	0.0001	110.9	111.8	0.020
21	29	-0.42	982.0	13.4	1315.0	7.8	2295.2	0.0	0.0000	95.3	97.2	0.004
21	25	0.74	982.0	13.4	1133.6	5.8	2114.6	0.0	0.0001	-85.3	-84.3	0.009
19	30	0.84	937.9	1.3	1329.7	112.2	2268.6	0.0	0.0000	68.7	67.7	0.012
19	26	-0.31	937.9	1.3	1202.3	2.0	2139.1	0.0	0.0000	-60.7	-59.8	0.005
18	34	1.33	829.6	14.7	1470.8	4.4	2288.7	0.0	0.0000	88.8	100.6	0.013
18	32	0.23	829.6	14.7	1414.2	6.4	2256.0	0.0	0.0000	56.1	43.9	0.005
18	31	-1.80	829.6	14.7	1387.5	1.5	2227.5	0.9	0.0013	27.6	17.2	0.105
18	30	47.33	829.6	14.7	1329.7	112.2	2154.6	109.2	0.1574	-45.3	-40.6	1.167
18	29	5.38	829.6	14.7	1315.0	7.8	2147.9	0.9	0.0013	-51.9	-55.2	0.097
18	28	5.50	829.6	14.7	1305.7	128.5	2137.5	0.6	0.0008	-62.4	-64.6	0.085
17	31	-0.43	843.8	10.8	1387.5	1.5	2223.1	0.0	0.0001	23.2	31.4	0.014
17	30	9.22	843.8	10.8	1329.7	112.2	2158.0	9.9	0.0143	-41.9	-26.4	0.349
17	29	1.06	843.8	10.8	1315.0	7.8	2142.3	0.0	0.0000	-57.6	-41.1	0.026
17	28	1.05	843.8	10.8	1305.7	128.5	2133.5	0.0	0.0000	-66.4	-50.4	0.021
16	31	-0.33	812.9	10.2	1387.5	1.5	2214.7	0.1	0.0001	14.8	0.6	0.605
16	30	5.87	812.9	10.2	1329.7	112.2	2149.9	1.9	0.0027	-50	-57.2	0.103
16	29	0.53	812.9	10.2	1315.0	7.8	2136.7	0.0	0.0000	-63.2	-71.9	0.007
16	28	0.86	812.9	10.2	1305.7	128.5	2126.0	0.0	0.0000	-73.9	-81.2	0.011
15	35	7.85	758.8	8.7	1511.4	91.2	2271.8	1.8	0.0027	71.9	70.4	0.112
15	34	-1.32	758.8	8.7	1470.8	4.4	2214.3	0.4	0.0005	14.4	29.8	0.045
15	31	2.47	758.8	8.7	1387.5	1.5	2153.0	0.6	0.0009	-46.9	-53.6	0.046
15	30	-54.47	758.8	8.7	1329.7	112.2	2082.2	18.7	0.0270	-117.7	-111.4	0.489
15	29	-6.39	758.8	8.7	1315.0	7.8	2074.2	0.2	0.0002	-125.7	-126.1	0.051
14	35	0.39	704.5	0.0	1511.4	91.2	2217.0	0.1	0.0001	17.2	16	0.024
14	33	-0.42	704.5	0.0	1457.8	9.7	2161.0	0.0	0.0001	-38.9	-37.6	0.011
13	36	-0.51	644.3	0.4	1589.3	5.7	2232.4	0.0	0.0000	32.5	33.7	0.015
12	37	0.92	625.5	19.3	1624.5	2.8	2249.0	0.1	0.0002	49.2	50.2	0.018
12	36	1.28	625.5	19.3	1589.3	5.7	2212.7	0.7	0.0011	12.8	14.9	0.086
12	35	-4.20	625.5	19.3	1511.4	91.2	2138.4	1.0	0.0015	-61.5	-62.9	0.067
12	34	0.79	625.5	19.3	1470.8	4.4	2081.2	0.0	0.0000	-118.6	-103.5	0.008
3	38	-4.30	132.3	0.7	2199.9	693.9	2324.3	0.5	0.0008	124.4	132.3	0.032

6-31+G(d,p)

i	j	K_{ijk} / cm^{-1}	ω(i) / cm^{-1}	I(i) / km mol^{-1}	ω(j) / cm^{-1}	I(j) / km mol^{-1}	ω(ij) / cm^{-1}	I(ij) / km mol^{-1}	I(ij) / I(k)	Δω'	Δω	TFR
25	25	-32.88	1128.6	19.6	1128.6	19.6	2252.5	10.1	0.0137	68.0	72.7	0.453
24	24	-0.93	1114.1	8.4	1114.1	8.4	2230.8	0.0	0.0000	46.3	43.7	0.021
23	23	0.58	1039.3	3.3	1039.3	3.3	2054.8	0.1	0.0001	-129.7	-105.9	0.005
25	26	-11.92	1128.6	19.6	1187.9	2.4	2310.6	1.1	0.0015	126.2	132.0	0.090
24	26	-0.85	1114.1	8.4	1187.9	2.4	2299.7	0.4	0.0006	115.2	117.5	0.007
24	25	-3.28	1114.1	8.4	1128.6	19.6	2241.4	0.1	0.0002	57.0	58.2	0.056
23	27	0.54	1039.3	3.3	1204.0	2.8	2231.0	0.0	0.0001	46.5	58.9	0.009
23	26	0.48	1039.3	3.3	1187.9	2.4	2211.9	0.0	0.0000	27.5	42.7	0.011
23	25	0.72	1039.3	3.3	1128.6	19.6	2156.7	0.4	0.0006	-27.7	-16.6	0.044
22	29	-0.70	1006.3	2.0	1311.4	40.5	2305.6	0.3	0.0004	121.1	133.3	0.005
22	27	-0.29	1006.3	2.0	1204.0	2.8	2205.7	0.0	0.0000	21.3	25.9	0.011
22	26	0.86	1006.3	2.0	1187.9	2.4	2185.0	1.4	0.0019	0.5	9.8	0.088
22	25	2.93	1006.3	2.0	1128.6	19.6	2129.0	0.7	0.0010	-55.4	-49.6	0.059
22	24	-0.62	1006.3	2.0	1114.1	8.4	2115.8	0.0	0.0000	-68.7	-64.0	0.010
21	30	0.62	967.7	4.1	1328.7	23.5	2301.1	0.0	0.0000	116.6	111.9	0.006
21	29	-0.23	967.7	4.1	1311.4	40.5	2278.3	0.0	0.0000	93.9	94.6	0.002
21	28	0.22	967.7	4.1	1276.8	13.9	2272.0	0.0	0.0001	87.5	60.1	0.004
21	27	-0.23	967.7	4.1	1204.0	2.8	2177.7	0.1	0.0001	-6.8	-12.7	0.018
21	26	-0.52	967.7	4.1	1187.9	2.4	2159.1	0.4	0.0005	-25.4	-28.9	0.018
19	30	0.76	923.2	1.6	1328.7	23.5	2250.8	0.0	0.0000	66.4	67.4	0.011
19	29	0.23	923.2	1.6	1311.4	40.5	2231.1	0.0	0.0000	46.6	50.1	0.005
19	26	-0.27	923.2	1.6	1187.9	2.4	2109.1	0.0	0.0000	-75.4	-73.4	0.004
18	34	-1.28	834.7	2.2	1479.2	4.2	2300.8	0.0	0.0000	116.3	129.4	0.010
18	33	0.21	834.7	2.2	1431.9	5.4	2239.6	0.0	0.0000	55.1	82.1	0.003
18	32	-0.46	834.7	2.2	1367.9	7.9	2245.2	0.0	0.0001	60.8	18.1	0.026
18	31	2.24	834.7	2.2	1404.2	5.3	2217.2	1.0	0.0014	32.8	54.5	0.041
18	30	-47.90	834.7	2.2	1328.7	23.5	2146.5	237.7	0.3234	-37.9	-21.1	2.270
18	29	-6.34	834.7	2.2	1311.4	40.5	2136.8	2.5	0.0033	-47.7	-38.4	0.165
18	28	-7.40	834.7	2.2	1276.8	13.9	2127.9	2.1	0.0029	-56.6	-72.9	0.101
17	31	-0.26	833.0	33.8	1404.2	5.3	2210.3	0.0	0.0000	25.8	52.8	0.005
17	30	4.87	833.0	33.8	1328.7	23.5	2150.9	6.1	0.0083	-33.6	-22.8	0.213
17	29	0.68	833.0	33.8	1311.4	40.5	2131.4	0.0	0.0000	-53.1	-40.1	0.017
17	28	0.74	833.0	33.8	1276.8	13.9	2120.9	0.0	0.0000	-63.5	-74.7	0.010
16	35	-0.51	792.7	11.0	1499.2	45.7	2294.8	0.0	0.0000	110.3	107.5	0.005
16	33	0.23	792.7	11.0	1431.9	5.4	2204.6	0.0	0.0000	20.1	40.2	0.006
16	31	-0.27	792.7	11.0	1404.2	5.3	2184.0	0.0	0.0001	-0.5	12.5	0.022
16	30	3.38	792.7	11.0	1328.7	23.5	2124.9	1.0	0.0014	-59.5	-63.1	0.054
16	29	0.31	792.7	11.0	1311.4	40.5	2106.6	0.0	0.0000	-77.9	-80.3	0.004
16	28	0.67	792.7	11.0	1276.8	13.9	2096.3	0.0	0.0000	-88.2	-114.9	0.006
15	35	7.54	753.9	11.4	1499.2	45.7	2249.8	1.6	0.0022	65.3	68.7	0.110

i	j	K_{ijk} / cm^{-1}	ω(i) / cm^{-1}	I(i) / km mol^{-1}	ω(j) / cm^{-1}	I(j) / km mol^{-1}	ω(ij) / cm^{-1}	I(ij) / km mol^{-1}	I(ij) / I(k)	Δω'	Δω	TFR
15	34	-1.28	753.9	11.4	1479.2	4.2	2222.6	0.3	0.0004	38.2	48.6	0.026
15	31	2.85	753.9	11.4	1404.2	5.3	2138.7	1.1	0.0014	-45.7	-26.3	0.108
15	30	-54.12	753.9	11.4	1328.7	23.5	2073.1	29.2	0.0397	-111.4	-101.9	0.531
15	29	-7.55	753.9	11.4	1311.4	40.5	2059.0	0.3	0.0005	-125.5	-119.2	0.063
14	35	0.27	679.8	0.7	1499.2	45.7	2174.2	0.0	0.0000	-10.3	-5.4	0.049
14	33	0.45	679.8	0.7	1431.9	5.4	2085.9	0.1	0.0001	-98.5	-72.8	0.006
13	37	0.22	642.9	0.3	1615.7	3.5	2254.7	0.0	0.0000	70.2	74.2	0.003
13	36	-0.57	642.9	0.3	1581.9	4.9	2223.4	0.0	0.0000	39.0	40.3	0.014
13	35	0.29	642.9	0.3	1499.2	45.7	2136.9	0.0	0.0000	-47.5	-42.3	0.007
12	37	1.01	610.1	21.1	1615.7	3.5	2225.4	0.1	0.0002	40.9	41.4	0.025
12	36	1.49	610.1	21.1	1581.9	4.9	2192.5	0.7	0.0010	8.0	7.5	0.199
12	35	-4.21	610.1	21.1	1499.2	45.7	2106.8	1.3	0.0018	-77.7	-75.1	0.056
12	34	0.81	610.1	21.1	1479.2	4.2	2080.3	0.0	0.0000	-104.1	-95.2	0.008
3	38	-5.36	126.8	0.7	2184.5	735.1	2300.2	0.6	0.0008	115.8	126.8	0.042

6-31++G(d,p)

i	j	K_{ijk} / cm^{-1}	ω(i) / cm^{-1}	I(i) / km mol^{-1}	ω(j) / cm^{-1}	I(j) / km mol^{-1}	ω(ij) / cm^{-1}	I(ij) / km mol^{-1}	I(ij) / I(k)	Δω'	Δω	TFR
25	25	-33.39	1130.9	14.1	1130.9	14.1	2260.8	10.5	0.0141	76.6	77.7	0.430
24	24	-0.75	1127.4	5.7	1127.4	5.7	2257.5	0.0	0.0000	73.4	70.6	0.011
23	23	0.60	1055.6	4.8	1055.6	4.8	2088.8	0.1	0.0001	-95.4	-72.9	0.008
24	25	-1.96	1127.4	5.7	1130.9	14.1	2259.1	0.0	0.0000	74.9	74.1	0.026
23	27	0.75	1055.6	4.8	1207.9	2.0	2250.2	0.1	0.0001	66.1	79.4	0.009
23	26	0.70	1055.6	4.8	1202.3	1.2	2246.9	0.0	0.0000	62.8	73.8	0.010
23	25	1.03	1055.6	4.8	1130.9	14.1	2177.4	0.8	0.0010	-6.7	2.4	0.428
22	28	0.24	1012.8	5.9	1293.1	79.0	2313.9	0.0	0.0000	129.7	121.8	0.002
22	26	0.96	1012.8	5.9	1202.3	1.2	2216.2	1.9	0.0025	32.1	31	0.031
22	25	2.95	1012.8	5.9	1130.9	14.1	2146.2	0.7	0.0009	-38	-40.4	0.073
22	24	-0.72	1012.8	5.9	1127.4	5.7	2142.5	0.0	0.0001	-41.6	-43.9	0.016
21	29	-0.46	991.1	28.8	1318.1	68.2	2310.7	0.0	0.0000	126.5	125	0.004
21	28	-0.21	991.1	28.8	1293.1	79.0	2292.5	0.0	0.0000	108.3	100.1	0.002
21	25	0.71	991.1	28.8	1130.9	14.1	2123.1	0.0	0.0001	-61.1	-62.1	0.012
19	30	0.90	939.4	1.9	1330.2	72.5	2267.3	0.0	0.0000	83.2	85.4	0.011
19	26	-0.29	939.4	1.9	1202.3	1.2	2142.6	0.0	0.0000	-41.5	-42.5	0.007
18	34	-1.28	834.5	3.2	1482.6	36.7	2295.5	0.0	0.0000	111.4	132.9	0.010
18	32	-0.47	834.5	3.2	1403.6	15.2	2254.3	0.0	0.0000	70.1	54	0.009
18	31	1.85	834.5	3.2	1387.1	10.3	2232.5	0.8	0.0010	48.4	37.4	0.050
18	30	-47.67	834.5	3.2	1330.2	72.5	2146.0	226.6	0.3061	-38.2	-19.4	2.452
18	29	-5.14	834.5	3.2	1318.1	68.2	2151.4	1.7	0.0023	-32.8	-31.6	0.163
18	28	-6.05	834.5	3.2	1293.1	79.0	2131.5	1.4	0.0019	-52.6	-56.6	0.107

i	j	K_{ijk} / cm^{-1}	ω(i) / cm^{-1}	I(i) / km mol^{-1}	ω(j) / cm^{-1}	I(j) / km mol^{-1}	ω(ij) / cm^{-1}	I(ij) / km mol^{-1}	I(ij) / I(k)	Δω'	Δω	TFR
17	31	-0.36	835.9	30.3	1387.1	10.3	2227.6	0.0	0.0000	43.5	38.9	0.009
17	30	6.49	835.9	30.3	1330.2	72.5	2151.7	10.1	0.0136	-32.4	-18	0.360
17	29	0.69	835.9	30.3	1318.1	68.2	2148.1	0.0	0.0000	-36.1	-30.1	0.023
17	28	0.83	835.9	30.3	1293.1	79.0	2126.3	0.0	0.0000	-57.8	-55.1	0.015
16	33	0.23	803.5	11.3	1450.7	34.6	2250.9	0.0	0.0000	66.8	70	0.003
16	31	-0.32	803.5	11.3	1387.1	10.3	2212.7	0.1	0.0001	28.6	6.4	0.050
16	30	5.13	803.5	11.3	1330.2	72.5	2137.6	2.3	0.0031	-46.6	-50.5	0.102
16	29	0.41	803.5	11.3	1318.1	68.2	2134.2	0.0	0.0000	-50	-62.6	0.007
16	28	0.81	803.5	11.3	1293.1	79.0	2113.5	0.0	0.0000	-70.6	-87.6	0.009
15	35	7.64	757.8	8.9	1508.5	53.2	2264.9	1.8	0.0024	80.8	82.1	0.093
15	34	-1.31	757.8	8.9	1482.6	36.7	2221.0	0.3	0.0004	36.8	56.2	0.023
15	31	2.53	757.8	8.9	1387.1	10.3	2158.4	0.9	0.0012	-25.8	-39.3	0.064
15	30	-54.54	757.8	8.9	1330.2	72.5	2076.0	29.1	0.0393	-108.2	-96.1	0.567
15	29	-6.07	757.8	8.9	1318.1	68.2	2077.9	0.2	0.0003	-106.3	-108.3	0.056
15	28	-9.30	757.8	8.9	1293.1	79.0	2058.3	0.5	0.0007	-125.8	-133.3	0.070
14	35	0.42	698.0	0.2	1508.5	53.2	2206.4	0.0	0.0001	22.3	22.3	0.019
14	33	0.46	698.0	0.2	1450.7	34.6	2137.0	0.1	0.0001	-47.1	-35.4	0.013
13	37	0.23	642.7	0.6	1611.1	3.7	2254.8	0.0	0.0000	70.7	69.7	0.003
13	36	0.49	642.7	0.6	1581.3	5.4	2223.0	0.0	0.0000	38.8	39.9	0.012
12	37	1.00	622.0	24.0	1611.1	3.7	2235.1	0.1	0.0002	50.9	49	0.020
12	36	-1.47	622.0	24.0	1581.3	5.4	2201.3	0.7	0.0009	17.2	19.1	0.077
12	35	-4.25	622.0	24.0	1508.5	53.2	2129.0	1.4	0.0019	-55.2	-53.7	0.079
12	34	0.84	622.0	24.0	1482.6	36.7	2085.3	0.0	0.0000	-98.9	-79.6	0.011
3	38	-5.35	135.7	1.6	2184.2	740.3	2307.1	0.6	0.0008	123	135.7	0.039

6-311G(d,p)

i	j	K_{ijk} / cm^{-1}	ω(i) / cm^{-1}	I(i) / km mol^{-1}	ω(j) / cm^{-1}	I(j) / km mol^{-1}	ω(ij) / cm^{-1}	I(ij) / km mol^{-1}	I(ij) / I(k)	Δω'	Δω	TFR
25	25	-32.15	1128.6	8.9163	1128.6	8.9163	2254.7	9.6531	0.0131	67.1	69.6	0.462
24	24	-1.15	1130.3	14.0172	1130.3	14.0172	2259.9	0.0140	0.0000	72.3	73.1	0.016
23	23	0.52	1091.0	3.6344	1091.0	3.6344	2092.6	0.0602	0.0001	-95	-5.7	0.091
24	25	-2.43	1130.3	14.0172	1128.6	8.9163	2257.1	0.0726	0.0001	69.5	71.3	0.034
23	27	0.75	1091.0	3.6344	1205.8	4.5593	2250.9	0.0769	0.0001	63.3	109.1	0.007
23	26	0.69	1091.0	3.6344	1203.1	1.7391	2248.7	0.0321	0.0000	61.1	106.5	0.007
23	25	0.96	1091.0	3.6344	1128.6	8.9163	2176.2	0.3157	0.0004	-11.4	32	0.030
22	28	1.07	1019.1	3.5745	1284.2	37.7391	2305.4	0.0025	0.0000	117.8	115.7	0.009
22	26	1.08	1019.1	3.5745	1203.1	1.7391	2221.3	6.5051	0.0088	33.7	34.7	0.031
22	25	2.73	1019.1	3.5745	1128.6	8.9163	2148.3	0.4771	0.0006	-39.2	-39.9	0.069
22	24	-0.61	1019.1	3.5745	1130.3	14.0172	2149.1	0.0253	0.0000	-38.5	-38.1	0.016
21	30	-3.15	990.2	0.8277	1324.9	57.5403	2317.5	0.1440	0.0002	129.9	127.5	0.025

i	j	K_{ijk} / cm^{-1}	ω(i) / cm^{-1}	I(i) / km mol^{-1}	ω(j) / cm^{-1}	I(j) / km mol^{-1}	ω(ij) / cm^{-1}	I(ij) / km mol^{-1}	I(ij) / I(k)	Δω’	Δω	TFR
21	29	-0.42	990.2	0.8277	1322.2	32.2631	2315.4	0.0023	0.0000	127.8	124.9	0.003
21	25	0.98	990.2	0.8277	1128.6	8.9163	2122.8	0.0562	0.0001	-64.8	-68.7	0.014
19	30	-0.98	905.4	0.4143	1324.9	57.5403	2261.9	0.0106	0.0000	74.3	42.7	0.023
19	26	0.33	905.4	0.4143	1203.1	1.7391	2138.8	0.0068	0.0000	-48.8	-79.0	0.004
18	34	-1.32	831.9	1.7915	1490.3	4.2758	2293.7	0.0223	0.0000	106.1	134.7	0.010
18	32	-0.38	831.9	1.7915	1385.5	3.3697	2250.0	0.0301	0.0000	62.4	29.9	0.013
18	31	2.08	831.9	1.7915	1405.5	1.5175	2228.5	1.1808	0.0016	40.9	49.9	0.042
18	30	-48.25	831.9	1.7915	1324.9	57.5403	2144.5	144.9548	0.1961	-43.1	-30.8	1.565
18	29	-2.15	831.9	1.7915	1322.2	32.2631	2151.9	0.2635	0.0004	-35.7	-33.4	0.064
18	28	-4.80	831.9	1.7915	1284.2	37.7391	2116.3	0.3334	0.0005	-71.3	-71.5	0.067
17	31	-0.55	843.2	34.1399	1405.5	1.5175	2222.6	0.0749	0.0001	35.0	61.2	0.009
17	30	10.31	843.2	34.1399	1324.9	57.5403	2147.1	18.4066	0.0249	-40.5	-19.5	0.529
17	29	0.45	843.2	34.1399	1322.2	32.2631	2147.0	0.0095	0.0000	-40.6	-22.1	0.021
17	28	1.03	843.2	34.1399	1284.2	37.7391	2111.3	0.0249	0.0000	-76.3	-60.2	0.017
16	34	0.23	803.5	5.1162	1490.3	4.2758	2283.7	0.0011	0.0000	96.1	106.3	0.002
16	33	0.21	803.5	5.1162	1459.7	16.6768	2279.5	0.0041	0.0000	91.9	75.7	0.003
16	31	-0.38	803.5	5.1162	1405.5	1.5175	2218.2	0.0661	0.0001	30.6	21.5	0.018
16	30	6.12	803.5	5.1162	1324.9	57.5403	2142.7	3.6493	0.0049	-44.9	-59.2	0.103
16	28	0.69	803.5	5.1162	1284.2	37.7391	2107.5	0.0152	0.0000	-80.1	-99.9	0.007
15	35	7.63	760.0	3.8398	1501.8	48.7380	2259.9	1.6935	0.0023	72.3	74.2	0.103
15	34	-1.29	760.0	3.8398	1490.3	4.2758	2222.9	0.2918	0.0004	35.3	62.8	0.021
15	31	2.77	760.0	3.8398	1405.5	1.5175	2157.2	0.8044	0.0011	-30.4	-22.1	0.125
15	30	-54.76	760.0	3.8398	1324.9	57.5403	2077.2	23.9474	0.0324	-110.4	-102.7	0.533
15	29	-1.75	760.0	3.8398	1322.2	32.2631	2081.7	0.0152	0.0000	-105.9	-105.4	0.017
14	35	0.45	711.5	0.4986	1501.8	48.7380	2210.1	0.0324	0.0000	22.5	25.7	0.018
14	33	0.49	711.5	0.4986	1459.7	16.6768	2170.8	0.1135	0.0002	-16.8	-16.3	0.030
13	36	0.58	642.6	0.0200	1573.1	4.7042	2215.9	0.0089	0.0000	28.3	28.2	0.021
13	35	0.27	642.6	0.0200	1501.8	48.7380	2141.7	0.0012	0.0000	-45.9	-43.2	0.006
13	34	-0.24	642.6	0.0200	1490.3	4.2758	2105.6	0.0194	0.0000	-82.0	-54.6	0.004
12	37	1.00	630.6	19.4882	1611.4	2.7279	2241.2	0.1235	0.0002	53.6	54.4	0.018
12	36	-1.15	630.6	19.4882	1573.1	4.7042	2203.4	0.5457	0.0007	15.8	16.1	0.071
12	35	-4.05	630.6	19.4882	1501.8	48.7380	2130.7	1.2127	0.0016	-56.9	-55.2	0.073
12	34	0.72	630.6	19.4882	1490.3	4.2758	2094.5	0.0034	0.0000	-93.1	-66.6	0.011

6-311+G(d,p)

i	j	K_{ijk} / cm^{-1}	ω(i) / cm^{-1}	I(i) / km mol^{-1}	ω(j) / cm^{-1}	I(j) / km mol^{-1}	ω(ij) / cm^{-1}	I(ij) / km mol^{-1}	I(ij) / I(k)	Δω'	Δω	TFR
26	26	-4.30	1042.8	14.4	1042.8	14.4	2199.1	0.0	0.0001	22.1	-91.5	0.0
25	25	-31.39	1125.2	13.9	1125.2	13.9	2250.5	9.1	0.0122	73.4	73.4	0.4
24	24	-1.14	1147.9	1.9	1147.9	1.9	2201.5	0.0	0.0000	24.4	118.8	0.0
23	23	0.52	1055.9	4.4	1055.9	4.4	2085.4	0.0	0.0001	-91.6	-65.3	0.0
25	26	-11.52	1125.2	13.9	1042.8	14.4	2226.7	1.0	0.0013	49.7	-9.0	1.3
24	26	-0.81	1147.9	1.9	1042.8	14.4	2200.8	0.5	0.0007	23.8	13.7	0.1
24	25	-2.98	1147.9	1.9	1125.2	13.9	2226.0	0.1	0.0001	48.9	96.1	0.0
23	27	0.74	1055.9	4.4	1205.3	2.8	2235.6	0.1	0.0001	58.6	84.1	0.0
23	26	0.66	1055.9	4.4	1042.8	14.4	2144.9	0.0	0.0000	-32.2	-78.4	0.0
23	25	0.93	1055.9	4.4	1125.2	13.9	2170.7	2.1	0.0028	-6.3	4.0	0.2
22	30	-10.68	1035.4	1.3	1323.4	132.6	2295.4	0.4	0.0006	118.3	181.8	0.1
22	29	-0.35	1035.4	1.3	1260.6	1.6	2220.4	0.3	0.0004	43.4	119.0	0.0
22	28	0.89	1035.4	1.3	1288.1	30.8	2260.4	0.0	0.0000	83.3	146.5	0.0
22	26	0.83	1035.4	1.3	1042.8	14.4	2073.4	0.5	0.0006	-103.7	-98.8	0.0
22	25	2.51	1035.4	1.3	1125.2	13.9	2101.3	0.7	0.0009	-75.8	-16.4	0.2
22	24	-0.60	1035.4	1.3	1147.9	1.9	2074.3	0.0	0.0001	-102.7	6.3	0.1
21	30	-1.76	862.3	16.5	1323.4	132.6	2266.9	0.1	0.0001	89.9	8.7	0.2
21	29	-0.44	862.3	16.5	1260.6	1.6	2191.0	0.0	0.0000	14.0	-54.1	0.0
21	25	0.55	862.3	16.5	1125.2	13.9	2072.9	0.0	0.0001	-104.2	-189.5	0.0
19	30	0.98	930.0	2.9	1323.4	132.6	2238.5	0.0	0.0000	61.5	76.3	0.0
18	34	-1.33	835.9	7.4	1169.9	11.3	2240.1	0.0	0.0000	63.0	-171.2	0.0
18	32	-0.38	835.9	7.4	1485.7	6.2	2218.8	0.0	0.0000	41.7	144.5	0.0
18	31	2.09	835.9	7.4	1389.7	1.9	2173.1	0.8	0.0011	-3.9	48.6	0.0
18	30	-48.58	835.9	7.4	1323.4	132.6	2138.6	238.6	0.3213	-38.4	-17.8	2.7
18	29	-2.29	835.9	7.4	1260.6	1.6	2077.6	0.6	0.0008	-99.5	-80.6	0.0
18	28	-5.82	835.9	7.4	1288.1	30.8	2115.3	0.9	0.0012	-61.7	-53.0	0.1
17	35	-0.84	825.2	26.4	1497.4	25.7	2300.0	0.0	0.0000	122.9	145.6	0.0
17	31	-0.44	825.2	26.4	1389.7	1.9	2164.4	0.0	0.0000	-12.7	37.9	0.0
17	30	7.96	825.2	26.4	1323.4	132.6	2140.9	24.6	0.0331	-36.2	-28.4	0.3
17	29	0.34	825.2	26.4	1260.6	1.6	2069.7	0.0	0.0000	-107.4	-91.2	0.0
17	28	0.96	825.2	26.4	1288.1	30.8	2107.3	0.0	0.0000	-69.7	-63.7	0.0
16	35	-0.61	783.7	10.0	1497.4	25.7	2267.6	0.0	0.0000	90.6	104.0	0.0
16	31	-0.32	783.7	10.0	1389.7	1.9	2132.4	0.0	0.0000	-44.7	-3.7	0.1
16	30	4.63	783.7	10.0	1323.4	132.6	2110.1	2.7	0.0037	-67.0	-70.0	0.1
16	28	0.64	783.7	10.0	1288.1	30.8	2076.2	0.0	0.0000	-100.9	-105.3	0.0
15	35	7.40	734.4	4.0	1497.4	25.7	2213.9	1.4	0.0019	36.9	54.7	0.1
15	34	-1.34	734.4	4.0	1169.9	11.3	2144.5	0.2	0.0002	-32.5	-272.7	0.0
15	31	2.76	734.4	4.0	1389.7	1.9	2079.1	1.2	0.0016	-97.9	-52.9	0.1
15	30	-55.71	734.4	4.0	1323.4	132.6	2048.8	36.3	0.0489	-128.2	-119.2	0.5
14	35	0.37	680.8	0.5	1497.4	25.7	2159.5	0.0	0.0000	-17.6	1.1	0.3
14	33	-0.50	680.8	0.5	1435.1	6.7	2050.8	0.2	0.0002	-126.2	-61.2	0.0
13	36	-0.57	643.8	0.0	1574.9	10.1	2217.0	0.0	0.0000	39.9	41.7	0.0
13	35	0.27	643.8	0.0	1497.4	25.7	2122.0	0.0	0.0000	-55.0	-35.9	0.0
12	37	1.02	626.2	23.6	1596.9	8.8	2221.7	0.1	0.0002	44.6	46.0	0.0
12	36	1.27	626.2	23.6	1574.9	10.1	2198.6	0.4	0.0005	21.5	24.1	0.1
12	35	-4.01	626.2	23.6	1497.4	25.7	2105.0	1.6	0.0022	-72.1	-53.5	0.1
5	38	22.06	37.0	0.9	2177.1	742.4	2203.0	0.4	0.0006	25.9	37.0	0.6
3	38	-5.23	91.7	3.8	2177.1	742.4	2258.8	0.6	0.0009	81.7	91.7	0.1

6-311++G(d,p)

i	j	K_{ijk} / cm^{-1}	ω(i) / cm^{-1}	I(i) / km mol^{-1}	ω(j) / cm^{-1}	I(j) / km mol^{-1}	ω(ij) / cm^{-1}	I(ij) / km mol^{-1}	I(ij) / I(k)	Δω'	Δω	TFR
25	25	-31.23	1128.5	6.7	1128.5	6.7	2254.4	9.0	0.0122	76.2	78.7	0.397
24	24	-1.33	1128.7	16.8	1128.7	16.8	2258.1	0.0	0.0000	79.9	79.1	0.017
23	23	0.48	1055.6	4.6	1055.6	4.6	2094.4	0.0	0.0001	-83.8	-67.0	0.007
24	25	-3.73	1128.7	16.8	1128.5	6.7	2256.2	0.2	0.0003	78.0	78.9	0.047
23	27	0.61	1055.6	4.6	1204.2	4.1	2250.2	0.0	0.0001	72.0	81.6	0.008
23	26	0.52	1055.6	4.6	1195.1	2.4	2243.1	0.0	0.0000	64.9	72.5	0.007
23	25	0.76	1055.6	4.6	1128.5	6.7	2177.0	1.6	0.0022	-1.2	5.9	0.130
22	28	0.78	1030.8	2.3	1282.1	37.4	2298.7	0.0	0.0000	120.5	134.7	0.006
22	27	-0.26	1030.8	2.3	1204.2	4.1	2219.9	0.0	0.0000	41.7	56.8	0.005
22	26	0.80	1030.8	2.3	1195.1	2.4	2210.8	0.5	0.0006	32.6	47.7	0.017
22	25	2.50	1030.8	2.3	1128.5	6.7	2144.4	0.7	0.0010	-33.8	-19.0	0.132
22	24	-0.52	1030.8	2.3	1128.7	16.8	2144.4	0.0	0.0000	-33.8	-18.8	0.028
21	27	-0.22	981.1	0.2	1204.2	4.1	2191.9	0.1	0.0001	13.7	7.1	0.030
21	26	-0.38	981.1	0.2	1195.1	2.4	2184.2	0.6	0.0007	6.0	-2.0	0.192
19	30	0.83	928.7	1.4	1321.8	83.4	2252.2	0.0	0.0000	74.0	72.3	0.011
19	26	-0.26	928.7	1.4	1195.1	2.4	2125.6	0.0	0.0000	-52.6	-54.4	0.005
18	34	-1.35	832.6	4.4	1471.6	4.6	2272.3	0.0	0.0000	94.1	126.1	0.011
18	32	-0.31	832.6	4.4	1396.9	2.1	2240.3	0.0	0.0000	62.1	51.4	0.006
18	31	2.25	832.6	4.4	1392.0	0.5	2223.5	0.9	0.0012	45.3	46.4	0.049
18	30	-48.73	832.6	4.4	1321.8	83.4	2140.1	249.2	0.3376	-38.2	-23.8	2.052
18	29	-2.61	832.6	4.4	1319.7	55.6	2150.6	0.7	0.0010	-27.6	-25.8	0.101
18	28	-6.45	832.6	4.4	1282.1	37.4	2114.0	1.1	0.0015	-64.2	-63.5	0.102
17	33	0.22	833.4	39.8	1431.5	3.8	2273.7	0.0	0.0000	95.5	86.7	0.003
17	31	-0.36	833.4	39.8	1392.0	0.5	2218.2	0.0	0.0000	40.0	47.2	0.008
17	30	6.57	833.4	39.8	1321.8	83.4	2146.1	16.5	0.0223	-32.1	-23.0	0.286
17	29	0.36	833.4	39.8	1319.7	55.6	2146.1	0.0	0.0000	-32.1	-25.1	0.014
17	28	0.88	833.4	39.8	1282.1	37.4	2109.6	0.0	0.0000	-68.6	-62.7	0.014
16	35	-0.50	794.0	9.8	1501.8	41.7	2301.5	0.0	0.0000	123.3	117.7	0.004
16	31	-0.28	794.0	9.8	1392.0	0.5	2193.9	0.0	0.0000	15.7	7.8	0.036
16	30	3.58	794.0	9.8	1321.8	83.4	2121.9	1.7	0.0024	-56.3	-62.3	0.057
16	28	0.54	794.0	9.8	1282.1	37.4	2084.9	0.0	0.0000	-93.3	-102.0	0.005
15	35	7.33	761.8	8.0	1501.8	41.7	2261.8	1.4	0.0019	83.6	85.4	0.086
15	34	-1.35	761.8	8.0	1471.6	4.6	2202.7	0.2	0.0002	24.5	55.2	0.025
15	31	2.91	761.8	8.0	1392.0	0.5	2155.2	1.3	0.0018	-23.1	-24.5	0.119
15	30	-55.60	761.8	8.0	1321.8	83.4	2075.7	36.5	0.0495	-102.5	-94.6	0.588
15	29	-2.48	761.8	8.0	1319.7	55.6	2081.5	0.0	0.0001	-96.7	-96.7	0.026
14	35	0.31	686.6	0.4	1501.8	41.7	2185.8	0.0	0.0000	7.6	10.3	0.030
14	33	0.49	686.6	0.4	1431.5	3.8	2134.4	0.2	0.0002	-43.9	-60.0	0.008
13	36	0.61	645.7	0.0	1572.6	6.5	2218.5	0.0	0.0000	40.3	40.2	0.015
13	35	0.36	645.7	0.0	1501.8	41.7	2145.4	0.0	0.0000	-32.8	-30.6	0.012
13	34	-0.23	645.7	0.0	1471.6	4.6	2086.5	0.0	0.0000	-91.7	-60.8	0.004
12	37	1.03	632.0	22.6	1608.4	2.1	2239.2	0.1	0.0002	61.0	62.2	0.017
12	36	-1.29	632.0	22.6	1572.6	6.5	2204.0	0.4	0.0005	25.8	26.4	0.049
12	35	-4.02	632.0	22.6	1501.8	41.7	2132.3	1.6	0.0022	-45.9	-44.4	0.091
12	34	0.74	632.0	22.6	1471.6	4.6	2073.1	0.0	0.0000	-105.1	-74.6	0.010

6-311++G(df,pd)

i	j	K_{ijk} / cm^{-1}	ω(i) / cm^{-1}	I(i) / km mol^{-1}	ω(j) / cm^{-1}	I(j) / km mol^{-1}	ω(ij) / cm^{-1}	I(ij) / km mol^{-1}	I(ij) / I(k)	Δω'	Δω	TFR
25	25	-31.65	1128.0	4.2	1128.0	4.2	2254.9	8.4	0.0180	77.1	78.2	0.405
24	24	-1.61	1119.5	12.4	1119.5	12.4	2241.9	0.0	0.0000	64.2	61.3	0.026
23	23	0.46	1053.7	4.3	1053.7	4.3	2088.7	0.0	0.0001	-89.1	-70.4	0.007
25	26	-11.16	1128.0	4.2	1170.7	0.6	2296.7	0.8	0.0018	118.9	120.8	0.092
24	26	-1.48	1119.5	12.4	1170.7	0.6	2289.1	0.6	0.0012	111.4	112.4	0.013
24	25	-4.77	1119.5	12.4	1128.0	4.2	2248.3	0.3	0.0007	70.6	69.7	0.068
23	27	0.62	1053.7	4.3	1204.7	2.9	2246.8	0.0	0.0001	69.0	80.6	0.008
23	26	0.50	1053.7	4.3	1170.7	0.6	2214.3	0.0	0.0000	36.6	46.5	0.011
23	25	0.76	1053.7	4.3	1128.0	4.2	2174.6	137.7	0.2954	-3.2	3.9	0.198
22	28	1.15	959.6	1.2	1281.6	35.8	2292.5	0.0	0.0000	114.7	63.4	0.018
22	26	0.68	959.6	1.2	1170.7	0.6	2177.0	0.2	0.0004	-0.8	-47.6	0.014
22	25	2.34	959.6	1.2	1128.0	4.2	2137.9	1.0	0.0021	-39.9	-90.2	0.026
22	24	-0.48	959.6	1.2	1119.5	12.4	2129.4	0.0	0.0001	-48.4	-98.7	0.005
21	30	-0.56	1030.8	1.6	1323.8	99.8	2300.4	0.0	0.0001	122.6	176.9	0.003
21	29	-0.42	1030.8	1.6	1305.0	18.9	2277.8	0.0	0.0000	100.1	158.1	0.003
21	27	-0.23	1030.8	1.6	1204.7	2.9	2179.2	0.1	0.0002	1.4	57.8	0.004
21	26	-0.37	1030.8	1.6	1170.7	0.6	2143.8	227.8	0.4890	-34.0	23.7	0.016
21	25	0.26	1030.8	1.6	1128.0	4.2	2106.2	0.0	0.0001	-71.6	-19.0	0.014
19	30	0.80	911.7	3.9	1323.8	99.8	2254.5	0.0	0.0000	76.7	57.8	0.014
19	26	-0.25	911.7	3.9	1170.7	0.6	2098.0	0.0	0.0000	-79.8	-95.4	0.003
18	34	-0.93	828.5	36.5	1466.2	9.1	2266.0	0.0	0.0000	88.2	116.9	0.008
18	33	0.30	828.5	36.5	1420.5	4.2	2256.9	0.0	0.0000	79.2	71.3	0.004
18	32	-0.40	828.5	36.5	1392.8	1.5	2244.9	0.0	0.0001	67.1	43.6	0.009
18	31	1.87	828.5	36.5	1366.5	4.7	2211.9	0.5	0.0011	34.1	17.2	0.109
18	30	-36.63	828.5	36.5	1323.8	99.8	2141.7	216.4	0.4643	-36.1	-25.5	1.439
18	29	-2.35	828.5	36.5	1305.0	18.9	2136.7	1.1	0.0023	-41.0	-44.2	0.053
18	28	-4.43	828.5	36.5	1281.6	35.8	2117.4	0.6	0.0013	-60.3	-67.7	0.065
17	34	0.77	846.4	3.5	1466.2	9.1	2263.0	0.0	0.0000	85.2	134.9	0.006
17	32	0.27	846.4	3.5	1392.8	1.5	2242.4	0.0	0.0001	64.6	61.5	0.004
17	31	-1.73	846.4	3.5	1366.5	4.7	2209.2	0.4	0.0009	31.5	35.1	0.049
17	30	32.43	846.4	3.5	1323.8	99.8	2154.5	3.5	0.0075	-23.2	-7.5	4.302
17	29	2.10	846.4	3.5	1305.0	18.9	2134.1	0.8	0.0017	-43.6	-26.3	0.080
17	28	3.93	846.4	3.5	1281.6	35.8	2115.0	0.4	0.0009	-62.8	-49.7	0.079
16	35	-0.53	784.9	11.3	1498.9	85.5	2284.2	0.0	0.0000	106.5	106.0	0.005
16	31	-0.33	784.9	11.3	1366.5	4.7	2165.6	0.0	0.0000	-12.1	-26.4	0.013
16	30	4.12	784.9	11.3	1323.8	99.8	2111.2	5.4	0.0117	-66.6	-69.1	0.060
16	28	0.56	784.9	11.3	1281.6	35.8	2073.2	0.0	0.0000	-104.6	-111.3	0.005
15	35	7.21	753.2	10.1	1498.9	85.5	2253.7	1.2	0.0026	76.0	74.4	0.097
15	34	-1.20	753.2	10.1	1466.2	9.1	2189.1	0.1	0.0003	11.3	41.7	0.029
15	31	3.26	753.2	10.1	1366.5	4.7	2136.5	1.9	0.0041	-41.3	-58.1	0.056
15	30	-56.11	753.2	10.1	1323.8	99.8	2072.8	42.5	0.0913	-104.9	-100.8	0.557
15	29	-3.03	753.2	10.1	1305.0	18.9	2059.7	0.1	0.0002	-118.0	-119.5	0.025
14	35	0.29	695.3	0.1	1498.9	85.5	2190.9	0.0	0.0000	13.2	16.5	0.017
14	33	0.49	695.3	0.1	1420.5	4.2	2118.3	0.2	0.0005	-59.5	-61.9	0.008
13	36	-0.59	647.1	0.1	1571.5	3.8	2218.3	0.0	0.0000	40.6	40.8	0.015
13	35	0.36	647.1	0.1	1498.9	85.5	2142.8	0.0	0.0000	-35.0	-31.7	0.011
12	37	1.04	630.9	23.4	1608.5	4.1	2235.6	0.1	0.0003	57.9	61.6	0.017
12	36	1.19	630.9	23.4	1571.5	3.8	2201.4	0.3	0.0006	23.6	24.6	0.048
12	35	-3.93	630.9	23.4	1498.9	85.5	2127.2	2.0	0.0044	-50.6	-48.0	0.082
12	34	0.69	630.9	23.4	1466.2	9.1	2063.1	0.0	0.0000	-114.7	-80.7	0.009
3	38	-5.29	125.4	0.7	2177.8	466.0	2289.6	0.7	0.0014	111.9	125.4	0.042

APPENDIX C

VIBRATIONAL MODES OF 4-AZIDOACETANILIDE THAT OCCUR WITHIN ±130 CM^{-1}

FROM THE FUNDAMENTAL VIBRATION FOR SEVEN BASIS SETS IN NNDMA

i, j, k : vibrational modes ; where k = 49 (azide asymmetric stretch)

i = j → overtone & i ≠ j → combination band

K_{ijk} : cubic force constant

TFR : third-order Fermi resonance

ω(i), ω(j), ω(k) : anharmonic frequencies of i, j & k th mode

ω(ij) : anharmonic frequency of ij th mode

I(i), I(j), I(k) : anharmonic intensities of i, j & k th mode

I(ij) : anharmonic intensity of ij th mode

Δω' : ω(ij) - ω(k)

Δω : ω(i) + ω(j) - ω(k)

6-31G(d,p)

i	j	K_{ijk} / cm^{-1}	ω(i) / cm^{-1}	I(i) / km mol^{-1}	ω(j) / cm^{-1}	I(j) / km mol^{-1}	ω(ij) / cm^{-1}	I(ij) / km mol^{-1}	I(ij) / I(k)	Δω'	Δω	TFR
33	33	-35.89	1138.1	8.1	1138.1	8.1	2261.8	11.7	0.0204	66.7	81	0.443
32	32	-0.93	1095.2	22.9	1095.2	22.9	2206.7	0.0	0.0000	11.6	-4.6	0.202
33	34	-13.97	1138.1	8.1	1163.1	5.7	2294.6	1.6	0.0027	99.5	106.1	0.132
32	34	-1.09	1095.2	22.9	1163.1	5.7	2265.7	0.5	0.0008	70.6	63.3	0.017
32	33	-4.89	1095.2	22.9	1138.1	8.1	2234.2	0.4	0.0007	39.1	38.2	0.128
31	35	-0.22	1033.5	10.4	1224.3	10.0	2259.7	0.0	0.0001	64.6	62.7	0.003
31	34	-0.25	1033.5	10.4	1163.1	5.7	2193.7	0.0	0.0000	-1.4	1.5	0.165
30	36	-0.63	1019.2	28.3	1276.4	77.3	2292.4	0.3	0.0006	97.3	100.4	0.006
30	35	-0.69	1019.2	28.3	1224.3	10.0	2244.5	0.1	0.0002	49.4	48.3	0.014
30	34	0.72	1019.2	28.3	1163.1	5.7	2179	4.1	0.0070	-16.1	-12.8	0.056
30	33	3.19	1019.2	28.3	1138.1	8.1	2147.9	0.8	0.0014	-47.2	-37.9	0.084
30	32	-0.44	1019.2	28.3	1095.2	22.9	2118.6	0.0	0.0000	-76.5	-80.7	0.005
29	36	-1.03	1008.1	0.1	1276.4	77.3	2287.4	0.1	0.0002	92.3	89.4	0.012

i	j	K_{ijk} / cm^{-1}	ω(i) / cm^{-1}	I(i) / km mol^{-1}	ω(j) / cm^{-1}	I(j) / km mol^{-1}	ω(ij) / cm^{-1}	I(ij) / km mol^{-1}	I(ij) / I(k)	Δω'	Δω	TFR
29	34	0.82	1008.1	0.1	1163.1	5.7	2173.7	3.5	0.0060	-21.4	-23.9	0.034
29	33	2.32	1008.1	0.1	1138.1	8.1	2143.2	0.3	0.0004	-51.9	-48.9	0.047
29	32	-0.61	1008.1	0.1	1095.2	22.9	2113.2	0.0	0.0001	-81.9	-91.8	0.007
28	39	1.67	925.2	5.1	1332.9	8.7	2259.1	0.1	0.0001	64.0	63.0	0.027
28	38	0.37	925.2	5.1	1316.3	39.3	2250	0.0	0.0000	54.9	46.4	0.008
28	36	0.54	925.2	5.1	1276.4	77.3	2205.4	0.0	0.0000	10.3	6.5	0.083
28	35	0.27	925.2	5.1	1224.3	10.0	2156.6	0.0	0.0001	-38.5	-45.6	0.006
28	34	-0.36	925.2	5.1	1163.1	5.7	2091.6	0.0	0.0000	-103.5	-106.8	0.003
27	39	-0.27	899.1	1.5	1332.9	8.7	2237.2	0.0	0.0000	42.1	37.0	0.007
27	35	0.30	899.1	1.5	1224.3	10.0	2134.9	0.1	0.0001	-60.2	-71.7	0.004
26	42	-0.23	935.5	8.1	1352.9	28.0	2298.4	0.0	0.0000	103.3	93.3	0.002
26	39	-4.84	935.5	8.1	1332.9	8.7	2257	1.0	0.0017	61.9	73.3	0.066
26	38	-1.73	935.5	8.1	1316.3	39.3	2245.1	0.1	0.0002	50.0	56.7	0.031
26	37	0.88	935.5	8.1	1320.2	41.5	2239.2	0.1	0.0002	44.1	60.7	0.014
26	36	-0.37	935.5	8.1	1276.4	77.3	2202.3	0.1	0.0001	7.2	16.8	0.022
26	35	0.41	935.5	8.1	1224.3	10.0	2155.6	0.6	0.0011	-39.5	-35.3	0.012
26	34	0.51	935.5	8.1	1163.1	5.7	2088.7	0.1	0.0001	-106.4	-96.5	0.005
25	44	-1.14	834	7.0	1466.4	40.4	2277.9	0.0	0.0001	82.8	105.3	0.011
25	42	-0.22	834	7.0	1352.9	28.0	2190.2	0.0	0.0000	-4.9	-8.3	0.026
25	41	-1.05	834	7.0	1411.8	2.2	2228.7	0.0	0.0000	33.6	50.7	0.021
25	40	0.79	834	7.0	1366.8	95.0	2182.9	0.1	0.0002	-12.2	5.7	0.139
25	39	-9.97	834	7.0	1332.9	8.7	2147.6	44.2	0.0768	-47.5	-28.2	0.354
25	38	-1.79	834	7.0	1316.3	39.3	2137.6	0.1	0.0002	-57.5	-44.8	0.04
25	36	-1.53	834	7.0	1276.4	77.3	2095.3	0.0	0.0000	-99.8	-84.7	0.018
24	44	4.14	802.7	9.9	1466.4	40.4	2271.7	0.2	0.0003	76.6	74.1	0.056
24	43	-0.51	802.7	9.9	1439.9	2.6	2245.5	0.0	0.0000	50.4	47.5	0.011
24	42	0.80	802.7	9.9	1352.9	28.0	2184.2	0.0	0.0000	-10.9	-39.5	0.02
24	41	4.37	802.7	9.9	1411.8	2.2	2223.3	1.8	0.0031	28.2	19.5	0.224
24	40	-3.10	802.7	9.9	1366.8	95.0	2179.2	111.8	0.1941	-15.9	-25.5	0.121
24	39	51.38	802.7	9.9	1332.9	8.7	2134.2	44.1	0.0765	-60.9	-59.4	0.865
24	38	10.33	802.7	9.9	1316.3	39.3	2132	2.2	0.0039	-63.1	-76.1	0.136
24	37	-0.78	802.7	9.9	1320.2	41.5	2126	0.0	0.0000	-69.1	-72.1	0.011
24	36	9.23	802.7	9.9	1276.4	77.3	2088.6	0.8	0.0014	-106.5	-116.0	0.08
23	45	0.52	772.5	1.2	1507.3	120.2	2273.3	0.0	0.0000	78.2	84.7	0.006
23	44	-0.34	772.5	1.2	1466.4	40.4	2233.7	0.0	0.0000	38.6	43.8	0.008
23	40	0.31	772.5	1.2	1366.8	95.0	2138.6	39.8	0.0690	-56.5	-55.8	0.006
23	39	-4.55	772.5	1.2	1332.9	8.7	2104	1.6	0.0028	-91.1	-89.7	0.051
23	38	-1.15	772.5	1.2	1316.3	39.3	2095.5	0.0	0.0000	-99.6	-106.3	0.011
22	45	5.20	754.6	11.6	1507.3	120.2	2262.9	0.3	0.0006	67.8	66.8	0.078
22	44	-2.12	754.6	11.6	1466.4	40.4	2221.6	1.6	0.0027	26.5	25.9	0.082
22	43	0.33	754.6	11.6	1439.9	2.6	2194.8	0.1	0.0001	-0.3	-0.7	0.486
22	42	-0.41	754.6	11.6	1352.9	28.0	2134.6	0.1	0.0003	-60.5	-87.7	0.005
22	41	-2.31	754.6	11.6	1411.8	2.2	2173.2	1.5	0.0026	-21.9	-28.7	0.08
22	40	1.43	754.6	11.6	1366.8	95.0	2125.7	0.3	0.0005	-69.4	-73.7	0.019
22	39	-36.17	754.6	11.6	1332.9	8.7	2090.1	14.1	0.0245	-105.0	-107.6	0.336
21	46	-1.06	707.9	12.7	1591.1	1.4	2297.7	0.0	0.0000	102.6	103.9	0.01
21	45	-3.03	707.9	12.7	1507.3	120.2	2207.9	1.4	0.0024	12.8	20.1	0.151

i	j	K_{ijk} / cm^{-1}	ω(i) / cm^{-1}	I(i) / km mol^{-1}	ω(j) / cm^{-1}	I(j) / km mol^{-1}	ω(ij) / cm^{-1}	I(ij) / km mol^{-1}	I(ij) / I(k)	Δω'	Δω	TFR
21	44	2.07	707.9	12.7	1466.4	40.4	2168.3	1.1	0.0019	-26.8	-20.8	0.1
21	43	-0.42	707.9	12.7	1439.9	2.6	2141.7	0.1	0.0001	-53.4	-47.3	0.009
21	41	1.28	707.9	12.7	1411.8	2.2	2118.5	0.0	0.0000	-76.6	-75.4	0.017
20	47	1.16	676.3	4.2	1612.4	2.2	2288	0.0	0.0000	92.9	93.6	0.012
20	46	-1.58	676.3	4.2	1591.1	1.4	2267.6	0.1	0.0001	72.5	72.3	0.022
20	45	-4.91	676.3	4.2	1507.3	120.2	2177.5	207.2	0.3599	-17.6	-11.5	0.427
20	44	2.92	676.3	4.2	1466.4	40.4	2135.8	0.3	0.0005	-59.3	-52.4	0.056
20	43	-0.39	676.3	4.2	1439.9	2.6	2109.3	0.0	0.0000	-85.8	-79.0	0.005
20	41	1.34	676.3	4.2	1411.8	2.2	2087.1	0.0	0.0000	-108.0	-107.0	0.013
19	47	0.36	642.2	2.3	1612.4	2.2	2261.2	0.0	0.0000	66.1	59.5	0.006
19	46	0.70	642.2	2.3	1591.1	1.4	2241.6	0.1	0.0001	46.5	38.2	0.018
19	45	1.34	642.2	2.3	1507.3	120.2	2151.1	0.1	0.0002	-44.0	-45.6	0.029
19	44	-0.98	642.2	2.3	1466.4	40.4	2110.1	0.2	0.0003	-85.0	-86.5	0.011
18	47	1.00	673.4	138.8	1612.4	2.2	2276.2	0.0	0.0001	81.1	90.7	0.011
18	44	0.65	673.4	138.8	1466.4	40.4	2124.3	0.1	0.0001	-70.8	-55.3	0.012
18	43	-0.28	673.4	138.8	1439.9	2.6	2097.2	0.0	0.0000	-97.9	-81.8	0.003
17	47	-0.40	542.4	7.0	1612.4	2.2	2151.4	0.3	0.0005	-43.7	-40.3	0.01
16	48	0.35	565.5	7.3	1711.8	1.6	2251.5	0.0	0.0000	56.4	82.2	0.004
16	47	0.89	565.5	7.3	1612.4	2.2	2153	0.1	0.0002	-42.1	-17.2	0.052
16	46	-0.25	565.5	7.3	1591.1	1.4	2131.5	0.0	0.0000	-63.6	-38.5	0.007
15	48	0.40	522.8	9.9	1711.8	1.6	2244.9	0.0	0.0000	49.8	39.5	0.01
15	47	0.54	522.8	9.9	1612.4	2.2	2146	0.1	0.0002	-49.1	-59.9	0.009
14	48	0.79	531.9	33.4	1711.8	1.6	2245.4	0.1	0.0002	50.3	48.6	0.016
14	47	1.97	531.9	33.4	1612.4	2.2	2145.6	1.3	0.0023	-49.5	-50.8	0.039
14	46	0.34	531.9	33.4	1591.1	1.4	2123.9	0.0	0.0000	-71.2	-72.1	0.005
13	48	0.34	484.7	12.0	1711.8	1.6	2203.8	0.2	0.0003	8.7	1.4	0.241
13	47	0.81	484.7	12.0	1612.4	2.2	2107	0.2	0.0004	-88.1	-98.0	0.008
12	48	0.27	413.3	5.8	1711.8	1.6	2117.3	0.0	0.0000	-77.8	-70.0	0.004
10	48	0.40	377	2.7	1711.8	1.6	2087.5	0.0	0.0001	-107.6	-106.3	0.004
3	49	-0.56	50.2	1.1	2195.1	575.9	2264.5	0.6	0.0010	69.4	50.2	0.011
2	49	-0.92	-14.4	5.9	2195.1	575.9	2173.9	0.2	0.0003	-21.2	-14.4	0.064

6-31+G(d,p)

i	j	K_{ijk} / cm^{-1}	ω(i) / cm^{-1}	I(i) / km mol^{-1}	ω(j) / cm^{-1}	I(j) / km mol^{-1}	ω(ij) / cm^{-1}	I(ij) / km mol^{-1}	I(ij) / I(k)	Δω'	Δω	TFR
33	33	-36.68	1131.4	15.0	1131.4	15.0	2262.7	12.8	0.0	81.8	82	0.447
32	32	-1.09	1094.2	7.6	1094.2	7.6	2222.1	0.0	0.0	41.3	7.6	0.144
33	34	-13.01	1131.4	15.0	1171.5	0.4	2285.9	1.4	0.0	105	122.1	0.107
32	34	-0.98	1094.2	7.6	1171.5	0.4	2262.6	0.6	0.0	81.7	84.9	0.012
32	33	-4.51	1094.2	7.6	1131.4	15.0	2242.6	0.3	0.0	61.8	44.8	0.101
31	35	-0.26	1031.6	8.6	1220.7	33.8	2250.2	0.0	0.0	69.3	71.4	0.004
31	34	-0.24	1031.6	8.6	1171.5	0.4	2184.9	0.0	0.0	4	22.2	0.011
30	35	-0.60	1017.2	15.0	1220.7	33.8	2235.2	0.2	0.0	54.3	57	0.010
30	33	0.99	1017.2	15.0	1131.4	15.0	2148.2	0.2	0.0	-32.7	-32.3	0.031
29	35	-0.34	1003.4	17.6	1220.7	33.8	2221.6	0.0	0.0	40.7	43.3	0.008

i	j	K_{ijk} / cm^{-1}	ω(i) / cm^{-1}	I(i) / km mol^{-1}	ω(j) / cm^{-1}	I(j) / km mol^{-1}	ω(ij) / cm^{-1}	I(ij) / km mol^{-1}	I(ij) / I(k)	Δω'	Δω	TFR
29	34	0.79	1003.4	17.6	1171.5	0.4	2153.9	2.1	0.0	-27.0	-5.9	0.133
29	33	3.67	1003.4	17.6	1131.4	15.0	2134.4	1.4	0.0	-46.5	-46.0	0.080
29	32	-0.81	1003.4	17.6	1094.2	7.6	2110.9	0.0	0.0	-69.9	-83.2	0.010
28	39	-1.59	944.3	0.6	1324.2	9.5	2265.9	0.0	0.0	85.0	87.6	0.018
28	38	-0.63	944.3	0.6	1312.6	47.0	2254.9	0.0	0.0	74.0	76.0	0.008
28	37	-0.33	944.3	0.6	1304.9	1.3	2241.9	0.0	0.0	61.1	68.2	0.005
28	36	-0.28	944.3	0.6	1293.8	0.3	2238.3	0.0	0.0	57.4	57.1	0.005
28	35	-0.30	944.3	0.6	1220.7	33.8	2160.8	20.9	0.0	-20.1	-15.9	0.019
28	34	0.36	944.3	0.6	1171.5	0.4	2094.1	0.0	0.0	-86.8	-65.1	0.006
28	33	0.75	944.3	0.6	1131.4	15.0	2073.8	0.0	0.0	-107.1	-105.2	0.007
27	35	0.31	919.4	1.1	1220.7	33.8	2141.9	0.1	0.0	-39.0	-40.8	0.008
26	40	-0.22	903.7	2.4	1359.7	63.3	2263.9	0.4	0.0	83.0	82.5	0.003
26	39	-3.89	903.7	2.4	1324.2	9.5	2230.5	0.6	0.0	49.6	47.0	0.083
26	38	-2.09	903.7	2.4	1312.6	47.0	2217.2	0.0	0.0	36.3	35.4	0.059
26	37	-0.35	903.7	2.4	1304.9	1.3	2206.5	0.2	0.0	25.6	27.7	0.013
26	36	0.40	903.7	2.4	1293.8	0.3	2202.7	0.0	0.0	21.8	16.6	0.024
26	35	0.51	903.7	2.4	1220.7	33.8	2123.7	0.7	0.0	-57.2	-56.4	0.009
25	44	-1.28	835.9	3.5	1423.7	16.9	2254.1	0.1	0.0	73.2	78.7	0.016
25	41	-0.95	835.9	3.5	1394.6	14.2	2229.9	0.0	0.0	49.0	49.7	0.019
25	40	0.86	835.9	3.5	1359.7	63.3	2187.2	0.1	0.0	6.3	14.7	0.058
25	39	-9.87	835.9	3.5	1324.2	9.5	2152.6	8.3	0.0	-28.3	-20.8	0.476
25	38	-3.02	835.9	3.5	1312.6	47.0	2140.0	2.0	0.0	-40.9	-32.3	0.093
25	37	-1.20	835.9	3.5	1304.9	1.3	2130.0	0.1	0.0	-50.9	-40.1	0.030
25	36	-0.93	835.9	3.5	1293.8	0.3	2127.0	0.0	0.0	-53.9	-51.2	0.018
24	44	3.97	808.9	7.7	1423.7	16.9	2236.0	0.2	0.0	55.1	51.7	0.077
24	43	-0.22	808.9	7.7	1436.3	22.1	2250.6	0.0	0.0	69.7	64.3	0.003
24	42	0.60	808.9	7.7	1466.0	37.0	2268.7	0.0	0.0	87.8	94.0	0.006
24	41	3.57	808.9	7.7	1394.6	14.2	2212.2	0.9	0.0	31.3	22.6	0.158
24	40	-3.18	808.9	7.7	1359.7	63.3	2170.3	6.1	0.0	-10.5	-12.3	0.258
24	39	48.86	808.9	7.7	1324.2	9.5	2127.7	102.3	0.1	-53.2	-47.8	1.023
24	38	16.49	808.9	7.7	1312.6	47.0	2122.8	18.7	0.0	-58.1	-59.4	0.278
24	37	6.37	808.9	7.7	1304.9	1.3	2111.3	1.0	0.0	-69.6	-67.1	0.095
24	36	5.72	808.9	7.7	1293.8	0.3	2107.4	0.9	0.0	-73.4	-78.2	0.073
23	45	-0.73	785.5	3.5	1501.0	54.4	2280.9	0.0	0.0	100.0	105.6	0.007
23	44	0.41	785.5	3.5	1423.7	16.9	2207.3	0.0	0.0	26.4	28.3	0.015
23	41	0.60	785.5	3.5	1394.6	14.2	2184.8	0.1	0.0	3.9	-0.8	0.793
23	40	-0.31	785.5	3.5	1359.7	63.3	2142.0	0.4	0.0	-38.9	-35.7	0.009
23	39	5.60	785.5	3.5	1324.2	9.5	2107.4	4.7	0.0	-73.5	-71.2	0.079
23	38	1.72	785.5	3.5	1312.6	47.0	2096.1	0.2	0.0	-84.8	-82.8	0.021
23	37	0.97	785.5	3.5	1304.9	1.3	2084.8	0.1	0.0	-96.1	-90.5	0.011
23	36	0.82	785.5	3.5	1293.8	0.3	2080.6	0.0	0.0	-100.2	-101.6	0.008
22	45	4.93	756.8	11.7	1501.0	54.4	2262.4	0.3	0.0	81.5	76.9	0.064
22	44	-2.11	756.8	11.7	1423.7	16.9	2188.8	1.4	0.0	7.9	-0.4	5.334
22	43	0.24	756.8	11.7	1436.3	22.1	2202.8	0.0	0.0	21.9	12.2	0.020
22	42	-0.31	756.8	11.7	1466.0	37.0	2220.4	0.1	0.0	39.5	41.9	0.008
22	41	-1.88	756.8	11.7	1394.6	14.2	2164.8	30.1	0.0	-16.1	-29.5	0.064
22	40	1.56	756.8	11.7	1359.7	63.3	2120.5	0.3	0.0	-60.3	-64.4	0.024
22	39	-35.47	756.8	11.7	1324.2	9.5	2085.1	23.0	0.0	-95.8	-99.9	0.355
22	38	-12.72	756.8	11.7	1312.6	47.0	2075.8	4.7	0.0	-105.1	-111.5	0.114

i	j	K_{ijk} / cm^{-1}	ω(i) / cm^{-1}	I(i) / km mol^{-1}	ω(j) / cm^{-1}	I(j) / km mol^{-1}	ω(ij) / cm^{-1}	I(ij) / km mol^{-1}	I(ij) / I(k)	Δω’	Δω	TFR
21	45	-3.12	708.3	13.1	1501.0	54.4	2205.8	1.2	0.0	24.9	28.4	0.110
21	44	2.28	708.3	13.1	1423.7	16.9	2134.0	3.6	0.0	-46.9	-48.9	0.047
21	43	-0.37	708.3	13.1	1436.3	22.1	2147.7	0.1	0.0	-33.1	-36.3	0.010
21	42	0.29	708.3	13.1	1466.0	37.0	2165.5	0.0	0.0	-15.4	-6.6	0.045
21	41	1.02	708.3	13.1	1394.6	14.2	2109.4	0.0	0.0	-71.4	-78.0	0.013
20	47	1.05	678.0	25.2	1602.8	4.7	2279.1	0.0	0.0	98.2	99.9	0.011
20	46	1.76	678.0	25.2	1586.6	5.3	2262.4	0.1	0.0	81.6	83.7	0.021
20	45	-4.66	678.0	25.2	1501.0	54.4	2173.4	39.6	0.0	-7.5	-1.9	2.511
20	44	2.82	678.0	25.2	1423.7	16.9	2100.6	0.5	0.0	-80.3	-79.2	0.036
20	42	0.38	678.0	25.2	1466.0	37.0	2132.5	0.0	0.0	-48.4	-36.9	0.010
20	41	0.70	678.0	25.2	1394.6	14.2	2076.1	0.0	0.0	-104.8	-108.3	0.006
19	47	0.30	641.3	4.2	1602.8	4.7	2254.3	0.0	0.0	73.4	63.2	0.005
19	46	-0.84	641.3	4.2	1586.6	5.3	2238.4	0.1	0.0	57.5	47.1	0.018
19	45	1.41	641.3	4.2	1501.0	54.4	2150.0	0.2	0.0	-30.9	-38.5	0.037
19	44	-1.00	641.3	4.2	1423.7	16.9	2077.5	0.2	0.0	-103.4	-115.9	0.009
18	47	0.96	666.0	100.3	1602.8	4.7	2262.2	0.0	0.0	81.3	87.9	0.011
18	46	0.23	666.0	100.3	1586.6	5.3	2245.0	0.0	0.0	64.2	71.7	0.003
18	44	0.67	666.0	100.3	1423.7	16.9	2082.1	0.1	0.0	-98.8	-91.2	0.007
18	43	-0.28	666.0	100.3	1436.3	22.1	2096.9	0.0	0.0	-83.9	-78.6	0.004
18	42	0.30	666.0	100.3	1466.0	37.0	2115.2	0.0	0.0	-65.7	-48.9	0.006
17	48	-0.33	545.1	10.2	1645.2	100.3	2182.8	0.0	0.0	1.9	9.3	0.035
17	47	-0.58	545.1	10.2	1602.8	4.7	2140.5	0.7	0.0	-40.4	-33.1	0.018
16	48	0.39	571.2	23.0	1645.2	100.3	2186.3	2.2	0.0	5.4	35.5	0.011
16	47	0.88	571.2	23.0	1602.8	4.7	2144.6	0.1	0.0	-36.3	-6.9	0.127
16	46	0.31	571.2	23.0	1586.6	5.3	2126.7	0.0	0.0	-54.2	-23.1	0.013
15	48	0.41	511.6	4.8	1645.2	100.3	2170.3	0.7	0.0	-10.6	-24.2	0.017
15	47	0.52	511.6	4.8	1602.8	4.7	2127.9	0.1	0.0	-53.0	-66.5	0.008
14	48	0.88	519.5	18.3	1645.2	100.3	2179.2	0.6	0.0	-1.6	-16.2	0.055
14	47	2.44	519.5	18.3	1602.8	4.7	2136.6	2.1	0.0	-44.3	-58.6	0.042
13	47	-0.50	484.9	10.0	1602.8	4.7	2100.3	0.1	0.0	-80.6	-93.3	0.005
5	49	-6.92	113.8	1.5	2180.9	858.6	2286.1	0.4	0.0	105.2	113.8	0.061
3	49	-0.75	68.6	5.2	2180.9	858.6	2237.6	0.7	0.0	56.8	68.6	0.011
2	49	-1.17	14.6	0.5	2180.9	858.6	2219.8	0.3	0.0	39.0	14.6	0.080
1	49	-1.30	160.2	3.0	2180.9	858.6	2257.8	1.6	0.0	77.0	160.2	0.008

6-31++G(d,p)

i	j	K_{ijk} / cm^{-1}	ω(i) / cm^{-1}	I(i) / km mol^{-1}	ω(j) / cm^{-1}	I(j) / km mol^{-1}	ω(ij) / cm^{-1}	I(ij) / km mol^{-1}	I(ij) / I(k)	Δω’	Δω	TFR
33	33	-36.66	1131.4	11.0	1131.4	11.0	2263.1	12.8	0.0148	81.3	81.0	0.452
32	32	-1.10	1096.3	9.8	1096.3	9.8	2218.3	0.0	0.0000	36.6	10.9	0.101
33	34	-13.10	1131.4	11.0	1171.9	2.0	2290.1	1.4	0.0016	108.4	121.5	0.108
32	34	-1.00	1096.3	9.8	1171.9	2.0	2264.8	0.6	0.0007	83.1	86.5	0.012
32	33	-4.54	1096.3	9.8	1131.4	11.0	2240.9	0.3	0.0004	59.2	45.9	0.099
31	35	-0.26	1031.8	1.4	1223.6	38.3	2253.1	0.0	0.0000	71.3	73.7	0.004

i	j	K_{ijk} / cm^{-1}	ω(i) / cm^{-1}	I(i) / km mol^{-1}	ω(j) / cm^{-1}	I(j) / km mol^{-1}	ω(ij) / cm^{-1}	I(ij) / km mol^{-1}	I(ij) / I(k)	Δω'	Δω	TFR
31	34	-0.24	1031.8	1.4	1171.9	2.0	2189.3	0.0	0.0000	7.5	21.9	0.011
30	35	-0.60	1017.4	15.6	1223.6	38.3	2238.0	0.2	0.0002	56.3	59.3	0.010
30	33	1.04	1017.4	15.6	1131.4	11.0	2148.6	0.2	0.0002	-33.2	-32.9	0.032
29	35	-0.31	1007.1	1.2	1223.6	38.3	2228.9	0.0	0.0000	47.2	49.0	0.006
29	34	0.79	1007.1	1.2	1171.9	2.0	2163.0	2.0	0.0023	-18.7	-2.8	0.285
29	33	3.64	1007.1	1.2	1131.4	11.0	2139.0	1.4	0.0016	-42.7	-43.3	0.084
29	32	-0.81	1007.1	1.2	1096.3	9.8	2113.7	0.0	0.0001	-68.0	-78.4	0.010
28	39	-1.60	944.2	0.7	1323.7	15.3	2265.3	0.0	0.0001	83.5	86.2	0.019
28	38	-0.62	944.2	0.7	1313.5	99.8	2254.5	0.0	0.0000	72.8	76.0	0.008
28	37	-0.31	944.2	0.7	1303.2	2.4	2241.5	0.0	0.0000	59.8	65.7	0.005
28	36	-0.31	944.2	0.7	1296.8	33.6	2236.8	0.0	0.0000	55.1	59.3	0.005
28	35	-0.31	944.2	0.7	1223.6	38.3	2162.2	22.9	0.0263	-19.6	-13.9	0.022
28	34	0.36	944.2	0.7	1171.9	2.0	2096.9	0.0	0.0000	-84.8	-65.7	0.005
28	33	0.76	944.2	0.7	1131.4	11.0	2072.6	0.0	0.0000	-109.1	-106.2	0.007
27	39	-0.24	916.9	1.8	1323.7	15.3	2244.9	0.0	0.0000	63.1	58.9	0.004
27	38	-0.20	916.9	1.8	1313.5	99.8	2233.6	0.0	0.0000	51.9	48.7	0.004
27	35	0.30	916.9	1.8	1223.6	38.3	2141.5	0.1	0.0002	-40.2	-41.1	0.007
26	40	-0.22	899.1	2.3	1359.9	42.7	2261.8	0.4	0.0004	80.1	77.3	0.003
26	39	-3.85	899.1	2.3	1323.7	15.3	2228.8	0.6	0.0006	47.1	41.1	0.094
26	38	-2.08	899.1	2.3	1313.5	99.8	2215.7	0.0	0.0000	34.0	30.9	0.067
26	37	-0.40	899.1	2.3	1303.2	2.4	2204.9	0.2	0.0002	23.2	20.6	0.019
26	36	0.37	899.1	2.3	1296.8	33.6	2200.2	0.0	0.0000	18.5	14.2	0.026
26	35	0.51	899.1	2.3	1223.6	38.3	2124.0	0.7	0.0008	-57.7	-58.9	0.009
25	44	-1.26	834.3	5.6	1426.3	15.1	2253.6	0.1	0.0001	71.9	78.9	0.016
25	41	-0.92	834.3	5.6	1394.0	15.6	2228.0	0.0	0.0000	46.3	46.7	0.020
25	40	0.83	834.3	5.6	1359.9	42.7	2185.9	0.1	0.0001	4.2	12.5	0.066
25	39	-9.54	834.3	5.6	1323.7	15.3	2151.7	6.3	0.0073	-30.1	-23.7	0.403
25	38	-2.89	834.3	5.6	1313.5	99.8	2139.5	1.9	0.0022	-42.2	-33.9	0.085
25	37	-1.10	834.3	5.6	1303.2	2.4	2129.3	0.1	0.0001	-52.5	-44.2	0.025
25	36	-1.00	834.3	5.6	1296.8	33.6	2125.0	0.0	0.0000	-56.7	-50.6	0.020
24	44	3.98	811.0	7.9	1426.3	15.1	2237.8	0.2	0.0002	56.1	55.6	0.072
24	43	-0.21	811.0	7.9	1439.7	13.5	2253.4	0.0	0.0000	71.7	69.0	0.003
24	42	0.60	811.0	7.9	1462.1	37.1	2266.3	0.0	0.0000	84.6	91.3	0.007
24	41	3.57	811.0	7.9	1394.0	15.6	2212.7	0.9	0.0011	31.0	23.3	0.153
24	40	-3.16	811.0	7.9	1359.9	42.7	2171.2	5.9	0.0068	-10.5	-10.9	0.290
24	39	48.86	811.0	7.9	1323.7	15.3	2129.0	104.0	0.1198	-52.8	-47.0	1.039
24	38	16.37	811.0	7.9	1313.5	99.8	2124.4	18.4	0.0212	-57.4	-57.2	0.286
24	37	5.96	811.0	7.9	1303.2	2.4	2112.9	0.9	0.0010	-68.8	-67.5	0.088
24	36	6.27	811.0	7.9	1296.8	33.6	2108.0	1.1	0.0013	-73.7	-73.9	0.085
23	45	-0.74	785.8	3.2	1499.5	99.9	2278.3	0.0	0.0000	96.6	103.6	0.007

i	j	K_{ijk} / cm^{-1}	ω(i) / cm^{-1}	I(i) / km mol^{-1}	ω(j) / cm^{-1}	I(j) / km mol^{-1}	ω(ij) / cm^{-1}	I(ij) / km mol^{-1}	I(ij) / I(k)	Δω'	Δω	TFR
23	44	0.42	785.8	3.2	1426.3	15.1	2206.6	0.0	0.0000	24.9	30.4	0.014
23	41	0.61	785.8	3.2	1394.0	15.6	2182.5	0.1	0.0002	0.8	-1.8	0.333
23	40	-0.30	785.8	3.2	1359.9	42.7	2140.3	0.4	0.0004	-41.4	-36.0	0.008
23	39	5.72	785.8	3.2	1323.7	15.3	2106.2	5.1	0.0059	-75.5	-72.2	0.079
23	38	1.75	785.8	3.2	1313.5	99.8	2095.1	0.2	0.0002	-86.6	-82.4	0.021
23	37	0.92	785.8	3.2	1303.2	2.4	2083.8	0.1	0.0001	-97.9	-92.7	0.010
23	36	0.92	785.8	3.2	1296.8	33.6	2077.6	0.0	0.0001	-104.1	-99.1	0.009
22	45	4.91	755.8	11.1	1499.5	99.9	2264.2	0.3	0.0003	82.5	73.6	0.067
22	44	-2.10	755.8	11.1	1426.3	15.1	2192.4	1.4	0.0016	10.7	0.4	4.812
22	43	0.24	755.8	11.1	1439.7	13.5	2207.3	0.0	0.0000	25.5	13.8	0.017
22	42	-0.31	755.8	11.1	1462.1	37.1	2219.9	0.1	0.0001	38.2	36.2	0.009
22	41	-1.87	755.8	11.1	1394.0	15.6	2167.0	31.7	0.0365	-14.7	-31.8	0.059
22	40	1.53	755.8	11.1	1359.9	42.7	2123.2	0.3	0.0003	-58.6	-66.0	0.023
22	39	-35.40	755.8	11.1	1323.7	15.3	2088.2	23.0	0.0265	-93.5	-102.2	0.346
22	38	-12.62	755.8	11.1	1313.5	99.8	2079.1	4.7	0.0054	-102.6	-112.4	0.112
21	46	-1.20	706.4	14.1	1586.8	1.4	2291.1	0.0	0.0000	109.3	111.4	0.011
21	45	2.99	706.4	14.1	1499.5	99.9	2203.4	1.0	0.0011	21.7	24.1	0.124
21	44	-2.18	706.4	14.1	1426.3	15.1	2133.1	4.9	0.0056	-48.6	-49.1	0.045
21	43	0.35	706.4	14.1	1439.7	13.5	2147.9	0.1	0.0001	-33.8	-35.7	0.010
21	42	-0.28	706.4	14.1	1462.1	37.1	2160.5	0.0	0.0000	-21.2	-13.3	0.021
21	41	-1.00	706.4	14.1	1394.0	15.6	2106.6	0.0	0.0000	-75.1	-81.3	0.012
20	47	1.07	677.0	20.8	1603.3	14.1	2279.6	0.0	0.0000	97.8	98.6	0.011
20	46	1.80	677.0	20.8	1586.8	1.4	2262.9	0.1	0.0001	81.2	82.0	0.022
20	45	-4.75	677.0	20.8	1499.5	99.9	2172.9	29.7	0.0342	-8.8	-5.3	0.896
20	44	2.90	677.0	20.8	1426.3	15.1	2101.8	0.5	0.0006	-79.9	-78.4	0.037
20	42	0.39	677.0	20.8	1462.1	37.1	2129.7	0.0	0.0000	-52.0	-42.7	0.009
20	41	0.73	677.0	20.8	1394.0	15.6	2076.0	0.0	0.0000	-105.7	-110.7	0.007
19	47	0.29	641.9	2.5	1603.3	14.1	2252.8	0.0	0.0000	71.0	63.6	0.005
19	46	-0.84	641.9	2.5	1586.8	1.4	2236.8	0.1	0.0001	55.1	47.0	0.018
19	45	1.40	641.9	2.5	1499.5	99.9	2147.7	0.2	0.0002	-34.0	-40.3	0.035
19	44	-1.01	641.9	2.5	1426.3	15.1	2076.9	0.2	0.0002	-104.8	-113.5	0.009
18	47	0.97	667.8	98.5	1603.3	14.1	2265.4	0.0	0.0001	83.7	89.5	0.011
18	44	0.66	667.8	98.5	1426.3	15.1	2086.2	0.1	0.0001	-95.6	-87.6	0.008
18	43	-0.28	667.8	98.5	1439.7	13.5	2102.0	0.0	0.0000	-79.7	-74.2	0.004
18	42	0.30	667.8	98.5	1462.1	37.1	2114.9	0.0	0.0000	-66.8	-51.8	0.006
17	48	-0.33	547.6	18.3	1645.4	395.9	2183.8	0.0	0.0000	2.1	11.2	0.030
17	47	-0.59	547.6	18.3	1603.3	14.1	2142.5	0.7	0.0008	-39.3	-30.8	0.019
16	48	0.41	568.7	20.3	1645.4	395.9	2185.1	2.3	0.0026	3.4	32.4	0.013
16	47	0.89	568.7	20.3	1603.3	14.1	2144.4	0.1	0.0001	-37.3	-9.6	0.093
16	46	0.32	568.7	20.3	1586.8	1.4	2126.4	0.0	0.0000	-55.3	-26.2	0.012

i	j	K_{ijk} / cm^{-1}	ω(i) / cm^{-1}	I(i) / km mol^{-1}	ω(j) / cm^{-1}	I(j) / km mol^{-1}	ω(ij) / cm^{-1}	I(ij) / km mol^{-1}	I(ij) / I(k)	Δω'	Δω	TFR
15	48	0.39	513.9	4.2	1645.4	395.9	2169.9	0.6	0.0007	-11.8	-22.4	0.017
15	47	0.47	513.9	4.2	1603.3	14.1	2128.3	0.1	0.0001	-53.4	-64.5	0.007
14	48	0.88	517.7	17.7	1645.4	395.9	2176.3	0.6	0.0006	-5.4	-18.7	0.047
14	47	2.42	517.7	17.7	1603.3	14.1	2134.5	2.0	0.0023	-47.2	-60.7	0.040
13	47	-0.59	487.5	9.8	1603.3	14.1	2105.1	0.1	0.0001	-76.6	-90.9	0.007
5	49	-6.91	114.6	1.1	2181.7	868.0	2286.7	0.4	0.0005	104.9	114.6	0.060
3	49	-0.73	71.9	5.3	2181.7	868.0	2236.9	0.7	0.0008	55.2	71.9	0.010
2	49	-1.14	12.9	0.5	2181.7	868.0	2225.6	0.3	0.0003	43.9	12.9	0.088
1	49	-1.27	155.7	2.1	2181.7	868.0	2256.4	1.6	0.0018	74.7	155.7	0.008

6-311G(d,p)

i	j	K_{ijk} / cm^{-1}	ω(i) / cm^{-1}	I(i) / km mol^{-1}	ω(j) / cm^{-1}	I(j) / km mol^{-1}	ω(ij) / cm^{-1}	I(ij) / km mol^{-1}	I(ij) / I(k)	Δω'	Δω	TFR
33	33	-34.63	1129.2	4.5	1129.2	4.5	2266.7	11.2	0.0972	80.4	72.3	0.479
32	32	-1.32	1134.2	12.1	1134.2	12.1	2272.6	0.0	0.0001	86.4	82.3	0.016
29	29	-0.86	1085.2	32.3	1085.2	32.3	2143.7	0.3	0.0028	-42.5	-15.9	0.054
32	33	-5.38	1134.2	12.1	1129.2	4.5	2268.8	0.5	0.0047	82.5	77.3	0.070
31	35	-0.23	1035.7	7.5	1219.2	31.2	2257.7	0.0	0.0003	71.5	68.6	0.003
31	34	-0.25	1035.7	7.5	1201.1	8.4	2233.3	0.0	0.0000	47.1	50.5	0.005
30	34	0.88	1016.9	3.2	1201.1	8.4	2213.8	10.3	0.0894	27.6	31.7	0.028
30	33	3.51	1016.9	3.2	1129.2	4.5	2152.3	1.0	0.0090	-33.9	-40.1	0.088
30	32	-0.75	1016.9	3.2	1134.2	12.1	2152.7	0.0	0.0003	-33.6	-35.1	0.021
29	35	-0.58	1085.2	32.3	1219.2	31.2	2292.4	0.2	0.0015	106.1	118.1	0.005
29	33	0.68	1085.2	32.3	1129.2	4.5	2206.5	0.1	0.0009	20.2	28.2	0.024
28	39	-1.68	927.0	3.2	1327.8	14.8	2255.4	0.1	0.0004	69.2	68.5	0.024
28	38	-0.33	927.0	3.2	1306.0	3.9	2248.6	0.0	0.0000	62.3	46.8	0.007
28	37	-0.42	927.0	3.2	1323.2	319.8	2246.2	0.0	0.0000	60.0	63.9	0.007
28	36	-0.33	927.0	3.2	1295.4	3.0	2229.2	0.0	0.0000	43.0	36.1	0.009
28	35	-0.31	927.0	3.2	1219.2	31.2	2147.5	45.1	0.3901	-38.8	-40.1	0.008
28	34	0.34	927.0	3.2	1201.1	8.4	2122.2	0.0	0.0002	-64.1	-58.2	0.006
27	39	-0.32	906.7	2.1	1327.8	14.8	2241.6	0.0	0.0000	55.4	48.3	0.007
27	35	0.24	906.7	2.1	1219.2	31.2	2133.9	0.1	0.0010	-52.3	-60.3	0.004
26	39	-3.78	922.8	1.5	1327.8	14.8	2252.7	0.5	0.0042	66.5	64.4	0.059
26	38	-1.62	922.8	1.5	1306.0	3.9	2244.6	0.0	0.0002	58.4	42.6	0.038
26	35	0.58	922.8	1.5	1219.2	31.2	2142.7	0.7	0.0061	-43.5	-44.2	0.013
26	34	0.45	922.8	1.5	1201.1	8.4	2120.0	0.1	0.0007	-66.2	-62.3	0.007
25	44	-0.77	813.0	13.5	1458.5	17.9	2277.7	0.0	0.0003	91.5	85.3	0.009
25	41	-0.46	813.0	13.5	1397.6	0.6	2212.5	0.0	0.0000	26.2	24.4	0.019
25	40	0.52	813.0	13.5	1380.8	31.1	2195.0	0.1	0.0005	8.8	7.6	0.068
25	39	-4.71	813.0	13.5	1327.8	14.8	2140.7	211.4	1.8274	-45.6	-45.4	0.104
25	38	-0.56	813.0	13.5	1306.0	3.9	2135.1	0.0	0.0001	-51.1	-67.2	0.008
25	37	-0.55	813.0	13.5	1323.2	319.8	2133.5	0.0	0.0000	-52.8	-50.1	0.011
25	36	-0.33	813.0	13.5	1295.4	3.0	2115.3	0.0	0.0000	-71.0	-77.8	0.004

i	j	K_{ijk} / cm^{-1}	ω(i) / cm^{-1}	I(i) / km mol^{-1}	ω(j) / cm^{-1}	I(j) / km mol^{-1}	ω(ij) / cm^{-1}	I(ij) / km mol^{-1}	I(ij) / I(k)	Δω'	Δω	TFR
24	44	4.29	837.5	11.9	1458.5	17.9	2288.4	0.2	0.0021	102.2	109.8	0.039
24	41	3.44	837.5	11.9	1397.6	0.6	2223.6	1.0	0.0086	37.4	48.9	0.070
24	40	-3.89	837.5	11.9	1380.8	31.1	2207.6	83.1	0.7180	21.4	32.1	0.121
24	39	53.07	837.5	11.9	1327.8	14.8	2140.7	17.3	0.1495	-45.5	-20.9	2.534
24	38	8.80	837.5	11.9	1306.0	3.9	2145.2	1.7	0.0144	-41.0	-42.7	0.206
24	37	9.02	837.5	11.9	1323.2	319.8	2143.4	1.4	0.0124	-42.9	-25.6	0.353
24	36	5.05	837.5	11.9	1295.4	3.0	2125.6	0.3	0.0022	-60.6	-53.4	0.095
23	45	0.94	771.6	4.7	1511.6	6.8	2275.0	0.0	0.0004	88.8	97.0	0.010
23	44	-0.69	771.6	4.7	1458.5	17.9	2239.5	0.0	0.0000	53.3	43.9	0.016
23	41	-0.37	771.6	4.7	1397.6	0.6	2174.3	0.1	0.0006	-11.9	-17.0	0.022
23	40	0.69	771.6	4.7	1380.8	31.1	2156.7	10.9	0.0943	-29.6	-33.8	0.021
23	39	-8.61	771.6	4.7	1327.8	14.8	2102.5	10.0	0.0867	-83.7	-86.8	0.099
23	38	-1.60	771.6	4.7	1306.0	3.9	2096.1	0.0	0.0004	-90.1	-108.6	0.015
23	37	-1.53	771.6	4.7	1323.2	319.8	2093.7	0.0	0.0003	-92.6	-91.5	0.017
22	45	4.71	767.3	5.7	1511.6	6.8	2274.7	0.2	0.0022	88.5	92.6	0.051
22	44	-2.03	767.3	5.7	1458.5	17.9	2238.8	1.3	0.0110	52.6	39.6	0.051
22	42	-0.32	767.3	5.7	1554.0	10.3	2293.8	0.1	0.0006	107.6	135.1	0.002
22	41	-1.64	767.3	5.7	1397.6	0.6	2173.0	4.3	0.0372	-13.2	-21.3	0.077
22	40	1.75	767.3	5.7	1380.8	31.1	2154.1	0.3	0.0027	-32.2	-38.1	0.046
22	39	-34.18	767.3	5.7	1327.8	14.8	2099.5	17.0	0.1470	-86.7	-91.1	0.375
22	38	-6.14	767.3	5.7	1306.0	3.9	2094.9	1.3	0.0109	-91.3	-112.9	0.054
22	37	-6.84	767.3	5.7	1323.2	319.8	2092.6	1.4	0.0125	-93.6	-95.8	0.071
21	45	2.94	712.5	58.8	1511.6	6.8	2220.4	0.6	0.0050	34.1	37.9	0.077
21	44	-2.06	712.5	58.8	1458.5	17.9	2184.9	67.7	0.5848	-1.3	-15.2	0.136
21	42	-0.24	712.5	58.8	1554.0	10.3	2240.8	0.0	0.0001	54.6	80.3	0.003
21	41	-0.91	712.5	58.8	1397.6	0.6	2119.1	0.0	0.0001	-67.1	-76.1	0.012
21	40	1.31	712.5	58.8	1380.8	31.1	2103.2	0.0	0.0004	-83.0	-92.8	0.014
20	47	1.20	684.9	20.4	1603.5	2.4	2291.7	0.0	0.0002	105.5	102.2	0.012
20	46	-1.59	684.9	20.4	1578.7	0.7	2264.9	0.1	0.0004	78.7	77.4	0.021
20	45	-4.87	684.9	20.4	1511.6	6.8	2190.3	715.8	6.1867	4.1	10.3	0.474
20	44	2.98	684.9	20.4	1458.5	17.9	2152.7	0.6	0.0055	-33.5	-42.8	0.070
20	42	0.41	684.9	20.4	1554.0	10.3	2208.9	0.0	0.0001	22.7	52.7	0.008
20	41	0.79	684.9	20.4	1397.6	0.6	2087.5	0.0	0.0002	-98.7	-103.7	0.008
19	47	0.51	729.5	34.8	1603.5	2.4	2292.0	0.0	0.0000	105.7	146.8	0.003
19	46	0.67	729.5	34.8	1578.7	0.7	2268.2	0.0	0.0004	81.9	122.0	0.005
19	45	1.22	729.5	34.8	1511.6	6.8	2190.3	0.2	0.0014	4.1	54.9	0.022
19	44	-0.71	729.5	34.8	1458.5	17.9	2157.3	0.1	0.0011	-28.9	1.8	0.387
18	47	0.90	648.6	9.0	1603.5	2.4	2284.9	0.0	0.0003	98.6	65.8	0.014
18	46	-0.28	648.6	9.0	1578.7	0.7	2260.5	0.0	0.0001	74.3	41.1	0.007
18	44	0.92	648.6	9.0	1458.5	17.9	2149.3	0.2	0.0015	-36.9	-79.1	0.012
18	42	0.25	648.6	9.0	1554.0	10.3	2201.7	0.0	0.0001	15.5	16.4	0.015
18	41	0.71	648.6	9.0	1397.6	0.6	2081.6	0.0	0.0001	-104.7	-140.0	0.005
17	47	-0.42	742.9	79.2	1603.5	2.4	2200.4	0.3	0.0030	14.2	160.1	0.003
17	45	0.59	742.9	79.2	1511.6	6.8	2097.9	0.0	0.0001	-88.3	68.3	0.009
16	47	0.93	542.3	8.3	1603.5	2.4	2205.7	0.1	0.0010	19.4	-40.5	0.023
16	46	-0.35	542.3	8.3	1578.7	0.7	2179.9	0.0	0.0003	-6.3	-65.2	0.005

i	j	K_{ijk} / cm^{-1}	ω(i) / cm^{-1}	I(i) / km mol^{-1}	ω(j) / cm^{-1}	I(j) / km mol^{-1}	ω(ij) / cm^{-1}	I(ij) / km mol^{-1}	I(ij) / I(k)	Δω'	Δω	TFR
15	48	0.32	538.4	12.1	1707.2	278.8	2259.4	0.0	0.0000	73.2	59.4	0.005
15	47	0.28	538.4	12.1	1603.5	2.4	2161.3	0.0	0.0003	-24.9	-44.4	0.006
14	48	0.93	605.7	5.6	1707.2	278.8	2272.5	90.8	0.7845	86.3	126.7	0.007
14	47	2.22	605.7	5.6	1603.5	2.4	2173.5	1.7	0.0143	-12.7	23.0	0.097
14	46	0.42	605.7	5.6	1578.7	0.7	2147.8	0.0	0.0003	-38.5	-1.8	0.234
13	48	-0.34	471.2	37.3	1707.2	278.8	2256.0	3.0	0.0262	69.8	-7.8	0.044
13	47	-0.80	471.2	37.3	1603.5	2.4	2158.2	0.2	0.0017	-28.0	-111.5	0.007
11	48	-0.27	518.9	62.0	1707.2	278.8	2139.4	0.1	0.0007	-46.9	39.9	0.007
10	48	0.44	384.3	6.1	1707.2	278.8	2101.1	0.0	0.0004	-85.1	-94.7	0.005
8	48	-0.34	350.2	3.2	1707.2	278.8	2132.1	0.2	0.0018	-54.1	-128.8	0.003
3	49	-0.61	63.8	3.4	2186.2	115.7	2218.4	0.6	0.0049	32.1	63.8	0.010
2	49	-1.17	100.5	5.7	2186.2	115.7	2232.5	0.1	0.0011	46.3	100.5	0.012

6-311+G(d,p)

i	j	K_{ijk} / cm^{-1}	ω(i) / cm^{-1}	I(i) / km mol^{-1}	ω(j) / cm^{-1}	I(j) / km mol^{-1}	ω(ij) / cm^{-1}	I(ij) / km mol^{-1}	I(ij) / I(k)	Δω'	Δω	TFR
33	33	34.82	1126.8	17.6	1126.8	17.6	2244.6	11.2	0.0236	70.7	79.8	0.437
32	32	1.40	1098.5	17.2	1098.5	17.2	2237.0	0.0	0.0000	63.1	23.0	0.061
33	34	-12.53	1126.8	17.6	1174.1	1.4	2281.3	1.2	0.0025	107.4	127.1	0.099
32	34	1.20	1098.5	17.2	1174.1	1.4	2276.8	0.7	0.0016	102.9	98.7	0.012
32	33	-5.23	1098.5	17.2	1126.8	17.6	2239.8	0.4	0.0009	66.0	51.4	0.102
31	35	-0.26	1032.7	16.4	1212.3	11.1	2249.2	0.0	0.0001	75.3	71.1	0.004
31	34	-0.26	1032.7	16.4	1174.1	1.4	2191.8	0.0	0.0000	17.9	32.9	0.008
30	35	-0.54	1011.3	26.8	1212.3	11.1	2223.2	0.2	0.0003	49.3	49.8	0.011
30	33	-0.21	1011.3	26.8	1126.8	17.6	2130.5	0.0	0.0001	-43.4	-35.8	0.006
30	32	0.23	1011.3	26.8	1098.5	17.2	2124.1	0.0	0.0001	-49.8	-64.1	0.004
29	36	-1.33	999.5	0.5	1282.2	48.5	2286.5	0.0	0.0000	112.7	107.8	0.012
29	35	-0.21	999.5	0.5	1212.3	11.1	2219.5	0.0	0.0000	45.6	37.9	0.006
29	34	0.66	999.5	0.5	1174.1	1.4	2160.3	0.6	0.0013	-13.6	-0.3	2.437
29	33	-3.35	999.5	0.5	1126.8	17.6	2126.6	1.6	0.0034	-47.2	-47.6	0.070
29	32	-0.73	999.5	0.5	1098.5	17.2	2119.5	0.0	0.0001	-54.4	-75.9	0.010
28	39	1.64	980.4	0.7	1315.6	61.3	2288.4	0.0	0.0001	114.5	122.1	0.013
28	38	0.53	980.4	0.7	1305.8	2.5	2277.3	0.0	0.0000	103.5	112.3	0.005
28	37	0.37	980.4	0.7	1301.8	219.3	2272.3	0.0	0.0000	98.4	108.3	0.003
28	36	-0.25	980.4	0.7	1282.2	48.5	2258.4	0.0	0.0000	84.6	88.7	0.003
28	35	0.29	980.4	0.7	1212.3	11.1	2188.8	0.1	0.0002	15.0	18.8	0.015
28	34	-0.36	980.4	0.7	1174.1	1.4	2131.8	0.0	0.0001	-42.0	-19.4	0.018
28	33	0.75	980.4	0.7	1126.8	17.6	2096.3	0.0	0.0000	-77.6	-66.7	0.011
27	35	-0.29	925.4	2.0	1212.3	11.1	2146.5	0.3	0.0006	-27.4	-36.1	0.008
26	39	3.30	900.1	4.6	1315.6	61.3	2217.9	0.4	0.0008	44.0	41.9	0.079
26	38	1.75	900.1	4.6	1305.8	2.5	2205.0	0.1	0.0001	31.2	32.1	0.054
26	35	-0.60	900.1	4.6	1212.3	11.1	2117.3	0.7	0.0016	-56.6	-61.4	0.010
26	34	-0.33	900.1	4.6	1174.1	1.4	2060.4	0.1	0.0002	-113.4	-99.6	0.003

i	j	K_{ijk} / cm^{-1}	ω(i) / cm^{-1}	I(i) / km mol^{-1}	ω(j) / cm^{-1}	I(j) / km mol^{-1}	ω(ij) / cm^{-1}	I(ij) / km mol^{-1}	I(ij) / I(k)	Δω'	Δω	TFR
25	44	1.03	849.2	26.0	1415.3	2.1	2255.9	0.1	0.0001	82.0	90.5	0.011
25	41	0.60	849.2	26.0	1386.3	12.5	2241.9	0.0	0.0000	68.0	61.6	0.010
25	40	0.69	849.2	26.0	1371.2	70.4	2216.2	0.1	0.0002	42.3	46.5	0.015
25	39	7.05	849.2	26.0	1315.6	61.3	2160.1	12.2	0.0257	-13.8	-9.1	0.773
25	38	1.57	849.2	26.0	1305.8	2.5	2148.9	0.6	0.0013	-25.0	-18.9	0.083
25	37	0.84	849.2	26.0	1301.8	219.3	2144.8	0.0	0.0001	-29.1	-22.9	0.037
25	36	-0.53	849.2	26.0	1282.2	48.5	2129.5	0.0	0.0000	-44.4	-42.6	0.012
25	35	0.57	849.2	26.0	1212.3	11.1	2061.0	0.0	0.0001	-112.9	-112.4	0.005
24	44	-4.07	817.2	0.8	1415.3	2.1	2225.2	0.2	0.0004	51.3	58.6	0.069
24	42	-0.48	817.2	0.8	1423.8	3.8	2240.0	0.0	0.0000	66.2	67.1	0.007
24	41	-3.02	817.2	0.8	1386.3	12.5	2210.4	0.7	0.0014	36.6	29.7	0.102
24	40	-3.42	817.2	0.8	1371.2	70.4	2184.6	6.1	0.0129	10.7	14.6	0.235
24	39	-51.93	817.2	0.8	1315.6	61.3	2119.2	51.8	0.1091	-54.7	-41.0	1.266
24	38	-13.89	817.2	0.8	1305.8	2.5	2117.3	12.0	0.0253	-56.6	-50.8	0.273
24	37	-8.30	817.2	0.8	1301.8	219.3	2111.1	2.6	0.0054	-62.8	-54.8	0.151
24	36	4.35	817.2	0.8	1282.2	48.5	2097.6	0.4	0.0008	-76.3	-74.5	0.058
23	44	-0.31	802.9	3.5	1415.3	2.1	2216.0	0.0	0.0000	42.1	44.3	0.007
23	41	-0.45	802.9	3.5	1386.3	12.5	2202.0	0.1	0.0002	28.1	15.3	0.030
23	40	-0.25	802.9	3.5	1371.2	70.4	2176.1	0.2	0.0004	2.2	0.2	1.360
23	39	-4.49	802.9	3.5	1315.6	61.3	2119.3	4.4	0.0092	-54.5	-55.4	0.081
23	38	-1.04	802.9	3.5	1305.8	2.5	2108.8	0.1	0.0002	-65.1	-65.2	0.016
23	37	-0.79	802.9	3.5	1301.8	219.3	2103.2	0.0	0.0001	-70.6	-69.2	0.011
23	36	0.63	802.9	3.5	1282.2	48.5	2086.4	0.1	0.0002	-87.5	-88.8	0.007
22	45	-4.60	759.6	13.0	1492.0	169.8	2256.7	0.2	0.0005	82.8	77.7	0.059
22	44	2.04	759.6	13.0	1415.3	2.1	2177.9	1.2	0.0025	4.1	1.0	2.130
22	42	0.24	759.6	13.0	1423.8	3.8	2191.8	0.0	0.0001	17.9	9.5	0.025
22	41	1.47	759.6	13.0	1386.3	12.5	2162.9	495.6	1.0426	-11.0	-28.0	0.052
22	40	1.62	759.6	13.0	1371.2	70.4	2134.6	0.3	0.0006	-39.3	-43.1	0.038
22	39	35.18	759.6	13.0	1315.6	61.3	2078.1	26.9	0.0566	-95.7	-98.7	0.356
22	38	10.17	759.6	13.0	1305.8	2.5	2069.2	3.4	0.0071	-104.6	-108.5	0.094
22	37	6.61	759.6	13.0	1301.8	219.3	2063.3	1.2	0.0026	-110.6	-112.5	0.059
21	46	-1.20	710.6	14.5	1576.1	1.5	2284.7	0.0	0.0001	110.8	112.8	0.011
21	45	-2.95	710.6	14.5	1492.0	169.8	2200.8	0.6	0.0012	27.0	28.8	0.102
21	44	2.17	710.6	14.5	1415.3	2.1	2122.9	0.1	0.0002	-50.9	-48.0	0.045
21	41	0.77	710.6	14.5	1386.3	12.5	2107.1	0.0	0.0000	-66.8	-76.9	0.010
21	40	1.23	710.6	14.5	1371.2	70.4	2081.7	0.0	0.0001	-92.1	-92.1	0.013
20	47	-1.04	674.5	6.2	1593.8	1.8	2271.1	0.0	0.0001	97.3	94.4	0.011
20	46	1.73	674.5	6.2	1576.1	1.5	2248.2	0.1	0.0001	74.4	76.6	0.023
20	45	4.64	674.5	6.2	1492.0	169.8	2165.0	42.4	0.0892	-8.9	-7.4	0.629
20	44	-2.83	674.5	6.2	1415.3	2.1	2086.1	0.9	0.0018	-87.7	-84.2	0.034
20	42	-0.31	674.5	6.2	1423.8	3.8	2100.5	0.0	0.0000	-73.3	-75.6	0.004
20	41	-0.43	674.5	6.2	1386.3	12.5	2071.0	0.0	0.0000	-102.9	-113.1	0.004
19	47	-0.34	643.8	1.8	1593.8	1.8	2237.1	0.0	0.0000	63.2	63.8	0.005
19	46	-0.76	643.8	1.8	1576.1	1.5	2218.1	0.0	0.0001	44.3	46.0	0.017
19	45	-1.21	643.8	1.8	1492.0	169.8	2132.0	0.2	0.0005	-41.9	-38.0	0.032
18	48	-0.34	601.0	28.1	1643.2	342.2	2242.0	0.1	0.0002	68.1	70.3	0.005

i	j	K_{ijk} / cm^{-1}	ω(i) / cm^{-1}	I(i) / km mol^{-1}	ω(j) / cm^{-1}	I(j) / km mol^{-1}	ω(ij) / cm^{-1}	I(ij) / km mol^{-1}	I(ij) / I(k)	Δω’	Δω	TFR
18	47	-0.91	601.0	28.1	1593.8	1.8	2199.7	0.0	0.0001	25.8	21.0	0.044
18	46	0.25	601.0	28.1	1576.1	1.5	2179.0	0.0	0.0000	5.1	3.2	0.079
17	48	0.28	548.0	11.3	1643.2	342.2	2177.9	0.0	0.0001	4.1	17.3	0.016
17	47	0.52	548.0	11.3	1593.8	1.8	2135.4	0.6	0.0013	-38.4	-32.0	0.016
16	48	-0.28	518.3	7.2	1643.2	342.2	2151.6	162.1	0.3410	-22.3	-12.4	0.022
16	47	-0.67	518.3	7.2	1593.8	1.8	2109.4	0.1	0.0001	-64.4	-61.7	0.011
16	46	0.37	518.3	7.2	1576.1	1.5	2088.0	0.0	0.0001	-85.9	-79.5	0.005
15	48	-0.50	528.9	17.3	1643.2	342.2	2150.5	3.6	0.0076	-23.3	-1.8	0.281
15	47	-0.67	528.9	17.3	1593.8	1.8	2108.5	0.1	0.0003	-65.4	-51.1	0.013
14	48	-0.95	450.3	109.2	1643.2	342.2	2113.0	0.7	0.0014	-60.9	-80.4	0.012
14	47	-2.59	450.3	109.2	1593.8	1.8	2070.6	2.2	0.0046	-103.2	-129.8	0.020
5	49	6.65	157.0	3.5	2173.9	475.4	2281.6	0.4	0.0009	107.7	157.0	0.042
2	49	1.20	41.4	3.9	2173.9	475.4	2208.3	0.4	0.0008	34.5	41.4	0.029
1	49	1.36	22.4	1.6	2173.9	475.4	2189.3	1.7	0.0035	15.4	22.4	0.061

6-311++G(d,p)

i	j	K_{ijk} / cm^{-1}	ω(i) / cm^{-1}	I(i) / km mol^{-1}	ω(j) / cm^{-1}	I(j) / km mol^{-1}	ω(ij) / cm^{-1}	I(ij) / km mol^{-1}	I(ij) / I(k)	Δω’	Δω	TFR
33	33	-34.83	1125.8	16.6	1125.8	16.6	2244.9	11.3	0.0314	74.6	81.3	0.428
32	32	-1.39	1096.2	18.1	1096.2	18.1	2221.8	0.0	0.0000	51.5	22.1	0.063
33	34	-12.57	1125.8	16.6	1164.6	0.8	2276.0	1.2	0.0033	105.7	120.1	0.105
32	34	-1.19	1096.2	18.1	1164.6	0.8	2263.7	0.7	0.0020	93.5	90.5	0.013
32	33	-5.20	1096.2	18.1	1125.8	16.6	2232.4	0.4	0.0012	62.2	51.7	0.101
31	35	-0.26	1027.2	10.3	1219.6	22.4	2244.6	0.0	0.0001	74.4	76.6	0.003
31	34	-0.25	1027.2	10.3	1164.6	0.8	2180.4	0.0	0.0000	10.1	21.6	0.012
30	35	-0.53	1013.9	32.5	1219.6	22.4	2228.7	0.2	0.0004	58.4	63.2	0.008
30	32	0.26	1013.9	32.5	1096.2	18.1	2120.6	0.0	0.0001	-49.6	-60.2	0.004
29	35	-0.22	999.3	0.4	1219.6	22.4	2219.3	0.0	0.0001	49.1	48.6	0.004
29	34	0.65	999.3	0.4	1164.6	0.8	2153.5	0.6	0.0017	-16.8	-6.4	0.102
29	33	3.33	999.3	0.4	1125.8	16.6	2125.2	1.6	0.0045	-45.0	-45.2	0.074
29	32	-0.72	999.3	0.4	1096.2	18.1	2110.4	0.0	0.0001	-59.8	-74.8	0.010
28	39	-1.64	956.4	0.2	1316.3	32.4	2269.4	0.0	0.0001	99.1	102.5	0.016
28	38	-0.52	956.4	0.2	1306.6	2.2	2259.1	0.0	0.0000	88.8	92.8	0.006
28	37	-0.37	956.4	0.2	1295.5	134.9	2245.1	0.0	0.0000	74.8	81.7	0.005
28	36	-0.25	956.4	0.2	1281.7	69.5	2238.8	0.0	0.0000	68.6	67.9	0.004
28	35	-0.29	956.4	0.2	1219.6	22.4	2170.5	0.1	0.0002	0.2	5.7	0.050
28	34	0.36	956.4	0.2	1164.6	0.8	2106.0	0.0	0.0001	-64.3	-49.2	0.007
28	33	0.75	956.4	0.2	1125.8	16.6	2076.7	0.0	0.0000	-93.5	-88.1	0.009
27	35	0.28	928.2	1.3	1219.6	22.4	2147.0	0.3	0.0008	-23.3	-22.4	0.012
26	39	-3.30	900.6	5.4	1316.3	32.4	2219.1	0.4	0.0010	48.9	46.6	0.071
26	38	-1.74	900.6	5.4	1306.6	2.2	2207.0	0.1	0.0002	36.8	36.9	0.047
26	35	0.60	900.6	5.4	1219.6	22.4	2119.2	0.7	0.0021	-51.0	-50.1	0.012

i	j	K_{ijk} / cm^{-1}	ω(i) / cm^{-1}	I(i) / km mol^{-1}	ω(j) / cm^{-1}	I(j) / km mol^{-1}	ω(ij) / cm^{-1}	I(ij) / km mol^{-1}	I(ij) / I(k)	Δω'	Δω	TFR
25	44	-1.01	837.9	23.4	1418.6	1.1	2248.6	0.1	0.0002	78.3	86.3	0.012
25	41	-0.59	837.9	23.4	1388.2	10.4	2231.8	0.0	0.0000	61.5	55.9	0.011
25	40	0.67	837.9	23.4	1362.8	87.7	2196.2	0.1	0.0002	25.9	30.4	0.022
25	39	-6.81	837.9	23.4	1316.3	32.4	2150.7	3.5	0.0098	-19.5	-16.0	0.425
25	38	-1.50	837.9	23.4	1306.6	2.2	2139.9	0.6	0.0016	-30.4	-25.7	0.058
25	37	-0.82	837.9	23.4	1295.5	134.9	2127.3	0.0	0.0001	-42.9	-36.8	0.022
25	36	-0.51	837.9	23.4	1281.7	69.5	2119.2	0.0	0.0000	-51.0	-50.6	0.010
24	44	-4.06	811.6	4.6	1418.6	1.1	2227.6	0.2	0.0005	57.4	59.9	0.068
24	42	-0.48	811.6	4.6	1427.7	3.1	2241.0	0.0	0.0000	70.7	69.1	0.007
24	41	-3.01	811.6	4.6	1388.2	10.4	2210.2	0.7	0.0018	39.9	29.5	0.102
24	40	3.40	811.6	4.6	1362.8	87.7	2175.0	6.1	0.0171	4.8	4.1	0.828
24	39	-51.90	811.6	4.6	1316.3	32.4	2118.8	43.9	0.1223	-51.5	-42.4	1.225
24	38	-13.78	811.6	4.6	1306.6	2.2	2118.2	11.6	0.0324	-52.1	-52.0	0.265
24	37	-8.37	811.6	4.6	1295.5	134.9	2103.9	2.6	0.0072	-66.3	-63.1	0.133
24	36	-4.38	811.6	4.6	1281.7	69.5	2097.1	0.4	0.0011	-73.1	-77.0	0.057
23	44	0.27	795.4	15.0	1418.6	1.1	2207.8	0.0	0.0000	37.5	43.8	0.006
23	41	0.42	795.4	15.0	1388.2	10.4	2191.2	0.1	0.0002	21.0	13.4	0.031
23	40	-0.22	795.4	15.0	1362.8	87.7	2155.1	0.2	0.0004	-15.2	-12.1	0.018
23	39	4.02	795.4	15.0	1316.3	32.4	2109.0	3.4	0.0095	-61.3	-58.5	0.069
23	38	0.91	795.4	15.0	1306.6	2.2	2099.1	0.1	0.0002	-71.2	-68.2	0.013
23	37	0.71	795.4	15.0	1295.5	134.9	2084.9	0.0	0.0001	-85.3	-79.3	0.009
23	36	0.59	795.4	15.0	1281.7	69.5	2075.4	0.1	0.0002	-94.9	-93.1	0.006
22	45	4.59	760.7	12.0	1492.0	37.8	2255.1	0.2	0.0006	84.9	82.4	0.056
22	44	-2.02	760.7	12.0	1418.6	1.1	2179.0	1.2	0.0033	8.7	9.0	0.223
22	42	-0.24	760.7	12.0	1427.7	3.1	2191.4	0.0	0.0001	21.2	18.2	0.013
22	41	-1.46	760.7	12.0	1388.2	10.4	2160.4	380.0	1.0595	-9.8	-21.4	0.068
22	40	1.60	760.7	12.0	1362.8	87.7	2123.7	0.3	0.0008	-46.6	-46.8	0.034
22	39	-35.10	760.7	12.0	1316.3	32.4	2077.0	26.8	0.0747	-93.2	-93.3	0.376
22	38	-10.08	760.7	12.0	1306.6	2.2	2068.8	3.3	0.0093	-101.4	-103.0	0.098
21	45	2.90	709.7	12.5	1492.0	37.8	2201.1	0.5	0.0014	30.9	31.4	0.092
21	44	-2.14	709.7	12.5	1418.6	1.1	2126.2	464.1	1.2938	-44.0	-42.0	0.051
21	41	-0.78	709.7	12.5	1388.2	10.4	2107.3	0.0	0.0000	-62.9	-72.4	0.011
21	40	1.20	709.7	12.5	1362.8	87.7	2072.6	0.0	0.0001	-97.7	-97.8	0.012
20	47	1.05	674.9	6.9	1593.3	2.3	2272.3	0.0	0.0001	102.0	98.0	0.011
20	46	1.76	674.9	6.9	1577.1	1.4	2249.8	0.1	0.0002	79.6	81.8	0.021
20	45	-4.70	674.9	6.9	1492.0	37.8	2165.8	42.8	0.1192	-4.4	-3.3	1.416
20	44	2.87	674.9	6.9	1418.6	1.1	2089.5	0.9	0.0024	-80.7	-76.7	0.037
20	42	0.31	674.9	6.9	1427.7	3.1	2102.5	0.0	0.0000	-67.8	-67.6	0.005
20	41	0.44	674.9	6.9	1388.2	10.4	2071.8	0.0	0.0000	-98.5	-107.1	0.004
19	47	0.33	645.1	2.0	1593.3	2.3	2238.5	0.0	0.0000	68.2	68.1	0.005
19	46	-0.77	645.1	2.0	1577.1	1.4	2219.9	0.0	0.0001	49.7	51.9	0.015
19	45	1.21	645.1	2.0	1492.0	37.8	2133.0	0.2	0.0006	-37.2	-33.2	0.037
18	48	0.34	595.8	30.5	1644.0	206.1	2241.2	0.1	0.0002	70.9	69.5	0.005

i	j	K_{ijk} / cm^{-1}	ω(i) / cm^{-1}	I(i) / km mol^{-1}	ω(j) / cm^{-1}	I(j) / km mol^{-1}	ω(ij) / cm^{-1}	I(ij) / km mol^{-1}	I(ij) / I(k)	Δω'	Δω	TFR
18	47	0.92	595.8	30.5	1593.3	2.3	2196.0	0.0	0.0001	25.7	18.9	0.049
18	46	0.24	595.8	30.5	1577.1	1.4	2175.7	0.0	0.0000	5.4	2.7	0.091
17	48	-0.28	548.8	12.8	1644.0	206.1	2180.3	0.0	0.0001	10.0	22.5	0.012
17	47	-0.51	548.8	12.8	1593.3	2.3	2134.9	0.6	0.0016	-35.3	-28.1	0.018
16	48	0.42	531.7	15.8	1644.0	206.1	2143.1	29.1	0.0811	-27.2	5.4	0.078
16	47	0.85	531.7	15.8	1593.3	2.3	2098.5	0.1	0.0003	-71.8	-45.2	0.019
16	46	0.41	531.7	15.8	1577.1	1.4	2077.4	0.0	0.0001	-92.8	-61.4	0.007
15	48	0.38	496.8	2.7	1644.0	206.1	2140.4	1.1	0.0030	-29.8	-29.5	0.013
15	47	0.41	496.8	2.7	1593.3	2.3	2094.9	0.1	0.0002	-75.3	-80.2	0.005
14	48	0.95	440.5	112.5	1644.0	206.1	2110.4	0.7	0.0019	-59.8	-85.8	0.011
14	47	2.59	440.5	112.5	1593.3	2.3	2065.1	2.2	0.0061	-105.1	-136.4	0.019
13	47	-0.26	487.6	10.1	1593.3	2.3	2095.7	0.0	0.0001	-74.5	-89.3	0.003
2	49	-1.21	-9.5	2.0	2170.3	358.8	2152.1	0.4	0.0011	-18.1	-9.5	0.127
1	49	-1.36	-78.8	39.0	2170.3	358.8	2082.3	1.6	0.0044	-88.0	-78.8	0.017

6-311++G(df,pd)

i	j	K_{ijk} / cm^{-1}	ω(i) / cm^{-1}	I(i) / km mol^{-1}	ω(j) / cm^{-1}	I(j) / km mol^{-1}	ω(ij) / cm^{-1}	I(ij) / km mol^{-1}	I(ij) / I(k)	Δω'	Δω	TFR
33	33	35.03	1127.4	15.1	1127.4	15.1	2253.5	10.4	0.0118	80.3	81.6	0.429
32	32	1.90	1103.9	11.5	1103.9	11.5	2251.5	0.0	0.0000	78.3	34.5	0.055
32	33	-6.73	1103.9	11.5	1127.4	15.1	2251.7	0.7	0.0007	78.5	58.1	0.116
31	35	-0.24	1032.7	14.4	1217.8	15.6	2248.8	0.0	0.0000	75.5	77.3	0.003
31	34	-0.27	1032.7	14.4	1191.9	1.3	2201.1	0.0	0.0000	27.9	51.4	0.005
30	34	0.59	1010.1	8.0	1191.9	1.3	2180.3	0.3	0.0003	7.1	28.8	0.020
30	33	-2.87	1010.1	8.0	1127.4	15.1	2138.6	1.7	0.0020	-34.6	-35.7	0.080
30	32	-0.67	1010.1	8.0	1103.9	11.5	2134.8	0.1	0.0001	-38.4	-59.3	0.011
29	35	-0.56	1018.8	20.6	1217.8	15.6	2233.8	0.2	0.0002	60.6	63.4	0.009
29	33	-1.41	1018.8	20.6	1127.4	15.1	2143.5	0.5	0.0006	-29.7	-26.9	0.052
28	39	1.63	957.0	1.1	1321.1	73.1	2274.6	0.0	0.0000	101.4	104.9	0.016
28	38	0.53	957.0	1.1	1312.5	7.4	2264.7	0.0	0.0000	91.5	96.4	0.005
28	37	0.46	957.0	1.1	1305.2	110.2	2259.2	0.0	0.0000	86.0	89.0	0.005
28	36	-0.25	957.0	1.1	1287.2	1.3	2239.2	0.0	0.0000	66.0	71.0	0.003
28	35	0.28	957.0	1.1	1217.8	15.6	2171.9	0.0	0.0000	-1.3	1.6	0.177
28	34	-0.37	957.0	1.1	1191.9	1.3	2123.5	0.1	0.0001	-49.7	-24.2	0.015
28	33	0.75	957.0	1.1	1127.4	15.1	2081.4	0.0	0.0000	-91.8	-88.8	0.008
27	35	-0.28	927.4	1.2	1217.8	15.6	2151.2	14.0	0.0159	-22.0	-28.0	0.010
26	39	2.91	905.1	3.6	1321.1	73.1	2227.6	0.3	0.0003	54.4	53.0	0.055
26	38	1.75	905.1	3.6	1312.5	7.4	2216.0	0.1	0.0001	42.8	44.4	0.039
26	35	-0.66	905.1	3.6	1217.8	15.6	2123.4	0.8	0.0010	-49.8	-50.3	0.013
26	34	-0.32	905.1	3.6	1191.9	1.3	2077.0	0.1	0.0001	-96.2	-76.2	0.004
25	44	0.77	838.4	12.6	1433.8	8.5	2260.8	0.1	0.0001	87.6	99.0	0.008

i	j	K_{ijk} / cm^{-1}	ω(i) / cm^{-1}	I(i) / km mol^{-1}	ω(j) / cm^{-1}	I(j) / km mol^{-1}	ω(ij) / cm^{-1}	I(ij) / km mol^{-1}	I(ij) / I(k)	Δω'	Δω	TFR
25	41	0.48	838.4	12.6	1393.5	6.7	2234.2	0.0	0.0000	61.0	58.7	0.008
25	40	0.51	838.4	12.6	1356.4	5.4	2188.7	0.1	0.0001	15.5	21.7	0.024
25	39	4.71	838.4	12.6	1321.1	73.1	2154.2	28.7	0.0325	-19.0	-13.6	0.346
25	38	1.00	838.4	12.6	1312.5	7.4	2144.7	1.7	0.0019	-28.5	-22.2	0.045
25	37	0.66	838.4	12.6	1305.2	110.2	2140.4	0.1	0.0001	-32.8	-29.6	0.022
25	36	-0.31	838.4	12.6	1287.2	1.3	2119.9	0.0	0.0000	-53.3	-47.6	0.007
24	44	3.68	816.9	7.3	1433.8	8.5	2240.6	0.1	0.0002	67.4	77.5	0.047
24	43	0.39	816.9	7.3	1428.4	9.6	2249.5	0.0	0.0000	76.3	72.1	0.005
24	42	0.46	816.9	7.3	1462.2	51.7	2270.7	0.0	0.0000	97.5	105.9	0.004
24	41	3.21	816.9	7.3	1393.5	6.7	2214.1	0.6	0.0007	40.9	37.2	0.086
24	40	3.51	816.9	7.3	1356.4	5.4	2170.1	4.1	0.0046	-3.1	0.2	19.820
24	39	51.93	816.9	7.3	1321.1	73.1	2124.2	141.0	0.1598	-49.0	-35.2	1.477
24	38	13.86	816.9	7.3	1312.5	7.4	2124.2	18.2	0.0207	-49.0	-43.7	0.317
24	37	10.61	816.9	7.3	1305.2	110.2	2118.4	6.5	0.0073	-54.8	-51.1	0.208
24	36	-3.98	816.9	7.3	1287.2	1.3	2099.4	0.4	0.0004	-73.8	-69.1	0.058
23	41	-0.22	783.9	4.6	1393.5	6.7	2186.6	0.1	0.0001	13.4	4.2	0.053
23	39	-0.27	783.9	4.6	1321.1	73.1	2106.7	0.0	0.0000	-66.5	-68.2	0.004
23	36	0.28	783.9	4.6	1287.2	1.3	2070.5	0.1	0.0001	-102.7	-102.1	0.003
22	45	-4.52	758.3	15.0	1501.2	116.0	2262.7	0.2	0.0002	89.5	86.4	0.052
22	44	1.71	758.3	15.0	1433.8	8.5	2191.9	1.0	0.0011	18.7	18.9	0.090
22	42	0.23	758.3	15.0	1462.2	51.7	2220.7	0.0	0.0000	47.5	47.3	0.005
22	41	1.54	758.3	15.0	1393.5	6.7	2164.4	12.7	0.0144	-8.8	-21.4	0.072
22	40	1.64	758.3	15.0	1356.4	5.4	2118.4	0.3	0.0004	-54.8	-58.4	0.028
22	39	34.74	758.3	15.0	1321.1	73.1	2082.3	31.4	0.0356	-90.9	-93.8	0.371
22	38	9.95	758.3	15.0	1312.5	7.4	2074.6	3.4	0.0039	-98.6	-102.3	0.097
22	37	8.27	758.3	15.0	1305.2	110.2	2069.1	2.2	0.0025	-104.1	-109.7	0.075
21	45	-2.87	714.6	11.4	1501.2	116.0	2212.2	0.4	0.0004	39.0	42.7	0.067
21	44	1.92	714.6	11.4	1433.8	8.5	2142.2	10.8	0.0122	-31.0	-24.8	0.078
21	41	0.86	714.6	11.4	1393.5	6.7	2114.5	0.0	0.0000	-58.7	-65.1	0.013
21	40	1.23	714.6	11.4	1356.4	5.4	2070.8	0.0	0.0000	-102.4	-102.1	0.012
20	47	-1.11	684.4	13.6	1595.5	1.8	2282.4	0.0	0.0000	109.2	106.8	0.010
20	46	1.66	684.4	13.6	1578.4	2.2	2261.3	0.0	0.0000	88.1	89.7	0.018
20	45	4.70	684.4	13.6	1501.2	116.0	2183.0	11.3	0.0128	9.8	12.5	0.377
20	44	-2.64	684.4	13.6	1433.8	8.5	2112.4	1.1	0.0012	-60.8	-55.0	0.048
20	43	-0.27	684.4	13.6	1428.4	9.6	2120.3	0.0	0.0000	-52.9	-60.4	0.004
20	42	-0.29	684.4	13.6	1462.2	51.7	2142.1	0.0	0.0000	-31.1	-26.6	0.011
20	41	-0.59	684.4	13.6	1393.5	6.7	2085.3	0.0	0.0000	-87.9	-95.3	0.006
19	47	-0.59	715.2	168.5	1595.5	1.8	2278.7	0.0	0.0000	105.5	137.6	0.004
19	46	-0.66	715.2	168.5	1578.4	2.2	2260.5	0.0	0.0000	87.3	120.5	0.005
19	45	-1.26	715.2	168.5	1501.2	116.0	2180.4	0.6	0.0006	7.2	43.3	0.029
19	44	0.59	715.2	168.5	1433.8	8.5	2110.8	0.1	0.0001	-62.4	-24.2	0.024
18	47	-0.85	647.1	2.7	1595.5	1.8	2275.2	0.1	0.0001	102.0	69.4	0.012
18	46	0.39	647.1	2.7	1578.4	2.2	2256.7	0.0	0.0000	83.5	52.3	0.007

i	j	K_{ijk} / cm^{-1}	ω(i) / cm^{-1}	I(i) / km mol^{-1}	ω(j) / cm^{-1}	I(j) / km mol^{-1}	ω(ij) / cm^{-1}	I(ij) / km mol^{-1}	I(ij) / I(k)	Δω'	Δω	TFR
18	44	-0.88	647.1	2.7	1433.8	8.5	2105.0	0.2	0.0002	-68.2	-92.3	0.009
18	42	-0.26	647.1	2.7	1462.2	51.7	2134.7	0.0	0.0000	-38.5	-63.9	0.004
18	41	-0.74	647.1	2.7	1393.5	6.7	2079.3	0.0	0.0000	-93.9	-132.6	0.006
17	48	0.32	551.2	20.0	1643.3	0.2	2185.1	0.0	0.0000	11.9	21.3	0.015
17	47	0.57	551.2	20.0	1595.5	1.8	2138.9	1.0	0.0011	-34.3	-26.5	0.021
16	48	-0.49	624.4	12.2	1643.3	0.2	2220.2	0.7	0.0008	47.0	94.4	0.005
16	47	-0.94	624.4	12.2	1595.5	1.8	2174.6	0.2	0.0002	1.4	46.7	0.020
16	46	0.41	624.4	12.2	1578.4	2.2	2154.7	0.1	0.0001	-18.5	29.6	0.014
16	45	-0.27	624.4	12.2	1501.2	116.0	2075.8	0.1	0.0001	-97.4	-47.6	0.006
15	48	-0.27	540.8	6.0	1643.3	0.2	2189.2	1.1	0.0012	16.0	10.8	0.025
14	48	-0.88	527.4	14.4	1643.3	0.2	2209.0	0.8	0.0009	35.8	-2.6	0.338
14	47	-2.52	527.4	14.4	1595.5	1.8	2162.4	2.3	0.0027	-10.8	-50.3	0.050
14	45	-0.32	527.4	14.4	1501.2	116.0	2063.5	0.1	0.0001	-109.7	-144.6	0.002
3	49	0.65	74.9	6.8	2173.2	882.6	2227.6	0.7	0.0008	54.4	74.9	0.009
2	49	1.18	10.6	0.3	2173.2	882.6	2219.8	0.4	0.0004	46.6	10.6	0.111
1	49	1.33	175.5	5.8	2173.2	882.6	2257.8	1.8	0.0020	84.6	175.5	0.008

APPENDIX D

VIBRATIONAL MODES OF 4-AZIDOACETANILIDE THAT OCCUR WITHIN ±130 CM^{-1}

FROM THE FUNDAMENTAL VIBRATION FOR SEVEN BASIS SETS IN THF

i, j, k : vibrational modes ; where k = 49 (azide asymmetric stretch)

i = j → overtone & i ≠ j → combination band

K_{ijk} : cubic force constant

TFR : third-order Fermi resonance

ω(i), ω(j), ω(k) : anharmonic frequencies of i, j & k th mode

ω(ij) : anharmonic frequency of ij th mode

I(i), I(j), I(k) : anharmonic intensities of i, j & k th mode

I(ij) : anharmonic intensity of ij th mode

Δω' : ω(ij) - ω(k)

Δω : ω(i) + ω(j) - ω(k)

6-31G(d,p)

i	j	K_{ijk} / cm^{-1}	ω(i) / cm^{-1}	I(i) / km mol^{-1}	ω(j) / cm^{-1}	I(j) / km mol^{-1}	ω(ij) / cm^{-1}	I(ij) / km mol^{-1}	I(ij) / I(k)	Δω'	Δω	TFR
33	33	36.38	1136.2	12.3	1136.2	12.3	2271.0	12.0	0.0157	71.7	73.0	0.498
32	32	1.00	1127.6	9.8	1127.6	9.8	2259.0	0.0	0.0000	59.7	56.0	0.018
32	33	4.65	1127.6	9.8	1136.2	12.3	2264.4	0.4	0.0005	65.1	64.5	0.072
31	35	-0.20	1031.0	17.9	1228.4	13.8	2256.3	0.0	0.0000	57.0	60.1	0.003
31	34	-0.24	1031.0	17.9	1190.6	3.5	2215.4	0.0	0.0000	16.1	22.3	0.011
30	35	-0.73	1032.8	26.7	1228.4	13.8	2260.6	0.1	0.0001	61.4	62.0	0.012
30	34	0.79	1032.8	26.7	1190.6	3.5	2221.5	0.9	0.0012	22.2	24.1	0.033
30	33	2.92	1032.8	26.7	1136.2	12.3	2168.9	0.6	0.0008	-30.4	-30.3	0.096
30	32	-0.32	1032.8	26.7	1127.6	9.8	2161.5	0.0	0.0000	-37.7	-38.8	0.008
29	36	-0.96	1014.1	5.3	1294.0	410.1	2307.2	0.1	0.0002	107.9	108.8	0.009
29	34	0.97	1014.1	5.3	1190.6	3.5	2201.6	1.2	0.0016	2.3	5.4	0.180
29	33	2.48	1014.1	5.3	1136.2	12.3	2150.3	0.3	0.0003	-49.0	-49.1	0.051

i	j	K_{ijk} / cm^{-1}	ω(i) / cm^{-1}	I(i) / km mol^{-1}	ω(j) / cm^{-1}	I(j) / km mol^{-1}	ω(ij) / cm^{-1}	I(ij) / km mol^{-1}	I(ij) / I(k)	Δω'	Δω	TFR
29	32	-0.55	1014.1	5.3	1127.6	9.8	2141.7	0.0	0.0000	-57.6	-57.6	0.010
28	39	-1.72	922.0	7.1	1336.5	2.5	2263.1	0.1	0.0001	63.8	59.2	0.029
28	38	-0.34	922.0	7.1	1312.1	6.5	2255.4	0.0	0.0000	56.2	34.8	0.010
28	36	-0.56	922.0	7.1	1294.0	410.1	2224.7	0.0	0.0000	25.4	16.7	0.034
28	35	-0.23	922.0	7.1	1228.4	13.8	2158.7	0.0	0.0000	-40.5	-48.9	0.005
28	34	0.32	922.0	7.1	1190.6	3.5	2119.3	0.0	0.0000	-79.9	-86.7	0.004
27	35	-0.25	901.7	1.4	1228.4	13.8	2134.9	0.1	0.0001	-64.3	-69.2	0.004
26	39	5.09	943.2	7.7	1336.5	2.5	2263.6	1.1	0.0015	64.3	80.4	0.063
26	38	1.68	943.2	7.7	1312.1	6.5	2252.8	0.2	0.0002	53.5	56.0	0.030
26	37	-0.90	943.2	7.7	1328.5	236.9	2253.1	0.1	0.0001	53.8	72.4	0.012
26	36	0.41	943.2	7.7	1294.0	410.1	2224.4	0.0	0.0001	25.2	37.9	0.011
26	35	-0.43	943.2	7.7	1228.4	13.8	2160.0	0.6	0.0008	-39.3	-27.7	0.016
26	34	-0.44	943.2	7.7	1190.6	3.5	2119.5	0.1	0.0001	-79.7	-65.5	0.007
25	44	1.06	836.0	7.3	1485.0	43.8	2297.6	0.0	0.0000	98.3	121.8	0.009
25	43	-0.29	836.0	7.3	1451.1	25.0	2279.5	0.0	0.0000	80.3	87.8	0.003
25	42	0.24	836.0	7.3	1396.4	6.8	2224.5	0.0	0.0000	25.2	33.2	0.007
25	41	1.13	836.0	7.3	1419.7	2.9	2236.4	0.0	0.0000	37.2	56.5	0.020
25	40	0.74	836.0	7.3	1365.9	184.8	2187.7	0.1	0.0002	-11.6	2.6	0.284
25	39	9.45	836.0	7.3	1336.5	2.5	2153.5	27.4	0.0358	-45.7	-26.8	0.353
25	38	1.58	836.0	7.3	1312.1	6.5	2144.7	0.1	0.0001	-54.6	-51.2	0.031
25	37	-0.24	836.0	7.3	1328.5	236.9	2145.8	0.0	0.0000	-53.4	-34.8	0.007
25	36	1.40	836.0	7.3	1294.0	410.1	2116.4	0.0	0.0000	-82.9	-69.3	0.020
24	44	-4.10	804.4	24.5	1485.0	43.8	2291.3	0.2	0.0002	92.0	90.1	0.045
24	43	1.13	804.4	24.5	1451.1	25.0	2274.0	0.0	0.0000	74.7	56.2	0.020
24	42	-0.98	804.4	24.5	1396.4	6.8	2218.7	0.0	0.0000	19.4	1.6	0.630
24	41	-4.77	804.4	24.5	1419.7	2.9	2230.6	2.4	0.0032	31.4	24.8	0.192
24	40	-3.09	804.4	24.5	1365.9	184.8	2183.1	4.1	0.0053	-16.1	-29.0	0.106
24	39	-51.77	804.4	24.5	1336.5	2.5	2138.5	64.2	0.0839	-60.8	-58.4	0.886
24	38	-9.99	804.4	24.5	1312.1	6.5	2138.7	1.6	0.0021	-60.6	-82.8	0.121
24	37	1.63	804.4	24.5	1328.5	236.9	2138.7	0.0	0.0000	-60.6	-66.4	0.024
24	36	-8.62	804.4	24.5	1294.0	410.1	2109.2	0.5	0.0007	-90.0	-100.9	0.085
23	45	-0.72	773.3	7.5	1513.9	80.5	2285.7	0.0	0.0000	86.5	88.0	0.008
23	44	0.41	773.3	7.5	1485.0	43.8	2253.5	0.0	0.0000	54.2	59.1	0.007
23	41	0.36	773.3	7.5	1419.7	2.9	2192.3	0.1	0.0001	-7.0	-6.2	0.058
23	40	0.36	773.3	7.5	1365.9	184.8	2143.2	1.4	0.0019	-56.1	-60.1	0.006
23	39	5.29	773.3	7.5	1336.5	2.5	2109.3	1.7	0.0023	-90.0	-89.5	0.059
23	38	1.18	773.3	7.5	1312.1	6.5	2102.8	0.0	0.0000	-96.5	-113.9	0.010
22	45	-5.30	761.5	9.6	1513.9	80.5	2271.5	0.3	0.0004	72.2	76.2	0.070
22	44	2.09	761.5	9.6	1485.0	43.8	2237.5	1.6	0.0021	38.2	47.2	0.044
22	43	-0.64	761.5	9.6	1451.1	25.0	2219.8	0.2	0.0003	20.6	13.3	0.048
22	42	0.53	761.5	9.6	1396.4	6.8	2165.0	0.3	0.0003	-34.2	-41.3	0.013
22	41	2.56	761.5	9.6	1419.7	2.9	2177.1	1.0	0.0013	-22.2	-18.0	0.142
22	40	1.43	761.5	9.6	1365.9	184.8	2126.7	0.3	0.0004	-72.6	-71.9	0.020
22	39	36.03	761.5	9.6	1336.5	2.5	2092.1	12.1	0.0158	-107.2	-101.3	0.356
21	46	1.05	706.2	16.1	1596.0	10.6	2300.5	0.0	0.0000	101.2	102.9	0.010
21	45	3.09	706.2	16.1	1513.9	80.5	2214.7	1.7	0.0022	15.5	20.9	0.148
21	44	-2.00	706.2	16.1	1485.0	43.8	2182.5	0.6	0.0008	-16.7	-8.1	0.247
21	43	0.71	706.2	16.1	1451.1	25.0	2164.8	0.1	0.0001	-34.4	-42.0	0.017

i	j	K_{ijk} / cm^{-1}	ω(i) / cm^{-1}	I(i) / km mol^{-1}	ω(j) / cm^{-1}	I(j) / km mol^{-1}	ω(ij) / cm^{-1}	I(ij) / km mol^{-1}	I(ij) / I(k)	Δω'	Δω	TFR
21	42	-0.46	706.2	16.1	1396.4	6.8	2109.8	0.0	0.0000	-89.4	-96.6	0.005
21	41	-1.47	706.2	16.1	1419.7	2.9	2120.6	0.0	0.0000	-78.7	-73.4	0.020
20	47	-1.19	683.0	12.4	1611.2	3.5	2297.8	0.0	0.0000	98.6	95.0	0.013
20	46	1.53	683.0	12.4	1596.0	10.6	2279.8	0.0	0.0001	80.6	79.8	0.019
20	45	4.94	683.0	12.4	1513.9	80.5	2194.1	70.3	0.0919	-5.1	-2.3	2.176
20	44	-2.86	683.0	12.4	1485.0	43.8	2159.8	0.2	0.0003	-39.4	-31.2	0.092
20	43	0.80	683.0	12.4	1451.1	25.0	2142.1	0.0	0.0000	-57.1	-65.2	0.012
20	41	-1.56	683.0	12.4	1419.7	2.9	2098.7	0.0	0.0000	-100.5	-96.5	0.016
19	47	-0.38	650.0	1.5	1611.2	3.5	2273.6	0.0	0.0000	74.3	62.0	0.006
19	46	-0.66	650.0	1.5	1596.0	10.6	2256.3	0.1	0.0001	57.1	46.8	0.014
19	45	-1.40	650.0	1.5	1513.9	80.5	2170.0	0.1	0.0001	-29.3	-35.3	0.040
19	44	0.95	650.0	1.5	1485.0	43.8	2136.8	0.2	0.0002	-62.4	-64.3	0.015
18	47	-0.97	702.2	81.3	1611.2	3.5	2302.1	0.0	0.0000	102.8	114.2	0.008
18	44	-0.60	702.2	81.3	1485.0	43.8	2166.5	0.1	0.0001	-32.8	-12.0	0.050
18	43	0.34	702.2	81.3	1451.1	25.0	2147.0	0.0	0.0000	-52.2	-46.0	0.007
18	42	-0.27	702.2	81.3	1396.4	6.8	2091.3	0.0	0.0000	-107.9	-100.6	0.003
18	41	-0.83	702.2	81.3	1419.7	2.9	2104.6	0.0	0.0000	-94.6	-77.3	0.011
17	48	0.33	551.7	9.9	1725.5	164.5	2269.4	0.0	0.0000	70.2	77.9	0.004
17	47	0.40	551.7	9.9	1611.2	3.5	2158.8	0.3	0.0003	-40.5	-36.4	0.011
16	48	-0.29	593.6	15.5	1725.5	164.5	2279.3	0.0	0.0000	80.1	119.8	0.002
16	47	-0.83	593.6	15.5	1611.2	3.5	2168.6	0.1	0.0001	-30.6	5.5	0.149
16	46	0.25	593.6	15.5	1596.0	10.6	2149.5	0.0	0.0000	-49.7	-9.7	0.026
15	48	-0.38	528.4	2.3	1725.5	164.5	2273.3	0.0	0.0000	74.0	54.6	0.007
15	47	-0.55	528.4	2.3	1611.2	3.5	2162.2	0.1	0.0001	-37.0	-59.7	0.009
14	48	-0.75	548.8	39.4	1725.5	164.5	2274.6	0.0	0.0000	75.4	75.1	0.010
14	47	-1.93	548.8	39.4	1611.2	3.5	2162.3	1.2	0.0016	-37.0	-39.2	0.049
14	46	-0.31	548.8	39.4	1596.0	10.6	2143.2	0.0	0.0000	-56.1	-54.4	0.006
13	48	0.32	483.7	12.9	1725.5	164.5	2227.7	0.1	0.0001	28.4	9.9	0.033
13	47	0.76	483.7	12.9	1611.2	3.5	2119.0	0.2	0.0002	-80.3	-104.3	0.007
12	48	-0.28	418.0	6.7	1725.5	164.5	2135.5	0.0	0.0000	-63.8	-55.8	0.005
10	48	0.38	379.1	3.1	1725.5	164.5	2104.9	0.0	0.0000	-94.4	-94.6	0.004
2	49	0.80	33.7	9.0	2199.3	765.3	2233.2	0.2	0.0003	34.0	33.7	0.024
1	49	1.02	-71.4	65.8	2199.3	765.3	2120.8	1.1	0.0015	-78.4	-71.4	0.014

6-31+G(d,p)

i	j	K_{ijk} / cm^{-1}	ω(i) / cm^{-1}	I(i) / km mol^{-1}	ω(j) / cm^{-1}	I(j) / km mol^{-1}	ω(ij) / cm^{-1}	I(ij) / km mol^{-1}	I(ij) / I(k)	Δω'	Δω	TFR
33	33	37.10	1133.9	15.1	1133.9	15.1	2265.9	13.0	0.0452	79.5	81.4	0.456
32	32	1.35	1096.1	10.2	1096.1	10.2	2228.8	0.0	0.0000	42.4	5.7	0.235
33	34	-13.39	1133.9	15.1	1173.3	1.5	2289.1	1.4	0.0049	102.6	120.8	0.111
32	34	1.40	1096.1	10.2	1173.3	1.5	2267.1	0.6	0.0021	80.6	82.9	0.017
32	33	-4.33	1096.1	10.2	1133.9	15.1	2247.5	0.3	0.0010	61.1	43.6	0.099
31	35	-0.23	1039.8	3.7	1223.6	16.9	2262.9	0.0	0.0001	76.5	76.9	0.003
31	34	-0.22	1039.8	3.7	1173.3	1.5	2195.1	0.0	0.0000	8.7	26.6	0.008
30	35	-0.61	1010.0	18.0	1223.6	16.9	2232.5	0.2	0.0005	46.1	47.2	0.013

i	j	K_{ijk} / cm^{-1}	ω(i) / cm^{-1}	I(i) / km mol^{-1}	ω(j) / cm^{-1}	I(j) / km mol^{-1}	ω(ij) / cm^{-1}	I(ij) / km mol^{-1}	I(ij) / I(k)	Δω'	Δω	TFR
30	33	-0.86	1010.0	18.0	1133.9	15.1	2143.6	0.1	0.0004	-42.8	-42.5	0.020
29	35	-0.43	1008.0	12.5	1223.6	16.9	2229.5	0.0	0.0001	43.1	45.1	0.010
29	34	1.01	1008.0	12.5	1173.3	1.5	2159.4	10.3	0.0357	-27.0	-5.2	0.196
29	33	-3.65	1008.0	12.5	1133.9	15.1	2140.1	1.1	0.0038	-46.3	-44.5	0.082
29	32	-0.64	1008.0	12.5	1096.1	10.2	2118.3	0.0	0.0001	-68.2	-82.4	0.008
28	39	1.68	959.0	0.1	1325.0	79.6	2278.8	0.1	0.0002	92.4	97.6	0.017
28	38	0.57	959.0	0.1	1311.5	29.0	2265.4	0.0	0.0000	79.0	84.1	0.007
28	37	-0.27	959.0	0.1	1305.8	0.6	2255.7	0.0	0.0000	69.3	78.4	0.003
28	36	0.41	959.0	0.1	1296.6	45.6	2252.1	0.0	0.0000	65.6	69.1	0.006
28	35	0.26	959.0	0.1	1223.6	16.9	2176.4	0.9	0.0029	-10.0	-3.9	0.066
28	34	-0.28	959.0	0.1	1173.3	1.5	2108.2	0.0	0.0000	-78.3	-54.2	0.005
28	33	0.87	959.0	0.1	1133.9	15.1	2087.3	0.0	0.0001	-99.1	-93.5	0.009
27	38	0.21	918.6	2.3	1311.5	29.0	2235.6	0.0	0.0001	49.2	43.7	0.005
27	35	-0.26	918.6	2.3	1223.6	16.9	2146.9	0.1	0.0003	-39.5	-44.3	0.006
26	39	3.92	900.6	0.5	1325.0	79.6	2226.8	0.6	0.0020	40.4	39.2	0.100
26	38	1.96	900.6	0.5	1311.5	29.0	2209.9	0.0	0.0001	23.4	25.8	0.076
26	37	-0.45	900.6	0.5	1305.8	0.6	2203.7	0.2	0.0007	17.3	20.0	0.023
26	36	-0.22	900.6	0.5	1296.6	45.6	2199.3	0.0	0.0000	12.8	10.8	0.020
26	35	-0.56	900.6	0.5	1223.6	16.9	2122.5	0.7	0.0024	-63.9	-62.2	0.009
25	44	1.18	838.9	18.8	1424.7	8.9	2251.0	0.1	0.0002	64.5	77.2	0.015
25	41	1.00	838.9	18.8	1380.1	47.6	2235.8	0.0	0.0000	49.4	32.6	0.031
25	40	0.85	838.9	18.8	1370.2	64.7	2202.6	0.1	0.0003	16.2	22.8	0.037
25	39	9.32	838.9	18.8	1325.0	79.6	2157.8	185.6	0.6428	-28.6	-22.5	0.415
25	38	2.53	838.9	18.8	1311.5	29.0	2144.2	0.7	0.0026	-42.2	-35.9	0.071
25	37	-0.93	838.9	18.8	1305.8	0.6	2137.3	0.0	0.0001	-49.1	-41.7	0.022
25	36	1.07	838.9	18.8	1296.6	45.6	2133.8	0.0	0.0001	-52.7	-50.9	0.021
24	44	-3.93	815.6	1.3	1424.7	8.9	2227.3	0.2	0.0006	40.8	53.8	0.073
24	43	0.36	815.6	1.3	1434.9	3.4	2248.0	0.0	0.0000	61.6	64.1	0.006
24	42	-0.67	815.6	1.3	1464.2	11.5	2265.0	0.0	0.0000	78.6	93.4	0.007
24	41	-3.75	815.6	1.3	1380.1	47.6	2214.5	1.1	0.0038	28.1	9.2	0.408
24	40	-3.33	815.6	1.3	1370.2	64.7	2181.9	11.3	0.0392	-4.5	-0.6	5.366
24	39	-49.94	815.6	1.3	1325.0	79.6	2130.4	23.0	0.0796	-56.0	-45.9	1.089
24	38	-15.35	815.6	1.3	1311.5	29.0	2123.1	10.7	0.0371	-63.3	-59.3	0.259
24	37	5.21	815.6	1.3	1305.8	0.6	2115.0	0.5	0.0017	-71.4	-65.0	0.080
24	36	-6.43	815.6	1.3	1296.6	45.6	2110.6	0.8	0.0029	-75.9	-74.3	0.087
23	45	0.41	789.2	3.7	1506.4	7.6	2292.9	0.0	0.0000	106.5	109.2	0.004
23	44	-0.23	789.2	3.7	1424.7	8.9	2204.7	0.0	0.0000	18.3	27.5	0.008
23	41	-0.34	789.2	3.7	1380.1	47.6	2192.6	0.1	0.0004	6.2	-17.1	0.020
23	39	-3.81	789.2	3.7	1325.0	79.6	2115.6	1.7	0.0058	-70.8	-72.2	0.053
23	38	-1.06	789.2	3.7	1311.5	29.0	2101.9	0.1	0.0003	-84.6	-85.6	0.012
23	37	0.58	789.2	3.7	1305.8	0.6	2093.9	0.1	0.0002	-92.5	-91.4	0.006
23	36	-0.49	789.2	3.7	1296.6	45.6	2088.9	0.0	0.0000	-97.6	-100.6	0.005
22	45	-5.05	760.4	6.7	1506.4	7.6	2270.7	0.3	0.0010	84.3	80.4	0.063
22	44	2.03	760.4	6.7	1424.7	8.9	2182.4	1.4	0.0048	-4.0	-1.4	1.502
22	43	-0.28	760.4	6.7	1434.9	3.4	2202.2	0.1	0.0002	15.8	8.9	0.032
22	42	0.36	760.4	6.7	1464.2	11.5	2219.6	0.1	0.0003	33.2	38.2	0.009
22	41	2.00	760.4	6.7	1380.1	47.6	2169.1	6.7	0.0231	-17.3	-46.0	0.044
22	40	1.64	760.4	6.7	1370.2	64.7	2134.0	0.3	0.0010	-52.4	-55.8	0.029

i	j	K_{ijk} / cm^{-1}	ω(i) / cm^{-1}	I(i) / km mol^{-1}	ω(j) / cm^{-1}	I(j) / km mol^{-1}	ω(ij) / cm^{-1}	I(ij) / km mol^{-1}	I(ij) / I(k)	Δω’	Δω	TFR
22	39	35.50	760.4	6.7	1325.0	79.6	2089.9	18.9	0.0656	-96.5	-101.0	0.351
22	38	11.63	760.4	6.7	1311.5	29.0	2077.9	3.7	0.0129	-108.5	-114.5	0.102
21	46	1.21	710.4	24.8	1587.0	3.9	2294.6	0.0	0.0001	108.1	111.0	0.011
21	45	3.19	710.4	24.8	1506.4	7.6	2211.7	1.5	0.0052	25.3	30.4	0.105
21	44	-2.19	710.4	24.8	1424.7	8.9	2124.9	1.9	0.0067	-61.5	-51.3	0.043
21	43	0.42	710.4	24.8	1434.9	3.4	2144.6	0.1	0.0003	-41.8	-41.0	0.010
21	42	-0.32	710.4	24.8	1464.2	11.5	2161.3	0.0	0.0001	-25.1	-11.7	0.027
21	41	-1.10	710.4	24.8	1380.1	47.6	2111.2	0.0	0.0000	-75.3	-95.9	0.011
21	40	-1.27	710.4	24.8	1370.2	64.7	2078.9	0.0	0.0001	-107.5	-105.7	0.012
20	47	-1.07	675.8	5.8	1605.6	3.7	2281.8	0.0	0.0001	95.3	95.0	0.011
20	46	1.66	675.8	5.8	1587.0	3.9	2263.1	0.1	0.0002	76.7	76.4	0.022
20	45	4.70	675.8	5.8	1506.4	7.6	2178.9	733.6	2.5403	-7.5	-4.2	1.121
20	44	-2.79	675.8	5.8	1424.7	8.9	2090.5	0.4	0.0012	-95.9	-85.9	0.033
20	43	0.29	675.8	5.8	1434.9	3.4	2110.7	0.0	0.0000	-75.7	-75.6	0.004
20	42	-0.43	675.8	5.8	1464.2	11.5	2128.1	0.0	0.0000	-58.3	-46.3	0.009
20	41	-0.78	675.8	5.8	1380.1	47.6	2076.9	0.0	0.0000	-109.5	-130.5	0.006
19	46	-0.81	640.4	1.4	1587.0	3.9	2243.1	0.1	0.0002	56.7	41.0	0.020
19	45	-1.46	640.4	1.4	1506.4	7.6	2158.8	0.2	0.0006	-27.6	-39.7	0.037
18	44	-0.58	707.5	133.7	1424.7	8.9	2105.6	0.1	0.0002	-80.8	-54.2	0.011
18	43	0.30	707.5	133.7	1434.9	3.4	2126.4	0.0	0.0001	-60.0	-44.0	0.007
18	42	-0.30	707.5	133.7	1464.2	11.5	2143.5	0.0	0.0001	-42.9	-14.6	0.020
18	41	-0.78	707.5	133.7	1380.1	47.6	2094.2	0.0	0.0000	-92.2	-98.8	0.008
17	48	0.36	543.4	13.5	1657.7	161.6	2193.1	0.0	0.0001	6.7	14.7	0.025
17	47	0.58	543.4	13.5	1605.6	3.7	2142.5	0.5	0.0018	-43.9	-37.4	0.015
16	48	-0.37	526.5	30.2	1657.7	161.6	2221.7	2.8	0.0096	35.3	-2.2	0.170
16	47	-0.78	526.5	30.2	1605.6	3.7	2172.3	0.1	0.0002	-14.2	-54.3	0.014
16	46	0.29	526.5	30.2	1587.0	3.9	2152.3	0.0	0.0001	-34.1	-72.9	0.004
15	48	-0.35	515.9	4.5	1657.7	161.6	2186.2	6.6	0.0228	-0.2	-12.8	0.027
15	47	-0.39	515.9	4.5	1605.6	3.7	2135.5	0.1	0.0002	-50.9	-65.0	0.006
14	48	-0.93	633.1	14.2	1657.7	161.6	2228.0	0.7	0.0024	41.6	104.5	0.009
14	47	-2.33	633.1	14.2	1605.6	3.7	2177.2	1.8	0.0062	-9.2	52.3	0.045
13	48	0.32	489.1	4.7	1657.7	161.6	2161.0	0.1	0.0002	-25.4	-39.6	0.008
13	47	0.68	489.1	4.7	1605.6	3.7	2111.4	0.1	0.0005	-75.0	-91.7	0.007
3	49	0.62	77.9	6.3	2186.4	288.8	2250.0	0.6	0.0021	63.6	77.9	0.008
2	49	1.04	39.2	1.3	2186.4	288.8	2239.6	0.3	0.0012	53.2	39.2	0.027

6-31++G(d,p)

i	j	K_{ijk} / cm^{-1}	ω(i) / cm^{-1}	I(i) / km mol^{-1}	ω(j) / cm^{-1}	I(j) / km mol^{-1}	ω(ij) / cm^{-1}	I(ij) / km mol^{-1}	I(ij) / I(k)	Δω’	Δω	TFR
33	33	37.07	1134.0	11.5	1134.0	11.5	2265.4	13.0	0.0181	80.2	82.8	0.448
32	32	1.34	1094.1	8.0	1094.1	8.0	2222.2	0.0	0.0000	37.0	3.0	0.441
33	34	-13.48	1134.0	11.5	1173.4	1.7	2291.0	1.4	0.0020	105.8	122.2	0.110
32	34	1.40	1094.1	8.0	1173.4	1.7	2265.8	0.6	0.0009	80.6	82.3	0.017
32	33	-4.33	1094.1	8.0	1134.0	11.5	2244.0	0.3	0.0004	58.8	42.9	0.101
31	35	-0.23	1035.6	7.9	1224.1	40.0	2259.5	0.0	0.0000	74.3	74.4	0.003

i	j	K_{ijk} / cm^{-1}	ω(i) / cm^{-1}	I(i) / km mol^{-1}	ω(j) / cm^{-1}	I(j) / km mol^{-1}	ω(ij) / cm^{-1}	I(ij) / km mol^{-1}	I(ij) / I(k)	Δω'	Δω	TFR
31	34	-0.22	1035.6	7.9	1173.4	1.7	2193.4	0.0	0.0000	8.2	23.7	0.009
30	35	-0.61	1006.5	25.7	1224.1	40.0	2229.5	0.2	0.0002	44.3	45.3	0.014
30	33	-0.88	1006.5	25.7	1134.0	11.5	2139.9	0.1	0.0002	-45.3	-44.8	0.020
29	35	-0.41	1010.7	0.4	1224.1	40.0	2232.9	0.0	0.0000	47.7	49.5	0.008
29	34	1.02	1010.7	0.4	1173.4	1.7	2164.7	9.5	0.0133	-20.5	-1.2	0.868
29	33	-3.62	1010.7	0.4	1134.0	11.5	2142.7	1.1	0.0015	-42.5	-40.6	0.089
29	32	-0.65	1010.7	0.4	1094.1	8.0	2117.9	0.0	0.0000	-67.3	-80.4	0.008
28	39	1.69	961.5	0.2	1323.1	108.7	2276.2	0.1	0.0001	91.0	99.4	0.017
28	38	0.56	961.5	0.2	1311.1	73.7	2263.2	0.0	0.0000	78.0	87.4	0.006
28	37	-0.26	961.5	0.2	1304.9	737.6	2254.0	0.0	0.0000	68.8	81.2	0.003
28	36	0.43	961.5	0.2	1297.9	1440.6	2249.5	0.0	0.0000	64.3	74.2	0.006
28	35	0.26	961.5	0.2	1224.1	40.0	2175.3	0.9	0.0012	-9.9	0.4	0.700
28	34	-0.27	961.5	0.2	1173.4	1.7	2108.7	0.0	0.0000	-76.5	-50.3	0.005
28	33	0.87	961.5	0.2	1134.0	11.5	2085.4	0.0	0.0000	-99.8	-89.7	0.010
27	38	0.22	912.8	3.2	1311.1	73.7	2229.5	0.0	0.0000	44.2	38.7	0.006
27	35	-0.25	912.8	3.2	1224.1	40.0	2141.9	0.1	0.0001	-43.3	-48.3	0.005
26	39	3.89	896.8	0.1	1323.1	108.7	2225.2	0.6	0.0008	40.0	34.7	0.112
26	38	1.94	896.8	0.1	1311.1	73.7	2208.7	0.0	0.0000	23.5	22.6	0.086
26	37	-0.47	896.8	0.1	1304.9	737.6	2203.1	0.2	0.0003	17.8	16.4	0.029
26	35	-0.56	896.8	0.1	1224.1	40.0	2122.3	0.7	0.0010	-62.9	-64.4	0.009
25	44	1.17	839.4	12.8	1425.0	15.4	2249.4	0.1	0.0001	64.2	79.2	0.015
25	41	0.97	839.4	12.8	1380.9	46.2	2232.1	0.0	0.0000	46.9	35.1	0.028
25	40	0.82	839.4	12.8	1364.7	31.7	2195.9	0.1	0.0001	10.7	19.0	0.043
25	39	9.03	839.4	12.8	1323.1	108.7	2154.3	183.9	0.2562	-30.9	-22.7	0.398
25	38	2.43	839.4	12.8	1311.1	73.7	2141.2	0.7	0.0010	-44.0	-34.7	0.070
25	37	-0.86	839.4	12.8	1304.9	737.6	2134.8	0.0	0.0000	-50.4	-40.9	0.021
25	36	1.09	839.4	12.8	1297.9	1440.6	2130.2	0.0	0.0000	-55.0	-47.8	0.023
24	44	-3.95	816.9	3.8	1425.0	15.4	2228.2	0.2	0.0002	43.0	56.7	0.070
24	43	0.35	816.9	3.8	1430.8	6.6	2245.9	0.0	0.0000	60.7	62.5	0.006
24	42	-0.67	816.9	3.8	1458.4	22.3	2257.5	0.0	0.0000	72.3	90.2	0.007
24	41	-3.75	816.9	3.8	1380.9	46.2	2213.3	1.1	0.0015	28.1	12.6	0.298
24	40	-3.31	816.9	3.8	1364.7	31.7	2177.6	11.0	0.0154	-7.6	-3.5	0.934
24	39	-49.96	816.9	3.8	1323.1	108.7	2129.3	71.7	0.0999	-55.9	-45.2	1.106
24	38	-15.26	816.9	3.8	1311.1	73.7	2122.4	10.6	0.0147	-62.8	-57.2	0.267
24	37	4.95	816.9	3.8	1304.9	737.6	2115.0	0.4	0.0006	-70.2	-63.4	0.078
24	36	-6.72	816.9	3.8	1297.9	1440.6	2109.7	0.9	0.0012	-75.6	-70.3	0.095
23	45	0.39	786.0	4.3	1502.3	71.8	2284.4	0.0	0.0000	99.2	103.1	0.004
23	44	-0.22	786.0	4.3	1425.0	15.4	2199.9	0.0	0.0000	14.7	25.7	0.009
23	41	-0.33	786.0	4.3	1380.9	46.2	2185.5	0.1	0.0001	0.3	-18.4	0.018
23	39	-3.68	786.0	4.3	1323.1	108.7	2108.8	1.6	0.0022	-76.4	-76.1	0.048
23	38	-1.02	786.0	4.3	1311.1	73.7	2095.4	0.1	0.0001	-89.8	-88.2	0.012
23	37	0.55	786.0	4.3	1304.9	737.6	2088.0	0.1	0.0001	-97.2	-94.3	0.006
23	36	-0.50	786.0	4.3	1297.9	1440.6	2082.1	0.0	0.0000	-103.1	-101.3	0.005
22	45	-5.03	754.0	8.7	1502.3	71.8	2268.9	0.3	0.0004	83.7	71.2	0.071
22	44	2.03	754.0	8.7	1425.0	15.4	2184.2	1.4	0.0019	-1.0	-6.2	0.327

i	j	K_{ijk} / cm^{-1}	ω(i) / cm^{-1}	I(i) / km mol^{-1}	ω(j) / cm^{-1}	I(j) / km mol^{-1}	ω(ij) / cm^{-1}	I(ij) / km mol^{-1}	I(ij) / I(k)	Δω'	Δω	TFR
22	43	-0.28	754.0	8.7	1430.8	6.6	2201.0	0.0	0.0001	15.8	-0.4	0.723
22	42	0.36	754.0	8.7	1458.4	22.3	2212.6	0.1	0.0001	27.4	27.3	0.013
22	41	1.99	754.0	8.7	1380.9	46.2	2168.8	6.7	0.0094	-50.3	-16.4	0.040
22	40	1.62	754.0	8.7	1364.7	31.7	2130.7	0.3	0.0004	-66.4	-54.6	0.024
22	39	35.40	754.0	8.7	1323.1	108.7	2089.8	18.9	0.0263	-108.1	-95.4	0.328
22	38	11.54	754.0	8.7	1311.1	73.7	2078.2	3.7	0.0051	-120.1	-107.0	0.096
21	46	1.16	709.0	12.9	1586.7	3.5	2292.7	0.0	0.0000	110.5	107.5	0.010
21	45	3.07	709.0	12.9	1502.3	71.8	2207.8	1.2	0.0017	26.1	22.6	0.117
21	44	-2.11	709.0	12.9	1425.0	15.4	2124.4	2.4	0.0033	-51.2	-60.8	0.041
21	43	0.40	709.0	12.9	1430.8	6.6	2141.1	0.1	0.0001	-45.4	-44.1	0.009
21	42	-0.31	709.0	12.9	1458.4	22.3	2152.5	0.0	0.0000	-17.7	-32.7	0.017
21	41	-1.08	709.0	12.9	1380.9	46.2	2107.7	0.0	0.0000	-95.3	-77.5	0.011
20	47	-1.09	675.0	5.2	1604.1	4.2	2280.6	0.0	0.0000	93.9	95.4	0.012
20	46	1.70	675.0	5.2	1586.7	3.5	2262.8	0.1	0.0001	76.4	77.6	0.022
20	45	4.79	675.0	5.2	1502.3	71.8	2175.6	21.7	0.0302	-7.9	-9.6	0.608
20	44	-2.87	675.0	5.2	1425.0	15.4	2091.4	0.4	0.0005	-85.3	-93.8	0.034
20	43	0.30	675.0	5.2	1430.8	6.6	2108.5	0.0	0.0000	-79.4	-76.7	0.004
20	42	-0.45	675.0	5.2	1458.4	22.3	2120.1	0.0	0.0000	-51.8	-65.1	0.009
20	41	-0.81	675.0	5.2	1380.9	46.2	2075.7	0.0	0.0000	-129.3	-109.5	0.006
19	46	-0.80	642.2	0.9	1586.7	3.5	2241.8	0.1	0.0001	43.6	56.6	0.018
19	45	-1.45	642.2	0.9	1502.3	71.8	2155.3	0.2	0.0002	-40.7	-29.9	0.036
18	44	-0.56	711.7	165.6	1425.0	15.4	2112.9	0.1	0.0001	-48.5	-72.3	0.012
18	43	0.29	711.7	165.6	1430.8	6.6	2130.5	0.0	0.0000	-42.7	-54.7	0.007
18	42	-0.29	711.7	165.6	1458.4	22.3	2142.0	0.0	0.0000	-15.0	-43.2	0.020
18	41	-0.77	711.7	165.6	1380.9	46.2	2099.2	0.0	0.0000	-92.6	-86.0	0.008
17	48	0.37	543.0	14.4	1657.8	65.9	2192.9	0.0	0.0001	15.7	7.7	0.023
17	47	0.59	543.0	14.4	1604.1	4.2	2141.4	0.5	0.0007	-38.0	-43.8	0.015
16	48	-0.38	523.9	30.2	1657.8	65.9	2226.1	3.7	0.0052	-3.5	40.9	0.108
16	47	-0.78	523.9	30.2	1604.1	4.2	2175.5	0.1	0.0001	-57.2	-9.7	0.014
16	46	0.30	523.9	30.2	1586.7	3.5	2156.2	0.0	0.0000	-74.7	-29.0	0.004
15	48	-0.33	516.5	3.7	1657.8	65.9	2186.8	3.8	0.0053	-10.8	1.6	0.031
15	47	-0.36	516.5	3.7	1604.1	4.2	2134.8	0.0	0.0001	-64.5	-50.4	0.006
14	48	-0.91	644.6	13.4	1657.8	65.9	2230.6	0.7	0.0010	117.3	45.4	0.008
14	47	-2.30	644.6	13.4	1604.1	4.2	2178.5	1.7	0.0024	63.6	-6.7	0.036
13	48	0.36	486.7	7.6	1657.8	65.9	2161.4	0.1	0.0001	-40.7	-23.8	0.009
13	47	0.80	486.7	7.6	1604.1	4.2	2110.6	0.2	0.0003	-94.4	-74.6	0.008
3	49	0.61	73.2	8.8	2185.2	717.9	2243.3	0.6	0.0009	73.2	58.1	0.008
2	49	1.02	36.8	1.8	2185.2	717.9	2233.2	0.3	0.0004	36.8	48.0	0.028

6-311G(d,p)

i	j	K_{ijk} / cm^{-1}	ω(i) / cm^{-1}	I(i) / km mol^{-1}	ω(j) / cm^{-1}	I(j) / km mol^{-1}	ω(ij) / cm^{-1}	I(ij) / km mol^{-1}	I(ij) / I(k)	Δω'	Δω	TFR
33	33	34.95	1133.1	15.5	1133.1	15.5	2263.5	11.2	0.0370	79.2	81.9	0.427
32	32	1.39	1129.2	5.6	1129.2	5.6	2269.6	0.0	0.0001	85.3	74.0	0.019
32	33	-5.13	1129.2	5.6	1133.1	15.5	2266.0	0.5	0.0016	81.7	78.0	0.066
31	34	-0.24	1033.3	7.4	1199.9	6.2	2225.7	0.0	0.0000	41.5	48.9	0.005
30	34	1.02	1022.0	7.2	1199.9	6.2	2214.9	0.2	0.0008	30.6	37.6	0.027
30	33	-3.39	1022.0	7.2	1133.1	15.5	2152.2	0.8	0.0026	-32.1	-29.2	0.116
30	32	-0.66	1022.0	7.2	1129.2	5.6	2152.9	0.0	0.0001	-31.4	-33.2	0.020
29	35	-0.60	1012.3	10.6	1218.1	31.2	2231.1	0.2	0.0006	46.8	46.0	0.013
29	33	-0.94	1012.3	10.6	1133.1	15.5	2146.6	0.1	0.0004	-37.7	-38.9	0.024
28	39	1.73	918.3	3.0	1325.3	52.0	2246.0	0.1	0.0002	61.7	59.3	0.029
28	38	0.23	918.3	3.0	1304.2	10.1	2224.9	0.0	0.0000	40.6	38.2	0.006
28	37	0.45	918.3	3.0	1313.6	1260.5	2233.3	0.0	0.0000	49.0	47.6	0.009
28	36	-0.37	918.3	3.0	1294.5	2.1	2214.6	0.0	0.0000	30.3	28.4	0.013
28	35	0.25	918.3	3.0	1218.1	31.2	2138.4	0.5	0.0017	-45.9	-48.0	0.005
28	34	-0.24	918.3	3.0	1199.9	6.2	2115.1	0.0	0.0000	-69.2	-66.1	0.004
27	34	-0.27	896.3	1.6	1199.9	6.2	2095.4	0.0	0.0001	-88.9	-88.1	0.003
26	39	3.88	913.2	1.7	1325.3	52.0	2231.9	0.5	0.0017	47.6	54.2	0.072
26	38	1.53	913.2	1.7	1304.2	10.1	2209.2	0.0	0.0001	24.9	33.2	0.046
26	37	0.24	913.2	1.7	1313.6	1260.5	2218.5	0.0	0.0001	34.2	42.6	0.006
26	35	-0.62	913.2	1.7	1218.1	31.2	2122.0	0.7	0.0023	-62.3	-53.0	0.012
26	34	-0.36	913.2	1.7	1199.9	6.2	2101.8	0.1	0.0002	-82.5	-71.2	0.005
25	44	0.72	809.1	17.7	1460.8	13.8	2268.6	0.0	0.0001	84.3	85.6	0.008
25	41	0.53	809.1	17.7	1397.5	1.2	2209.0	0.0	0.0000	24.7	22.3	0.024
25	40	0.48	809.1	17.7	1354.3	8.5	2163.3	0.1	0.0002	-21.0	-20.8	0.023
25	39	4.21	809.1	17.7	1325.3	52.0	2134.6	74.8	0.2476	-49.7	-49.9	0.084
25	38	0.36	809.1	17.7	1304.2	10.1	2114.2	0.0	0.0000	-70.1	-70.9	0.005
25	37	0.49	809.1	17.7	1313.6	1260.5	2123.3	0.0	0.0000	-61.0	-61.5	0.008
25	36	-0.32	809.1	17.7	1294.5	2.1	2103.6	0.0	0.0000	-80.7	-80.7	0.004
24	44	-4.30	829.1	11.5	1460.8	13.8	2270.9	0.2	0.0008	86.6	105.6	0.041
24	42	-0.75	829.1	11.5	1476.9	116.4	2273.0	0.0	0.0000	88.7	121.7	0.006
24	41	-3.67	829.1	11.5	1397.5	1.2	2212.5	1.2	0.0039	28.2	42.3	0.087
24	40	-3.99	829.1	11.5	1354.3	8.5	2168.5	314.6	1.0410	-15.8	-0.9	4.421
24	39	-53.06	829.1	11.5	1325.3	52.0	2128.7	51.4	0.1701	-55.5	-29.9	1.774
24	38	-8.22	829.1	11.5	1304.2	10.1	2116.4	1.1	0.0035	-67.9	-51.0	0.161
24	37	-8.42	829.1	11.5	1313.6	1260.5	2125.5	0.9	0.0031	-58.8	-41.6	0.203
24	36	5.01	829.1	11.5	1294.5	2.1	2106.2	0.2	0.0006	-78.1	-60.8	0.082
23	45	-1.44	758.5	1.4	1512.6	78.0	2267.2	0.1	0.0003	82.9	86.8	0.017
23	44	0.96	758.5	1.4	1460.8	13.8	2224.2	0.0	0.0000	39.9	35.0	0.028
23	41	0.75	758.5	1.4	1397.5	1.2	2165.0	0.1	0.0003	-19.3	-28.4	0.026
23	40	0.94	758.5	1.4	1354.3	8.5	2119.1	0.2	0.0005	-65.2	-71.5	0.013

i	j	K_{ijk} / cm^{-1}	ω(i) / cm^{-1}	I(i) / km mol^{-1}	ω(j) / cm^{-1}	I(j) / km mol^{-1}	ω(ij) / cm^{-1}	I(ij) / km mol^{-1}	I(ij) / I(k)	Δω’	Δω	TFR
23	39	11.48	758.5	1.4	1325.3	52.0	2089.7	14.5	0.0481	-94.6	-100.5	0.114
23	37	2.04	758.5	1.4	1313.6	1260.5	2077.3	0.1	0.0002	-107	-112.2	0.018
22	45	-4.86	753.4	16.1	1512.6	78.0	2265.1	0.3	0.0008	80.8	81.7	0.059
22	44	2.04	753.4	16.1	1460.8	13.8	2221.6	1.3	0.0044	37.3	29.9	0.068
22	42	0.40	753.4	16.1	1476.9	116.4	2221.9	0.1	0.0003	37.6	46	0.009
22	41	1.82	753.4	16.1	1397.5	1.2	2161.8	2.2	0.0073	-22.5	-33.4	0.055
22	40	1.84	753.4	16.1	1354.3	8.5	2114.4	0.3	0.0010	-69.9	-76.6	0.024
22	39	34.06	753.4	16.1	1325.3	52.0	2085.2	14.6	0.0484	-99	-105.6	0.323
22	37	6.42	753.4	16.1	1313.6	1260.5	2074.6	1.3	0.0043	-109.7	-117.2	0.055
21	46	-1.06	711.9	14.5	1578.6	1.5	2288.5	0.0	0.0001	104.3	106.2	0.010
21	45	-3.06	711.9	14.5	1512.6	78.0	2213.7	0.7	0.0022	29.4	40.2	0.076
21	44	2.04	711.9	14.5	1460.8	13.8	2170.6	11.1	0.0368	-13.7	-11.6	0.176
21	42	0.28	711.9	14.5	1476.9	116.4	2171.4	0.0	0.0000	-12.9	4.5	0.063
21	41	1.08	711.9	14.5	1397.5	1.2	2110.8	0.0	0.0000	-73.5	-74.9	0.014
20	47	-1.23	683.5	18.1	1603.5	1.3	2288.3	0.0	0.0001	104.1	102.7	0.012
20	46	1.53	683.5	18.1	1578.6	1.5	2260.5	0.1	0.0002	76.2	77.8	0.020
20	45	4.94	683.5	18.1	1512.6	78.0	2187.6	219.1	0.7249	3.3	11.8	0.420
20	44	-3.00	683.5	18.1	1460.8	13.8	2142.5	0.5	0.0016	-41.8	-40	0.075
20	42	-0.47	683.5	18.1	1476.9	116.4	2144.1	0.0	0.0000	-40.2	-23.9	0.020
20	41	-0.94	683.5	18.1	1397.5	1.2	2083.1	0.0	0.0001	-101.2	-103.4	0.009
19	47	-0.43	643.5	3.6	1603.5	1.3	2273.5	0.0	0.0000	89.2	62.8	0.007
19	46	-0.64	643.5	3.6	1578.6	1.5	2248.7	0.1	0.0002	64.4	37.9	0.017
19	45	-1.27	643.5	3.6	1512.6	78.0	2172.4	0.1	0.0005	-11.9	-28.1	0.045
19	44	0.78	643.5	3.6	1460.8	13.8	2132.1	0.1	0.0005	-52.2	-79.9	0.010
18	47	-0.91	706.3	117.7	1603.5	1.3	2280.4	0.0	0.0001	96.1	125.6	0.007
18	46	0.25	706.3	117.7	1578.6	1.5	2255.0	0.0	0.0000	70.7	100.7	0.003
18	44	-0.83	706.3	117.7	1460.8	13.8	2138.8	0.1	0.0004	-45.5	-17.2	0.048
18	42	-0.26	706.3	117.7	1476.9	116.4	2135.5	0.0	0.0000	-48.8	-1	0.250
18	41	-0.73	706.3	117.7	1397.5	1.2	2076.2	0.0	0.0000	-108.1	-80.5	0.009
17	48	0.34	546.6	19.7	1699.3	255.2	2238.5	0.0	0.0001	54.2	61.6	0.006
17	47	0.43	546.6	19.7	1603.5	1.3	2145.0	0.3	0.0009	-39.3	-34.1	0.013
16	48	-0.39	526.6	19.6	1699.3	255.2	2268.5	0.0	0.0001	84.2	41.5	0.009
16	47	-0.86	526.6	19.6	1603.5	1.3	2175.1	0.1	0.0002	-9.2	-54.2	0.016
16	46	0.36	526.6	19.6	1578.6	1.5	2148.4	0.0	0.0001	-35.9	-79.1	0.005
15	48	-0.30	537.9	11.9	1699.3	255.2	2245.8	0.0	0.0000	61.5	52.8	0.006
15	47	-0.28	537.9	11.9	1603.5	1.3	2151.7	0.0	0.0001	-32.6	-42.9	0.006
14	48	-0.89	634.0	6.9	1699.3	255.2	2271.4	1.6	0.0055	87.1	149	0.006
14	47	-2.18	634.0	6.9	1603.5	1.3	2176.0	1.5	0.0051	-8.3	53.3	0.041
14	46	-0.39	634.0	6.9	1578.6	1.5	2149.4	0.0	0.0001	-34.9	28.4	0.014
14	45	-0.30	634.0	6.9	1512.6	78.0	2074.8	0.1	0.0003	-109.5	-37.7	0.008
13	48	0.34	470.3	6.6	1699.3	255.2	2179.8	1.2	0.0040	-4.4	-14.8	0.023
13	47	0.79	470.3	6.6	1603.5	1.3	2088.1	0.2	0.0006	-96.1	-110.5	0.007

i	j	K_{ijk} / cm^{-1}	ω(i) / cm^{-1}	I(i) / km mol^{-1}	ω(j) / cm^{-1}	I(j) / km mol^{-1}	ω(ij) / cm^{-1}	I(ij) / km mol^{-1}	I(ij) / I(k)	Δω'	Δω	TFR
6	42	-0.51	598.3	22.2	1476.9	116.4	2074.4	2.2	0.0073	-109.9	-109.1	0.005
3	49	0.57	28.2	1.1	2184.3	302.2	2206.3	0.5	0.0017	22.1	28.2	0.020
2	49	1.09	-12.0	1.9	2184.3	302.2	2166.2	0.1	0.0003	-18.1	-12.0	0.091
1	49	0.95	14.0	0.6	2184.3	302.2	2197.8	1.3	0.0044	13.5	14.0	0.068

6-311+G(d,p)

i	j	K_{ijk} / cm^{-1}	ω(i) / cm^{-1}	I(i) / km mol^{-1}	ω(j) / cm^{-1}	I(j) / km mol^{-1}	ω(ij) / cm^{-1}	I(ij) / km mol^{-1}	I(ij) / I(k)	Δω'	Δω	TFR
34	34	5.11	1103.4	26.5	1103.4	26.5	2208.2	0.1	0.0001	33.8	32.3	0.158
33	33	35.16	1136.7	4.0	1136.7	4.0	2239.0	11.3	0.0142	64.6	99.1	0.355
32	32	1.61	1045.4	50.1	1045.4	50.1	2111.8	0.0	0.0000	-62.6	-83.6	0.019
33	34	-12.93	1136.7	4.0	1103.4	26.5	2225.5	1.2	0.0015	51.1	65.7	0.197
32	35	-0.56	1045.4	50.1	1208.6	57.9	2266.5	0.0	0.0000	92.1	79.6	0.007
32	34	1.56	1045.4	50.1	1103.4	26.5	2158.1	0.7	0.0009	-16.3	-25.7	0.061
32	33	-5.12	1045.4	50.1	1136.7	4.0	2175.5	0.4	0.0005	1.1	7.7	0.663
31	37	-0.28	1010.7	3.3	1233.6	478.1	2252.6	0.0	0.0000	78.2	69.8	0.004
31	35	-0.24	1010.7	3.3	1208.6	57.9	2223.5	0.0	0.0000	49.0	44.8	0.005
31	34	-0.23	1010.7	3.3	1103.4	26.5	2117.7	0.0	0.0000	-56.7	-60.4	0.004
30	38	1.34	983.6	792.4	1294.1	112.6	2271.5	0.5	0.0006	97.1	103.2	0.013
30	37	0.60	983.6	792.4	1233.6	478.1	2220.6	0.2	0.0002	46.2	42.7	0.014
30	36	0.30	983.6	792.4	1288.5	58.2	2261.2	0.1	0.0001	86.8	97.6	0.003
30	35	-0.51	983.6	792.4	1208.6	57.9	2192.0	0.1	0.0002	17.5	17.8	0.029
30	34	-0.22	983.6	792.4	1103.4	26.5	2085.7	0.0	0.0000	-88.7	-87.5	0.002
30	33	0.27	983.6	792.4	1136.7	4.0	2101.2	0.0	0.0000	-73.2	-54.1	0.005
29	38	-2.72	992.6	1063.8	1294.1	112.6	2282.6	0.5	0.0006	108.2	112.3	0.024
29	37	-1.72	992.6	1063.8	1233.6	478.1	2229.7	0.2	0.0002	55.3	51.8	0.033
29	36	-1.32	992.6	1063.8	1288.5	58.2	2269.1	0.0	0.0000	94.7	106.7	0.012
29	35	-0.34	992.6	1063.8	1208.6	57.9	2201.2	0.0	0.0000	26.8	26.8	0.013
29	34	0.80	992.6	1063.8	1103.4	26.5	2092.5	1.1	0.0014	-81.9	-78.4	0.010
29	33	-3.33	992.6	1063.8	1136.7	4.0	2110.5	1.3	0.0016	-63.9	-45.1	0.074
28	39	1.70	947.4	6.7	1312.7	93.1	2248.2	0.0	0.0001	73.7	85.7	0.020
28	38	0.43	947.4	6.7	1294.1	112.6	2229.6	0.0	0.0000	55.1	67.1	0.006
28	37	0.46	947.4	6.7	1233.6	478.1	2177.6	0.0	0.0000	3.2	6.6	0.070
28	36	-0.27	947.4	6.7	1288.5	58.2	2217.5	0.0	0.0000	43.1	61.5	0.004
28	35	0.22	947.4	6.7	1208.6	57.9	2147.2	0.1	0.0002	-27.2	-18.4	0.012
27	38	0.20	875.9	5.6	1294.1	112.6	2188.6	0.0	0.0000	14.2	-4.4	0.046
26	44	0.77	898.2	14.5	1369.6	85.1	2271.9	0.3	0.0004	97.5	93.3	0.008
26	43	-0.42	898.2	14.5	1411.2	15.5	2250.5	0.0	0.0000	76.1	134.9	0.003
26	39	3.32	898.2	14.5	1312.7	93.1	2206.3	0.4	0.0005	31.9	36.5	0.091
26	38	1.63	898.2	14.5	1294.1	112.6	2186.1	0.0	0.0001	11.7	17.8	0.091
26	35	-0.66	898.2	14.5	1208.6	57.9	2104.5	0.7	0.0009	-69.9	-67.6	0.010
25	44	0.96	829.8	21.0	1369.6	85.1	2201.5	0.1	0.0001	27.1	25.0	0.038
25	41	0.69	829.8	21.0	1398.8	1.8	2213.6	0.0	0.0000	39.2	54.2	0.013
25	40	0.66	829.8	21.0	1355.1	17.5	2170.1	0.1	0.0001	-4.3	10.5	0.063

i	j	K_{ijk} / cm^{-1}	ω(i) / cm^{-1}	I(i) / km mol^{-1}	ω(j) / cm^{-1}	I(j) / km mol^{-1}	ω(ij) / cm^{-1}	I(ij) / km mol^{-1}	I(ij) / I(k)	Δω'	Δω	TFR
25	39	6.54	829.8	21.0	1312.7	93.1	2133.0	1.5	0.0018	-41.4	-31.9	0.205
25	38	1.23	829.8	21.0	1294.1	112.6	2114.3	0.2	0.0002	-60.1	-50.5	0.024
25	36	-0.50	829.8	21.0	1288.5	58.2	2101.9	0.0	0.0000	-72.5	-56.2	0.009
24	45	-5.64	806.2	1.4	1487.9	21.1	2280.7	1.6	0.0020	106.3	119.6	0.047
24	44	4.03	806.2	1.4	1369.6	85.1	2184.3	0.2	0.0003	9.9	1.3	2.994
24	42	0.55	806.2	1.4	1250.9	150.1	2117.1	0.0	0.0000	-57.3	-117.4	0.005
24	41	3.21	806.2	1.4	1398.8	1.8	2196.4	0.8	0.0010	22.0	30.6	0.105
24	40	3.53	806.2	1.4	1355.1	17.5	2153.3	9.8	0.0123	-21.2	-13.1	0.269
24	39	52.78	806.2	1.4	1312.7	93.1	2107.5	52.4	0.0659	-66.9	-55.5	0.950
24	38	12.79	806.2	1.4	1294.1	112.6	2096.7	6.6	0.0083	-77.7	-74.2	0.172
24	36	-4.20	806.2	1.4	1288.5	58.2	2084.2	0.3	0.0003	-90.3	-79.8	0.053
23	45	0.25	774.5	6.7	1487.9	21.1	2238.5	0.0	0.0000	64.1	87.9	0.003
23	39	-3.18	774.5	6.7	1312.7	93.1	2074.2	1.6	0.0021	-100.2	-87.3	0.036
22	45	-4.74	734.6	12.9	1487.9	21.1	2229.3	0.2	0.0003	54.9	48.1	0.099
22	44	1.97	734.6	12.9	1369.6	85.1	2133.8	1.2	0.0015	-40.6	-70.2	0.028
22	42	0.28	734.6	12.9	1250.9	150.1	2065.1	0.0	0.0000	-109.3	-189.0	0.001
22	41	1.61	734.6	12.9	1398.8	1.8	2144.7	37.0	0.0465	-29.7	-41.0	0.039
22	40	1.66	734.6	12.9	1355.1	17.5	2099.5	0.3	0.0003	-74.9	-84.7	0.020
21	46	-1.17	700.4	10.7	1572.4	2.4	2272.7	0.0	0.0000	98.2	98.4	0.012
21	45	-3.08	700.4	10.7	1487.9	21.1	2178.2	0.7	0.0008	3.8	13.8	0.223
21	44	2.10	700.4	10.7	1369.6	85.1	2083.2	43.5	0.0547	-91.2	-104.5	0.020
21	41	0.90	700.4	10.7	1398.8	1.8	2093.9	0.0	0.0000	-80.5	-75.3	0.012
20	47	-1.06	665.6	4.8	1601.2	10.2	2257.7	0.0	0.0000	83.3	92.4	0.011
20	46	1.62	665.6	4.8	1572.4	2.4	2233.6	0.1	0.0001	59.2	63.7	0.025
20	45	4.69	665.6	4.8	1487.9	21.1	2140.2	115.1	0.1448	-34.2	-20.9	0.224
19	47	-0.25	636.1	4.0	1601.2	10.2	2227.9	0.0	0.0000	53.5	62.9	0.004
19	46	-0.73	636.1	4.0	1572.4	2.4	2207.8	0.0	0.0001	33.4	34.1	0.021
19	45	-1.27	636.1	4.0	1487.9	21.1	2111.2	0.2	0.0002	-63.2	-50.4	0.025
18	48	-0.39	578.1	24.7	1648.5	135.7	2225.3	0.1	0.0001	50.9	52.2	0.007
18	47	-0.90	578.1	24.7	1601.2	10.2	2174.4	0.0	0.0000	-0.1	4.8	0.185
17	48	0.33	537.1	9.7	1648.5	135.7	2166.2	0.0	0.0000	-8.2	11.2	0.030
17	47	0.53	537.1	9.7	1601.2	10.2	2113.8	0.5	0.0006	-60.7	-36.2	0.015
16	48	-0.39	518.7	54.9	1648.5	135.7	2120.3	0.3	0.0003	-54.2	-7.2	0.054
16	47	-0.77	518.7	54.9	1601.2	10.2	2068.7	0.1	0.0001	-105.7	-54.5	0.014
15	48	-0.40	466.2	37.3	1648.5	135.7	2125.0	3.0	0.0038	-49.4	-59.8	0.007
15	47	-0.45	466.2	37.3	1601.2	10.2	2072.7	0.1	0.0001	-101.7	-107.1	0.004
14	48	-1.01	384.8	55.5	1648.5	135.7	2090.2	0.9	0.0011	-84.3	-141.1	0.007
13	47	0.35	483.7	5.7	1601.2	10.2	2077.2	0.0	0.0000	-97.3	-89.5	0.004
5	49	6.41	82.0	0.5	2174.4	795.2	2249.7	0.4	0.0005	75.3	82.0	0.078

6-311++G(d,p)

i	j	K_{ijk} / cm^{-1}	ω(i) / cm^{-1}	I(i) / km mol^{-1}	ω(j) / cm^{-1}	I(j) / km mol^{-1}	ω(ij) / cm^{-1}	I(ij) / km mol^{-1}	I(ij) / I(k)	Δω’	Δω	TFR
34	34	5.12	1155.3	1.5	1155.3	1.5	2257.8	0.1	0.0002	83.7	136.5	0.038
33	33	35.16	1125.8	10.3	1125.8	10.3	2248.9	11.3	0.0194	74.8	77.5	0.454
32	32	1.59	1069.7	20.2	1069.7	20.2	2190.9	0.0	0.0000	16.8	-34.8	0.046
33	34	-12.98	1125.8	10.3	1155.3	1.5	2255.2	1.2	0.0021	81.0	107.0	0.121
32	34	1.55	1069.7	20.2	1155.3	1.5	2223.0	0.7	0.0012	48.8	50.9	0.030
32	33	-5.10	1069.7	20.2	1125.8	10.3	2219.9	0.4	0.0007	45.7	21.4	0.239
31	35	-0.24	1030.9	10.8	1214.2	17.5	2244.5	0.0	0.0001	70.3	71.0	0.003
31	34	-0.23	1030.9	10.8	1155.3	1.5	2160.9	0.0	0.0000	-13.3	12.1	0.019
30	35	-0.48	1010.8	30.5	1214.2	17.5	2217.6	0.1	0.0002	43.5	50.8	0.009
30	34	-0.28	1010.8	30.5	1155.3	1.5	2133.8	0.1	0.0001	-40.3	-8.1	0.035
30	33	0.55	1010.8	30.5	1125.8	10.3	2129.4	0.0	0.0000	-44.7	-37.5	0.015
30	32	0.36	1010.8	30.5	1069.7	20.2	2098.4	0.0	0.0001	-75.8	-93.7	0.004
29	37	-1.66	990.3	0.9	1270.8	12.1	2275.2	0.2	0.0004	101.1	87.0	0.019
29	36	-1.30	990.3	0.9	1292.5	5.2	2276.1	0.0	0.0000	101.9	108.6	0.012
29	35	-0.36	990.3	0.9	1214.2	17.5	2209.1	0.0	0.0001	35.0	30.3	0.012
29	34	0.77	990.3	0.9	1155.3	1.5	2123.1	1.0	0.0018	-51.0	-28.6	0.027
29	33	-3.28	990.3	0.9	1125.8	10.3	2120.8	1.3	0.0022	-53.3	-58.0	0.056
29	32	-0.55	990.3	0.9	1069.7	20.2	2088.5	0.0	0.0000	-85.6	-114.2	0.005
28	39	1.70	954.8	0.2	1315.0	38.3	2253.5	0.0	0.0001	79.3	95.7	0.018
28	38	0.43	954.8	0.2	1299.1	21.2	2237.4	0.0	0.0000	63.3	79.7	0.005
28	37	0.46	954.8	0.2	1270.8	12.1	2221.1	0.0	0.0000	47.0	51.5	0.009
28	36	-0.27	954.8	0.2	1292.5	5.2	2222.3	0.0	0.0000	48.2	73.1	0.004
28	35	0.22	954.8	0.2	1214.2	17.5	2153.2	0.1	0.0002	-20.9	-5.2	0.042
28	34	-0.24	954.8	0.2	1155.3	1.5	2068.6	0.0	0.0000	-105.5	-64.0	0.004
28	33	0.88	954.8	0.2	1125.8	10.3	2065.5	0.0	0.0000	-108.6	-93.5	0.009
27	38	0.21	882.9	2.8	1299.1	21.2	2199.8	0.0	0.0001	25.7	7.8	0.027
26	44	0.77	900.9	4.3	1367.1	42.9	2277.8	0.3	0.0005	103.7	93.9	0.008
26	39	3.32	900.9	4.3	1315.0	38.3	2209.4	0.4	0.0006	35.2	41.8	0.079
26	38	1.62	900.9	4.3	1299.1	21.2	2191.7	0.0	0.0001	17.5	25.9	0.063
26	35	-0.66	900.9	4.3	1214.2	17.5	2108.3	0.7	0.0013	-65.8	-59.0	0.011
25	44	0.94	832.6	19.7	1367.1	42.9	2209.4	0.1	0.0001	35.2	25.6	0.037
25	41	0.68	832.6	19.7	1406.4	5.4	2217.6	0.0	0.0000	43.5	64.9	0.010
25	40	0.64	832.6	19.7	1357.9	23.6	2184.7	0.1	0.0001	10.5	16.4	0.039
25	39	6.32	832.6	19.7	1315.0	38.3	2137.8	1.3	0.0022	-36.3	-26.5	0.239
25	38	1.18	832.6	19.7	1299.1	21.2	2121.7	0.2	0.0003	-52.4	-42.4	0.028
25	37	0.82	832.6	19.7	1270.8	12.1	2106.8	0.0	0.0000	-67.4	-70.6	0.012
25	36	-0.48	832.6	19.7	1292.5	5.2	2106.3	0.0	0.0000	-67.8	-49.0	0.010
24	44	4.03	808.4	3.9	1367.1	42.9	2192.7	0.2	0.0003	18.5	1.4	2.948
24	42	0.55	808.4	3.9	1430.4	3.0	2235.5	0.0	0.0000	61.4	64.7	0.008
24	41	3.20	808.4	3.9	1406.4	5.4	2201.0	0.8	0.0013	26.8	40.7	0.079
24	40	3.52	808.4	3.9	1357.9	23.6	2168.3	9.9	0.0170	-5.8	-7.8	0.451
24	39	52.73	808.4	3.9	1315.0	38.3	2112.3	45.5	0.0781	-61.9	-50.7	1.040
24	38	12.77	808.4	3.9	1299.1	21.2	2104.7	6.6	0.0113	-69.5	-66.7	0.192
24	37	8.16	808.4	3.9	1270.8	12.1	2088.4	1.8	0.0030	-85.7	-94.9	0.086
24	36	-4.18	808.4	3.9	1292.5	5.2	2089.1	0.3	0.0004	-85.0	-73.2	0.057

i	j	K_{ijk} / cm^{-1}	ω(i) / cm^{-1}	I(i) / km mol^{-1}	ω(j) / cm^{-1}	I(j) / km mol^{-1}	ω(ij) / cm^{-1}	I(ij) / km mol^{-1}	I(ij) / I(k)	Δω'	Δω	TFR
23	39	-2.66	781.8	4.9	1315.0	38.3	2080.9	1.1	0.0019	-93.2	-77.3	0.034
23	38	-0.61	781.8	4.9	1299.1	21.2	2065.1	0.0	0.0001	-109.0	-93.3	0.007
22	45	-4.73	736.9	9.7	1490.1	42.2	2245.3	0.2	0.0004	71.2	52.9	0.090
22	44	1.96	736.9	9.7	1367.1	42.9	2143.6	1.2	0.0020	-30.5	-70.1	0.028
22	42	0.28	736.9	9.7	1430.4	3.0	2185.1	0.0	0.0001	11.0	-6.8	0.041
22	41	1.60	736.9	9.7	1406.4	5.4	2150.7	41.7	0.0715	-23.4	-30.8	0.052
22	40	1.66	736.9	9.7	1357.9	23.6	2116.0	0.3	0.0005	-58.1	-79.3	0.021
22	39	34.96	736.9	9.7	1315.0	38.3	2068.5	22.0	0.0377	-105.6	-122.2	0.286
21	46	-1.17	704.4	12.4	1575.3	1.6	2279.5	0.0	0.0001	105.4	105.6	0.011
21	45	-3.05	704.4	12.4	1490.1	42.2	2193.1	0.6	0.0011	19.0	20.3	0.150
21	44	2.07	704.4	12.4	1367.1	42.9	2091.8	116.1	0.1991	-82.3	-102.6	0.020
21	43	-0.22	704.4	12.4	1416.4	15.2	2117.7	0.1	0.0002	-56.4	-53.3	0.004
21	41	0.91	704.4	12.4	1406.4	5.4	2098.9	0.0	0.0000	-75.3	-63.4	0.014
21	40	1.25	704.4	12.4	1357.9	23.6	2066.6	0.0	0.0001	-107.6	-111.8	0.011
20	47	-1.07	674.8	5.7	1590.9	5.4	2266.7	0.0	0.0000	92.6	91.6	0.012
20	46	1.65	674.8	5.7	1575.3	1.6	2246.1	0.1	0.0001	71.9	76.0	0.022
20	45	4.76	674.8	5.7	1490.1	42.2	2160.6	111.9	0.1920	-13.5	-9.3	0.514
20	42	-0.37	674.8	5.7	1430.4	3.0	2100.2	0.0	0.0000	-74.0	-69.0	0.005
20	41	-0.54	674.8	5.7	1406.4	5.4	2065.8	0.0	0.0000	-108.3	-93.0	0.006
19	47	-0.25	645.0	4.4	1590.9	5.4	2234.3	0.0	0.0000	60.1	61.8	0.004
19	46	-0.73	645.0	4.4	1575.3	1.6	2217.6	0.0	0.0001	43.5	46.2	0.016
19	45	-1.27	645.0	4.4	1490.1	42.2	2128.9	0.2	0.0003	-45.2	-39.1	0.033
18	48	-0.39	580.9	14.1	1650.0	161.8	2231.2	0.1	0.0001	57.1	56.8	0.007
18	47	-0.90	580.9	14.1	1590.9	5.4	2178.1	0.0	0.0001	4.0	-2.3	0.391
17	48	0.33	543.8	8.7	1650.0	161.8	2176.3	0.0	0.0001	2.2	19.8	0.017
17	47	0.53	543.8	8.7	1590.9	5.4	2121.8	0.5	0.0008	-52.3	-39.4	0.013
16	48	-0.47	533.0	25.5	1650.0	161.8	2130.8	0.5	0.0008	-43.3	8.9	0.053
16	47	-0.85	533.0	25.5	1590.9	5.4	2077.5	0.1	0.0002	-96.6	-50.2	0.017
15	48	-0.31	518.7	2.5	1650.0	161.8	2165.8	202.8	0.3480	-8.3	-5.3	0.058
15	47	-0.28	518.7	2.5	1590.9	5.4	2111.1	0.0	0.0001	-63.1	-64.5	0.004
14	48	-1.00	391.7	75.6	1650.0	161.8	2102.6	0.9	0.0016	-71.5	-132.3	0.008
13	47	0.41	477.6	20.9	1590.9	5.4	2083.4	0.0	0.0001	-90.7	-105.6	0.004
5	49	6.41	129.8	2.0	2174.1	582.8	2279.3	0.4	0.0007	105.2	129.8	0.049
2	49	1.16	-38.1	10.1	2174.1	582.8	2129.4	0.3	0.0005	-44.7	-38.1	0.031
1	49	1.29	-100.8	62.4	2174.1	582.8	2066.5	1.5	0.0025	-107.6	-100.8	0.013

6-311++G(df,pd)

i	j	K_{ijk} / cm^{-1}	ω(i) / cm^{-1}	I(i) / km mol^{-1}	ω(j) / cm^{-1}	I(j) / km mol^{-1}	ω(ij) / cm^{-1}	I(ij) / km mol^{-1}	I(ij) / I(k)	Δω'	Δω	TFR
33	33	35.54	1128.1	10.6	1128.1	10.6	2255.1	10.5	0.0135	85.5	86.5	0.411
32	32	2.02	1101.3	13.3	1101.3	13.3	2236.0	0.0	0.0000	66.4	33.0	0.061
32	33	-6.32	1101.3	13.3	1128.1	10.6	2245.2	0.6	0.0007	75.6	59.8	0.106
31	35	-0.22	1037.2	12.8	1218.9	24.0	2256.5	0.0	0.0000	86.9	86.5	0.002
31	34	-0.24	1037.2	12.8	1182.6	1.4	2202.8	0.0	0.0000	33.2	50.2	0.005
30	34	0.78	1010.7	15.0	1182.6	1.4	2176.0	0.4	0.0005	6.4	23.7	0.033

i	j	K_{ijk} / cm^{-1}	ω(i) / cm^{-1}	I(i) / km mol^{-1}	ω(j) / cm^{-1}	I(j) / km mol^{-1}	ω(ij) / cm^{-1}	I(ij) / km mol^{-1}	I(ij) / I(k)	Δω'	Δω	TFR
30	33	-2.79	1010.7	15.0	1128.1	10.6	2140.3	1.2	0.0016	-29.3	-30.8	0.090
30	32	-0.54	1010.7	15.0	1101.3	13.3	2127.7	0.0	0.0000	-41.9	-57.6	0.009
29	35	-0.59	1017.1	12.9	1218.9	24.0	2233.3	0.2	0.0002	63.7	66.4	0.009
29	33	-1.38	1017.1	12.9	1128.1	10.6	2142.6	0.4	0.0005	-27.0	-24.4	0.057
28	39	1.72	970.3	0.1	1318.8	93.3	2278.6	0.0	0.0001	109.0	119.5	0.014
28	38	0.41	970.3	0.1	1311.8	100.1	2270.4	0.0	0.0000	100.8	112.5	0.004
28	37	0.53	970.3	0.1	1303.1	177.9	2263.2	0.0	0.0000	93.6	103.7	0.005
28	36	-0.27	970.3	0.1	1286.4	1.5	2244.6	0.0	0.0000	75.0	87.0	0.003
28	35	0.22	970.3	0.1	1218.9	24.0	2179.4	0.0	0.0000	9.8	19.6	0.011
28	34	-0.28	970.3	0.1	1182.6	1.4	2124.9	0.0	0.0000	-44.7	-16.8	0.016
28	33	0.87	970.3	0.1	1128.1	10.6	2088.4	0.0	0.0000	-81.2	-71.3	0.012
27	35	-0.22	917.6	2.2	1218.9	24.0	2144.2	0.9	0.0011	-25.4	-33.1	0.007
26	39	2.97	898.8	1.6	1318.8	93.3	2221.1	0.3	0.0003	51.5	48.1	0.062
26	38	1.61	898.8	1.6	1311.8	100.1	2211.3	0.1	0.0001	41.7	41.0	0.039
26	35	-0.71	898.8	1.6	1218.9	24.0	2120.4	0.8	0.0011	-49.2	-51.8	0.014
26	34	-0.23	898.8	1.6	1182.6	1.4	2067.7	0.1	0.0001	-101.9	-88.2	0.003
25	44	0.71	842.5	10.6	1429.4	15.3	2251.3	0.0	0.0001	81.7	102.3	0.007
25	41	0.54	842.5	10.6	1383.1	19.7	2232.5	0.0	0.0000	62.9	56.0	0.010
25	40	0.51	842.5	10.6	1365.6	43.9	2200.6	0.1	0.0001	31.0	38.4	0.013
25	39	4.42	842.5	10.6	1318.8	93.3	2153.8	37.9	0.0489	-15.8	-8.3	0.532
25	38	0.73	842.5	10.6	1311.8	100.1	2145.9	0.3	0.0004	-23.7	-15.3	0.048
25	37	0.64	842.5	10.6	1303.1	177.9	2139.6	0.0	0.0000	-30.0	-24.1	0.026
25	36	-0.31	842.5	10.6	1286.4	1.5	2120.8	0.0	0.0000	-48.8	-40.8	0.008
24	44	-3.61	819.4	5.9	1429.4	15.3	2221.5	0.1	0.0002	51.9	79.2	0.046
24	43	-0.31	819.4	5.9	1422.1	3.0	2236.7	0.0	0.0000	67.1	71.9	0.004
24	42	-0.53	819.4	5.9	1461.5	49.4	2262.0	0.0	0.0000	92.4	111.3	0.005
24	41	-3.40	819.4	5.9	1383.1	19.7	2203.6	0.7	0.0009	34.0	32.9	0.103
24	40	-3.59	819.4	5.9	1365.6	43.9	2172.2	5.8	0.0075	2.6	15.4	0.234
24	39	-52.34	819.4	5.9	1318.8	93.3	2115.1	89.4	0.1153	-54.5	-31.4	1.669
24	38	-12.11	819.4	5.9	1311.8	100.1	2116.5	9.1	0.0117	-53.1	-38.4	0.315
24	37	-10.27	819.4	5.9	1303.1	177.9	2108.8	4.2	0.0054	-60.8	-47.1	0.218
24	36	3.79	819.4	5.9	1286.4	1.5	2091.4	0.3	0.0003	-78.2	-63.8	0.059
23	44	0.57	752.8	8.7	1429.4	15.3	2199.0	0.0	0.0000	29.4	12.6	0.045
23	41	0.41	752.8	8.7	1383.1	19.7	2181.0	0.1	0.0001	11.4	-33.7	0.012
23	40	0.54	752.8	8.7	1365.6	43.9	2149.0	0.1	0.0002	-20.6	-51.2	0.010
23	39	7.30	752.8	8.7	1318.8	93.3	2101.9	21.8	0.0281	-67.7	-97.9	0.075
23	38	1.73	752.8	8.7	1311.8	100.1	2093.9	0.1	0.0002	-75.6	-105.0	0.016
23	37	1.56	752.8	8.7	1303.1	177.9	2086.2	0.1	0.0001	-83.4	-113.7	0.014
23	36	-0.35	752.8	8.7	1286.4	1.5	2067.7	0.0	0.0001	-101.9	-130.4	0.003
22	45	-4.67	776.7	6.3	1502.5	87.6	2266.1	0.2	0.0003	96.5	109.6	0.043
22	44	1.66	776.7	6.3	1429.4	15.3	2183.1	1.0	0.0012	13.5	36.5	0.045
22	42	0.28	776.7	6.3	1461.5	49.4	2221.6	0.0	0.0000	52.0	68.7	0.004
22	41	1.69	776.7	6.3	1383.1	19.7	2162.8	70.6	0.0911	-6.8	-9.8	0.172
22	40	1.72	776.7	6.3	1365.6	43.9	2130.0	0.3	0.0004	-39.6	-27.3	0.063
22	39	34.75	776.7	6.3	1318.8	93.3	2082.5	26.1	0.0336	-87.1	-74.0	0.469
22	38	8.62	776.7	6.3	1311.8	100.1	2076.4	2.4	0.0030	-93.2	-81.1	0.106
22	37	8.02	776.7	6.3	1303.1	177.9	2069.1	2.0	0.0026	-100.5	-89.8	0.089

i	j	K_{ijk} / cm^{-1}	ω(i) / cm^{-1}	I(i) / km mol^{-1}	ω(j) / cm^{-1}	I(j) / km mol^{-1}	ω(ij) / cm^{-1}	I(ij) / km mol^{-1}	I(ij) / I(k)	Δω'	Δω	TFR
21	45	-2.98	717.7	16.2	1502.5	87.6	2214.7	0.4	0.0005	45.1	50.6	0.059
21	44	1.87	717.7	16.2	1429.4	15.3	2132.3	36.7	0.0474	-37.3	-22.5	0.083
21	41	0.97	717.7	16.2	1383.1	19.7	2112.7	0.0	0.0000	-56.9	-68.8	0.014
21	40	1.27	717.7	16.2	1365.6	43.9	2081.4	0.0	0.0000	-88.2	-86.3	0.015
20	46	1.55	682.4	4.4	1579.0	2.5	2259.4	0.0	0.0001	89.8	91.9	0.017
20	45	4.76	682.4	4.4	1502.5	87.6	2181.7	16.9	0.0218	12.1	15.3	0.310
20	44	-2.63	682.4	4.4	1429.4	15.3	2098.6	0.8	0.0010	-71.0	-57.7	0.045
20	42	-0.34	682.4	4.4	1461.5	49.4	2137.9	0.0	0.0000	-31.7	-25.6	0.013
20	41	-0.70	682.4	4.4	1383.1	19.7	2079.4	0.0	0.0000	-90.2	-104.1	0.007
19	46	-0.64	647.1	1.2	1579.0	2.5	2269.3	0.0	0.0000	99.7	56.5	0.011
19	45	-1.31	647.1	1.2	1502.5	87.6	2189.5	0.4	0.0005	19.9	-20.0	0.066
19	44	0.69	647.1	1.2	1429.4	15.3	2107.4	0.1	0.0002	-62.2	-93.1	0.007
18	44	-0.78	755.5	184.5	1429.4	15.3	2126.6	0.1	0.0002	-43.0	15.3	0.051
18	42	-0.27	755.5	184.5	1461.5	49.4	2166.5	0.0	0.0000	-3.1	47.4	0.006
18	41	-0.78	755.5	184.5	1383.1	19.7	2109.7	0.0	0.0000	-59.9	-31.0	0.025
18	40	-0.39	755.5	184.5	1365.6	43.9	2078.1	0.0	0.0000	-91.5	-48.6	0.008
17	48	0.35	550.9	14.9	1654.1	109.1	2193.9	0.0	0.0001	24.3	35.3	0.010
17	47	0.55	550.9	14.9	1597.7	0.9	2140.7	0.7	0.0009	-28.9	-21.0	0.026
16	48	-0.43	536.9	30.6	1654.1	109.1	2261.3	0.1	0.0001	91.7	21.4	0.020
16	47	-0.80	536.9	30.6	1597.7	0.9	2209.3	0.1	0.0001	39.7	-35.0	0.023
16	46	0.40	536.9	30.6	1579.0	2.5	2186.9	0.0	0.0001	17.3	-53.6	0.007
14	48	-0.94	705.0	37.6	1654.1	109.1	2274.3	1.2	0.0016	104.7	189.5	0.005
14	47	-2.46	705.0	37.6	1597.7	0.9	2220.8	2.1	0.0027	51.2	133.1	0.019
14	45	-0.28	705.0	37.6	1502.5	87.6	2119.5	0.1	0.0001	-50.1	37.9	0.007
11	48	0.35	412.2	0.8	1654.1	109.1	2071.7	0.1	0.0001	-97.9	-103.3	0.003
2	49	1.02	96.7	8.2	2169.6	775.3	2224.8	0.4	0.0005	55.2	96.7	0.011

APPENDIX E

VIBRATIONAL MODES OF 4-AZIDO-N-PHENYLMALEIMIDE (ISOMER 1) THAT OCCUR WITHIN ±130 CM^{-1} FROM THE FUNDAMENTAL VIBRATION FOR SEVEN BASIS SETS IN NNDMA

i, j, k : vibrational modes ; where k = 54 (azide asymmetric stretch)

i = j → overtone & i ≠ j → combination band

K_{ijk} : cubic force constant

TFR : third-order Fermi resonance

ω(i), ω(j), ω(k) : anharmonic frequencies of i, j & k th mode

ω(ij) : anharmonic frequency of ij th mode

I(i), I(j), I(k) : anharmonic intensities of i, j & k th mode

I(ij) : anharmonic intensity of ij th mode

Δω’ : ω(ij) - ω(k)

Δω : ω(i) + ω(j) - ω(k)

6-31G(d,p)

i	j	K_{ijk} / cm^{-1}	ω(i) / cm^{-1}	I(i) / km mol^{-1}	ω(j) / cm^{-1}	I(j) / km mol^{-1}	ω(ij) / cm^{-1}	I(ij) / km mol^{-1}	I(ij) / I(k)	Δω’	Δω	TFR
39	39	-36.22	1137.3	46.2	1137.3	46.2	2272.9	12.2	0.0247	69.1	70.8	0.511
38	38	-3.87	1139.7	18.4	1139.7	18.4	2269.3	0.3	0.0007	65.5	75.6	0.051
37	37	-1.27	1120.0	18.0	1120	18.0	2251.2	0.0	0.0000	47.4	36.2	0.035
36	36	-0.26	1058.0	9.5	1058	9.5	2106.9	0.3	0.0007	-96.9	-87.8	0.003
39	40	-13.95	1137.3	46.2	1196.3	12.5	2333.5	1.8	0.0037	129.8	129.8	0.107
38	40	-2.60	1139.7	18.4	1196.3	12.5	2333.5	0.3	0.0006	129.7	132.2	0.020
38	39	-7.14	1139.7	18.4	1137.3	46.2	2272.8	1.5	0.0031	69.1	73.2	0.097
37	39	-1.93	1120.0	18.0	1137.3	46.2	2262.5	0.0	0.0000	58.7	53.5	0.036
37	38	0.46	1120.0	18.0	1139.7	18.4	2259.9	0.4	0.0008	56.1	55.9	0.008
36	42	0.24	1058.0	9.5	1292.5	6.9	2335.9	0.1	0.0002	132.2	146.7	0.002
36	41	-0.46	1058.0	9.5	1212	10.6	2267	0.1	0.0002	63.2	66.2	0.007
36	40	0.75	1058.0	9.5	1196.3	12.5	2251.7	0.0	0.0000	47.9	50.5	0.015

i	j	K_{ijk} / cm^{-1}	ω(i) / cm^{-1}	I(i) / km mol^{-1}	ω(j) / cm^{-1}	I(j) / km mol^{-1}	ω(ij) / cm^{-1}	I(ij) / km mol^{-1}	I(ij) / I(k)	Δω'	Δω	TFR
36	39	2.45	1058.0	9.5	1137.3	46.2	2193.2	217.1	0.4388	-10.5	-8.5	0.288
36	38	0.46	1058.0	9.5	1139.7	18.4	2191.1	2.3	0.0047	-12.7	-6.1	0.076
35	42	0.25	1025.3	5.1	1292.5	6.9	2319.5	0.7	0.0014	115.7	114.0	0.002
35	39	-0.73	1025.3	5.1	1137.3	46.2	2164.8	0.2	0.0004	-38.9	-41.2	0.018
35	38	0.69	1025.3	5.1	1139.7	18.4	2160.4	1.4	0.0028	-43.4	-38.8	0.018
35	37	-0.34	1025.3	5.1	1120	18.0	2151.4	0.5	0.0010	-52.4	-58.5	0.006
34	44	-0.59	1018.2	0.7	1313.1	31.7	2332.4	0.1	0.0002	128.6	127.5	0.005
34	43	-0.23	1018.2	0.7	1317.4	259.2	2334.7	0.1	0.0002	130.9	131.7	0.002
34	41	-0.55	1018.2	0.7	1212	10.6	2230	0.0	0.0000	26.2	26.4	0.021
34	40	1.29	1018.2	0.7	1196.3	12.5	2214.3	2.7	0.0055	10.5	10.7	0.121
34	39	3.62	1018.2	0.7	1137.3	46.2	2155.3	0.8	0.0015	-48.4	-48.3	0.075
34	38	0.35	1018.2	0.7	1139.7	18.4	2153.7	0.0	0.0001	-50.0	-45.9	0.008
34	37	-0.83	1018.2	0.7	1120	18.0	2142.6	0.1	0.0001	-61.1	-65.6	0.013
33	45	-0.20	961.0	0.7	1328.2	97.6	2288.2	0.0	0.0000	84.5	85.5	0.002
32	46	-0.21	961.4	14.5	1374	31.8	2331.2	0.0	0.0000	127.4	131.6	0.002
32	45	0.75	961.4	14.5	1328.2	97.6	2282.7	0.0	0.0000	78.9	85.9	0.009
32	44	-0.22	961.4	14.5	1313.1	31.7	2271.9	0.0	0.0001	68.2	70.8	0.003
32	43	-0.65	961.4	14.5	1317.4	259.2	2273.8	0.0	0.0001	70.1	75.0	0.009
32	41	-0.23	961.4	14.5	1212	10.6	2167.4	0.2	0.0004	-36.4	-30.3	0.008
32	40	0.25	961.4	14.5	1196.3	12.5	2152.7	0.0	0.0000	-51.1	-46.0	0.005
32	39	0.79	961.4	14.5	1137.3	46.2	2093.7	0.0	0.0000	-110.1	-105.1	0.008
32	38	0.29	961.4	14.5	1139.7	18.4	2091.6	0.1	0.0001	-112.2	-102.6	0.003
31	46	-0.29	948.3	1.1	1374	31.8	2328.2	0.0	0.0000	124.4	118.6	0.002
31	45	1.26	948.3	1.1	1328.2	97.6	2279.7	0.0	0.0000	76.0	72.8	0.017
31	43	-0.78	948.3	1.1	1317.4	259.2	2270.5	0.0	0.0000	66.7	61.9	0.013
31	39	0.60	948.3	1.1	1137.3	46.2	2090.6	0.0	0.0000	-113.1	-118.1	0.005
30	40	-0.23	946.6	1.9	1196.3	12.5	2143.1	0.0	0.0000	-60.7	-60.8	0.004
30	37	-0.32	946.6	1.9	1120	18.0	2071.7	0.1	0.0001	-132.1	-137.1	0.002
29	46	-0.75	840.4	73.5	1374	31.8	2214.6	0.4	0.0007	10.8	10.7	0.070
29	45	3.02	840.4	73.5	1328.2	97.6	2166.4	1.1	0.0022	-37.3	-35.1	0.086
29	44	0.63	840.4	73.5	1313.1	31.7	2156.5	0.0	0.0000	-47.3	-50.2	0.013
29	43	0.46	840.4	73.5	1317.4	259.2	2158.9	0.1	0.0001	-44.9	-46.0	0.010
28	46	0.70	828.3	22.6	1374	31.8	2202.4	11.4	0.0230	-1.3	-1.4	0.489
28	45	-3.02	828.3	22.6	1328.2	97.6	2154.8	0.5	0.0011	-49.0	-47.2	0.064
28	44	-0.67	828.3	22.6	1313.1	31.7	2144.4	0.0	0.0000	-59.4	-62.3	0.011
28	43	-0.36	828.3	22.6	1317.4	259.2	2145.9	0.0	0.0000	-57.9	-58.1	0.006
27	48	6.80	818.7	2.6	1516	107.6	2335.4	1.9	0.0038	131.6	131.0	0.052
27	47	0.48	818.7	2.6	1438.1	1.2	2259.6	0.0	0.0001	55.9	53.0	0.009
27	46	15.12	818.7	2.6	1374	31.8	2192.6	176.6	0.3570	-11.2	-11.1	1.368
27	45	-57.35	818.7	2.6	1328.2	97.6	2136.7	57.6	0.1165	-67.0	-56.8	1.009
27	44	-12.59	818.7	2.6	1313.1	31.7	2135.4	2.8	0.0058	-68.4	-71.9	0.175
27	43	-6.90	818.7	2.6	1317.4	259.2	2137.2	0.7	0.0014	-66.5	-67.7	0.102
27	42	2.76	818.7	2.6	1292.5	6.9	2114.9	0.1	0.0003	-88.8	-92.6	0.030

i	j	K_{ijk} / cm^{-1}	ω(i) / cm^{-1}	I(i) / km mol^{-1}	ω(j) / cm^{-1}	I(j) / km mol^{-1}	ω(ij) / cm^{-1}	I(ij) / km mol^{-1}	I(ij) / I(k)	Δω'	Δω	TFR
26	48	-0.30	820.5	2.6	1516	107.6	2335.2	0.0	0.0000	131.5	132.8	0.002
26	46	-0.83	820.5	2.6	1374	31.8	2195	6.5	0.0132	-8.7	-9.3	0.090
26	45	1.44	820.5	2.6	1328.2	97.6	2146.5	0.1	0.0001	-57.2	-55	0.026
26	44	0.24	820.5	2.6	1313.1	31.7	2137.2	0.0	0.0001	-66.6	-70.1	0.003
26	43	0.40	820.5	2.6	1317.4	259.2	2138.4	0.0	0.0000	-65.4	-65.9	0.006
25	48	-0.46	759.5	4.1	1516	107.6	2275.5	0.1	0.0001	71.8	71.8	0.006
25	46	-2.48	759.5	4.1	1374	31.8	2133.5	0.8	0.0015	-70.3	-70.2	0.035
25	45	5.14	759.5	4.1	1328.2	97.6	2086	0.1	0.0003	-117.7	-116	0.044
25	44	1.24	759.5	4.1	1313.1	31.7	2075.7	0.0	0.0001	-128.1	-131.1	0.009
25	43	0.76	759.5	4.1	1317.4	259.2	2076.9	0.0	0.0000	-126.9	-126.9	0.006
24	48	0.30	716.5	13.8	1516	107.6	2229.2	0.0	0.0001	25.5	28.7	0.010
23	50	-0.61	715.1	10.8	1612	2.2	2322.4	0.0	0.0000	118.6	123.3	0.005
23	49	-2.36	715.1	10.8	1596.2	1.8	2306.1	0.1	0.0002	102.3	107.5	0.022
23	48	6.71	715.1	10.8	1516	107.6	2226.1	10.0	0.0201	22.4	27.3	0.246
23	47	1.30	715.1	10.8	1438.1	1.2	2150	0.1	0.0002	-53.7	-50.6	0.026
23	46	10.52	715.1	10.8	1374	31.8	2084.5	0.2	0.0005	-119.3	-114.7	0.092
21	50	-0.27	644.6	3.1	1612	2.2	2255.7	0.0	0.0000	51.9	52.9	0.005
21	48	1.08	644.6	3.1	1516	107.6	2159.6	0.1	0.0002	-44.1	-43.1	0.025
21	47	0.40	644.6	3.1	1438.1	1.2	2083.3	0.1	0.0001	-120.4	-121.1	0.003
20	49	0.93	643.0	1.8	1596.2	1.8	2240.4	0.1	0.0003	36.6	35.5	0.026
20	48	-1.99	643.0	1.8	1516	107.6	2158.9	0.2	0.0003	-44.8	-44.8	0.045
20	47	-0.96	643.0	1.8	1438.1	1.2	2082.3	0.1	0.0002	-121.4	-122.7	0.008
18	52	0.26	585.1	5.9	1739.8	71.7	2323	0.0	0.0000	119.3	121.1	0.002
17	50	0.90	547.2	9.6	1612	2.2	2158	0.9	0.0017	-45.8	-44.5	0.020
15	52	-0.24	517.6	2.5	1739.8	71.7	2257.1	0.0	0.0001	53.3	53.6	0.004
5	54	-3.60	125.0	5.8	2203.8	494.8	2312	0.3	0.0006	108.2	125	0.029
2	54	-0.76	62.2	1.0	2203.8	494.8	2256.8	0.1	0.0002	53	62.2	0.012
1	54	-0.82	16.7	0.3	2203.8	494.8	2214	1.4	0.0029	10.2	16.7	0.049

6-31+G(d,p)

i	j	K_{ijk} / cm^{-1}	ω(i) / cm^{-1}	I(i) / km mol^{-1}	ω(j) / cm^{-1}	I(j) / km mol^{-1}	ω(ij) / cm^{-1}	I(ij) / km mol^{-1}	I(ij) / I(k)	Δω'	Δω	TFR
39	39	39.19	1127.3	9.7	1127.3	9.7	2252.2	15.7	0.0196	68.1	70.6	0.555
38	38	2.54	1122.0	35.0	1122.0	35.0	2239.4	0.6	0.0007	55.4	59.9	0.042
37	37	1.38	1114.4	23.8	1114.4	23.8	2241.5	0.0	0.0000	57.5	44.8	0.031
36	36	0.26	1078.0	12.0	1078.0	12.0	2159.9	0.3	0.0004	-24.1	-28.0	0.009
35	35	0.72	1033.1	13.3	1033.1	13.3	2064.7	0.1	0.0002	-119.3	-117.7	0.006
39	40	12.81	1127.3	9.7	1176.4	4.0	2297.8	1.8	0.0023	113.8	119.7	0.107
38	40	1.12	1122.0	35.0	1176.4	4.0	2293.7	0.1	0.0002	109.7	114.4	0.010
38	39	3.13	1122.0	35.0	1127.3	9.7	2249.4	0.4	0.0004	65.4	65.2	0.048
37	39	0.40	1114.4	23.8	1127.3	9.7	2245.4	0.0	0.0000	61.4	57.7	0.007

i	j	K_{ijk} / cm^{-1}	ω(i) / cm^{-1}	I(i) / km mol^{-1}	ω(j) / cm^{-1}	I(j) / km mol^{-1}	ω(ij) / cm^{-1}	I(ij) / km mol^{-1}	I(ij) / I(k)	Δω'	Δω	TFR
36	41	0.51	1078.0	12.0	1204.9	16.1	2282.8	0.1	0.0001	98.8	98.9	0.005
36	40	-0.88	1078.0	12.0	1176.4	4.0	2249.3	0.0	0.0000	65.3	70.4	0.012
36	39	-2.86	1078.0	12.0	1127.3	9.7	2205.4	13.0	0.0162	21.4	21.3	0.134
36	38	-0.25	1078.0	12.0	1122.0	35.0	2200.6	0.4	0.0005	16.6	16.0	0.016
35	39	0.34	1033.1	13.3	1127.3	9.7	2160.4	0.1	0.0001	-23.7	-23.6	0.014
35	38	-0.76	1033.1	13.3	1122.0	35.0	2151.3	2.2	0.0027	-32.7	-28.9	0.026
34	44	0.31	1011.3	1.2	1307.2	160.8	2316.1	0.1	0.0001	132.1	134.6	0.002
34	41	0.39	1011.3	1.2	1204.9	16.1	2215.8	0.0	0.0000	31.8	32.3	0.012
34	40	-1.02	1011.3	1.2	1176.4	4.0	2182.0	25.9	0.0323	-2.0	3.8	0.272
34	39	-3.32	1011.3	1.2	1127.3	9.7	2138.0	0.9	0.0011	-46.0	-45.4	0.073
34	37	0.82	1011.3	1.2	1114.4	23.8	2130.1	0.0	0.0001	-53.9	-58.2	0.014
33	45	-0.53	961.0	1.0	1325.6	124.5	2281.4	0.0	0.0000	97.3	102.7	0.005
33	44	-0.26	961.0	1.0	1307.2	160.8	2264.7	0.0	0.0000	80.7	84.3	0.003
33	39	0.43	961.0	1.0	1127.3	9.7	2085.6	0.0	0.0000	-98.4	-95.7	0.004
31	45	0.97	949.7	8.4	1325.6	124.5	2271.8	0.0	0.0000	87.8	91.3	0.011
31	44	-0.60	949.7	8.4	1307.2	160.8	2254.9	0.0	0.0001	70.9	73.0	0.008
31	43	-0.76	949.7	8.4	1300.6	0.2	2252.3	0.1	0.0001	68.2	66.3	0.011
31	41	-0.31	949.7	8.4	1204.9	16.1	2152.0	0.4	0.0005	-32.0	-29.4	0.011
31	40	0.48	949.7	8.4	1176.4	4.0	2120.2	0.0	0.0000	-63.8	-57.9	0.008
31	39	0.97	949.7	8.4	1127.3	9.7	2076.3	0.0	0.0000	-107.7	-107.0	0.009
31	37	0.27	949.7	8.4	1114.4	23.8	2067.9	0.1	0.0001	-116.1	-119.9	0.002
30	45	0.37	927.6	4.0	1325.6	124.5	2252.4	0.0	0.0000	68.4	69.2	0.005
30	38	0.29	927.6	4.0	1122.0	35.0	2051.8	0.1	0.0001	-132.2	-134.5	0.002
29	46	-0.39	834.0	53.9	1370.2	74.7	2207.5	0.1	0.0002	23.5	20.2	0.019
29	45	2.23	834.0	53.9	1325.6	124.5	2152.7	1.9	0.0024	-31.3	-24.4	0.092
29	44	0.57	834.0	53.9	1307.2	160.8	2137.4	0.1	0.0001	-46.6	-42.8	0.013
28	46	-4.09	825.9	338.5	1370.2	74.7	2202.5	7.9	0.0099	18.5	12.1	0.339
28	45	19.18	825.9	338.5	1325.6	124.5	2146.8	47.4	0.0591	-37.2	-32.5	0.590
28	44	4.44	825.9	338.5	1307.2	160.8	2133.0	0.5	0.0007	-51.0	-50.9	0.087
28	43	1.91	825.9	338.5	1300.6	0.2	2129.7	0.1	0.0001	-54.3	-57.6	0.033
28	42	-0.39	825.9	338.5	1312.3	46.0	2135.4	0.0	0.0000	-48.6	-45.9	0.008
27	48	-6.13	818.9	146.7	1499.7	201.6	2317.7	1.7	0.0021	133.7	134.6	0.046
27	46	-11.35	818.9	146.7	1370.2	74.7	2197.0	74.4	0.0927	13.0	5.1	2.214
27	45	54.12	818.9	146.7	1325.6	124.5	2130.6	102.9	0.1283	-53.4	-39.5	1.370
27	44	12.59	818.9	146.7	1307.2	160.8	2124.1	3.9	0.0049	-59.9	-57.9	0.218
27	43	5.44	818.9	146.7	1300.6	0.2	2121.9	0.6	0.0008	-62.1	-64.5	0.084
27	42	-1.15	818.9	146.7	1312.3	46.0	2127.8	0.0	0.0001	-56.2	-52.8	0.022
26	48	0.63	790.0	14.1	1499.7	201.6	2291.5	0.0	0.0000	107.5	105.7	0.006
26	46	0.75	790.0	14.1	1370.2	74.7	2170.1	0.8	0.0010	-14.0	-23.8	0.032
26	45	-4.94	790.0	14.1	1325.6	124.5	2115.2	2.2	0.0027	-68.9	-68.4	0.072
26	44	-1.11	790.0	14.1	1307.2	160.8	2099.9	0.0	0.0001	-84.1	-86.8	0.013
26	43	-0.52	790.0	14.1	1300.6	0.2	2096.8	0.0	0.0000	-87.2	-93.4	0.006
25	48	0.27	764.0	2.2	1499.7	201.6	2264.2	0.0	0.0000	80.2	79.7	0.003
25	46	1.65	764.0	2.2	1370.2	74.7	2140.3	0.6	0.0007	-43.7	-49.8	0.033

i	j	K_{ijk} / cm^{-1}	ω(i) / cm^{-1}	I(i) / km mol^{-1}	ω(j) / cm^{-1}	I(j) / km mol^{-1}	ω(ij) / cm^{-1}	I(ij) / km mol^{-1}	I(ij) / I(k)	Δω’	Δω	TFR
25	45	-3.74	764.0	2.2	1325.6	124.5	2086.8	0.1	0.0001	-97.2	-94.4	0.040
25	44	-0.97	764.0	2.2	1307.2	160.8	2071.3	0.0	0.0000	-112.7	-112.8	0.009
25	43	-0.43	764.0	2.2	1300.6	0.2	2067.6	0.0	0.0000	-116.4	-119.5	0.004
23	50	0.36	709.7	14.4	1604.4	25.6	2311.5	0.0	0.0000	127.5	130.1	0.003
23	49	2.50	709.7	14.4	1583.6	1.2	2293.6	0.1	0.0001	109.6	109.3	0.023
23	48	-6.45	709.7	14.4	1499.7	201.6	2207.4	6.7	0.0084	23.4	25.4	0.254
23	47	-1.23	709.7	14.4	1423.1	1.3	2131.2	0.1	0.0002	-52.8	-51.1	0.024
23	46	-8.75	709.7	14.4	1370.2	74.7	2084.8	0.3	0.0003	-99.2	-104.0	0.084
21	49	0.29	646.8	2.3	1583.6	1.2	2232.7	0.0	0.0000	48.7	46.4	0.006
21	48	0.50	646.8	2.3	1499.7	201.6	2145.8	0.1	0.0001	-38.2	-37.5	0.013
21	47	0.33	646.8	2.3	1423.1	1.3	2069.3	0.1	0.0001	-114.7	-114.0	0.003
20	49	1.15	643.8	2.0	1583.6	1.2	2231.0	0.1	0.0002	46.9	43.4	0.026
20	48	-2.51	643.8	2.0	1499.7	201.6	2143.6	0.5	0.0006	-40.4	-40.5	0.062
20	47	-0.95	643.8	2.0	1423.1	1.3	2066.7	0.0	0.0001	-117.3	-117.1	0.008
19	49	-0.27	617.5	0.7	1583.6	1.2	2204.0	0.0	0.0000	20.0	17.1	0.016
17	50	-0.76	543.0	8.8	1604.4	25.6	2146.5	0.7	0.0009	-37.5	-36.6	0.021
15	52	-0.34	504.9	7.0	1706.5	944.5	2211.7	0.0	0.0000	27.7	27.4	0.012
11	52	0.39	363.9	0.8	1706.5	944.5	2070.2	0.1	0.0001	-113.8	-113.7	0.003
5	54	4.76	107.9	7.6	2184.0	802.1	2283.6	0.4	0.0005	99.6	107.9	0.044
1	54	1.15	-7.9	0.4	2184.0	802.1	2167.8	1.9	0.0024	-16.2	-7.9	0.146

6-31++G(d,p)

i	j	K_{ijk} / cm^{-1}	ω(i) / cm^{-1}	I(i) / km mol^{-1}	ω(j) / cm^{-1}	I(j) / km mol^{-1}	ω(ij) / cm^{-1}	I(ij) / km mol^{-1}	I(ij) / I(k)	Δω’	Δω	TFR
39	39	39.16	1126.5	109.2	1126.5	109.2	2252.2	15.6	0.0197	68.5	69.2	0.565
38	38	2.50	1123.2	13.7	1123.2	13.7	2244.4	0.6	0.0007	60.6	62.7	0.040
37	37	1.37	1115.5	65.8	1115.5	65.8	2244.3	0.0	0.0000	60.5	47.2	0.029
36	36	0.26	1076.4	12.6	1076.4	12.6	2154.9	0.3	0.0004	-28.9	-30.9	0.008
35	35	0.71	1032.3	12.4	1032.3	12.4	2064.3	0.1	0.0002	-119.4	-119.1	0.006
39	40	12.95	1126.5	109.2	1185.8	13.3	2306.6	1.9	0.0024	122.8	128.5	0.101
38	40	1.04	1123.2	13.7	1185.8	13.3	2305.9	0.1	0.0002	122.1	125.3	0.008
38	39	2.87	1123.2	13.7	1126.5	109.2	2251.9	0.3	0.0004	68.2	66	0.044
37	39	0.40	1115.5	65.8	1126.5	109.2	2246.8	0.0	0.0000	63.1	58.2	0.007
36	41	0.50	1076.4	12.6	1204.8	18.6	2279.9	0.1	0.0001	96.1	97.5	0.005
36	40	-0.90	1076.4	12.6	1185.8	13.3	2255.9	0.0	0.0000	72.2	78.5	0.011
36	39	-2.88	1076.4	12.6	1126.5	109.2	2203.1	12.5	0.0158	19.4	19.2	0.150
36	38	-0.23	1076.4	12.6	1123.2	13.7	2200.7	0.4	0.0005	16.9	15.9	0.015
35	39	0.34	1032.3	12.4	1126.5	109.2	2160.2	0.1	0.0001	-23.5	-24.9	0.014
35	38	-0.76	1032.3	12.4	1123.2	13.7	2153.6	2.1	0.0027	-30.2	-28.2	0.027
34	44	0.32	1013.0	0.7	1301.7	107.0	2314.5	0.1	0.0001	130.8	130.9	0.002
34	41	0.38	1013.0	0.7	1204.8	18.6	2216.6	0.0	0.0000	32.8	34.1	0.011
34	40	-1.03	1013.0	0.7	1185.8	13.3	2192.6	31.4	0.0396	8.8	15	0.069
34	39	-3.29	1013.0	0.7	1126.5	109.2	2139.4	0.9	0.0011	-44.3	-44.3	0.074
34	37	0.82	1013.0	0.7	1115.5	65.8	2132.9	0.0	0.0001	-50.8	-55.3	0.015
33	45	-0.51	956.8	1.9	1325.4	163.0	2273.9	0.0	0.0000	90.1	98.5	0.005
33	44	-0.26	956.8	1.9	1301.7	107.0	2253.9	0.0	0.0000	70.2	74.7	0.003

i	j	K_{ijk} / cm^{-1}	ω(i) / cm^{-1}	I(i) / km mol^{-1}	ω(j) / cm^{-1}	I(j) / km mol^{-1}	ω(ij) / cm^{-1}	I(ij) / km mol^{-1}	I(ij) / I(k)	Δω'	Δω	TFR
33	39	0.42	956.8	1.9	1126.5	109.2	2077.8	0.0	0.0000	-106	-100.5	0.004
31	45	0.93	950.1	5.8	1325.4	163.0	2272.4	0.0	0.0000	88.7	91.8	0.010
31	44	-0.60	950.1	5.8	1301.7	107.0	2252.4	0.0	0.0001	68.6	68	0.009
31	43	-0.77	950.1	5.8	1300.7	0.6	2253.0	0.1	0.0001	69.2	67	0.011
31	41	-0.30	950.1	5.8	1204.8	18.6	2151.8	0.4	0.0005	-32	-28.8	0.010
31	40	0.49	950.1	5.8	1185.8	13.3	2129.6	0.0	0.0000	-54.2	-47.9	0.010
31	39	0.99	950.1	5.8	1126.5	109.2	2076.6	0.0	0.0000	-107.1	-107.2	0.009
31	37	0.26	950.1	5.8	1115.5	65.8	2069.7	0.1	0.0001	-114.1	-118.2	0.002
30	45	0.35	915.4	2.3	1325.4	163.0	2244.1	0.0	0.0000	60.3	57.1	0.006
29	46	-0.37	831.5	82.8	1374.3	165.1	2199.8	0.1	0.0002	16.1	22.1	0.017
29	45	2.14	831.5	82.8	1325.4	163.0	2145.6	1.8	0.0023	-38.2	-26.8	0.080
29	44	0.56	831.5	82.8	1301.7	107.0	2127.0	0.1	0.0001	-56.8	-50.6	0.011
28	46	-4.10	824.5	8.6	1374.3	165.1	2200.5	7.7	0.0097	16.7	15.1	0.272
28	45	19.33	824.5	8.6	1325.4	163.0	2145.3	48.1	0.0606	-38.4	-33.8	0.571
28	44	4.52	824.5	8.6	1301.7	107.0	2128.2	0.6	0.0007	-55.5	-57.6	0.078
28	43	1.97	824.5	8.6	1300.7	0.6	2128.3	0.1	0.0001	-55.4	-58.6	0.034
28	42	-0.36	824.5	8.6	1310.8	44.1	2131.4	0.0	0.0000	-52.3	-48.4	0.007
27	48	-6.09	819.3	25.1	1497.7	170.1	2316.9	1.7	0.0021	133.2	133.3	0.046
27	46	-11.22	819.3	25.1	1374.3	165.1	2197.8	70.8	0.0892	14	9.9	1.138
27	45	53.83	819.3	25.1	1325.4	163.0	2131.7	109.2	0.1375	-52	-39	1.379
27	44	12.64	819.3	25.1	1301.7	107.0	2122.2	4.0	0.0050	-61.5	-62.8	0.201
27	43	5.54	819.3	25.1	1300.7	0.6	2123.4	0.7	0.0008	-60.3	-63.8	0.087
27	42	-1.05	819.3	25.1	1310.8	44.1	2127.0	0.0	0.0000	-56.7	-53.6	0.020
26	48	0.74	766.0	15.9	1497.7	170.1	2269.8	0.0	0.0000	86.1	79.9	0.009
26	46	0.96	766.0	15.9	1374.3	165.1	2151.1	1.0	0.0013	-32.7	-43.5	0.022
26	45	-5.98	766.0	15.9	1325.4	163.0	2096.6	3.3	0.0042	-87.2	-92.4	0.065
26	44	-1.37	766.0	15.9	1301.7	107.0	2074.8	0.1	0.0001	-108.9	-116.1	0.012
26	43	-0.63	766.0	15.9	1300.7	0.6	2077.5	0.0	0.0000	-106.3	-117.1	0.005
25	48	0.26	764.3	2.2	1497.7	170.1	2262.8	0.0	0.0000	79	78.2	0.003
25	46	1.64	764.3	2.2	1374.3	165.1	2140.4	0.6	0.0007	-43.4	-45.2	0.036
25	45	-3.64	764.3	2.2	1325.4	163.0	2087.5	0.1	0.0001	-96.3	-94	0.039
25	44	-0.95	764.3	2.2	1301.7	107.0	2068.7	0.0	0.0000	-115	-117.8	0.008
25	43	-0.43	764.3	2.2	1300.7	0.6	2068.3	0.0	0.0000	-115.5	-118.8	0.004
23	50	0.35	709.3	14.5	1604.7	24.4	2311.8	0.0	0.0000	128	130.2	0.003
23	49	2.51	709.3	14.5	1583.8	0.9	2293.8	0.1	0.0001	110.1	109.3	0.023
23	48	-6.45	709.3	14.5	1497.7	170.1	2205.6	6.8	0.0086	21.9	23.3	0.277
23	47	-1.24	709.3	14.5	1422.1	5.1	2130.5	0.1	0.0002	-53.2	-52.3	0.024
23	46	-8.70	709.3	14.5	1374.3	165.1	2084.6	0.3	0.0003	-99.1	-100.1	0.087
21	49	0.27	646.5	2.2	1583.8	0.9	2232.6	0.0	0.0000	48.8	46.5	0.006
21	48	0.52	646.5	2.2	1497.7	170.1	2143.7	0.1	0.0001	-40	-39.6	0.013
21	47	0.34	646.5	2.2	1422.1	5.1	2068.3	0.1	0.0001	-115.4	-115.1	0.003
20	49	1.15	645.7	2.0	1583.8	0.9	2232.1	0.1	0.0002	48.3	45.7	0.025
20	48	-2.52	645.7	2.0	1497.7	170.1	2142.7	0.5	0.0006	-41.1	-40.4	0.062
20	47	-0.96	645.7	2.0	1422.1	5.1	2067.0	0.1	0.0001	-116.8	-116	0.008
19	49	-0.27	613.1	0.7	1583.8	0.9	2200.7	0.0	0.0000	17	13.1	0.020
17	50	-0.77	542.9	9.4	1604.7	24.4	2146.6	0.7	0.0009	-37.1	-36.2	0.021
15	52	-0.34	497.4	5.1	1706.5	949.7	2204.2	0.0	0.0000	20.5	20.2	0.017
11	52	0.38	364.8	0.9	1706.5	949.7	2071.1	0.1	0.0001	-112.6	-112.4	0.003
6	54	6.18	141.3	6.7	2183.7	794.3	2316.3	0.1	0.0002	132.6	141.3	0.044
5	54	4.73	107.2	7.3	2183.7	794.3	2282.3	0.4	0.0005	98.6	107.2	0.044
1	54	1.28	-29.7	2.4	2183.7	794.3	2145.3	2.1	0.0026	-38.5	-29.7	0.043

6-311G(d,p)

i	j	K_{ijk} / cm^{-1}	ω(i) / cm^{-1}	I(i) / km mol^{-1}	ω(j) / cm^{-1}	I(j) / km mol^{-1}	ω(ij) / cm^{-1}	I(ij) / km mol^{-1}	I(ij) / I(k)	Δω'	Δω	TFR
39	39	-36.23	1132.0	33.4	1132.0	33.4	2261.7	12.6	0.0261	73.1	75.5	0.480
38	38	-2.53	1133.0	37.4	1133.0	37.4	2261.5	0.2	0.0005	72.9	77.4	0.033
37	37	-1.55	1105.0	9.1	1105.0	9.1	2214.0	0.1	0.0001	25.4	21.3	0.073
36	36	-0.29	1067.0	13.0	1067.0	13.0	2133.4	0.5	0.0009	-55.2	-54.6	0.005
35	35	-0.58	1030.5	6.2	1030.5	6.2	2058.6	0.1	0.0002	-130.0	-127.6	0.005
39	40	-13.89	1132.0	33.4	1182.0	11.9	2313.5	1.8	0.0038	124.8	125.5	0.111
38	40	-1.19	1133.0	37.4	1182.0	11.9	2315.0	0.3	0.0006	126.4	126.5	0.009
38	39	-4.07	1133.0	37.4	1132.0	33.4	2262.9	0.5	0.0010	74.2	76.4	0.053
37	41	-0.24	1105.0	9.1	1202.2	12.9	2308.0	0.8	0.0017	119.4	118.6	0.002
37	39	-1.56	1105.0	9.1	1132.0	33.4	2239.1	0.0	0.0001	50.5	48.4	0.032
37	38	0.76	1105.0	9.1	1133.0	37.4	2236.5	0.5	0.0010	47.9	49.4	0.015
36	41	-0.40	1067.0	13.0	1202.2	12.9	2268.3	0.1	0.0002	79.7	80.6	0.005
36	40	0.80	1067.0	13.0	1182.0	11.9	2248.3	0.0	0.0000	59.6	60.4	0.013
36	39	2.65	1067.0	13.0	1132.0	33.4	2198.7	226.9	0.4702	10.1	10.4	0.254
36	38	0.22	1067.0	13.0	1133.0	37.4	2197.6	0.1	0.0003	9.0	11.4	0.019
35	42	0.40	1030.5	6.2	1293.0	83.1	2322.4	0.4	0.0007	133.8	134.9	0.003
35	39	-0.65	1030.5	6.2	1132.0	33.4	2162.1	0.1	0.0003	-26.6	-26.1	0.025
35	38	0.59	1030.5	6.2	1133.0	37.4	2159.1	1.0	0.0020	-29.5	-25.1	0.024
35	37	-0.38	1030.5	6.2	1105.0	9.1	2135.5	0.7	0.0014	-53.1	-53.1	0.007
34	43	0.21	1021.8	0.2	1300.4	5.7	2320.6	0.0	0.0000	132.0	133.6	0.002
34	42	-0.66	1021.8	0.2	1293.0	83.1	2311.9	0.0	0.0000	123.3	126.2	0.005
34	41	-0.30	1021.8	0.2	1202.2	12.9	2223.2	0.0	0.0000	34.6	35.5	0.008
34	40	1.08	1021.8	0.2	1182.0	11.9	2203.3	33.9	0.0702	14.7	15.3	0.07
34	39	3.13	1021.8	0.2	1132.0	33.4	2152.9	0.8	0.0016	-35.7	-34.8	0.09
34	37	-0.85	1021.8	0.2	1105.0	9.1	2128.3	0.1	0.0002	-60.4	-61.8	0.014
33	45	-0.25	964.3	0.4	1320.0	207.9	2285.9	0.0	0.0000	97.3	95.7	0.003
32	45	0.23	975.1	3.4	1320.0	207.9	2276.3	0.0	0.0000	87.6	106.5	0.002
32	39	-0.31	975.1	3.4	1132.0	33.4	2086.7	0.0	0.0000	-101.9	-81.5	0.004
31	44	0.56	946.9	14.1	1317.4	5.8	2263.9	0.0	0.0000	75.2	75.6	0.007
31	43	0.71	946.9	14.1	1300.4	5.7	2244.6	0.3	0.0007	56.0	58.6	0.012
31	42	-0.77	946.9	14.1	1293.0	83.1	2237.4	0.2	0.0003	48.8	51.2	0.015
31	41	0.21	946.9	14.1	1202.2	12.9	2147.0	0.4	0.0008	-41.6	-39.5	0.005
31	40	-0.28	946.9	14.1	1182.0	11.9	2128.6	0.0	0.0001	-60.0	-59.7	0.005
31	39	-1.29	946.9	14.1	1132.0	33.4	2078.7	0.0	0.0000	-109.9	-109.7	0.012
29	46	-0.67	833.6	56.7	1354.2	80.2	2193.8	0.1	0.0003	5.1	-0.7	0.929
29	45	2.42	833.6	56.7	1320.0	207.9	2154.6	2.6	0.0054	-34.0	-35.0	0.069
29	43	0.36	833.6	56.7	1300.4	5.7	2134.1	0.1	0.0001	-54.5	-54.6	0.007
29	42	-0.27	833.6	56.7	1293.0	83.1	2126.3	0.0	0.0000	-62.4	-62.0	0.004
28	46	0.33	848.5	40.3	1354.2	80.2	2193.5	0.1	0.0003	4.9	14.1	0.023
28	45	-1.32	848.5	40.3	1320.0	207.9	2154.2	0.3	0.0005	-34.4	-20.1	0.065
27	48	6.56	819.1	7.7	1503.6	210.5	2321.4	1.9	0.0040	132.8	134.1	0.049
27	47	0.42	819.1	7.7	1429.5	0.1	2248.0	0.0	0.0001	59.4	60.0	0.007
27	46	17.17	819.1	7.7	1354.2	80.2	2176.3	168.2	0.3485	-12.3	-15.3	1.125
27	45	-58.45	819.1	7.7	1320.0	207.9	2128.2	83.6	0.1732	-60.5	-49.5	1.18
27	44	1.12	819.1	7.7	1317.4	5.8	2135.9	0.0	0.0000	-52.8	-52.1	0.022
27	43	-6.47	819.1	7.7	1300.4	5.7	2118.5	0.6	0.0012	-70.1	-69.2	0.094
27	42	7.44	819.1	7.7	1293.0	83.1	2110.1	0.7	0.0014	-78.5	-76.5	0.097
26	45	-0.68	786.8	12.5	1320.0	207.9	2122.1	0.0	0.0001	-66.5	-81.9	0.008

i	j	K_{ijk} / cm^{-1}	ω(i) / cm^{-1}	I(i) / km mol^{-1}	ω(j) / cm^{-1}	I(j) / km mol^{-1}	ω(ij) / cm^{-1}	I(ij) / km mol^{-1}	I(ij) / I(k)	Δω’	Δω	TFR
25	48	-0.39	768.8	2.6	1503.6	210.5	2272.4	0.1	0.0001	83.8	83.8	0.005
25	46	-2.61	768.8	2.6	1354.2	80.2	2128.5	1.1	0.0022	-60.1	-65.6	0.04
25	45	4.97	768.8	2.6	1320.0	207.9	2089.8	0.2	0.0004	-98.8	-99.8	0.05
25	43	0.64	768.8	2.6	1300.4	5.7	2068.6	0.0	0.0000	-120.0	-119.5	0.005
25	42	-0.74	768.8	2.6	1293.0	83.1	2061.2	0.0	0.0000	-127.4	-126.8	0.006
23	50	-0.54	712.9	16.2	1601.6	0.7	2316.2	0.0	0.0000	127.6	125.9	0.004
23	49	-2.34	712.9	16.2	1575.2	5.1	2289.1	0.1	0.0002	100.4	99.5	0.024
23	48	6.58	712.9	16.2	1503.6	210.5	2215.3	6.8	0.0142	26.7	27.9	0.236
23	47	1.27	712.9	16.2	1429.5	0.1	2142.0	0.1	0.0002	-46.7	-46.2	0.027
23	46	11.87	712.9	16.2	1354.2	80.2	2072.7	0.3	0.0006	-115.9	-121.5	0.098
21	49	0.23	648.0	4.9	1575.2	5.1	2220.4	0.0	0.0000	31.7	34.6	0.007
21	48	0.56	648.0	4.9	1503.6	210.5	2145.9	0.1	0.0001	-42.7	-37.0	0.015
20	49	0.83	640.2	2.0	1575.2	5.1	2219.1	0.1	0.0002	30.5	26.8	0.031
20	48	-2.03	640.2	2.0	1503.6	210.5	2145.1	0.3	0.0006	-43.5	-44.8	0.045
20	47	-0.98	640.2	2.0	1429.5	0.1	2071.0	0.1	0.0001	-117.7	-119.0	0.008
19	49	-0.26	619.8	0.8	1575.2	5.1	2200.9	0.0	0.0000	12.3	6.4	0.04
18	52	0.25	582.9	11.7	1723.5	376.8	2304.2	0.0	0.0001	115.6	117.8	0.002
18	48	0.25	582.9	11.7	1503.6	210.5	2085.7	0.0	0.0000	-102.9	-102.1	0.002
17	50	0.92	545.3	13.1	1601.6	0.7	2149.3	0.9	0.0019	-39.3	-41.7	0.022
17	49	-0.25	545.3	13.1	1575.2	5.1	2122.1	0.0	0.0001	-66.5	-68.1	0.004
15	52	-0.29	513.2	15.6	1723.5	376.8	2239.2	0.0	0.0001	50.6	48.0	0.006
14	53	0.26	442.1	1.1	1775.8	1.6	2235.4	0.0	0.0000	46.8	29.3	0.009
6	54	-6.02	145.9	1.5	2188.6	482.6	2307.0	0.1	0.0002	118.4	145.9	0.041
5	54	-3.69	108.7	8.7	2188.6	482.6	2285.1	0.3	0.0007	96.5	108.7	0.034
1	54	1.00	1.2	0.1	2188.6	482.6	2176.8	1.6	0.0033	-11.8	1.2	0.857

6-311+G(d,p)

i	j	K_{ijk} / cm^{-1}	ω(i) / cm^{-1}	I(i) / km mol^{-1}	ω(j) / cm^{-1}	I(j) / km mol^{-1}	ω(ij) / cm^{-1}	I(ij) / km mol^{-1}	I(ij) / I(k)	Δω’	Δω	TFR
39	39	-37.52	1128.2	39.0	1128.2	39.0	2253.9	14.1	0.0179	76.4	78.8	0.476
38	38	-2.26	1122.9	7.4	1122.9	7.4	2245.2	0.4	0.0006	67.7	68.3	0.033
37	37	-1.58	1112.9	49.4	1112.9	49.4	2241.1	0.0	0.0000	63.6	48.2	0.033
36	36	-0.27	1081.7	13.1	1081.7	13.1	2168.8	0.4	0.0005	-8.7	-14.1	0.019
35	35	-0.67	1037.3	9.6	1037.3	9.6	2073.0	0.1	0.0001	-104.5	-103.0	0.007
38	39	1.11	1122.9	7.4	1128.2	39.0	2252.5	0.1	0.0001	75.0	73.6	0.015
37	39	-0.58	1112.9	49.4	1128.2	39.0	2247.7	0.0	0.0000	70.3	63.5	0.009
37	38	-0.27	1112.9	49.4	1122.9	7.4	2242.0	0.2	0.0003	64.5	58.3	0.005
36	41	-0.48	1081.7	13.1	1210.3	4.9	2285.2	0.1	0.0001	107.7	114.5	0.004
36	40	0.94	1081.7	13.1	1191.1	25.7	2273.1	0.0	0.0000	95.6	95.3	0.010
36	39	2.92	1081.7	13.1	1128.2	39.0	2209.9	12.0	0.0153	32.4	32.3	0.090
35	39	-0.32	1037.3	9.6	1128.2	39.0	2165.4	0.1	0.0001	-12.1	-12.1	0.027
35	38	-0.64	1037.3	9.6	1122.9	7.4	2158.6	1.6	0.0020	-18.8	-17.3	0.037
35	37	-0.30	1037.3	9.6	1112.9	49.4	2156.3	0.4	0.0005	-21.2	-27.4	0.011
34	42	-0.78	1017.4	1.3	1288.5	148.5	2302.3	0.0	0.0000	124.8	128.4	0.006
34	41	-0.33	1017.4	1.3	1210.3	4.9	2219.0	0.0	0.0000	41.5	50.2	0.007
34	40	0.98	1017.4	1.3	1191.1	25.7	2207.5	7.9	0.0100	30.1	31.0	0.032
34	39	2.77	1017.4	1.3	1128.2	39.0	2143.5	0.8	0.0010	-34.0	-32.0	0.087
34	37	-0.74	1017.4	1.3	1112.9	49.4	2135.0	0.0	0.0001	-42.5	-47.3	0.016
33	45	-0.64	979.6	0.1	1322.3	114.8	2293.9	0.0	0.0000	116.4	124.4	0.005
33	42	0.27	979.6	0.1	1288.5	148.5	2262.7	0.0	0.0000	85.2	90.6	0.003
33	39	0.44	979.6	0.1	1128.2	39.0	2102.4	0.0	0.0000	-75.1	-69.7	0.006

i	j	K_{ijk} / cm^{-1}	ω(i) / cm^{-1}	I(i) / km mol^{-1}	ω(j) / cm^{-1}	I(j) / km mol^{-1}	ω(ij) / cm^{-1}	I(ij) / km mol^{-1}	I(ij) / I(k)	Δω'	Δω	TFR
31	44	-0.35	952.4	3.0	1308.3	19.0	2268.4	0.0	0.0000	90.9	83.2	0.004
31	43	0.34	952.4	3.0	1313.0	22.5	2268.6	0.2	0.0003	91.1	87.9	0.004
31	42	-0.67	952.4	3.0	1288.5	148.5	2245.0	0.0	0.0000	67.5	63.4	0.011
31	41	0.23	952.4	3.0	1210.3	4.9	2159.2	0.2	0.0002	-18.2	-14.8	0.016
31	40	-0.43	952.4	3.0	1191.1	25.7	2148.3	0.0	0.0000	-29.2	-34.0	0.013
31	39	-0.90	952.4	3.0	1128.2	39.0	2085.0	0.0	0.0000	-92.5	-96.9	0.009
30	45	0.28	955.8	13.6	1322.3	114.8	2277.8	0.0	0.0000	100.3	100.6	0.003
30	44	0.34	955.8	13.6	1308.3	19.0	2270.6	0.0	0.0000	93.1	86.6	0.004
30	43	-0.29	955.8	13.6	1313.0	22.5	2270.5	0.3	0.0003	93.0	91.3	0.003
30	42	0.63	955.8	13.6	1288.5	148.5	2247.0	0.0	0.0000	69.5	66.8	0.009
30	40	0.35	955.8	13.6	1191.1	25.7	2150.4	0.0	0.0000	-27.1	-30.5	0.011
30	39	0.79	955.8	13.6	1128.2	39.0	2086.9	0.0	0.0000	-90.6	-93.5	0.008
30	38	-0.27	955.8	13.6	1122.9	7.4	2082.4	0.2	0.0002	-95.1	-98.8	0.003
29	46	-0.38	851.3	67.8	1370.0	137.9	2213.9	0.1	0.0002	36.4	43.9	0.009
29	45	1.93	851.3	67.8	1322.3	114.8	2164.4	3.1	0.0040	-13.1	-3.9	0.502
29	43	0.22	851.3	67.8	1313.0	22.5	2159.0	0.1	0.0001	-18.5	-13.2	0.017
29	42	-0.28	851.3	67.8	1288.5	148.5	2134.5	0.0	0.0000	-43.0	-37.7	0.007
28	46	-0.76	835.6	22.6	1370.0	137.9	2206.9	0.2	0.0003	29.4	28.2	0.027
28	45	3.19	835.6	22.6	1322.3	114.8	2157.9	3.2	0.0040	-19.6	-19.6	0.163
28	42	-0.50	835.6	22.6	1288.5	148.5	2128.4	0.0	0.0000	-49.1	-53.4	0.009
27	47	0.31	821.0	5.0	1418.8	13.6	2240.3	0.0	0.0000	62.8	62.3	0.005
27	46	13.20	821.0	5.0	1370.0	137.9	2191.3	128.3	0.1627	13.8	13.6	0.972
27	45	-58.84	821.0	5.0	1322.3	114.8	2126.4	152.6	0.1934	-51.1	-34.1	1.723
27	44	0.55	821.0	5.0	1308.3	19.0	2132.4	0.0	0.0000	-45.1	-48.1	0.011
27	43	-4.25	821.0	5.0	1313.0	22.5	2133.5	0.4	0.0005	-43.9	-43.5	0.098
27	42	9.67	821.0	5.0	1288.5	148.5	2108.2	1.6	0.0020	-69.3	-68.0	0.142
26	46	1.01	821.1	3.5	1370.0	137.9	2191.4	1.9	0.0024	13.9	13.7	0.074
26	45	-5.79	821.1	3.5	1322.3	114.8	2140.7	3.5	0.0045	-36.7	-34.1	0.170
26	43	-0.39	821.1	3.5	1313.0	22.5	2135.0	0.0	0.0000	-42.5	-43.4	0.009
26	42	0.96	821.1	3.5	1288.5	148.5	2109.7	0.0	0.0001	-67.8	-67.9	0.014
25	48	0.22	777.4	0.6	1504.3	180.3	2280.9	0.0	0.0000	103.4	104.2	0.002
25	46	1.63	777.4	0.6	1370.0	137.9	2145.6	0.7	0.0009	-31.9	-30.0	0.054
25	45	-3.45	777.4	0.6	1322.3	114.8	2097.0	0.1	0.0002	-80.5	-77.8	0.044
25	43	-0.28	777.4	0.6	1313.0	22.5	2090.3	0.0	0.0000	-87.2	-87.1	0.003
25	42	0.65	777.4	0.6	1288.5	148.5	2067.3	0.0	0.0000	-110.2	-111.6	0.006
24	45	0.42	728.0	11.5	1322.3	114.8	2047.1	0.1	0.0001	-130.4	-127.2	0.003
23	50	-0.26	711.1	15.1	1595.7	12.1	2308.0	0.0	0.0000	130.5	129.4	0.002
23	49	-2.44	711.1	15.1	1575.4	3.5	2288.8	0.1	0.0001	111.3	109.0	0.022
23	48	6.31	711.1	15.1	1504.3	180.3	2215.6	4.5	0.0057	38.1	37.9	0.166
23	47	1.32	711.1	15.1	1418.8	13.6	2133.9	0.2	0.0002	-43.6	-47.6	0.028
23	46	9.58	711.1	15.1	1370.0	137.9	2081.6	0.3	0.0004	-95.9	-96.3	0.099
21	49	0.35	652.0	1.8	1575.4	3.5	2226.4	0.0	0.0000	49.0	49.9	0.007
21	48	0.36	652.0	1.8	1504.3	180.3	2152.7	0.0	0.0001	-24.8	-21.2	0.017
20	49	1.00	648.1	2.8	1575.4	3.5	2223.3	0.1	0.0001	45.8	46.0	0.022
20	48	-2.35	648.1	2.8	1504.3	180.3	2150.0	0.7	0.0008	-27.5	-25.1	0.094
20	47	-0.95	648.1	2.8	1418.8	13.6	2066.7	0.0	0.0001	-110.8	-110.6	0.009
19	49	-0.34	624.6	0.8	1575.4	3.5	2203.7	0.0	0.0000	26.3	22.5	0.015
17	50	0.79	546.7	7.7	1595.7	12.1	2143.4	0.8	0.0010	-34.1	-35.1	0.023
17	48	-1.12	546.7	7.7	1504.3	180.3	2050.6	0.1	0.0001	-126.9	-126.5	0.009
15	52	-0.34	523.5	7.8	1699.8	923.0	2221.7	0.0	0.0000	44.2	45.8	0.008
14	53	0.26	439.7	0.2	1770.0	0.5	2218.7	0.0	0.0000	41.2	32.3	0.008
11	52	0.41	373.4	0.9	1699.8	923.0	2074.6	0.1	0.0002	-102.8	-104.3	0.004
5	54	-4.35	112.3	6.4	2177.5	788.8	2290.1	0.4	0.0005	112.7	112.3	0.039

6-311++G(d,p)

i	j	K_{ijk} / cm^{-1}	ω(i) / cm^{-1}	I(i) / km mol^{-1}	ω(j) / cm^{-1}	I(j) / km mol^{-1}	ω(ij) / cm^{-1}	I(ij) / km mol^{-1}	I(ij) / I(k)	Δω'	Δω	TFR
39	39	37.50	1130.0	46.4	1130.0	46.4	2256.4	14.1	0.0185	81.7	85.3	0.439
38	38	2.23	1112.5	70.2	1112.5	70.2	2268.8	0.5	0.0006	94.2	50.4	0.044
37	37	1.47	1165.5	9.1	1165.5	9.1	2292.1	0.0	0.0000	117.5	156.3	0.009
36	36	0.27	1082.6	14.7	1082.6	14.7	2170.7	0.4	0.0005	-4.0	-9.4	0.028
35	35	0.67	1040.2	0.9	1040.2	0.9	2073.5	0.1	0.0001	-101.1	-94.3	0.007
34	34	-0.56	1034.0	11.7	1034.0	11.7	2058.8	0.0	0.0000	-115.9	-106.7	0.005
38	39	-1.14	1112.5	70.2	1130.0	46.4	2265.6	0.1	0.0001	90.9	67.9	0.017
37	39	0.65	1165.5	9.1	1130.0	46.4	2274.1	0.0	0.0000	99.4	120.8	0.005
37	38	0.31	1165.5	9.1	1112.5	70.2	2279.7	0.2	0.0003	105.0	103.4	0.003
36	41	0.46	1082.6	14.7	1199.3	32.5	2292.4	0.1	0.0001	117.7	107.3	0.004
36	40	-0.93	1082.6	14.7	1240.0	4.8	2309.3	0.0	0.0000	134.6	147.9	0.006
36	39	-2.94	1082.6	14.7	1130.0	46.4	2212.2	12.1	0.0158	37.5	38.0	0.077
35	39	0.33	1040.2	0.9	1130.0	46.4	2167.0	0.1	0.0001	-7.7	-4.5	0.073
35	38	0.64	1040.2	0.9	1112.5	70.2	2170.7	1.6	0.0021	-4.0	-22.0	0.029
35	37	0.29	1040.2	0.9	1165.5	9.1	2181.7	0.4	0.0005	7.0	31.0	0.009
34	41	0.28	1034.0	11.7	1199.3	32.5	2238.8	0.0	0.0000	64.2	58.6	0.005
34	40	-0.93	1034.0	11.7	1240.0	4.8	2257.6	6.8	0.0089	82.9	99.3	0.009
34	39	-2.79	1034.0	11.7	1130.0	46.4	2158.2	0.8	0.0011	-16.5	-10.7	0.262
34	37	0.80	1034.0	11.7	1165.5	9.1	2174.4	0.0	0.0001	-0.2	24.8	0.032
33	42	0.28	1020.9	3.4	1290.3	82.7	2303.8	0.0	0.0000	129.1	136.5	0.002
33	39	0.51	1020.9	3.4	1130.0	46.4	2144.0	0.0	0.0000	-30.6	-23.8	0.022
31	44	0.55	950.1	14.6	1352.2	2.7	2302.3	0.0	0.0000	127.7	127.7	0.004
31	43	-0.45	950.1	14.6	1313.3	38.9	2264.7	0.4	0.0006	90.0	88.7	0.005
31	42	0.89	950.1	14.6	1290.3	82.7	2241.1	0.1	0.0001	66.4	65.7	0.014
31	41	-0.22	950.1	14.6	1199.3	32.5	2160.3	0.3	0.0004	-14.4	-25.3	0.009
31	40	0.47	950.1	14.6	1240.0	4.8	2179.2	0.0	0.0000	4.6	15.4	0.031
31	39	1.22	950.1	14.6	1130.0	46.4	2081.7	0.0	0.0000	-93.0	-94.6	0.013
30	42	0.21	987.0	3.7	1290.3	82.7	2289.8	0.0	0.0000	115.1	102.7	0.002
30	38	-0.34	987.0	3.7	1112.5	70.2	2137.1	0.1	0.0001	-37.6	-75.1	0.004
29	46	-0.36	860.3	21.7	1372.6	160.6	2240.7	0.1	0.0002	66.0	58.2	0.006
29	45	1.97	860.3	21.7	1318.2	118.6	2191.5	3.4	0.0044	16.9	3.9	0.510
29	42	-0.29	860.3	21.7	1290.3	82.7	2160.4	0.0	0.0000	-14.2	-24.1	0.012
28	46	-0.77	847.7	50.0	1372.6	160.6	2223.3	0.2	0.0003	48.6	45.6	0.017
28	45	3.22	847.7	50.0	1318.2	118.6	2174.5	3.2	0.0042	-0.1	-8.8	0.366
28	43	0.22	847.7	50.0	1313.3	38.9	2169.6	0.0	0.0000	-5.0	-13.7	0.016
28	42	-0.50	847.7	50.0	1290.3	82.7	2143.9	0.0	0.0000	-30.8	-36.7	0.014
28	40	-0.30	847.7	50.0	1240.0	4.8	2081.3	0.0	0.0000	-93.4	-87.0	0.003
27	47	-0.35	819.0	6.0	1429.3	4.8	2248.7	0.0	0.0000	74.0	73.6	0.005
27	46	-13.11	819.0	6.0	1372.6	160.6	2191.7	124.7	0.1634	17.0	16.9	0.777
27	45	58.78	819.0	6.0	1318.2	118.6	2126.1	179.8	0.2355	-48.6	-37.5	1.568
27	44	-0.58	819.0	6.0	1352.2	2.7	2169.7	0.0	0.0000	-5.0	-3.5	0.168
27	43	4.22	819.0	6.0	1313.3	38.9	2134.0	0.4	0.0005	-40.7	-42.4	0.099
27	42	-9.71	819.0	6.0	1290.3	82.7	2107.7	1.6	0.0021	-67.0	-65.4	0.148
27	40	-5.54	819.0	6.0	1240.0	4.8	2047.5	0.0	0.0001	-127.2	-115.7	0.048
26	46	1.12	903.1	29.5	1372.6	160.6	2255.0	2.3	0.0030	80.3	100.9	0.011
26	45	-6.04	903.1	29.5	1318.2	118.6	2205.0	3.9	0.0051	30.4	46.6	0.130
26	43	-0.45	903.1	29.5	1313.3	38.9	2198.8	0.0	0.0000	24.1	41.7	0.011
26	42	1.01	903.1	29.5	1290.3	82.7	2172.5	0.0	0.0001	-2.2	18.7	0.054
26	40	0.28	903.1	29.5	1240.0	4.8	2113.6	0.0	0.0000	-61.1	-31.7	0.009
25	48	0.22	778.1	0.0	1518.4	150.3	2296.7	0.0	0.0000	122.0	121.9	0.002
25	46	1.61	778.1	0.0	1372.6	160.6	2148.1	0.7	0.0009	-26.6	-24.0	0.067

i	j	K_{ijk} / cm^{-1}	ω(i) / cm^{-1}	I(i) / km mol^{-1}	ω(j) / cm^{-1}	I(j) / km mol^{-1}	ω(ij) / cm^{-1}	I(ij) / km mol^{-1}	I(ij) / I(k)	Δω'	Δω	TFR
25	45	-3.42	778.1	0.0	1318.2	118.6	2099.8	0.1	0.0002	-74.9	-78.3	0.044
25	43	-0.28	778.1	0.0	1313.3	38.9	2092.9	0.0	0.0000	-81.8	-83.2	0.003
25	42	0.65	778.1	0.0	1290.3	82.7	2068.9	0.0	0.0000	-105.8	-106.2	0.006
24	45	0.51	733.3	14.1	1318.2	118.6	2055.1	0.1	0.0001	-119.6	-123.2	0.004
23	49	2.46	711.6	17.7	1578.9	3.5	2291.9	0.1	0.0001	117.3	115.8	0.021
23	48	-6.33	711.6	17.7	1518.4	150.3	2230.0	4.6	0.0060	55.3	55.3	0.114
23	47	-1.32	711.6	17.7	1429.3	4.8	2142.9	0.2	0.0002	-31.8	-33.8	0.039
23	46	-9.54	711.6	17.7	1372.6	160.6	2082.6	0.3	0.0004	-92.0	-90.5	0.105
23	44	-0.72	711.6	17.7	1352.2	2.7	2062.2	0.0	0.0000	-112.4	-110.9	0.006
21	49	0.32	651.8	1.9	1578.9	3.5	2231.0	0.0	0.0000	56.3	56.0	0.006
21	48	0.41	651.8	1.9	1518.4	150.3	2169.0	0.1	0.0001	-5.7	-4.5	0.092
20	49	0.99	646.6	2.2	1578.9	3.5	2226.6	0.1	0.0001	51.9	50.8	0.019
20	48	-2.32	646.6	2.2	1518.4	150.3	2164.4	0.6	0.0008	-10.2	-9.7	0.239
20	47	-0.98	646.6	2.2	1429.3	4.8	2075.8	0.0	0.0001	-98.9	-98.7	0.010
19	49	-0.33	629.1	0.6	1578.9	3.5	2209.6	0.0	0.0000	35.0	33.3	0.010
17	50	-0.78	549.4	9.9	1600.8	9.8	2151.7	0.8	0.0010	-22.9	-24.5	0.032
17	48	1.04	549.4	9.9	1518.4	150.3	2068.9	0.1	0.0001	-105.8	-106.9	0.010
15	52	-0.34	561.9	0.9	1699.6	948.8	2254.3	0.0	0.0000	79.6	86.7	0.004
14	53	-0.26	445.8	0.4	1772.5	0.3	2231.0	0.0	0.0000	56.3	43.6	0.006
14	50	0.28	445.8	0.4	1600.8	9.8	2051.9	0.0	0.0000	-122.7	-128.0	0.002
12	50	0.42	461.1	1.2	1600.8	9.8	2060.1	0.0	0.0000	-114.6	-112.8	0.004
11	52	0.41	376.5	0.9	1699.6	948.8	2075.8	0.1	0.0002	-98.9	-98.7	0.004
10	52	0.30	345.2	4.5	1699.6	948.8	2044.7	0.0	0.0000	-130.0	-129.9	0.002
5	54	4.34	125.8	11.6	2174.7	763.1	2294.8	0.4	0.0005	120.1	125.8	0.035

6-311++G(df,pd)

i	j	K_{ijk} / cm^{-1}	ω(i) / cm^{-1}	I(i) / km mol^{-1}	ω(j) / cm^{-1}	I(j) / km mol^{-1}	ω(ij) / cm^{-1}	I(ij) / km mol^{-1}	I(ij) / I(k)	Δω'	Δω	TFR
39	39	37.99	1124.8	36.3	1124.8	36.3	2247.0	12.7	0.0176	73.9	76.5	0.497
38	38	2.13	1110.6	17.3	1110.6	17.3	2223.0	0.2	0.0003	49.9	48.2	0.044
37	37	1.75	1108.2	33.4	1108.2	33.4	2216.5	0.1	0.0001	43.4	43.2	0.040
36	36	0.33	1085.7	14.7	1085.7	14.7	2176.2	0.4	0.0005	3.2	-1.7	0.187
35	35	0.70	1035.7	11.1	1035.7	11.1	2069.9	0.1	0.0002	-103.2	-101.6	0.007
39	40	12.68	1124.8	36.3	1165.3	3.9	2288.7	1.6	0.0022	115.6	117.0	0.108
38	40	0.42	1110.6	17.3	1165.3	3.9	2275.6	0.3	0.0004	102.5	102.9	0.004
38	39	1.23	1110.6	17.3	1124.8	36.3	2236.9	0.0	0.0001	63.8	62.3	0.020
37	39	0.65	1108.2	33.4	1124.8	36.3	2232.9	0.0	0.0001	59.9	59.8	0.011
37	38	-0.39	1108.2	33.4	1110.6	17.3	2218.7	0.3	0.0005	45.7	45.7	0.009
36	41	0.46	1085.7	14.7	1202.9	17.5	2288.6	0.1	0.0001	115.5	115.5	0.004
36	40	-0.99	1085.7	14.7	1165.3	3.9	2250.3	0.0	0.0000	77.3	77.9	0.013
36	39	-3.18	1085.7	14.7	1124.8	36.3	2210.5	4.1	0.0058	37.4	37.4	0.085
35	39	0.35	1035.7	11.1	1124.8	36.3	2160.4	0.1	0.0001	-12.6	-12.6	0.028
35	38	-0.58	1035.7	11.1	1110.6	17.3	2145.9	1.3	0.0018	-27.2	-26.7	0.022
35	37	0.45	1035.7	11.1	1108.2	33.4	2142.4	0.8	0.0012	-30.7	-29.2	0.016
34	42	-1.26	1014.7	1.0	1285.0	62.2	2297.5	0.0	0.0000	124.5	126.6	0.010
34	41	0.27	1014.7	1.0	1202.9	17.5	2217.4	0.0	0.0000	44.3	44.5	0.006
34	40	-0.88	1014.7	1.0	1165.3	3.9	2178.3	0.7	0.0010	5.2	6.9	0.127
34	39	-2.50	1014.7	1.0	1124.8	36.3	2138.9	1.0	0.0014	-34.1	-33.6	0.074
34	38	0.34	1014.7	1.0	1110.6	17.3	2126.5	0.0	0.0000	-46.6	-47.8	0.007
34	37	0.65	1014.7	1.0	1108.2	33.4	2122.7	0.1	0.0001	-50.4	-50.2	0.013

i	j	K_{ijk} / cm^{-1}	ω(i) / cm^{-1}	I(i) / km mol^{-1}	ω(j) / cm^{-1}	I(j) / km mol^{-1}	ω(ij) / cm^{-1}	I(ij) / km mol^{-1}	I(ij) / I(k)	Δω'	Δω	TFR
33	45	-0.60	978.9	1.9	1318.7	124.5	2293.3	0.0	0.0000	120.2	124.5	0.005
33	42	-0.25	978.9	1.9	1285.0	62.2	2260.1	0.0	0.0000	87.0	90.8	0.003
33	39	0.40	978.9	1.9	1124.8	36.3	2099.8	0.0	0.0000	-73.2	-69.4	0.006
31	45	0.30	952.6	3.0	1318.7	124.5	2274.0	0.0	0.0000	100.9	98.2	0.003
31	38	0.23	952.6	3.0	1110.6	17.3	2067.7	0.0	0.0001	-105.3	-109.8	0.002
30	45	-0.34	947.9	11.4	1318.7	124.5	2266.1	0.0	0.0000	93.0	93.5	0.004
30	44	-0.54	947.9	11.4	1307.6	4.6	2255.1	0.0	0.0000	82.0	82.4	0.007
30	43	-0.30	947.9	11.4	1316.3	0.8	2263.1	0.5	0.0007	90.0	91.1	0.003
30	42	-1.02	947.9	11.4	1285.0	62.2	2232.3	0.0	0.0000	59.2	59.8	0.017
30	41	-0.28	947.9	11.4	1202.9	17.5	2148.8	0.4	0.0005	-24.3	-22.3	0.013
30	40	0.57	947.9	11.4	1165.3	3.9	2112.3	0.0	0.0000	-60.8	-59.9	0.010
30	39	1.32	947.9	11.4	1124.8	36.3	2072.5	0.0	0.0000	-100.6	-100.4	0.013
29	46	-0.27	843.1	15.6	1355.3	74.5	2208.4	0.1	0.0002	35.3	25.3	0.011
29	45	1.44	843.1	15.6	1318.7	124.5	2163.9	144.5	0.2007	-9.1	-11.3	0.128
29	42	0.22	843.1	15.6	1285.0	62.2	2131.3	0.0	0.0000	-41.8	-45.0	0.005
28	46	-0.70	858.1	85.6	1355.3	74.5	2212.3	0.1	0.0002	39.2	40.3	0.017
28	45	2.81	858.1	85.6	1318.7	124.5	2168.8	7.5	0.0104	-4.3	3.7	0.753
28	42	0.38	858.1	85.6	1285.0	62.2	2136.4	0.0	0.0000	-36.7	-30.0	0.013
27	48	-1.16	804.8	7.0	1496.6	173.8	2305.6	0.1	0.0001	132.6	128.3	0.009
27	46	-3.13	804.8	7.0	1355.3	74.5	2173.1	3.6	0.0050	0.0	-13.0	0.240
27	45	12.27	804.8	7.0	1318.7	124.5	2127.5	41.2	0.0572	-45.6	-49.6	0.247
27	43	0.55	804.8	7.0	1316.3	0.8	2128.4	0.0	0.0000	-44.7	-52.0	0.011
27	42	1.86	804.8	7.0	1285.0	62.2	2094.6	0.1	0.0001	-78.4	-83.3	0.022
26	46	-13.39	817.8	5.5	1355.3	74.5	2178.9	95.9	0.1332	5.8	0.0	892.798
26	45	57.89	817.8	5.5	1318.7	124.5	2120.7	117.0	0.1625	-52.4	-36.6	1.582
26	44	1.01	817.8	5.5	1307.6	4.6	2122.0	0.1	0.0001	-51.1	-47.7	0.021
26	43	2.53	817.8	5.5	1316.3	0.8	2132.9	0.2	0.0003	-40.2	-38.9	0.065
26	42	8.75	817.8	5.5	1285.0	62.2	2098.5	1.4	0.0019	-74.6	-70.3	0.124
25	48	0.23	778.0	3.1	1496.6	173.8	2275.7	0.0	0.0000	102.6	101.5	0.002
25	46	1.73	778.0	3.1	1355.3	74.5	2140.8	0.8	0.0011	-32.3	-39.8	0.043
25	45	-3.61	778.0	3.1	1318.7	124.5	2097.6	0.2	0.0002	-75.5	-76.4	0.047
25	42	-0.64	778.0	3.1	1285.0	62.2	2065.1	0.0	0.0000	-108.0	-110.1	0.006
23	50	0.25	712.5	23.3	1589.8	4.4	2301.0	0.0	0.0000	127.9	129.3	0.002
23	49	2.32	712.5	23.3	1572.4	3.1	2285.2	0.1	0.0001	112.1	111.8	0.021
23	48	-6.26	712.5	23.3	1496.6	173.8	2207.9	2.8	0.0039	34.8	36.0	0.174
23	47	-1.14	712.5	23.3	1415.6	4.6	2128.2	0.2	0.0002	-44.8	-44.9	0.025
23	46	-10.00	712.5	23.3	1355.3	74.5	2074.3	0.4	0.0006	-98.8	-105.3	0.095
21	49	0.44	652.8	3.9	1572.4	3.1	2220.0	0.0	0.0000	47.0	52.1	0.008
20	49	0.90	640.3	0.3	1572.4	3.1	2217.9	0.1	0.0001	44.8	39.6	0.023
20	48	-2.33	640.3	0.3	1496.6	173.8	2141.5	1.1	0.0015	-31.6	-36.2	0.064
20	47	-0.89	640.3	0.3	1415.6	4.6	2060.6	0.0	0.0000	-112.5	-117.2	0.008
19	49	-0.35	630.3	0.6	1572.4	3.1	2204.5	0.0	0.0000	31.5	29.7	0.012
17	50	-0.81	540.3	8.2	1589.8	4.4	2130.8	1.0	0.0013	-42.2	-42.9	0.019
15	52	-0.32	509.4	10.9	1702.2	45.7	2216.5	0.0	0.0000	43.4	38.5	0.008
14	53	0.26	439.3	0.7	1768.1	0.9	2221.2	0.0	0.0000	48.2	34.3	0.008
11	52	0.39	371.0	1.3	1702.2	45.7	2073.0	0.1	0.0002	-100.1	-99.9	0.004
10	53	-0.29	330.6	6.0	1768.1	0.9	2112.8	0.0	0.0000	-60.3	-74.4	0.004
6	54	6.27	108.0	0.8	2173.1	719.8	2265.1	0.1	0.0002	92.0	108.0	0.058
5	54	4.38	118.2	11.2	2173.1	719.8	2277.0	0.4	0.0005	103.9	118.2	0.037
1	54	1.13	-8.1	0.4	2173.1	719.8	2154.5	2.0	0.0028	-18.6	-8.1	0.140

APPENDIX F

VIBRATIONAL MODES OF 4-AZIDO-N-PHENYLMALEIMIDE (ISOMER 1) THAT OCCUR WITHIN ±130 CM^{-1} FROM THE FUNDAMENTAL VIBRATION FOR SEVEN BASIS SETS IN THF

i, j, k : vibrational modes ; where k = 54 (azide asymmetric stretch)

i = j → overtone & i ≠ j → combination band

K_{ijk} : cubic force constant

TFR : third-order Fermi resonance

ω(i), ω(j), ω(k) : anharmonic frequencies of i, j & k th mode

ω(ij) : anharmonic frequency of ij th mode

I(i), I(j), I(k) : anharmonic intensities of i, j & k th mode

I(ij) : anharmonic intensity of ij th mode

Δω' : ω(ij) - ω(k)

Δω : ω(i) + ω(j) - ω(k)

6-31G(d,p)

i	j	K_{ijk} / cm^{-1}	ω(i) / cm^{-1}	I(i) / km mol^{-1}	ω(j) / cm^{-1}	I(j) / km mol^{-1}	ω(ij) / cm^{-1}	I(ij) / km mol^{-1}	I(ij) / I(k)	Δω'	Δω	TFR
39	39	-36.15	1147.1	17.7	1147.1	17.7	2289.7	12.0	0.0267	93.4	98.0	0.369
38	38	-3.98	1144.5	13.0	1144.5	13.0	2279.6	0.3	0.0006	83.3	92.8	0.043
37	37	-1.59	1116.5	22.0	1116.5	22.0	2245.7	0.0	0.0000	49.4	36.7	0.043
36	36	-0.30	1061.7	10.4	1061.7	10.4	2119.4	0.4	0.0008	-76.8	-72.9	0.004
35	35	-0.61	1028.7	7.4	1028.7	7.4	2055.8	0.2	0.0004	-140.5	-138.8	0.004
39	40	-14.16	1147.1	17.7	1193.1	11.0	2341.9	1.8	0.0041	145.7	144.0	0.098
38	40	-3.01	1144.5	13.0	1193.1	11.0	2338.3	0.3	0.0007	142.0	141.4	0.021
38	39	-7.31	1144.5	13.0	1147.1	17.7	2286.1	1.6	0.0035	89.9	95.4	0.077
37	40	-0.48	1116.5	22.0	1193.1	11.0	2320.4	0.5	0.0011	124.1	113.3	0.004
37	39	-1.68	1116.5	22.0	1147.1	17.7	2268.4	0.0	0.0000	72.2	67.3	0.025
37	38	0.36	1116.5	22.0	1144.5	13.0	2262.3	0.4	0.0010	66.0	64.7	0.006
36	41	-0.50	1061.7	10.4	1216.4	1.3	2274.2	0.1	0.0002	77.9	81.8	0.006
36	40	0.82	1061.7	10.4	1193.1	11.0	2257.7	0.0	0.0001	61.5	58.5	0.014
36	39	2.37	1061.7	10.4	1147.1	17.7	2207.7	24.8	0.0552	11.4	12.5	0.189
36	38	0.50	1061.7	10.4	1144.5	13.0	2202.1	1.0	0.0021	5.8	10.0	0.050

i	j	K_{ijk} / cm^{-1}	ω(i) / cm^{-1}	I(i) / km mol^{-1}	ω(j) / cm^{-1}	I(j) / km mol^{-1}	ω(ij) / cm^{-1}	I(ij) / km mol^{-1}	I(ij) / I(k)	Δω'	Δω	TFR
35	42	0.25	1028.7	7.4	1300.7	8.0	2327.3	0.7	0.0015	131	133.2	0.002
35	39	-0.71	1028.7	7.4	1147.1	17.7	2174.5	0.2	0.0004	-21.8	-20.4	0.035
35	38	0.63	1028.7	7.4	1144.5	13.0	2166.5	1.2	0.0027	-29.8	-23	0.027
35	37	-0.44	1028.7	7.4	1116.5	22.0	2149.8	0.6	0.0012	-46.5	-51.1	0.009
34	44	-0.73	1023.5	0.2	1313.4	19.7	2342.5	0.1	0.0002	146.2	140.6	0.005
34	41	-0.73	1023.5	0.2	1216.4	1.3	2236.7	0.1	0.0001	40.4	43.6	0.017
34	40	1.56	1023.5	0.2	1193.1	11.0	2219.7	3.2	0.0071	23.4	20.4	0.077
34	39	3.47	1023.5	0.2	1147.1	17.7	2169.3	0.6	0.0014	-27	-25.6	0.135
34	38	0.45	1023.5	0.2	1144.5	13.0	2164.2	0.0	0.0001	-32.1	-28.2	0.016
34	37	-0.61	1023.5	0.2	1116.5	22.0	2145.8	0.0	0.0001	-50.5	-56.3	0.011
34	35	-0.26	1023.5	0.2	1028.7	7.4	2052.1	0.0	0.0001	-144.2	-144	0.002
33	45	-0.20	981.8	3.2	1331.6	161.6	2314.0	0.0	0.0000	117.7	117.1	0.002
32	46	-0.38	948.5	4.8	1374.5	91.1	2326.6	0.0	0.0000	130.4	126.7	0.003
32	45	1.31	948.5	4.8	1331.6	161.6	2282.9	0.0	0.0000	86.6	83.8	0.016
32	43	-0.88	948.5	4.8	1322.2	17.3	2271.2	0.0	0.0001	74.9	74.4	0.012
32	41	-0.31	948.5	4.8	1216.4	1.3	2162.4	0.4	0.0008	-33.9	-31.4	0.010
32	40	0.23	948.5	4.8	1193.1	11.0	2147.2	0.0	0.0000	-49.1	-54.7	0.004
32	39	0.92	948.5	4.8	1147.1	17.7	2096.8	0.0	0.0000	-99.5	-100.7	0.009
32	38	0.35	948.5	4.8	1144.5	13.0	2090.7	0.1	0.0002	-105.6	-103.2	0.003
31	45	0.64	961.3	7.9	1331.6	161.6	2290.7	0.0	0.0000	94.4	96.6	0.007
31	43	-0.23	961.3	7.9	1322.2	17.3	2279.0	0.0	0.0000	82.7	87.2	0.003
29	46	-0.69	849.6	69.6	1374.5	91.1	2218.9	0.4	0.0009	22.6	27.8	0.025
29	45	2.81	849.6	69.6	1331.6	161.6	2175.6	0.7	0.0017	-20.7	-15.1	0.187
29	44	0.66	849.6	69.6	1313.4	19.7	2164.9	0.0	0.0000	-31.4	-33.3	0.020
28	46	6.61	834.2	5.6	1374.5	91.1	2214.1	25.2	0.0561	17.8	12.4	0.533
28	45	-24.52	834.2	5.6	1331.6	161.6	2168.3	31.0	0.0691	-28	-30.5	0.804
28	44	-5.33	834.2	5.6	1313.4	19.7	2159.3	0.4	0.0010	-37	-48.7	0.110
28	43	-2.66	834.2	5.6	1322.2	17.3	2159.2	0.1	0.0003	-37.1	-39.9	0.067
28	42	1.12	834.2	5.6	1300.7	8.0	2140.3	0.0	0.0000	-56	-61.4	0.018
28	41	-1.02	834.2	5.6	1216.4	1.3	2051.3	0.0	0.0000	-145	-145.7	0.007
27	48	-6.42	825.4	0.1	1517.6	101.8	2343.3	1.5	0.0034	147	146.8	0.044
27	47	-0.26	825.4	0.1	1440.4	0.7	2267.8	0.0	0.0001	71.6	69.5	0.004
27	46	-14.25	825.4	0.1	1374.5	91.1	2205.8	230.5	0.5140	9.5	3.6	3.942
27	45	52.03	825.4	0.1	1331.6	161.6	2148.4	97.4	0.2173	-47.8	-39.3	1.325
27	44	11.27	825.4	0.1	1313.4	19.7	2146.6	2.1	0.0046	-49.7	-57.5	0.196
27	43	5.71	825.4	0.1	1322.2	17.3	2146.8	0.4	0.0009	-49.5	-48.6	0.117
27	42	-2.34	825.4	0.1	1300.7	8.0	2127.6	0.1	0.0002	-68.7	-70.2	0.033
26	46	-0.88	805.5	2.1	1374.5	91.1	2181.9	1.9	0.0041	-14.4	-16.4	0.054
26	45	1.87	805.5	2.1	1331.6	161.6	2138.7	0.1	0.0002	-57.6	-59.2	0.032
26	44	0.46	805.5	2.1	1313.4	19.7	2128.2	0.0	0.0001	-68.1	-77.4	0.006
25	48	-0.49	761.3	4.1	1517.6	101.8	2278.9	0.1	0.0001	82.6	82.6	0.006
25	46	-2.50	761.3	4.1	1374.5	91.1	2135.9	0.7	0.0015	-60.4	-60.5	0.041
25	45	5.19	761.3	4.1	1331.6	161.6	2093.3	0.1	0.0003	-103	-103.4	0.050
25	44	1.23	761.3	4.1	1313.4	19.7	2082.2	0.0	0.0001	-114.1	-121.6	0.010
25	43	0.70	761.3	4.1	1322.2	17.3	2081.9	0.0	0.0000	-114.4	-112.8	0.006
25	42	-0.27	761.3	4.1	1300.7	8.0	2061.3	0.0	0.0000	-135	-134.3	0.002
24	48	0.26	718.6	10.6	1517.6	101.8	2232.7	0.0	0.0001	36.4	40	0.007
24	46	0.24	718.6	10.6	1374.5	91.1	2093.1	0.4	0.0009	-103.1	-103.2	0.002
24	45	-0.76	718.6	10.6	1331.6	161.6	2049.9	0.1	0.0002	-146.4	-146.1	0.005
23	50	-0.69	707.0	16.0	1615.1	9.3	2322.4	0.0	0.0001	126.2	125.8	0.005
23	49	-2.31	707.0	16.0	1596.6	1.8	2303.8	0.1	0.0002	107.5	107.3	0.022
23	48	6.79	707.0	16.0	1517.6	101.8	2225.2	11.6	0.0259	28.9	28.4	0.239

i	j	K_{ijk} / cm^{-1}	ω(i) / cm^{-1}	I(i) / km mol^{-1}	ω(j) / cm^{-1}	I(j) / km mol^{-1}	ω(ij) / cm^{-1}	I(ij) / km mol^{-1}	I(ij) / I(k)	Δω'	Δω	TFR
23	47	1.22	707.0	16.0	1440.4	0.7	2149.4	0.1	0.0002	-46.9	-48.9	0.025
23	46	10.87	707.0	16.0	1374.5	91.1	2082.8	0.2	0.0005	-113.4	-114.8	0.095
21	50	-0.25	643.2	2.2	1615.1	9.3	2256.8	0.0	0.0000	60.5	62.0	0.004
21	48	0.88	643.2	2.2	1517.6	101.8	2159.7	0.1	0.0002	-36.6	-35.5	0.025
21	47	0.30	643.2	2.2	1440.4	0.7	2083.8	0.1	0.0002	-112.5	-112.7	0.003
20	50	-0.23	641.0	3.1	1615.1	9.3	2256.0	0.0	0.0000	59.7	59.8	0.004
20	49	-0.94	641.0	3.1	1596.6	1.8	2238.7	0.2	0.0003	42.4	41.3	0.023
20	48	2.18	641.0	3.1	1517.6	101.8	2158.9	0.2	0.0004	-37.4	-37.7	0.058
20	47	0.88	641.0	3.1	1440.4	0.7	2082.6	0.1	0.0002	-113.7	-114.9	0.008
18	52	0.26	583.3	5.8	1748.4	235.1	2329.6	0.0	0.0001	133.3	135.4	0.002
18	48	0.32	583.3	5.8	1517.6	101.8	2101.0	0.0	0.0000	-95.3	-95.4	0.003
17	50	0.92	546.3	6.7	1615.1	9.3	2160.8	0.8	0.0018	-35.5	-34.9	0.026
17	48	-0.77	546.3	6.7	1517.6	101.8	2063.1	0.0	0.0000	-133.1	-132.3	0.006
14	50	0.49	434.7	4.8	1615.1	9.3	2049.5	0.0	0.0000	-146.8	-146.5	0.003
5	54	-3.48	128.8	4.1	2196.3	448.4	2314.2	0.3	0.0006	117.9	128.8	0.027
2	54	-0.74	86.7	2.7	2196.3	448.4	2283.3	0.1	0.0003	87.0	86.7	0.009
1	54	0.95	39.4	0.4	2196.3	448.4	2240.8	1.3	0.0029	44.6	39.4	0.024

6-31+G(d,p)

i	j	K_{ijk} / cm^{-1}	ω(i) / cm^{-1}	I(i) / km mol^{-1}	ω(j) / cm^{-1}	I(j) / km mol^{-1}	ω(ij) / cm^{-1}	I(ij) / km mol^{-1}	I(ij) / I(k)	Δω'	Δω	TFR
39	39	38.91	1137.1	31.1	1137.1	31.1	2273.2	15.2	0.0217	87.4	88.4	0.440
38	38	2.68	1120.2	37.7	1120.2	37.7	2249.4	0.5	0.0007	63.6	54.6	0.049
37	37	1.09	1143.8	8.2	1143.8	8.2	2277.3	0.0	0.0000	91.5	101.8	0.011
36	36	0.26	1086.7	14.9	1086.7	14.9	2177.6	0.3	0.0004	-8.2	-12.4	0.021
35	35	0.70	1032.7	15.5	1032.7	15.5	2062.8	0.2	0.0002	-123.0	-120.5	0.006
34	34	-0.48	1023.0	1.0	1023.0	1.0	2046.2	0.0	0.0000	-139.6	-139.8	0.003
38	41	-0.50	1120.2	37.7	1215.0	3.4	2335.4	1.6	0.0023	149.6	149.4	0.003
38	40	1.29	1120.2	37.7	1199.2	14.0	2332.0	0.1	0.0002	146.1	133.6	0.010
38	39	3.84	1120.2	37.7	1137.1	31.1	2264.5	0.5	0.0007	78.7	71.5	0.054
37	39	0.85	1143.8	8.2	1137.1	31.1	2274.5	0.0	0.0000	88.7	95.1	0.009
37	38	-0.29	1143.8	8.2	1120.2	37.7	2264.2	0.1	0.0002	78.4	78.2	0.004
36	41	0.47	1086.7	14.9	1215.0	3.4	2296.9	0.1	0.0001	111.1	115.9	0.004
36	40	-0.80	1086.7	14.9	1199.2	14.0	2289.6	0.0	0.0000	103.8	100.1	0.008
36	39	-2.77	1086.7	14.9	1137.1	31.1	2224.0	19.9	0.0284	38.2	38.0	0.073
36	38	-0.29	1086.7	14.9	1120.2	37.7	2213.5	1.3	0.0019	27.6	21.1	0.014
35	39	0.44	1032.7	15.5	1137.1	31.1	2169.8	0.1	0.0001	-16.0	-16.0	0.028
35	38	-0.78	1032.7	15.5	1120.2	37.7	2155.2	1.9	0.0028	-30.7	-32.9	0.024
34	44	0.28	1023.0	1.0	1306.0	151.1	2332.3	0.1	0.0001	146.5	143.2	0.002
34	41	0.38	1023.0	1.0	1215.0	3.4	2233.8	0.0	0.0000	47.9	52.2	0.007
34	40	-0.96	1023.0	1.0	1199.2	14.0	2227.0	5.2	0.0074	41.2	36.4	0.026
34	39	-3.31	1023.0	1.0	1137.1	31.1	2160.6	0.8	0.0012	-25.2	-25.7	0.129
34	37	0.81	1023.0	1.0	1143.8	8.2	2160.5	0.0	0.0001	-25.3	-19.0	0.043
33	45	-0.35	913.1	11.1	1323.3	56.4	2266.9	0.0	0.0000	81.1	50.6	0.007
33	44	-0.26	913.1	11.1	1306.0	151.1	2250.8	0.0	0.0000	65.0	33.3	0.008
33	39	0.29	913.1	11.1	1137.1	31.1	2077.6	0.0	0.0000	-108.2	-135.6	0.002
31	46	0.29	948.3	9.3	1371.9	10.7	2326.9	0.0	0.0000	141.1	134.4	0.002
31	45	-1.11	948.3	9.3	1323.3	56.4	2276.2	0.0	0.0000	90.4	85.8	0.013

i	j	K_{ijk} / cm^{-1}	ω(i) / cm^{-1}	I(i) / km mol^{-1}	ω(j) / cm^{-1}	I(j) / km mol^{-1}	ω(ij) / cm^{-1}	I(ij) / km mol^{-1}	I(ij) / I(k)	Δω'	Δω	TFR
31	44	0.49	948.3	9.3	1306.0	151.1	2260.0	0.0	0.0000	74.2	68.5	0.007
31	43	0.86	948.3	9.3	1331.6	60.1	2274.5	0.0	0.0001	88.7	94.1	0.009
31	41	0.24	948.3	9.3	1215.0	3.4	2158.5	0.3	0.0005	-27.3	-22.5	0.011
31	40	-0.35	948.3	9.3	1199.2	14.0	2152.9	0.0	0.0000	-32.9	-38.3	0.009
31	39	-0.99	948.3	9.3	1137.1	31.1	2087.2	0.0	0.0000	-98.6	-100.4	0.010
30	45	0.54	971.6	7.9	1323.3	56.4	2271.8	0.0	0.0000	86.0	109.1	0.005
30	38	0.24	971.6	7.9	1120.2	37.7	2071.7	0.1	0.0001	-114.1	-94.0	0.003
29	48	-0.36	788.0	3.5	1513.6	157.9	2334.5	0.0	0.0000	148.7	115.8	0.003
29	46	-0.40	788.0	3.5	1371.9	10.7	2199.6	0.1	0.0002	13.8	-25.8	0.015
29	45	2.18	788.0	3.5	1323.3	56.4	2148.8	1.2	0.0018	-37.0	-74.5	0.029
29	44	0.53	788.0	3.5	1306.0	151.1	2133.8	0.0	0.0001	-52.0	-91.8	0.006
29	43	0.26	788.0	3.5	1331.6	60.1	2149.3	0.0	0.0000	-36.5	-66.1	0.004
28	46	-2.27	836.1	54.6	1371.9	10.7	2202.3	3.5	0.0051	16.5	22.2	0.102
28	45	9.63	836.1	54.6	1323.3	56.4	2151.7	10.1	0.0145	-34.1	-26.4	0.364
28	44	2.18	836.1	54.6	1306.0	151.1	2137.2	0.1	0.0002	-48.6	-43.7	0.050
28	43	0.88	836.1	54.6	1331.6	60.1	2150.9	0.0	0.0000	-34.9	-18.1	0.049
27	48	-6.71	819.7	3.3	1513.6	157.9	2331.5	1.8	0.0026	145.7	147.5	0.046
27	46	-12.97	819.7	3.3	1371.9	10.7	2199.1	161.4	0.2311	13.3	5.8	2.226
27	45	56.83	819.7	3.3	1323.3	56.4	2133.7	112.2	0.1606	-52.1	-42.8	1.328
27	44	13.04	819.7	3.3	1306.0	151.1	2129.3	3.8	0.0055	-56.6	-60.1	0.217
27	43	5.30	819.7	3.3	1331.6	60.1	2144.5	0.5	0.0008	-41.3	-34.5	0.154
27	42	-1.32	819.7	3.3	1317.8	70.5	2137.2	0.0	0.0001	-48.6	-48.3	0.027
26	46	0.27	860.8	57.1	1371.9	10.7	2214.7	0.8	0.0012	28.9	46.9	0.006
26	45	-2.62	860.8	57.1	1323.3	56.4	2163.9	0.5	0.0007	-21.9	-1.7	1.516
26	44	-0.62	860.8	57.1	1306.0	151.1	2149.2	0.0	0.0000	-36.7	-19.0	0.032
26	40	0.30	860.8	57.1	1199.2	14.0	2043.5	0.0	0.0000	-142.3	-125.8	0.002
25	48	-0.34	762.1	1.6	1513.6	157.9	2275.4	0.0	0.0001	89.6	89.9	0.004
25	46	-1.90	762.1	1.6	1371.9	10.7	2138.8	0.6	0.0009	-47.0	-51.7	0.037
25	45	4.18	762.1	1.6	1323.3	56.4	2088.9	0.1	0.0002	-96.9	-100.4	0.042
25	44	1.05	762.1	1.6	1306.0	151.1	2073.9	0.0	0.0000	-111.9	-117.6	0.009
25	43	0.48	762.1	1.6	1331.6	60.1	2087.4	0.0	0.0000	-98.4	-92.0	0.005
24	48	0.23	702.8	54.5	1513.6	157.9	2211.4	0.0	0.0000	25.6	30.5	0.008
23	50	0.46	710.9	11.9	1608.7	25.0	2315.1	0.0	0.0000	129.2	133.7	0.003
23	49	2.48	710.9	11.9	1585.8	2.2	2294.8	0.1	0.0001	109.0	110.8	0.022
23	48	-6.65	710.9	11.9	1513.6	157.9	2219.6	8.2	0.0118	33.8	38.6	0.172
23	47	-1.11	710.9	11.9	1432.9	0.2	2140.0	0.1	0.0001	-45.8	-42.0	0.027
23	46	-9.45	710.9	11.9	1371.9	10.7	2084.7	0.2	0.0003	-101.1	-103.0	0.092
21	48	0.57	649.0	2.6	1513.6	157.9	2161.1	0.1	0.0001	-24.7	-23.2	0.024
21	47	0.35	649.0	2.6	1432.9	0.2	2081.2	0.1	0.0001	-104.6	-103.9	0.003
20	49	1.05	641.7	1.6	1585.8	2.2	2230.7	0.1	0.0002	44.9	41.7	0.025
20	48	-2.39	641.7	1.6	1513.6	157.9	2154.5	0.4	0.0005	-31.3	-30.5	0.078
20	47	-0.89	641.7	1.6	1432.9	0.2	2074.3	0.0	0.0001	-111.5	-111.2	0.008
17	50	-0.78	546.9	7.5	1608.7	25.0	2153.9	0.7	0.0010	-31.9	-30.2	0.026
17	48	0.92	546.9	7.5	1513.6	157.9	2058.1	0.1	0.0001	-127.7	-125.3	0.007
15	52	-0.29	510.0	12.9	1714.2	714.8	2230.2	0.0	0.0000	44.4	38.4	0.008
14	50	0.30	445.0	0.2	1608.7	25.0	2053.4	0.0	0.0000	-132.4	-132.2	0.002
11	52	0.32	368.0	1.3	1714.2	714.8	2081.9	0.1	0.0001	-103.9	-103.6	0.003
6	54	6.02	155.9	4.7	2185.8	698.6	2332.1	0.1	0.0002	146.3	155.9	0.039
5	54	4.49	125.4	7.7	2185.8	698.6	2296.0	0.3	0.0005	110.2	125.4	0.036
1	54	1.43	-0.5	0.0	2185.8	698.6	2175.3	1.6	0.0024	-10.5	-0.5	3.160

6-31++G(d,p)

i	j	K_{ijk} / cm^{-1}	ω(i) / cm^{-1}	I(i) / km mol^{-1}	ω(j) / cm^{-1}	I(j) / km mol^{-1}	ω(ij) / cm^{-1}	I(ij) / km mol^{-1}	I(ij) / I(k)	Δω'	Δω	TFR
41	41	-0.46	1034.8	512.5	1034.8	512.5	2270.6	0.0	0.0000	95.2	-105.7	0.004
38	38	-2.65	1149.5	276.3	1149.5	276.3	2278.5	0.5	0.0007	103.1	123.5	0.021
37	37	-1.07	1134.7	27.7	1134.7	27.7	2256.2	0.0	0.0000	80.8	94.0	0.011
35	35	-0.69	1026.5	155.8	1026.5	155.8	2037.1	0.2	0.0002	-138.3	-122.4	0.006
40	41	1.20	1224.8	19.3	1034.8	512.5	2312.2	0.0	0.0000	136.9	84.3	0.014
38	41	0.47	1149.5	276.3	1034.8	512.5	2275.4	1.6	0.0020	100.0	8.9	0.053
38	40	-1.26	1149.5	276.3	1224.8	19.3	2319.6	0.1	0.0002	144.2	198.9	0.006
37	38	0.31	1134.7	27.7	1149.5	276.3	2268.2	0.1	0.0002	92.8	108.8	0.003
35	39	-0.49	1026.5	155.8	1299.6	29.1	2275.3	0.1	0.0002	99.9	150.7	0.003
35	38	0.78	1026.5	155.8	1149.5	276.3	2156.9	1.9	0.0025	-18.5	0.6	1.398
34	41	-0.33	1172.9	143.8	1034.8	512.5	2293.3	0.0	0.0000	117.9	32.4	0.010
34	37	-0.84	1172.9	143.8	1134.7	27.7	2297.9	0.0	0.0001	122.5	132.2	0.006
33	44	-0.26	885.9	59.0	1285.3	118.5	2244.8	0.0	0.0000	69.4	-4.2	0.062
33	39	0.34	885.9	59.0	1299.6	29.1	2179.7	0.0	0.0000	4.4	10.2	0.034
31	44	0.48	918.9	117.2	1285.3	118.5	2259.0	0.0	0.0000	83.6	28.9	0.017
31	43	0.88	918.9	117.2	1315.4	80.6	2251.9	0.0	0.0001	76.5	58.9	0.015
31	41	0.23	918.9	117.2	1034.8	512.5	2078.6	0.3	0.0004	-96.8	-221.6	0.001
31	40	-0.35	918.9	117.2	1224.8	19.3	2120.7	0.0	0.0000	-54.7	-31.7	0.011
31	39	-1.00	918.9	117.2	1299.6	29.1	2201.4	0.0	0.0000	26.0	43.2	0.023
29	44	0.52	1017.8	92.5	1285.3	118.5	2238.7	0.0	0.0001	63.3	127.7	0.004
29	43	0.24	1017.8	92.5	1315.4	80.6	2232.9	0.0	0.0000	57.5	157.8	0.001
29	39	-0.53	1017.8	92.5	1299.6	29.1	2194.3	0.0	0.0000	18.9	142.0	0.004
29	38	-0.25	1017.8	92.5	1149.5	276.3	2064.9	0.0	0.0000	-110.5	-8.2	0.030
29	30	3.54	1017.8	92.5	1318.0	327.4	2212.7	0.1	0.0001	37.3	160.3	0.022
28	46	-2.37	754.9	238.5	1467.3	44.5	2273.0	4.0	0.0051	97.6	46.8	0.051
28	45	10.14	754.9	238.5	1413.2	186.9	2271.4	11.6	0.0151	96.0	-7.3	1.379
28	44	2.32	754.9	238.5	1285.3	118.5	2159.1	0.1	0.0002	-16.3	-135.2	0.017
28	43	0.95	754.9	238.5	1315.4	80.6	2151.3	0.0	0.0000	-24.1	-105.1	0.009
28	39	-3.02	754.9	238.5	1299.6	29.1	2103.2	0.1	0.0002	-72.2	-120.9	0.025
28	30	-0.53	754.9	238.5	1318.0	327.4	2130.4	0.0	0.0000	-45.0	-102.5	0.005
27	46	12.88	834.2	362.5	1467.3	44.5	2252.4	155.6	0.2016	77.0	126.2	0.102
27	45	-56.66	834.2	362.5	1413.2	186.9	2251.0	94.3	0.1221	75.6	72.0	0.787
27	44	-13.13	834.2	362.5	1285.3	118.5	2134.8	3.9	0.0051	-40.6	-55.8	0.235
27	43	-5.41	834.2	362.5	1315.4	80.6	2128.5	0.5	0.0007	-46.9	-25.8	0.210
27	42	1.29	834.2	362.5	1314.1	7.9	2133.9	0.0	0.0001	-41.5	-27.0	0.048
27	39	16.87	834.2	362.5	1299.6	29.1	2077.5	3.6	0.0047	-97.9	-41.5	0.406
27	36	-0.82	834.2	362.5	1237.8	58.2	2049.6	0.0	0.0000	-125.8	-103.4	0.008
27	30	-0.42	834.2	362.5	1318.0	327.4	2108.3	0.2	0.0002	-67.1	-23.2	0.018
26	46	0.33	786.2	177.7	1467.3	44.5	2253.2	1.0	0.0012	77.8	78.2	0.004
26	45	-2.88	786.2	177.7	1413.2	186.9	2251.5	0.6	0.0008	76.1	24.0	0.120
26	44	-0.67	786.2	177.7	1285.3	118.5	2144.4	0.0	0.0000	-31.0	-103.8	0.006
26	39	0.73	786.2	177.7	1299.6	29.1	2081.9	0.0	0.0000	-93.5	-89.5	0.008
26	30	3.73	786.2	177.7	1318.0	327.4	2121.7	0.1	0.0001	-53.7	-71.2	0.052
25	46	-1.91	935.9	90.7	1467.3	44.5	2307.1	0.7	0.0009	131.7	227.9	0.008
25	45	4.07	935.9	90.7	1413.2	186.9	2317.5	0.1	0.0002	142.1	173.7	0.023
25	44	1.05	935.9	90.7	1285.3	118.5	2222.7	0.0	0.0000	47.3	45.9	0.023
25	43	0.54	935.9	90.7	1315.4	80.6	2208.7	0.0	0.0000	33.3	75.9	0.007
25	40	-0.67	935.9	90.7	1224.8	19.3	2074.1	0.0	0.0000	-101.3	-14.6	0.046
25	39	-1.06	935.9	90.7	1299.6	29.1	2144.6	0.0	0.0000	-30.8	60.2	0.018

i	j	K_{ijk} / cm^{-1}	ω(i) / cm^{-1}	I(i) / km mol^{-1}	ω(j) / cm^{-1}	I(j) / km mol^{-1}	ω(ij) / cm^{-1}	I(ij) / km mol^{-1}	I(ij) / I(k)	Δω'	Δω	TFR
25	37	0.29	935.9	90.7	1134.7	27.7	2029.4	0.0	0.0000	-146.0	-104.8	0.003
23	47	1.12	815.0	91.5	1422.2	160.1	2175.9	0.1	0.0001	0.5	61.8	0.018
23	46	9.41	815.0	91.5	1467.3	44.5	2192.0	0.3	0.0003	16.6	106.9	0.088
23	45	-40.45	815.0	91.5	1413.2	186.9	2186.5	6.3	0.0081	11.1	52.8	0.767
23	44	-11.49	815.0	91.5	1285.3	118.5	2070.2	0.8	0.0010	-105.1	-75.1	0.153
23	43	-5.30	815.0	91.5	1315.4	80.6	2062.7	0.1	0.0002	-112.7	-45.0	0.118
23	42	1.16	815.0	91.5	1314.1	7.9	2068.6	0.0	0.0000	-106.7	-46.3	0.025
22	30	0.52	340.2	87.5	1318.0	327.4	2120.7	6.9	0.0090	-54.7	-517.2	0.001
21	48	0.59	628.5	87.6	1611.6	75.2	2261.3	0.1	0.0001	85.9	64.6	0.009
21	47	0.35	628.5	87.6	1422.2	160.1	2071.1	0.1	0.0001	-104.3	-124.7	0.003
21	46	0.47	628.5	87.6	1467.3	44.5	2080.6	0.5	0.0006	-94.8	-79.6	0.006
21	45	2.40	628.5	87.6	1413.2	186.9	2077.8	0.0	0.0000	-97.6	-133.8	0.018
20	49	1.05	652.5	29.7	1606.8	10.7	2290.2	0.1	0.0002	114.8	83.9	0.013
20	48	-2.40	652.5	29.7	1611.6	75.2	2302.2	0.4	0.0005	126.8	88.6	0.027
20	47	-0.90	652.5	29.7	1422.2	160.1	2105.7	0.0	0.0001	-69.7	-100.7	0.009
20	46	-4.55	652.5	29.7	1467.3	44.5	2122.0	1.6	0.0021	-53.4	-55.6	0.082
20	45	14.03	652.5	29.7	1413.2	186.9	2119.7	0.2	0.0003	-55.7	-109.8	0.128
18	45	-0.84	449.2	63.3	1413.2	186.9	2044.7	0.0	0.0000	-130.7	-313.1	0.003
17	50	0.76	555.6	0.9	1688.6	12.0	2259.6	0.7	0.0010	84.2	68.9	0.011
17	48	-0.93	555.6	0.9	1611.6	75.2	2183.3	0.1	0.0001	7.9	-8.2	0.114
15	52	-0.29	209.9	63.6	1712.1	604.5	2185.3	0.0	0.0000	9.9	-253.4	0.001
14	49	-1.46	256.4	191.8	1606.8	10.7	2034.9	0.0	0.0001	-140.5	-312.1	0.005
13	48	0.72	535.2	25.3	1611.6	75.2	2032.6	0.0	0.0000	-142.8	-28.6	0.025
12	50	0.48	688.3	159.8	1688.6	12.0	2170.9	0.0	0.0000	-4.5	201.5	0.002
11	52	0.32	417.3	5.2	1712.1	604.5	2134.5	0.1	0.0001	-40.8	-46.0	0.007
11	49	-0.96	417.3	5.2	1606.8	10.7	2026.8	0.0	0.0000	-148.6	-151.3	0.006

6-311G(d,p)

i	j	K_{ijk} / cm^{-1}	ω(i) / cm^{-1}	I(i) / km mol^{-1}	ω(j) / cm^{-1}	I(j) / km mol^{-1}	ω(ij) / cm^{-1}	I(ij) / km mol^{-1}	I(ij) / I(k)	Δω'	Δω	TFR
39	39	35.70	1133.9	32.3	1133.9	32.3	2266.6	11.8	0.0185	76.9	78.1	0.457
38	38	2.91	1122.6	30.8	1122.6	30.8	2247.0	0.1	0.0002	57.3	55.6	0.052
37	37	1.80	1102.6	42.6	1102.6	42.6	2204.5	0.1	0.0001	14.9	15.5	0.116
36	36	0.34	1034.0	12.9	1034.0	12.9	2053.0	0.5	0.0007	-136.7	-121.7	0.003
39	41	-4.33	1133.9	32.3	1204.8	4.7	2337.7	0.1	0.0002	148.0	149.0	0.029
39	40	14.27	1133.9	32.3	1180.4	12.5	2313.2	1.8	0.0028	123.5	124.6	0.115
38	41	-0.58	1122.6	30.8	1204.8	4.7	2327.2	0.9	0.0014	137.5	137.8	0.004
38	40	1.99	1122.6	30.8	1180.4	12.5	2303.6	0.4	0.0006	113.9	113.4	0.018
38	39	5.42	1122.6	30.8	1133.9	32.3	2258.2	0.8	0.0012	68.5	66.8	0.081
37	40	0.26	1102.6	42.6	1180.4	12.5	2281.9	0.5	0.0008	92.3	93.4	0.003
37	39	1.63	1102.6	42.6	1133.9	32.3	2237.3	0.0	0.0000	47.6	46.8	0.035
37	38	-0.62	1102.6	42.6	1122.6	30.8	2224.6	0.5	0.0008	34.9	35.6	0.017
36	43	0.89	1034.0	12.9	1298.1	94.2	2302.8	0.1	0.0001	113.1	142.4	0.006
36	42	-0.83	1034.0	12.9	1265.5	4.0	2301.8	0.1	0.0001	112.1	109.8	0.008
36	41	0.43	1034.0	12.9	1204.8	4.7	2233.0	0.1	0.0002	43.3	49.1	0.009
36	40	-0.87	1034.0	12.9	1180.4	12.5	2208.9	0.0	0.0000	19.2	24.7	0.035
36	39	-2.57	1034.0	12.9	1133.9	32.3	2164.3	1.2	0.0018	-25.4	-21.8	0.118
36	38	-0.34	1034.0	12.9	1122.6	30.8	2153.9	0.2	0.0003	-35.8	-33.1	0.010
35	42	-0.39	1017.6	2.9	1265.5	4.0	2298.7	0.4	0.0006	109.0	93.4	0.004

i	j	K_{ijk} / cm^{-1}	ω(i) / cm^{-1}	I(i) / km mol^{-1}	ω(j) / cm^{-1}	I(j) / km mol^{-1}	ω(ij) / cm^{-1}	I(ij) / km mol^{-1}	I(ij) / I(k)	Δω'	Δω	TFR
35	39	0.70	1017.6	2.9	1133.9	32.3	2154.5	0.1	0.0002	-35.2	-38.2	0.018
35	38	-0.52	1017.6	2.9	1122.6	30.8	2142.3	0.8	0.0012	-47.4	-49.5	0.011
35	37	0.46	1017.6	2.9	1102.6	42.6	2120.8	0.7	0.0012	-68.9	-69.5	0.007
34	45	9.36	1011.2	0.5	1319.9	218.5	2331.4	0.4	0.0006	141.7	141.4	0.066
34	43	-0.36	1011.2	0.5	1298.1	94.2	2294.0	0.0	0.0000	104.4	119.7	0.003
34	42	0.66	1011.2	0.5	1265.5	4.0	2289.7	0.0	0.0000	100.0	87.1	0.008
34	41	0.45	1011.2	0.5	1204.8	4.7	2214.8	0.0	0.0000	25.1	26.4	0.017
34	40	-1.32	1011.2	0.5	1180.4	12.5	2189.1	45.1	0.0705	-0.6	2.0	0.668
34	39	-3.07	1011.2	0.5	1133.9	32.3	2145.6	0.6	0.0010	-44.1	-44.6	0.069
34	37	0.70	1011.2	0.5	1102.6	42.6	2113.5	0.1	0.0001	-76.2	-75.8	0.009
33	45	-0.24	943.9	0.6	1319.9	218.5	2265.9	0.0	0.0000	76.2	74.1	0.003
32	40	-0.23	955.0	0.2	1180.4	12.5	2133.7	0.0	0.0001	-55.9	-54.2	0.004
31	44	0.52	942.7	15.4	1311.2	16.3	2253.5	0.0	0.0000	63.9	64.3	0.008
31	43	-0.75	942.7	15.4	1298.1	94.2	2224.1	0.3	0.0004	34.4	51.2	0.015
31	42	0.71	942.7	15.4	1265.5	4.0	2220.7	0.2	0.0003	31.0	18.6	0.038
31	41	-0.28	942.7	15.4	1204.8	4.7	2144.2	0.4	0.0006	-45.5	-42.1	0.007
31	40	0.32	942.7	15.4	1180.4	12.5	2121.4	0.0	0.0001	-68.3	-66.5	0.005
31	39	1.28	942.7	15.4	1133.9	32.3	2077.0	0.0	0.0000	-112.7	-113.1	0.011
31	38	0.25	942.7	15.4	1122.6	30.8	2065.8	0.1	0.0001	-123.9	-124.3	0.002
30	37	0.29	943.5	6.7	1102.6	42.6	2046.3	0.1	0.0001	-143.4	-143.6	0.002
29	48	-0.36	830.3	71.4	1505.2	191.8	2334.6	0.0	0.0000	144.9	145.8	0.002
29	46	-0.66	830.3	71.4	1356.5	21.4	2190.3	0.1	0.0002	0.6	-2.9	0.229
29	45	2.14	830.3	71.4	1319.9	218.5	2150.3	1.6	0.0025	-39.4	-39.5	0.054
29	43	0.33	830.3	71.4	1298.1	94.2	2113.1	0.1	0.0001	-76.6	-61.2	0.005
28	48	0.32	813.3	20.4	1505.2	191.8	2317.5	0.0	0.0000	127.8	128.8	0.002
28	46	0.58	813.3	20.4	1356.5	21.4	2173.5	0.5	0.0008	-16.2	-19.9	0.029
28	45	-1.96	813.3	20.4	1319.9	218.5	2133.3	0.5	0.0007	-56.4	-56.5	0.035
28	43	-0.27	813.3	20.4	1298.1	94.2	2096.1	0.0	0.0000	-93.6	-78.3	0.003
28	42	0.22	813.3	20.4	1265.5	4.0	2092.5	0.0	0.0000	-97.2	-110.9	0.002
27	48	-6.83	817.5	4.7	1505.2	191.8	2321.1	1.9	0.0030	131.4	133.0	0.051
27	47	-0.30	817.5	4.7	1425.8	3.3	2242.6	0.0	0.0000	53.0	53.6	0.006
27	46	-18.13	817.5	4.7	1356.5	21.4	2175.1	145.4	0.2275	-14.6	-15.7	1.155
27	45	58.44	817.5	4.7	1319.9	218.5	2126.4	88.6	0.1386	-63.3	-52.3	1.117
27	44	2.11	817.5	4.7	1311.2	16.3	2128.1	0.1	0.0001	-61.6	-61.0	0.035
27	43	6.54	817.5	4.7	1298.1	94.2	2100.5	0.5	0.0008	-89.2	-74.1	0.088
27	42	-6.55	817.5	4.7	1265.5	4.0	2096.4	0.5	0.0008	-93.3	-106.7	0.061
26	48	-0.25	809.1	1.2	1505.2	191.8	2313.7	0.0	0.0000	124.0	124.6	0.002
26	46	-0.72	809.1	1.2	1356.5	21.4	2169.7	1.9	0.0030	-20.0	-24.1	0.030
25	48	-0.43	771.1	3.1	1505.2	191.8	2275.9	0.1	0.0001	86.2	86.6	0.005
25	46	-2.69	771.1	3.1	1356.5	21.4	2130.9	1.0	0.0015	-58.8	-62.1	0.043
25	45	5.02	771.1	3.1	1319.9	218.5	2091.3	0.2	0.0003	-98.4	-98.7	0.051
25	43	0.65	771.1	3.1	1298.1	94.2	2054.7	0.0	0.0000	-135.0	-120.5	0.005
25	42	-0.66	771.1	3.1	1265.5	4.0	2051.2	0.0	0.0000	-138.5	-153.1	0.004
24	48	0.22	727.2	7.8	1505.2	191.8	2230.6	0.0	0.0000	40.9	42.8	0.005
23	50	0.62	713.3	12.2	1598.0	4.0	2313.6	0.0	0.0000	123.9	121.6	0.005
23	49	2.25	713.3	12.2	1573.9	1.5	2289.9	0.1	0.0001	100.2	97.5	0.023
23	48	-6.64	713.3	12.2	1505.2	191.8	2215.3	7.6	0.0119	25.6	28.8	0.230
23	47	-1.19	713.3	12.2	1425.8	3.3	2136.8	0.1	0.0002	-52.9	-50.6	0.024
23	46	-12.50	713.3	12.2	1356.5	21.4	2071.3	0.3	0.0004	-118.4	-119.9	0.104
21	49	0.25	645.3	4.4	1573.9	1.5	2216.6	0.0	0.0000	26.9	29.5	0.009
21	48	0.43	645.3	4.4	1505.2	191.8	2141.3	0.0	0.0001	-48.4	-39.2	0.011
20	50	0.22	639.8	0.6	1598.0	4.0	2245.1	0.0	0.0000	55.4	48.1	0.005
20	49	0.79	639.8	0.6	1573.9	1.5	2221.6	0.1	0.0001	31.9	24.0	0.033
20	48	-2.07	639.8	0.6	1505.2	191.8	2146.7	0.2	0.0004	-43.0	-44.7	0.046
20	47	-0.91	639.8	0.6	1425.8	3.3	2067.6	0.0	0.0001	-122.1	-124.1	0.007

i	j	K_{ijk} / cm^{-1}	ω(i) / cm^{-1}	I(i) / km mol^{-1}	ω(j) / cm^{-1}	I(j) / km mol^{-1}	ω(ij) / cm^{-1}	I(ij) / km mol^{-1}	I(ij) / I(k)	Δω'	Δω	TFR
18	52	-0.26	578.9	7.5	1727.8	1579.4	2304.3	0.0	0.0000	114.6	117.0	0.002
17	50	-0.92	545.1	11.4	1598.0	4.0	2147.4	0.8	0.0013	-42.3	-46.6	0.020
17	48	0.54	545.1	11.4	1505.2	191.8	2048.5	0.0	0.0000	-141.2	-139.4	0.004
15	52	-0.25	515.3	5.2	1727.8	1579.4	2243.7	0.0	0.0001	54.0	53.4	0.005
10	52	0.31	328.3	3.4	1727.8	1579.4	2055.9	0.1	0.0001	-133.8	-133.6	0.002
6	54	5.93	143.6	3.4	2189.7	639.0	2321.7	0.1	0.0001	132.0	143.6	0.041
5	54	3.55	125.2	5.8	2189.7	639.0	2294.7	0.3	0.0005	105.0	125.2	0.028
2	54	-0.72	30.1	0.8	2189.7	639.0	2218.4	0.1	0.0002	28.7	30.1	0.024

6-311+G(d,p)

i	j	K_{ijk} / cm^{-1}	ω(i) / cm^{-1}	I(i) / km mol^{-1}	ω(j) / cm^{-1}	I(j) / km mol^{-1}	ω(ij) / cm^{-1}	I(ij) / km mol^{-1}	I(ij) / I(k)	Δω'	Δω	TFR
39	39	-37.29	1129.1	24.3	1129.1	24.3	2314.6	13.9	0.0247	133.3	76.9	0.485
38	38	-2.20	1120.3	91.2	1120.3	91.2	2285.6	0.4	0.0006	104.3	59.2	0.037
37	37	-1.41	1152.2	1.2	1152.2	1.2	2314.0	0.0	0.0000	132.7	123.1	0.011
36	36	-0.27	1083.3	16.0	1083.3	16.0	2173.8	0.4	0.0007	-7.5	-14.7	0.019
35	35	-0.65	1035.5	4.7	1035.5	4.7	2069.9	0.1	0.0002	-111.4	-110.2	0.006
34	34	0.48	1029.6	7.7	1029.6	7.7	2105.1	0.0	0.0001	-76.2	-122.1	0.004
38	39	-1.83	1120.3	91.2	1129.1	24.3	2302.7	0.1	0.0002	121.4	68.1	0.027
37	39	-0.81	1152.2	1.2	1129.1	24.3	2316.0	0.0	0.0001	134.7	100	0.008
37	38	0.55	1152.2	1.2	1120.3	91.2	2299.8	0.3	0.0006	118.5	91.2	0.006
36	41	-0.44	1083.3	16.0	1185.8	21.1	2316.2	0.1	0.0001	134.9	87.8	0.005
36	39	2.84	1083.3	16.0	1129.1	24.3	2242.7	17.5	0.0311	61.4	31.1	0.091
35	42	0.36	1035.5	4.7	1294.7	124.9	2330.2	0.2	0.0004	148.9	148.9	0.002
35	39	-0.41	1035.5	4.7	1129.1	24.3	2193.9	0.1	0.0001	12.6	-16.6	0.025
35	38	0.66	1035.5	4.7	1120.3	91.2	2176.8	1.3	0.0024	-4.5	-25.5	0.026
35	37	-0.34	1035.5	4.7	1152.2	1.2	2190.7	0.5	0.0010	9.4	6.5	0.053
34	41	-0.33	1029.6	7.7	1185.8	21.1	2285.4	0.0	0.0000	104.1	34.1	0.010
34	40	0.92	1029.6	7.7	1379.4	7.2	2307.3	19.2	0.0341	126	227.7	0.004
34	39	2.78	1029.6	7.7	1129.1	24.3	2211.6	0.7	0.0013	30.3	-22.6	0.123
34	37	-0.69	1029.6	7.7	1152.2	1.2	2210.3	0.0	0.0001	29	0.5	1.307
33	45	-0.40	954.5	0.9	1314.5	202.3	2279.1	0.0	0.0000	97.8	87.7	0.005
33	39	0.25	954.5	0.9	1129.1	24.3	2109.1	0.0	0.0000	-72.2	-97.7	0.003
31	44	0.48	948.5	4.1	1405.4	211.9	2329.0	0.0	0.0001	147.6	172.6	0.003
31	43	-0.56	948.5	4.1	1311.4	10.7	2263.7	0.4	0.0006	82.4	78.5	0.007
31	42	0.82	948.5	4.1	1294.7	124.9	2239.7	0.1	0.0002	58.4	61.8	0.013
31	41	-0.22	948.5	4.1	1185.8	21.1	2176.8	0.3	0.0006	-4.6	-47.1	0.005
31	40	0.41	948.5	4.1	1379.4	7.2	2198.5	0.0	0.0000	17.2	146.5	0.003
31	39	1.22	948.5	4.1	1129.1	24.3	2104.9	0.0	0.0000	-76.5	-103.7	0.012
30	45	0.43	930.1	7.1	1314.5	202.3	2265.0	0.0	0.0000	83.6	63.3	0.007
30	44	0.24	930.1	7.1	1405.4	211.9	2321.5	0.0	0.0000	140.2	154.2	0.002
30	39	0.30	930.1	7.1	1129.1	24.3	2095.6	0.0	0.0000	-85.8	-122.1	0.002
29	46	-0.46	850.4	82.0	1354.1	37.9	2202.6	0.1	0.0002	21.3	23.2	0.020
29	45	2.14	850.4	82.0	1314.5	202.3	2166.9	2.8	0.0050	-14.5	-16.4	0.131
29	43	0.32	850.4	82.0	1311.4	10.7	2159.2	0.1	0.0001	-22.1	-19.5	0.016
29	42	-0.30	850.4	82.0	1294.7	124.9	2133.6	0.0	0.0000	-47.8	-36.2	0.008
28	46	-0.52	826.8	11.5	1354.1	37.9	2194.2	0.2	0.0003	12.8	-0.4	1.287
28	45	1.78	826.8	11.5	1314.5	202.3	2158.4	0.8	0.0014	-22.9	-39.9	0.045
27	46	14.66	824.4	6.9	1354.1	37.9	2190.9	282.6	0.5027	9.5	-2.9	5.115
27	45	-59.05	824.4	6.9	1314.5	202.3	2135.7	177.2	0.3153	-42.4	-45.6	1.392
27	44	-0.75	824.4	6.9	1405.4	211.9	2207.1	0.0	0.0000	48.5	25.8	0.015
27	43	-5.24	824.4	6.9	1311.4	10.7	2143.1	0.5	0.0009	-45.6	-38.2	0.115

i	j	K_{ijk} / cm^{-1}	ω(i) / cm^{-1}	I(i) / km mol^{-1}	ω(j) / cm^{-1}	I(j) / km mol^{-1}	ω(ij) / cm^{-1}	I(ij) / km mol^{-1}	I(ij) / I(k)	Δω'	Δω	TFR
27	42	8.80	824.4	6.9	1294.7	124.9	2116.9	1.2	0.0021	-64.4	-62.3	0.141
27	41	-1.28	824.4	6.9	1185.8	21.1	2056.2	0.0	0.0000	-125.1	-171.2	0.007
27	40	5.58	824.4	6.9	1379.4	7.2	2077.4	0.0	0.0001	-103.9	22.4	0.249
26	47	0.22	801.7	3.2	1441.7	73.1	2259.3	0.1	0.0001	77.9	62.0	0.004
26	46	0.72	801.7	3.2	1354.1	37.9	2172.2	4.5	0.0080	-9.1	-25.6	0.028
26	45	-4.18	801.7	3.2	1314.5	202.3	2136.6	1.5	0.0026	-44.7	-65.1	0.064
26	43	-0.29	801.7	3.2	1311.4	10.7	2128.0	0.0	0.0000	-53.4	-68.3	0.004
26	42	0.59	801.7	3.2	1294.7	124.9	2101.3	0.0	0.0000	-80.0	-85.0	0.007
26	40	0.45	801.7	3.2	1379.4	7.2	2064.3	0.0	0.0000	-117.1	-0.3	1.591
25	48	-0.28	770.9	2.6	1543.4	79.6	2308.2	0.0	0.0001	126.8	133.0	0.002
25	46	-1.95	770.9	2.6	1354.1	37.9	2133.8	0.8	0.0014	-47.5	-56.3	0.035
25	45	3.98	770.9	2.6	1314.5	202.3	2098.8	0.2	0.0003	-82.6	-95.9	0.042
25	43	0.41	770.9	2.6	1311.4	10.7	2089.7	0.0	0.0000	-91.7	-99.0	0.004
25	42	-0.68	770.9	2.6	1294.7	124.9	2065.4	0.0	0.0000	-116.0	-115.8	0.006
24	48	0.25	726.7	9.4	1543.4	79.6	2262.8	0.0	0.0000	81.5	88.8	0.003
24	45	-0.60	726.7	9.4	1314.5	202.3	2054.1	0.1	0.0001	-127.2	-140.1	0.004
24	43	-0.24	726.7	9.4	1311.4	10.7	2045.8	0.0	0.0000	-135.5	-143.2	0.002
23	49	-2.43	732.7	7.9	1585.4	6.5	2318.8	0.1	0.0002	137.5	136.8	0.018
23	48	6.53	732.7	7.9	1543.4	79.6	2272.1	5.4	0.0096	90.8	94.8	0.069
23	47	1.17	732.7	7.9	1441.7	73.1	2184.5	0.1	0.0002	3.1	-6.9	0.171
23	46	10.49	732.7	7.9	1354.1	37.9	2098.0	0.3	0.0006	-83.4	-94.5	0.111
23	45	-41.20	732.7	7.9	1314.5	202.3	2057.7	7.2	0.0128	-123.6	-134.1	0.307
23	44	-0.36	732.7	7.9	1405.4	211.9	2118.2	0.0	0.0000	-63.2	-43.2	0.008
23	43	-4.90	732.7	7.9	1311.4	10.7	2054.2	0.2	0.0003	-127.1	-137.2	0.036
21	49	0.24	652.3	3.6	1585.4	6.5	2237.0	0.0	0.0000	55.6	56.4	0.004
21	48	0.46	652.3	3.6	1543.4	79.6	2188.7	0.0	0.0001	7.4	14.4	0.032
21	47	0.25	652.3	3.6	1441.7	73.1	2100.7	0.1	0.0001	-80.6	-87.3	0.003
20	49	0.92	648.3	1.9	1585.4	6.5	2233.4	0.1	0.0001	52.0	52.4	0.018
20	48	-2.23	648.3	1.9	1543.4	79.6	2185.6	0.5	0.0008	4.2	10.4	0.214
20	47	-0.88	648.3	1.9	1441.7	73.1	2097.1	0.0	0.0001	-84.2	-91.3	0.010
19	49	-0.23	626.9	0.4	1585.4	6.5	2212.3	0.0	0.0000	31.0	31.0	0.008
17	50	0.81	551.6	13.0	1608.1	8.1	2156.3	0.8	0.0014	-25.0	-21.7	0.037
17	48	-0.84	551.6	13.0	1543.4	79.6	2088.6	0.1	0.0001	-92.7	-86.3	0.010
15	52	-0.29	516.4	11.4	1707.9	705.9	2231.2	0.0	0.0001	49.8	43.0	0.007
14	53	-0.26	467.8	0.3	1776.4	0.4	2248.5	0.0	0.0000	67.2	62.9	0.004
14	50	0.31	467.8	0.3	1608.1	8.1	2071.4	0.0	0.0000	-109.9	-105.5	0.003
14	49	1.51	467.8	0.3	1585.4	6.5	2050.9	0.0	0.0001	-130.4	-128.2	0.012
11	52	0.33	373.3	1.1	1707.9	705.9	2081.5	0.1	0.0002	-99.8	-100.1	0.003
1	54	1.31	34.9	0.5	2181.3	562.0	2208.7	1.8	0.0032	27.3	34.9	0.038

6-311++G(d,p)

i	j	K_{ijk} / cm^{-1}	ω(i) / cm^{-1}	I(i) / km mol^{-1}	ω(j) / cm^{-1}	I(j) / km mol^{-1}	ω(ij) / cm^{-1}	I(ij) / km mol^{-1}	I(ij) / I(k)	Δω'	Δω	TFR
39	39	37.24	1130.9	25.8	1130.9	25.8	2289.6	13.7	0.0223	114.0	86.2	0.432
38	38	2.20	1154.0	6.6	1154.0	6.6	2272.2	0.4	0.0006	96.6	132.3	0.017
37	37	1.41	1116.5	72.1	1116.5	72.1	2285.4	0.0	0.0000	109.8	57.5	0.024
36	36	0.27	1081.1	17.1	1081.1	17.1	2166.1	0.4	0.0006	-9.5	-13.3	0.020
35	35	0.65	1032.3	3.4	1032.3	3.4	2066.5	0.1	0.0002	-109.1	-111.1	0.006
34	34	-0.48	1034.2	6.6	1034.2	6.6	2078.8	0.0	0.0000	-96.8	-107.2	0.004
38	39	1.84	1154.0	6.6	1130.9	25.8	2283.3	0.1	0.0002	107.7	109.3	0.017

i	j	K_{ijk} / cm^{-1}	ω(i) / cm^{-1}	I(i) / km mol^{-1}	ω(j) / cm^{-1}	I(j) / km mol^{-1}	ω(ij) / cm^{-1}	I(ij) / km mol^{-1}	I(ij) / I(k)	Δω'	Δω	TFR
37	39	0.84	1116.5	72.1	1130.9	25.8	2289.0	0.0	0.0000	113.4	71.8	0.012
37	38	-0.54	1116.5	72.1	1154.0	6.6	2278.6	0.3	0.0005	103.0	94.9	0.006
36	41	0.44	1081.1	17.1	1193.9	17.7	2300.6	0.1	0.0001	125.0	99.5	0.004
36	40	-0.86	1081.1	17.1	1283.2	6.1	2309.7	0.0	0.0000	134.1	188.8	0.005
36	39	-2.84	1081.1	17.1	1130.9	25.8	2226.4	17.4	0.0284	50.8	36.5	0.078
35	39	0.41	1032.3	3.4	1130.9	25.8	2179.6	0.1	0.0001	4.0	-12.4	0.033
35	38	-0.66	1032.3	3.4	1154.0	6.6	2168.4	1.3	0.0022	-7.2	10.6	0.062
35	37	0.34	1032.3	3.4	1116.5	72.1	2174.6	0.5	0.0009	-1.0	-26.8	0.013
34	41	0.32	1034.2	6.6	1193.9	17.7	2260.3	0.0	0.0000	84.7	52.6	0.006
34	40	-0.92	1034.2	6.6	1283.2	6.1	2271.1	16.2	0.0265	95.5	141.8	0.006
34	39	-2.76	1034.2	6.6	1130.9	25.8	2185.8	0.7	0.0012	10.2	-10.5	0.264
34	37	0.69	1034.2	6.6	1116.5	72.1	2182.6	0.0	0.0001	7.0	-24.9	0.028
33	45	-0.42	954.1	3.6	1320.4	192.5	2268.2	0.0	0.0000	92.6	99.0	0.004
33	39	0.26	954.1	3.6	1130.9	25.8	2090.1	0.0	0.0000	-85.4	-90.6	0.003
31	44	-0.50	945.3	2.5	1377.0	59.7	2303.9	0.0	0.0001	128.3	146.7	0.003
31	43	0.57	945.3	2.5	1310.6	2.4	2258.0	0.4	0.0006	82.5	80.2	0.007
31	42	-0.84	945.3	2.5	1292.4	188.8	2237.5	0.1	0.0002	61.9	62.1	0.013
31	41	0.21	945.3	2.5	1193.9	17.7	2163.4	0.3	0.0005	-12.2	-36.4	0.006
31	40	-0.42	945.3	2.5	1283.2	6.1	2174.2	0.0	0.0000	-1.3	52.9	0.008
31	39	-1.24	945.3	2.5	1130.9	25.8	2090.8	0.0	0.0000	-84.7	-99.4	0.012
30	45	0.42	908.5	1.8	1320.4	192.5	2241.2	0.0	0.0000	65.6	53.3	0.008
30	37	-0.23	908.5	1.8	1116.5	72.1	2059.4	0.1	0.0001	-116.2	-150.6	0.001
29	46	-0.46	845.6	75.5	1351.8	0.9	2191.7	0.1	0.0002	16.1	21.8	0.021
29	45	2.13	845.6	75.5	1320.4	192.5	2153.4	2.8	0.0046	-22.2	-9.5	0.223
29	43	0.32	845.6	75.5	1310.6	2.4	2146.2	0.1	0.0001	-29.3	-19.4	0.016
29	42	-0.30	845.6	75.5	1292.4	188.8	2124.0	0.0	0.0000	-51.6	-37.5	0.008
28	46	-0.54	823.1	10.7	1351.8	0.9	2193.3	0.2	0.0003	17.8	-0.7	0.762
28	45	1.90	823.1	10.7	1320.4	192.5	2155.2	0.9	0.0014	-20.4	-32.1	0.059
28	42	-0.23	823.1	10.7	1292.4	188.8	2126.3	0.0	0.0000	-49.3	-60.1	0.004
28	40	-0.24	823.1	10.7	1283.2	6.1	2061.7	0.0	0.0000	-113.9	-69.3	0.003
27	47	-0.21	816.5	5.3	1437.8	13.4	2255.9	0.0	0.0001	80.3	78.7	0.003
27	46	-14.61	816.5	5.3	1351.8	0.9	2180.8	280.2	0.4566	5.2	-7.3	2.010
27	45	58.96	816.5	5.3	1320.4	192.5	2125.6	127.1	0.2071	-50.0	-38.6	1.526
27	44	0.64	816.5	5.3	1377.0	59.7	2175.3	0.0	0.0000	-0.2	17.9	0.036
27	43	5.20	816.5	5.3	1310.6	2.4	2131.1	0.5	0.0008	-44.5	-48.5	0.107
27	42	-8.79	816.5	5.3	1292.4	188.8	2108.3	1.2	0.0019	-67.2	-66.6	0.132
27	41	1.26	816.5	5.3	1193.9	17.7	2036.4	0.0	0.0000	-139.2	-165.1	0.008
27	40	-5.58	816.5	5.3	1283.2	6.1	2046.3	0.0	0.0001	-129.2	-75.9	0.074
26	48	0.43	768.9	9.1	1526.2	135.5	2298.2	0.0	0.0000	122.6	119.5	0.004
26	47	0.23	768.9	9.1	1437.8	13.4	2215.3	0.1	0.0001	39.7	31.1	0.007
26	46	0.85	768.9	9.1	1351.8	0.9	2136.1	5.2	0.0085	-39.4	-54.9	0.015
26	45	-4.70	768.9	9.1	1320.4	192.5	2097.9	1.8	0.0030	-77.7	-86.3	0.054
26	43	-0.34	768.9	9.1	1310.6	2.4	2089.9	0.0	0.0000	-85.7	-96.2	0.004
26	42	0.67	768.9	9.1	1292.4	188.8	2066.7	0.0	0.0000	-108.9	-114.3	0.006
25	48	-0.28	770.3	2.7	1526.2	135.5	2294.3	0.0	0.0001	118.8	120.9	0.002
25	46	-1.94	770.3	2.7	1351.8	0.9	2131.1	0.8	0.0013	-44.5	-53.5	0.036
25	45	3.96	770.3	2.7	1320.4	192.5	2093.6	0.2	0.0003	-82.0	-84.9	0.047
25	43	0.40	770.3	2.7	1310.6	2.4	2084.9	0.0	0.0000	-90.6	-94.7	0.004
25	42	-0.68	770.3	2.7	1292.4	188.8	2064.1	0.0	0.0000	-111.5	-112.9	0.006
24	48	0.23	720.1	4.2	1526.2	135.5	2242.9	0.0	0.0000	67.4	70.8	0.003
24	45	-0.50	720.1	4.2	1320.4	192.5	2042.9	0.1	0.0001	-132.7	-135.0	0.004
24	43	-0.23	720.1	4.2	1310.6	2.4	2035.1	0.0	0.0000	-140.4	-144.9	0.002
23	50	0.39	722.1	16.5	1601.8	4.8	2322.4	0.0	0.0000	146.8	148.3	0.003
23	49	2.42	722.1	16.5	1579.9	5.6	2302.4	0.1	0.0001	126.8	126.4	0.019
23	48	-6.53	722.1	16.5	1526.2	135.5	2245.7	5.4	0.0087	70.2	72.8	0.090
23	47	-1.19	722.1	16.5	1437.8	13.4	2162.2	0.1	0.0002	-13.4	-15.6	0.076

i	j	K_{ijk} / cm^{-1}	ω(i) / cm^{-1}	I(i) / km mol^{-1}	ω(j) / cm^{-1}	I(j) / km mol^{-1}	ω(ij) / cm^{-1}	I(ij) / km mol^{-1}	I(ij) / I(k)	Δω'	Δω	TFR
23	46	-10.47	722.1	16.5	1351.8	0.9	2082.9	0.3	0.0005	-92.6	-101.7	0.103
23	45	41.23	722.1	16.5	1320.4	192.5	2040.2	7.1	0.0116	-135.4	-133.0	0.310
23	44	0.28	722.1	16.5	1377.0	59.7	2081.3	0.0	0.0000	-94.3	-76.5	0.004
23	43	4.86	722.1	16.5	1310.6	2.4	2037.2	0.2	0.0002	-138.4	-142.9	0.034
21	49	0.23	651.1	3.4	1579.9	5.6	2232.2	0.0	0.0000	56.6	55.4	0.004
21	48	0.48	651.1	3.4	1526.2	135.5	2174.3	0.1	0.0001	-1.3	1.7	0.280
21	47	0.25	651.1	3.4	1437.8	13.4	2090.3	0.1	0.0001	-85.3	-86.7	0.003
20	49	0.92	645.2	1.4	1579.9	5.6	2226.6	0.1	0.0001	51.0	49.5	0.019
20	48	-2.23	645.2	1.4	1526.2	135.5	2169.1	0.5	0.0008	-6.5	-4.2	0.534
20	47	-0.88	645.2	1.4	1437.8	13.4	2084.7	0.0	0.0001	-90.9	-92.6	0.010
19	49	-0.23	625.0	0.5	1579.9	5.6	2206.9	0.0	0.0000	31.3	29.3	0.008
17	50	-0.81	549.3	12.2	1601.8	4.8	2150.7	0.8	0.0013	-24.9	-24.5	0.033
17	48	0.84	549.3	12.2	1526.2	135.5	2073.0	0.1	0.0001	-102.5	-100.0	0.008
15	52	-0.29	501.7	5.0	1707.7	667.1	2209.3	0.0	0.0001	33.8	33.9	0.009
14	53	0.25	456.9	0.1	1775.2	0.5	2239.2	0.0	0.0000	63.6	56.5	0.005
14	50	-0.30	456.9	0.1	1601.8	4.8	2058.6	0.0	0.0000	-117.0	-116.9	0.003
14	49	-1.51	456.9	0.1	1579.9	5.6	2037.9	0.0	0.0001	-137.7	-138.8	0.011
11	52	0.33	367.7	1.4	1707.7	667.1	2075.6	0.1	0.0002	-100.0	-100.2	0.003
1	54	1.31	-84.3	10.7	2175.6	613.7	2078.7	1.7	0.0028	-96.9	-84.3	0.016

6-311++G(df,pd)

i	j	K_{ijk} / cm^{-1}	ω(i) / cm^{-1}	I(i) / km mol^{-1}	ω(j) / cm^{-1}	I(j) / km mol^{-1}	ω(ij) / cm^{-1}	I(ij) / km mol^{-1}	I(ij) / I(k)	Δω'	Δω	TFR
39	39	37.89	1135.0	20.8	1135.0	20.8	2267.7	12.7	0.0197	89.4	91.6	0.414
38	38	1.99	1144.6	27.5	1144.6	27.5	2276.6	0.2	0.0003	98.2	110.9	0.018
37	37	1.63	1107.5	75.1	1107.5	75.1	2231.8	0.1	0.0001	53.4	36.6	0.045
36	36	0.32	1086.5	16.8	1086.5	16.8	2178.2	0.4	0.0006	-0.2	-5.3	0.061
35	35	0.68	1033.7	11.7	1033.7	11.7	2065.8	0.1	0.0002	-112.6	-111.1	0.006
34	34	-0.50	1027.1	0.8	1027.1	0.8	2054.5	0.0	0.0000	-123.9	-124.1	0.004
38	39	2.18	1144.6	27.5	1135.0	20.8	2273.3	0.1	0.0002	94.9	101.2	0.022
37	39	0.87	1107.5	75.1	1135.0	20.8	2251.4	0.0	0.0001	73.0	64.1	0.014
37	38	-0.63	1107.5	75.1	1144.6	27.5	2253.2	0.3	0.0005	74.8	73.7	0.009
36	41	0.42	1086.5	16.8	1198.6	15.0	2294.4	0.1	0.0001	116.0	106.8	0.004
36	40	-0.91	1086.5	16.8	1217.8	2.9	2294.7	0.0	0.0000	116.3	126.0	0.007
36	39	-3.08	1086.5	16.8	1135.0	20.8	2221.6	5.5	0.0085	43.2	43.1	0.071
35	42	0.41	1033.7	11.7	1291.8	69.4	2325.3	0.1	0.0002	146.9	147.0	0.003
35	39	0.45	1033.7	11.7	1135.0	20.8	2168.6	0.1	0.0002	-9.8	-9.7	0.046
35	38	-0.60	1033.7	11.7	1144.6	27.5	2169.9	1.1	0.0017	-8.4	-0.1	6.645
35	37	0.47	1033.7	11.7	1107.5	75.1	2147.9	0.9	0.0014	-30.5	-37.3	0.013
34	42	-1.24	1027.1	0.8	1291.8	69.4	2316.0	0.0	0.0000	137.6	140.5	0.009
34	41	0.25	1027.1	0.8	1198.6	15.0	2235.1	0.0	0.0000	56.8	47.4	0.005
34	40	-0.82	1027.1	0.8	1217.8	2.9	2236.2	1.0	0.0015	57.8	66.6	0.012
34	39	-2.52	1027.1	0.8	1135.0	20.8	2162.1	0.8	0.0012	-16.3	-16.2	0.155
34	38	0.31	1027.1	0.8	1144.6	27.5	2165.8	0.0	0.0000	-12.5	-6.6	0.047
34	37	0.63	1027.1	0.8	1107.5	75.1	2143.7	0.1	0.0001	-34.7	-43.8	0.015
34	35	0.23	1027.1	0.8	1033.7	11.7	2060.7	0.0	0.0000	-117.7	-117.6	0.002
33	45	-0.41	972.7	0.1	1319.8	186.1	2293.4	0.0	0.0000	115.1	114.2	0.004
33	39	0.24	972.7	0.1	1135.0	20.8	2107.5	0.0	0.0000	-70.8	-70.7	0.003
31	45	0.42	963.7	26.0	1319.8	186.1	2284.6	0.0	0.0000	106.2	105.1	0.004
31	37	-0.25	963.7	26.0	1107.5	75.1	2079.9	0.1	0.0001	-98.5	-107.2	0.002
30	44	-0.62	947.3	19.2	1341.6	50.5	2288.7	0.0	0.0000	110.4	110.5	0.006

i	j	K_{ijk} / cm^{-1}	ω(i) / cm^{-1}	I(i) / km mol^{-1}	ω(j) / cm^{-1}	I(j) / km mol^{-1}	ω(ij) / cm^{-1}	I(ij) / km mol^{-1}	I(ij) / I(k)	Δω'	Δω	TFR
30	43	-0.37	947.3	19.2	1320.2	3.2	2264.8	0.4	0.0007	86.5	89.2	0.004
30	42	-0.96	947.3	19.2	1291.8	69.4	2237.5	0.0	0.0001	59.2	60.7	0.016
30	40	0.41	947.3	19.2	1217.8	2.9	2155.3	0.0	0.0000	-23.0	-13.2	0.031
30	39	1.33	947.3	19.2	1135.0	20.8	2082.2	0.0	0.0000	-96.2	-96.1	0.014
29	46	-0.34	855.2	56.6	1359.0	88.5	2209.3	0.1	0.0001	30.9	35.8	0.009
29	45	1.66	855.2	56.6	1319.8	186.1	2167.2	12.4	0.0192	-11.2	-3.4	0.486
29	43	0.21	855.2	56.6	1320.2	3.2	2167.4	0.1	0.0001	-10.9	-3.0	0.072
29	42	0.26	855.2	56.6	1291.8	69.4	2137.7	0.0	0.0000	-40.7	-31.4	0.008
28	46	-0.54	831.1	34.9	1359.0	88.5	2193.6	0.1	0.0002	15.2	11.7	0.046
28	45	1.85	831.1	34.9	1319.8	186.1	2151.9	1.8	0.0028	-26.4	-27.5	0.067
27	46	-14.09	819.3	7.7	1359.0	88.5	2187.7	180.1	0.2789	9.3	-0.1	105.926
27	45	55.34	819.3	7.7	1319.8	186.1	2130.6	127.4	0.1973	-47.7	-39.3	1.408
27	43	2.86	819.3	7.7	1320.2	3.2	2142.4	0.2	0.0003	-35.9	-38.9	0.074
27	42	8.26	819.3	7.7	1291.8	69.4	2112.0	1.1	0.0017	-66.4	-67.3	0.123
27	41	0.87	819.3	7.7	1198.6	15.0	2030.1	0.0	0.0000	-148.2	-160.5	0.005
27	40	-5.33	819.3	7.7	1217.8	2.9	2031.3	0.0	0.0001	-147.0	-141.3	0.038
26	46	4.99	831.8	3.2	1359.0	88.5	2199.5	29.9	0.0462	21.1	12.4	0.402
26	45	-20.91	831.8	3.2	1319.8	186.1	2154.6	63.0	0.0975	-23.8	-26.8	0.781
26	43	-1.02	831.8	3.2	1320.2	3.2	2156.8	0.0	0.0000	-21.6	-26.3	0.039
26	42	-3.08	831.8	3.2	1291.8	69.4	2126.3	0.2	0.0003	-52.1	-54.8	0.056
26	41	-0.41	831.8	3.2	1198.6	15.0	2044.5	0.0	0.0000	-133.9	-148.0	0.003
26	40	2.03	831.8	3.2	1217.8	2.9	2047.8	0.0	0.0000	-130.6	-128.8	0.016
25	48	-0.28	773.6	3.2	1514.4	144.9	2287.7	0.0	0.0001	109.3	109.6	0.003
25	46	-1.99	773.6	3.2	1359.0	88.5	2135.8	0.8	0.0013	-42.6	-45.8	0.043
25	45	4.03	773.6	3.2	1319.8	186.1	2094.5	0.2	0.0003	-83.8	-85.0	0.047
25	43	0.24	773.6	3.2	1320.2	3.2	2093.1	0.0	0.0000	-85.2	-84.5	0.003
25	42	0.70	773.6	3.2	1291.8	69.4	2065.3	0.0	0.0000	-113.1	-113.0	0.006
24	45	-0.38	731.3	0.7	1319.8	186.1	2052.4	0.1	0.0001	-126.0	-127.3	0.003
23	50	0.36	712.5	13.2	1602.0	7.3	2317.9	0.0	0.0000	139.5	136.1	0.003
23	49	2.30	712.5	13.2	1578.3	3.8	2293.1	0.1	0.0001	114.7	112.4	0.020
23	48	-6.42	712.5	13.2	1514.4	144.9	2226.8	3.3	0.0052	48.4	48.5	0.132
23	47	-1.00	712.5	13.2	1433.2	0.1	2146.7	0.1	0.0002	-31.7	-32.6	0.031
23	46	-10.75	712.5	13.2	1359.0	88.5	2076.1	0.4	0.0005	-102.3	-106.9	0.101
23	45	41.55	712.5	13.2	1319.8	186.1	2029.5	7.7	0.0120	-148.8	-146.1	0.284
23	44	0.28	712.5	13.2	1341.6	50.5	2054.6	0.0	0.0000	-123.8	-124.3	0.002
23	43	2.85	712.5	13.2	1320.2	3.2	2034.0	0.1	0.0001	-144.4	-145.6	0.020
21	49	0.35	649.8	2.1	1578.3	3.8	2226.1	0.0	0.0000	47.7	49.7	0.007
20	49	-0.81	646.1	3.2	1578.3	3.8	2226.6	0.1	0.0001	48.2	46.0	0.018
20	48	2.20	646.1	3.2	1514.4	144.9	2160.2	0.7	0.0011	-18.2	-17.9	0.123
20	47	0.84	646.1	3.2	1433.2	0.1	2079.1	0.0	0.0000	-99.2	-99.0	0.008
19	49	-0.24	613.8	1.9	1578.3	3.8	2198.6	0.0	0.0000	20.2	13.7	0.018
17	50	-0.81	549.3	11.1	1602.0	7.3	2155.3	0.9	0.0014	-23.0	-27.0	0.030
17	48	0.78	549.3	11.1	1514.4	144.9	2063.7	0.1	0.0001	-114.7	-114.7	0.007
15	52	-0.25	525.0	6.8	1711.3	742.9	2251.6	0.0	0.0000	73.2	57.9	0.004
14	53	0.25	450.9	0.2	1774.6	0.5	2236.0	0.0	0.0000	57.6	47.2	0.005
14	50	-0.31	450.9	0.2	1602.0	7.3	2055.4	0.0	0.0000	-122.9	-125.4	0.002
14	49	-1.52	450.9	0.2	1578.3	3.8	2031.4	0.0	0.0001	-147.0	-149.2	0.010
11	52	0.32	371.2	1.6	1711.3	742.9	2082.2	0.1	0.0002	-96.2	-96.0	0.003
10	53	-0.29	339.3	3.5	1774.6	0.5	2124.6	0.0	0.0000	-53.7	-64.4	0.005
5	54	4.25	132.4	7.4	2178.4	645.8	2297.2	0.3	0.0005	118.8	132.4	0.032
1	54	1.25	19.4	0.5	2178.4	645.8	2189.2	1.8	0.0028	10.9	19.4	0.065

APPENDIX G

VIBRATIONAL MODES OF 4-AZIDO-N-PHENYLMALEIMIDE (ISOMER 2) THAT OCCUR WITHIN ±130 CM^{-1} FROM THE FUNDAMENTAL VIBRATION FOR SEVEN BASIS SETS IN NNDMA

i, j, k : vibrational modes ; where k = 54 (azide asymmetric stretch)

i = j → overtone & i ≠ j → combination band

K_{ijk} : cubic force constant

TFR : third-order Fermi resonance

ω(i), ω(j), ω(k) : anharmonic frequencies of i, j & k th mode

ω(ij) : anharmonic frequency of ij th mode

I(i), I(j), I(k) : anharmonic intensities of i, j & k th mode

I(ij) : anharmonic intensity of ij th mode

Δω’ : ω(ij) - ω(k)

Δω : ω(i) + ω(j) - ω(k)

6-31G(d,p)

i	j	K_{ijk} / cm^{-1}	ω(i) / cm^{-1}	I(i) / km mol^{-1}	ω(j) / cm^{-1}	I(j) / km mol^{-1}	ω(ij) / cm^{-1}	I(ij) / km mol^{-1}	I(ij) / I(k)	Δω’	Δω	TFR
39	39	-36.23	1139.0	66.0	1139.0	66.0	2276.4	12.2	0.0278	73.7	75.2	0.482
38	38	-3.89	1141.4	13.9	1141.4	13.9	2267.7	0.3	0.0007	64.9	80.0	0.049
37	37	-1.26	1119.1	28.1	1119.1	28.1	2251.0	0.0	0.0000	48.2	35.4	0.036
36	36	-0.26	1057.2	9.7	1057.2	9.7	2102.3	0.3	0.0008	-100.5	-88.4	0.003
39	40	-13.95	1139.0	66.0	1195.8	10.7	2334.9	1.8	0.0042	132.1	132.0	0.106
38	40	-2.62	1141.4	13.9	1195.8	10.7	2332.2	0.3	0.0006	129.4	134.4	0.020
38	39	-7.19	1141.4	13.9	1139.0	66.0	2273.9	1.6	0.0036	71.1	77.6	0.093
37	39	-1.94	1119.1	28.1	1139.0	66.0	2264.2	0.0	0.0000	61.4	55.3	0.035
37	38	0.46	1119.1	28.1	1141.4	13.9	2259.0	0.4	0.0009	56.2	57.7	0.008
36	42	0.24	1057.2	9.7	1290.3	3.7	2331.7	0.1	0.0002	129.0	144.7	0.002
36	41	0.46	1057.2	9.7	1212.0	9.7	2264.8	0.1	0.0002	62.0	66.4	0.007
36	40	-0.75	1057.2	9.7	1195.8	10.7	2249.0	0.0	0.0000	46.2	50.2	0.015
36	39	-2.46	1057.2	9.7	1139.0	66.0	2192.9	218.3	0.4955	-9.9	-6.6	0.371
36	38	-0.47	1057.2	9.7	1141.4	13.9	2188.1	2.4	0.0054	-14.6	-4.2	0.110
35	42	-0.25	1024.6	4.6	1290.3	3.7	2318.5	0.7	0.0016	115.8	112.1	0.002
35	39	-0.73	1024.6	4.6	1139.0	66.0	2167.5	0.2	0.0004	-35.3	-39.2	0.019
35	38	0.69	1024.6	4.6	1141.4	13.9	2160.4	1.4	0.0031	-42.3	-36.8	0.019

i	j	K_{ijk} / cm^{-1}	ω(i) / cm^{-1}	I(i) / km mol^{-1}	ω(j) / cm^{-1}	I(j) / km mol^{-1}	ω(ij) / cm^{-1}	I(ij) / km mol^{-1}	I(ij) / I(k)	Δω’	Δω	TFR
35	37	-0.33	1024.6	4.6	1119.1	28.1	2152.1	0.5	0.0011	-50.6	-59.1	0.006
34	44	-0.60	1018.5	0.6	1313.2	40.8	2332.5	0.1	0.0003	129.7	128.9	0.005
34	43	-0.24	1018.5	0.6	1318.1	210.0	2335.7	0.1	0.0002	132.9	133.8	0.002
34	41	-0.55	1018.5	0.6	1212.0	9.7	2230.3	0.0	0.0000	27.5	27.7	0.020
34	40	1.29	1018.5	0.6	1195.8	10.7	2214.1	2.7	0.0061	11.3	11.5	0.112
34	39	3.63	1018.5	0.6	1139.0	66.0	2157.4	0.8	0.0017	-45.3	-45.3	0.080
34	38	0.36	1018.5	0.6	1141.4	13.9	2153.3	0.0	0.0001	-49.5	-42.9	0.008
34	37	-0.83	1018.5	0.6	1119.1	28.1	2142.9	0.1	0.0001	-59.9	-65.2	0.013
33	45	-0.20	956.9	1.2	1331.4	40.4	2285.4	0.0	0.0000	82.6	85.6	0.002
32	46	-0.21	961.9	15.5	1373.1	33.9	2331.4	0.0	0.0000	128.6	132.2	0.002
32	45	0.77	961.9	15.5	1331.4	40.4	2284.8	0.0	0.0000	82.0	90.5	0.008
32	44	-0.22	961.9	15.5	1313.2	40.8	2272.5	0.0	0.0001	69.8	72.3	0.003
32	43	-0.66	961.9	15.5	1318.1	210.0	2275.3	0.0	0.0001	72.6	77.2	0.008
32	41	-0.23	961.9	15.5	1212.0	9.7	2168.1	0.2	0.0005	-34.6	-28.9	0.008
32	40	0.25	961.9	15.5	1195.8	10.7	2153.0	0.0	0.0000	-49.8	-45.1	0.006
32	39	0.80	961.9	15.5	1139.0	66.0	2096.3	0.0	0.0000	-106.5	-101.9	0.008
32	38	0.29	961.9	15.5	1141.4	13.9	2091.6	0.1	0.0001	-111.2	-99.5	0.003
31	46	-0.29	951.9	2.8	1373.1	33.9	2328.8	0.0	0.0000	126.0	122.2	0.002
31	45	1.25	951.9	2.8	1331.4	40.4	2282.1	0.0	0.0000	79.4	80.5	0.016
31	43	-0.77	951.9	2.8	1318.1	210.0	2272.3	0.0	0.0000	69.5	67.2	0.011
31	39	0.58	951.9	2.8	1139.0	66.0	2093.6	0.0	0.0000	-109.2	-111.9	0.005
30	40	-0.23	942.9	0.8	1195.8	10.7	2140.9	0.0	0.0001	-61.9	-64.1	0.004
30	37	-0.32	942.9	0.8	1119.1	28.1	2070.0	0.1	0.0001	-132.8	-140.8	0.002
29	46	-0.76	840.1	52.2	1373.1	33.9	2213.8	0.4	0.0008	11.0	10.5	0.072
29	45	3.05	840.1	52.2	1331.4	40.4	2167.4	1.1	0.0025	-35.3	-31.2	0.098
29	44	0.64	840.1	52.2	1313.2	40.8	2156.0	0.0	0.0000	-46.7	-49.4	0.013
29	43	0.46	840.1	52.2	1318.1	210.0	2159.3	0.1	0.0002	-43.5	-44.6	0.010
28	46	0.61	825.5	43.7	1373.1	33.9	2198.9	8.3	0.0189	-3.9	-4.2	0.147
28	45	-2.68	825.5	43.7	1331.4	40.4	2153.1	0.4	0.0010	-49.7	-45.8	0.058
28	44	-0.60	825.5	43.7	1313.2	40.8	2141.1	0.0	0.0000	-61.7	-64.0	0.009
28	43	-0.32	825.5	43.7	1318.1	210.0	2143.6	0.0	0.0000	-59.2	-59.2	0.005
27	48	6.80	819.6	1.7	1515.5	108.1	2335.8	1.9	0.0043	133.0	132.3	0.051
27	47	0.48	819.6	1.7	1437.9	1.3	2260.5	0.0	0.0001	57.7	54.7	0.009
27	46	15.10	819.6	1.7	1373.1	33.9	2192.4	224.7	0.5099	-10.4	-10.1	1.494
27	45	-57.35	819.6	1.7	1331.4	40.4	2138.4	67.3	0.1528	-64.3	-51.8	1.107
27	44	-12.65	819.6	1.7	1313.2	40.8	2136.1	2.9	0.0065	-66.6	-70.0	0.181
27	43	-6.93	819.6	1.7	1318.1	210.0	2138.9	0.7	0.0016	-63.9	-65.1	0.107
27	42	-2.76	819.6	1.7	1290.3	3.7	2114.2	0.1	0.0003	-88.6	-92.9	0.030
26	48	-0.30	820.0	3.0	1515.5	108.1	2334.2	0.0	0.0000	131.4	132.7	0.002
26	46	-0.83	820.0	3.0	1373.1	33.9	2194.0	6.6	0.0150	-8.8	-9.7	0.085
26	45	1.43	820.0	3.0	1331.4	40.4	2147.3	0.1	0.0001	-55.4	-51.4	0.028
26	44	0.24	820.0	3.0	1313.2	40.8	2136.5	0.0	0.0001	-66.3	-69.5	0.004
26	43	0.40	820.0	3.0	1318.1	210.0	2138.6	0.0	0.0000	-64.2	-64.7	0.006
25	48	-0.46	756.2	4.2	1515.5	108.1	2271.7	0.1	0.0001	68.9	69.0	0.007
25	46	-2.47	756.2	4.2	1373.1	33.9	2129.6	0.8	0.0017	-73.2	-73.4	0.034
25	45	5.14	756.2	4.2	1331.4	40.4	2084.0	0.1	0.0003	-118.8	-115.1	0.045
25	44	1.25	756.2	4.2	1313.2	40.8	2072.2	0.0	0.0001	-130.5	-133.3	0.009
25	43	0.76	756.2	4.2	1318.1	210.0	2074.3	0.0	0.0000	-128.5	-128.4	0.006
24	48	0.29	718.8	12.1	1515.5	108.1	2231.0	0.0	0.0001	28.2	31.5	0.009
23	50	-0.61	708.2	15.2	1612.3	1.7	2322.7	0.0	0.0001	119.9	117.7	0.005
23	49	-2.36	708.2	15.2	1596.2	2.2	2306.1	0.1	0.0002	103.4	101.6	0.023
23	48	6.71	708.2	15.2	1515.5	108.1	2225.7	9.9	0.0225	22.9	20.9	0.321
23	47	1.31	708.2	15.2	1437.9	1.3	2150.0	0.1	0.0002	-52.8	-56.7	0.023
23	46	10.50	708.2	15.2	1373.1	33.9	2084.0	0.2	0.0005	-118.8	-121.5	0.086
21	50	-0.27	645.3	4.5	1612.3	1.7	2255.4	0.0	0.0000	52.6	54.8	0.005
21	48	1.09	645.3	4.5	1515.5	108.1	2158.5	0.1	0.0002	-44.3	-42.0	0.026

i	j	K_{ijk} / cm^{-1}	ω(i) / cm^{-1}	I(i) / km mol^{-1}	ω(j) / cm^{-1}	I(j) / km mol^{-1}	ω(ij) / cm^{-1}	I(ij) / km mol^{-1}	I(ij) / I(k)	Δω'	Δω	TFR
21	47	0.40	645.3	4.5	1437.9	1.3	2082.6	0.1	0.0002	-120.1	-119.7	0.003
20	49	0.93	642.8	1.0	1596.2	2.2	2240.1	0.1	0.0003	37.3	36.3	0.026
20	48	-1.99	642.8	1.0	1515.5	108.1	2158.1	0.2	0.0004	-44.7	-44.4	0.045
20	47	-0.96	642.8	1.0	1437.9	1.3	2082.0	0.1	0.0002	-120.8	-122.1	0.008
18	52	0.26	584.4	6.2	1740.5	75.4	2323.1	0.0	0.0001	120.4	122.2	0.002
17	50	0.90	546.7	10.9	1612.3	1.7	2158.2	0.9	0.0019	-44.6	-43.8	0.021
15	52	0.24	519.7	3.2	1740.5	75.4	2260.0	0.0	0.0001	57.3	57.5	0.004
5	54	-3.58	124.2	5.6	2202.8	440.6	2307.8	0.3	0.0007	105.0	124.2	0.029
2	54	-0.76	60.9	1.2	2202.8	440.6	2254.0	0.1	0.0003	51.2	60.9	0.012
1	54	0.82	14.9	0.3	2202.8	440.6	2209.6	1.4	0.0033	6.8	14.9	0.055

6-31+G(d,p)

i	j	K_{ijk} / cm^{-1}	ω(i) / cm^{-1}	I(i) / km mol^{-1}	ω(j) / cm^{-1}	I(j) / km mol^{-1}	ω(ij) / cm^{-1}	I(ij) / km mol^{-1}	I(ij) / I(k)	Δω'	Δω	TFR
39	39	-39.19	1131.9	9.9	1131.9	9.9	2254.7	15.7	0.0197	72.4	81.5	0.481
38	38	-2.55	1124.4	21.3	1124.4	21.3	2240.1	0.6	0.0007	57.7	66.4	0.038
37	37	-1.37	1116.7	9.4	1116.7	9.4	2256.4	0.0	0.0000	74.1	51.0	0.027
36	36	-0.26	1077.3	12.3	1077.3	12.3	2158.3	0.3	0.0004	-24.1	-27.7	0.009
35	35	-0.72	1033.2	13.5	1033.2	13.5	2064.9	0.1	0.0002	-117.5	-115.9	0.006
39	40	-12.78	1131.9	9.9	1187.7	4.7	2311.2	1.8	0.0023	128.8	137.3	0.093
38	40	-1.14	1124.4	21.3	1187.7	4.7	2306.6	0.1	0.0002	124.2	129.8	0.009
38	39	-3.19	1124.4	21.3	1131.9	9.9	2251.0	0.4	0.0005	68.6	74.0	0.043
37	39	-0.41	1116.7	9.4	1131.9	9.9	2254.2	0.0	0.0000	71.8	66.3	0.006
36	41	0.51	1077.3	12.3	1205.3	14.1	2282.4	0.1	0.0001	100.0	100.2	0.005
36	40	-0.88	1077.3	12.3	1187.7	4.7	2260.6	0.0	0.0000	78.2	82.7	0.011
36	39	-2.86	1077.3	12.3	1131.9	9.9	2206.0	13.0	0.0162	23.6	26.9	0.106
36	38	-0.25	1077.3	12.3	1124.4	21.3	2200.2	0.4	0.0005	17.8	19.3	0.013
35	39	-0.35	1033.2	13.5	1131.9	9.9	2161.7	0.1	0.0001	-20.7	-17.2	0.020
35	38	0.76	1033.2	13.5	1124.4	21.3	2151.7	2.2	0.0027	-30.7	-24.7	0.031
34	41	-0.39	1014.4	1.4	1205.3	14.1	2219.1	0.0	0.0000	36.7	37.2	0.010
34	40	1.02	1014.4	1.4	1187.7	4.7	2197.5	27.1	0.0339	15.1	19.7	0.052
34	39	3.32	1014.4	1.4	1131.9	9.9	2142.4	0.9	0.0012	-40.0	-36.1	0.092
34	37	-0.83	1014.4	1.4	1116.7	9.4	2140.7	0.0	0.0001	-41.7	-51.3	0.016
33	45	-0.53	959.4	1.4	1325.3	105.4	2278.3	0.0	0.0000	95.9	102.4	0.005
33	44	0.26	959.4	1.4	1305.9	149.2	2261.5	0.0	0.0000	79.2	82.9	0.003
33	39	0.42	959.4	1.4	1131.9	9.9	2083.6	0.0	0.0000	-98.8	-91.0	0.005
31	45	-0.96	950	7.9	1325.3	105.4	2272.3	0.0	0.0000	89.9	93.0	0.010
31	44	-0.59	950	7.9	1305.9	149.2	2255.4	0.0	0.0001	73.0	73.5	0.008
31	43	0.77	950	7.9	1313.3	59.1	2258.2	0.1	0.0001	75.8	80.9	0.009
31	41	0.31	950	7.9	1205.3	14.1	2152.6	0.4	0.0005	-29.8	-27.1	0.011
31	40	-0.48	950	7.9	1187.7	4.7	2132.5	0.0	0.0000	-49.9	-44.6	0.011
31	39	-0.97	950	7.9	1131.9	9.9	2077.8	0.0	0.0000	-104.6	-100.4	0.010
31	37	-0.27	950	7.9	1116.7	9.4	2075.3	0.1	0.0001	-107.0	-115.7	0.002
30	45	0.37	919.1	4.7	1325.3	105.4	2246.0	0.0	0.0000	63.6	62.1	0.006
29	46	-0.39	833.9	127.0	1385.4	89.5	2204.4	0.1	0.0002	22.0	36.9	0.011
29	45	2.26	833.9	127.0	1325.3	105.4	2149.9	2.0	0.0024	-32.5	-23.2	0.098
29	44	-0.58	833.9	127.0	1305.9	149.2	2134.5	0.1	0.0001	-47.9	-42.6	0.014
28	46	-4.00	826.5	301.8	1385.4	89.5	2203.1	7.6	0.0095	20.7	29.6	0.135
28	45	18.72	826.5	301.8	1325.3	105.4	2147.8	45.2	0.0566	-34.6	-30.5	0.614
28	44	-4.33	826.5	301.8	1305.9	149.2	2133.8	0.5	0.0006	-48.6	-50.0	0.087
28	43	1.90	826.5	301.8	1313.3	59.1	2136.0	0.1	0.0001	-46.3	-42.6	0.045
28	42	0.39	826.5	301.8	1305.4	0.6	2136.0	0.0	0.0000	-46.4	-50.5	0.008
27	46	11.39	817.9	174.9	1385.4	89.5	2196.1	75.4	0.0944	13.7	21.0	0.543

i	j	K_{ijk} / cm^{-1}	ω(i) / cm^{-1}	I(i) / km mol^{-1}	ω(j) / cm^{-1}	I(j) / km mol^{-1}	ω(ij) / cm^{-1}	I(ij) / km mol^{-1}	I(ij) / I(k)	Δω'	Δω	TFR
27	45	-54.27	817.9	174.9	1325.3	105.4	2129.7	108.0	0.1353	-52.7	-39.1	1.388
27	44	12.63	817.9	174.9	1305.9	149.2	2123.4	4.0	0.0050	-59.0	-58.6	0.216
27	43	-5.55	817.9	174.9	1313.3	59.1	2126.8	0.7	0.0008	-55.6	-51.2	0.108
27	42	-1.17	817.9	174.9	1305.4	0.6	2126.9	0.0	0.0001	-55.5	-59.1	0.020
26	48	0.63	776.4	12.6	1501.8	158.9	2283.3	0.0	0.0000	100.9	95.7	0.007
26	46	0.76	776.4	12.6	1385.4	89.5	2159.7	0.8	0.0010	-22.7	-20.6	0.037
26	45	-4.98	776.4	12.6	1325.3	105.4	2104.9	2.2	0.0028	-77.4	-80.7	0.062
26	44	1.12	776.4	12.6	1305.9	149.2	2089.6	0.1	0.0001	-92.8	-100.1	0.011
26	43	-0.53	776.4	12.6	1313.3	59.1	2091.8	0.0	0.0000	-90.6	-92.8	0.006
25	48	0.28	764.1	2.2	1501.8	158.9	2267.0	0.0	0.0000	84.6	83.4	0.003
25	46	1.66	764.1	2.2	1385.4	89.5	2140.4	0.6	0.0007	-41.9	-32.9	0.051
25	45	-3.75	764.1	2.2	1325.3	105.4	2087.2	0.1	0.0001	-95.2	-93.0	0.040
25	44	0.97	764.1	2.2	1305.9	149.2	2071.6	0.0	0.0000	-110.8	-112.5	0.009
25	43	-0.44	764.1	2.2	1313.3	59.1	2073.4	0.0	0.0000	-109.0	-105.1	0.004
23	50	-0.36	707.8	15.1	1604.6	25.2	2310.0	0.0	0.0000	127.6	130.0	0.003
23	49	-2.51	707.8	15.1	1584.2	1.2	2292.3	0.1	0.0001	109.9	109.6	0.023
23	48	6.45	707.8	15.1	1501.8	158.9	2208.5	6.7	0.0084	26.1	27.2	0.237
23	47	1.24	707.8	15.1	1425.2	2.8	2131.5	0.1	0.0002	-50.9	-49.4	0.025
23	46	8.75	707.8	15.1	1385.4	89.5	2083.2	0.3	0.0003	-99.2	-89.2	0.098
21	49	0.28	647.8	2.0	1584.2	1.2	2234.2	0.0	0.0000	51.8	49.7	0.006
21	48	0.50	647.8	2.0	1501.8	158.9	2149.6	0.1	0.0001	-32.8	-32.8	0.015
21	47	0.34	647.8	2.0	1425.2	2.8	2072.4	0.1	0.0001	-110.0	-109.4	0.003
20	49	1.15	643	2.1	1584.2	1.2	2229.6	0.1	0.0002	47.2	44.8	0.026
20	48	-2.51	643	2.1	1501.8	158.9	2144.5	0.5	0.0006	-37.9	-37.6	0.067
20	47	-0.96	643	2.1	1425.2	2.8	2067.0	0.1	0.0001	-115.4	-114.2	0.008
19	49	-0.27	615.9	0.5	1584.2	1.2	2203.9	0.0	0.0000	21.5	17.7	0.015
17	50	0.77	539.3	10.3	1604.6	25.2	2143.2	0.7	0.0009	-39.2	-38.4	0.020
15	52	0.34	502.1	5.7	1706.6	944.2	2208.8	0.0	0.0000	26.4	26.4	0.013
11	52	-0.38	364.6	0.6	1706.6	944.2	2071.1	0.1	0.0001	-111.3	-111.2	0.003
6	54	-6.18	137.6	6.9	2182.4	798.5	2311.9	0.1	0.0002	129.6	137.6	0.045
5	54	-4.73	99.7	6.3	2182.4	798.5	2271.5	0.4	0.0005	89.1	99.7	0.047
1	54	1.19	-27.8	2.0	2182.4	798.5	2145.0	1.9	0.0024	-37.4	-27.8	0.043

6-31++G(d,p)

i	j	K_{ijk} / cm^{-1}	ω(i) / cm^{-1}	I(i) / km mol^{-1}	ω(j) / cm^{-1}	I(j) / km mol^{-1}	ω(ij) / cm^{-1}	I(ij) / km mol^{-1}	I(ij) / I(k)	Δω'	Δω	TFR
39	39	39.14	1126.9	107.7	1126.9	107.7	2251.6	15.6	0.0196	69.0	71.2	0.550
38	38	2.51	1123.1	17.9	1123.1	17.9	2244.4	0.6	0.0007	61.8	63.5	0.040
37	37	1.37	1114.4	12.0	1114.4	12.0	2247.2	0.0	0.0000	64.6	46.1	0.030
36	36	0.26	1076.4	12.2	1076.4	12.2	2154.8	0.3	0.0004	-27.8	-29.8	0.009
35	35	0.71	1032.3	13.1	1032.3	13.1	2064.4	0.1	0.0002	-118.2	-117.9	0.006
39	40	12.95	1126.9	107.7	1188.5	5.4	2306.9	1.9	0.0024	124.3	132.8	0.098
38	40	1.06	1123.1	17.9	1188.5	5.4	2306.6	0.1	0.0002	124.0	128.9	0.008
38	39	2.93	1123.1	17.9	1126.9	107.7	2251.6	0.3	0.0004	69.0	67.3	0.044
37	39	0.40	1114.4	12.0	1126.9	107.7	2248.0	0.0	0.0000	65.4	58.6	0.007
36	41	-0.50	1076.4	12.2	1204.9	18.1	2279.8	0.1	0.0001	97.2	98.7	0.005
36	40	0.90	1076.4	12.2	1188.5	5.4	2256.5	0.0	0.0000	73.9	82.3	0.011
36	39	2.88	1076.4	12.2	1126.9	107.7	2202.8	12.5	0.0157	20.2	20.7	0.139
36	38	0.24	1076.4	12.2	1123.1	17.9	2200.7	0.4	0.0005	18.1	16.8	0.014
35	39	0.35	1032.3	13.1	1126.9	107.7	2160.0	0.1	0.0001	-22.6	-23.4	0.015

i	j	K_{ijk} / cm^{-1}	ω(i) / cm^{-1}	I(i) / km mol^{-1}	ω(j) / cm^{-1}	I(j) / km mol^{-1}	ω(ij) / cm^{-1}	I(ij) / km mol^{-1}	I(ij) / I(k)	Δω'	Δω	TFR
35	38	-0.76	1032.3	13.1	1123.1	17.9	2153.6	2.1	0.0027	-29.0	-27.2	0.028
34	44	-0.33	1013.0	1.0	1301.3	102.7	2314.8	0.1	0.0001	132.2	131.7	0.002
34	41	0.38	1013.0	1.0	1204.9	18.1	2216.9	0.0	0.0000	34.3	35.3	0.011
34	40	-1.03	1013.0	1.0	1188.5	5.4	2193.6	31.3	0.0394	11.0	18.9	0.055
34	39	-3.28	1013.0	1.0	1126.9	107.7	2139.5	0.9	0.0011	-43.1	-42.7	0.077
34	37	0.82	1013.0	1.0	1114.4	12.0	2134.8	0.0	0.0001	-47.8	-55.2	0.015
33	45	-0.51	958.0	1.9	1325.7	161.3	2274.3	0.0	0.0000	91.7	101.2	0.005
33	44	0.26	958.0	1.9	1301.3	102.7	2254.3	0.0	0.0000	71.7	76.7	0.003
33	39	0.42	958.0	1.9	1126.9	107.7	2077.8	0.0	0.0000	-104.8	-97.7	0.004
31	45	0.94	950.1	6.1	1325.7	161.3	2272.5	0.0	0.0000	89.9	93.2	0.010
31	44	0.60	950.1	6.1	1301.3	102.7	2252.4	0.0	0.0001	69.8	68.8	0.009
31	43	-0.77	950.1	6.1	1301.4	1.9	2253.6	0.1	0.0001	71.0	68.9	0.011
31	41	-0.30	950.1	6.1	1204.9	18.1	2151.8	0.4	0.0005	-30.8	-27.6	0.011
31	40	0.49	950.1	6.1	1188.5	5.4	2130.3	0.0	0.0000	-52.3	-44.0	0.011
31	39	0.99	950.1	6.1	1126.9	107.7	2076.4	0.0	0.0000	-106.2	-105.6	0.009
31	37	0.26	950.1	6.1	1114.4	12.0	2071.2	0.1	0.0001	-111.4	-118.1	0.002
30	45	0.35	914.4	2.3	1325.7	161.3	2243.9	0.0	0.0000	61.3	57.6	0.006
29	46	-0.37	831.4	76.8	1373.8	169.0	2199.2	0.1	0.0002	16.6	22.6	0.016
29	45	2.15	831.4	76.8	1325.7	161.3	2145.6	1.8	0.0023	-37.0	-25.5	0.084
29	44	-0.56	831.4	76.8	1301.3	102.7	2126.9	0.1	0.0001	-55.7	-49.9	0.011
28	46	-4.13	823.9	12.8	1373.8	169.0	2199.2	7.8	0.0098	16.6	15.1	0.273
28	45	19.46	823.9	12.8	1325.7	161.3	2144.6	48.8	0.0613	-38.0	-33.0	0.590
28	44	-4.56	823.9	12.8	1301.3	102.7	2127.5	0.6	0.0007	-55.1	-57.4	0.079
28	43	1.98	823.9	12.8	1301.4	1.9	2128.2	0.1	0.0001	-54.4	-57.3	0.035
28	42	0.36	823.9	12.8	1310.7	48.4	2130.8	0.0	0.0000	-51.8	-48.0	0.007
27	48	6.08	817.8	25.4	1497.7	169.0	2315.4	1.7	0.0021	132.9	133.0	0.046
27	46	11.21	817.8	25.4	1373.8	169.0	2195.7	70.5	0.0886	13.1	9.1	1.235
27	45	-53.78	817.8	25.4	1325.7	161.3	2130.3	107.4	0.1350	-52.3	-39.0	1.378
27	44	12.66	817.8	25.4	1301.3	102.7	2120.7	4.0	0.0050	-61.9	-63.4	0.200
27	43	-5.53	817.8	25.4	1301.4	1.9	2122.5	0.6	0.0008	-60.1	-63.4	0.087
27	42	-1.04	817.8	25.4	1310.7	48.4	2125.6	0.0	0.0000	-57.0	-54.0	0.019
26	48	0.73	765.9	15.5	1497.7	169.0	2269.7	0.0	0.0000	87.1	81.0	0.009
26	46	0.96	765.9	15.5	1373.8	169.0	2150.4	1.0	0.0013	-32.2	-42.9	0.022
26	45	-5.95	765.9	15.5	1325.7	161.3	2096.4	3.3	0.0041	-86.2	-91.0	0.065
26	44	1.36	765.9	15.5	1301.3	102.7	2074.6	0.1	0.0001	-108.0	-115.4	0.012
26	43	-0.63	765.9	15.5	1301.4	1.9	2077.9	0.0	0.0000	-104.7	-115.3	0.005
25	48	0.26	763.1	2.2	1497.7	169.0	2261.6	0.0	0.0000	79.0	78.2	0.003
25	46	1.64	763.1	2.2	1373.8	169.0	2138.6	0.6	0.0007	-44.0	-45.7	0.036
25	45	-3.64	763.1	2.2	1325.7	161.3	2086.2	0.1	0.0001	-96.3	-93.8	0.039
25	44	0.95	763.1	2.2	1301.3	102.7	2067.4	0.0	0.0000	-115.2	-118.2	0.008
25	43	-0.43	763.1	2.2	1301.4	1.9	2067.6	0.0	0.0000	-115.0	-118.1	0.004
23	50	0.35	709.4	14.8	1605.0	23.2	2312.3	0.0	0.0000	129.7	131.8	0.003
23	49	2.51	709.4	14.8	1583.7	1.0	2293.8	0.1	0.0001	111.2	110.5	0.023
23	48	-6.45	709.4	14.8	1497.7	169.0	2205.7	6.8	0.0086	23.1	24.5	0.263
23	47	-1.24	709.4	14.8	1422.9	4.9	2131.4	0.1	0.0002	-51.2	-50.3	0.025
23	46	-8.69	709.4	14.8	1373.8	169.0	2084.2	0.3	0.0003	-98.4	-99.4	0.087
21	49	0.27	647.7	0.8	1583.7	1.0	2232.2	0.0	0.0000	49.6	48.8	0.006

i	j	K_{ijk} / cm^{-1}	ω(i) / cm^{-1}	I(i) / km mol^{-1}	ω(j) / cm^{-1}	I(j) / km mol^{-1}	ω(ij) / cm^{-1}	I(ij) / km mol^{-1}	I(ij) / I(k)	Δω'	Δω	TFR
21	48	0.52	647.7	0.8	1497.7	169.0	2143.4	0.1	0.0001	-39.2	-37.2	0.014
21	47	0.34	647.7	0.8	1422.9	4.9	2068.8	0.1	0.0001	-113.8	-112.0	0.003
20	49	1.15	645.3	3.4	1583.7	1.0	2232.2	0.1	0.0002	49.6	46.3	0.025
20	48	-2.52	645.3	3.4	1497.7	169.0	2142.9	0.5	0.0006	-39.7	-39.6	0.064
20	47	-0.96	645.3	3.4	1422.9	4.9	2067.9	0.1	0.0001	-114.7	-114.5	0.008
19	49	-0.27	610.5	0.7	1583.7	1.0	2199.1	0.0	0.0000	16.5	11.6	0.023
17	50	-0.77	543.2	9.3	1605.0	23.2	2147.4	0.7	0.0009	-35.2	-34.3	0.022
15	52	0.34	497.9	7.2	1706.4	950.0	2204.6	0.0	0.0000	22.0	21.7	0.016
11	52	-0.38	364.6	0.9	1706.4	950.0	2070.8	0.1	0.0001	-111.8	-111.6	0.003
6	54	6.18	139.7	6.6	2182.6	795.8	2313.6	0.1	0.0002	131.0	139.7	0.044
5	54	4.73	107.2	6.9	2182.6	795.8	2280.3	0.4	0.0005	97.7	107.2	0.044
1	54	1.29	-37.6	3.9	2182.6	795.8	2135.6	2.1	0.0026	-47.0	-37.6	0.034

6-311G(d,p)

i	j	K_{ijk} / cm^{-1}	ω(i) / cm^{-1}	I(i) / km mol^{-1}	ω(j) / cm^{-1}	I(j) / km mol^{-1}	ω(ij) / cm^{-1}	I(ij) / km mol^{-1}	I(ij) / I(k)	Δω'	Δω	TFR
39	39	-36.24	1129.8	28.8	1129.8	28.8	2257.3	12.6	0.0240	69.8	72.1	0.502
38	38	-2.54	1137.5	31.4	1137.5	31.4	2269.5	0.2	0.0005	82.0	87.5	0.029
37	37	-1.54	1107.0	16.2	1107.0	16.2	2220.6	0.1	0.0001	33.1	26.5	0.058
36	36	-0.29	1064.1	14.5	1064.1	14.5	2128.8	0.5	0.0009	-58.7	-59.2	0.005
35	35	-0.58	1030.8	6.4	1030.8	6.4	2057.1	0.1	0.0002	-130.5	-125.9	0.005
39	40	-13.90	1129.8	28.8	1186.3	13.7	2314.7	1.8	0.0035	127.1	128.6	0.108
38	39	-4.09	1137.5	31.4	1129.8	28.8	2264.6	0.5	0.0009	77.1	79.8	0.051
37	41	-0.25	1107.0	16.2	1202.0	12.5	2311.1	0.8	0.0015	123.5	121.5	0.002
37	39	-1.56	1107.0	16.2	1129.8	28.8	2240.2	0.0	0.0001	52.6	49.3	0.032
37	38	0.76	1107.0	16.2	1137.5	31.4	2243.9	0.5	0.0009	56.4	57.0	0.013
36	41	0.40	1064.1	14.5	1202.0	12.5	2265.8	0.1	0.0002	78.2	78.6	0.005
36	40	-0.80	1064.1	14.5	1186.3	13.7	2249.4	0.0	0.0000	61.8	62.9	0.013
36	39	-2.65	1064.1	14.5	1129.8	28.8	2194.2	248.8	0.4744	6.7	6.5	0.410
36	38	-0.22	1064.1	14.5	1137.5	31.4	2199.2	0.1	0.0003	11.7	14.1	0.016
35	42	-0.40	1030.8	6.4	1291.0	80.9	2320.4	0.4	0.0007	132.9	134.3	0.003
35	39	-0.65	1030.8	6.4	1129.8	28.8	2159.0	0.1	0.0002	-28.5	-26.9	0.024
35	38	0.59	1030.8	6.4	1137.5	31.4	2162.3	1.0	0.0019	-25.2	-19.2	0.031
35	37	-0.38	1030.8	6.4	1107.0	16.2	2138.0	0.7	0.0013	-49.5	-49.7	0.008
34	43	-0.21	1025.4	1.0	1299.8	7.0	2322.4	0.0	0.0000	134.8	137.6	0.002
34	42	0.66	1025.4	1.0	1291.0	80.9	2313.0	0.0	0.0000	125.5	128.9	0.005
34	41	-0.30	1025.4	1.0	1202.0	12.5	2225.3	0.0	0.0000	37.8	39.8	0.008
34	40	1.07	1025.4	1.0	1186.3	13.7	2209.2	31.5	0.0602	21.7	24.1	0.044
34	39	3.14	1025.4	1.0	1129.8	28.8	2153.0	0.8	0.0014	-34.6	-32.3	0.097
34	37	-0.85	1025.4	1.0	1107.0	16.2	2133.9	0.1	0.0001	-53.6	-55.1	0.015
34	35	-0.31	1025.4	1.0	1030.8	6.4	2052.7	0.0	0.0000	-134.8	-131.3	0.002
33	45	-0.25	962.5	0.6	1317.8	207.9	2282.4	0.0	0.0000	94.9	92.8	0.003
32	45	0.23	986.0	3.0	1317.8	207.9	2278.7	0.0	0.0000	91.2	116.2	0.002
32	39	-0.31	986.0	3.0	1129.8	28.8	2088.7	0.0	0.0000	-98.8	-71.7	0.004
31	44	-0.56	945.6	14.5	1320.8	4.4	2266.0	0.0	0.0000	78.5	78.8	0.007

i	j	K_{ijk} / cm^{-1}	ω(i) / cm^{-1}	I(i) / km mol^{-1}	ω(j) / cm^{-1}	I(j) / km mol^{-1}	ω(ij) / cm^{-1}	I(ij) / km mol^{-1}	I(ij) / I(k)	Δω'	Δω	TFR
31	43	-0.71	945.6	14.5	1299.8	7.0	2242.8	0.3	0.0006	55.2	57.8	0.012
31	42	0.77	945.6	14.5	1291.0	80.9	2235.0	0.2	0.0003	47.4	49.1	0.016
31	41	0.21	945.6	14.5	1202.0	12.5	2145.5	0.4	0.0007	-42.0	-39.9	0.005
31	40	-0.28	945.6	14.5	1186.3	13.7	2130.8	0.0	0.0001	-56.8	-55.6	0.005
31	39	-1.29	945.6	14.5	1129.8	28.8	2075.3	0.0	0.0000	-112.3	-112.1	0.012
29	46	-0.66	835.5	83.5	1370.8	114.8	2194.4	0.1	0.0002	6.8	18.8	0.035
29	45	2.41	835.5	83.5	1317.8	207.9	2153.5	2.5	0.0048	-34.0	-34.2	0.071
29	43	-0.36	835.5	83.5	1299.8	7.0	2134.1	0.1	0.0001	-53.4	-52.2	0.007
29	42	0.27	835.5	83.5	1291.0	80.9	2125.7	0.0	0.0000	-61.8	-61.0	0.004
28	46	0.32	860.6	14.7	1370.8	114.8	2196.7	0.1	0.0003	9.1	43.8	0.007
28	45	-1.29	860.6	14.7	1317.8	207.9	2155.7	0.2	0.0005	-31.9	-9.2	0.141
27	48	6.55	817.2	9.0	1505.0	201.6	2321.2	1.9	0.0036	133.6	134.6	0.049
27	47	0.43	817.2	9.0	1430.8	0.4	2247.4	0.0	0.0001	59.8	60.4	0.007
27	46	17.12	817.2	9.0	1370.8	114.8	2174.5	149.6	0.2853	-13.0	0.4	38.914
27	45	-58.45	817.2	9.0	1317.8	207.9	2125.0	75.5	0.1440	-62.6	-52.5	1.113
27	44	-1.14	817.2	9.0	1320.8	4.4	2137.3	0.0	0.0000	-50.2	-49.6	0.023
27	43	6.52	817.2	9.0	1299.8	7.0	2115.9	0.6	0.0011	-71.6	-70.6	0.092
27	42	-7.44	817.2	9.0	1291.0	80.9	2107.0	0.7	0.0013	-80.5	-79.3	0.094
26	45	-0.65	783.4	6.8	1317.8	207.9	2123.9	0.0	0.0001	-63.6	-86.4	0.008
25	48	-0.39	770.0	3.4	1505.0	201.6	2277.6	0.1	0.0001	90.1	87.4	0.004
25	46	-2.61	770.0	3.4	1370.8	114.8	2131.8	1.1	0.0020	-55.7	-46.8	0.056
25	45	4.97	770.0	3.4	1317.8	207.9	2091.5	0.2	0.0004	-96.1	-99.8	0.050
25	43	-0.65	770.0	3.4	1299.8	7.0	2071.4	0.0	0.0000	-116.1	-117.8	0.006
25	42	0.74	770.0	3.4	1291.0	80.9	2063.4	0.0	0.0000	-124.1	-126.5	0.006
23	50	-0.54	711.9	18.3	1601.6	1.0	2315.4	0.0	0.0000	127.9	125.9	0.004
23	49	-2.34	711.9	18.3	1575.9	6.2	2288.9	0.1	0.0002	101.4	100.2	0.023
23	48	6.58	711.9	18.3	1505.0	201.6	2216.0	6.9	0.0131	28.5	29.3	0.224
23	47	1.27	711.9	18.3	1430.8	0.4	2142.3	0.1	0.0002	-45.3	-44.9	0.028
23	46	11.84	711.9	18.3	1370.8	114.8	2071.5	0.3	0.0005	-116.0	-104.9	0.113
21	49	0.22	647.3	4.4	1575.9	6.2	2220.3	0.0	0.0000	32.8	35.7	0.006
21	48	0.58	647.3	4.4	1505.0	201.6	2146.7	0.1	0.0001	-40.8	-35.2	0.016
20	49	0.83	640.0	1.8	1575.9	6.2	2220.1	0.1	0.0002	32.6	28.4	0.029
20	48	-2.02	640.0	1.8	1505.0	201.6	2146.9	0.3	0.0005	-40.6	-42.5	0.048
20	47	-0.98	640.0	1.8	1430.8	0.4	2072.4	0.1	0.0001	-115.1	-116.7	0.008
19	49	-0.26	618.5	1.1	1575.9	6.2	2200.9	0.0	0.0000	13.4	6.8	0.038
18	52	0.25	582.5	10.9	1722.9	346.7	2303.2	0.0	0.0001	115.6	117.9	0.002
18	48	-0.25	582.5	10.9	1505.0	201.6	2086.9	0.0	0.0000	-100.6	-100.1	0.003
17	50	0.92	545.3	13.9	1601.6	1.0	2149.4	0.9	0.0017	-38.1	-40.7	0.023
17	49	-0.25	545.3	13.9	1575.9	6.2	2123.0	0.0	0.0001	-64.6	-66.4	0.004
15	52	0.29	516.4	11.0	1722.9	346.7	2239.8	0.0	0.0001	52.2	51.8	0.006
14	53	-0.26	447.9	0.1	1776.9	2.4	2238.4	0.0	0.0000	50.9	37.2	0.007
6	54	-6.02	148.6	1.5	2187.5	524.4	2305.6	0.1	0.0002	118.0	148.6	0.040
5	54	-3.69	119.3	4.5	2187.5	524.4	2283.4	0.3	0.0006	95.9	119.3	0.031
1	54	1.00	13.0	1.5	2187.5	524.4	2219.7	1.6	0.0031	32.2	13.0	0.077

6-311+G(d,p)

i	j	K_{ijk} / cm^{-1}	ω(i) / cm^{-1}	I(i) / km mol^{-1}	ω(j) / cm^{-1}	I(j) / km mol^{-1}	ω(ij) / cm^{-1}	I(ij) / km mol^{-1}	I(ij) / I(k)	Δω'	Δω	TFR
39	39	-37.54	1128.2	35.9	1128.2	35.9	2254.0	14.1	0.0178	78.5	80.9	0.464
38	38	-2.26	1125.2	3.2	1125.2	3.2	2246.7	0.4	0.0006	71.2	74.8	0.030
37	37	-1.58	1112.3	51.6	1112.3	51.6	2241.7	0.0	0.0000	66.2	49.0	0.032
36	36	-0.27	1081.6	13.2	1081.6	13.2	2168.6	0.4	0.0005	-6.9	-12.3	0.022
35	35	-0.67	1037.0	9.3	1037.0	9.3	2073.3	0.1	0.0001	-102.1	-101.4	0.007
38	39	1.12	1125.2	3.2	1128.2	35.9	2253.3	0.1	0.0001	77.8	77.9	0.014
37	39	-0.58	1112.3	51.6	1128.2	35.9	2248.1	0.0	0.0000	72.6	65.0	0.009
37	38	-0.27	1112.3	51.6	1125.2	3.2	2243.2	0.2	0.0003	67.7	61.9	0.004
36	41	0.48	1081.6	13.2	1211.7	3.0	2284.9	0.1	0.0001	109.4	117.8	0.004
36	40	-0.94	1081.6	13.2	1191.8	25.1	2276.9	0.0	0.0000	101.4	97.9	0.010
36	39	-2.92	1081.6	13.2	1128.2	35.9	2209.9	12.0	0.0151	34.4	34.3	0.085
35	39	-0.32	1037.0	9.3	1128.2	35.9	2165.6	0.1	0.0001	-9.8	-10.2	0.032
35	38	-0.64	1037.0	9.3	1125.2	3.2	2159.6	1.6	0.0020	-15.9	-13.3	0.048
35	37	-0.30	1037.0	9.3	1112.3	51.6	2156.8	0.4	0.0005	-18.7	-26.2	0.012
34	42	0.78	1016.8	1.3	1288.5	143.9	2302.8	0.0	0.0000	127.3	129.8	0.006
34	41	-0.33	1016.8	1.3	1211.7	3.0	2219.3	0.0	0.0000	43.8	53.0	0.006
34	40	0.98	1016.8	1.3	1191.8	25.1	2212.0	7.8	0.0098	36.6	33.1	0.030
34	39	2.77	1016.8	1.3	1128.2	35.9	2144.0	0.8	0.0010	-31.5	-30.5	0.091
34	37	-0.74	1016.8	1.3	1112.3	51.6	2135.8	0.0	0.0001	-39.7	-46.4	0.016
33	45	-0.64	980.0	0.1	1323.0	91.6	2293.5	0.0	0.0000	118.1	127.5	0.005
33	42	-0.27	980.0	0.1	1288.5	143.9	2262.5	0.0	0.0000	87.0	93.0	0.003
33	39	0.44	980.0	0.1	1128.2	35.9	2102.2	0.0	0.0000	-73.3	-67.3	0.007
31	44	-0.35	951.9	2.8	1311.6	36.7	2272.4	0.0	0.0000	97.0	88.0	0.004
31	43	-0.33	951.9	2.8	1312.8	20.6	2268.0	0.2	0.0003	92.5	89.2	0.004
31	42	0.66	951.9	2.8	1288.5	143.9	2244.6	0.0	0.0000	69.1	64.9	0.010
31	41	0.22	951.9	2.8	1211.7	3.0	2158.6	0.2	0.0002	-16.9	-11.9	0.019
31	40	-0.41	951.9	2.8	1191.8	25.1	2151.8	0.0	0.0000	-23.6	-31.8	0.013
31	39	-0.89	951.9	2.8	1128.2	35.9	2084.6	0.0	0.0000	-90.9	-95.4	0.009
30	45	0.28	955.0	13.5	1323.0	91.6	2276.4	0.0	0.0000	100.9	102.6	0.003
30	44	0.34	955.0	13.5	1311.6	36.7	2273.8	0.0	0.0000	98.3	91.2	0.004
30	43	0.29	955.0	13.5	1312.8	20.6	2268.9	0.3	0.0003	93.5	92.3	0.003
30	42	-0.65	955.0	13.5	1288.5	143.9	2245.8	0.0	0.0000	70.3	68.1	0.010
30	40	0.36	955.0	13.5	1191.8	25.1	2153.1	0.0	0.0000	-22.4	-28.6	0.012
30	39	0.81	955.0	13.5	1128.2	35.9	2085.7	0.0	0.0000	-89.8	-92.2	0.009
30	38	-0.27	955.0	13.5	1125.2	3.2	2081.9	0.2	0.0002	-93.5	-95.3	0.003
29	46	-0.38	850.4	66.7	1370.2	140.0	2213.5	0.1	0.0002	38.0	45.1	0.008
29	45	1.93	850.4	66.7	1323.0	91.6	2163.7	3.2	0.0040	-11.8	-2.1	0.930
29	43	-0.22	850.4	66.7	1312.8	20.6	2158.3	0.1	0.0001	-17.2	-12.3	0.018
29	42	0.28	850.4	66.7	1288.5	143.9	2134.1	0.0	0.0000	-41.4	-36.6	0.008
28	46	-0.76	835.6	22.5	1370.2	140.0	2206.5	0.2	0.0003	31.1	30.3	0.025
28	45	3.20	835.6	22.5	1323.0	91.6	2157.2	3.2	0.0040	-18.3	-16.9	0.189
28	42	0.50	835.6	22.5	1288.5	143.9	2128.0	0.0	0.0000	-47.5	-51.4	0.010
27	47	0.31	819.0	4.5	1418.9	12.5	2238.4	0.0	0.0000	62.9	62.4	0.005
27	46	13.18	819.0	4.5	1370.2	140.0	2189.3	126.8	0.1601	13.9	13.7	0.962
27	45	-58.84	819.0	4.5	1323.0	91.6	2124.2	151.3	0.1911	-51.2	-33.5	1.759
27	44	0.55	819.0	4.5	1311.6	36.7	2134.7	0.0	0.0000	-40.8	-44.9	0.012

i	j	K_{ijk} / cm^{-1}	ω(i) / cm^{-1}	I(i) / km mol^{-1}	ω(j) / cm^{-1}	I(j) / km mol^{-1}	ω(ij) / cm^{-1}	I(ij) / km mol^{-1}	I(ij) / I(k)	Δω'	Δω	TFR
27	43	4.26	819.0	4.5	1312.8	20.6	2131.3	0.4	0.0005	-44.2	-43.7	0.097
27	42	-9.69	819.0	4.5	1288.5	143.9	2106.1	1.6	0.0020	-69.3	-68.0	0.143
26	46	1.02	822.3	3.6	1370.2	140.0	2192.5	1.9	0.0024	17.1	17.0	0.060
26	45	-5.83	822.3	3.6	1323.0	91.6	2141.6	3.6	0.0045	-33.9	-30.2	0.193
26	43	0.39	822.3	3.6	1312.8	20.6	2135.8	0.0	0.0000	-39.6	-40.4	0.010
26	42	-0.97	822.3	3.6	1288.5	143.9	2110.8	0.0	0.0001	-64.7	-64.7	0.015
25	48	0.22	776.7	0.7	1504.4	177.9	2280.5	0.0	0.0000	105.0	105.6	0.002
25	46	1.63	776.7	0.7	1370.2	140.0	2145.1	0.7	0.0009	-30.4	-28.5	0.057
25	45	-3.45	776.7	0.7	1323.0	91.6	2096.2	0.1	0.0002	-79.3	-75.7	0.046
25	43	0.28	776.7	0.7	1312.8	20.6	2089.5	0.0	0.0000	-86.0	-86.0	0.003
25	42	-0.65	776.7	0.7	1288.5	143.9	2066.7	0.0	0.0000	-108.8	-110.2	0.006
24	45	0.41	727.2	12.5	1323.0	91.6	2046.0	0.1	0.0001	-129.4	-125.3	0.003
23	50	-0.26	710.2	15.5	1595.9	12.3	2307.2	0.0	0.0000	131.7	130.6	0.002
23	49	-2.44	710.2	15.5	1575.6	3.4	2288.0	0.1	0.0001	112.6	110.3	0.022
23	48	6.31	710.2	15.5	1504.4	177.9	2214.8	4.5	0.0057	39.3	39.1	0.161
23	47	1.32	710.2	15.5	1418.9	12.5	2133.1	0.2	0.0002	-42.4	-46.3	0.028
23	46	9.56	710.2	15.5	1370.2	140.0	2080.7	0.3	0.0004	-94.8	-95.1	0.101
21	49	0.35	652.3	2.2	1575.6	3.4	2227.2	0.0	0.0000	51.7	52.5	0.007
21	48	0.36	652.3	2.2	1504.4	177.9	2153.4	0.0	0.0001	-22.1	-18.8	0.019
20	49	1.00	648.0	2.6	1575.6	3.4	2223.4	0.1	0.0001	48.0	48.2	0.021
20	48	-2.35	648.0	2.6	1504.4	177.9	2150.1	0.7	0.0008	-25.4	-23.1	0.102
20	47	-0.95	648.0	2.6	1418.9	12.5	2066.7	0.0	0.0001	-108.7	-108.5	0.009
19	49	-0.34	625.1	0.8	1575.6	3.4	2204.4	0.0	0.0000	28.9	25.3	0.014
17	50	0.79	546.2	5.6	1595.9	12.3	2144.0	0.8	0.0010	-31.5	-33.3	0.024
17	48	-1.12	546.2	5.6	1504.4	177.9	2051.1	0.1	0.0001	-124.4	-124.9	0.009
15	52	0.34	522.5	8.0	1699.7	923.5	2220.9	0.0	0.0000	45.5	46.8	0.007
14	53	-0.26	439.6	0.2	1770.0	0.5	2219.6	0.0	0.0000	44.1	34.1	0.008
11	52	-0.41	373.3	1.1	1699.7	923.5	2073.6	0.1	0.0002	-101.9	-102.4	0.004
10	52	-0.30	342.0	4.2	1699.7	923.5	2041.9	0.0	0.0000	-133.6	-133.7	0.002
5	54	-4.35	127.7	6.9	2175.5	791.7	2285.7	0.4	0.0005	110.2	127.7	0.034

6-311++G(d,p)

i	j	K_{ijk} / cm^{-1}	ω(i) / cm^{-1}	I(i) / km mol^{-1}	ω(j) / cm^{-1}	I(j) / km mol^{-1}	ω(ij) / cm^{-1}	I(ij) / km mol^{-1}	I(ij) / I(k)	Δω'	Δω	TFR
39	39	-37.51	1124.4	36.9	1124.4	36.9	2245.4	14.0	0.0189	62.1	65.5	0.572
38	38	-2.24	1144.0	16.9	1144.0	16.9	2258.6	0.5	0.0006	75.3	104.7	0.021
37	37	-1.51	1108.5	60.5	1108.5	60.5	2275.7	0.0	0.0000	92.4	33.7	0.045
36	36	-0.27	1083.0	15.1	1083.0	15.1	2171.4	0.4	0.0005	-11.9	-17.2	0.015
35	35	-0.67	1036.7	9.4	1036.7	9.4	2072.5	0.1	0.0001	-110.7	-109.8	0.006
38	39	1.14	1144.0	16.9	1124.4	36.9	2255.0	0.1	0.0001	71.8	85.1	0.013
37	39	-0.63	1108.5	60.5	1124.4	36.9	2260.2	0.0	0.0000	77.0	49.6	0.013
37	38	-0.30	1108.5	60.5	1144.0	16.9	2266.2	0.2	0.0003	82.9	69.2	0.004
36	41	0.46	1083.0	15.1	1188.5	24.8	2295.3	0.1	0.0001	112.1	88.3	0.005
36	40	-0.93	1083.0	15.1	1250.2	6.6	2294.7	0.0	0.0000	111.5	150.0	0.006
36	39	-2.93	1083.0	15.1	1124.4	36.9	2207.2	12.0	0.0161	24.0	24.2	0.121
35	39	-0.33	1036.7	9.4	1124.4	36.9	2161.1	0.1	0.0001	-22.1	-22.1	0.015

i	j	K_{ijk} / cm^{-1}	ω(i) / cm^{-1}	I(i) / km mol^{-1}	ω(j) / cm^{-1}	I(j) / km mol^{-1}	ω(ij) / cm^{-1}	I(ij) / km mol^{-1}	I(ij) / I(k)	Δω'	Δω	TFR
35	38	-0.64	1036.7	9.4	1144.0	16.9	2165.1	1.6	0.0021	-18.2	-2.6	0.248
35	37	-0.29	1036.7	9.4	1108.5	60.5	2173.3	0.4	0.0005	-10.0	-38.1	0.008
34	42	0.79	1009.0	0.3	1288.9	95.8	2294.0	0.0	0.0000	110.7	114.7	0.007
34	41	-0.30	1009.0	0.3	1188.5	24.8	2219.4	0.0	0.0000	36.1	14.3	0.021
34	40	0.94	1009.0	0.3	1250.2	6.6	2219.3	6.8	0.0091	36.0	76.0	0.012
34	39	2.78	1009.0	0.3	1124.4	36.9	2130.7	0.8	0.0011	-52.6	-49.8	0.056
34	37	-0.78	1009.0	0.3	1108.5	60.5	2143.7	0.0	0.0001	-39.5	-65.7	0.012
33	42	-0.28	947.3	13.7	1288.9	95.8	2296.3	0.0	0.0000	113.1	53.0	0.005
33	39	0.49	947.3	13.7	1124.4	36.9	2132.3	0.0	0.0000	-51.0	-111.6	0.004
31	44	0.53	956.3	6.9	1342.0	12.9	2304.6	0.0	0.0000	121.3	115.0	0.005
31	43	0.44	956.3	6.9	1316.2	31.3	2281.6	0.4	0.0006	98.3	89.2	0.005
31	42	-0.89	956.3	6.9	1288.9	95.8	2255.2	0.1	0.0001	71.9	62.0	0.014
31	41	-0.24	956.3	6.9	1188.5	24.8	2178.5	0.3	0.0005	-4.7	-38.5	0.006
31	40	0.50	956.3	6.9	1250.2	6.6	2180.2	0.0	0.0000	-3.1	23.3	0.021
31	39	1.21	956.3	6.9	1124.4	36.9	2091.9	0.0	0.0000	-91.3	-102.6	0.012
30	42	-0.21	1080.8	40.4	1288.9	95.8	2297.3	0.0	0.0000	114.0	186.5	0.001
30	38	-0.32	1080.8	40.4	1144.0	16.9	2140.6	0.1	0.0001	-42.6	41.5	0.008
29	46	-0.37	825.3	4.8	1376.3	164.4	2242.3	0.1	0.0002	59.1	18.4	0.020
29	45	1.97	825.3	4.8	1314.4	140.2	2194.0	3.4	0.0046	10.8	-43.6	0.045
29	42	0.28	825.3	4.8	1288.9	95.8	2158.8	0.0	0.0000	-24.4	-69.0	0.004
28	46	-0.76	846.2	63.8	1376.3	164.4	2217.8	0.2	0.0003	34.6	39.2	0.019
28	45	3.21	846.2	63.8	1314.4	140.2	2169.9	3.2	0.0043	-13.3	-22.7	0.141
28	42	0.50	846.2	63.8	1288.9	95.8	2135.2	0.0	0.0000	-48.0	-48.2	0.010
28	40	-0.31	846.2	63.8	1250.2	6.6	2058.4	0.0	0.0000	-124.8	-86.9	0.004
27	47	0.35	818.0	4.5	1419.4	0.6	2246.4	0.0	0.0000	63.1	54.1	0.006
27	46	13.12	818.0	4.5	1376.3	164.4	2201.3	125.6	0.1693	18.0	11.0	1.190
27	45	-58.77	818.0	4.5	1314.4	140.2	2135.9	195.1	0.2630	-47.3	-50.9	1.155
27	44	0.59	818.0	4.5	1342.0	12.9	2164.0	0.0	0.0000	-19.3	-23.3	0.025
27	43	4.22	818.0	4.5	1316.2	31.3	2143.2	0.4	0.0005	-40.1	-49.0	0.086
27	42	-9.70	818.0	4.5	1288.9	95.8	2114.0	1.6	0.0021	-69.3	-76.3	0.127
26	46	1.12	984.2	29.3	1376.3	164.4	2291.7	2.3	0.0031	108.4	177.2	0.006
26	45	-6.14	984.2	29.3	1314.4	140.2	2242.6	4.1	0.0056	59.4	115.3	0.053
26	43	0.45	984.2	29.3	1316.2	31.3	2234.9	0.0	0.0000	51.7	117.2	0.004
26	42	-1.02	984.2	29.3	1288.9	95.8	2205.7	0.0	0.0001	22.5	89.9	0.011
26	40	0.34	984.2	29.3	1250.2	6.6	2131.6	0.0	0.0000	-51.6	51.2	0.007
26	37	-0.41	984.2	29.3	1108.5	60.5	2057.6	0.0	0.0000	-125.7	-90.6	0.004
25	48	0.22	775.1	0.2	1512.9	160.3	2289.1	0.0	0.0000	105.8	104.8	0.002
25	46	1.61	775.1	0.2	1376.3	164.4	2146.6	0.7	0.0009	-36.6	-31.9	0.051
25	45	-3.42	775.1	0.2	1314.4	140.2	2099.1	0.1	0.0002	-84.1	-93.8	0.036
25	43	0.28	775.1	0.2	1316.2	31.3	2091.0	0.0	0.0000	-92.3	-91.9	0.003
25	42	-0.65	775.1	0.2	1288.9	95.8	2064.2	0.0	0.0000	-119.0	-119.2	0.005
24	45	0.53	730.9	14.3	1314.4	140.2	2062.1	0.1	0.0001	-121.2	-138.0	0.004
23	50	-0.27	712.9	13.8	1597.6	10.7	2308.1	0.0	0.0000	124.8	127.2	0.002
23	49	-2.45	712.9	13.8	1583.7	2.8	2294.0	0.1	0.0001	110.7	113.3	0.022
23	48	6.33	712.9	13.8	1512.9	160.3	2224.6	4.6	0.0061	41.3	42.5	0.149
23	47	1.33	712.9	13.8	1419.4	0.6	2131.7	0.2	0.0002	-51.6	-51.0	0.026
23	46	9.54	712.9	13.8	1376.3	164.4	2083.3	0.3	0.0004	-99.9	-94.1	0.101
21	49	0.33	658.3	5.2	1583.7	2.8	2238.9	0.0	0.0000	55.6	58.7	0.006

i	j	K_{ijk} / cm^{-1}	ω(i) / cm^{-1}	I(i) / km mol^{-1}	ω(j) / cm^{-1}	I(j) / km mol^{-1}	ω(ij) / cm^{-1}	I(ij) / km mol^{-1}	I(ij) / I(k)	Δω'	Δω	TFR
21	48	0.40	658.3	5.2	1512.9	160.3	2169.6	0.1	0.0001	-13.7	-12.0	0.034
20	49	0.99	651.7	7.3	1583.7	2.8	2233.4	0.1	0.0001	50.2	52.1	0.019
20	48	-2.33	651.7	7.3	1512.9	160.3	2163.9	0.7	0.0009	-19.3	-18.6	0.125
20	47	-0.97	651.7	7.3	1419.4	0.6	2069.3	0.0	0.0001	-113.9	-112.2	0.009
19	49	-0.33	625.2	2.9	1583.7	2.8	2212.4	0.0	0.0000	29.1	25.7	0.013
17	50	0.79	525.7	7.9	1597.6	10.7	2149.0	0.8	0.0011	-34.3	-59.9	0.013
17	48	-1.07	525.7	7.9	1512.9	160.3	2065.0	0.1	0.0001	-118.3	-144.6	0.007
15	52	0.34	547.1	5.0	1699.4	950.2	2264.4	0.0	0.0000	81.1	63.2	0.005
14	53	-0.26	406.0	1.4	1772.5	0.3	2192.1	0.0	0.0000	8.8	-4.7	0.054
12	50	0.43	454.4	7.1	1597.6	10.7	2052.8	0.0	0.0000	-130.5	-131.2	0.003
11	52	-0.41	366.4	0.2	1699.4	950.2	2080.2	0.1	0.0002	-103.1	-117.5	0.003
5	54	-4.35	264.6	44.8	2183.3	741.7	2313.3	0.4	0.0005	130.0	264.6	0.016

APPENDIX H

VIBRATIONAL MODES OF 4-AZIDO-N-PHENYLMALEIMIDE (ISOMER 2) THAT OCCUR WITHIN ±130 CM^{-1} FROM THE FUNDAMENTAL VIBRATION FOR SEVEN BASIS SETS IN THF

i, j, k : vibrational modes ; where k = 54 (azide asymmetric stretch)

i = j → overtone & i ≠ j → combination band

K_{ijk} : cubic force constant

TFR : third-order Fermi resonance

ω(i), ω(j), ω(k) : anharmonic frequencies of i, j & k th mode

ω(ij) : anharmonic frequency of ij th mode

I(i), I(j), I(k) : anharmonic intensities of i, j & k th mode

I(ij) : anharmonic intensity of ij th mode

Δω' : ω(ij) - ω(k)

Δω : ω(i) + ω(j) - ω(k)

6-31G(d,p)

i	j	K_{ijk} / cm^{-1}	ω(i) / cm^{-1}	I(i) / km mol^{-1}	ω(j) / cm^{-1}	I(j) / km mol^{-1}	ω(ij) / cm^{-1}	I(ij) / km mol^{-1}	I(ij) / I(k)	Δω'	Δω	TFR
39	39	36.18	1142.9	21.9	1142.9	21.9	2286.1	12.0	0.0311	89.6	89.4	0.405
38	38	3.94	1141.4	40.1	1141.4	40.1	2279.4	0.3	0.0007	82.9	86.3	0.046
37	37	1.60	1120.6	26.0	1120.6	26.0	2251.9	0.0	0.0000	55.4	44.7	0.036
36	36	0.30	1061.8	10.7	1061.8	10.7	2119.4	0.4	0.0009	-77.0	-72.9	0.004
38	39	7.22	1141.4	40.1	1142.9	21.9	2284.2	1.5	0.0040	87.7	87.9	0.082
37	40	0.49	1120.6	26.0	1197.5	4.5	2327.6	0.5	0.0013	131.1	121.6	0.004
37	39	1.64	1120.6	26.0	1142.9	21.9	2269.7	0.0	0.0000	73.2	67.0	0.025
37	38	-0.38	1120.6	26.0	1141.4	40.1	2265.2	0.4	0.0011	68.7	65.5	0.006
36	41	-0.50	1061.8	10.7	1219.8	28.9	2276.9	0.1	0.0002	80.5	85.1	0.006
36	40	0.82	1061.8	10.7	1197.5	4.5	2261.7	0.0	0.0001	65.2	62.8	0.013
36	39	2.37	1061.8	10.7	1142.9	21.9	2205.3	127.2	0.3303	8.8	8.2	0.288
36	38	0.49	1061.8	10.7	1141.4	40.1	2202.0	0.9	0.0023	5.6	6.7	0.074
35	42	0.25	1029.1	6.9	1298.9	1.6	2327.2	0.7	0.0017	130.8	131.6	0.002
35	39	0.71	1029.1	6.9	1142.9	21.9	2173.0	0.2	0.0004	-23.5	-24.4	0.029
35	38	-0.63	1029.1	6.9	1141.4	40.1	2166.8	1.2	0.0031	-29.7	-26.0	0.024
35	37	0.45	1029.1	6.9	1120.6	26.0	2153.3	0.6	0.0015	-43.2	-46.8	0.010
34	41	0.73	1023.7	0.4	1219.8	26.0	2239.5	0.1	0.0002	43.0	47.0	0.016

i	j	K_{ijk} / cm^{-1}	ω(i) / cm^{-1}	I(i) / km mol^{-1}	ω(j) / cm^{-1}	I(j) / km mol^{-1}	ω(ij) / cm^{-1}	I(ij) / km mol^{-1}	I(ij) / I(k)	Δω'	Δω	TFR
34	40	-1.57	1023.7	0.4	1197.5	4.5	2223.7	3.2	0.0084	27.2	24.7	0.064
34	39	-3.47	1023.7	0.4	1142.9	21.9	2167.5	0.6	0.0016	-28.9	-29.9	0.116
34	38	-0.44	1023.7	0.4	1141.4	40.1	2164.2	0.0	0.0001	-32.3	-31.4	0.014
34	37	0.60	1023.7	0.4	1120.6	26.0	2148.9	0.0	0.0001	-47.6	-52.2	0.012
33	45	-0.20	983.5	3.3	1333.2	158.0	2315.0	0.0	0.0000	118.5	120.2	0.002
32	46	-0.38	951.6	4.4	1375.2	89.5	2328.0	0.0	0.0000	131.5	130.4	0.003
32	45	1.29	951.6	4.4	1333.2	158.0	2282.9	0.0	0.0000	86.5	88.3	0.015
32	43	-0.87	951.6	4.4	1327.0	0.7	2273.5	0.0	0.0001	77.0	82.2	0.011
32	41	-0.31	951.6	4.4	1219.8	28.9	2166.0	0.3	0.0009	-30.5	-25.0	0.012
32	40	0.23	951.6	4.4	1197.5	4.5	2151.9	0.0	0.0000	-44.6	-47.3	0.005
32	39	0.92	951.6	4.4	1142.9	21.9	2095.8	0.0	0.0000	-100.7	-101.9	0.009
32	38	0.35	951.6	4.4	1141.4	40.1	2091.4	0.1	0.0002	-105.1	-103.4	0.003
31	45	0.69	964.0	6.9	1333.2	158.0	2291.4	0.0	0.0000	94.9	100.7	0.007
31	43	-0.25	964.0	6.9	1327.0	0.7	2281.9	0.0	0.0000	85.4	94.6	0.003
29	46	-0.71	852.7	68.4	1375.2	89.5	2222.2	0.5	0.0012	25.7	31.4	0.023
29	45	2.89	852.7	68.4	1333.2	158.0	2177.6	0.8	0.0020	-18.9	-10.6	0.272
29	44	0.66	852.7	68.4	1314.0	120.5	2168.5	0.0	0.0000	-28.0	-29.7	0.022
29	43	0.23	852.7	68.4	1327.0	0.7	2169.8	0.1	0.0001	-26.7	-16.7	0.014
28	46	6.23	835.2	7.8	1375.2	89.5	2215.1	23.1	0.0600	18.7	13.9	0.447
28	45	-23.08	835.2	7.8	1333.2	158.0	2168.4	27.4	0.0712	-28.1	-28.1	0.821
28	44	-4.96	835.2	7.8	1314.0	120.5	2160.7	0.4	0.0010	-35.8	-47.2	0.105
28	43	-2.50	835.2	7.8	1327.0	0.7	2161.3	0.1	0.0003	-35.2	-34.2	0.073
28	42	-1.06	835.2	7.8	1298.9	1.6	2140.5	0.0	0.0000	-56.0	-62.3	0.017
27	47	-0.25	824.0	1.0	1440.4	0.7	2266.3	0.0	0.0001	69.9	68.0	0.004
27	46	-14.48	824.0	1.0	1375.2	89.5	2206.4	222.8	0.5786	9.9	2.8	5.228
27	45	52.70	824.0	1.0	1333.2	158.0	2146.5	87.6	0.2275	-50.0	-39.3	1.342
27	44	11.29	824.0	1.0	1314.0	120.5	2145.9	2.1	0.0054	-50.6	-58.4	0.193
27	43	5.79	824.0	1.0	1327.0	0.7	2146.8	0.4	0.0011	-49.7	-45.4	0.128
27	42	2.38	824.0	1.0	1298.9	1.6	2125.7	0.1	0.0002	-70.8	-73.5	0.032
26	46	-0.85	824.6	0.3	1375.2	89.5	2202.1	1.7	0.0045	5.6	3.4	0.254
26	45	1.78	824.6	0.3	1333.2	158.0	2157.7	0.1	0.0002	-38.8	-38.7	0.046
26	44	0.43	824.6	0.3	1314.0	120.5	2148.9	0.0	0.0001	-47.6	-57.8	0.007
25	48	-0.49	762.9	4.1	1518.8	102.2	2281.8	0.1	0.0002	85.3	85.3	0.006
25	46	-2.50	762.9	4.1	1375.2	89.5	2138.1	0.7	0.0018	-58.4	-58.3	0.043
25	45	5.20	762.9	4.1	1333.2	158.0	2094.2	0.1	0.0003	-102.3	-100.4	0.052
25	44	1.22	762.9	4.1	1314.0	120.5	2084.7	0.0	0.0001	-111.8	-119.5	0.010
25	43	0.70	762.9	4.1	1327.0	0.7	2085.0	0.0	0.0000	-111.5	-106.5	0.007
25	42	0.28	762.9	4.1	1298.9	1.6	2062.5	0.0	0.0000	-133.9	-134.6	0.002
24	48	0.23	722.6	7.8	1518.8	102.2	2238.0	0.0	0.0001	41.5	45.0	0.005
23	50	0.69	709.4	18.8	1615.2	6.4	2324.1	0.0	0.0001	127.6	128.1	0.005
23	49	2.30	709.4	18.8	1596.9	1.8	2305.6	0.1	0.0003	109.2	109.8	0.021
23	48	-6.79	709.4	18.8	1518.8	102.2	2227.9	11.8	0.0308	31.4	31.8	0.214
23	47	-1.21	709.4	18.8	1440.4	0.7	2150.9	0.1	0.0002	-45.5	-46.6	0.026
23	46	-10.91	709.4	18.8	1375.2	89.5	2084.9	0.2	0.0006	-111.6	-111.8	0.098
21	50	-0.25	643.7	2.3	1615.2	6.4	2257.3	0.0	0.0000	60.8	62.3	0.004
21	48	0.87	643.7	2.3	1518.8	102.2	2161.4	0.1	0.0002	-35.1	-34.0	0.026
21	47	0.30	643.7	2.3	1440.4	0.7	2084.3	0.1	0.0002	-112.2	-112.4	0.003
20	50	0.23	641.1	2.5	1615.2	6.4	2256.1	0.0	0.0000	59.6	59.8	0.004
20	49	0.94	641.1	2.5	1596.9	1.8	2239.0	0.2	0.0004	42.5	41.5	0.023
20	48	-2.19	641.1	2.5	1518.8	102.2	2160.1	0.2	0.0004	-36.4	-36.5	0.060
20	47	-0.88	641.1	2.5	1440.4	0.7	2082.6	0.1	0.0002	-113.8	-114.9	0.008
18	48	0.33	586.7	5.3	1518.8	102.2	2105.7	0.0	0.0000	-90.8	-90.9	0.004
17	50	-0.93	549.4	6.7	1615.2	6.4	2164.0	0.8	0.0021	-32.5	-31.9	0.029
17	48	0.78	549.4	6.7	1518.8	102.2	2067.6	0.0	0.0001	-128.9	-128.2	0.006
5	54	3.55	134.8	5.9	2196.5	385.2	2320.1	0.3	0.0007	123.6	134.8	0.026
2	54	-0.74	113.1	2.4	2196.5	385.2	2310.6	0.1	0.0004	114.2	113.1	0.007
1	54	0.97	39.3	0.4	2196.5	385.2	2243.2	1.3	0.0034	46.7	39.3	0.025

6-31+G(d,p)

i	j	K_{ijk} / cm^{-1}	ω(i) / cm^{-1}	I(i) / km mol^{-1}	ω(j) / cm^{-1}	I(j) / km mol^{-1}	ω(ij) / cm^{-1}	I(ij) / km mol^{-1}	I(ij) / I(k)	Δω'	Δω	TFR
39	39	-38.89	1136.9	31.3	1136.9	31.3	2273.1	15.2	0.0215	87.3	88.0	0.442
38	38	-2.68	1120.3	36.5	1120.3	36.5	2248.8	0.5	0.0007	63.1	54.8	0.049
37	37	-1.09	1143.1	8.3	1143.1	8.3	2276.6	0.0	0.0000	90.9	100.4	0.011
36	36	-0.26	1087.2	15.3	1087.2	15.3	2179.5	0.3	0.0004	-6.2	-11.4	0.023
35	35	-0.70	1033.3	16.4	1033.3	16.4	2062.3	0.2	0.0002	-123.5	-119.1	0.006
34	34	0.48	1022.8	1.0	1022.8	1.0	2045.8	0.0	0.0000	-140.0	-140.2	0.003
38	41	0.51	1120.3	36.5	1215.1	3.5	2335.3	1.6	0.0023	149.5	149.6	0.003
38	40	-1.30	1120.3	36.5	1198.5	14.2	2330.9	0.1	0.0002	145.2	133.0	0.010
38	39	-3.87	1120.3	36.5	1136.9	31.3	2264.1	0.5	0.0007	78.4	71.4	0.054
37	39	-0.84	1143.1	8.3	1136.9	31.3	2274.1	0.0	0.0000	88.4	94.2	0.009
37	38	0.29	1143.1	8.3	1120.3	36.5	2263.6	0.1	0.0002	77.8	77.6	0.004
36	41	0.47	1087.2	15.3	1215.1	3.5	2298.0	0.1	0.0001	112.3	116.5	0.004
36	40	-0.80	1087.2	15.3	1198.5	14.2	2289.8	0.0	0.0000	104.0	99.9	0.008
36	39	-2.77	1087.2	15.3	1136.9	31.3	2224.9	19.9	0.0283	39.1	38.3	0.072
36	38	-0.29	1087.2	15.3	1120.3	36.5	2214.1	1.3	0.0019	28.4	21.7	0.013
35	39	-0.44	1033.3	16.4	1136.9	31.3	2169.5	0.1	0.0001	-16.3	-15.5	0.029
35	38	0.78	1033.3	16.4	1120.3	36.5	2154.6	1.9	0.0027	-31.1	-32.2	0.024
34	44	-0.28	1022.8	1.0	1305.9	151.2	2332.0	0.1	0.0001	146.2	142.9	0.002
34	41	-0.39	1022.8	1.0	1215.1	3.5	2233.7	0.0	0.0000	47.9	52.2	0.007
34	40	0.97	1022.8	1.0	1198.5	14.2	2226.1	5.2	0.0073	40.3	35.5	0.027
34	39	3.31	1022.8	1.0	1136.9	31.3	2160.4	0.8	0.0011	-25.4	-26.1	0.127
34	37	-0.81	1022.8	1.0	1143.1	8.3	2159.9	0.0	0.0001	-25.8	-19.9	0.041
33	45	-0.35	897.0	15.8	1322.7	52.2	2257.4	0.0	0.0000	71.6	34.0	0.010
33	44	-0.26	897.0	15.8	1305.9	151.2	2241.2	0.0	0.0000	55.4	17.2	0.015
33	39	0.29	897.0	15.8	1136.9	31.3	2068.0	0.0	0.0000	-117.8	-151.8	0.002
31	46	0.29	947.2	7.8	1386.6	15.6	2326.3	0.0	0.0000	140.5	148.0	0.002
31	45	-1.11	947.2	7.8	1322.7	52.2	2275.7	0.0	0.0000	89.9	84.1	0.013
31	44	0.49	947.2	7.8	1305.9	151.2	2259.3	0.0	0.0000	73.6	67.3	0.007
31	43	0.86	947.2	7.8	1331.5	60.2	2273.4	0.0	0.0001	87.6	93.0	0.009
31	41	0.24	947.2	7.8	1215.1	3.5	2158.0	0.3	0.0005	-27.7	-23.5	0.010
31	40	-0.35	947.2	7.8	1198.5	14.2	2151.5	0.0	0.0000	-34.2	-40.1	0.009
31	39	-0.99	947.2	7.8	1136.9	31.3	2086.6	0.0	0.0000	-99.2	-101.7	0.010
30	45	0.53	974.5	9.4	1322.7	52.2	2268.3	0.0	0.0000	82.6	111.5	0.005
30	38	0.24	974.5	9.4	1120.3	36.5	2067.9	0.1	0.0001	-117.9	-91.0	0.003
29	48	-0.37	771.9	2.3	1513.0	161.2	2327.6	0.0	0.0000	141.8	99.1	0.004
29	46	-0.41	771.9	2.3	1386.6	15.6	2193.1	0.1	0.0002	7.4	-27.3	0.015
29	45	2.21	771.9	2.3	1322.7	52.2	2142.3	1.3	0.0018	-43.4	-91.2	0.024
29	44	0.54	771.9	2.3	1305.9	151.2	2127.3	0.0	0.0001	-58.5	-108.0	0.005
29	43	0.26	771.9	2.3	1331.5	60.2	2142.3	0.0	0.0000	-43.5	-82.3	0.003
28	46	-2.25	838.2	52.1	1386.6	15.6	2201.5	3.5	0.0049	15.8	39.1	0.058
28	45	9.55	838.2	52.1	1322.7	52.2	2150.9	10.0	0.0141	-34.8	-24.8	0.385
28	44	2.16	838.2	52.1	1305.9	151.2	2136.3	0.1	0.0002	-49.4	-41.6	0.052
28	43	0.87	838.2	52.1	1331.5	60.2	2149.6	0.0	0.0000	-36.2	-16.0	0.055
27	48	6.71	818.8	6.4	1513.0	161.2	2330.2	1.8	0.0026	144.4	146.1	0.046
27	46	12.97	818.8	6.4	1386.6	15.6	2198.2	160.9	0.2284	12.4	19.7	0.659
27	45	-56.85	818.8	6.4	1322.7	52.2	2133.0	108.5	0.1539	-52.8	-44.2	1.286
27	44	-13.05	818.8	6.4	1305.9	151.2	2128.3	3.8	0.0054	-57.5	-61.0	0.214
27	43	-5.29	818.8	6.4	1331.5	60.2	2143.1	0.5	0.0007	-42.7	-35.4	0.150
27	42	-1.32	818.8	6.4	1318.3	63.0	2136.9	0.0	0.0001	-48.9	-48.6	0.027
26	46	0.27	864.3	63.3	1386.6	15.6	2211.6	0.8	0.0012	25.8	65.1	0.004
26	45	-2.63	864.3	63.3	1322.7	52.2	2160.8	0.5	0.0007	-25.0	1.2	2.126
26	44	-0.62	864.3	63.3	1305.9	151.2	2145.9	0.0	0.0000	-39.8	-15.6	0.040
26	40	0.31	864.3	63.3	1198.5	14.2	2039.5	0.0	0.0000	-146.3	-123.0	0.002

i	j	K_{ijk} / cm^{-1}	ω(i) / cm^{-1}	I(i) / km mol^{-1}	ω(j) / cm^{-1}	I(j) / km mol^{-1}	ω(ij) / cm^{-1}	I(ij) / km mol^{-1}	I(ij) / I(k)	Δω'	Δω	TFR
25	48	-0.34	762.0	1.6	1513.0	161.2	2274.8	0.0	0.0001	89.0	89.2	0.004
25	46	-1.90	762.0	1.6	1386.6	15.6	2138.6	0.6	0.0009	-47.1	-37.2	0.051
25	45	4.18	762.0	1.6	1322.7	52.2	2088.7	0.1	0.0002	-97.0	-101.0	0.041
25	44	1.05	762.0	1.6	1305.9	151.2	2073.6	0.0	0.0000	-112.1	-117.9	0.009
25	43	0.48	762.0	1.6	1331.5	60.2	2086.6	0.0	0.0000	-99.1	-92.2	0.005
24	48	0.23	702.5	54.5	1513.0	161.2	2210.8	0.0	0.0000	25.0	29.7	0.008
23	50	-0.46	708.6	14.3	1608.2	30.6	2313.3	0.0	0.0000	127.5	131.1	0.004
23	49	-2.48	708.6	14.3	1585.4	2.2	2293.2	0.1	0.0001	107.4	108.3	0.023
23	48	6.65	708.6	14.3	1513.0	161.2	2217.9	8.2	0.0117	32.1	35.9	0.185
23	47	1.11	708.6	14.3	1432.4	0.2	2138.2	0.1	0.0001	-47.6	-44.7	0.025
23	46	9.44	708.6	14.3	1386.6	15.6	2083.4	0.2	0.0003	-102.4	-90.5	0.104
21	48	0.57	648.7	2.5	1513.0	161.2	2160.3	0.1	0.0001	-25.5	-24.1	0.024
21	47	0.35	648.7	2.5	1432.4	0.2	2080.3	0.1	0.0001	-105.4	-104.7	0.003
20	49	-1.05	641.2	1.5	1585.4	2.2	2229.9	0.1	0.0002	44.1	40.8	0.026
20	48	2.40	641.2	1.5	1513.0	161.2	2153.5	0.4	0.0005	-32.3	-31.6	0.076
20	47	0.89	641.2	1.5	1432.4	0.2	2073.2	0.0	0.0001	-112.5	-112.2	0.008
17	50	0.78	545.4	9.5	1608.2	30.6	2152.4	0.7	0.0010	-33.4	-32.2	0.024
17	48	-0.93	545.4	9.5	1513.0	161.2	2056.7	0.1	0.0001	-129.0	-127.4	0.007
15	52	0.29	508.7	14.2	1714.1	717.2	2226.4	0.0	0.0000	40.6	37.1	0.008
14	50	0.30	443.2	0.3	1608.2	30.6	2051.2	0.0	0.0000	-134.6	-134.4	0.002
11	52	-0.32	366.6	1.2	1714.1	717.2	2080.5	0.1	0.0001	-105.2	-105.0	0.003
6	54	6.02	154.2	5.4	2185.8	704.8	2330.5	0.1	0.0002	144.8	154.2	0.039
5	54	-4.50	121.6	6.1	2185.8	704.8	2293.1	0.3	0.0005	107.3	121.6	0.037
1	54	1.43	-13.0	0.5	2185.8	704.8	2162.9	1.6	0.0023	-22.8	-13.0	0.110
5	54	3.55	134.8	5.9	2196.5	385.2	2320.1	0.3	0.0007	123.6	134.8	0.026

6-31++G(d,p)

i	j	K_{ijk} / cm^{-1}	ω(i) / cm^{-1}	I(i) / km mol^{-1}	ω(j) / cm^{-1}	I(j) / km mol^{-1}	ω(ij) / cm^{-1}	I(ij) / km mol^{-1}	I(ij) / I(k)	Δω'	Δω	TFR
38	38	2.65	1135.6	35.0	1135.6	35.0	2270.4	0.5	0.0007	96.1	96.9	0.027
37	37	1.08	1148.3	242.4	1148.3	242.4	2265.8	0.0	0.0000	91.6	122.3	0.009
36	36	0.26	1080.1	1.7	1080.1	1.7	2173.2	0.3	0.0004	-1.0	-14.1	0.019
35	35	0.69	1025.4	39.8	1025.4	39.8	2050.0	0.2	0.0002	-124.2	-123.3	0.006
30	30	4.14	1155.4	74.8	1155.4	74.8	2292.9	0.5	0.0007	118.7	136.6	0.030
38	41	-0.47	1135.6	35.0	1106.7	155.4	2304.1	1.6	0.0021	129.9	68.1	0.007
37	38	-0.31	1148.3	242.4	1135.6	35.0	2269.0	0.1	0.0002	94.8	109.6	0.003
36	41	-0.46	1080.1	1.7	1106.7	155.4	2253.0	0.1	0.0001	78.7	12.5	0.036
36	40	0.82	1080.1	1.7	1222.8	10.7	2274.6	0.0	0.0000	100.4	128.6	0.006
36	38	0.28	1080.1	1.7	1135.6	35.0	2221.6	1.2	0.0015	47.4	41.4	0.007
35	39	0.49	1025.4	39.8	1285.9	45.4	2292.2	0.1	0.0002	117.9	137.1	0.004
35	38	-0.78	1025.4	39.8	1135.6	35.0	2159.3	1.9	0.0025	-15.0	-13.2	0.059
34	37	0.83	1194.5	61.8	1148.3	242.4	2311.5	0.0	0.0001	137.3	168.5	0.005
33	44	-0.26	931.5	5.2	1298.0	137.6	2257.2	0.0	0.0000	83.0	55.2	0.005
33	39	0.34	931.5	5.2	1285.9	45.4	2204.3	0.0	0.0000	30.1	43.1	0.008
31	46	-0.27	947.0	85.2	1359.7	90.7	2292.7	0.0	0.0000	118.5	132.5	0.002
31	44	-0.49	947.0	85.2	1298.0	137.6	2260.3	0.0	0.0000	86.1	70.8	0.007
31	43	-0.87	947.0	85.2	1315.7	36.8	2263.9	0.0	0.0001	89.7	88.5	0.010
31	41	-0.23	947.0	85.2	1106.7	155.4	2114.3	0.3	0.0004	-59.9	-120.5	0.002
31	40	0.35	947.0	85.2	1222.8	10.7	2137.7	0.0	0.0000	-36.5	-4.5	0.078
31	39	1.00	947.0	85.2	1285.9	45.4	2214.9	0.0	0.0000	40.7	58.7	0.017
30	38	0.25	1155.4	74.8	1135.6	35.0	2283.3	0.1	0.0001	109.1	116.7	0.002
29	46	-0.39	942.9	93.7	1359.7	90.7	2231.8	0.1	0.0002	57.5	128.4	0.003
29	44	0.53	942.9	93.7	1298.0	137.6	2200.5	0.0	0.0001	26.3	66.7	0.008

i	j	K_{ijk} / cm^{-1}	ω(i) / cm^{-1}	I(i) / km mol^{-1}	ω(j) / cm^{-1}	I(j) / km mol^{-1}	ω(ij) / cm^{-1}	I(ij) / km mol^{-1}	I(ij) / I(k)	Δω'	Δω	TFR
29	43	0.25	942.9	93.7	1315.7	36.8	2205.4	0.0	0.0000	31.2	84.4	0.003
29	39	-0.55	942.9	93.7	1285.9	45.4	2168.2	0.0	0.0000	-6.0	54.6	0.010
29	38	-0.25	942.9	93.7	1135.6	35.0	2024.3	0.0	0.0000	-150.0	-95.7	0.003
29	30	-3.53	942.9	93.7	1155.4	74.8	2033.8	0.1	0.0001	-140.4	-75.9	0.047
28	46	-2.38	781.9	113.5	1359.7	90.7	2185.6	3.7	0.0048	11.4	-32.6	0.073
28	45	10.16	781.9	113.5	1438.8	141.8	2275.6	11.7	0.0153	101.4	46.5	0.219
28	44	2.33	781.9	113.5	1298.0	137.6	2155.0	0.1	0.0002	-19.3	-94.3	0.025
28	43	0.96	781.9	113.5	1315.7	36.8	2157.9	0.0	0.0000	-16.4	-76.6	0.013
28	40	-0.96	781.9	113.5	1222.8	10.7	2031.2	0.0	0.0000	-143.0	-169.6	0.006
28	39	-3.03	781.9	113.5	1285.9	45.4	2111.2	0.1	0.0002	-63.0	-106.4	0.029
27	46	-12.82	816.3	305.2	1359.7	90.7	2168.8	147.4	0.1918	-5.4	1.7	7.384
27	45	56.66	816.3	305.2	1438.8	141.8	2257.5	78.3	0.1019	83.3	80.8	0.701
27	44	13.17	816.3	305.2	1298.0	137.6	2133.5	4.0	0.0051	-40.7	-60.0	0.220
27	43	5.42	816.3	305.2	1315.7	36.8	2137.8	0.6	0.0007	-36.4	-42.2	0.128
27	42	1.28	816.3	305.2	1316.4	1.8	2137.2	0.0	0.0001	-37.0	-41.6	0.031
27	39	-16.90	816.3	305.2	1285.9	45.4	2088.4	3.6	0.0047	-85.8	-72.0	0.235
26	46	0.33	831.9	198.9	1359.7	90.7	2182.6	0.9	0.0012	8.4	17.4	0.019
26	45	-2.91	831.9	198.9	1438.8	141.8	2267.6	0.6	0.0008	93.4	96.5	0.030
26	44	-0.68	831.9	198.9	1298.0	137.6	2152.1	0.0	0.0000	-22.1	-44.3	0.015
26	40	0.31	831.9	198.9	1222.8	10.7	2032.3	0.0	0.0000	-141.9	-119.5	0.003
26	39	0.74	831.9	198.9	1285.9	45.4	2101.8	0.0	0.0000	-72.5	-56.4	0.013
25	46	-1.85	947.4	14.1	1359.7	90.7	2265.8	0.6	0.0008	91.6	132.9	0.014
25	44	1.05	947.4	14.1	1298.0	137.6	2252.3	0.0	0.0000	78.1	71.2	0.015
25	43	0.54	947.4	14.1	1315.7	36.8	2249.0	0.0	0.0000	74.8	88.9	0.006
25	40	-0.67	947.4	14.1	1222.8	10.7	2119.4	0.0	0.0000	-54.8	-4.1	0.165
25	39	-1.06	947.4	14.1	1285.9	45.4	2186.3	0.0	0.0000	12.1	59.1	0.018
25	37	0.28	947.4	14.1	1148.3	242.4	2065.4	0.0	0.0000	-108.8	-78.6	0.004
24	29	-1.14	1641.0	2737.3	942.9	93.7	2244.0	2.0	0.0026	69.8	409.7	0.003
24	27	0.34	1641.0	2737.3	816.3	305.2	2177.4	0.0	0.0000	3.1	283.1	0.001
24	26	-0.93	1641.0	2737.3	831.9	198.9	2193.8	4.4	0.0058	19.6	298.7	0.003
23	47	-1.12	757.7	5.9	1426.5	13.5	2160.8	0.1	0.0001	-13.4	10.0	0.113
23	46	-9.37	757.7	5.9	1359.7	90.7	2080.2	0.2	0.0003	-94.1	-56.9	0.165
23	45	40.44	757.7	5.9	1438.8	141.8	2172.5	6.2	0.0081	-1.7	22.2	1.820
23	44	11.52	757.7	5.9	1298.0	137.6	2047.9	0.8	0.0010	-126.4	-118.6	0.097
23	43	5.30	757.7	5.9	1315.7	36.8	2051.1	0.1	0.0002	-123.2	-100.8	0.053
23	42	1.15	757.7	5.9	1316.4	1.8	2051.0	0.0	0.0000	-123.2	-100.2	0.011
23	24	0.37	757.7	5.9	1641.0	2737.3	2090.9	0.1	0.0002	-83.3	224.5	0.002
21	48	0.58	648.9	1.1	1615.6	108.8	2264.2	0.1	0.0001	90.0	90.4	0.006
21	47	0.35	648.9	1.1	1426.5	13.5	2075.2	0.1	0.0001	-99.0	-98.7	0.004
21	45	2.46	648.9	1.1	1438.8	141.8	2083.0	0.0	0.0000	-91.2	-86.5	0.028
20	49	1.05	643.0	18.8	1603.1	2.9	2264.6	0.1	0.0002	90.3	71.9	0.015
20	48	-2.40	643.0	18.8	1615.6	108.8	2287.6	0.4	0.0005	113.4	84.4	0.028
20	47	-0.90	643.0	18.8	1426.5	13.5	2092.3	0.0	0.0001	-81.9	-104.7	0.009
20	45	14.02	643.0	18.8	1438.8	141.8	2107.4	0.2	0.0003	-66.8	-92.4	0.152
19	45	-2.09	626.5	21.3	1438.8	141.8	2035.2	0.0	0.0000	-139.1	-108.9	0.019
18	45	-0.84	501.9	43.8	1438.8	141.8	2040.1	0.0	0.0000	-134.1	-233.5	0.004
17	50	-0.76	554.5	1.9	1698.3	9.9	2259.3	0.7	0.0010	85.1	78.5	0.010
17	48	0.94	554.5	1.9	1615.6	108.8	2177.2	0.1	0.0001	3.0	-4.1	0.229
15	52	0.29	598.3	75.0	1713.0	656.2	2210.0	0.0	0.0000	35.8	137.1	0.002
14	49	1.45	460.6	6.6	1603.1	2.9	2035.1	0.0	0.0001	-139.1	-110.6	0.013
13	48	-0.73	409.2	5.0	1615.6	108.8	2038.6	0.0	0.0001	-135.7	-149.4	0.005
12	50	0.48	340.5	40.4	1698.3	9.9	2157.4	0.0	0.0000	-16.8	-135.4	0.004
11	52	-0.32	382.8	3.1	1713.0	656.2	2112.4	0.1	0.0001	-61.8	-78.4	0.004
10	50	0.66	305.1	18.5	1698.3	9.9	2031.3	0.0	0.0000	-143.0	-170.8	0.004
5	54	4.49	144.4	4.5	2174.2	768.1	2305.3	0.3	0.0004	131.1	144.4	0.031
1	54	1.44	216.4	58.8	2174.2	768.1	2319.3	1.7	0.0022	145.1	216.4	0.007

6-311G(d,p)

i	j	K_{ijk} / cm^{-1}	ω(i) / cm^{-1}	I(i) / km mol^{-1}	ω(j) / cm^{-1}	I(j) / km mol^{-1}	ω(ij) / cm^{-1}	I(ij) / km mol^{-1}	I(ij) / I(k)	Δω'	Δω	TFR
39	39	-35.69	1133.7	21.1	1133.7	21.1	2265.1	11.9	0.0175	75.2	77.4	0.461
38	38	-2.91	1126.2	21.4	1126.2	21.4	2252.3	0.1	0.0002	62.4	62.5	0.047
37	37	-1.80	1103.5	42.6	1103.5	42.6	2205.4	0.1	0.0001	15.5	17.0	0.106
36	36	-0.34	1032.8	11.2	1032.8	11.2	2054.0	0.5	0.0007	-135.9	-124.3	0.003
35	35	-0.58	1021.6	2.1	1021.6	2.1	2040.7	0.1	0.0002	-149.2	-146.8	0.004
39	41	4.33	1133.7	21.1	1203.1	6.0	2335.2	0.1	0.0001	145.2	146.8	0.029
39	40	-14.26	1133.7	21.1	1181.1	0.9	2315.2	1.8	0.0027	125.3	124.9	0.114
38	41	0.58	1126.2	21.4	1203.1	6.0	2328.0	0.9	0.0013	138.1	139.4	0.004
38	40	-1.99	1126.2	21.4	1181.1	0.9	2309.4	0.4	0.0005	119.4	117.4	0.017
38	39	-5.43	1126.2	21.4	1133.7	21.1	2260.0	0.8	0.0012	70.1	70.0	0.078
37	40	-0.25	1103.5	42.6	1181.1	0.9	2285.4	0.5	0.0007	95.4	94.6	0.003
37	39	-1.63	1103.5	42.6	1133.7	21.1	2237.0	0.0	0.0000	47.0	47.2	0.035
37	38	0.62	1103.5	42.6	1126.2	21.4	2227.8	0.5	0.0007	37.9	39.8	0.016
36	43	-0.89	1032.8	11.2	1296.8	56.7	2302.8	0.1	0.0001	112.9	139.6	0.006
36	42	0.83	1032.8	11.2	1266.0	3.4	2301.2	0.1	0.0001	111.3	108.9	0.008
36	41	0.43	1032.8	11.2	1203.1	6.0	2231.6	0.1	0.0001	41.6	45.9	0.009
36	40	-0.87	1032.8	11.2	1181.1	0.9	2212.1	0.0	0.0000	22.1	24.0	0.036
36	39	-2.57	1032.8	11.2	1133.7	21.1	2163.9	1.0	0.0015	-26.0	-23.4	0.110
36	38	-0.34	1032.8	11.2	1126.2	21.4	2156.9	0.2	0.0003	-33.0	-30.9	0.011
35	42	-0.39	1021.6	2.1	1266.0	3.4	2298.7	0.4	0.0006	108.8	97.6	0.004
35	39	-0.69	1021.6	2.1	1133.7	21.1	2154.9	0.1	0.0002	-35.1	-34.7	0.020
35	38	0.52	1021.6	2.1	1126.2	21.4	2146.0	0.8	0.0012	-43.9	-42.1	0.012
35	37	-0.46	1021.6	2.1	1103.5	42.6	2122.4	0.7	0.0011	-67.6	-64.9	0.007
34	45	-9.36	1012.9	0.1	1320.0	235.8	2335.3	0.4	0.0006	145.3	143.0	0.065
34	43	-0.35	1012.9	0.1	1296.8	56.7	2296.5	0.0	0.0000	106.6	119.8	0.003
34	42	0.66	1012.9	0.1	1266.0	3.4	2291.5	0.0	0.0000	101.6	89.0	0.007
34	41	-0.45	1012.9	0.1	1203.1	6.0	2216.1	0.0	0.0000	26.1	26.1	0.017
34	40	1.32	1012.9	0.1	1181.1	0.9	2195.3	36.6	0.0541	5.4	4.1	0.319
34	39	3.07	1012.9	0.1	1133.7	21.1	2147.9	0.6	0.0009	-42.0	-43.3	0.071
34	37	-0.70	1012.9	0.1	1103.5	42.6	2117.2	0.1	0.0001	-72.7	-73.5	0.009
33	45	-0.24	940.2	0.7	1320.0	235.8	2263.2	0.0	0.0000	73.3	70.3	0.003
32	40	-0.23	957.0	0.6	1181.1	0.9	2138.8	0.0	0.0001	-51.1	-51.8	0.005
31	44	-0.52	942.7	15.5	1314.7	12.8	2256.9	0.0	0.0000	67.0	67.4	0.008
31	43	-0.75	942.7	15.5	1296.8	56.7	2223.4	0.3	0.0004	33.5	49.5	0.015
31	42	0.71	942.7	15.5	1266.0	3.4	2219.3	0.2	0.0003	29.4	18.7	0.038
31	41	0.28	942.7	15.5	1203.1	6.0	2142.4	0.4	0.0005	-47.6	-44.2	0.006
31	40	-0.32	942.7	15.5	1181.1	0.9	2124.1	0.0	0.0001	-65.8	-66.2	0.005
31	39	-1.28	942.7	15.5	1133.7	21.1	2076.2	0.0	0.0000	-113.8	-113.6	0.011
31	38	-0.25	942.7	15.5	1126.2	21.4	2068.3	0.1	0.0001	-121.6	-121.0	0.002
30	37	0.29	941.1	4.3	1103.5	42.6	2044.3	0.1	0.0001	-145.6	-145.4	0.002
29	48	-0.36	828.2	65.3	1505.8	190.9	2333.1	0.0	0.0000	143.2	144.1	0.003
29	46	-0.65	828.2	65.3	1354.4	30.9	2186.4	0.1	0.0002	-3.5	-7.3	0.089
29	45	2.12	828.2	65.3	1320.0	235.8	2149.0	1.5	0.0023	-40.9	-41.7	0.051
29	43	-0.33	828.2	65.3	1296.8	56.7	2110.5	0.1	0.0001	-79.4	-64.9	0.005
28	48	0.31	814.3	51.5	1505.8	190.9	2319.3	0.0	0.0000	129.3	130.1	0.002
28	46	0.56	814.3	51.5	1354.4	30.9	2172.7	0.5	0.0008	-17.2	-21.2	0.026
28	45	-1.90	814.3	51.5	1320.0	235.8	2135.1	0.4	0.0006	-54.8	-55.7	0.034
28	43	0.27	814.3	51.5	1296.8	56.7	2096.5	0.0	0.0000	-93.4	-78.9	0.003
28	42	-0.22	814.3	51.5	1266.0	3.4	2092.3	0.0	0.0000	-97.6	-109.6	0.002
27	48	6.82	817.9	5.2	1505.8	190.9	2322.1	1.9	0.0028	132.2	133.8	0.051
27	47	0.30	817.9	5.2	1429.0	2.4	2246.3	0.0	0.0000	56.4	57.0	0.005
27	46	18.08	817.9	5.2	1354.4	30.9	2174.1	115.6	0.1709	-15.8	-17.6	1.028
27	45	-58.44	817.9	5.2	1320.0	235.8	2127.5	92.1	0.1362	-62.4	-52.1	1.123

i	j	K_{ijk} / cm^{-1}	ω(i) / cm^{-1}	I(i) / km mol^{-1}	ω(j) / cm^{-1}	I(j) / km mol^{-1}	ω(ij) / cm^{-1}	I(ij) / km mol^{-1}	I(ij) / I(k)	Δω'	Δω	TFR
27	44	-2.11	817.9	5.2	1314.7	12.8	2132.0	0.1	0.0001	-57.9	-57.3	0.037
27	43	6.55	817.9	5.2	1296.8	56.7	2100.3	0.5	0.0007	-89.6	-75.3	0.087
27	42	-6.58	817.9	5.2	1266.0	3.4	2095.6	0.5	0.0007	-94.4	-106.0	0.062
26	48	-0.25	810.5	2.0	1505.8	190.9	2315.9	0.0	0.0000	125.9	126.4	0.002
26	46	-0.72	810.5	2.0	1354.4	30.9	2169.3	1.8	0.0027	-20.6	-25.0	0.029
26	45	0.95	810.5	2.0	1320.0	235.8	2131.7	0.0	0.0000	-58.3	-59.4	0.016
25	48	-0.43	770.9	3.2	1505.8	190.9	2276.3	0.1	0.0001	86.4	86.8	0.005
25	46	-2.69	770.9	3.2	1354.4	30.9	2128.8	1.0	0.0015	-61.1	-64.6	0.042
25	45	5.02	770.9	3.2	1320.0	235.8	2091.8	0.2	0.0003	-98.1	-99.1	0.051
25	43	-0.66	770.9	3.2	1296.8	56.7	2053.8	0.0	0.0000	-136.1	-122.3	0.005
25	42	0.66	770.9	3.2	1266.0	3.4	2049.6	0.0	0.0000	-140.3	-153.0	0.004
24	48	0.22	719.3	9.3	1505.8	190.9	2223.1	0.0	0.0000	33.2	35.1	0.006
23	50	-0.62	713.2	15.9	1598.6	1.7	2315.7	0.0	0.0000	125.8	121.9	0.005
23	49	-2.25	713.2	15.9	1573.4	1.9	2290.5	0.1	0.0001	100.5	96.7	0.023
23	48	6.63	713.2	15.9	1505.8	190.9	2216.9	7.7	0.0114	27.0	29.1	0.228
23	47	1.19	713.2	15.9	1429.0	2.4	2141.0	0.1	0.0001	-48.9	-47.8	0.025
23	46	12.46	713.2	15.9	1354.4	30.9	2070.5	0.3	0.0004	-119.5	-122.3	0.102
21	49	0.25	645.8	4.6	1573.4	1.9	2215.6	0.0	0.0000	25.7	29.3	0.009
21	48	0.43	645.8	4.6	1505.8	190.9	2141.3	0.0	0.0001	-48.6	-38.3	0.011
20	50	-0.22	640.0	1.1	1598.6	1.7	2246.0	0.0	0.0000	56.1	48.7	0.005
20	49	-0.79	640.0	1.1	1573.4	1.9	2221.0	0.1	0.0001	31.1	23.5	0.034
20	48	2.07	640.0	1.1	1505.8	190.9	2147.1	0.2	0.0004	-42.8	-44.1	0.047
20	47	0.91	640.0	1.1	1429.0	2.4	2070.6	0.0	0.0001	-119.4	-121.0	0.007
18	52	0.26	578.2	8.5	1726.0	85.0	2302.4	0.0	0.0000	112.5	114.3	0.002
17	50	0.92	545.3	11.2	1598.6	1.7	2148.7	0.8	0.0012	-41.2	-46.0	0.020
17	48	-0.55	545.3	11.2	1505.8	190.9	2049.3	0.0	0.0000	-140.7	-138.9	0.004
15	52	0.25	513.8	10.4	1726.0	85.0	2240.9	0.0	0.0001	51.0	49.9	0.005
14	50	-0.50	437.0	6.0	1598.6	1.7	2042.0	0.0	0.0000	-148.0	-154.4	0.003
10	52	-0.31	329.3	3.7	1726.0	85.0	2055.0	0.1	0.0001	-134.9	-134.6	0.002
6	54	-5.93	141.1	2.9	2189.9	676.4	2319.7	0.1	0.0001	129.8	141.1	0.042
5	54	-3.57	124.7	5.8	2189.9	676.4	2295.3	0.3	0.0004	105.3	124.7	0.029
2	54	-0.71	25.6	0.6	2189.9	676.4	2213.1	0.1	0.0002	23.1	25.6	0.028

6-311G+(d,p)

i	j	K_{ijk} / cm^{-1}	ω(i) / cm^{-1}	I(i) / km mol^{-1}	ω(j) / cm^{-1}	I(j) / km mol^{-1}	ω(ij) / cm^{-1}	I(ij) / km mol^{-1}	I(ij) / I(k)	Δω'	Δω	TFR
39	39	-37.26	1130.6	27.9	1130.6	27.9	2304.0	13.8	0.0239	124.6	81.7	0.456
38	38	-2.20	1152.2	4.6	1152.2	4.6	2279.1	0.4	0.0006	99.6	124.9	0.018
37	37	-1.41	1118.3	79.7	1118.3	79.7	2299.2	0.0	0.0000	119.8	57.2	0.025
36	36	-0.27	1082.8	18.3	1082.8	18.3	2169.4	0.4	0.0006	-10.1	-13.9	0.019
35	35	-0.65	1035.8	3.2	1035.8	3.2	2069.4	0.1	0.0002	-110.0	-107.9	0.006
34	34	0.48	1032.4	1.5	1032.4	1.5	2092.3	0.0	0.0001	-87.1	-114.6	0.004
38	39	-1.82	1152.2	4.6	1130.6	27.9	2294.1	0.1	0.0002	114.6	103.3	0.018
37	39	-0.81	1118.3	79.7	1130.6	27.9	2303.3	0.0	0.0001	123.8	69.5	0.012
37	38	0.55	1118.3	79.7	1152.2	4.6	2289.1	0.3	0.0006	109.6	91.1	0.006
36	41	0.44	1082.8	18.3	1190.8	20.5	2308.8	0.1	0.0001	129.3	94.1	0.005
36	40	-0.85	1082.8	18.3	1329.2	6.5	2322.5	0.0	0.0000	143.1	232.5	0.004
36	39	-2.84	1082.8	18.3	1130.6	27.9	2235.2	17.3	0.0300	55.8	33.9	0.084
35	39	-0.41	1035.8	3.2	1130.6	27.9	2188.3	0.1	0.0001	8.9	-13.1	0.031
35	38	0.66	1035.8	3.2	1152.2	4.6	2173.3	1.3	0.0023	-6.2	8.5	0.077
35	37	-0.34	1035.8	3.2	1118.3	79.7	2183.1	0.5	0.0009	3.6	-25.3	0.014

i	j	K_{ijk} / cm^{-1}	ω(i) / cm^{-1}	I(i) / km mol^{-1}	ω(j) / cm^{-1}	I(j) / km mol^{-1}	ω(ij) / cm^{-1}	I(ij) / km mol^{-1}	I(ij) / I(k)	Δω'	Δω	TFR
34	41	-0.33	1032.4	1.5	1190.8	20.5	2273.7	0.0	0.0000	94.2	43.8	0.007
34	40	0.92	1032.4	1.5	1329.2	6.5	2289.2	18.8	0.0327	109.7	182.1	0.005
34	39	2.77	1032.4	1.5	1130.6	27.9	2199.9	0.7	0.0013	20.4	-16.4	0.169
34	37	-0.69	1032.4	1.5	1118.3	79.7	2196.5	0.0	0.0001	17.0	-28.7	0.024
33	45	-0.40	952.3	0.2	1316.9	205.5	2276.4	0.0	0.0000	97.0	89.6	0.004
33	39	0.25	952.3	0.2	1130.6	27.9	2102.6	0.0	0.0000	-76.8	-96.6	0.003
31	44	-0.48	947.6	3.2	1390.3	201.4	2316.2	0.0	0.0001	136.7	158.4	0.003
31	43	-0.56	947.6	3.2	1311.4	4.7	2261.5	0.4	0.0006	82.0	79.6	0.007
31	42	0.82	947.6	3.2	1294.6	121.3	2239.3	0.1	0.0002	59.9	62.8	0.013
31	41	0.22	947.6	3.2	1190.8	20.5	2171.1	0.3	0.0006	-8.3	-41.0	0.005
31	40	-0.41	947.6	3.2	1329.2	6.5	2186.5	0.0	0.0000	7.0	97.3	0.004
31	39	-1.22	947.6	3.2	1130.6	27.9	2099.2	0.0	0.0000	-80.3	-101.2	0.012
30	45	0.43	931.2	7.2	1316.9	205.5	2261.8	0.0	0.0000	82.4	68.6	0.006
30	44	0.23	931.2	7.2	1390.3	201.4	2307.4	0.0	0.0000	127.9	142.0	0.002
30	39	0.29	931.2	7.2	1130.6	27.9	2088.6	0.0	0.0000	-90.8	-117.6	0.002
29	46	-0.45	848.8	79.8	1353.4	37.3	2200.7	0.1	0.0002	21.2	22.7	0.020
29	45	2.10	848.8	79.8	1316.9	205.5	2164.1	2.7	0.0047	-15.3	-13.9	0.151
29	43	-0.31	848.8	79.8	1311.4	4.7	2156.1	0.1	0.0001	-23.4	-19.3	0.016
29	42	0.30	848.8	79.8	1294.6	121.3	2132.3	0.0	0.0000	-47.1	-36.1	0.008
28	46	-0.53	823.6	13.8	1353.4	37.3	2193.3	0.2	0.0003	13.8	-2.4	0.218
28	45	1.85	823.6	13.8	1316.9	205.5	2156.8	0.8	0.0015	-22.7	-39.0	0.047
28	40	-0.23	823.6	13.8	1329.2	6.5	2071.2	0.0	0.0000	-108.3	-26.7	0.009
27	46	14.69	822.7	6.6	1353.4	37.3	2188.4	281.5	0.4893	9.0	-3.4	4.342
27	45	-59.05	822.7	6.6	1316.9	205.5	2133.0	165.4	0.2874	-46.5	-39.9	1.479
27	44	-0.74	822.7	6.6	1390.3	201.4	2193.0	0.0	0.0000	13.5	33.5	0.022
27	43	5.21	822.7	6.6	1311.4	4.7	2139.5	0.5	0.0008	-40.0	-45.4	0.115
27	42	-8.76	822.7	6.6	1294.6	121.3	2115.2	1.2	0.0020	-64.2	-62.1	0.141
27	41	-1.28	822.7	6.6	1190.8	20.5	2049.2	0.0	0.0000	-130.2	-166.0	0.008
27	40	5.57	822.7	6.6	1329.2	6.5	2064.0	0.0	0.0001	-115.5	-27.6	0.202
26	47	0.22	800.3	1.5	1440.3	41.5	2249.8	0.1	0.0001	70.3	61.1	0.004
26	46	0.72	800.3	1.5	1353.4	37.3	2166.4	4.4	0.0076	-13.0	-25.8	0.028
26	45	-4.17	800.3	1.5	1316.9	205.5	2130.1	1.5	0.0025	-49.4	-62.3	0.067
26	43	0.29	800.3	1.5	1311.4	4.7	2121.1	0.0	0.0000	-58.4	-67.8	0.004
26	42	-0.59	800.3	1.5	1294.6	121.3	2096.3	0.0	0.0000	-83.1	-84.5	0.007
26	40	0.44	800.3	1.5	1329.2	6.5	2047.3	0.0	0.0000	-132.2	-50.0	0.009
25	48	-0.28	770.4	2.7	1534.6	101.6	2301.3	0.0	0.0001	121.9	125.6	0.002
25	46	-1.95	770.4	2.7	1353.4	37.3	2132.6	0.8	0.0014	-46.9	-55.6	0.035
25	45	3.98	770.4	2.7	1316.9	205.5	2096.7	0.2	0.0003	-82.7	-92.2	0.043
25	43	-0.41	770.4	2.7	1311.4	4.7	2087.3	0.0	0.0000	-92.2	-97.6	0.004
25	42	0.68	770.4	2.7	1294.6	121.3	2064.9	0.0	0.0000	-114.6	-114.4	0.006
24	48	0.25	726.7	7.3	1534.6	101.6	2256.4	0.0	0.0000	76.9	81.9	0.003
24	45	-0.66	726.7	7.3	1316.9	205.5	2052.6	0.1	0.0001	-126.9	-135.9	0.005
24	43	0.25	726.7	7.3	1311.4	4.7	2043.9	0.0	0.0000	-135.5	-141.3	0.002
23	49	-2.42	732.0	5.5	1582.6	5.7	2312.9	0.1	0.0002	133.5	135.1	0.018
23	48	6.54	732.0	5.5	1534.6	101.6	2260.8	5.4	0.0093	81.3	87.1	0.075
23	47	1.17	732.0	5.5	1440.3	41.5	2175.3	0.1	0.0002	-4.1	-7.2	0.162
23	46	10.51	732.0	5.5	1353.4	37.3	2092.4	0.3	0.0005	-87.1	-94.1	0.112
23	45	-41.22	732.0	5.5	1316.9	205.5	2051.3	7.2	0.0125	-128.2	-130.7	0.315
23	44	-0.35	732.0	5.5	1390.3	201.4	2100.8	0.0	0.0000	-78.6	-57.2	0.006
23	43	4.88	732.0	5.5	1311.4	4.7	2047.4	0.2	0.0003	-132.0	-136.1	0.036
21	49	0.24	651.4	3.3	1582.6	5.7	2235.0	0.0	0.0000	55.5	54.5	0.004
21	48	0.46	651.4	3.3	1534.6	101.6	2181.4	0.0	0.0001	1.9	6.5	0.071
21	47	0.25	651.4	3.3	1440.3	41.5	2095.5	0.1	0.0001	-84.0	-87.8	0.003
20	49	0.92	646.3	1.7	1582.6	5.7	2230.3	0.1	0.0001	50.8	49.4	0.019
20	48	-2.23	646.3	1.7	1534.6	101.6	2177.0	0.5	0.0008	-2.4	1.5	1.523
20	47	-0.88	646.3	1.7	1440.3	41.5	2090.8	0.0	0.0001	-88.7	-92.9	0.009

i	j	K_{ijk} / cm^{-1}	ω(i) / cm^{-1}	I(i) / km mol^{-1}	ω(j) / cm^{-1}	I(j) / km mol^{-1}	ω(ij) / cm^{-1}	I(ij) / km mol^{-1}	I(ij) / I(k)	Δω'	Δω	TFR
19	49	-0.23	625.8	0.5	1582.6	5.7	2210.1	0.0	0.0000	30.7	29.0	0.008
17	50	0.81	548.8	12.6	1605.6	5.9	2152.2	0.8	0.0013	-27.2	-25.1	0.032
17	48	-0.84	548.8	12.6	1534.6	101.6	2079.3	0.1	0.0001	-100.2	-96.1	0.009
15	52	0.29	513.6	12.2	1707.7	688.2	2225.9	0.0	0.0001	46.4	41.8	0.007
14	53	0.26	460.8	0.5	1775.7	0.5	2242.8	0.0	0.0000	63.3	57.0	0.004
14	50	0.31	460.8	0.5	1605.6	5.9	2064.8	0.0	0.0000	-114.7	-113.0	0.003
14	49	1.51	460.8	0.5	1582.6	5.7	2044.4	0.0	0.0001	-135.1	-136.0	0.011
11	52	-0.33	370.6	0.9	1707.7	688.2	2078.5	0.1	0.0002	-101.0	-101.1	0.003
1	54	1.32	21.7	0.5	2179.5	575.2	2189.8	1.8	0.0032	10.4	21.7	0.061

6-311G++(d,p)

i	j	K_{ijk} / cm^{-1}	ω(i) / cm^{-1}	I(i) / km mol^{-1}	ω(j) / cm^{-1}	I(j) / km mol^{-1}	ω(ij) / cm^{-1}	I(ij) / km mol^{-1}	I(ij) / I(k)	Δω'	Δω	TFR
39	39	-37.25	1133.2	26.9	1133.2	26.9	2288.9	13.7	0.0223	110.3	87.8	0.424
38	38	-2.20	1153.8	8.2	1153.8	8.2	2269.2	0.4	0.0006	90.6	129.0	0.017
37	37	-1.41	1115.7	72.7	1115.7	72.7	2280.1	0.0	0.0000	101.5	52.8	0.027
36	36	-0.27	1082.0	17.1	1082.0	17.1	2169.0	0.4	0.0006	-9.6	-14.6	0.019
35	35	-0.65	1033.9	7.3	1033.9	7.3	2066.8	0.1	0.0002	-111.8	-110.8	0.006
34	34	0.48	1032.7	3.6	1032.7	3.6	2075.6	0.0	0.0000	-103.0	-113.2	0.004
38	39	-1.83	1153.8	8.2	1133.2	26.9	2281.5	0.1	0.0002	102.9	108.4	0.017
37	39	-0.84	1115.7	72.7	1133.2	26.9	2286.0	0.0	0.0000	107.4	70.3	0.012
37	38	0.54	1115.7	72.7	1153.8	8.2	2274.5	0.3	0.0005	95.9	90.9	0.006
36	41	0.44	1082.0	17.1	1194.5	17.1	2301.0	0.1	0.0001	122.4	97.9	0.004
36	40	-0.86	1082.0	17.1	1275.1	5.6	2308.9	0.0	0.0000	130.3	178.5	0.005
36	39	-2.84	1082.0	17.1	1133.2	26.9	2227.5	17.4	0.0284	48.9	36.6	0.078
35	42	-0.36	1033.9	7.3	1292.4	189.0	2327.6	0.2	0.0004	149.0	147.7	0.002
35	39	-0.41	1033.9	7.3	1133.2	26.9	2179.5	0.1	0.0001	0.9	-11.5	0.036
35	38	0.66	1033.9	7.3	1153.8	8.2	2167.1	1.3	0.0022	-11.5	9.1	0.072
35	37	-0.34	1033.9	7.3	1115.7	72.7	2172.2	0.5	0.0009	-6.4	-29.0	0.012
34	42	0.81	1032.7	3.6	1292.4	189.0	2328.5	0.0	0.0000	149.9	146.5	0.006
34	41	-0.32	1032.7	3.6	1194.5	17.1	2257.7	0.0	0.0000	79.1	48.6	0.007
34	40	0.92	1032.7	3.6	1275.1	5.6	2267.3	16.6	0.0270	88.7	129.2	0.007
34	39	2.76	1032.7	3.6	1133.2	26.9	2183.8	0.7	0.0012	5.3	-12.7	0.218
34	37	-0.69	1032.7	3.6	1115.7	72.7	2178.4	0.0	0.0001	-0.2	-30.2	0.023
33	45	-0.42	955.2	3.5	1320.9	213.4	2265.4	0.0	0.0000	86.9	97.6	0.004
33	39	0.26	955.2	3.5	1133.2	26.9	2087.1	0.0	0.0000	-91.5	-90.2	0.003
31	44	-0.50	944.7	2.7	1374.6	36.1	2300.9	0.0	0.0001	122.3	140.7	0.004
31	43	-0.57	944.7	2.7	1310.9	3.0	2257.4	0.4	0.0006	78.9	77.0	0.007
31	42	0.84	944.7	2.7	1292.4	189.0	2236.7	0.1	0.0002	58.1	58.5	0.014
31	41	0.21	944.7	2.7	1194.5	17.1	2162.0	0.3	0.0005	-16.6	-39.4	0.005
31	40	-0.42	944.7	2.7	1275.1	5.6	2171.6	0.0	0.0000	-6.9	41.2	0.010
31	39	-1.24	944.7	2.7	1133.2	26.9	2090.1	0.0	0.0000	-88.5	-100.7	0.012
30	45	0.41	899.0	1.8	1320.9	213.4	2235.4	0.0	0.0000	56.8	41.4	0.010
30	37	-0.23	899.0	1.8	1115.7	72.7	2051.0	0.1	0.0001	-127.6	-163.9	0.001
29	46	-0.47	847.1	74.2	1350.4	2.2	2189.5	0.1	0.0002	10.9	18.9	0.025
29	45	2.18	847.1	74.2	1320.9	213.4	2152.0	2.9	0.0047	-26.6	-10.5	0.206
29	43	-0.32	847.1	74.2	1310.9	3.0	2144.8	0.1	0.0001	-33.8	-20.6	0.016
29	42	0.31	847.1	74.2	1292.4	189.0	2122.2	0.0	0.0000	-56.3	-39.1	0.008
28	46	-0.53	825.0	8.2	1350.4	2.2	2192.2	0.2	0.0003	13.6	-3.2	0.166
28	45	1.85	825.0	8.2	1320.9	213.4	2154.9	0.8	0.0013	-23.7	-32.7	0.057
28	42	0.22	825.0	8.2	1292.4	189.0	2125.6	0.0	0.0000	-53.0	-61.2	0.004
28	40	-0.23	825.0	8.2	1275.1	5.6	2059.2	0.0	0.0000	-119.4	-78.5	0.003

i	j	K_{ijk} / cm^{-1}	ω(i) / cm^{-1}	I(i) / km mol^{-1}	ω(j) / cm^{-1}	I(j) / km mol^{-1}	ω(ij) / cm^{-1}	I(ij) / km mol^{-1}	I(ij) / I(k)	Δω'	Δω	TFR
27	47	0.21	818.9	6.2	1437.1	10.6	2257.6	0.0	0.0001	79.0	77.4	0.003
27	46	14.61	818.9	6.2	1350.4	2.2	2182.8	281.2	0.4579	4.2	-9.3	1.571
27	45	-58.96	818.9	6.2	1320.9	213.4	2128.5	126.0	0.2051	-50.1	-38.8	1.520
27	44	-0.65	818.9	6.2	1374.6	36.1	2175.5	0.0	0.0000	-3.1	14.9	0.043
27	43	5.20	818.9	6.2	1310.9	3.0	2133.8	0.5	0.0008	-44.8	-48.8	0.107
27	42	-8.80	818.9	6.2	1292.4	189.0	2110.8	1.2	0.0019	-67.8	-67.3	0.131
27	41	-1.26	818.9	6.2	1194.5	17.1	2038.3	0.0	0.0000	-140.3	-165.2	0.008
27	40	5.59	818.9	6.2	1275.1	5.6	2047.0	0.0	0.0001	-131.6	-84.6	0.066
26	48	0.43	755.5	10.8	1524.7	142.5	2287.6	0.0	0.0000	109.0	101.6	0.004
26	47	0.23	755.5	10.8	1437.1	10.6	2205.3	0.1	0.0001	26.7	14.0	0.016
26	46	0.86	755.5	10.8	1350.4	2.2	2126.4	5.4	0.0088	-52.2	-72.7	0.012
26	45	-4.74	755.5	10.8	1320.9	213.4	2088.9	1.8	0.0030	-89.7	-102.2	0.046
26	43	0.34	755.5	10.8	1310.9	3.0	2080.8	0.0	0.0000	-97.7	-112.2	0.003
26	42	-0.67	755.5	10.8	1292.4	189.0	2057.4	0.0	0.0000	-121.2	-130.8	0.005
25	48	-0.28	770.8	2.7	1524.7	142.5	2293.2	0.0	0.0001	114.7	116.9	0.002
25	46	-1.94	770.8	2.7	1350.4	2.2	2130.7	0.8	0.0013	-47.9	-57.4	0.034
25	45	3.96	770.8	2.7	1320.9	213.4	2094.0	0.2	0.0003	-84.5	-86.9	0.046
25	43	-0.40	770.8	2.7	1310.9	3.0	2085.2	0.0	0.0000	-93.4	-96.9	0.004
25	42	0.68	770.8	2.7	1292.4	189.0	2064.2	0.0	0.0000	-114.4	-115.4	0.006
24	48	0.23	720.6	4.7	1524.7	142.5	2241.8	0.0	0.0000	63.2	66.7	0.003
24	45	-0.46	720.6	4.7	1320.9	213.4	2043.4	0.1	0.0001	-135.2	-137.0	0.003
23	50	-0.39	720.4	3.6	1601.3	3.9	2324.5	0.0	0.0000	145.9	143.1	0.003
23	49	-2.42	720.4	3.6	1578.6	5.4	2304.0	0.1	0.0001	125.4	120.5	0.020
23	48	6.53	720.4	3.6	1524.7	142.5	2246.6	5.4	0.0087	68.0	66.5	0.098
23	47	1.19	720.4	3.6	1437.1	10.6	2163.6	0.1	0.0002	-15.0	-21.0	0.057
23	46	10.47	720.4	3.6	1350.4	2.2	2084.6	0.3	0.0005	-94.0	-107.7	0.097
23	45	-41.22	720.4	3.6	1320.9	213.4	2042.7	7.1	0.0116	-135.9	-137.2	0.300
23	44	-0.28	720.4	3.6	1374.6	36.1	2081.1	0.0	0.0000	-97.5	-83.6	0.003
23	43	4.87	720.4	3.6	1310.9	3.0	2039.5	0.2	0.0002	-139.1	-147.2	0.033
21	49	0.23	652.1	3.3	1578.6	5.4	2232.3	0.0	0.0000	53.7	52.1	0.004
21	48	0.48	652.1	3.3	1524.7	142.5	2173.7	0.1	0.0001	-4.9	-1.8	0.263
21	47	0.25	652.1	3.3	1437.1	10.6	2090.2	0.1	0.0001	-88.4	-89.4	0.003
20	49	0.92	645.4	1.5	1578.6	5.4	2225.9	0.1	0.0001	47.3	45.4	0.020
20	48	-2.23	645.4	1.5	1524.7	142.5	2167.7	0.5	0.0008	-10.9	-8.5	0.262
20	47	-0.88	645.4	1.5	1437.1	10.6	2083.8	0.0	0.0001	-94.8	-96.1	0.009
19	49	-0.23	627.0	0.5	1578.6	5.4	2207.9	0.0	0.0000	29.3	27.0	0.009
17	50	0.81	548.6	12.0	1601.3	3.9	2149.5	0.8	0.0013	-29.1	-28.7	0.028
17	48	-0.84	548.6	12.0	1524.7	142.5	2070.7	0.1	0.0001	-107.9	-105.3	0.008
15	52	0.29	493.7	15.6	1707.6	664.3	2215.8	0.0	0.0001	37.2	22.7	0.013
14	53	0.25	454.1	0.2	1774.5	0.4	2236.5	0.0	0.0000	57.9	50.0	0.005
14	50	0.30	454.1	0.2	1601.3	3.9	2055.8	0.0	0.0000	-122.8	-123.2	0.002
14	49	1.51	454.1	0.2	1578.6	5.4	2034.6	0.0	0.0001	-144.0	-145.9	0.010
11	52	-0.33	369.6	1.3	1707.6	664.3	2076.9	0.1	0.0002	-101.7	-101.4	0.003
1	54	1.31	-1.7	0.1	2178.6	614.1	2165.7	1.8	0.0029	-12.9	-1.7	0.779

6-311G++(df,pd)

i	j	K_{ijk} / cm^{-1}	ω(i) / cm^{-1}	I(i) / km mol^{-1}	ω(j) / cm^{-1}	I(j) / km mol^{-1}	ω(ij) / cm^{-1}	I(ij) / km mol^{-1}	I(ij) / I(k)	Δω'	Δω	TFR
39	39	37.90	1134.4	16.3	1134.4	16.3	2266.5	12.7	0.0178	89.4	91.7	0.413
38	38	1.99	1126.8	20.2	1126.8	20.2	2256.4	0.2	0.0003	79.4	76.5	0.026
37	37	1.65	1103.4	104.6	1103.4	104.6	2205.6	0.1	0.0001	28.6	29.8	0.055
36	36	0.32	1085.4	16.9	1085.4	16.9	2176.1	0.4	0.0006	-0.9	-6.3	0.051
35	35	0.68	1033.3	12.8	1033.3	12.8	2063.9	0.1	0.0002	-113.1	-110.4	0.006

i	j	K_{ijk} / cm^{-1}	ω(i) / cm^{-1}	I(i) / km mol^{-1}	ω(j) / cm^{-1}	I(j) / km mol^{-1}	ω(ij) / cm^{-1}	I(ij) / km mol^{-1}	I(ij) / I(k)	Δω’	Δω	TFR
34	34	-0.52	1021.4	1.9	1021.4	1.9	2039.6	0.0	0.0000	-137.5	-134.3	0.004
39	40	12.85	1134.4	16.3	1179.6	17.4	2313.3	1.5	0.0021	136.2	136.9	0.094
38	40	0.60	1126.8	20.2	1179.6	17.4	2309.2	0.3	0.0004	132.1	129.3	0.005
38	39	2.30	1126.8	20.2	1134.4	16.3	2262.7	0.1	0.0002	85.6	84.1	0.027
37	39	0.90	1103.4	104.6	1134.4	16.3	2237.9	0.0	0.0001	60.8	60.7	0.015
37	38	-0.64	1103.4	104.6	1126.8	20.2	2229.6	0.3	0.0005	52.5	53.2	0.012
36	41	-0.42	1085.4	16.9	1202.0	2.1	2285.1	0.1	0.0001	108.1	110.3	0.004
36	40	0.91	1085.4	16.9	1179.6	17.4	2263.9	0.0	0.0000	86.9	87.9	0.010
36	39	3.09	1085.4	16.9	1134.4	16.3	2219.8	5.3	0.0075	42.7	42.7	0.072
35	42	-0.41	1033.3	12.8	1290.5	60.3	2323.1	0.1	0.0001	146.1	146.7	0.003
35	39	0.47	1033.3	12.8	1134.4	16.3	2167.1	0.1	0.0002	-10.0	-9.4	0.050
35	38	-0.60	1033.3	12.8	1126.8	20.2	2159.1	1.1	0.0015	-18.0	-17.0	0.036
35	37	0.48	1033.3	12.8	1103.4	104.6	2134.0	0.9	0.0013	-43.0	-40.3	0.012
34	42	1.23	1021.4	1.9	1290.5	60.3	2307.4	0.0	0.0000	130.3	134.8	0.009
34	41	0.24	1021.4	1.9	1202.0	2.1	2219.6	0.0	0.0000	42.6	46.3	0.005
34	40	-0.80	1021.4	1.9	1179.6	17.4	2198.2	0.9	0.0012	21.1	23.9	0.034
34	39	-2.54	1021.4	1.9	1134.4	16.3	2154.1	0.8	0.0012	-23.0	-21.3	0.119
34	38	0.33	1021.4	1.9	1126.8	20.2	2148.0	0.0	0.0000	-29.0	-28.9	0.011
34	37	0.65	1021.4	1.9	1103.4	104.6	2123.0	0.1	0.0001	-54.0	-52.3	0.012
34	35	0.23	1021.4	1.9	1033.3	12.8	2052.4	0.0	0.0000	-124.7	-122.4	0.002
33	45	-0.42	966.0	3.1	1315.1	174.2	2277.6	0.0	0.0000	100.5	104.1	0.004
33	42	0.21	966.0	3.1	1290.5	60.3	2251.6	0.0	0.0000	74.6	79.4	0.003
33	39	0.25	966.0	3.1	1134.4	16.3	2096.6	0.0	0.0000	-80.4	-76.7	0.003
31	45	0.44	943.3	19.9	1315.1	174.2	2264.9	0.0	0.0000	87.8	81.4	0.005
31	39	-0.25	943.3	19.9	1134.4	16.3	2083.6	0.0	0.0000	-93.5	-99.4	0.003
31	37	-0.25	943.3	19.9	1103.4	104.6	2052.2	0.1	0.0001	-124.8	-130.3	0.002
30	44	0.61	946.9	16.0	1317.1	8.3	2263.7	0.0	0.0000	86.6	87.0	0.007
30	43	-0.37	946.9	16.0	1318.5	3.2	2262.7	0.4	0.0006	85.6	88.4	0.004
30	42	-0.95	946.9	16.0	1290.5	60.3	2235.9	0.0	0.0001	58.8	60.3	0.016
30	40	-0.41	946.9	16.0	1179.6	17.4	2125.4	0.0	0.0000	-51.7	-50.6	0.008
30	39	-1.32	946.9	16.0	1134.4	16.3	2081.1	0.0	0.0000	-95.9	-95.8	0.014
29	46	-0.33	844.5	24.7	1357.2	65.3	2198.7	0.1	0.0001	21.6	24.6	0.013
29	45	1.64	844.5	24.7	1315.1	174.2	2153.1	12.3	0.0174	-24.0	-17.5	0.094
29	42	-0.26	844.5	24.7	1290.5	60.3	2127.7	0.0	0.0000	-49.4	-42.1	0.006
28	46	-0.53	820.3	86.0	1357.2	65.3	2181.0	0.1	0.0002	3.9	0.5	1.178
28	45	1.82	820.3	86.0	1315.1	174.2	2135.8	1.7	0.0025	-41.3	-41.6	0.044
27	48	6.06	809.2	5.4	1501.8	153.7	2316.2	1.5	0.0022	139.1	134.0	0.045
27	46	14.51	809.2	5.4	1357.2	65.3	2180.1	187.9	0.2644	3.0	-10.6	1.366
27	45	-57.06	809.2	5.4	1315.1	174.2	2120.9	87.8	0.1235	-56.2	-52.7	1.083
27	43	2.98	809.2	5.4	1318.5	3.2	2134.8	0.2	0.0003	-42.3	-49.3	0.060
27	42	8.56	809.2	5.4	1290.5	60.3	2104.9	1.2	0.0017	-72.2	-77.4	0.111
26	46	3.67	832.1	11.8	1357.2	65.3	2190.4	17.4	0.0245	13.3	12.2	0.300
26	45	-15.70	832.1	11.8	1315.1	174.2	2142.8	34.6	0.0487	-34.3	-29.9	0.525
26	43	0.77	832.1	11.8	1318.5	3.2	2147.9	0.0	0.0000	-29.1	-26.5	0.029
26	42	2.32	832.1	11.8	1290.5	60.3	2118.0	0.1	0.0001	-59.0	-54.5	0.043
26	41	-0.33	832.1	11.8	1202.0	2.1	2029.2	0.0	0.0000	-147.8	-143.0	0.002
25	48	-0.29	768.7	1.4	1501.8	153.7	2269.6	0.0	0.0000	92.5	93.5	0.003
25	46	-2.01	768.7	1.4	1357.2	65.3	2129.1	0.9	0.0012	-47.9	-51.1	0.039
25	45	4.10	768.7	1.4	1315.1	174.2	2084.4	0.2	0.0003	-92.7	-93.2	0.044
25	43	-0.25	768.7	1.4	1318.5	3.2	2086.5	0.0	0.0000	-90.5	-89.8	0.003
25	42	-0.71	768.7	1.4	1290.5	60.3	2059.2	0.0	0.0000	-117.8	-117.9	0.006
24	45	-0.43	730.1	7.9	1315.1	174.2	2046.9	0.1	0.0001	-130.1	-131.8	0.003
23	50	0.36	712.7	20.8	1597.1	9.3	2313.4	0.0	0.0000	136.4	132.7	0.003
23	49	2.30	712.7	20.8	1575.3	6.0	2291.3	0.1	0.0001	114.2	110.9	0.021
23	48	-6.41	712.7	20.8	1501.8	153.7	2214.0	3.2	0.0045	36.9	37.4	0.171
23	47	-1.01	712.7	20.8	1424.7	2.5	2139.5	0.1	0.0002	-37.6	-39.7	0.025

i	**j**	**K_{ijk} / cm^{-1}**	**ω(i) / cm^{-1}**	**I(i) / km mol^{-1}**	**ω(j) / cm^{-1}**	**I(j) / km mol^{-1}**	**ω(ij) / cm^{-1}**	**I(ij) / km mol^{-1}**	**I(ij) / I(k)**	**Δω'**	**Δω**	**TFR**
23	46	-10.76	712.7	20.8	1357.2	65.3	2075.0	0.4	0.0005	-102.1	-107.2	0.100
23	44	0.26	712.7	20.8	1317.1	8.3	2030.4	0.0	0.0000	-146.7	-147.3	0.002
23	43	-2.89	712.7	20.8	1318.5	3.2	2032.9	0.1	0.0001	-144.2	-145.9	0.020
21	49	0.34	651.1	3.3	1575.3	6.0	2218.4	0.0	0.0000	41.4	49.3	0.007
20	49	0.80	644.1	3.0	1575.3	6.0	2222.5	0.1	0.0001	45.5	42.4	0.019
20	48	-2.19	644.1	3.0	1501.8	153.7	2145.3	0.7	0.0010	-31.8	-31.1	0.070
20	47	-0.85	644.1	3.0	1424.7	2.5	2069.7	0.0	0.0000	-107.4	-108.3	0.008
19	49	-0.24	599.2	5.0	1575.3	6.0	2187.3	0.0	0.0000	10.2	-2.5	0.093
17	50	-0.81	552.9	9.0	1597.1	9.3	2152.4	0.9	0.0012	-24.7	-27.1	0.030
17	48	0.77	552.9	9.0	1501.8	153.7	2052.3	0.1	0.0001	-124.7	-122.4	0.006
15	52	0.25	509.1	10.1	1711.4	725.4	2255.2	0.0	0.0000	78.2	43.5	0.006
14	53	-0.25	448.9	0.5	1770.6	0.6	2233.6	0.0	0.0000	56.5	42.4	0.006
14	50	-0.33	448.9	0.5	1597.1	9.3	2047.8	0.0	0.0000	-129.3	-131.1	0.002
11	52	-0.32	370.6	1.2	1711.4	725.4	2082.2	0.1	0.0001	-94.8	-95.1	0.003
10	53	0.29	336.9	4.0	1770.6	0.6	2122.2	0.0	0.0000	-54.8	-69.6	0.004
6	54	6.14	146.7	6.3	2177.1	710.8	2313.6	0.1	0.0002	136.5	146.7	0.042
5	54	4.21	123.2	6.1	2177.1	710.8	2291.6	0.3	0.0005	114.5	123.2	0.034
1	54	1.27	2.7	0.1	2177.1	710.8	2171.3	1.7	0.0024	-5.8	2.7	0.473

VITA

Graduate School
Southern Illinois University Carbondale

Gammanage Sathya M. Perera

sathya.madhuwanthi93@gmail.com

University of Ruhuna
Bachelor of Science, Chemistry, May 2017

Thesis Paper Title:
Density functional theory studies of Fermi resonance in small aryl azide vibrational probes.

Major Professor: Lichang Wang

Publications:
Perera, S. M.; Hettiarachchi, S. R.; Hewage, J. W. Molecular Adsorption of H_2 on Small Neutral Silver-Copper Bimetallic Nanoparticles: A Search for Novel Hydrogen Storage. *ACS OMEGA* **2022**, 7, 2316-2330.

Presentations:
Perera, S. M.; Hettiarachchi, S. R.; Hewage, J. W. Silver-Copper Bimetallic Nanoclusters as Potential Candidates for Hydrogen Storage. Presented at the ACS Spring 2022 National Meeting, San Diego, USA, March 20-24, 2022.

Perera, S. M.; Moran S. D.; Wang, L. DFT Studies of Fermi Resonance in Azido Modified IR Tags. Presented at the ACS Spring 2022 National Meeting, San Diego, USA, March 20-24, 2022.